THE PHYSIOLOGICAL REGULATION OF ENERGY METABOLISM IN INSECTS

EDITED BY: Bin Tang, Fernando Ariel Genta, Kai Lu and Oleh Lushchak
PUBLISHED IN: Frontiers in Physiology

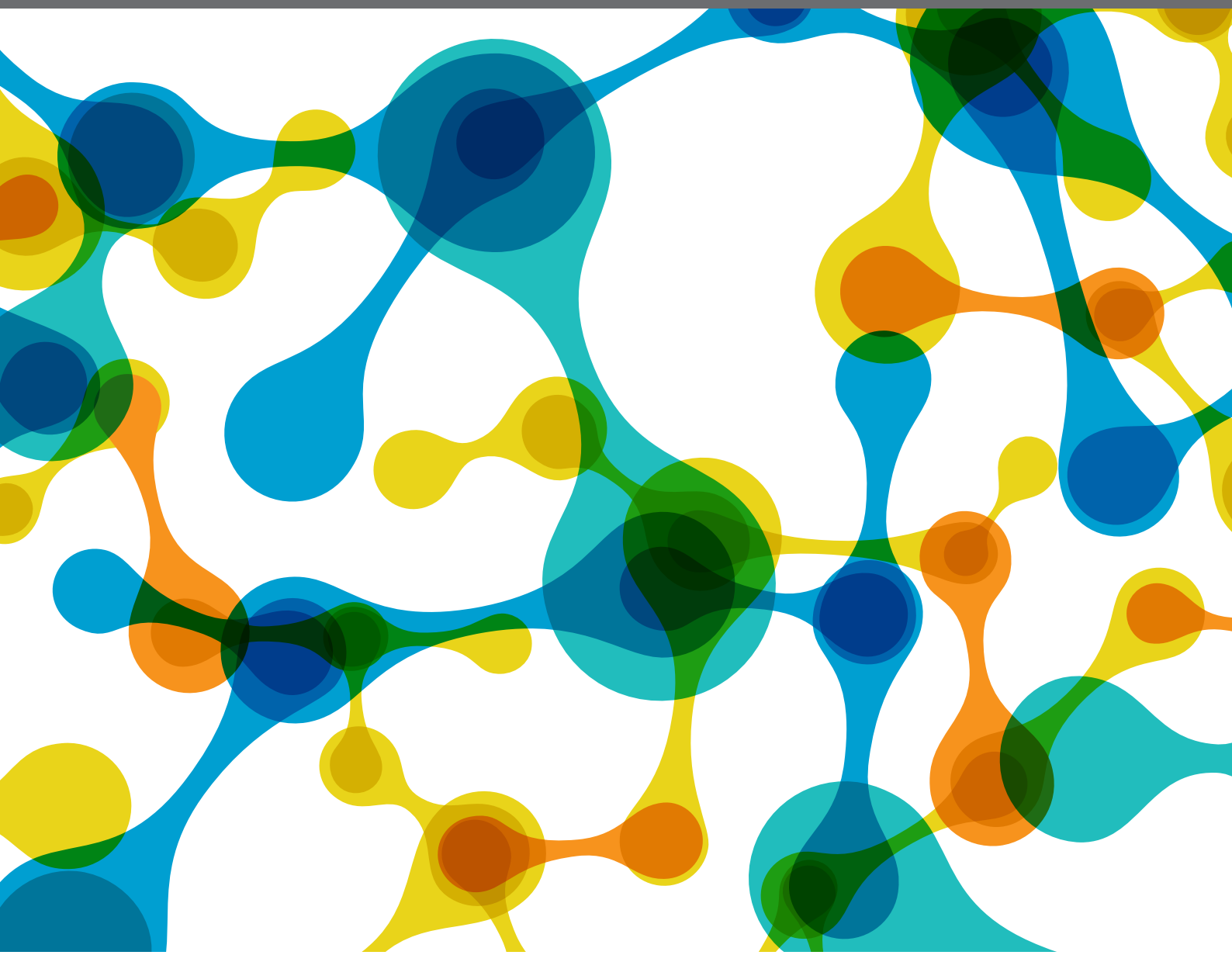

frontiers Research Topics

frontiers

ISSN 1664-8714
ISBN 978-2-88966-887-8
DOI 10.3389/978-2-88966-887-8

About Frontiers

Frontiers is more than just an open-access publisher of scholarly articles: it is a pioneering approach to the world of academia, radically improving the way scholarly research is managed. The grand vision of Frontiers is a world where all people have an equal opportunity to seek, share and generate knowledge. Frontiers provides immediate and permanent online open access to all its publications, but this alone is not enough to realize our grand goals.

Frontiers Journal Series

The Frontiers Journal Series is a multi-tier and interdisciplinary set of open-access, online journals, promising a paradigm shift from the current review, selection and dissemination processes in academic publishing. All Frontiers journals are driven by researchers for researchers; therefore, they constitute a service to the scholarly community. At the same time, the Frontiers Journal Series operates on a revolutionary invention, the tiered publishing system, initially addressing specific communities of scholars, and gradually climbing up to broader public understanding, thus serving the interests of the lay society, too.

Dedication to Quality

Each Frontiers article is a landmark of the highest quality, thanks to genuinely collaborative interactions between authors and review editors, who include some of the world's best academicians. Research must be certified by peers before entering a stream of knowledge that may eventually reach the public - and shape society; therefore, Frontiers only applies the most rigorous and unbiased reviews.
Frontiers revolutionizes research publishing by freely delivering the most outstanding research, evaluated with no bias from both the academic and social point of view. By applying the most advanced information technologies, Frontiers is catapulting scholarly publishing into a new generation.

What are Frontiers Research Topics?

Frontiers Research Topics are very popular trademarks of the Frontiers Journals Series: they are collections of at least ten articles, all centered on a particular subject. With their unique mix of varied contributions from Original Research to Review Articles, Frontiers Research Topics unify the most influential researchers, the latest key findings and historical advances in a hot research area! Find out more on how to host your own Frontiers Research Topic or contribute to one as an author by contacting the Frontiers Editorial Office: frontiersin.org/about/contact

THE PHYSIOLOGICAL REGULATION OF ENERGY METABOLISM IN INSECTS

Topic Editors:
Bin Tang, Hangzhou Normal University, China
Fernando Ariel Genta, Oswaldo Cruz Foundation (Fiocruz), Brazil
Kai Lu, Fujian Agriculture and Forestry University, China
Oleh Lushchak, Vasyl Stefanyk Precarpathian National University, Ukraine

Citation: Tang, B., Genta, F. A., Lu, K., Lushchak, O., eds. (2021). The Physiological Regulation of Energy Metabolism in Insects. Lausanne: Frontiers Media SA.
doi: 10.3389/978-2-88966-887-8

Table of Contents

frontiers in Physiology

ORIGINAL RESEARCH
published: 20 August 2020
doi: 10.3389/fphys.2020.01071

Roles of the *PTP61F* Gene in Regulating Energy Metabolism of *Tribolium castaneum* (Coleoptera: Tenebrionidae)

Kang-Kang Xu[1†], Bi-Ying Pan[2†], Yuan-Yuan Wang[1], Qian-Qian Ren[1] and Can Li[1]*

[1] Guizhou Provincial Key Laboratory for Rare Animal and Economic Insect of the Mountainous Region, Guizhou Provincial Engineering Research Center for Biological Resources Protection and Efficient Utilization of the Mountainous Region, College of Biology and Environmental Engineering, Guiyang University, Guiyang, China, [2] College of Life and Environmental Sciences, Hangzhou Normal University, Hangzhou, China

Protein tyrosine phosphatase 1B (PTP1B) is a negative regulator in the insulin signaling pathway. It belongs to a class of non-receptor phosphatases of protein tyrosine phosphatase and can catalyze the dephosphorylation of tyrosine to regulate cell differentiation, growth, and metabolism. However, few studies have focused on the role of PTP1B in regulating energy metabolism of insects. In this study, we investigated the expression profiles and the functions of a *PTP1B* gene (designated *TcPTP61F*) in the red flour beetle *Tribolium castaneum*. Quantitative real-time PCR analyzed showed that *TcPTP61F* was highly expressed in the pupal and adult stages. In adult tissues, *TcPTP61F* was prominently expressed in the tarsus and head. RNA interference-mediated silencing of *TcPTP61F* reduced the expression of eight genes in trehalose metabolic and glycolytic pathways. *TcPTP61F* depletion also caused a significant change in the distribution of trehalose, glucose, and glycogen. Additionally, knockdown of *TcPTP61F* inhibited the pyruvate kinase (PK) activity and significantly decreased the adenosine triphosphate (ATP) level. The results suggest that *TcPTP61F* is indispensible for trehalose and energy metabolism of *T. castaneum*.

Keywords: *Tribolium castaneum*, protein tyrosine phosphatase, RNA interference, trehalose metabolism, energy metabolism

OPEN ACCESS

Edited by:
Kai Lu,
Fujian Agriculture and Forestry University, China

Reviewed by:
Shunhua Gui,
Ghent University, Belgium
Honggang Tian,
Northwest A&F University, China
Hamzeh Izadi,
Vali-E-Asr University of Rafsanjan, Iran

***Correspondence:**
Can Li
lican790108@163.com

[†]These authors have contributed equally to this work

Specialty section:
This article was submitted to Invertebrate Physiology, a section of the journal Frontiers in Physiology

Received: *23 June 2020*
Accepted: *04 August 2020*
Published: *20 August 2020*

Citation:
Xu K-K, Pan B-Y, Wang Y-Y, Ren Q-Q and Li C (2020) Roles of the PTP61F Gene in Regulating Energy Metabolism of Tribolium castaneum (Coleoptera: Tenebrionidae). Front. Physiol. 11:1071. doi: 10.3389/fphys.2020.01071

INTRODUCTION

Insects need a continuous supply of energy to maintain their metabolism and activity. Energy metabolism in the insect body is constant. Insects directly use trehalose as their main energy source and it serves as the main sugar component of insect hemolymph (Yasugi et al., 2017). Trehalose is a highly stable, non-reducing disaccharide formed by two glucose molecules. It is found in a variety of organisms including bacteria, yeast, fungi, nematodes, insects, and some other invertebrates, but not in mammals (Elbein et al., 2003). In addition to playing a crucial role as an immediate source of energy, trehalose also plays important functions in insect response to stresses such as high or low temperatures, poor nutrition or starvation, oxidation, high osmotic pressure, toxic substances, and UV-B irradiation (Tamang et al., 2017; Chen J. X. et al., 2018). Under the catalysis of trehalose phosphate synthase (TPS), uridine diphosphate (UDP) glucose (UDP-glucose) and glucose-6-phosphate (G-6-P) synthesize trehalose-6-phosphate, which is then dephosphorylated

under the action of 6-trehalose phosphate esterase (TPP) to produce trehalose. This is the most important path of trehalose synthesis in insects (Shukla et al., 2015; Tang et al., 2017; Chen J. X. et al., 2018).

When energy is needed, trehalose is hydrolyzed into glucose under the catalysis of trehalase (TRE), the only enzyme known to irreversibly degrade trehalose (Barraza and Sánchez, 2013). Glucose then enters the glycolysis-tricarboxylic acid (glycolysis-TCA) cycle. In the glycolysis pathway, glucose serves as the initial substrate and is converted into pyruvate by a series of enzymes, including hexokinase (HK), glucose-6-phosphate isomerase (G6PI), phosphofructokinase (PFK), and pyruvate kinase (PK) (Hu et al., 2016). Pyruvate can be further converted into acetyl-coenzyme A (acetyl-CoA), which can combine with oxaloacetic acid to enter TCA cycle and finally be oxidized to CO_2, H_2O, and adenosine triphosphate (ATP) (Hu et al., 2016). Insects could adapt to various physiological activities by regulating the rate of the glycolysis-TCA cycle. For example, some insects reduce the expression of glycolysis or TCA metabolic enzyme genes in the early pupal stage which saves energy for the development of new organs. These species include *Drosophila melanogaster*, *Bombyx mori*, and *Spodoptera litura* (White et al., 1999; Tian et al., 2010; Hu et al., 2016).

Insulin is important in regulating glucose homeostasis, lipid metabolism, and energy balance (White, 1998; Czech and Corvera, 1999). It can increase the transport of glucose and the synthesis of glycogen, diminish gluconeogenesis, inhibit glycogenolysis, and regulate the expression of many genes (Lochhead et al., 2001; Vital et al., 2010). Components of the insulin signaling pathway are extremely conserved in organisms as distantly related as humans, *D. melanogaster*, and *Caenorhabditis elegans* (Leevers, 2001). In *Aedes aegypti*, upstream components of the insulin signaling pathway, such as phosphatidylinositol 3-kinase (PI3K) (Pri-Tal et al., 2008) and protein kinase B (AKT) (Riehle and Brown, 2003), have been associated with glucose metabolism. The insulin signaling pathway not only controls the metabolic balance of blood glucose but also directly regulates juvenile hormones and ecdysone, which control insect development, metamorphosis, and reproduction (Satake et al., 1997; Vital et al., 2010; Kim and Hong, 2015).

Protein tyrosine phosphatases (PTPs, EC 3.1.3.48) are a large family of enzymes that regulate insulin signal transduction and are also involved in cell signal transduction and cell cycles (Klaman et al., 2000; Tonks, 2006). The PTP family is composed of four different subfamilies, classes I, II, III and IV (Sacco et al., 2012). Class I Cys-PTPs are the largest group of PTPs and could be divided into "classical" and dual specificity phosphatases, in which classical phosphatases are strictly devoted to the dephosphorylation of phosphotyrosine residues (Alonso et al., 2004). The family genes additionally participate in other physiological activities and metabolic processes such as cell differentiation, transformation, growth, reproduction, and immunity (Abaskharoun et al., 2010; Bao et al., 2011; Alho et al., 2013; Agouni et al., 2014). Protein tyrosine phosphatase 1B (PTP1B) is involved in the regulation of insulin action and other signal transduction pathways. PTP1B is a major regulator of energy balance, insulin sensitivity, and fat storage in insect body. In *Locusta migratoria tibetensis*, PTPN1-encoded insulin receptor inhibitor tyrosine protein phosphatase non-receptor type PTP1B is a negative regulator of the insulin pathway, and it plays an important role in response to hypoxic stress (Ding et al., 2018). The homologous gene of *PTP1B* in *D. melanogaster* encoded by PTP61F specifically targets to Dock and enhances the signal selectivity of insulin receptor (Wu et al., 2011).

The red flour beetle, *Tribolium castaneum* (Herbst) (Coleoptera: Tenebrionidae), is a worldwide pest of stored grains (Mehmood et al., 2018; Chen Q. W. et al., 2018). It has glands that secrete a liquid which causes a moldy smell in flour and this secretion also contains the carcinogen benzoquinone (Boateng and Obengofori, 2008). Control of *T. castaneum* in stored products and grain is primarily by fumigants and sprays, but insecticide resistance is now a major problem (Pimentel et al., 2010; Perkin and Oppert, 2019). Most importantly, *T. castaneum* is a model insect often used for research on gene function (Lorenzen et al., 2007). To date, few studies have evaluated the role of PTP1B in regulating energy metabolism in insects. In this present study, we identified and obtained a *PTP1B* gene (*TcPTP61F*) from *T. castaneum* and analyzed its expression patterns in different developmental stages and tissues. We used RNA interference *in vivo* to efficiently disrupt the *TcPTP61F* gene function in order to clarify its role in regulating the energy metabolism of *T. castaneum*.

MATERIALS AND METHODS

Insect and Sample Preparation

The laboratory stock colony of *T. castaneum* were raised on whole wheat flour containing 5% yeast in an incubator at 28 ± 1°C and 65 ± 5% relative humidity under a constant 24 h dark (0L:24D).

In the tissue-specific experiment, the adults (male to female ratio 1:1) were used for tissue dissection. The antennae, head, wing, tarsus, epidermis, midgut, and fat body of *T. castaneum* were dissected under a stereomicroscope (Olympus SZX12, Tokyo, Japan). Pools of 200 individuals were used to prepare each body part. Samples at different developmental stages, including early larvae (EL, 2nd instar), middle larvae (ML, 5th instar), and late larvae (LL, 8th instar); early pupae (EP, 1st day), middle pupae (MP, 3rd day), and late pupae (LP, 5th day); and early adults (EA, 1st day), middle adults (MA, 3rd day), and late adults (LA, 5th day) were collected separately. *T. castaneum* used for the microinjection of double-stranded RNA (dsRNA) were the 1st day of the 8th instar larvae, and the insects at 48 and 72 h after injection were collected for determination of gene expression, carbohydrate content, and ATP content. Ten individuals were used for gene expression, and 20 for carbohydrate, and ATP contents, respectively. All above the samples were immediately frozen in liquid nitrogen and stored at -80°C. All of the experiments were repeated three times.

RNA Isolation and cDNA Synthesis

Total RNA was isolated from each sample by using the MiniBEST Universal Extraction Kit (TaKaRa, Dalian, China),

following the manufacturer's instructions. Total RNA integrity was evaluated using 1% agarose gel electrophoresis, and the RNA concentration and purity were determined by a NanoDrop 2000C Spectrophotometer (Thermo Fisher Scientific, Waltham, MA, United States). First-strand complementary DNA (cDNA) synthesis was performed using the PrimeScript® RT Reagent Kit (TaKaRa, Dalian, China) following manufacturer's instructions.

Synthesis and Injection of dsRNA

RNAi was used to study the potential function of *TcPTP61F* in *T. castaneum*. The dsRNA primers (**Table 1**) for *TcPTP61F* and green fluorescent protein (*GFP*, as control) were designed using E-RNAi[1]. The PCR products were subject to T cloning, followed by a subsequent amplification with primers containing the T7 promoter sequence. Cross-PCR reactions were performed using a T7 RiboMAX^{TM} Express RNAi System kit (Promega, Madison, WI, United States) to synthesize dsRNA. The dsRNA was diluted with nuclease-free water to a final concentration of 2 μg/μL. Using a Nanoliter 2010 injector (World Precision Instruments, Sarasota, FL, United States), 200 ng of ds*TcPTP61F* or ds*GFP* was slowly injected into the hemocoel between the third and fourth abdominal segments of each 1st day of the 8th instar larvae. Three biological replicates (each with at least 50 larvae) were treated by ds*TcPTP61F* and ds*GFP* injection. The insects treated with dsRNA were reared under the same conditions as mentioned above.

Quantitative Real-Time Polymerase Chain Reaction (qPCR)

The qPCR was conducted to confirm the relative expression levels of *PTP61F* in various developmental phases and tissues. At 48 and 72 h after dsRNA injection, the insects from each treatment were collected for qPCR to assess the efficiency of the RNAi. After *PTP61F* was knocked down, transcript levels of six trehalose metabolic pathway genes, including five trehalases (*TcTre1-1*, *TcTre1-2*, *TcTre1-3*, *TcTre1-4*, and *TcTre2*) and trehalose-6-phosphate synthase gene (*TcTPS*); and glycolytic pathway genes, such as hexokinases (*TcHK1* and *TcHK2*) and glucose-6-phosphate isomerase (*TcG6PI*); and pyruvate kinase gene (*TcPK*) were detected by qPCR after injection. The qPCR was carried out on a CFX-96 real-time detection system (Bio-Rad, Hercules, CA, United States) in a 20 μL reaction containing 1 μL (100 ng/μL) cDNA, 1 μL (10 μM) each primer (**Table 1**), 7 μL nuclease-free water, and 10 μL of GoTaq® qPCR MasterMix (Promega). The reaction was performed under the following conditions: pre-incubation at 95°C for 2 min, followed by 40 cycles of 95°C for 30 s and annealing at 60°C for 30 s, with a melting curve at 65–95°C. Amplification of *Ribosomal Protein L13a* (*RPL13a*) was used as an internal control. All of the experiments were performed in triplicate, with two technical replicates each. The $2^{-\Delta\Delta CT}$ method was used for the analysis of relative gene expression (Livak and Schmittgen, 2001).

[1]http://www.dkfz.de/signaling/e-rnai3/idseq.php

Analysis of Trehalose, Glucose, and Glycogen Contents

Twenty individuals, collected after injection, were used to measured trehalose, glucose and glycogen contents. The anthrone-sulfuric acid method was used to measure the trehalose content (Leyva et al., 2008). The assay of glucose and glycogen contents was performed according to the previously described methods (Zhang et al., 2017). Three independent biological replicates were used for assays. Briefly, the samples were homogenized in 200 μL phosphate buffer saline (PBS; pH 7.0), then 800 μL PBS was added up to 1 mL. Subsequently, the homogenate was centrifuged at 1,000 g for 20 min at 4°C. The supernatant (300 μL) was taken to detect concentrations of protein, trehalose, and glycogen as described below. Then 350 μL of the supernatant was removed and ultracentrifuged at 20,800 g for 60 min at 4°C. The supernatant (300 μL) obtained from ultracentrifugation was used to determine the concentration of protein and glucose. The sediment was suspended in PBS (300 μL) then used for the determination of protein and glucose contents. The glucose content was determined using a glucose (GO) Assay Kit (Sigma-Aldrich, St. Louis, MO, United States) according to manufacturer instructions. As for the determination of glycogen content, the methods were similar to the methods of glucose content measurement unless the samples required 4 h decomposition reaction by amyloglucosidase (catalog no. 10115, Sigma-Aldrich). The protein content was determined using the BCA Protein Assay Kit (Beyotime, China).

Determination of PK Activity and Measurement of ATP Content

The beetles were mixed into physiological saline (g:mL = 1:9) for grinding and crushing to obtain a 10% homogenate. The 10% homogenate was prepared with physiological saline, and the experiment was conducted according to the instruction on the Pyruvate Kinase Assay Kit (No. A076-1-1, Nanjing Jiancheng Bioengineering Institute) to determinate the PK activity. Measurement of ATP content was determined according to the instruction of ATP Assay Kit (No. A095-1-1, Nanjing Jiancheng Bioengineering Institute).

Statistical Analyses

All of the data were presented as mean ± standard error (SE) and were analyzed using SPSS version 20 software (SPSS Inc., Chicago, IL, United States). A one-way analysis of variance (ANOVA) followed by a least significant difference (LSD) test was used for comparing the differences among more than two samples. Differences between two groups were compared using Student's *t*-test ($^{*}P < 0.05$, $^{**}P < 0.01$).

RESULTS

The Developmental and Tissue Expression Profiles of *TcPTP61F*

We measured the expression level of *TcPTP61F* in the antenna, head, wing, tarsus, epidermis, midgut, and fat body from adult

TABLE 1 | Primers used to synthesize dsRNA and analyze transcript levels.

Application of primers	Gene name	Forward primer (5′–3′)	Reverse primer (5′-3′)	Length (bp)
dsRNA synthesis	*TcPTP61F*	T7-GTCATCGGGCAATAACATC	T7-ATATCTCGGGACTCTTTCGT	584
	GFP	T7-AAGGGCGAGGAGCTGTTCACCG	T7-CAGCAGGACCATGTGATCGCGC	256
qPCR analysis	*TcPTP61F*	CCAAATATCCCCAAGAGC	GACTATCGGAACGCAAATC	151
	TcTre1-1	AACGACTCGCAATGGCTGG	CGGAGGCGTAGTGGAATAGAG	127
	TcTre1-2	GTGCCCAATGGGTTTATCG	CAACCACAACACTTCCTTCG	261
	TcTre1-3	CCTCTCATTCGTCACAAGCG	AAGCGTTTGATTTCTTTGCG	205
	TcTre1-4	ACGGTGCCCGCATCTACTA	GTGTAGGTGGTCCCGTTCTTG	187
	TcTre2	CTCAGCCTGGCCCTTAGTTG	GGAGTCCTCGTAGATGCGTT	120
	TcTPS	CGATTCGTACTACAACGGCTGC	GTGGTGTAGCATTGCCAGTGC	105
	TcHK1	CGCACCGAATGCCAGAATC	GACCCACCCGACATCGATT	141
	TcHK2	CGAATCGGCCTAATAGTTGGC	GACGGAGCCCTCGATTTCAT	155
	TcG6PI	GTGATGCCGGAGGTGAAT	CACGTCGGTGATGGGCTT	112
	TcPK	CAATTTTACCGCATCTCAAC	GTCTCCATCATTTTCTCCAAC	240
	TcRPL13a	ACCATATGACCGCAGGAAAC	GGTGAATGGAGCCACTTGTT	250

T7:GGATCCTAATACGACTCACTATAGG.

T. castaneum to study tissue-specific expression profiles of *TcPTP61F* (**Figure 1A**). Among the seven tissues, the highest expression level of *TcPTP61F* was detected in the tarsus, followed by the head and epidermis; expression was relatively lower in the other tissues. As for developmental expression profiles illustrated in **Figure 1B**, the mRNA of *TcPTP61F* was highly expressed in the pupal and adult stages was stable at a low expression level in larvae. The results showed that the expression of *TcPTP61F* varied across developmental stages and among many tissues.

Evaluation of the Efficiency of RNAi Knockdown by ds*TcPTP61F*

To determine the effect of RNAi, the relative expression level of *TcPTP61F* were detected by qPCR. The results showed that the expression level of *TcPTP61F* was significantly decreased at 48 and 72 h after ds*TcPTP61F* injection ($P < 0.01$) (**Figure 2**), and the interference efficiency were 88.14 and 94.29%, respectively, indicating the successful inhibition of the target genes.

Effects on the Relative Expression Levels of Genes in the Trehalose Metabolic Pathway Following *TcPTP61F* Knockdown

The results showed that the mRNA levels of *TcTre1-1*, *TcTre1-4*, *TcTre2*, and *TcTPS* decreased significantly at 48 and 72 h after *TcPTP61F* was inhibited ($P < 0.05$) (**Figures 3A,D–F**). The expression levels of *TcTre1-2* and *TcTre1-3* decreased at 48 h but increased significantly at 72 h after injection of ds*TcPTP61F* ($P < 0.01$) (**Figures 3B,C**).

Effects on the Content of Trehalose, Glucose, and Glycogen Following ds*TcPTP61F* Injection

The content of trehalose increased 52.62% at 48 h after injection with ds*TcPTP61F* ($P < 0.01$) and then was restored to a normal level at 72 h compared to the ds*GFP* group (**Figure 4A**). In contrast, the glycogen and glucose contents significantly increased at 72 h after *TcPTP61F* was knocked down ($P < 0.05$) (**Figures 4B,C**). The glycogen content was stable at 48 h after ds*TcPTP61F* injection (**Figure 4B**), whereas the glucose content decreased significantly ($P < 0.05$) (**Figure 4C**).

Effects of *TcPTP61F* Knockdown on the Relative Expression of Critical Genes in the Glycolytic Pathway

After *TcPTP61F* was knocked down, the relative expressions of *HK1* and *HK2* were significantly downregulated at 48 and 72 h ($P < 0.01$) (**Figures 5A,B**). In addition, the relative expression of *G6PI* was significantly downregulated at 48 h, but upregulated sharply at 72 h ($P < 0.01$) (**Figure 5C**).

Effects on the Enzyme Activity of PK and ATP Content After *TcPTP61F* Knockdown

When *TcPTP61F* was inhibited, the enzyme activity of PK significantly decreased at 48 and 72 h, especially it was decreased at 48 h by 42.03% compared to the ds*GFP* group ($P < 0.05$) (**Figure 6A**). Consistently, the mRNA level of *TcPK* was significantly down-regulated at 48 and 72 h after *TcPTP61F* suppression ($P < 0.01$) (**Figure 6B**). The ATP content decreased 63.61 and 23.15% at 48 and 72 h after ds*TcPTP61F* injection, respectively (**Figure 7**).

DISCUSSION

Protein phosphorylation and dephosphorylation is one of the most important biochemical reactions in the body and plays a role in regulating cell growth, proliferation, differentiation, and immunity (Mustelin et al., 2005; Tonks, 2006). Protein tyrosine phosphatase is a type of superfamily phosphatase that changes its phosphate by specifically catalyzing the removal of phosphate groups on phosphorylated modified tyrosine residues to control cell function (Tonks, 2006).

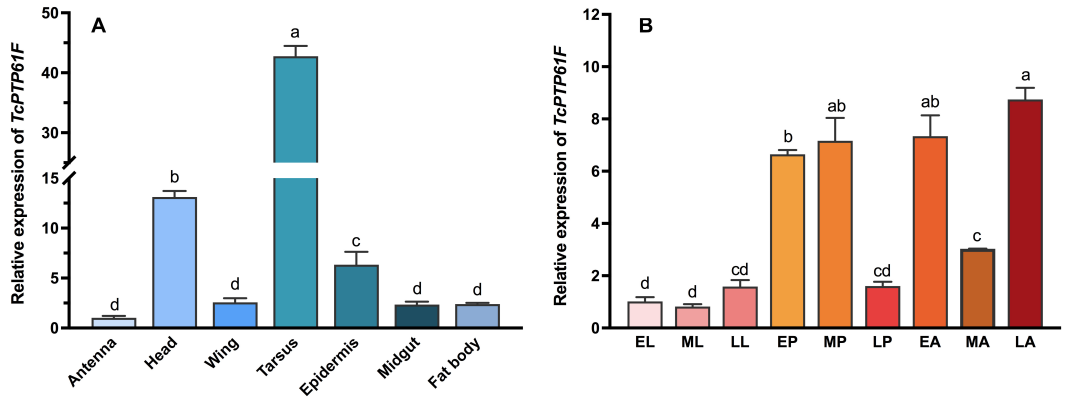

FIGURE 1 | Relative expression levels of *TcPTP61F* in different tissues **(A)** and different developmental stages **(B)** of *Tribolium castaneum*. EL, ML, LL, EP, MP, LP, EA, MA, and LA represent early instar larvae, middle instar larvae, late instar larvae, early pupae, middle pupae, late pupae, early adults, middle adults, and late adults, respectively. Different letters above bars indicate significant differences based on one-way ANOVA followed by a least significance difference test ($P < 0.05$).

Although the amino acid sequences and substrates of PTPs differ, most PTPs have a conserved structural motif (Motif) (H/V) C (X) R (S/T) (**Supplementary Figure S1**), and this structural phantom plays a key role in the catalytic activity of PTP (Wang et al., 2014). The amino acid sequences of PTP1B in several insect species contain a catalytic domain of protein tyrosine phosphatase (PTPc) (**Supplementary Figure S2**).

PTP1B is a ubiquitously expressed intracellular protein tyrosine phosphatase (Forsell et al., 2000). It is common in the testis, kidney, spleen, muscle, heart, liver, and brain of mice (Miyasaka and Li, 1992). However, there are few studies of PTP1B in insects. In *A. aegypti*, it has been reported to occur in all tissues, and it is highly expressed in the ovaries (Moretti et al., 2014). In this study, we found that *TcPTP61F* is expressed in a variety of *T. castaneum* tissues. This study did not evaluate the *T. castaneum* ovary but it showed that *TcPTP61F* was highly expressed in the tarsus and the head. Muscle has been revealed as one of the insulin's key target tissues (Saltiel and Kahn, 2001; Biddinger and Kahn, 2006), and it is known that tarsus contains a great number of muscle, which may be the main reason of the high expression of *TcPTP61F* in tarsus. Like the mosquito, the head of *T. castaneum* is also composed of many different structures and tissues, and responsible for several physiological processes (Predel et al., 2010). Meanwhile, phosphorylation of tyrosine residues induces phosphotyrosine (pTyr) signaling pathways are important signal transduction systems for many cellular functions such as protein synthesis and cell proliferation. Further studies are required to clarify the roles of *TcPTP61F* in the tarsus and head of *T. castaneum*. In the developmental pattern of *TcPTP61F*, we found relatively lower expression in the larval stage, but higher expression in the pupal and adult stages, which demonstrates differences in *TcPTP61F* at different developmental stages. A transient increase occurred in the total tyrosine phosphorylation of the *A. aegypti* head during the first days after adult emergence (Jablonka et al., 2011), and our results are consistent with the those in *A. aegypti*.

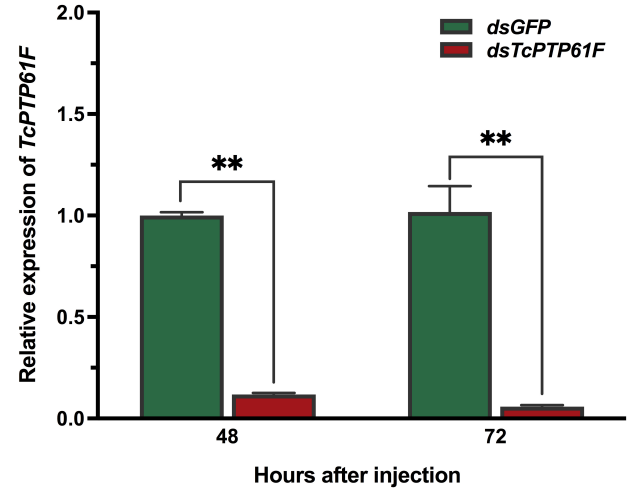

FIGURE 2 | Relative expression levels of *TcPTP61F* at 48 and 72 h after *TcPTP61F* or *GFP* dsRNA injection. Significant differences between the RNAi group and the control group were determined using Student's *t*-test (**$p < 0.01$).

PTP1B is a member of the PTPs family and plays a key regulatory role in insulin and leptin signaling. By catalyzing the dephosphorylation of phosphotyrosine (pTyr), it maintains the level of phosphorylation of protein tyrosine together with protein tyrosine kinase (PTKs) (Tiganis and Bennett, 2007). PTP1B regulates the insulin signaling pathway with tissue specificity. The lack of T-cell protein tyrosine phosphatase (TCPTP) in the muscles of mice does not alter insulin signaling and glucose homeostasis (Loh et al., 2012). RNAi is an effective means to inhibit gene expression through dsRNA injection and it is widely used to study gene function (Prentice et al., 2017). To explore the potential role of *TcPTP61F* in *T. castaneum*, we knocked down *TcPTP61F* using RNAi technology. The expression of *TcPTP61F* decreased significantly at 48 and 72 h following ds*TcPTP61F* injection. Trehalose can provide energy to promote

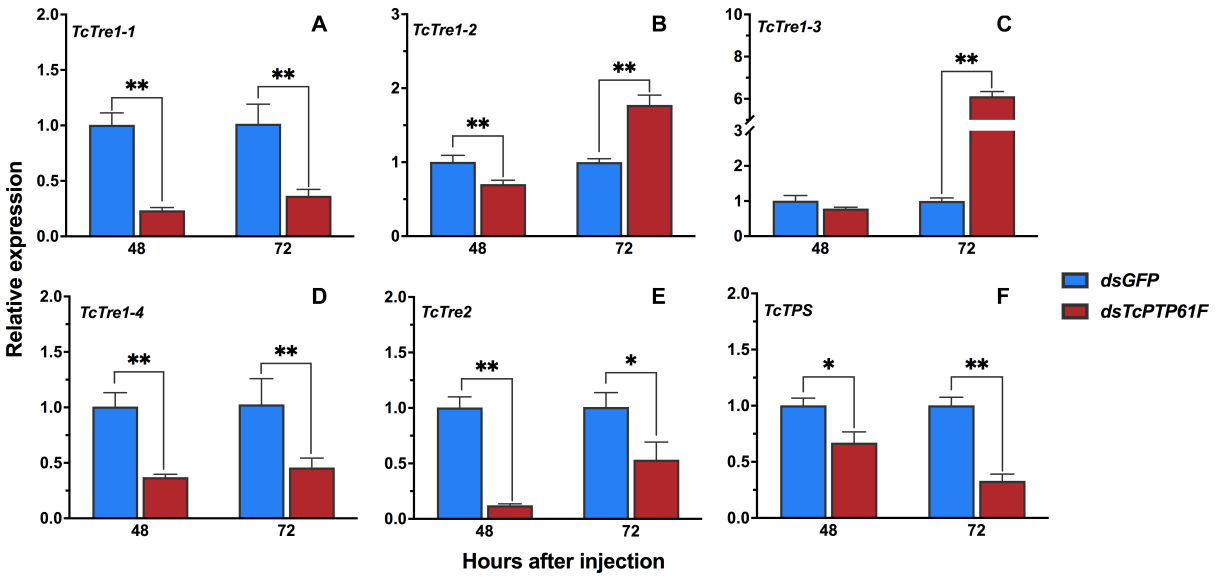

FIGURE 3 | Effects of *TcPTP61F* knockdown on the expressions of six trehalose metabolic pathway genes. The relative expression levels of five trehalases (*TcTre*, **A–E**) and one trehalose-6-phosphate synthases (*TcTPS*, **F**) at 48 and 72 h after *TcPTP61F* or *GFP* dsRNA injection. The expression values were calculated by comparison to the ds*GFP* group, which was normalized at 1. Significant differences were identified by Student's *t*-test (*$P < 0.05$, **$P < 0.01$).

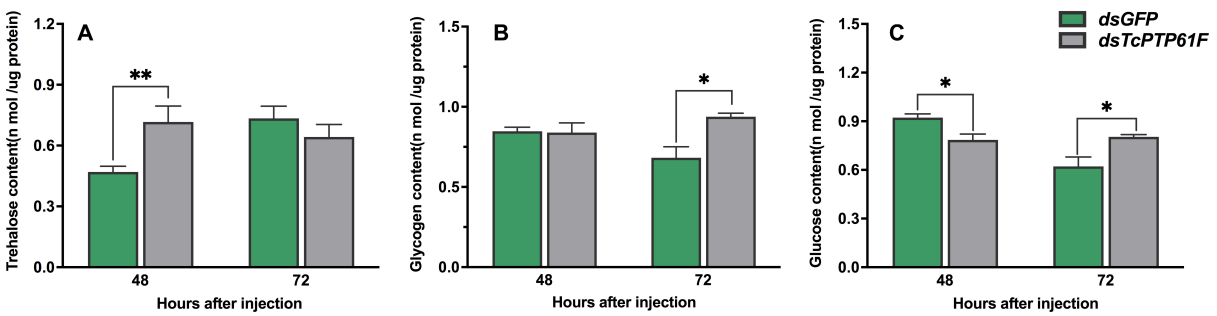

FIGURE 4 | Effects of *TcPTP61F* knockdown on content of trehalase **(A)**, glycogen **(B)**, and glucose **(C)**. Significant differences were identified by Student's *t*-test (*$P < 0.05$, **$P < 0.01$).

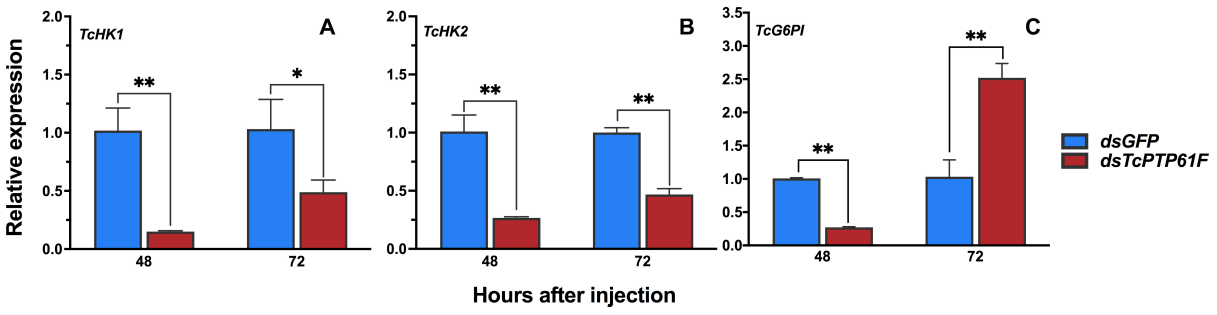

FIGURE 5 | Effects of *TcPTP61F* knockdown on the expressions of three glycolytic pathway pathway genes. The relative expression levels of *TcHK1* **(A)**, *TcHK2* **(B)**, and *TcG6PI* **(C)** at 48 and 72 h after *TcPTP61F* or *GFP* dsRNA injection. Significant differences were identified by Student's *t*-test (*$P < 0.05$, **$P < 0.01$).

development, metamorphosis, stress recovery, chitin synthesis, and flight (Wegener et al., 2003, 2010; Tatun et al., 2014; Shukla et al., 2015; Tang et al., 2017; Zhang et al., 2017). In addition, trehalase is critical to the role of trehalose in insect physiology because it is required for regulation of metabolism and glucose generation (Shukla et al., 2015). Therefore, we tested the gene

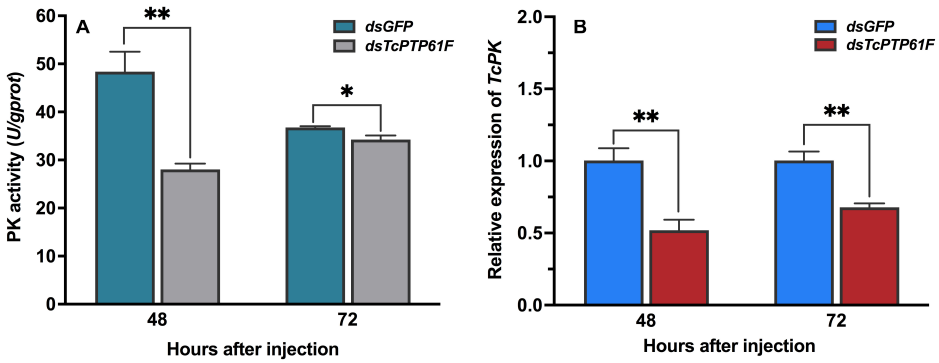

FIGURE 6 | Effect of *TcPTP61F* knockdown on pyruvate kinase activity **(A)** and expression of *TcPK* gene **(B)**. Significant differences were identified by Student's *t*-test (*$P < 0.05$, **$P < 0.01$).

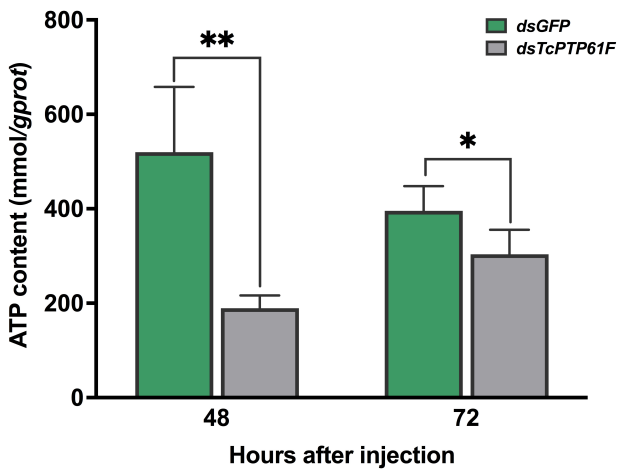

FIGURE 7 | Effect of *TcPTP61F* knockdown on content of adenosine triphosphate (ATP). Significant differences were identified by Student's *t*-test (*$P < 0.05$, **$P < 0.01$).

expression of the trehalose metabolism pathway of *T. castaneum* after RNAi and found that almost all *Tre* and *TPS* genes were significantly downregulated. However, *TcTre1-2* and *TcTre1-3* increased at 72 h after injection. These results suggest that the inhibition of *TcPTP61F* effected the regulation of the trehalose metabolism pathway. To further analyze its effect on trehalose metabolism, we tested the trehalose content and found that the synthesis of trehalose increased significantly at 48 h and returned to normal levels at 72 h (**Figure 4A**). This finding may be the result of the conversion of these three kinds of sugars. From the results of glucose and glycogen, we observed that trehalose accumulated at 48 h and was converted into glucose and glycogen after 72 h, resulting in a significant increase in glycogen and glucose content at 72 h (**Figures 4B,C**). The increased expression of *TcTre1-2* and *TcTre1-3* might be main cause of the destruction of glucose hemostasis. These results all indicate that the silencing of *TcPTP61F* can have an effect on trehalose metabolism.

Glycolysis is an important method of energy metabolism and it involves the process of glucose decomposed into pyruvate, under an anaerobic environment, by a series of enzymes (Sunna et al., 1997). Among these enzymes, hexokinase (HK) is the first rate-limiting enzyme in the glycolytic pathway, which plays a key role in glucose homeostasis and energy metabolism through glucose (Glc) phosphorylation and Glc signaling (Ge et al., 2019). Therefore, we tested the expression of *HK* to investigate the effect of ds*TcPTP61F* injection on the glucose homeostasis and energy metabolism of *T. castaneum*. The results showed that the expression of two *TcHK* genes in *T. castaneum* was significantly downregulated (**Figures 5A,B**). However, the glucose content decreases significantly at 48 h, it may be due to less glucose being synthesized. Furthermore, the glucose content increased significantly after RNAi at 72 h, which may be caused by the decomposition of a large amount of trehalose.

The PK enzyme catalyzes the conversion of phosphoenolpyruvate and ADP to pyruvate and ATP in glycolysis, and pyruvate can be further converted into acetyl-CoA that can combine with oxaloacetic acid to enter the TCA cycle (Israelsen and Vander Heiden, 2015). The TCA cycle, together with the subsequent electron transport chain, is one of the main metabolic pathways that provides energy to support cellular homeostasis under aerobic conditions (Gaster et al., 2012). Our results showed that PK enzyme activity was significantly reduced after *TcPTP61F* knockdown. Adenosine triphosphate has a fundamental intracellular role and is the direct energy source of most activities in living cells (Bodin and Burnstock, 2001). In this study, after *TcPTP61F* knockdown, the ATP content was significantly decreased both at 48 and 72 h.

Based on our results and previous studies, we propose a hypothesis for the roles of *TcPTP61F* in regulating energy metabolism of *T. castaneum* (**Figure 8**). PTP61F acts as insulin receptor inhibitor that causes changes in the distribution of trehalose, glucose, and glycogen as well as a decreased glycolysis level. Downregulation of *TcPTP61F* caused a decreased ATP content. The inhibition of *TcPTP61F* resulted in disorders of energy metabolism in *T. castaneum*.

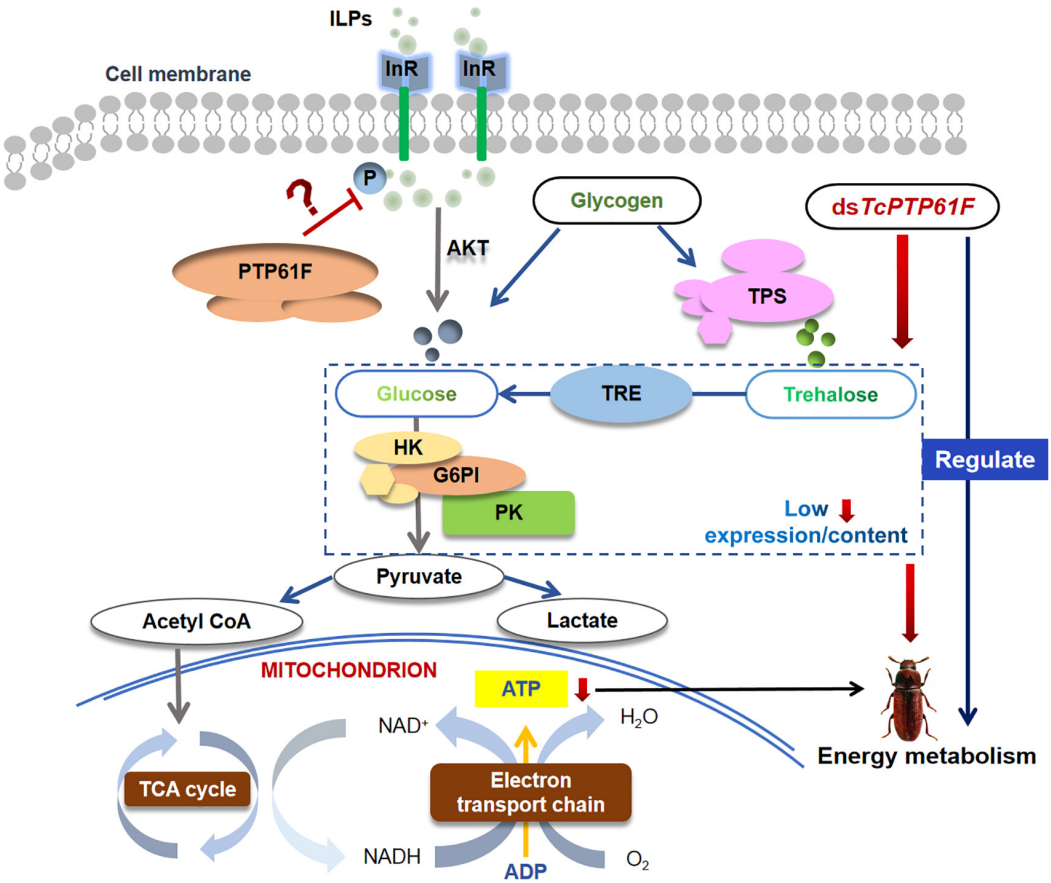

FIGURE 8 | Schematic description of the hypothesis for the roles of *TcPTP61F* in regulating energy metabolism of *T. castaneum*. PTP61F acts as insulin receptor inhibitor causes changes in the distribution of trehalose, glucose, and glycogen as well as a decreased glycolysis level. Downregulation of *TcPTP61F* caused a decreased ATP content. The inhibition of *TcPTP61F* resulted in disorders of energy metabolism in *T. castaneum*.

DATA AVAILABILITY STATEMENT

The raw data supporting the conclusions of this article will be made available by the authors, without undue reservation, to any qualified researcher.

AUTHOR CONTRIBUTIONS

K-KX, B-YP, and CL conceived and designed the experiments, and wrote the manuscript. B-YP, Y-YW, and Q-QR performed the experiments. CL revised the manuscript. All authors gave final approval for the publication. All authors contributed to the article and approved the submitted version.

FUNDING

This study was supported by the National Natural Science Foundation of China (31960542), the Discipline and Master's Site Construction Project of Guiyang University by Guiyang City Financial Support Guiyang University (SH-2020), the Program for Science and Technology Youth Talents in Department of Education in Guizhou Province (2018298), the Training Program for High Level Innovative Talents of Guizhou Province (20164020), and the Program for First-Class Discipline Construction in Guizhou Province (201785).

SUPPLEMENTARY MATERIAL

The Supplementary Material for this article can be found online at: https://www.frontiersin.org/articles/10.3389/fphys.2020.01071/full#supplementary-material

FIGURE S1 | Multiple alignments of the amino acid sequence of *TcPTP61F* with homologs from other insect species. Identical and similar amino acids are marked with the same color. Gaps have been introduced to permit alignment. The heights of the pink bars below the aligned sequences represent the degree of similarity of the amino acids. The red box indicate the conserved catalytic cysteine. TcPTP61F (*Tribolium castaneum*; GenBank accession number: XP_008190655.1), DmPTP61F (*Drosophila melanogaster*; NP_476688.1), AgPTP61F1 (*Anoplophora glabripennis*; XP_018577682.1), DvPTP61F1 (*Diabrotica virgifera*; XP_028144768.1), LmPTPN1 (*Locusta migratoria*; AYI50186.1), LdPTP61F1(*Leptinotarsa decemlineata*; XP_023013201.1), AtPTP61F1(*Aethina tumida*; XP_019879072.1), NvPTP61F1(*Nicrophorus vespilloides*; XP_017775944.1), and OtPTP61F1(*Onthophagus taurus*; XP_022904338.1).

FIGURE S2 | Domain organization of PTP61Fs from *T. castaneum* and other insect speicies. The domain organization was generated with the SMART tool (http://smart.embl-heidelberg.de/) by using the protein sequences. The dark blue frame indicate the protein tyrosine coiled-coiloscioled-coliatase, catalytic domain (PTPc), and the light blue frame indicates the amino acid responsible for the recognition of Y-coiled-coiloscioled-coliatase. Structure of the coiled-coil and transmembrane region of PTP61Fs are represented as yellow ellipse and green polygon, respectively.

REFERENCES

Abaskharoun, M., Bellemare, M., Lau, E., and Margolis, R. U. (2010). Glypican-1, phosphacan/receptor protein-tyrosine phosphatase-ζ/β and its ligand, tenascin-C, are expressed by neural stem cells and neural cells derived from embryonic stem cells. *ASN Neuro*. 2:e00039. doi: 10.1042/AN20100001

Agouni, A., Tual-Chalot, S., Chalopin, M., Duluc, L., Mody, N., Martinez, C., et al. (2014). Hepatic protein tyrosine phosphatase 1B (PTP1B) deficiency protects against obesity-induced endothelial dysfunction. *Biochem. Pharmacol.* 92, 607-617. doi: 10.1016/j.bcp.2014.10.008

Alho, I., Costa, L., Bicho, M., and Coelho, C. (2013). The role of low-molecular-weight protein tyrosine phosphatase (LMW-PTP ACP1) in oncogenesis. *Tumor. Biol.* 34, 1979–1989. doi: 10.1007/s13277-013-0784-1

Alonso, A., Sasin, J., Bottini, N., Ilan, F., Iddo, F., Andrei, O., et al. (2004). Protein tyrosine phosphatases in the human genome. *Cell* 117, 699-711. doi: 10.1016/j.cell.2004.05.018

Bao, Y. Y., Xue, J., Wu, W. J., Wang, Y., Lv, Z. Y., and Zhang, C. X. (2011). An immune-induced reeler protein is involved in the *Bombyx mori* melanization cascade. *Insect. Biochem. Mol. Biol.* 41, 696–706. doi: 10.1016/j.ibmb.2011.05.001

Barraza, A., and Sánchez, F. (2013). Trehalases: a neglected carbon metabolism regulator? *Plant Signal. Behav.* 8:e24778. doi: 10.4161/psb.24778

Baum, J. A., Bogaert, T., Clinton, W., Heck, G. R., Feldmann, P., Ilagan, O., et al. (2007). Control of coleopteran insect pests through RNA interference. *Nat. Biotechnol.* 25, 1322–1326. doi: 10.1038/nbt1359

Biddinger, S. B., and Kahn, C. R. (2006). From mice to men: insights into the insulin resistance syndromes. *Annu. Rev. Physiol.* 68, 123-158. doi: 10.1146/annurev.physiol.68.040104.124723

Boateng, B. A., and Obengofori, D. (2008). "Major stored product arthropod pests," in *Post-Harvest Science and Technology*, eds E. W. Cornelius, D. Obeng-Ofori (Accra: Smartline Publishing Limited), 67–91.

Bodin, P., and Burnstock, G. (2001). Purinergic signalling: ATP release. *Neurochem. Res.* 26, 959–969. doi: 10.1023/a:1012388618693

Chen, J. X., Lyu, Z. H., Wang, C.Y., Cheng, J., and Lin, T. (2018). RNA interference of a trehalose-6-phosphate synthase gene reveals its roles in the biosynthesis of chitin and lipids in *Heortia vitessoides* (Lepidoptera: Crambidae). *Insect Sci.* 27, 212–223. doi: 10.1111/1744-7917.12650

Chen, Q. W., Jin, S., Zhang, L., Shen, Q. D., Wei, P., Wei, C. M., et al. (2018). Regulatory functions of trehalose-6-phosphate synthase in the chitin biosynthesis pathway in *Tribolium castaneum* (Coleoptera: Tenebrionidae) revealed by RNA interference. *Bull. Entomol. Res.* 108, 388–399. doi: 10.1017/S000748531700089X

Czech, M. P., and Corvera, S. (1999). Signaling mechanisms that regulate glucose transport. *J. Biol. Chem.* 274, 1865–1868. doi: 10.1074/jbc.274.4.1865

Ding, D., Liu, G. J., Hou, L., Gui, W. Y., Chen, B., and Kang, L. (2018). Genetic variation in PTPN1 contributes to metabolic adaptation to high-altitude hypoxia in Tibetan migratory locusts. *Nat. Commun.* 26:4991. doi: 10.1038/s41467-018-07529-8

Elbein, A. D., Pan, Y. T., Pastuszak, I., and Carroll, D. (2003). New insights on trehalose: a multifunctional molecule. *Glycobiology* 13, 17R–27R. doi: 10.1093/glycob/cwg047

Forsell, P. A., Boie, Y., Montalibet, J., Collins, S., and Kennedy, B. P. (2000). Genomic characterization of the human and mouse protein tyrosine phosphatase-1B genes. *Gene* 260, 145–153. doi: 10.1016/s0378-1119(00)00464-9

Gaster, M., Nehlin, J. O., and Minet, A. D. (2012). Impaired TCA cycle flux in mitochondria in skeletal muscle from type 2 diabetic subjects: marker or maker of the diabetic phenotype? *Arch. Physiol. Biochem.* 118, 156–189. doi: 10.3109/13813455.2012.656653

Ge, L. Q., Gu, H. T., Li, X., Zheng, S., Zhou, Z., Miao, H., et al. (2019). Silencing of triazophos-induced Hexokinase-1-like reduces fecundity in *Nilaparvata lugens* (Stål) (Hemiptera: Delphacidae). *Pestic. Biochem. Physiol.* 153, 176–184. doi: 10.1016/j.pestbp.2018.11.016

Hendriks, W. J. A. J., Elson, A., Harroch, S., Pulido, R., Stoker, A., and den Hertog, J. (2013). Protein tyrosine phosphatases in health and disease. *FEBS J.* 280, 708–730. doi: 10.1111/febs.12000

Hu, D., Luo, W., Fan, L. F., Liu, F. L., Gu, J., Deng, H. M., et al. (2016). Dynamics and regulation of glycolysis-tricarboxylic acid metabolism in the midgut of *Spodoptera litura* during metamorphosis. *Insect. Mol. Biol.* 25, 153–162. doi: 10.1111/imb.12208

Israelsen, W. J., and Vander Heiden, M. G. (2015). Pyruvate kinase: function, regulation and role in cancer. *Semin. Cell Dev. Biol.* 43, 43–51. doi: 10.1016/j.semcdb.2015.08.004

Jablonka, W., Senna, R., Nahu, T., Ventura, G., Menezes, L., and Silva-Neto, M. A. (2011). A transient increase in total head phosphotyrosine levels is observed upon the emergence of *Aedes aegypti* from the pupal stage. *Mem. Inst. Oswaldo Cruz* 106:546–552. doi: 10.1590/s0074-02762011000500005

Kim, Y., and Hong, Y. (2015). Regulation of hemolymph trehalose level by an insulin-like peptide through diel feeding rhythm of the beet armyworm, *Spodoptera exigua*. *Peptides* 68, 91–98. doi: 10.1016/j.peptides.2015.02.003

Klaman, L. D., Boss, O., Peroni, O. D., Kim, J. K., Martino, J. L., Zabolotny, J. M., et al. (2000). Increased energy expenditure, decreased adiposity, and tissue-specific insulin sensitivity in protein-tyrosine phosphatase 1B-deficient mice. *Mol. Cell. Biol.* 20, 5479–5489. doi: 10.1128/mcb.20.15.5479-5489.2000

Leevers, S. J. (2001). Growth control: invertebrate insulin surprises! *Curr. Biol.* 11, R209–R212. doi: 10.1016/s0960-9822(01)00107-5

Leyva, A., Quintana, A., Sánchez, M., Rodríguez, E. N., Cremata, J., and Sánchez, J. C. (2008). Rapid and sensitive anthrone-sulfuric acid assay in microplate format to quantify carbohydrate in biopharmaceutical products: method devlopment and validation. *Biologicals* 36, 134–141. doi: 10.1016/j.biologicals.2007.09.001

Livak, K. J., and Schmittgen, T. D. (2001). Analysis of relative gene expression data using real-time quantitative PCR and the $2^{-\Delta\Delta CT}$ method. *Methods* 25, 402–408. doi: 10.1006/meth.2001.1262

Lochhead, P. A., Coghlan, M., Rice, S. Q., and Sutherland, C. (2001). Inhibition of GSK-3 selectively reduces glucose-6-phosphatase and phosphatase and phosphoenolypyruvate carboxykinase gene expression. *Diabetes* 50, 937–946. doi: 10.2337/diabetes.50.5.937

Loh, K., Merry, T. L., Galic, S., Wu, B. J., Watt, M. J., Zhang, S., et al. (2012). T cell protein tyrosine phosphatase (TCPTP) deficiency in muscle does not alter insulin signalling and glucose homeostasis. *Diabetologia* 55, 468–478. doi: 10.1007/s00125-011-2386-z

Lorenzen, M. D., Kimzey, T., Shippy, T. D., Brown, S. J., Denell, R. E., and Beeman, R. W. (2007). PiggyBac-based insertional mutagenesis in *Tribolium castaneum* using donor/helper hybrids. *Insect Mol. Biol.* 16, 265–275. doi: 10.1111/j.1365-2583.2007.00727.x

Mehmood, K., Husain, M., Aslam, M., Ahmedani, M. S., Aulahk, A. M., and Shaheen, F. A. (2018). Changes in the nutritional composition of maize flour due to *Tribolium castaneum* infestation and application of carbon dioxide to manage this pest. *Environ. Sci. Pollut. Res.* 25, 18540–18547. doi: 10.1007/s11356-018-2063-6

Miyasaka, H., and Li, S. S. (1992). The cDNA cloning, nucleotide sequence and expression of an intracellular protein tyrosine phosphatase from mouse testis. *Biochem. Biophys. Res. Commun.* 185, 818–825. doi: 10.1016/0006-291x(92)91700-z

Moretti, D. M., Ahuja, L. G., Nunes, R. D., Cudischevitch, C. O., Daumas-Filho, C. R. O., Medeiros-Castro, P., et al. (2014). Molecular analysis of *Aedes aegypti* classical protein tyrosine phosphatases uncovers an ortholog of mammalian PTP-1B implicated in the control of egg production in mosquitoes. *PLoS One* 9:e104878. doi: 10.1371/journal.pone.0104878

Mustelin, T., Vang, T., and Bottini, N. (2005). Protein tyrosine phosphatases and the immune response. *Nat. Rev. Immunol.* 5, 43–57. doi: 10.1038/nri1530

Noh, M. Y., Beeman, R. W., and Arakane, Y. (2012). RNAi-based functional genomics in *Tribolium castaneum* and possible application for controlling insect pests. *Entomol. Res.* 42, 1–10. doi: 10.1111/j.1748-5967.2011.00437.x

Perkin, L. C., and Oppert, B. (2019). Gene expression in *Tribolium castaneum* life stages: identifying a species-specific target for pest control applications. *Peer J.* 7:e6946. doi: 10.7717/peerj.6946

Pimentel, M. A. G., Faroni, L. R. D. A., da Silva, F. H., Basista, M. D., and Guedes, R. N. (2010). Spread of phosphine resistance among brazilian populations of three species of stored product insects. *Neotrop. Entomol.* 39, 101–107. doi: 10.1590/s1519-566x2010000100014

Predel, R., Neupert, S., Garczynski, S. F., Crim, J. W., Brown, M. R., Russell, W. K., et al. (2010). Neuropeptidomics of the mosquito *Aedes aegypti*. *J. Proteome. Res.* 9, 2006-2015. doi: 10.1021/pr901187p

Prentice, K., Christiaens, O., Pertry, I., Bailey, A., Niblett, C., Ghislain, M., et al. (2017). RNAi-based gene silencing through dsRNA injection or ingestion against the African sweet potato weevil *Cylas puncticollis* (Coleoptera: Brentidae). *Pest Manag. Sci.* 73, 44–52. doi: 10.1002/ps.4337

Pri-Tal, B. M., Brown, J. M., and Riehle, M. A. (2008). Identification and characterization of the catalytic subunit of phosphatidylinositol 3-kinase in the yellow fever mosquito *Aedes aegypti*. *Insect Biochem. Mol. Biol.* 38, 932–939. doi: 10.1016/j.ibmb.2008.07.004

Riehle, M. A., and Brown, M. R. (2003). Molecular analysis of the serine/threonine kinase Akt and its expression in the mosquito *Aedes aegypti*. *Insect Mol. Biol.* 12, 225–232. doi: 10.1046/j.1365-2583.2003.00405.x

Sacco, F., Perfetto, L., Castagnoli, L., Cesareni, G. (2012). The human phosphatase interactome: an intricate family portrait. *FEBS Lett.* 586, 2732-2739. doi: 10.1016/j.febslet.2012.05.008

Saltiel, A. R., and Kahn, C. R. (2001). Insulin signalling and the regulation of glucose and lipid metabolism. *Nature* 414, 799-806. doi: 10.1038/414799a

Satake, S., Masumura, M., Ishizaki, H., Nagata, K., Kataoka, H., Suzuki, A., et al. (1997). Bombyxin, an insulin-related peptide of insects, reduces the major storage carbohydrates in the silk worm *Bombyx mori*. *Comp. Biochem. Physiol. B Biochem. Mol. Biol.* 118, 349–357. doi: 10.1016/s0305-0491(97)00166-1

Shukla, E., Thorat, L. J., Nath, B. B., and Gaikwad, S. M. (2015). Insect trehalase: physiological significance and potential applications. *Glycobiology* 25, 357–367. doi: 10.1093/glycob/cwu125

Sunna, A., Moracci, M., Rossi, M., and Antranikian, G. (1997). Glycosyl hydrolases from hyperthermophiles. *Extremophiles* 1, 27–13. doi: 10.1007/s007920050009

Tamang, A. M., Kalra, B., and Parkash, R. (2017). Cold and desiccation stress induced changes in the accumulation and utilization of proline and trehalose in seasonal populations of *Drosophila immigrans*. *Comp. Biochem. Physiol. A Mol. Integr. Physiol.* 203, 304–313. doi: 10.1016/j.cbpa.2016.10.011

Tang, B., Wei, P., Zhao, L. N., Shi, Z. K., Shen, Q. D., Yang, M. M., et al. (2016). Knockdown of five trehalase genes using RNA interference regulates the gene expression of the chitin biosynthesis pathway in *Tribolium castaneum*. *BMC Biotechnol.* 6:67. doi: 10.1186/s12896-016-0297-2

Tang, B., Yang, M. M., Shen, Q. D., Xu, Y. X., Wang, H. J., and Wang, S. G. (2017). Suppressing the activity of trehalase with validamycin disrupts the trehalose and chitin biosynthesis pathways in the rice brown planthopper, *Nilaparvata lugens*. *Pestic. Biochem. Physiol.* 137, 81–90. doi: 10.1016/j.pestbp.2016.10.003

Tatun, N., Wangsantitham, O.,Tungjitwitayakul, J., and Sakurai, S. (2014). Trehalase activity in fungus-growing termite, *Odontotermes feae* (Isoptera: Termitideae) and inhibitory effect of validamycin. *J. Econ. Entomol.* 107, 1224–1232. doi: 10.1603/ec14051

Tian, L., Guo, E. E., Wang, S., Liu, S. M., Jiang, R. J., Cao, Y., et al. (2010). Developmental regulation of glycolysis by 20-hydroxyecdysone and juvenile hormone in fat body tissues of the silkworm, *Bombyx mori*. *J. Mol. Cell Biol.* 2, 255–263. doi: 10.1093/jmcb/mjq020

Tiganis, T., and Bennett, A. M. (2007). Protein tyrosine phosphatase function: the substrate perspective. *Biochem. J.* 402, 1–15. doi: 10.1042/BJ20061548

Tonks, N. K. (2006). Protein tyrosine phosphatases: from genes, to function, to disease. *Nat. Rev. Mol. Cell Biol.* 7, 833–846. doi: 10.1038/nrm2039

Tsou, R. C., and Bence, K. K. (2013). Central regulation of metabolism by protein tyrosine phosphatases. *Front. Neurosci.* 6:192. doi: 10.3389/fnins.2012.00192

Vital, W., Rezende, G. L., Abreu, L., Moraes, J., Lemos, F. J. A., Jr., et al. (2010). Germ band retraction as a landmark in glucose metabolism during *Aedes aegypti* embryogenesis. *BMC Dev. Biol.* 10, 25. doi: 10.1186/1471-213X-10-25

Wang, Y. J., He, H. W., Liu, L. N., Gao, C. Y., Xu, S., Zhao, P., et al. (2014). Inactivation and unfolding of protein tyrosine phosphatase from *Thermus thermophilus* HB27 during urea and guanidine hydrochloride denaturation. *PLoS One* 9:e107932. doi: 10.1371/journal.pone.0107932

Wegener, G., Macho, C., Schlöder, P., Kamp, G., and Ando, O. (2010). Long-term effects of the trehalase inhibitor trehazolin on trehalase activity in locust flight muscle. *J. Exp. Biol.* 213, 3852–3857. doi: 10.1242/jeb.042028

Wegener, G., Tschiedel, V., Schlöder, P., and Ando, O. (2003). The toxic and lethal effects of the trehalase inhibitor trehazolin in locusts are caused by hypoglycaemia. *J. Exp. Biol.* 206, 1233–1240. doi: 10.1242/jeb.00217

White, K. P., Rifkin, S. A., Hurban, P., and Hogness, D. S. (1999). Microarray analysis of *Drosophila* development during metamorphosis. *Science* 286, 2179–2184. doi: 10.1126/science.286.5447.2179

White, M. F. (1998). The IRS-signalling system: a network of docking proteins that mediate insulin action. *Mol. Cell. Biochem.* 182, 3–11.

Wu, C. L., Buszard, B., Teng, C. H., Chen, W. L., Warr, C. G., Tiganis, T., et al. (2011). Dock/Nck facilitates PTP61F/PTP1B regulation of insulin signalling. *Biochem. J.* 439, 151–159. doi: 10.1042/BJ20110799

Yasugi, T., Yamada, T., and Nishimura, T. (2017). Adaptation to dietary conditions by trehalose metabolism in *Drosophila*. *Sci. Rep.* 7:1619. doi: 10.1038/s41598-017-01754-9

Zhang, L., Qiu, L. Y.,Yang, H. L., Wang, H. J., Zhou, M., Wang, S. G., et al. (2017). Study on the effect of wing bud chitin metabolism and its developmental network genes in the brown planthopper, *Nilaparvata lugens*, by knockdown of *TRE* gene. *Front. Physiol.* 8:750. doi: 10.3389/fphys.2017.00750

Conflict of Interest: The authors declare that the research was conducted in the absence of any commercial or financial relationships that could be construed as a potential conflict of interest.

frontiers in Physiology

ORIGINAL RESEARCH
published: 15 September 2020
doi: 10.3389/fphys.2020.574851

The Effect of Different Dietary Sugars on the Development and Fecundity of *Harmonia axyridis*

Yan Li[1], Shasha Wang[1], Yongkang Liu[1], Yuting Lu[1], Min Zhou[1], Su Wang[2] and Shigui Wang[1]**

[1] College of Life and Environmental Sciences, Hangzhou Normal University, Hangzhou, China, [2] Institute of Plant and Environment Protection, Beijing Academy of Agricultural and Forestry Sciences, Beijing, China

OPEN ACCESS

Edited by:
Kai Lu,
Fujian Agriculture and Forestry University, China

Reviewed by:
Hao-Sen Li,
Sun Yat-sen University, China
Hamzeh Izadi,
Vali-E-Asr University of Rafsanjan, Iran
Senthil Kumar Nachimuthu,
Mizoram University, India

***Correspondence:**
Su Wang
anthocoridae@163.com
Shigui Wang
sgwang@hznu.edu.cn;
sgwang@mail.hz.zj.cn

Specialty section:
This article was submitted to Invertebrate Physiology, a section of the journal Frontiers in Physiology

Received: *21 June 2020*
Accepted: *25 August 2020*
Published: *15 September 2020*

Citation:
Li Y, Wang S, Liu Y, Lu Y, Zhou M, Wang S and Wang S (2020) The Effect of Different Dietary Sugars on the Development and Fecundity of Harmonia axyridis. Front. Physiol. 11:574851. doi: 10.3389/fphys.2020.574851

The aim of this study was to screen synergistic substances included in existing artificial feeds in order to improve the fertility and survival rate of *Harmonia axyridis* (Pallas) (Coleoptera: Coccinellidae), an efficient pest predator. To this end, we analyzed the potential effects of glucose and trehalose on the growth, development, and reproduction of *H. axyridis* and evaluated the effect of three different artificial feeds on the energy stress of *H. axyridis*. The artificial diets contained fresh pork liver, honey, sucrose, vitamin C, and royal jelly, which was marked it as Diet1. The glucose was added to diet1, which was marked it as diet2, while adding trehalose to diet1 was marked as diet3. The pre-oviposition period of *H. axyridis* on Diet 1 was slower than that of Diet 2 and Diet 3. Additionally, the spawning quantity and incubation rate of insects on Diet 2 and Diet 3 were significantly higher than that of those on Diet 1. Finally, the larval developmental time on Diet 1 was significantly slower than that of Diet 2 and Diet 3. These results indicate that the addition of an appropriate amount of glucose or trehalose may affect positively the growth, development, and reproduction of *H. axyridis*. In addition, further studies showed that ATP, amino acids and fatty acids content in the *H. axyridis* also increased after the addition of the synergistic substance. All these results show that proper adjustment of stored energy anabolic and catabolism is important to maintain the metabolic balance of the insect's entire life cycle and the addition of glucose or trehalose has a certain effect on the life indicators of *H. axyridis.*

Keywords: *Harmonia axyridis*, artificial diets, glucose, trehalose, fecundity

INTRODUCTION

Agricultural and forestry crop pests seriously threaten the quality and yield of agricultural production, causing huge economic losses (Hansen et al., 1999). Although chemical control is used for the direct elimination or extermination of agricultural and forestry crop pests, the use of pesticides on a large scale causes severe environmental pollution, endangers human health (Youn et al., 2003; Katsarou et al., 2005; Garratt and Kennedy, 2006), and results in the resistance of many pests (Puinean et al., 2010; Kavi et al., 2014; Bass et al., 2015; Saddiq et al., 2015). It is well-known

that natural enemy insects are important biological agents in global agricultural ecosystems (Juen et al., 2012; Lu et al., 2012). However, they often face seasonal natural food shortages. In addition, the manual feeding of natural food requires the maintenance of a three-level nutrition chain, which increases both the feeding and the biological control cost (Liu et al., 2013). An artificial diet is the key to avoid the seasonal restrictions of natural food and meet the needs of various experiments. Agricultural pests, such as Hemiptera, Coleoptera, Lepidoptera, and a variety of economic insects, such as the *Asian corn borer* (Fadamiro et al., 2005) are some of the insect species fed artificial diets.

Harmonia axyridis (Pallas) (Coleoptera: Coccinellidae) is an efficient pest predator (Koch, 2003). A large number of studies have shown that *H. axyridis* is an important insect in the integrated pest management strategy (Brown et al., 2011; Castro et al., 2011; Luo et al., 2014). As early as 1916, *H. axyridis* was released as a biological control insect in orchards, farms, and greenhouses (Michaud, 2002; Majerus et al., 2006; Brown et al., 2011; Van, 2012), but so far there are still natural prey that cannot sustain the ladybugs throughout the year (Zhang et al., 2014). It is difficult to maintain a sufficient *H. axyridis* supply in the biological control of insects, especially when it comes to large-scale breeding populations in laboratories (Zazycki et al., 2015). In large-scale insect propagation, feeding aphid diets in captivity is an expensive and time-consuming method (Bonte et al., 2010). Therefore, it is necessary to develop artificial diets that *H. axyridis* can be supplemented with, in order to achieve the low-cost and continuous expansion of this insect that will facilitate the effective control of pests (Cheng et al., 2018). In response to this problem, various artificial insect diets have been exploited and proposed (Cohen, 2001; Castane and Zapata, 2005). Research on artificial diets for *H. axyridis* has ranged from exploring original insect source components such as *Tenebrio molitor* and *Trichogramma dendrolimi* Matsumura (Guo and Wan, 2001) to non-insect sources with fresh pig liver as the main component. Many studies have proposed that although insects can be bred with artificial feedstuffs with some success, in many cases they lose their ability to adapt and reproduce, which has led to a delayed development and lower fertility (Denno and Fagan, 2003; Wilder et al., 2011; Schmidt et al., 2012). The previous research, suggested that the main reason for the decline in the hatchability and reproductive capacity of *Spodoptera exigua* was long-term indoor mating, in subsequent research, these decreases were attributed to irrational feed nutrition (Li et al., 2002).

Studies on *Microplitis mediator* in bee cocoons have revealed that feeding glucose can enhance the reproductive efficiency and potential of the bees. It has been suggested that the main reason for this is that a carbohydrate food supplement provides mature eggs with the energy they need as they do not need to resort to their lipid reserves to acquire energy; additionally, the accumulation of lipids in the female's body is directly used in oogenesis and egg maturation (Huang et al., 2015). Glucose is the most widely used sugar by insects for energy production and the supply of large molecular precursors and is a signaling molecule in the liver and adipose tissue (Vaulont et al., 2000). As a direct energy substance, glucose can be used better by females for egg maturation (Huang et al., 2015). Some reports showed that glucose metabolism and its regulation are particularly important for termite reproduction; glucose is particularly important for feeding adult females as it provides them with energy for reproduction and promotes egg maturation (Thompson, 2003). The energy metabolism of insects, which is otherwise similar to that of other animals, has a unique feature; the synthesis and utilization of trehalose (Tang et al., 2010). The regulation of trehalose metabolism and the control of glucose utilization are important in terms of energy (Tang et al., 2010). Trehalose can effectively prevent the denaturation and functionality loss of proteins under adverse conditions (Haque et al., 2015). In addition, studies have shown that the trehalose content affects food choices and feeding behavior. The physiological role of trehalose as insects' blood sugar during their reproductive processes has been reported previously (Lu et al., 2019). A parallel relationship between the hemolymph trehalose levels and ovarian maturation was observed, suggesting that trehalose supplies the energy required for the reproductive cycle processes (Huang and Lee, 2011). Trehalose is a readily accessible energy source that can be used as required (Shi et al., 2017).

In addition, studies have shown that the main parts of insects that produce and store glycogen and trehalose are fat bodies, ovaries, and flying muscles (Tang et al., 2012). Trehalose is the energy fuel for vitellogenin (Vg) formation and oocyte maturation (Lu et al., 2019). Therefore, it is speculated that eating artificial feedstuffs with glucose or trehalose could provide insects with sufficient energy to act on the ovary, thereby promoting the development of their ovaries and increasing spawning. The population proliferation of insects is based on individual reproduction, and reproductive success depends on the Vg synthesis of the fat body and on oocyte development (Tufail and Takeda, 2008; Tufail et al., 2010). Vg is the main storage protein precursor of the ova of many animals, the energy reserve of many ovipara (Zhang et al., 2017), and plays an important role in the reproduction of oviparous vertebrates and invertebrates (Liu et al., 2013).

The aim of this study was to supplement insect diets with potentially synergistic substances while meeting their minimum nutritional requirements. Additionally, we aimed to discover and screen more effective and high-quality artificial feedstuffs for natural enemy insects that would lead to higher proliferation, thereby providing technical support for their release. Based on previous reference on artificial feedstuffs (Yang et al., 2013), we used glucose and trehalose as energy supplying nutrients for insects. By measuring the growth, development, reproductive ability, and substance content indicators in the bodies of *H. axyridis*, we evaluated the potential role of glucose and trehalose on their growth, development, and reproduction.

MATERIALS AND METHODS

Insects

Harmonia axyridis individuals were raised in the Key Laboratory of Animal Adaptation and Evolution of Hangzhou Normal

University. All insects were bred in a growth chamber maintained at 23 ± 2°C, with 68 ± 5% relative humidity (RH), and a photoperiod of 16:8 h (L: D). *H. axyridis* individuals were fed *Aphis medicaginis* at a fixed time every day. After oviposition, the eggs were collected 2–3 times daily and placed in a 7 cm Petri dish containing filter paper; distilled water was sprayed onto the filter paper once a day to preserve its humidity. After the eggs hatched, we used a writing brush to gently move the hatched larvae into individual larva rearing boxes containing aphids or artificial feedstuffs (4 cm × 3 cm × 2 cm). It was necessary to keep them alone in order to prevent cannibalism and competition among individuals. After being reared to emergence, the adults (12 females and 8 males in each box) were placed in adult feeding boxes containing aphids or artificial diets. The diet in all feeding boxes was changed once a day and wet cotton balls were replenished.

Preparation of Artificial Diets

In this experiment, we used the artificial feed formula prepared by Yang et al. (2013) as reference material; we adapted it by optimizing the addition of ingredients and improving their ratio (Yang et al., 2013). Three artificial feed formulae were designed, namely Diet 1, Diet 2 and Diet 3, CK represents *Aphis medicaginis* used as the control. The raw materials were weighed and mixed according to the number of insects in each group, in order to prepare a semi-fluid feed and were stored in a refrigerator at −20°C. For a detailed component analysis of each formula, see **Table 1**.

Experimental Method

Determination of the Tissue and Hemolymph Sugar Contents of *H. axyridis* Larvae

At least 50 early fourth instar larvae were collected from each of the three groups, which fed with Diet 1, Diet 2, and Diet 3. After having fed for 12, 24, and 48 h, the larvae were placed on ice. After the larval ability decreased, their feet were punctured by a medical anatomical needle. Hemolymph was collected with a capillary tube and transferred to an Eppendorf (EP) tube (Eppendorf, Hamburg, Germany) containing anticoagulant (Wang et al., 2007). Each tube contained the hemolymph of seven larvae. After hemolymph extraction, the tissue of larvae was placed into a new EP tube; each tube contained the tissue of three larvae. Each of the experiments was performed in three biological replicates and three technical replicates.

TABLE 1 | Specific ingredients of the artificial feed formula of the *H. axyridis*.

Ingridients	Diet 1	Diet 2	Diet 3
Fresh pork liver	64%	64%	64%
Honey	13.5%	13.5%	13.5%
Vitamin C	3.5%	3.5%	3.5%
Sugar	13.5%	13.5%	13.5%
Royal jelly	5.5%	5.5%	5.5%
Glucose	–	12%	–
Trehalose	–	–	20%

The above samples were ground with phosphate buffered saline (PBS) and sonicated. Subsequently, 350 μL of the supernatant was collected and ultracentrifuged at 20,800 *g* for 60 min at 4°C. The remaining supernatant was used to determine the protein, trehalose, and glycogen contents. The trehalose content was measured using the anthrone method. Briefly, we took 30 μL of the centrifuged supernatant sample, added 30 μL of 1% H_2SO_4, placed it in a water bath at 90°C for 10 min, and then in an ice bath for 3 min. After adding 30 μL of 30% KOH, the sample was incubated again at 90°C in a water bath for 10 min and in an ice bath for 3 min. Then, 600 μL of developer was added and the sample was placed in a water bath at 90°C for 10 min and then cooled in an ice bath. The absorbance of the sample was measured at 630 nm using a microplate reader. A glucose assay kit (Sigma-Aldrich, St. Louis, MO, United States) was used to measure the glucose content by taking 150 μL of 20,800 *g* centrifuged supernatant and 20,800 *g* of pellet suspension, according to the manufacturer's instructions. After incubation in water bath at 37°C for 30 min, 300 μL of 2N H_2SO_4 was added to stop the reaction, and the absorbance of the samples was measured at 540 nm using a microplate reader. For the determination of the glycogen contents, 160 μL of supernatant obtained after centrifugation at 1,000 *g* was added to 600 μL of anthrone sulfate reagent, and the mixture was incubated at 90°C for 10 min and then cooled in an ice bath. The absorbance of the sample was measured at 625 nm using a microplate reader. The protein content was determined using the BCA Protein Assay Kit (Beyotime, Shanghai, China).

Observation of the Developmental Duration and the Body Weight Index of *H. axyridis* Larvae

At least 100 eggs were collected from each group. We measured the developmental period from the first instar to the pupal stage and monitored the development of *H. axyridis* every day. At the same time, the body weight of the larvae that fed on different artificial feeds was recorded. Electronic scales (METTLER TOLEDO, Shanghai, China) were used to weigh the first, second, third, and fourth instar larvae. As the larvae were small, 10 larvae that fed on the same feed and were at the same developmental stage were weighed each time. Then, we recorded the average weight of the three groups; the above experiment was repeated three times.

Observations on the Pre-oviposition, Oviposition Rate, and Fecundity of *H. axyridis*

We collected at least 50 pairs of *H. axyridis* adults from each group. Each group was provided with five feeding boxes for 42 days. The time from the first day of the emergence of *H. axyridis* to the oviposition time was considered as the pre-oviposition. Then, the daily oviposition of adults that had fed on different diets and aphids was counted and recorded. We recorded the average of three breeding rounds as the final spawning result. From each round, we selected approximately 100 eggs and repeated this process three times per group. Then, we calculated the hatchability of the eggs by observing and recording the number of first instar larvae after 1 day of incubation.

Determination of the Sugar and Substance Contents of *H. axyridis* Adults

We collected at least 50 pairs of the adults from each group at the beginning of the emergence stage. Then, we measured the sugar and substance contents of females that had fed for 48 and 72 h. The sugar content detection method was the same as the one described in Section "Determination of the Tissue and Hemolymph Sugar Contents of *H. axyridis* Larvae." We used the GLYCERINE kit, the Non-esterified Free fatty acids assay kit (NEFA), and the Total Amino Acid assay kit to measure the glycerine, free fatty acid, and adenosine 5′-triphosphate (ATP) contents. The above kits are collected from Nanjing Jiancheng Bioengineering Institute.

Ovarian Development in *H. axyridis* Adults

We collected at least 50 pairs of the adults from each group at the beginning of the emergence stage and fed them Diet 1, Diet 2, and Diet 3. The ovaries of *H. axyridis* that had fed for 3, 5, and 7 days were dissected. The vivisection of female *H. axyridis* was conducted in saline; first, we cut off their wings and head and then we attached the insect bodies to the anatomical box (AGAR dish). Under the Leica EZ4HD stereoscopic microscope (Leica, Wetzlar, Germany), we cut along the middle back of the adults to the end of the abdomen and removed the organs and tissues of non-reproductive systems, such as the digestive tract and the fat body.

Determination of the Relative Expression of the VgR and Vgs Genes in *H. axyridis*

We collected at least 50 pairs of the adults from each group at the beginning of the emergence stage. Ha-rp49 was used as an internal reference gene and detected the relative expression of the *VgR*, *Vg1*, and *Vg2* genes in their adults.

First, total RNA was extracted from the adults of *H. axyridis* by a Trizol-based method. Each tube sample was homogenized with 800 μL of TRIzol reagent (Invitrogen, Carlsbad, CA, United States) according to the manufacturer's instructions. A Thermo Scientific NanoDrop 2000 UV-Vis spectrophotometer (Thermo Fisher Scientific, Inc., Waltham, MA, United States) was used to determine the RNA quality and quantity. Complementary DNA (cDNA) was synthesized from 1 μg of total RNA using the PrimeScript^{TM}RT reagent Kit with gDNA Eraser (perfect Real Time) (Takara Bio, Inc., Kusatsu, Japan) according to the manufacturer's protocol.

The cDNA was diluted fivefold for subsequent quantitative real-time polymerase chain reaction (qRT-PCR) analyses. qRT-PCR was carried out in 20 μL reactions containing 1.0 μL cDNA, 10 μL SYBR Green Premix Ex Taq (Takara Bio, Inc.), 1 μL forward primer (10 μM), 1 μL reverse primer (10 μM), and 7 μL nuclease free water using the Bio-Rad CFX96^{TM} Real-Time PCR Detection System (Bio-Rad Laboratories, Inc., Hercules, CA, United States). Then, we conducted a melting curve analysis (from 60 to 95°C) to ensure the consistency and specificity of the amplified product. All samples were normalized to the threshold cycle value for QHa-rp49 mRNA, which was chosen as an invariant control. Information on the primer sequences of the *H. axyridis* genes is shown in **Table 2**.

TABLE 2 | Sequences of qRT-PCR primers for *VgR* and *Vgs* genes.

Gene	Forward (5′–3′)	Reverse (5′–3′)
HaVgR	TGTAGGAGGCGAAGCAATGAT	TGGGATGTGACAGGGAAATAA
HaVg1	GCAACAGAGTCCGTGGTCTTT	GCTGCTTTCACCGTTCTTCAA
HaVg2	CAATCAAAACTCAAGCA AGGAGA	GTCAAAAACTGGATGGAC AACAA
QHarp49	GCGATCGCTATGGAAAACTC	TACGATTTTGCATCAACAGT

Statistical Analyses

All the data were analyzed using a one-way ANOVA with the statistical software package version 7.0 (StatSoft, Inc., Tulsa, United States). Multiple comparisons of means were conducted using Tukey's test. Differences between means were deemed to be significant when $P \leq 0.05$. Statistical analysis was performed with STATISTICA 8.0 and Sigma Plot 10.0. The qRT-PCR data were processed using the $2^{-\Delta\Delta CT}$ method (Livak and Schmittgen, 2001).

RESULTS

Tissue and Hemolymph Sugar Contents of *H. axyridis* Larvae

The tissue and hemolymph glycogen content after 24 and 48 h feeding on the Diet 2 and Diet 3 were significantly higher than that of the Diet 1 ($P < 0.05$) (**Figures 1A,D**). The trehalose content in the tissues of larvae fed on Diet 1 for 24 and 48 h Diet 1 was significantly lower than that of the Diet 2 and Diet 3 ($P < 0.05$) (**Figure 1B**). The trehalose content in the hemolymph of the Diet 1 was lower than that of the Diet 2 and Diet 3 ($P < 0.05$) (**Figure 1E**). The glucose content in the tissues of all groups did not change significantly after having fed for 24 h. However, the glucose level of Diet 1 was significantly lower than those of Diet 2 and Diet 3 ($P < 0.05$) after 48 h (**Figure 1C**). After 12 and 24 h of feeding, the glucose content in the hemolymph of Diet 1 was significantly lower than that of Diet 2 and Diet 3, while there were no significant differences among the insects of the three groups after they had fed for 48 h ($P < 0.05$) (**Figure 1F**).

Developmental Time and Larval Weight

We observed and recorded the developmental time of the larvae and pupae that had fed on different artificial diets. As is shown in **Figure 2**, the effect of different diets on the developmental time of the larvae was significant ($P < 0.05$). The developmental times of the larvae fed on of Diet 2 and Diet3 were much shorter than that of Diet 1 (25.8, 24.5, and 28.1 days, respectively). The developmental time of each of the aforementioned groups was longer than that of the group that fed on aphids, which was about 21.5 days. As is presented in **Table 3**, the *H. axyridis* that fed on the three diets were lighter than those that fed on aphids. Additionally, Diet 2 and Diet 3 individuals weighed more than Diet 1 individuals. More specifically, the differences were

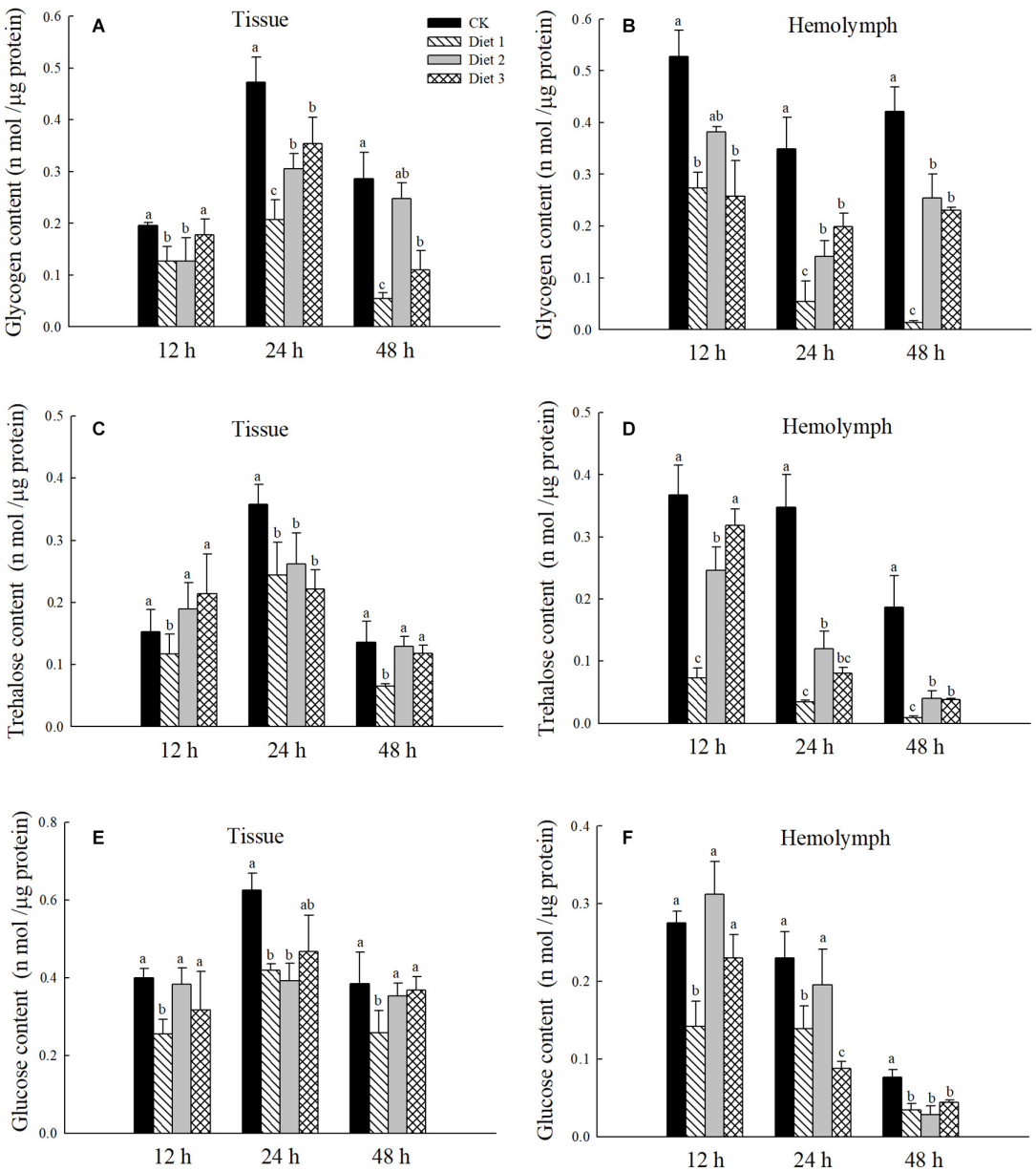

FIGURE 1 | After 12, 24, and 48 h of fed with three kinds of artificial feedstuffs, the sugar content in the larval tissue and hemolymph of *H. axyridis*. **(A)** The glycogen content in the tissue. **(B)** The trehalose content in the tissue. **(C)** The glucose content in the tissue. **(D)** The glycogen content in the hemolymph. **(E)** The trehalose content in the hemolymph. **(F)** The glucose content in the hemolymph. Line bars represent standard error of the mean. Bars with different letters are significantly different (Tukey–Kramer tests, $P < 0.05$). Numbers of samples for each treatment of hemolymph = 7. Sample size for each treatment of tissue = 3.

significant at the third and fourth instar and at the pupal stage ($P < 0.05$). On weight of with different lowercase letters are significantly different.

Pre-oviposition Period, Fecundity, and Hatching Rate Indicators of *H. axyridis* Adults

The results presented in **Figure 3** show that the different artificial diets had a significant effect on the pre- oviposition, egg production, and hatching rate of *H. axyridis* ($P < 0.05$). The pre-oviposition period on Diet 1 (15.33 ± 1.52 days) was longer than that of Diet 2 and Diet 3 (13.33 ± 1.17 and 11.75 ± 1.72 days, respectively) (**Figure 3A**). Additionally, the fecundity (**Figure 3B**) and the incubation fertility (**Figure 3C**) of Diet 2 (483.50 ± 70.88 eggs per female, 81.69 ± 10.60%) and Diet 3 (527.66 ± 49.65 eggs per female, 87.00 ± 12.64%) were significantly higher than those of Diet 1 individuals (236.92 ± 32.56 eggs per female, 60.67 ± 15.23%).

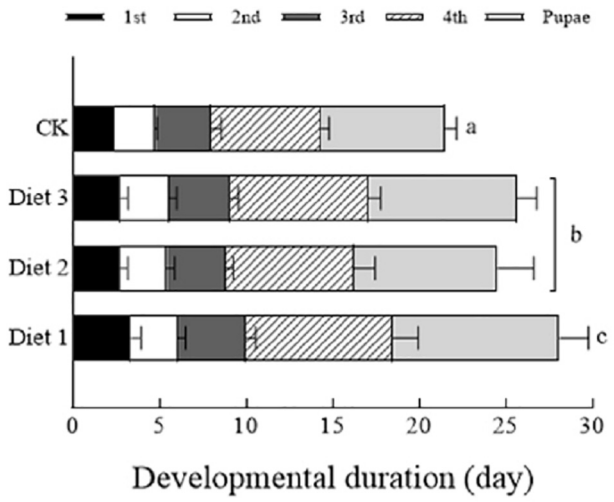

FIGURE 2 | Development periods of larvae to pupae after feeding with different artificial feeds. The "1st" represents the 1st instar larval stage, "2nd" represents the 2nd instar larval stage, "3rd" represents the 3rd instar larval stage, "4th" represents the 4th instar larval stage, and "Pupae" represents the entire pupal stage. Line bars represent standard error of the mean. Bars with different letters are significantly different (Tukey–Kramer tests, $P < 0.05$). Sample size for each treatment = 30.

Chemical Contents of Adults

The glycogen content on Diet 2 and Diet 3 was significantly higher than that of Diet 1 ($P < 0.05$; **Figure 4A**). In all time treatments, i.e., 48 and 72 h feeding on different artificial diets, trehalose and glycogen contents of the adults fed on Diet 2 and Diet 3 were significantly higher than that of Diet 1 ($P < 0.05$; **Figures 4B,C**).

In addition, we tested the content of associated chemical in adult *H. axyridis* after 48 and 72 h of feeding on different artificial diets. As is shown in **Figure 5**, after 72 h feeding on Diet 2 and Diet3 the ATP content of the adults was significantly higher than that on the adults fed with Diet 1 while there was no significant difference after feeding for 48 h ($P < 0.05$; **Figure 5A**). After 48 and 72 h feeding on Diet 2 and Diet 3, the fatty acid content was significantly higher than that of Diet 1 ($P < 0.05$; **Figure 5B**); In this experiment, there was no significant difference among the total amino acid contents of the three groups after they had fed on an artificial diet for 48 and 72 h ($P < 0.05$; **Figure 5C**). Finally, the glycerol content of Diet 2 and Diet 3 individuals, after they had fed for 48 and 72 h, was significantly higher than that of Diet 1 individuals ($P < 0.05$; **Figure 5D**).

Ovarian Development of the Adults

Our results showed that the development of *H. axyridis*' ovaries that fed on aphids was obviously better than that of the artificialy-fed groups. The ovarian development of Diet 2 and Diet 3 insects was significantly better than that of Diet 1 insects (**Figure 6**).

Relative Expression of *VgR* and *Vgs* in *H. axyridis* Adults

We tested the relative expression levels of the *VgR*, *Vg1*, and *Vg2* genes in *H. axyridis* adult that fed on different artificial diets for 24 and 48 h. The *VgR* gene expression in Diet 2 individuals was significantly higher than it was in Diet 1 individuals ($P < 0.05$; **Figure 7A**). Additionally, there was no significant difference

TABLE 3 | Effect of different artificial diets on weight of *Harmonia axyridis* pupae.

Prescriptions	1st (mg)	2nd (mg)	3rd (mg)	4th (mg)	Pupae (mg)
Aphis medicaginis	0.68 ± 0.071 a	2.3 ± 0.90 a	10 ± 0.48 a	17.97 ± 0.14 a	23.622 ± 0.84 a
Diet 1	0.63 ± 0.64 a	1.2 ± 0.41 c	4.1 ± 0.42 d	10.74 ± 0.32 c	19.467 ± 0.76 b
Diet 2	0.64 ± 0.020 a	1.6 ± 0.20 b	8.7 ± 0.35 a	15.58 ± 0.24 b	22.833 ± 0.50 a
Diet 3	0.66 ± 0.03a	1.9 ± 0. 37 ab	6.6 ± 0. 24 c	16.03 ± 0. 31 b	21.967 ± 0. 16 a

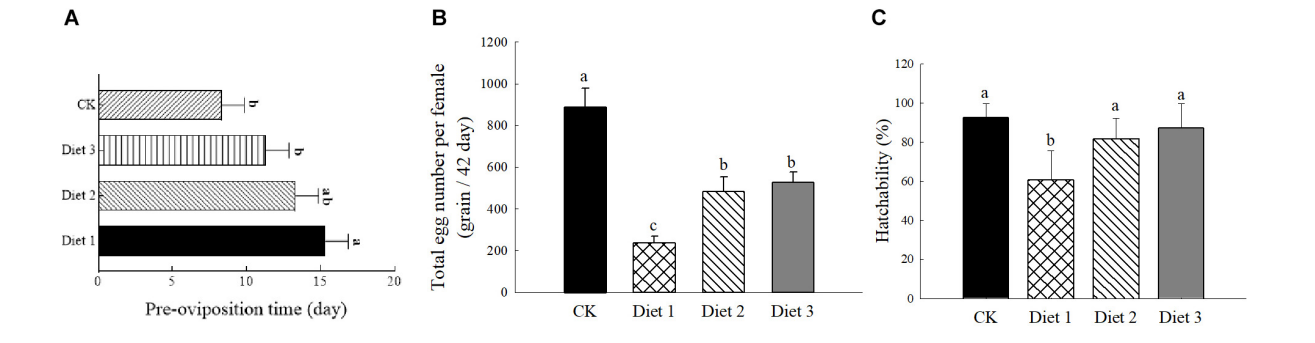

FIGURE 3 | Pre-laying period, egg-laying number and hatching rate of *H. axyridis*. **(A)** Pre-oviposition period, numbers of samples for each treatment = 36. **(B)** In a single trial lasting 42 days of eggs laid by *H. axyridis*, numbers of samples for each treatment = 36. **(C)** Hatching rate, numbers of samples for each treatment = 50. Line bars represent standard error of the mean. Bars with different letters are significantly different (Tukey–Kramer tests, $P < 0.05$).

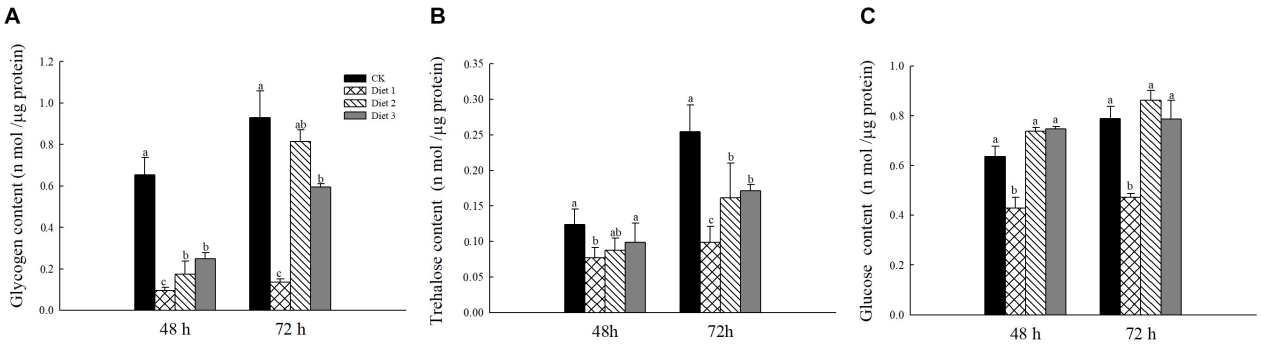

FIGURE 4 | Sugar content in female *H. axyridis* after 48 and 72 h of feeding on artificial feedstuffs. **(A)** represents the glycogen content. **(B)** Represents the trehalose content. **(C)** Represents the glucose content. Line bars represent standard error of the mean. Bars with different letters are significantly different (Tukey–Kramer tests, $P < 0.05$).

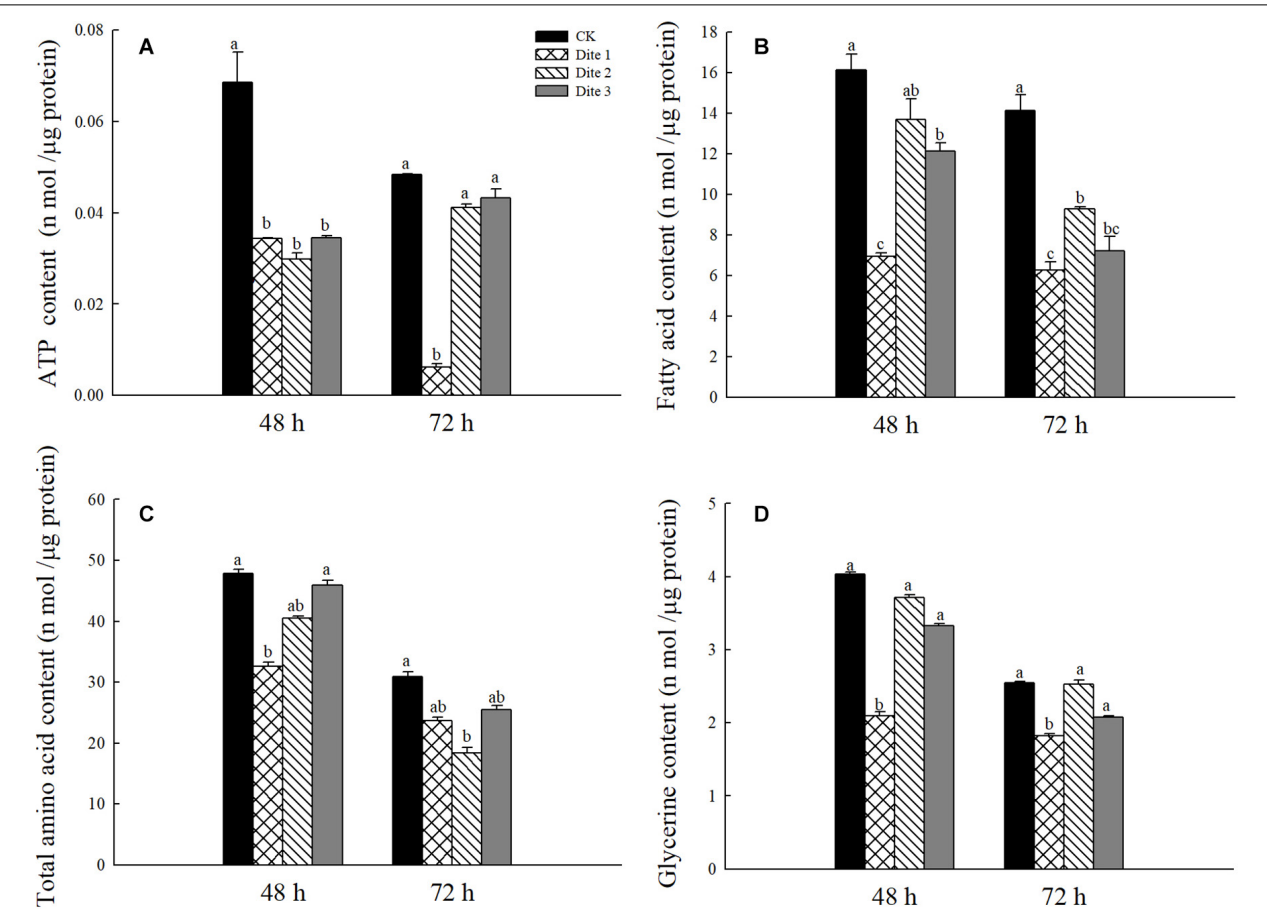

FIGURE 5 | Substance content in female *H. axyridis* after feeding on artificial feedstuffs for 48 and 72 h. **(A)** ATP content. **(B)** Fatty acid content. **(C)** Total amino acid content. **(D)** Glycerin content. Line bars represent standard error of the mean. Bars with different letters are significantly different (Tukey–Kramer tests, $P < 0.05$).

between the Diet 1 and Diet 3 groups. Regarding the relative expression of the *Vg1* and *Vg2* genes, the gene expression of Diet 2 and Diet 3 was significantly higher than that of Diet 1 insects. The gene expressions of all artificial feed groups were significantly lower than those of the CK group ($P < 0.05$; **Figures 7B,C**).

DISCUSSION

The results of this study showed that the trehalose, glucose, and glycogen contents in the hemolymph and tissues of larvae that fed on artificial Diet 2 and Diet 3 increased, indicating that the addition of glucose and trehalose has a certain impact on the

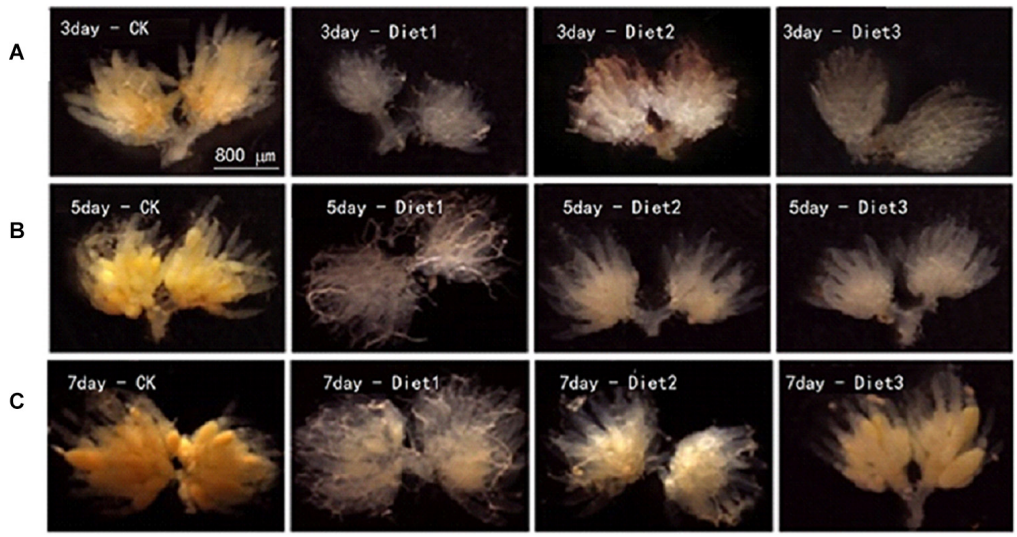

FIGURE 6 | Ovaries development of *H. axyridis*. Dissecting the ovaries of female *H. axyridis* in saline, after the wings were cut off, the back of the ladybird was gently made open. Remove non-reproductive tissues and organs such as fat body and digestive tract and intact ovaries could be seen at the end of the abdomen. **(A)** The ovarian anatomy of *H. axyridis* on the 3rd day after feeding. **(B)** The ovarian anatomy of *H. axyridis* on the 5th day after feeding. **(C)** The ovarian anatomy of the *H. axyridis* after 7th day after feeding.

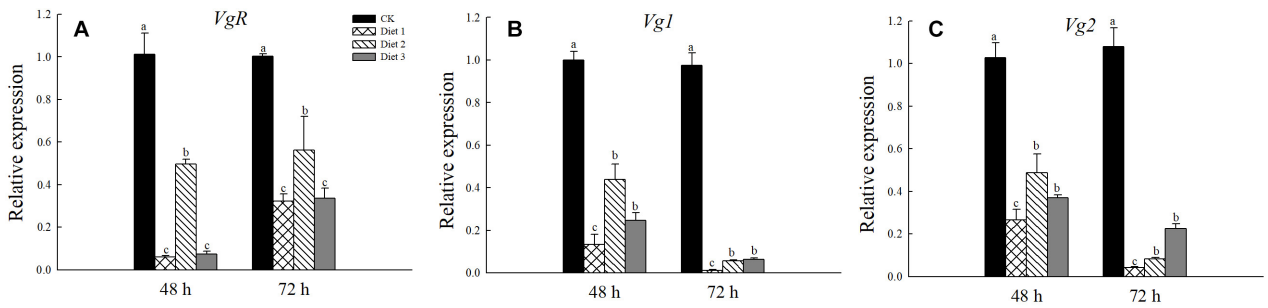

FIGURE 7 | Relative expression levels of *VgR*, *Vg1*, and *Vg2* after fed for 48 and 72 h. **(A)** Relative expression of *VgR* gene. **(B)** Relative expression of *Vg1*gene. **(C)** Relative expression of *Vg2*gene. Line bars represent standard error of the mean. Bars with different letters are significantly different (Tukey–Kramer tests, $P < 0.05$).

life indicators of *H. axyridis*. Glycogen plays a regulatory role in insect development, affecting larval development and the ability to pupate (Yee et al., 2012; Puggioli et al., 2013). There are differences in the developmental time and viability of pupa and adult insects fed different artificial feedstuffs (Silva et al., 2009), this was confirmed by our study. In this study, the weight of larvae fed on Diet 2 and Diet 3 was significantly higher than that of those that fed on Diet 1. Additionally, the developmental period of larvae fed on Diet 2 and Diet 3 was extended significantly. Adding an appropriate amount of energy substances such as glucose or trehalose can help insects grow and develop. It has been reported that the health indicators of larvae affect the fecundity of adults (Leuck and Perkins, 1972).

It has been suggested that the growth and reproduction of insect populations are important indicators for analyzing and understanding insect artificial diet (Bellows et al., 1992). In this study, although the *H. axyridis* on Diet 1 reproduced and laid eggs, their fecundity was relatively lower than that of those fed on Diet 2 and Diet 3. This could be a result of the amount of nutrients and energy in their diet that were not enough for them to grow and reproduce. After adding glucose or trehalose to the pork liver diet, not only the pre-oviposition period shortened, but also the fecundity and fertility of the eggs increased. When newly hatched larvae have sufficient food resources, their mortality rate will decrease as they develop faster, which reduces damage during development (Lucas, 2005; Lebreton et al., 2015). The apparent benefits on the reproductive ability of insects that fed on artificial feedstuffs containing glucose or trehalose that were observed in the experiments described in this paper, are inconsistent with the results of a previous study, which reported that feeding *Cydia pomonella* with sugars (Siekmann et al., 2001) can extend their lives but cannot increase their or their eggs' fertility (Savary et al., 2019). However, the results of increased fertility obtained in this study are consistent with earlier reports

of increased fertility caused by feeding sugar (Fadamiro and Heimpel, 2001). In parasitic bees, the benefits of glucose on health-related characteristics such as longevity and fertility are well-documented (Desouhant et al., 2010).

Trehalose has been reported as the dominant sugar in the insect hemolymph and other tissues (Van Handel, 1969) as it provides energy for targeted activities (Lu et al., 2019). In our study, we detected that the ATP content in the Diet 2 and Diet 3 groups was significantly higher than that in the Diet 1 group. In addition, studies have reported that developing insect embryos use glycogen to generate ATP energy and produce biomolecules required for cell proliferation and differentiation to maintain the embryonic development (Tennessen et al., 2011). Further metabolic analysis has shown that glycogen stored in oocytes is consumed during embryogenesis (Matsuda et al., 2015). In this study, we found that the glycogen content of Diet 2 and Diet 3 adults was significantly higher than that of Diet 1 adults. This is relatively consistent with the results of the larval glycogen content. At the same time, the overall glucose content increased. The glucose increase could have been caused by the conversion of glycogen to glucose (Fraga et al., 2013). Prolonged starvation reduces trehalose and glucose levels (Schilman and Roces, 2008; Laparie et al., 2012). The ovary is a reproductive organ that plays a vital role in population reproduction (Koch, 2003). There is high correlation between trehalose levels and spawning. Decreasing trehalose levels will delay the production of oocysts (Huang and Lee, 2011). The results of the ovarian development map showed that the ovarian development of the Diet 1 group was significantly more stunted than that of the Diet 2 and Diet 3 groups. The development of the ovary can be based on the presence or absence of egg chambers, transparent ovaries or yolk deposition, etc., to determine whether the development is good at the normal development stage (Chen et al., 2015). This suggests that trehalose may be an important energy fuel during spawning.

The relative gene expression of *VgR*, *Vg1*, and *Vg2* of insects that fed on Diet 2 and Diet 3 was significantly higher than that of those that fed on Diet 1. Oviposition is one of the most energy-demanding activities of adult female insects. During the development of oocytes, Vg is synthesized in the fat body, secreted into hemolymph, and enters developing oocytes through endocytosis mediated by the VgR (Tufail and Takeda, 2008). Therefore, the inadequate trehalose intake by the egg cells, which could inhibit the expression of *Vg*, may be the main reason for the delayed oviposition of *H. axyridis*. Research on *Drosophila* has suggested that the higher expression rate of *Vg* (vitellogenin precursor) leads to an increase in egg maturation and fertility (Drapeau et al., 2006). Up to now, *Vg* has been widely studied in insects, with its direct physiological function being to provide nutrition for developing embryos (Tufail and Takeda, 2008). In our study, the addition of glucose or trehalose increased the *Vg* expression. Researchers have discovered that *Vg* is involved in the maturation and development of oocytes and is, therefore, a key factor in insect reproduction. Additionally, *Vg* has been studied in many insects, including Lepidoptera, Diptera, Hymenoptera, and Hemiptera (Raviv et al., 2006).

It is well-known that the activity of any insect is closely associated with its energy metabolism (Wong et al., 2016); additionally, the metabolism of fatty and amino acids affects the release of insect hormones (Van der Horst, 2003). Owing to the limited ability of the ovaries to synthesize lipids, the formation and mobilization of lipid reserves in the fat body is also critical for egg maturation. It has been reported that glucose is not only a major energy source, but also promotes the synthesis of most molecules such as amino acids, nucleotides, and fatty acids (Saltiel and Kahn, 2001). In our study, the fatty acid content of adult *H. axyridis* increased after adding glucose or trehalose to their diets (**Figure 5B**), which could also explain their improved ovarian development and fertility. During the development of insect oocytes, the developing oocytes accumulate a large amount of energy reserves from the hemolymph, such as lipids and proteins; essentially, reserves in the fat body that are essential for the development and reproduction of adults are mobilized (Tufail and Takeda, 2008). Excess glucose obtained from the diet is stored as branched-chain polysaccharide glycogen or as triglycerides in the body to satisfy future energy needs (Saltiel and Kahn, 2001; Chng et al., 2017). In this study, the glycerol content of the insects increased with the consumption of artificial feedstuff containing glucose or trehalose, indicating that the proper adjustment of the stored energy's anabolism and catabolism is critical to preserve the insect's metabolic balance throughout its life cycle (Mattila and Hietakangas, 2017). Moreover, studies have shown that insects with insufficient energy supply mobilize glycogen and triglycerides stored in their fat bodies (Bede et al., 2007; Konuma et al., 2012; Park et al., 2013). The lipid reserves of hungry females gradually decrease, while the lipid reserves of hungry males remain stable, indicating that nutrient reserves (lipids and glycogen) may be used when females spawn (Fadamiro et al., 2005). The fat content and fatty acid composition of insects depend on the composition of their feedstuffs and on the feeding conditions (Van Broekhoven et al., 2015), it follows that larvae fed low nutritional quality foods may use their fat reserves as energy, thereby reducing their fat content (St-Hilaire et al., 2007).

Therefore, the selection of a suitable artificial diet as larval food is the basis for the breeding success of *H. axyridis*. Research has indicated that there is an energetic cost to the act of reproduction (Wu et al., 2008) and several studies have shown that sugar has a positive effect on insect survival or fertility (Fadamiro and Heimpel, 2001). In addition, glucose increases mating events (Lebreton et al., 2015), which may contribute to the increase in spawning. Moreover, studies have shown that glucose can promote gastrointestinal motility, intestinal transport, and excretion (Chng et al., 2017), although these topics require further study.

CONCLUSION

Our results demonstrated that glucose and trehalose contributed to the growth, development and reproduction of *H. axyridis*, which may be due to their roles in energy. The reproduction of *H. axyridis* was elevated with addition of glucose and trehalose in our study. Adult reproduction depends on energy consumption and accumulation in the early stages of insect development, and

the more is energy, the strong is reproduction. Therefore, the selection of suitable artificial diet as larval food is the basis for the success of *H. axyridis* breeding.

DATA AVAILABILITY STATEMENT

All datasets generated for this study are included in the article/supplementary material.

AUTHOR CONTRIBUTIONS

SGW and SW conceived the design and manuscript structure design. YL, YKL, YTL, SSW, and MZ contributed to the current articles collection and trehalose metabolism genes' analysis. YL, SW, and SGW wrote the manuscript. All authors contributed to the article and approved the submitted version.

FUNDING

This work was supported by National Key Research and Development Program of China (Grant No. 2017YFD0201000), Hangzhou Science and Technology Development Program of China (Grant No. 20190101A01), Beijing Key Laboratory of Environment-Friendly Management on Fruit Disease and Pests in North China (Grant No. BZ0432), Beijing Technology Program (Grant No. D171100001617003), Technical Innovation Program of Beijing Academy of Agricultural and Forest Science (Grant No. 20170107), and Youth Scientific Research Fund of Beijing Academy of Agricultural and Forestry Science (Grant No. QNJJ201725).

REFERENCES

Bass, C., Denholm, I., Williamson, M. S., and Nauen, R. (2015). The global status of insect resistance to neonicotinoid insecticides. *Pestic. Biochem. Physiol.* 121, 78–87. doi: 10.1016/j.pestbp.2015.04.004

Bede, J. C., McNeil, J. N., and Tobe, S. S. (2007). The role of neuropeptides in caterpillar nutritional ecology. *Peptides* 28, 185–196. doi: 10.1016/j.peptides

Bellows, T. S., Van Driesche, R. G., and Elkinton, J. S. (1992). Life-Table construction and analysis in the evaluation of natural enemies. *Annu. Rev. Entomol.* 37, 587–612. doi: 10.1146/annurev.en.37.010192.003103

Bonte, M., Samih, M. A., and Clercq, P. D. (2010). Development and reproduction of *Adalia bipunctata* on factitious and artificial foods. *Biocontrol.* 55, 485–491. doi: 10.1007/s10526-010-9266-1

Brown, P. M. J., Thomas, C. E., Lombaert, E., Jeffries, D. L., Estoup, A., and Handley, L. J. L. (2011). The global spread of Harmonia axyridis (Coleoptera: Coccinellidae): distribution, dispersal and routes of invasion. *Biocontrol.* 56, 623–641. doi: 10.1007/s10526-011-9379-1

Castane, C., and Zapata, R. (2005). Rearing the predatory bug Macrolophus caliginosus on a meat based diet. *Biocontrol* 34, 66–72. doi: 10.1016/j.biocontrol

Castro, C. F., Almeida, L. M., and Penteado, S. R. C. (2011). The impact of temperature on biological aspects and life table of Harmonia axyridis (Pallas) (Coleoptera: Coccinellidae). *Fla. Entomol.* 94, 923–932. doi: 10.2307/23065850

Chen, J., Wu, C. J., Zhang, Q. W., Ma, Z., Sun, H. K., and He, Y. Z. (2015). Ovarian development and oogenesis of Harmonia axyridis Pallas. *J. Plant Prot.* 42, 237–243.

Cheng, Y., Zhi, J., Li, F., Li, W., and Zhou, Y. (2018). Improving the artificial diet for adult of seven spotted ladybird beetle Coccinella septempunctata L. *(Coleoptera: Coccinellidae) with orthogonal design. Bull. Entomol. Res.* 108, 337–343. doi: 10.1017/S0007485317000797

Chng, W. A., Hietakangas, V., and Lemaitre, B. (2017). Physiological adaptations to sugar intake: new paradigms from Drosophila melanogaster. *Trends Endocrinol. Metab.* 28, 131–142. doi: 10.1016/j.tem.2016.11.003

Cohen, A. C. (2001). Formalizing insect rearing and artificial diet technology. *Ame Entomol.* 47, 198–206. doi: 10.1093/ae/47.4.198

Denno, R. F., and Fagan, W. F. (2003). Might nitrogen limitation promote omnivory among carnivorous arthropods? Comment. *Ecology* 84, 2522–2531. doi: 10.1890/09-2080.1

Desouhant, E., Lucchetta, P., Giron, D., and Bernstein, C. (2010). Feeding activity pattern in a parasitic wasp when foraging in the field. *Ecol. Res.* 25, 419–428. doi: 10.1007/s11284-009-0671-9

Drapeau, M. D., Albert, S., Kucharski, R., Prusko, C., and Maleszka, R. (2006). Evolution of the yellow/major royal jelly protein family and the emergence of social behavior in honey bees. *Genome Res.* 16, 1385–1394. doi: 10.1101/gr.5012006

Fadamiro, H. Y., Chen, L., Onagbola, E. O., and Graham, L. (2005). Lifespan and patterns of accumulation and mobilization of nutrients in the sugar-fed phorid fly, *Pseudacteon tricuspis*. *Physiolog. Entomol.* 30, 212–224. doi: 10.1111/j.1365-3032.2005.00449.x

Fadamiro, H. Y., and Heimpel, G. E. (2001). Effects of Partial Sugar Deprivation on Lifespan and Carbohydrate Mobilization in the Parasitoid Macrocentrus grandii (Hymenoptera: Braconidae). *Ann. Entomol. Soc. Am.* 94, 909–916. doi: 10.1603/0013-8746(2001)094[0909:eopsdo]2.0.co;2

Fraga, A., Ribeiro, L., Lobato, M., Santos, V., Silva, J. R., Gomes, H., et al. (2013). Glycogen and Glucose Metabolism Are Essential for Early Embryonic Development of the Red Flour Beetle *Tribolium castaneum*. *PLoS One* 8:e65125. doi: 10.1371/journal.pone.0065125

Garratt, J., and Kennedy, A. (2006). Use of models to assess the reduction in contamination of water bodies by agricultural pesticides through the implementation of policy instruments: a case study of the Voluntary Initiative in the UK. *Pest Manag. Sci.* 62, 1138-1149. doi: 10.1002/ps.1284

Guo, J. Y., and Wan, F. H. (2001). Effect of three diets on development and fecundity of the ladybeetles Harmonia axyridis and Propylaea japonica. *Chin. J. Biol. Cont.* 17, 116–120. doi: 10.16409/j.cnki.2095-039x

Hansen, D. L., Brodsgaard, H. F., and Enkegaard, A. (1999). Life table characteristics of Macrolophus caliginosus preying upon Tetra urticae. *Entomol. Exp. Appl.* 9, 269–275.

Haque, M. A., Chen, J., Aldred, P., and Adhikari, B. (2015). Drying and denaturation characteristics of whey protein isolate in the presence of lactose and trehalose. *Food Chem.* 177, 8–16. doi: 10.1016/j.foodchem.2014.12.064

Huang, J. H., and Lee, H. J. (2011). RNA interference unveils functions of the hypertrehalosemic hormone on cyclic fluctuation of hemolymph trehalose and oviposition in the virgin female Blattella germanica. *J. Insect Physiol.* 57, 858–864. doi: 10.1016/j.jinsphys

Huang, J. J., Ding, B. J., Shu, X. H., and Liu, Y. H. (2015). Effects of different sugars on longevity and egg mature of Microplitis mediator. *J. Environ. Entomol.* 37, 617–622.

Juen, A., Hogendoorn, K. M. G., Schmidt, O., and Keller, M. A. (2012). Analysing the diets of invertebrate predators using terminal restriction fragments. *J. Pest Sci.* 85, 89–100. doi: 10.1007/s10340-011-0406-x

Katsarou, I., Margaritopoulos, J. T., Tsitsipis, J. A., Perdikis, D. C., and Zarpas, K. D. (2005). Effect of temperature on development, growth and feeding of Coccinella septempunctata and Hippodamia convergens reared on the tobacco aphid, Myzus persicaenicotianae. *Biocontrol* 50, 565–588. doi: 10.1007/s10526-004-2838-1

Kavi, L. A., Kaufman, P. E., and Scott, J. G. (2014). Genetics and mechanisms of imidacloprid resistance in house flies. *Pestic. Biochem. Physiol.* 109, 64–69. doi: 10.1016/j.pestbp.2014.01.006

Koch, R. L. (2003). The multicolored Asian lady beetle, Harmonia axyridis: a review of its biology, uses in biological control, and non-target impacts. *J. Insect Sci.* 3:32. doi: 10.1093/jis/3.1.32

Konuma, T., Morooka, N., Nagasawa, H., and Nagata, S. (2012). Knockdown of the adipokinetic hormone receptor increases feeding frequency in the two-spotted

cricket Gryllus bimaculatus. *Endocrinology* 153, 3111–3122. doi: 10.1210/en.2011-1533

Laparie, M., Larvor, V., Frenot, Y., and Renault, D. (2012). Starvation resistance and effects of diet on energy reserves in a predatory ground beetle (Merizodus soledadinus; Carabidae) invading the Kerguelen Islands. *Comp. Biochem. Physiol. A. Mol. Integr. Physiol.* 161, 122–129. doi: 10.1016/j.cbpa.2011.09.011

Lebreton, S., Trona, F., Borrero-Echeverry, F., Bilz, F., Grabe, V., Becher, P. G., et al. (2015). Feeding regulates sex pheromone attraction and courtship in Drosophila females. *Sci. Rep.* 5:13132. doi: 10.1038/srep13132

Leuck, D. B., and Perkins, W. D. (1972). A method of estimating fall armyworm progeny reduction when evaluating control achieved by host-plant resistance. *J. Econ. Entomol.* 65, 482–483. doi: 10.1093/jee/65.2.482

Li, G. H., Pang, Y., Chen, Q., Su, Z. J., and Wen, X. Z. (2002). Studies on the artificial diet for beet armyworm, Spodoptera exigua. *Chin. J. Biol. Cont.* 18, 132–134. doi: 10.16409/j.cnki.2095-039x.2002.03.008

Liu, H. L., Zheng, L. M., Liu, Q. Q., Quan, F. S., and Zhang, Y. (2013). Studies on the transcriptomes of non-model organisms. *Hereditas* 35, 955–970. doi: 10.3724/sp.j.1005.2013.00955

Livak, K. J., and Schmittgen, T. D. (2001). Analysis of relative gene expression data using real-time quantitative PCR and the 2-11CT method. *Methods* 25, 402–408. doi: 10.1006/meth

Lu, K., Wang, Y., Chen, X., Zhang, X., Li, W., Cheng, Y., et al. (2019). Adipokinetic hormone receptor mediates trehalose homeostasis to promote vitellogenin uptake by oocytes in Nilaparvata lugens. *Front. Physiol.* 9:1904. doi: 10.3389/fphys.2018.01904

Lu, Y., Wu, K., Jiang, Y., Guo, Y., and Desneux, N. (2012). Widespread adoption of Bt cotton and insecticide decrease promotes biocontrol services. *Nature* 487, 362–365. doi: 10.1038/nature11153

Lucas, É (2005). Intraguild predation among aphidophagous predators. *Eur. J. Entomol.* 102, 351–364. doi: 10.14411/eje.2005.052

Luo, S. P., Naranjo, S. E., and Wu, K. M. (2014). Biological control of cotton pests in China. *Biol. Control.* 68, 6–14. doi: 10.1016/j.biocontrol.2013.06.004

Majerus, M., Strawson, V., and Roy, H. (2006). The potential impacts of the arrival of the harlequin ladybird, Harmonia axyridis (Pallas) (Coleoptera: Coccinellidae), in Britain. *J. Econ. Entomol.* 31, 207–215. doi: 10.1111/j.1365-2311.2006.00734.x

Matsuda, H., Yamada, T., Yoshida, M., and Nishimura, T. (2015). Flies without trehalose. *J. Biol. Chem.* 290, 1244–1255. doi: 10.1074/jbc.M114.619411

Mattila, J., and Hietakangas, V. (2017). Regulation of carbohydrate energy metabolism in Drosophila melanogaster. *Genetics* 207, 1231–1253. doi: 10.1534/genetics.117.199885

Michaud, J. P. (2002). Invasion of the Florida citrus ecosystem by Harmonia axyridis (Coleoptera: Coccinellidae) and asymmetric competition with a native species, Cycloneda sanguinea. *Environ. Entomol.* 31, 827–835. doi: 10.1603/0046-225X-31.5.827

Park, M. S., Park, P., and Takeda, M. (2013). Roles of fat body trophocytes, mycetocytes and urocytes in the American cockroach, Periplaneta americana under starvation conditions: an ultrastructural study. *Arthropod Struct. Dev.* 42, 287–295. doi: 10.1016/j.asd.2013.03.004

Puggioli, A., Balestrino, F., Damiens, D., Lees, R. S., Soliban, S. M., Madakacherry, O., et al. (2013). Efficiency of three diets for larval development in mass rearing *Aedes albopictus* (Diptera: Culicidae). *J. Med. Entomol.* 50, 819–825. doi: 10.1603/me13011

Puinean, A. M., Denholm, I., Millar, N. S., Nauen, R., and Williamson, M. S. (2010). Characterisation of imidacloprid resistance mechanisms in the brown planthopper, Nilaparvata lugens Stål (Hemiptera: Delphacidae). *Pestic. Biochem. Physiol.* 97, 129–132. doi: 10.1016/j.pestbp.2009.06.008

Raviv, S., Parnes, S., Segall, C., Davis, C., and Sagi, A. (2006). Complete sequence of Litopenaeus vannamei (Crustacea: Decapoda) vitellogenin cDNA and its expression in endocrinologically induced sub-adult females. *Gen. Comp. Endocrinol.* 145, 39–50. doi: 10.1016/j.ygcen.2005.06.009

Saddiq, B., Shad, S. A., Aslam, M., Ijaz, M., and Abbas, N. (2015). Monitoring resistance of Phenacoccus solenopsis Tinsley (Homoptera: pseudococcidae) to new chemical insecticides in Punjab, Pakistan. *Crop Prot.* 74, 24–29. doi: 10.1016/j.cropro.2015.03.026

Saltiel, A. R., and Kahn, C. R. (2001). Insulin signalling and the regulation of glucose and lipid metabolism. *Nature* 414, 799–806. doi: 10.1038/414799a

Savary, S., Willocquet, L., Pethybridge, S. J., Esker, P., McRoberts, N., and Nelson, A. (2019). The global burden of pathogens and pests on major food crops. *Nat. Ecol. Evol.* 3, 430–439. doi: 10.1038/s41559-018-0793-y

Schilman, P. E., and Roces, F. (2008). Haemolymph sugar levels in a nectar-feeding ant: dependence on metabolic expenditure and carbohydrate deprivation. *J. Comp. Physiol. B.* 178, 157–165. doi: 10.1007/s00360-007-0207-y

Schmidt, J. M., Sebastian, P., Wilder, S. M., and Rypstra, A. L. (2012). The nutritional content of prey affects the foraging of a generalist arthropod predator. *PLoS One* 7:e49223. doi: 10.1371/journal.pone.0049223

Shi, Z. K., Wang, S., Wang, S. G., Zhang, L., Xu, Y. X., Guo, X. J., et al. (2017). Effects of starvation on the carbohydrate metabolism in Harmonia axyridis (Pallas). *Biol. Open.* 15 6, 1096–1103. doi: 10.1242/bio.025189

Siekmann, G., Tenhumberg, B., and Keller, M. A. (2001). Feeding and survival in parasitic wasps: sugar concentration and timing matter. *Oikos* 95, 425–430. doi: 10.1034/j.1600-0706.2001.950307.x

Silva, R. B., Zanuncio, J. C., Serrão, J. E., Lima, E. R., Figueiredo, M. L. C., and Cruz, I. (2009). Suitability of different artificial diets for development and survival of stages of the predaceous ladybird beetle Eriopis connexa. *Phytoparasitica* 37, 115–123. doi: 10.1007/s12600-008-0015-2

St-Hilaire, S., Cranfill, K., McGuire, M. A., Mosley, E. E., Tomberlin, J. K., Newton, L., et al. (2007). Fish offal recycling by the black soldier fly produces a foodstuff high in omega-3 fatty acids. *J. World Aquac. Soc.* 38, 309–313. doi: 10.1111/j.1749-7345.2007.00101.x

Tang, B., Chen, J., Yao, Q., Pan, Z., Xu, W., Wang, S., et al. (2010). Characterization of a trehalose-6-phosphate synthase gene from Spodoptera exigua and its function identification through RNA interference. *J. Insect Physiol.* 56, 813–821. doi: 10.1016/j.jinsphys.2010.02.009

Tang, B., Xu, Q., Zou, Q., Fang, Q., Wang, S. G., and Ye, G. Y. (2012). Sequencing and characterization of glycogen synthase and glycogen phosphorylase genes from Spodoptera exigua and analysis of their function in starvation and excessive sugar intake. *Arch. Insect Biochem. Physiol.* 80, 42–62. doi: 10.1002/arch.21027

Tennessen, J. M., Baker, K. D., Lam, G., Evans, J., and Thummel, C. S. (2011). The Drosophila estrogen-related receptor directs a metabolic switch that supports developmental growth. *Cell Metab.* 13, 139–148. doi: 10.1016/j.cmet.2011.01.005

Thompson, S. N. (2003). Trehalose – the insect 'blood' sugar. *Adv. Insect. Physiol* 31, 205–285.

Tufail, M., Naeemullah, M., Elmogy, M., Sharma, P. N., Takeda, M., and Nakamura, C. (2010). Molecular cloning, transcriptional regulation, and differential expression profiling of vitellogenin in two wing-morphs of the brown planthopper, Nilaparvata lugens Stål (Hemiptera: Delphacidae). *Insect Mol. Biol.* 19, 787–798. doi: 10.1111/j.1365-2583.2010.01035.x

Tufail, M., and Takeda, M. (2008). Molecular characteristics of insect vitellogenins. *J. Insect Physiol.* 54, 1447–1458. doi: 10.1016/j.jinsphys.2008.08.007

Van, J. C. (2012). The state of commercial augmentative biological control: plenty of natural enemies, but a frustrating lack of uptake. *Biocontrol* 57, 1–20. doi: 10.1007/s10526-011-9395-1

Van Broekhoven, S., Oonincx, D. G., van Huis, A., and van Loon, J. J. (2015). Growth performance and feed conversion efficiency of three edible mealworm species (Coleoptera: Tenebrionidae) on diets composed of organic by-products. *J. Insect Physiol.* 73, 1–10. doi: 10.1016/j.jinsphys.2014.12.005

Van der Horst, D. J. (2003). Insect adipokinetic hormones: release and integration of flight energy metabolism. *Comp. Biochem. Physiol. B. Biochem. Mol. Biol.* 136, 217–226. doi: 10.1016/s1096-4959(03)00151-9

Van Handel, E. (1969). Metabolism of hexoses in the intact mosquito: exclusion of glucose and trehalose as intermediates. *Comp. Biochem. Physiol.* 29, 413–421. doi: 10.1016/0010-406x(69)91760-5

Vaulont, S., Vasseur-Cognet, M., and Kahn, A. F. (2000). Glucose regulation of gene transcription. *J. Biol. Chem.* 275, 555–558. doi: 10.1074/jbc.R000016200

Wang, C., Cao, Y., Wang, Z., Yin, Y., Peng, G., Li, Z., et al. (2007). Differentially-expressed glycoproteins in Locusta migratoria hemolymph infected with Metarhizium anisopliae. *J. Invertebr. Pathol.* 96, 230–236. doi: 10.1016/j.jip.2007.05.012

Wilder, S. M., Holway, D. A., Suarez, A. V., and Eubanks, M. D. (2011). Macronutrient content of plant-based food affects growth of a carnivorous arthropod. *Ecology* 92, 325–332. doi: 10.1890/10-0623.1

Wong, S. C., Oksanen, A., Mattila, A. L., Lehtonen, R., Niitepõld, K., and Hanski, I. (2016). Effects of ambient and preceding temperatures and metabolic genes on flight metabolism in the Glanville fritillary butterfly. *J. Insect Physiol.* 85, 23–31. doi: 10.1016/j.jinsphys.2015.11.015

Wu, H. P., Meng, L., and Li, B. P. (2008). Effects of feeding frequency and sugar concentrations on lifetime reproductive success of Meteorus pulchricornis (Hymenoptera: Braconidae). *Biol. Cont.* 45, 353–359. doi: 10.1016/j.biocontrol.2008.01.017

Yang, H., Xiong, J. W., and Zhang, F. (2013). Advances of artificial diet for Harminia axyridis. *J. Mou. Agr. Biol.* 22, 169–172. doi: 10.15958/j.cnki.sdnyswxb.2003.02.016

Yee, D. A., Juliano, S. A., and Vamosi, S. M. (2012). Seasonal photoperiods alter developmental time and mass of an invasive mosquito, *Aedes albopictus* (Diptera: Culicidae), across its north-south range in the United States. *J. Med. Entomol.* 49, 825–832. doi: 10.1603/me11132

Youn, Y. N., Seo, M. J., Shin, J. G., Jang, C., and Yu, Y. M. (2003). Toxicity of greenhouse pesticides to multicolored Asian lady beetles, Harmonia axyridis (Coleoptera:Coccinellidae). *Biocontrol* 28:170. doi: 10.1016/s1049-9644(03)00098-7

Zazycki, L. C. F., Semedo, R. E. S., Silva, A., Bisognin, A. Z., Bernardi, O., Garcia, M. S., et al. (2015). Biology and fertility life table of Eriopis connexa, Harmonia axyridis and Olla v-nigrum (Coleoptera: Coccinellidae). *Braz. J. Biol.* 75, 969–973. doi: 10.1590/1519-6984.03814

Zhang, L. S., Chen, H. Y., and Li, B. P. (2014). *Mass rearing and utilization of insect natural enemies*, 1st Edn. Beijing: China Agriculture Scientech Press.

Zhang, T., Zhang, G., Zeng, F., Mao, J., Liang, H., and Liu, F. (2017). Molecular cloning of the vitellogenin gene and the effects of vitellogenin protein expression on the physiology of Harmonia axyridis (Coleoptera: Coccinellidae). *Sci. Rep.* 7:13926. doi: 10.1038/s41598-017-14339-3

Conflict of Interest: The authors declare that the research was conducted in the absence of any commercial or financial relationships that could be construed as a potential conflict of interest.

frontiers in Physiology

ORIGINAL RESEARCH
published: 17 September 2020
doi: 10.3389/fphys.2020.575485

Regulation of Carbohydrate Metabolism by Trehalose-6-Phosphate Synthase 3 in the Brown Planthopper, *Nilaparvata lugens*

Sha-Sha Wang[1,2†], Guo-Yong Li[1†], Yong-Kang Liu[2], Yu-Jia Luo[2], Cai-Di Xu[2], Can Li[1] and Bin Tang[1,2*]*

[1] Guizhou Provincial Key Laboratory for Rare Animal and Economic Insect of the Mountainous Region, Department of Biology and Engineering of Environment, Guiyang University, Guiyang, China, [2] College of Life and Environmental Sciences, Hangzhou Normal University, Hangzhou, China

OPEN ACCESS

Edited by:
Peng He,
Guizhou University, China

Reviewed by:
Zhongxiang Sun,
Fujian Agriculture and Forestry University, China
Bimalendu B. Nath,
Savitribai Phule Pune University, India

***Correspondence:**
Can Li
Lican790108@163.com
Bin Tang
tbzm611@yahoo.com

[†] These authors have contributed equally to this work

Specialty section:
This article was submitted to Invertebrate Physiology, a section of the journal Frontiers in Physiology

Received: *23 June 2020*
Accepted: *25 August 2020*
Published: *17 September 2020*

Citation:
Wang S-S, Li G-Y, Liu Y-K, Luo Y-J, Xu C-D, Li C and Tang B (2020) Regulation of Carbohydrate Metabolism by Trehalose-6-Phosphate Synthase 3 in the Brown Planthopper, Nilaparvata lugens. Front. Physiol. 11:575485. doi: 10.3389/fphys.2020.575485

Nilaparvata lugens (Stål) (Hemiptera: Delphacidae) is one of the pests that harm rice. In this paper, a new trehalose-6-phosphate synthase gene, *TPS3*, was identified by transcriptome sequencing and gene cloning. To explore its role in the energy metabolism of *N. lugens* we examined the carbohydrate contents at different stages of development, the tissue expression of *TPS*, and some physiological and biochemical indicators by injecting dsTPS3 and dsTPSs (a proportional mixture of dsTPS1, dsTPS2, and dsTPS3). The glucose content at the fifth instar was significantly higher than that in the fourth instar and the adult stages. The trehalose and glycogen contents before molting were higher than those after molting. *TPS1*, *TPS2,* and *TPS3* were expressed in the head, leg, wing bud, and cuticle, with the highest expression in the wing bud. In addition, compared with the control group, the glucose content increased significantly at 48 h after RNA interference, and the trehalose content decreased significantly after 72 h. qRT-PCR showed that the expression level of *UGPase* decreased significantly at 48 h after injection, whereas *GS* expression increased significantly at 48 h after injecting dsTPS3. After dsTPS injection, the expression levels of *PPGM2*, *UGPase*, *GP*, and *GS* increased significantly at 72 h. After interfering with the expression of *TPS3* gene alone, *UGPase* expression decreased significantly at 48 h, and *GS* expression increased significantly at 72 h. Finally, combined with the digital gene expression and pathway analysis, 1439 and 1346 genes were upregulated, and 2127 and 1927 genes were downregulated in the dsTPS3 and dsTPSs groups, respectively. The function of most differential genes was concentrated in sugar metabolism, lipid metabolism, and amino acid metabolism. The results indicated that *TPS3* plays a key role in the energy metabolism of *N. lugens* and confirmed that *TPS3* is a feasible target gene for RNA interference in *N. lugens*. Simultaneously, they provide a theoretical basis for the development and utilization of *TPS3* to control pests.

Keywords: delphacidae, trehalose-6-phosphate synthase, trehalose metabolism, glycogen, RNA interference

INTRODUCTION

Crops are often attacked by various agricultural pests, resulting in decreased yield and quality of agricultural products. Therefore, agricultural pests are one of the factors that constrain global agricultural development. Nearly half the global population consumes rice, especially Chinese residents (Sun et al., 2019). Locusts can pose a major threat to rice, and destruction of produce by locusts occurs in frequent bursts. Among them, *Nilaparvata lugens* (Stål) (Hemiptera: Delphacidae) is one of the most destructive pests of rice (Yang et al., 2019). This insect can use its probe to pierce the sheath phloem sap and absorb vascular fluids containing sucrose, amino acids, potassium, and ATP from vascular bundles (Hayashi and Chino, 1990). In addition to extracting nutrients from the vascular bundle, it can transmit viruses such as rice ragged stunt virus (RRSV) and rice grassy stunt virus to rice plants (Hibino, 1996; Wang et al., 2016). The use of large amounts of chemical pesticides is well known to the human body and the environment. It would be great to develop a new type of green pesticide to control pests by blocking the energy metabolism of planthoppers.

For all organisms, continuation of life is inseparable from energy metabolism. In mammals, glucose is the energy source and metabolic intermediate of living cells and is called the "fuel of life." Glucose is also an important source of energy in insects. After feeding, the carbohydrates in food are absorbed by cells and produce energy through the glycolytic pathway; the excess glucose in circulation is stored in the form of trehalose and glycogen (Roach et al., 2012; Yamada et al., 2018). Glycogen is synthesized and stored in several tissues, including the muscles and fat body (Yamada et al., 2018). Glycogen metabolism is controlled by two enzymes, glycogen synthase (GS) and glycogen phosphorylase (GP). GP catalyzes the rate-limiting cleavage of glucose monomers at the ends of glycogen branches (Roach et al., 2012; Zhang et al., 2017; Yamada et al., 2019). In addition to glycogen, the concentration of the non-reducing disaccharide, trehalose, in insect hemolymph is maintained at a high level (Becker et al., 1996; Shukla et al., 2015). At the beginning of the 19th century, Wiggers first discovered this sugar in rye ergot; it was subsequently reported in mushrooms (Elbein et al., 2003; Shukla et al., 2015). Trehalose was also found in bacteria, plants, insects, and other organisms (Argüelles, 2014; Lunn et al., 2014; Shukla et al., 2015). Trehalose plays a variety of important roles in these organisms; for example, it acts as a structural component in bacterial cell walls, as a growth regulator and carbon source in plants and fungi, as an energy source in insects, and as a compatible solute against environmental stress (Crowe et al., 1984; Asano, 2003). In insects, trehalose is the main hemolymph sugar and is synthesized in the fat body. Two enzymes are involved in this synthetic pathway, namely trehalose-6-phosphate synthase (TPS) and trehalose 6-phosphate phosphatase (TPP). TPS catalyzes glucose transfer from uridine diphosphate glucose (UDP-glucose) to glucose-6-phosphate to form trehalose-6-phosphate (T-6-P) and UDP, whereas TPP dephosphorylates T-6-P to trehalose and inorganic phosphate (Shukla et al., 2015).

Trehalose-6-phosphate synthase genes have been cloned in many insects such as *Apis mellifera*, *Tribolium castaneum*, *Musca domestica*, and *Heortia vitessoides* (Chen et al., 2018, 2020; Łopieńska-Biernat et al., 2018; Zhang D. W. et al., 2019). As a tool for knocking out individual gene expression after transcription, RNA interference (RNAi) has been used to control the expression of specific genes in many experimental organisms (Mello and Conte, 2004; Han, 2018). A large number of studies on *TPS* have shown that *TPS* plays an important role in the growth and development of organisms. For example, when *TPS* expression in insects was inhibited, insects showed death and deformity phenotypes, indicating that *TPS* affects insect energy metabolism and chitin metabolism (Xiong et al., 2016; Chen et al., 2018, 2020). In addition, *TPS* acts as an inducible anti-stress gene that takes part in immune defense in *M. domestica* via synthesizing its product trehalose (Zhang D. W. et al., 2019). *TPS1* and *TPS2* have been reported in *N. lugens*, and related studies have been carried out on these genes (Yang et al., 2017). In this study, we cloned a new *TPS* named *TPS3*. This study used RNAi to explore the effects of *TPS3* gene on energy metabolism, and to evaluate whether *TPS3* has the theoretical potential as a target gene for controlling brown planthoppers.

MATERIALS AND METHODS

Insect and Material Collection

The brown planthoppers (*N. lugens*) collected from the Zhejiang Academy of Agricultural Sciences were kept in the laboratory of the author. The brown planthopper and rice were tested and cultivated in an artificial climate chamber. Brown planthopper feeding conditions: temperature 26 ± 1°C, photoperiod 16 h: 8 h (light: dark), relative humidity 70%.

The rice variety used to raise the brown planthopper was TN1 (Taichung Native 1). Rice planting steps: First, the rice seeds were soaked in warm water at about 70°C for 10 min, followed by soaking in tap water and placing them in an artificial climate incubator at 30°C for 24 h. Then, the water was drained, rinsed with tap water, and the seeds were wrapped with wet gauze, and placed in a 30°C artificial climate incubator for 24–48 h. After the seeds germinated, we planted them in plastic pots and fertilized them appropriately. After the seedlings grew to about 10 cm, they were transferred to the field for cultivation. After rice was grown to the middle of the tillering, it was moved to the insect cage; the rice plants were replaced every 2–3 days.

From the fourth instar nymph to the third day of the adult, the developmental expression materials of the brown planthopper were collected every 12 h. Three biological replicates were performed at each developmental stage, and seven planthoppers were collected for each replicate. The expression material of the brown planthopper tissue was taken from the adult stage and dissected under the Leica EZ4 dissecting microscope to obtain the planthopper head, foot, wing bud, and epidermis. Three biological replicates were performed for each tissue material, and more than 200 individuals were collected for each replicate.

RNA Extraction and cDNA Synthesis

Total RNA was isolated from whole brown planthopper using TRIzol reagent (Invitrogen, Carlsbad, CA, United States) according to the method described by Yang et al. (2017). After extraction, the RNA quality was first determined by agarose gel electrophoresis, and the purity and concentration of the isolated RNA were determined spectrophotometrically using a NanoDrop™ 2000 (Thermo Scientific, Wilmington, United States). The remaining RNA was stored in a −80°C freezer. The first strand of cDNA was synthesized using the TaKaRa PrimeScript™ RT reagent Kit with the gDNA Eraser kit (TaKaRa, Dalian, China) that includes the removal reaction and reverse transcription reaction of genomic DNA. The specific experimental method can be found in the kit manual. The cDNA was stored in a refrigerator at −20°C.

Double-Stranded RNA Synthesis

First, the dsRNA primer of *N. lugens TPS3* (GenBank: KU556827.1) gene was designed using Primer Premier 5 software. The T7 sequence was 5′-GGATCCTAATACGACTCACTATAGG-3′. In addition, the dsRNA primer of *GFP*, *TPS1* (GenBank: GQ397450.1), and *TPS2* (GenBank: KU556826.1) genes were used as described by Yang et al. (2017). Specific primer sequences are shown in **Table 1**.

The T7 RiboMAX™ Express RNAi System is an *in vitro* transcription system that synthesizes milligrams of dsRNA in a short period of time. Moreover, the synthesized dsRNA does not contain the contamination of proteins and other components, and it was suitable for RNAi of the brown planthopper *TPS* gene in this study. The two complementary RNA strands were synthesized using plasmid DNA as a template, and the single-stranded RNA then generates double-stranded RNA after annealing. The DNA template and single-stranded RNA remaining in the reaction are removed by nuclease digestion, and the resulting dsRNA is purified by precipitation with isopropanol to obtain a dsRNA that can be used for RNAi experiments.

TABLE 1 | Primers used for dsTPS1, dsTPS2, dsTPS3 and dsGFP.

Primer name	Primer Sequence (5′-3′)
dsNITPS1-F	ACCAGGAGTTGAAGGAGGAG
dsNITPS1-R	GCTATGGGCACCCTGATC
dsNITPS1-FT	GGATCCTAATACGACTCACTATAGGACCAGGAGTTGAAGGAGGAG
dsNITPS1-RT	GGATCCTAATACGACTCACTATAGGGCTATGGGCACCCTGATC
dsNITPS2-F	CACCAAAGGTCTAAGGCACA
dsNITPS2-R	TCCCTACGAGATCAACGATG
dsNITPS2-FT	GGATCCTAATACGACTCACTATAGGCACCAAAGGTCTAAGGCACA
dsNITPS2-RT	GGATCCTAATACGACTCACTATAGGTCCCTACGAGATCAACGATG
dsNITPS3-F	GAGTCTGACCTGATAGCCTTTA
dsNITPS3-R	ATCGGAGTCCATTTAGTTGT
dsNITPS3-FT	GGATCCTAATACGACTCACTATAGGGAGTCTGACCTGATAGCCTTTA
dsNITPS3-RT	GGATCCTAATACGACTCACTATAGGATCGGAGTCCATTTAGTTGT
dsNIGFP-F	AAGGGCGAGGAGCTGTTCACCG
dsNIGFP-R	CAGCAGGACCATGTGATCGCGC
dsNIGFP-FT	GGATCCTAATACGACTCACTATAGGAAGGGCGAGGAGCTGTTCACCG
dsNIGFP-RT	GGATCCTAATACGACTCACTATAGGCAGCAGGACCATGTGATCGCGC

Microinjection

The injection volume was 200 ng of dsRNA per brown planthopper, and the injection was performed in the fifth instar nymph of brown planthopper, and the injection site was the lateral epidermis between the two pairs of hind limbs in the thorax of the brown planthopper. The number of injections per treatment group was 50–100 planthoppers, and three biological replicates were performed. The microinjection system was first adjusted, the nitrogen pressure was adjusted to a suitable scale, and the volume of each dsRNA injected was determined under a microscope using standard capillaries. The brown planthoppers were then immobilized with carbon dioxide, and placed ventral-side up on a pre-prepared agarose plate. The insect was then injected under a microscope, and successfully injected brown planthoppers were transferred to a glass tube containing fresh rice for subsequent experiments.

Quantitative Real-Time PCR

The primers required for Quantitative Real-time PCR (qRT-PCR) were first designed using Primer Premier 5 software. In this experiment, the brown planthopper *18S* gene was used as an internal reference gene (Yang et al., 2017). The detailed qRT-PCR primers are shown in **Table 2**.

qRT-PCR system preparation: SYBR Premix Ex Taq (10 μL), template cDNA (1 μL), forward primer (1 μL), reverse primer (1 μL); the volume was made up to 20 μL with sterile water. qRT-PCR system: pre-denaturation at 95°C for 3 min, denaturation at 95°C for 5 s and annealing at 55–60°C for 30 s (39 cycles), and a dissolution curve at 95°C for 5 s. The CT values of several genes were determined by qRT-PCR, then, the relative expression of target genes was calculated by the $2^{-\Delta\Delta CT}$ method (Livaka and Schmittgenb, 2001). All comparisons were performed with three biological replicates and three technical replicates.

Determination of Carbohydrate Contents

Material Handling Process

Seven individuals were placed in a mortar and ground with liquid nitrogen. The ground material was transferred to a 1.5 mL Eppendorf tube and 200 μL of phosphate-buffered saline (PBS, 20 mM, pH 6.0) was added and then sonicated in a sonicator. After complete crushing, 800 μL of PBS was added to the Eppendorf tube, and the material was centrifuged (4°C, 1000 × *g*) for 20 min. A portion of the supernatant after centrifugation was added to a new Eppendorf tube, and subjected to ultracentrifugation (4°C, 20800 × *g*) for 1 h; another portion was used to detect the trehalose content, glycogen content and protein content. The supernatant after the second centrifugation was used to determine the glucose content and protein content.

TABLE 2 | Primers used for qRT-PCR.

Primer name	Forward Primer (5′-3′)	Reverse Primer (5′-3′)
QNl18S	CGCTACTACCGATTGAA	GGAAACCTTGTTACGACTT
QNlTPS1	AAGACTGAGGCGAATGGT	AAGGTGGAAATGGAATGTG
QNlTPS2	AGAGTGGACCGCAACAACA	TCAACGCCGAGAATGACTT
QNlTPS3	GTGATGCGTCGGTGGCTAT	CCGTTCATCATTGGGCATAGT
QNlG-6-pase	TTTCGGCTCACTTCCCTC	GCAGTAATCAACATAGCACCT
QNlPPGM1	TAAAGCCAGTCATACCAG	TCGATAGATAGATTGAGGC
QNlPPGM2	ACAGCCAGTCACAATCCG	GGTAACAGCATCTGGAGC
QNlUGPase	GCACGGTGACTTCTACGA	TGAGGTCAACTGTGGCTC
QNlGP	GCTGCCTATGGCTATGGTATTC	TCTGAGTGTTGACCCACTTCTTG
QNlGS	GCTCCAAAGCCTATGTTTCTACT	TGGTAACCCCTGTCCCTCA

The anthrone method was used to measure the trehalose content in brown planthoppers. The specific experimental procedure is as follows: 10 μL of the test solution or trehalose standard solution was placed in a 1.5 mL Eppendorf tube. The trehalose concentrations used to generate the standard curve were 1.6, 0.8, 0.6, 0.4, 0.2, 0.1, and 0.05 mM. Next, 10 μL of 1% H_2SO_4 was added to each sample, and then placed in a water bath at 90°C for 10 min. After incubation in the water bath, the samples were placed on ice for 3 min, and 10 μL of 30% KOH was added. The mixture was then placed in a water bath at 90°C for 10 min, and cooled on ice for 3 min. Next, 200 μL of the developer (0.02 g anthrone dissolved in 80% H_2SO_4) was added to the EP tube and placed in a water bath at 90°C for 10 min. Finally, the samples were placed on ice for cooling, and absorbance at 630 nm was measured using a microplate reader. The glycogen content and glucose content were measured using the Glucose (GO) Assay Kit from Sigma-Aldrich. The test solution was first reacted with 0.1 U/L of starch transglucosidase at 40°C for 4 h, so that the glycogen was first converted to glucose, and the glucose content was then measured in the same manner. The assay was carried out according to the specified method (Yang et al., 2017). The protein concentration was determined using BCA protein assay kit (Pierce Biotechnology, Rockford, IL, United States). According to the number of samples, add 50 volumes of BCA A reagent to 1 volume of BCA B reagent to prepare an appropriate amount of BCA. Then, when the protein standard solution was completely dissolved, take out 10 μL of the standard solution and dilute it to 100 μL with PBS to make the final concentration 0.5 mg/mL. According to the kit instructions, prepare standard solutions of different concentrations to obtain a standard curve. Then add 200 μL of BCA to 20 μL of each sample solution and standard solution. After placing them in a constant temperature incubator at 37°C for 30 min, the absorbance was measured at 562 nm. The above experiments were carried out three biological replicates and three technical replicates.

DGE Sequencing and Analysis

The extracted RNA samples were sent to the Beijing Genomics Institution (BGI) for DGE sequencing. The instrument used was Hiseq2000 (Illumina, United States).

Brown planthoppers injected with dsGFP were used as the control group, and those in the experimental groups were injected with dsTPS3 and dsTPSs. Combined with the sequencing data from the previous study, the differential genes were screened by comparative analysis of sequencing data from the control group and the experimental group. The *P* value was then corrected by a multiple hypothesis test, and the threshold of the *P* value was controlled by the False Discovery Rate (FDR). In this study, only genes with an FDR less than or equal to 0.001 and in multiples of difference greater than or equal to 2 were selected for screening the differential genes.

Data Analysis

The data presented in the final result figures are expressed as the mean + standard error (SE) of three biological replicates. Differences were analyzed using Tukey's test of One-way ANOVA in IBM SPSS Statistics 20 (**$P < 0.01$; *$P < 0.05$). The analyzed data were plotted using the Grouped Error Bars chart option in the Vertical Bar Chart type of SigmaPlot 10.0 software.

RESULTS

Developmental Expression Pattern of Carbohydrates

The content of trehalose in the brown planthopper at 24 h in the fourth instar was lower than that at 48 h in the fourth instar (**Figure 1A**). At the fifth instar stage, the trehalose content at 24 h was significantly higher than that at 0, 12, 36, and 84 h (**Figure 1A**). For adults after emergence, the trehalose and glycogen contents were relatively low in the initial stage (0 to 36 h), but both sugar contents increased significantly after 48 h (**Figures 1A,B**). Finally, the glucose content was significantly higher than that at the fourth instar and adult stage in the 0–60 h phase of the fifth instar, and the glucose content in the adult stage was higher than that in the fourth instar stage (**Figure 1C**).

Tissue Expression Pattern of *TPS* Genes in *N. lugens* Adults

The expression level of *TPS* in the head was used as a control. As seen in **Figure 2**, the expression levels of three *TPS* genes in the wing bud group were higher than those in other tissues, and the expression level of *TPS3* in the leg and cuticle was significantly lower than that in the control group.

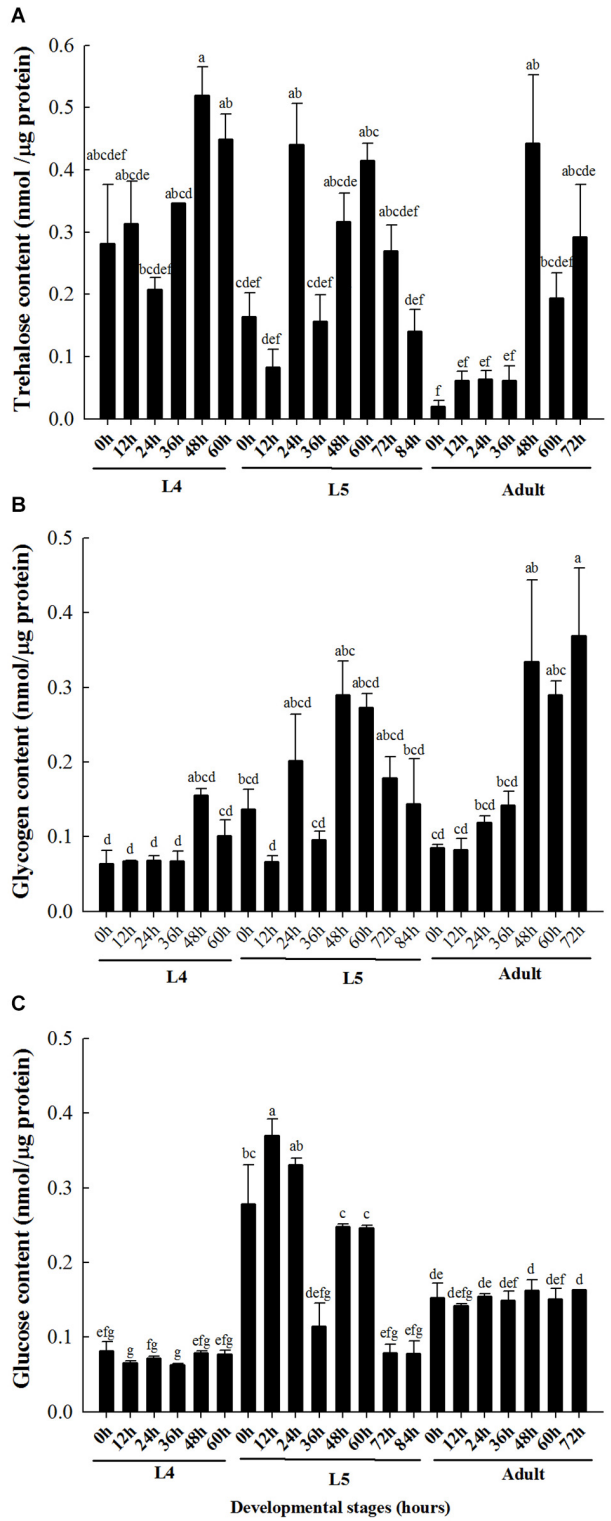

FIGURE 1 | Carbohydrate contents in different developmental stages of brown planthopper. **(A)** Trehalose content. **(B)** Glycogen content. **(C)** Glucose content. L4 indicates fourth instar larva and L5 indicates fifth instar larva. Each bar depicts the mean (+SE) of three biological replicates, with different letters above the error bars denoting significant differences between the means (Tukey's test, α = 0.05; each group was analyzed separately).

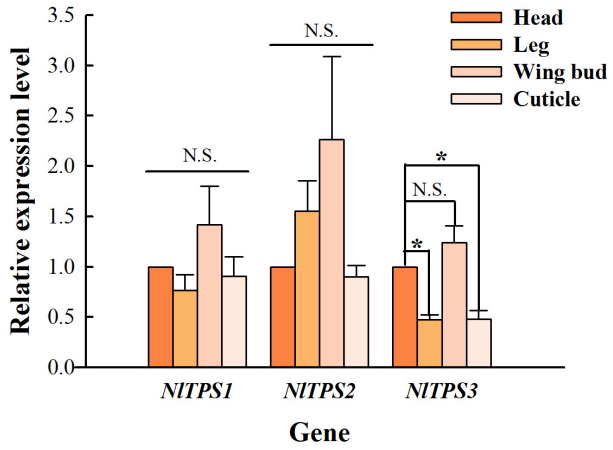

FIGURE 2 | Comparison of changes in relative expression levels of the three *TPS* genes in the adult tissues of brown planthopper. The expression levels of these genes were determined by qRT-PCR using the housekeeping gene *18S* as a reference. Each bar depicts the mean (+SE) of three biological replicates. The relative expression level of each gene in the head was used as the control (Tukey's test; $^*P < 0.05$, N.S. means no significant difference).

The Inhibitory Effect of dsRNA

The expression level of *TPS1* was significantly different from that of the control group only 72 h after the injection of dsTPSs, which showed an increase (**Figure 3A**). It can be seen from **Figure 3B** that when dsTPSs was injected for 48 h, the expression level of *TPS2* decreased significantly. When dsTPS3 or dsTPSs was injected into *N. lugens* for 48 h, the expression level of *TPS3* reduced by qRT-PCR detection (**Figure 3C**). Detecting the expression level at 72 h found that the expression level of *TPS3* in the dsTPS3 group was not significantly different from the control group, while the expression level of *TPS3* in the dsTPSs group was lower than that in the control group (**Figure 3C**).

Comparison of Differential Genes After RNAi

The results of DGE analysis showed that after dsTPS3 injection, 1439 genes were upregulated, and 2127 genes were downregulated. When dsTPSs were injected, 1346 genes were upregulated, and 1927 genes were downregulated (**Figure 4A**). Comparing the two injection groups, 1048 and 1584 genes were identical in the upregulated and downregulated genes, respectively (**Figure 4B**).

Significant Pathway Enrichment Analysis After RNAi

The results showed that more than 20 genes were involved in sugar metabolism, followed by more genes involved in amino acid metabolism and lipid metabolism. In addition, the genes involved in nucleotide metabolism, energy metabolism, and hormone metabolism are fewer than other pathways. Moreover, there are more than five genes in each group, and the functions of 15 or less genes are unknown (**Figure 5**).

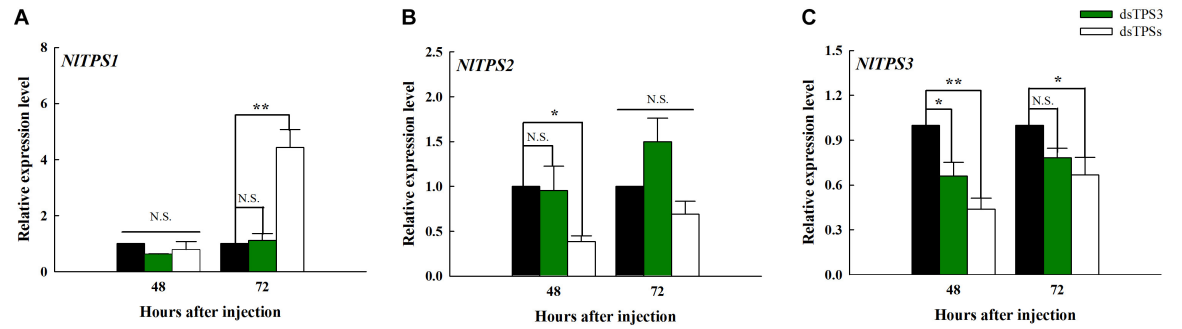

FIGURE 3 | Changes in the expression levels of the three *TPS* genes after RNAi at 48 and 72 h in the fifth instar nymph of brown planthopper. The relative expression levels of trehalose-6-phosphate synthase 1 gene (*TPS1*) **(A)**, trehalose-6-phosphate synthase 2 gene (*TPS2*) **(B)**, and trehalose-6-phosphate synthase 3 gene (*TPS3*) **(C)**. Each bar depicts the mean (+SE) from three biological replicates. The relative expression level of each gene after injection of dsGFP was used as the control (Tukey's test; $^{**}P < 0.01$, $^{*}P < 0.05$, N.S. means no significant difference).

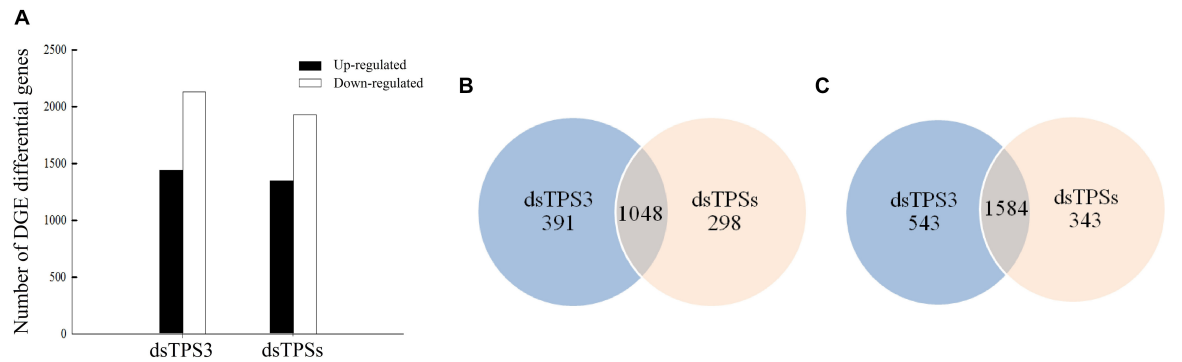

FIGURE 4 | The number of differentially expressed genes after dsTPS3 and dsTPSs injection compared to dsGFP. **(A)** The differential expression of single genes in the two DGE databases is plotted according to each treatment. **(B,C)** Comparison of the number of upregulated **(B)** and downregulated **(C)** unigenes from the two DGE databases for each of the treatments. Blue: the first DGE-seq database only; apricot: the second DGE-seq database only; overlap: both databases.

Changes in Carbohydrate Content After RNAi

After knocking down the single *TPS3* gene, the trehalose content was decreased significantly at 72 h (**Figure 6A**), and the glucose content in *N. lugens* was increased significantly at 48 h (**Figure 6B**). In addition, the trehalose and glucose contents were increased significantly at 48 h (**Figures 6A,B**), and the trehalose and glycogen contents were decreased significantly at 72 h after mixed interference with the *TPS1*, *TPS2*, and *TPS3* genes (**Figures 6A,C**).

Changes in the Expression Levels of Related Genes After RNAi

The relative expression levels of UDP-glucose pyrophosphorylase (UGPase) was decreased after 48 h of dsTPS3 and dsTPSs injection (**Figure 7C**). However, the relative expression level of *GS* was significantly increased after 48 h of interference with the expression of the *TPS3* gene alone (**Figure 7E**). The relative expression levels of phosphoglucomutase 2 gene (*PPGM2*), *UGPase*, GP, and GS were significantly increased at 72 h after mixed interference with *TPS1*, *TPS2*, and *TPS3* genes (**Figures 7B–E**). At 72 h after dsTPS injection, the expression level of UGPase was significantly decreased (**Figure 7C**), while the glucose-6-phosphatase gene (*G-6-Pase*) was increased significantly (**Figure 7F**).

DISCUSSION

Similar to glycogen metabolism, trehalose metabolism is controlled by two enzymes: TPS and trehalase (TRE) (Elbein et al., 2003). The carbohydrate metabolic rate is determined by the energy demand and is regulated by hormones (Arrese and Soulages, 2010). In mammals, the main nutrient in blood is glucose, and studies have determined that it is regulated by several hormones such as insulin and glucagon (Mochanová et al., 2018). The nutrient levels in the hemolymph of insects are mainly controlled by adipokinetic hormone (AKH) (Mochanová et al., 2018). Other hormones including octopamine, ecdysone, and insulin-like growth factor can regulate carbohydrate metabolism (Lorenz and Gäde, 2009; Arrese and Soulages, 2010; Kim and Neufeld, 2015; Jiang et al., 2017; Song et al., 2017; Kawabe et al., 2019). *A. mellifera* is a unique model system for aging and longevity studies. As a complete metamorphosis insect, the

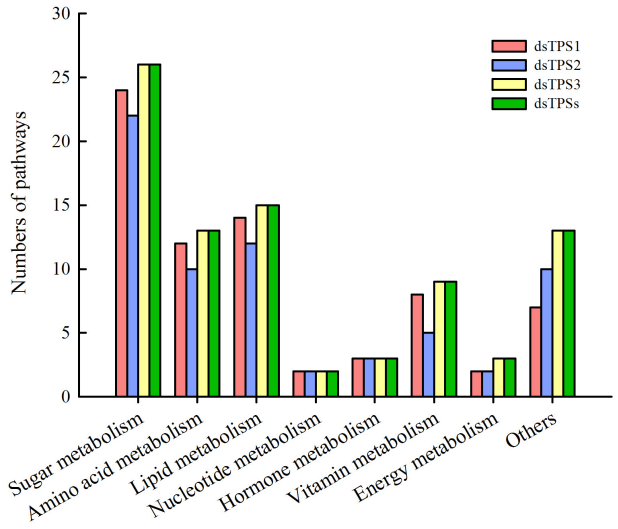

FIGURE 5 | Pathway enrichment analysis after RNAi. Red: dsTPS1 injection group; Blue: dsTPS2 injection group; Yellow: dsTPS3 injection group; Green: dsTPSs injection group.

entire developmental period includes the egg, larva (age 1–7), pupa, and adult stages (Lu et al., 2018). Studies on *A. mellifera* showed that the transcriptional expression levels of GS were particularly high in the 4th and 7th instar larvae, whereas the relative expression level of *GP* was lower in the 6th instar and newly emerged adults (Łopieńska-Biernat et al., 2018). Our experiments showed that the glycogen content was higher at the last stage of the brown planthopper larvae (**Figure 1**). The *TPS* developmental pattern of brown planthoppers from the first instar to the adult on day 15 was determined. The results showed that the expression level of *TPS* was constant and there was no significant difference between the ages (Chen et al., 2010). By aligning the sequences, we learned that they indicated the expression level of *TPS1* in the brown planthopper. Our results also indicate that trehalose can be detected from the 4th instar to the adult stage of brown planthopper, and its content increases before molting or emergence (**Figure 1**). Therefore, we speculated that energy reserves are accumulated to be used during metamorphosis as well as to provide reserves for the new adult. In addition to trehalose, the glycogen content increased in the late 5th and adult stages (**Figure 1**) and may also be similar to the effect of trehalose. The developmental expression pattern of *TPS* can also be detected in other insects. The highest level of *TPS* expression at one age of larval stage was found in *A. mellifera* and *Bactrocera minax* (Xiong et al., 2016; Łopieńska-Biernat et al., 2018). Differently, the highest expression was found in the adult stage of *M. domestica* (Zhang D. W. et al., 2019) and in the early pupa of *H. vitessoides* (Chen et al., 2020). In addition, the glucose content was low in the 4th instar, rich in the early 5th instar, and remained stable and abundant in the adult population. It is thus speculated that the newly emerged adult of brown planthoppers needs to consume more energy to maintain life and reproduction. In harsh conditions such as hunger and cold, glucose, trehalose, and glycogen are transformed into each other thereby maintaining the balance in the insect body and continuing life (Shi et al., 2017; Zhang Y. et al., 2019). Therefore, carbohydrates are an important source of energy and play an important role in insects.

The insect fat body is an important place for trehalose synthesis, like the liver in mammals (Candy and Kilby, 1959; Murphy and Wyatt, 1965; Friedman, 1968; Tang et al., 2018). Therefore, many studies have found that *TPS* mRNA expression can be detected in fat bodies (Cui and Xia, 2009; Xu et al., 2009; Chen et al., 2010; Tang et al., 2010; Xiong et al., 2016). Moreover, the expression level of TPS in the fat body is far higher than that in other tissues such as the epidermis, midgut, and the Malpighian tube in *Tribolium castaneum*, *B. minax*, *H. vitessoides*, and *N. lugens* (Chen et al., 2010, 2018, 2020; Xiong et al., 2016). In this experiment, only the expression levels of three *TPSs* in the head, leg, wing bud and cuticle of brown planthopper were determined. The *TPS* gene was found to be expressed in all the tissues examined (**Figure 2**), and similarly, the expression level of TPS was also detected in the head of *H. vitessoides* (Chen et al., 2020). Conversely, almost no *TPS* expression was detected in the epidermis of the brown planthopper (Chen et al., 2010). The reason for the contradiction between our results is that the age of the test insect is different, and the *TPS* expression in their tissues may thus, be different. In this study, the expression level in the wing bud was higher than that in the other three tissues (**Figure 2**), indicating that *TPS* is closely related to the energy consumption in brown planthopper flight. Similar studies are also available in other insects, for example, hemolymph trehalose is an important substrate for carbohydrate storage and flight in locusts (Wegener et al., 2010). Research has found that trehalose catabolism is lower in the flight muscles when the locusts are resting, but rapidly increases during flight (Jutsum and Goldsworthy, 1976; Van der Horst et al., 1978; Wegener, 1996; Mentel et al., 2003). In order to utilize muscle metabolism, trehalose must be hydrolyzed to glucose by TRE, and so, the potential activity of TRE in the flying muscle of locusts is high (Worm, 1981; Vaandrager et al., 1989; Becker et al., 1996; Wegener et al., 2003; Liebl et al., 2010). Therefore, we speculate that *TPS* will be expressed in the locust flying muscle to maintain the synthetic catabolism of trehalose. TRE activity in the homogenate of flying muscles from cockroaches, moths and locusts has been observed (Zebe and Mcshan, 1959; Gussin and Wyatt, 1965; Gilby et al., 1967; Candy, 1974).

In fact, in addition to trehalose synthesis in the fat body, the basic cells of the fat body are fat cells, characterized by the presence of many lipid droplets. The intermediate metabolism of most insects occurs in this organ including lipid and carbohydrate metabolism, protein synthesis, amino acid, and nitrogen metabolism. Therefore, fat bodies play an important role in insect life, and are a dynamic organization involving a variety of metabolic functions (Arrese and Soulages, 2010). Firstly, we checked the inhibitory effect of dsRNA, and the results showed that it can effectively inhibit the expression of target genes (**Figure 3**), which can be used in subsequent experiments. However, after the injection of dsTPS3, the relative expression levels of *TPS1* and *TPS2* were not different from those of the

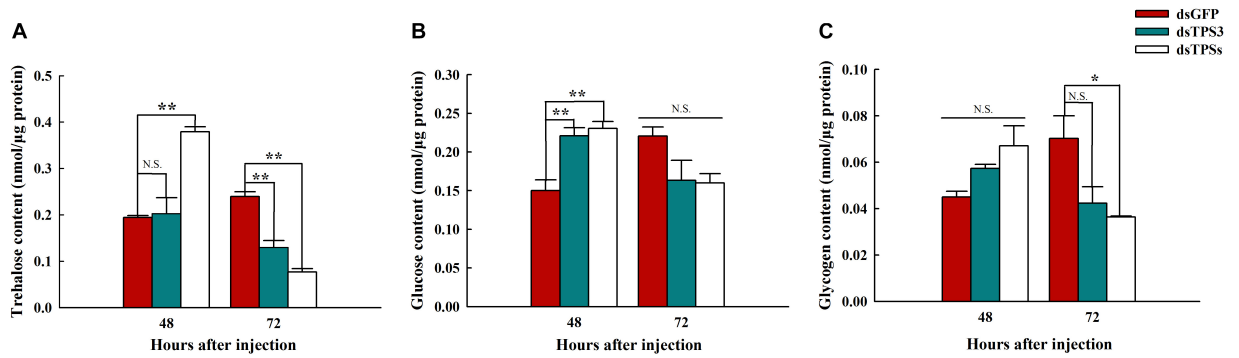

FIGURE 6 | Trehalose, glycogen, and glucose contents after RNAi at 48 and 72 h in the fifth instar nymph of brown planthopper. **(A)** Trehalose content. **(B)** Glucose content. **(C)** Glycogen content. All *Nilaparvata lugens* larvae were divided into three groups and injected with dsGFP, dsTPS3, or dsTPSs. Each bar depicts the mean (+SE) from three biological replicates. The carbohydrate content at 48 or 72 h after dsGFP injection was used as the control (Tukey's test; $^{**}P < 0.01$, $^{*}P < 0.05$, N.S. means no significant difference).

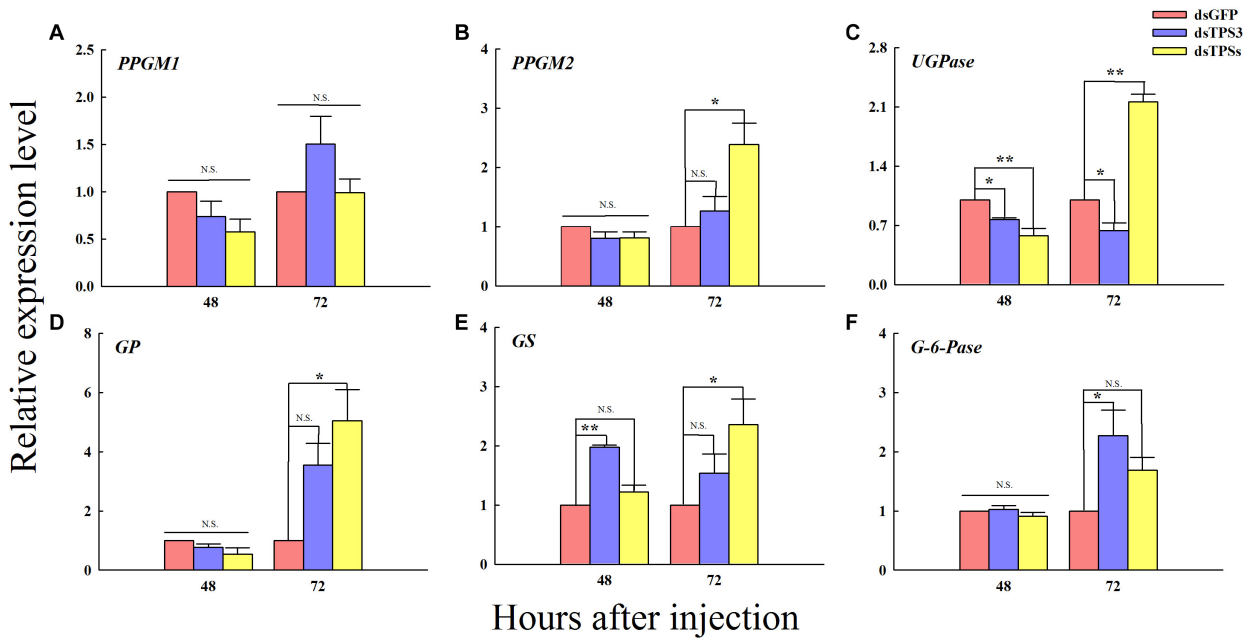

FIGURE 7 | Changes in the expression levels of related genes after RNAi at 48 and 72 h in the fifth instar nymph of brown planthopper. The relative expression levels of phosphoglucomutase 1 gene (*PPGM1*) **(A)**, phosphoglucomutase 2 gene (*PPGM2*) **(B)**, UDP-Glucose pyrophosphorylase gene (*UGPase*) **(C)**, glycogen phosphorylase gene (*GP*) **(D)**, glycogen synthase gene (*GS*) **(E)**, and glucose-6-phosphatase gene (*G-6-Pase*) **(F)**. Each bar depicts the mean (+SE) from three biological replicates. The relative expression level of each gene after injection of dsGFP was used as the control (Tukey's test; $^{**}P < 0.01$, $^{*}P < 0.05$, N.S. means no significant difference).

control group, indicating that there may be a compensation effect between the three *TPS* genes (**Figure 3**). Then in our experiments, differential genes between the dsTPS3 and dsTPSs groups were screened by DGE analysis. The experimental results showed 2632 identical differential genes between the two groups, of which 1048 were upregulated and 1564 were downregulated. Yang et al. (2017) carried out RNA interference on *TPS1* and *TPS2* in the brown planthopper, and also detected the expression of differential genes in the two treatments. The number of upregulated and downregulated genes in the dsTPS1 group were found to be more than those in the dsTPS2 group, and there were 212 upregulated genes and 268 downregulated genes in both groups. Compared with our results (**Figure 4**), the upregulated genes in the dsTPS3 group differed from those in the dsTPS1 and dsTPS2 groups by 703 and 933, respectively, and the downregulated genes differed by 1469 and 1808, respectively. In addition, the upregulated genes in the dsTPSs group differed by 610 and 840, respectively, from the dsTPS1 and dsTPS2 groups, and the downregulated genes differed by 1269 and 1608. From this point of view, inhibition of *TPS3*

gene expression or mixed inhibition of the three *TPS*, results in greater differential gene expression in the brown planthopper compared to that with inhibition of *TPS1* and *TPS2* alone. This result may indicate that the physiological roles of the three *TPS* genes in brown planthopper are different. In microorganisms, TPS and TPP are required for trehalose biosynthesis in yeast and filamentous fungi, including *Fusarium graminearum* (Song et al., 2014; Liu et al., 2019). Three mutants were obtained, a TPS mutant, a TPP mutant, and a double deletion of TPS and TPP (TPS-TPP mutant). None of these three mutants could synthesize trehalose. Compared with the wild type (WT), the lower number of specific genes in the TPS-TPP mutant indicated that double deletion of TPS and TPP resulted in altered expression of most genes detected in the TPS or TPP mutants. Differential genes were analyzed by the MIPS function, and the functional classification showed that compared with the WT, the differentially expressed genes with annotation function could be divided into 18 categories. The metabolic pathway constitutes the most affected of the three mutants, and the TPP mutant has the most genes in all categories. In addition, there were a large number of unknown genetic products (Song et al., 2014). Similar to our results, most functions of differential genes were aggregated by sugar metabolism, amino acid metabolism, and lipid metabolism, and the function of some genes was unknown. It is worth noting that the relative differences in nucleotide and hormone metabolism are nil among dsTPS1, dsTPS2 and dsTPS3 groups. So *TPS3* may play a greater role in general metabolic pathways, which are physiologically important to insects. In summary, when *TPS* expression is affected, the expression levels of genes involved in metabolism in the organism are upregulated or downregulated.

Whether in *T. castaneum* or the *B. minax*, the trehalose content was reduced after injection of dsTPS (Xiong et al., 2016; Chen et al., 2018). In addition, the same experimental results were achieved in *M. domestica* and *H. vitessoides* (Zhang D. W. et al., 2019; Chen et al., 2020). Although the trehalose content increased significantly after 48 h of the mixture of dsTPS1, dsTPS2, and dsTPS3 in our experiments, the trehalose content was decreased significantly after 72 h (**Figure 6**). The reason for our analysis was that the brown planthopper was stimulated in the early stage of RNAi, which made it synthesize trehalose to maintain normal metabolism, and its interference effect was more obvious. We also tested the changes in glycogen and glucose levels and found that the levels of both sugars were first increased and then decreased (**Figure 6**). In the study on *B. minax* and *H. vitessoides*, upon *TPS* inhibition by RNAi, the change in trehalose content and glucose content was the opposite, and the glucose content was increased compared with the control group (Xiong et al., 2016; Chen et al., 2020). Combined our experimental results indicate that upon blocking trehalose synthesis, insects will consume glucose and glycogen to replenish energy. However, not all insects show the same experimental results; for example, glucose fluctuated after treatment in *T. castaneum*, but showed no significant difference (Chen et al., 2018). It is thus suggested that there may be species-specific differences between different insects, which may also be related to experimental methods, suggesting that the ability of glucose to compensate for trehalose may not be so obvious. When *Maruca vitrata* was starved, the expression level of *TPS* was significantly higher than that in the feeding process, whereas the result of *TRE* was opposite to that of *TPS*. Moreover, after injection of dsTPS, the trehalose content decreased with the prolongation of injection time, but increased gradually after injection of dsTRE (Al Baki et al., 2018). In summary, the above results indicate that when the expression level of insect *TPS* was inhibited, trehalose synthesis was inhibited and the glucose content was increased.

In addition to the important role of the *TPS* gene in the trehalose metabolism pathway, there are several key genes in this pathway including *TRE*, Hexokinase (*HK*), Glucose-6-phosphate isomerase (*G6PI*), and so on. In previous studies on brown planthopper *TPS1* and *TPS2*, the expression levels of some genes in the pathway after RNAi showed a decrease (Yang et al., 2017). Similar results were obtained in this study. However, the difference was that although the expression levels of these genes were decreased in the early stage of RNAi, they were increased after 72 h, and some genes were even significantly higher than those in the control group (**Figure 7**). In particular, the *GS* gene showed a significant increase after RNAi (**Figure 7**), indicating that glycogen synthesis was promoted in the early stage of injection. Similarly, the expression of six chitin synthesis-related genes such as hexokinase 2 and glutamine-fructose-6-phosphate aminotransferase was suppressed at 48 and 72 h after dsTPS injection (Chen et al., 2018). Additionally, *TPS* silencing inhibited the expression of three key genes in the chitin biosynthesis pathway and exhibited 52% death and abnormal phenotypes in *B. minax* (Xiong et al., 2016). In *H. vitessoides*, silencing of *TPS* suppressed the expression of six key genes in the chitin biosynthesis pathway and one key gene related to lipid catabolism (Chen et al., 2020). In addition to the genes of the trehalose metabolic pathway, several genes were involved in chitin synthesis. From this point of view, inhibition of *TPS* expression by RNAi, would not only affect the energy metabolism of insects, but would also have different effects on chitin metabolism. Of course, some studies have detected the chitin content and deformity rate of insects after dsTPS injection such as in *T. castaneum*, *B. minax*, and *H. vitessoides* (Xiong et al., 2016; Chen et al., 2018, 2020). In our study, the results strongly suggest that TPS is essential for the normal growth and development of brown planthopper, providing a reference for further studies on the key genes involved in chitin and lipid metabolism to control insect development.

In summary, in *N. lugens*, the change in carbohydrate content was related to the molting of nymphs, and three *TPS* genes were expressed in the adult head, feet, wings, and epidermis. After inhibiting the expression of *TPS3* or *TPSs*, glucose accumulation was promoted in the early stage, and subsequently *N. lugens* consumed trehalose for energy.

DATA AVAILABILITY STATEMENT

The sequencing data has been deposited into the Sequence Read Archive (accession: PRJNA658271, https://www.ncbi.nlm.nih.gov/sra/PRJNA658271).

AUTHOR CONTRIBUTIONS

BT, CL, and C-DX contributed to the conceptualization, project administration, and supervision. S-SW, Y-KL, Y-JL, and G-YL contributed to the investigation and validation. S-SW, G-YL, CL, and BT contributed to the writing of the original draft. All authors contributed to the article and approved the submitted version.

FUNDING

This work was supported by the National Natural Science Foundation of China (Grant Nos. 31672081 and 31371996). Also we thank the Regional First-class Discipline Construction of Guizhou Province (No. [2017]85), Training Project for High-Level Innovative Talents in Guizhou Province (No. 2016 [4020]), and Program for Academician Workstation in Guiyang University (20195605) for financial support.

ACKNOWLEDGMENTS

We thank Dr. Qiang Fu (China National Rice Research Institute, Hangzhou, China) and Hong-Xing Xu (Zhejiang Academy of Agricultural Sciences, Hangzhou, China) for their kindly help.

SUPPLEMENTARY MATERIAL

The Supplementary Material for this article can be found online at: https://www.frontiersin.org/articles/10.3389/fphys.2020.575485/full#supplementary-material

REFERENCES

Al Baki, M. A., Jung, J. K., and Kim, Y. (2018). Regulation of hemolymph trehalose titers by insulin signaling in the legume pod borer, *Maruca vitrata* (Lepidoptera: Crambidae). *Peptides* 106, 28–36. doi: 10.1016/j.peptides.2018.06.006

Argüelles, J. C. (2014). Why can't vertebrates synthesize trehalose? *J. Mol. Evol.* 79, 111–116. doi: 10.1007/s00239-014-9645-9

Arrese, E. L., and Soulages, J. L. (2010). Insect fat body: energy, metabolism, and regulation. *Annu. Rev. Entomol.* 55, 207–225. doi: 10.1146/annurev-ento-112408-085356

Asano, A. (2003). Glycosidase inhibitors: update and perspectives on practical use. *Glycobiology* 13, 93–104. doi: 10.1002/3527601740.ch5

Becker, A., Schlöder, P., Steele, J. E., and Wegener, G. (1996). The regulation of trehalose metabolism in insects. *Experientia* 52, 433–439. doi: 10.1007/BF01919312

Candy, D. J. (1974). The control of muscle trehalase activity during locust flight. *Biochem. Soc. Trans.* 2, 1107–1109. doi: 10.1042/bst0021107

Candy, D. J., and Kilby, B. A. (1959). Site and mode of trehalose biosynthesis in the locust. *Nature* 183, 1594–1595. doi: 10.1038/1831594a0

Chen, J., Zhang, D., Yao, Q., Zhang, J., Dong, X., Tian, H., et al. (2010). Feeding-based RNA interference of a trehalose phosphate synthase gene in the brown planthopper, *Nilaparvata lugens*. *Insect Mol. Biol.* 19, 777–786. doi: 10.1111/j.1365-2583.2010.01038.x

Chen, J. X., Lyu, Z. H., Wang, C. Y., Cheng, J., and Lin, T. (2020). RNA interference of a trehalose-6-phosphate synthase gene reveals its roles in the biosynthesis of chitin and lipids in *Heortia vitessoides* (Lepidoptera: Crambidae). *Insect Sci.* 27, 212–223. doi: 10.1111/1744-7917.12650

Chen, Q. W., Jin, S., Zhang, L., Shen, Q. D., Wei, P., Wei, Z. M., et al. (2018). Regulatory functions of trehalose-6-phosphate synthase in the chitin biosynthesis pathway in *Tribolium castaneum* (Coleoptera: Tenebrionidae) revealed by RNA interference. *Bull. Entomol. Res.* 108, 388–399. doi: 10.1017/S000748531700089X

Crowe, J. H., Crowe, L. M., and Chapman, D. (1984). Preservation of membranes in anhydrobiotic organisms: the role of trehalose. *Science* 223, 701–703. doi: 10.1126/science.223.4637.701

Cui, S. Y., and Xia, Y. X. (2009). Isolation and characterization of the trehalose-6-phosphate synthase gene from *Locusta migratoria* manilensis. *Insect Sci.* 16, 287–295. doi: 10.1111/j.1744-7917.2009.01268.x

Elbein, A. D., Pan, Y. T., Pastuszak, I., and Carroll, D. (2003). New insights on trehalose: a multifunctional molecule. *Glycobiology* 13, 17R–27R.

Friedman, S. (1968). Trehalose regulation of glucose-6-phosphate hydrolysis in blowfly extracts. *Science* 159, 110–111. doi: 10.1126/science.159.3810.110

Gilby, A. R., Wyatt, S. S., and Wyatt, G. R. (1967). Trehalases from the cockroach, *Blaberus discoidalis*: activation, solubilization and properties of the muscle enzyme and some properties of the intestinal enzyme. *Acta Biochim. Pol.* 14, 83–100.

Gussin, A. E., and Wyatt, G. R. (1965). Membrane-bound trehalase from cecropia silkmoth muscle. *Arch. Biochem. Biophys.* 112, 626–634. doi: 10.1016/0003-9861(65)90106-2

Han, H. (2018). RNA interference to knock down gene expression. *Methods Mol. Biol.* 1706, 293–302. doi: 10.1007/978-1-4939-7471-9_16

Hayashi, H., and Chino, M. (1990). Chemical composition of phloem sap from the uppermost internode of the rice plant. *Plant Cell Physiol.* 31, 247–251.

Hibino, H. (1996). Biology and epidemiology of rice viruses. *Annu. Rev. Phytopathol.* 34, 249–274. doi: 10.1146/annurev.phyto.34.1.249

Jiang, J., Xu, Y., and Lin, X. (2017). Role of broad-complex (Br) and Krüppel homolog 1 (Kr-h1) in the ovary development of *Nilaparvata lugens*. *Front. Physiol.* 8:1013. doi: 10.3389/fphys.2017.01013

Jutsum, A. R., and Goldsworthy, G. J. (1976). Fuels for flight in Locusta. *J. Insect Physiol.* 22, 243–249. doi: 10.1016/0022-1910(76)90032-9

Kawabe, Y., Waterson, H., and Mizoguchi, A. (2019). Bombyxin (Bombyx insulin-like peptide) increases the respiration rate through facilitation of carbohydrate catabolism in *Bombyx mori*. *Front. Endocrinol.* 10:150. doi: 10.3389/fendo.2019.00150

Kim, J., and Neufeld, T. P. (2015). Dietary sugar promotes systemic TOR activation in Drosophila through AKH-dependent selective secretion of Dilp3. *Nat. Commun.* 6:6846. doi: 10.1038/ncomms7846

Liebl, M., Nelius, V., Kamp, G., Ando, O., and Wegener, G. (2010). Fate and effects of the trehalase inhibitor trehazolin in the migratory locust (*Locusta migratoria*). *J. Insect Physiol.* 56, 567–574. doi: 10.1016/j.jinsphys.2009.11.021

Liu, C., Chen, F., Zhang, J., Liu, L., Lei, H., Li, H., et al. (2019). Metabolic changes of *Fusarium graminearum* induced by TPS gene deletion. *J. Proteome Res.* 18, 3317–3327. doi: 10.1021/acs.jproteome.9b00259

Livaka, K. J., and Schmittgenb, T. D. (2001). Analysis of relative gene expression data using real-time quantitative PCR and the method. *Methods* 25, 402–408. doi: 10.1006/meth.2001.1262

Łopieńska-Biernat, E., Żółtowska, K., Zaobidna, E. A., Dmitryjuk, M., and Bąk, B. (2018). Developmental changes in gene expression and enzyme activities of anabolic and catabolic enzymes for storage carbohydrates in the honeybee, *Apis mellifera*. *Insectes Soc.* 65, 571–580. doi: 10.1007/s00040-018-0648-1

Lorenz, M. W., and Gäde, G. (2009). Hormonal regulation of energy metabolism in insects as a driving force for performance. *Integr. Comp. Biol.* 49, 380–392. doi: 10.1093/icb/icp019

Lu, C. Y., Qiu, J. T., and Hsu, C. Y. (2018). Cellular energy metabolism maintains young status in old queen honey bees (*Apis mellifera*). *Arch. Insect Biochem. Physiol.* 98:e21468. doi: 10.1002/arch.21468

Lunn, J. E., Delorge, I., Figueroa, C. M., Van Dijck, P., and Stitt, M. (2014). Trehalose metabolism in plants. *Plant J.* 79, 544–567. doi: 10.1111/tpj.12509

Mello, C. C., and Conte, D. Jr. (2004). Revealing the world of RNA interference. *Nature* 431, 338–342. doi: 10.1038/nature02872

Mentel, T., Duch, C., Stypa, H., Wegener, G., Müller, U., and Pflüger, H. J. (2003). Central modulatory neurons control fuel selection in flight muscle of migratory locust. *J. Neurosci.* 23, 1109–1113. doi: 10.1523/jneurosci.23-04-01109.2003

Mochanová, M., Tomčala, A., Svobodová, Z., and Kodrík, D. (2018). Role of adipokinetic hormone during starvation in Drosophila. *Comp. Biochem. Physiol. B Biochem. Mol. Biol.* 226, 26–35. doi: 10.1016/j.cbpb.2018.08.004

Murphy, T. A., and Wyatt, G. R. (1965). The enzymes of glycogen and trehalose synthesis in silk moth fat body. *J. Biol. Chem.* 240, 1500–1508.

Roach, P. J., Depaoli-Roach, A. A., Hurley, T. D., and Tagliabracci, V. S. (2012). Glycogen and its metabolism: some new developments and old themes. *Biochem. J.* 441, 763–787. doi: 10.1042/BJ20111416

Shi, Z. K., Wang, S., Wang, S. G., Zhang, L., Xu, Y. X., Guo, X. J., et al. (2017). Effects of starvation on the carbohydrate metabolism in *Harmonia axyridis* (Pallas). *Biol. Open* 6, 1096–1103. doi: 10.1242/bio.025189

Shukla, E., Thorat, L. J., Nath, B. B., and Gaikwad, S. M. (2015). Insect trehalase: physiological significance and potential applications. *Glycobiology* 25, 357–367. doi: 10.1093/glycob/cwu125

Song, W., Cheng, D., Hong, S., Sappe, B., Hu, Y., Wei, N., et al. (2017). Midgut-derived activin regulates glucagon-like action in the fat body and glycemic control. *Cell Metab.* 25, 386–399. doi: 10.1016/j.cmet.2017.01.002

Song, X. S., Li, H. P., Zhang, J. B., Song, B., Huang, T., Du, X. M., et al. (2014). Trehalose 6-phosphate phosphatase is required for development, virulence and mycotoxin biosynthesis apart from trehalose biosynthesis in *Fusarium graminearum*. *Fungal Genet. Biol.* 63, 24–41. doi: 10.1016/j.fgb.2013.11.005

Sun, L. J., Wang, J., Song, K., Sun, Y. F., Qin, Q., and Xue, Y. (2019). Transcriptome analysis of rice (*Oryza sativa* L.) shoots responsive to cadmium stress. *Sci. Rep.* 9:10177. doi: 10.1038/s41598-019-46684-w

Tang, B., Chen, J., Yao, Q., Pan, Z., Xu, W., Wang, S., et al. (2010). Characterization of a trehalose-6-phosphate synthase gene from *Spodoptera exigua* and its function identification through RNA interference. *J. Insect Physiol.* 56, 813–821. doi: 10.1016/j.jinsphys.2010.02.009

Tang, B., Wang, S., Wang, S. G., Wang, H. J., Zhang, J. Y., and Cui, S. Y. (2018). Invertebrate trehalose-6-phosphate synthase gene: genetic architecture, biochemistry, physiological function, and potential applications. *Front. Physiol.* 9:30. doi: 10.3389/fphys.2018.00030

Vaandrager, S. H., Haller, T. B., van Marrewijk, W. J. A., and Beenakkers, A. M. T. (1989). Fractionation and kinetic properties of trehalase from flight muscle and hemolymph of the locust, *Locusta migratoria*. *Insect Biochem.* 19, 89–94. doi: 10.1016/0020-1790(89)90013-9

Van der Horst, D. J., Van Doorn, J. M., and Beenakkers, A. M. T. (1978). Dynamics in the haemolymph trehalose pool during flight of the locust *Locusta migratoria*. *Insect Biochem.* 8, 413–416. doi: 10.1016/0020-1790(78)90053-7

Wang, S. L., Cheng, R. L., Lu, J. B., Yu, X. P., and Zhang, C. X. (2016). A Cripavirus in the brown planthopper, *Nilaparvata lugens*. *J. Gen. Virol.* 97, 706–714. doi: 10.1099/jgv.0.000394

Wegener, G. (1996). Flying insects: model systems in exercise physiology. *Experientia* 52, 404–412. doi: 10.1007/bf01919307

Wegener, G., Macho, C., Schlöder, P., Kamp, G., and Ando, O. (2010). Long-term effects of the trehalase inhibitor trehazolin on trehalase activity in locust flight muscle. *J. Exp. Biol.* 213, 3852–3857. doi: 10.1242/jeb.042028

Wegener, G., Tschiedel, V., Schlöder, P., and Ando, O. (2003). The toxic and lethal effects of the trehalase inhibitor trehazolin in locusts are caused by hypoglycaemia. *J. Exp. Biol.* 206, 1233–1240. doi: 10.1242/jeb.00217

Worm, R. A. A. (1981). Characterization of trehalase from locust flight muscle. *Comp. Biochem. Physiol.* 70B, 509–514. doi: 10.1016/0305-0491(81)90289-3

Xiong, K. C., Wang, J., Li, J. H., Deng, Y. Q., Pu, P., Fan, H., et al. (2016). RNA interference of a trehalose-6-phosphate synthase gene reveals its roles during larval-pupal metamorphosis in *Bactrocera minax* (Diptera: Tephritidae). *J. Insect Physiol.* 91-92, 84–92. doi: 10.1016/j.jinsphys.2016.07.003

Xu, J., Bao, B., Zhang, Z. F., Yi, Y. Z., and Xu, W. H. (2009). Identification of a novel gene encoding the trehalose phosphate synthase in the cotton bollworm, *Helicoverpa armigera*. *Glycobiology* 19, 250–257. doi: 10.1093/glycob/cwn127

Yamada, T., Habara, O., Kubo, H., and Nishimura, T. (2018). Fat body glycogen serves as a metabolic safeguard for the maintenance of sugar levels in Drosophila. *Development* 145:dev158865. doi: 10.1242/dev.158865

Yamada, T., Habara, O., Yoshii, Y., Matsushita, R., Kubo, H., Nojima, Y., et al. (2019). The role of glycogen in development and adult fitness in Drosophila. *Development* 146:dev176149. doi: 10.1242/dev.176149

Yang, M., Cheng, L., Yan, L. H., Shu, W., Wang, X. Y., and Qiu, Y. F. (2019). Mapping and characterization of a quantitative trait locus resistance to the brown planthopper in the rice variety IR64. *Hereditas* 156:22. doi: 10.1186/s41065-019-0098-4

Yang, M. M., Zhao, L. N., Shen, Q. D., Xie, G. Q., Wang, S. G., and Tang, B. (2017). Knockdown of two trehalose-6-phosphate synthases severely affects chitin metabolism gene expression in the brown planthopper *Nilaparvata lugens*. *Pest Manag. Sci.* 73, 206–216. doi: 10.1002/ps.4287

Zebe, E. C., and Mcshan, W. H. (1959). Trehalase in the thoracic muscles of the woodroach, *Leucophaea maderae*. *J. Cell Comp. Physiol.* 53, 21–29. doi: 10.1002/jcp.1030530104

Zhang, L., Wang, H. J., Chen, J. Y., Shen, Q. D., Wang, S. G., Xu, H. X., et al. (2017). Glycogen phosphorylase and glycogen synthase: gene cloning and expression analysis reveal their role in trehalose metabolism in the Brown Planthopper, *Nilaparvata lugens* Stål (Hemiptera: Delphacidae). *J. Insect Sci.* 17:42. doi: 10.1093/jisesa/iex015

Zhang, D. W., Xiao, Z. J., Zeng, B. P., Li, K., and Tang, Y. L. (2019). Insect behavior and physiological adaptation mechanisms under starvation stress. *Front. Physiol.* 10:163. doi: 10.3389/fphys.2019.00163

Zhang, Y., Wang, F., Feng, Q., Wang, H., Tang, T., Huang, D., et al. (2019). Involvement of trehalose-6-phosphate synthase in innate immunity of *Musca domestica*. *Dev. Comp. Immunol.* 91, 85–92. doi: 10.1016/j.dci.2018.10.010

Conflict of Interest: The authors declare that the research was conducted in the absence of any commercial or financial relationships that could be construed as a potential conflict of interest.

frontiers in Physiology

ORIGINAL RESEARCH
published: 25 September 2020
doi: 10.3389/fphys.2020.576617

The Diapause Lipidomes of Three Closely Related Beetle Species Reveal Mechanisms for Tolerating Energetic and Cold Stress in High-Latitude Seasonal Environments

Philipp Lehmann[1,2], Melissa Westberg[3], Patrik Tang[3,4], Leena Lindström[2] and Reijo Käkelä[3,5]*

[1] Department of Zoology, Stockholm University, Stockholm, Sweden, [2] Department of Biological and Environmental Science, University of Jyväskylä, Jyväskylä, Finland, [3] Molecular and Integrative Biosciences Research Programme, Faculty of Biological and Environmental Sciences, University of Helsinki, Helsinki, Finland, [4] Department of Biological Sciences, University of Bergen, Bergen, Norway, [5] Helsinki University Lipidomics Unit, Helsinki Institute for Life Science and Biocenter Finland, Helsinki, Finland

OPEN ACCESS

Edited by:
Bin Tang,
Hangzhou Normal University, China

Reviewed by:
Hamzeh Izadi,
Vali-E-Asr University of Rafsanjan, Iran
Umut Toprak,
Ankara University, Turkey

****Correspondence:***
Philipp Lehmann
philipp.lehmann@zoologi.su.se

Specialty section:
This article was submitted to Invertebrate Physiology, a section of the journal Frontiers in Physiology

Received: *26 June 2020*
Accepted: *01 September 2020*
Published: *25 September 2020*

Citation:
Lehmann P, Westberg M, Tang P, Lindström L and Käkelä R (2020) The Diapause Lipidomes of Three Closely Related Beetle Species Reveal Mechanisms for Tolerating Energetic and Cold Stress in High-Latitude Seasonal Environments. Front. Physiol. 11:576617. doi: 10.3389/fphys.2020.576617

During winter insects face energetic stress driven by lack of food, and thermal stress due to sub-optimal and even lethal temperatures. To survive, most insects living in seasonal environments such as high latitudes, enter diapause, a deep resting stage characterized by a cessation of development, metabolic suppression and increased stress tolerance. The current study explores physiological adaptations related to diapause in three beetle species at high latitudes in Europe. From an ecological perspective, the comparison is interesting since one species (*Leptinotarsa decemlineata*) is an invasive pest that has recently expanded its range into northern Europe, where a retardation in range expansion is seen. By comparing its physiological toolkit to that of two closely related native beetles (*Agelastica alni* and *Chrysolina polita*) with similar overwintering ecology and collected from similar latitude, we can study if harsh winters might be constraining further expansion. Our results suggest all species suppress metabolism during diapause and build large lipid stores before diapause, which then are used sparingly. In all species diapause is associated with temporal shifts in storage and membrane lipid profiles, mostly in accordance with the homeoviscous adaptation hypothesis, stating that low temperatures necessitate acclimation responses that increase fluidity of storage lipids, allowing their enzymatic hydrolysis, and ensure integral protein functions. Overall, the two native species had similar lipidomic profiles when compared to the invasive species, but all species showed specific shifts in their lipid profiles after entering diapause. Taken together, all three species show adaptations that improve energy saving and storage and membrane lipid fluidity during overwintering diapause. While the three species differed in the specific strategies used to increase lipid viscosity, the two native beetle species showed a more canalized lipidomic response, than the recent invader.

Since close relatives with similar winter ecology can have different winter ecophysiology, extrapolations among species should be done with care. Still, range expansion of the recent invader into high latitude habitats might indeed be retarded by lack of physiological tools to manage especially thermal stress during winter, but conversely species adapted to long cold winters may face these stressors as a consequence of ongoing climate warming.

Keywords: climate change, range expansion, abiotic stress, invasive species, pest insect

INTRODUCTION

Life in high latitude environments with large seasonal variation in abiotic and biotic environmental factors demands optimizing life-history and stress-tolerance according to prevalent conditions (Tauber et al., 1986; Schmidt-Nielsen, 1990). A major challenge is surviving winter, and many adaptations exist to this end, which can be grouped into three main categories: migrating to more benign environments (Dingle, 1978), tolerating the winter in an active state, often through structural, physiological and biochemical acclimatization (Leather, 1993) or spending winter in a resting state (Danks, 1987). Most small ectotherms, such as insects, spend winter in diapause, a pre-programmed deep resting stage, characterized by a cessation of reproductive and ontogenetic development, depressed metabolic rate and increased stress tolerance (Tauber et al., 1986; Denlinger and Lee, 2010; Tougeron, 2019).

One major challenge during diapause is surviving energetic stress. During diapause insects generally do not feed and are thus dependent on stored energy for survival (Hahn and Denlinger, 2007). Stored energy is accumulated prior to diapause, generally in the form of lipids, but to a smaller extent also as carbohydrates and proteins (Hahn and Denlinger, 2011). Energy stores are utilized to fuel basic metabolic needs during overwintering, but also to complete ontogenetic development, for reproductive maturation or for dispersal after overwintering (Koštál, 2006; Hahn and Denlinger, 2007; Sinclair, 2015). Some diapausing insects store significantly more chemical energy than non-overwintering counterparts, suggesting that they budget for winter-related expenses already during development. However, this is not always possible due to e.g. size constraints, which could limit the amount of extra energy that can be stored. Therefore there is a second, not mutually exclusive option, that diapause is associated with extreme metabolic suppression, which limits energy expenditure, often in a temperature-independent fashion (Williams et al., 2012, 2015; Lehmann et al., 2016; Lindestad et al., 2020).

Abbreviations: AB, Alder leaf beetle; Ster, cholesterol; CPB, Colorado potato beetle; DAG, diacylglycerol; DGC, discontinuous gas exchange; DBI, double bond index; DPB, dynamic phase behavior; ESI-MS, electrospray ionization mass spectrometry; HPTLC, high-performance thin-layer chromatography; HPA, homeophasic adaptation; HVA, homeoviscous adaptation; MB, Mint or Knotgrass leaf beetle; PC, phosphatidylcholines; PE, phosphatidylethanolamines; PI, phosphatidylinositols; PS, phosphatidylserines; PUFA, polyunsaturated fatty acids; SIMCA, soft independent modeling of class analogies; SM, sphingomyelins; PCA, principal component analyses; SE, sterol esters; TAG, triacylglycerols.

Diapause is also associated with cold stress (Denlinger and Lee, 2010). Low temperatures lead to among other, impaired enzyme function and ion homeostasis, and subzero temperatures are associated with the risk of ice formation, which is lethal without specialized adaptations (Toxopeus and Sinclair, 2018). Another central homeostasis issue is that, without compensating adaptations, decreasing temperatures reduce the viscosity of storage lipid droplets and cellular phospholipid membranes. The consequences would be impaired accessibility of the droplets for enzymatic hydrolysis deliberating fatty acids for energy, and compromised functions of multiple membrane proteins, respectively (Hazel, 1995). To prevent these adverse effects, ectotherms employ various biochemical structural modifications to maintain the optimal semifluid state of lipid membranes and droplets. These include increasing the average degree of lipid unsaturation, decreasing the average length of fatty acids, reshuffling fatty acids to produce new molecular species without affecting individual fatty acid proportions, head group re-structuring or changing the relative amount of cholesterol in membranes (Koštál, 2010). The various ways of biochemical acclimatization of lipid structures to maintain functionality as temperature decreases are often gathered under the umbrella term HVA, which include the HPA and the DPB theory (Sinensky, 1974; Lewis et al., 1989; Hazel, 1995). Central to all is the temperature-dependent dynamism in the lipid bilayer (Zehmer, 2005; Nickels et al., 2019). It should be stressed that there are several mechanisms by which proper lipid composition and physical properties are maintained, and that no clear taxonomic patterns exist, i.e., some animal groups employing only a certain acclimatization response (Koštál, 2010). Instead it seems as if many routes can lead to similar phenotypes.

During latitudinal range expansion, or as a consequence of climate change, ectothermic organisms can face changes in winter abiotic conditions, such as for instance length of the cold season, its average temperature, the temperature fluctuations or absolute minimum temperature (Bale and Hayward, 2010; Williams et al., 2014). These can act as expansion barriers if the organism cannot cope with the changing conditions, be this through general robustness, phenotypic plasticity or adaptation over generations (Urbanski et al., 2012). One species, that has rapidly expanded its range from relatively benign areas in Northern Mexico into habitats with stronger seasonality, is the invasive CPB, *Leptinotarsa decemlineata* (Say), a major pest of cultivated Solanaceous crops. The capacity of the CPB to overwinter in diapause, where cold tolerance is increased

(Boiteau and Coleman, 1996; Lehmann et al., 2015a) and energy consumption decreased through metabolic suppression (May, 1989; Piiroinen et al., 2011; Lehmann et al., 2015b), has been suggested to be of major importance for survival during the invasion into environments with progressively stronger seasonality (Kort, 1990; Alyokhin, 2009; Lehmann, 2013; Izzo et al., 2014). While range expansion in Europe has been rapid (Johnson, 1967), a retardation in expansion speed has been observed during the last 30 years at the northern range margin (EPPO, 2006; Lindström and Lehmann, 2015; Lehmann et al., 2020). This species therefore presents an interesting opportunity to understand factors and mechanisms facilitating and constraining latitudinal range-expansion. Here we compared diapause energetics and temporal changes in lipid composition during diapause in the invasive CPB and two native high-latitude chrysomelids, the MB *Chrysolina polita* (Linnaeus) and the AB *Agelastica alni* (Linnaeus). These are among the closest relatives to the CPB that can be found in the region, since there are no naturally occurring *Leptinotarsa* species in Europe (Silfverberg, 2011). These species overwinter as adults burrowed in the soil (Kort, 1990; Kölsch et al., 2002, Lehmann P, personal observation) and show the typical diapause ecophysiology common to Chrysomelids (Tauber et al., 1986; Hodek, 2012).

We investigate two major ecophysiological stressors during winter; energetic stress and cold stress. Energetic traits include (i) metabolic suppression, (ii) lipid store size, and (iii) lipid store utilization. While it is known that the CPB gathers TAG in its fat body during pre-diapause (Yocum et al., 2011a; Lehmann et al., 2012) it is not known how lipid quantity and quality changes temporally or compares to other high latitude chrysomelid beetles with similar overwintering ecology. For cold stress we study the effects of low temperature on lipid biology, and investigate (iv) HVA in storage and structural lipids. For utilization of lipid stores, even at very low rate under metabolic suppression, storage lipid molecules cannot solidify but have to remain in a semifluid state. This requires modifications in their molecular structure (Raclot et al., 2001; Rozsypal et al., 2014) and we here study average degree of acyl chain unsaturation (expressed as DBI) in TAG species. Similarly, most physiological functions of animals are dependent on the actions of integral membrane proteins, which require specific lipids to surround them (Marèelja, 1976; Wodtke, 1981) and we here study head-group restructurings (seen as changed phospholipid class ratios) and DBI of structural lipids. Lipidome differences in either storage or structural lipids between the invasive CPB and its native relatives related to winter energetics could be indicative of a physiological constraint that is limiting further range expansion, or alternatively tolerance against climate change in the present habitats.

MATERIALS AND METHODS

Study Animals and Rearing Conditions

The CPB were originally collected from fields near Petroskoi in Russian Karelia (61°49′N, 34°10′E) (N = 917) in the summer of 2006. These areas represent the current northernmost distribution of the species (EPPO, 2006). In each summer the overwintered CPB adults were maintained under a long-day photoperiod (18 h light, 23°C, 60% relative humidity) to ensure mating. Their offspring were then reared at a short-day photoperiod (12 h light 23°C, 60% relative humidity) and overwintered at 5°C in environmental chambers as described previously (Lehmann et al., 2012). We maintained a large and outbred population over the generations (at least 50 families per generation, over 1000 individuals) to minimize laboratory selection.

For the experiment, which was performed during the summer of 2012, unrelated CPB beetles were mated. Mated pairs were checked for deposited eggs daily. Larvae (10–15 per family) were reared on whole potato plants (which were covered in a plastic housing) in a greenhouse till adulthood at 23°C degrees, 60% relative humidity and 18 h light. The pots were checked daily for emerged adults, which were sexed and weighed (±0.1 mg, AM100; Mettler) and reared under a short-day photoperiod (12 h light). The MB and AB were collected the 14.08.2012 from two locations in central Finland (around lake Jyväsjärvi, 62°22′N, 25°73′E). We tracked the emergence of the summer generation, collected young adults during August and subsequently reared them under short-day photoperiods (12 h light) to induce overwintering. The AB and MB were maintained for 1 month at these conditions before the start of the experiment, to allow them to fully acclimate to the laboratory conditions, and undergo physiological preparation for diapause. A field survey conducted at the collection locations on a monthly basis showed that natural overwintering for the AB and MB was initiated in October (**Supplementary Figure S1**). Since we collected the beetles very early in the overwintering generation, several months before natural diapause initiation, and maintained them under the same conditions as the CPB in the laboratory, we are confident the diapause initiation program is comparable among the species. All beetles were fed *ad libitum* with fresh leaves, the CPB with potato (*Solanum tuberosum* of the van Gogh variety), the MB with mint (*Mentha arvensis*) and the AB with alder leaves (*Alnus glutinosa* and *Alnus incana*). Beetles were overwintered by decreasing temperature from 23° to 15°, 10° and finally to 5°C with 2 weeks at each intermediate temperature.

Adult beetles were sampled at three time-points during winter. First when the temperature had been lowered from 23°C to 15°C and adults had stopped feeding, but had not yet burrowed into the soil. Importantly, this means the first sampling point reflected when beetles had "chosen" to enter diapause, and thus should be physiologically prepared (Lehmann et al., 2014a, 2015a). The second time-point was 2 months and the third time-point 4 months after they had burrowed to the soil. Beetles were thus acclimated to 15°C in the first time-point and 5°C in the second and third time-point. The time-points were chosen to reflect different diapause phases, the first diapause initiation (0 months), the second diapause maintenance (2 months) and the third the transition between terminated diapause (4 months) and the following low temperature quiescence (Lefevere and De Kort, 1989; Koštál, 2006). Sample sizes for all analyses can be found in **Supplementary Table S1**.

Flow-Through Respirometry

Respirometry was performed by measuring gaseous carbon dioxide (CO_2) production at the three time-points described above. For the first time-point beetles were taken straight from the rearing conditions. For the second and third time-points beetles were first transferred to acclimate at 10°C for 24 h and then dug up from overwintering pots for respirometry. Beetles were kept in darkness throughout the acclimation and measurement process. CPB and MB were measured individually while AB were measured in same-sex pairs. This was done since these beetles primarily showed continuous respiration and the CO_2 amounts of single beetles generally were below our signal to noise threshold. CO_2 production was measured for 120 min with a Li-6252 CO_2 analyzer (LiCor, Lincoln, NE, United States) connected to a flow through respirometry system, as described previously (Lehmann et al., 2014a). Briefly, ambient air was scrubbed free of water vapor (Drierite; WA Hammond Drierite Co Ltd., Xenia, OH, United States) and CO_2 (Ascarite II; Acros Organics, Fisher Scientific, Pittsburgh, PA, United States) and pumped through the system (SS-2 pump; Sable Systems, Las Vegas, NV, United States) at a flow rate of 150 ml min^{-1} controlled by a mass flow controller (840 Series; Sierra Instruments Inc., Monterey, CA, United States). The respirometry chamber (volume 1.7 ml) was located inside a cabinet (PTC-1; Sable Systems) in which the temperature was set to 15°C and programmed with a temperature controller (Pelt-5; Sable Systems). Preliminary tests were performed to ensure that incurrent air temperature flowing through the respirometry chamber was stabilized with the ambient temperature in the cabinet. The respirometry data were baseline corrected and converted to mL CO_2 h^{-1} using the acquisition and analysis software ExpeData, version 1.1.15 (Sable Systems). Potential beetle movement was tracked with an infrared light scattering based activity detector (AD-1; Sable Systems). After the respirometry beetles were weighed (±0.1 mg, AM100; Mettler), and stored whole at −20°C until used for lipid analyses.

Total Lipid Extraction

Total lipids were extracted using the Folch method (Folch et al., 1957). First, whole frozen beetles were homogenized mechanically in 220 µl milli-Q water in Wheaton homogenizers (low extractable borosilicate glass mortar and PTFE pestle). Then 4.5 ml chloroform:methanol (2:1) was added, and the tubes were vortexed vigorously for 10 s. The homogenate was transferred to Kimax glass tubes and left at 23°C for 30 min in darkness, and centrifuged for 10 min at 3000 rpm to precipitate solid materials. The clear supernatant was moved to a new Kimax tube and 0.9 ml of milli-Q water was added. Following vigorous vortexing (10 s), tubes were again centrifuged for 10 min at 3000 rpm and the lower organic phase was collected to a new tube. This step was repeated on the original tube after substituting the collected lower phase with theoretical lower phase (2.25 ml chloroform/methanol/water 86:14:1). The pooled lower phases of the two extraction steps were vortexed, centrifuged as above, and the clear organic supernatant was moved to a new tube, and evaporated near to dryness under nitrogen stream after which 1 ml of chloroform:methanol (1:2) was added and the sample stored in 1.5 ml chromatography vials (Waters, Milford, MA, United States) for a maximum of 3 days at −20°C until analysis of the lipid class profiles by HPTLC. Aliquots of the extracts were stored at −80°C for mass spectrometric analysis of the detailed lipid species profiles.

Analysis of Lipid Classes Using High-Performance Thin-Layer Chromatography

Lipid class compositions were analyzed using HPTLC (technical details can be found in **Supplementary Table S2**). First, silica gel HPTLC 60 F254 plates (Merck, Darmstadt, Germany) were cleaned prior to analyses with chloroform/methanol/acetic acid/water (25:17.5:3.8:1.75) and stored in a desiccator. Samples were removed from the freezer, and dried under nitrogen. Then 500 µl of chloroform: methanol (1:2) was added, the vial vortexed, and samples applied on a silica plate with a Camag Automatic TLC Sampler 4 (Camag, Muttenz, Switzerland). For MB and AB 20 µl of sample was added, and for CPB only 15 µl, as the extract of these larger beetles had higher lipid concentrations. On each plate a range of storage (or neutral) lipid standards of known concentration were also sprayed (**Supplementary Table S3**). After spraying, the plate was dried for 5 min using a hair dryer. The plate was then placed in a horizontal through chamber (Camag, Horizontal Developing Chamber 2) and the storage lipids were eluted with hexane/diethyl ether/acetic acid/water (26:6:0.4:0.1). For the separation of phospholipids on another plate, samples and standards (**Supplementary Table S3**) were eluted with chloroform/methanol/acetic acid/water (25:17.5:3.8:1.75). The plate was dried for 5 min using a hairdryer and then developed by first dipping for 6 s (Camag, Chromatogram Immersion Device III) in an aqueous 3% copper sulfate and 8% phosphoric acid, dried for 5 min using a hairdryer, and finally heated in an oven set to 180°C until lipid bands were clearly visible (about 3–4 min). After development, plates were scanned with a Camag TLC plate scanner 3 at 254 nm using a deuterium lamp and with the lipid bands quantified by the Win-CATS 1.1.3.0 software. Resulting chromatographic peaks were identified by comparing their retention times against those of known standards. Then the peak areas were integrated and the amount of lipid per lipid class (in pmol) in the sample counted using the formula:

$$\text{pmol}[\text{sample}] = \text{area}[\text{sample}] \div \left(\text{area}\left[\text{standard}\right] \div \text{pmol}\left[\text{standard}\right]\right)$$

The relative concentrations of the lipid classes (molar percentage) were calculated by dividing the pmol content of a specific lipid class with the sum of pmol contents of all major lipid classes detected. In addition, lipid stores are primarily made up of TAG, but also DAG and SE are intrinsic to energy metabolism (Athenstaedt and Daum, 2006; Arrese and Soulages, 2010), and therefore these three lipid classes were summed for calculating total lipid store size in pmol per beetle. For the downstream statistical analyses, the storage lipid contents were corrected for

spraying amount differences, transformed to μmol and divided by beetle mass to yield relative storage lipid amount.

Analysis of Lipid Species Using Electrospray Ionization Mass Spectrometry

Individual lipid species of the main lipid classes were identified and quantified using ESI-MS. Sample extracts were removed from storage and brought to room temperature. Then 10 μl aliquots were dissolved in 60 μl chloroform/methanol 1:2 (by volume) and spiked with 3–6 μl cocktail of internal standards (**Supplementary Table S4**), the volume adjusted according to the lipid concentration of each sample. The sample solutions were infused into the electrospray source of an ion trap mass spectrometer (Esquire LC, Bruker-Franzen Analytik, Bremen, Germany) and spectra recorded by employing both positive and negative ionization mode in the range of m/z 500–1000 (technical details described in **Supplementary Table S5**). To confirm the identifications of glycerolipid species, additional ESI-MS/MS precursor or neutral loss scans were recorded for each sample type to verify phospholipid polar head groups (Brügger et al., 1997) and reveal the acyl chain assemblies of TAGs (Murphy et al., 2007) using a triple quadrupole mass spectrometer (Agilent 6490 Triple Quad LC/MS with iFunnel Technology; Agilent Technologies, Santa Clara, CA, United States). The ion trap ESI-MS spectra were processed by Bruker Daltonics (Billerica, MA, United States) data analysis software and the triple quadrupole ESI-MS/MS spectra by Agilent Mass Hunter software. The individual lipid species were quantified by using the internal standards (**Supplementary Table S4**) and LIMSA software (Haimi et al., 2006) and expressed in mole percentage (mol%). The lipid species were abbreviated as: [chain total carbon number]:[chain total number of double bonds].

Two indexes related to lipid viscosity or packing efficiency in membranes were calculated, the ratio of PE to PC (PE/PC), and average number of double bonds per acyl chain of the lipid species (DBI). The DBI was applied to lipid species to follow the original principle of DBI designed for fatty acids (Kates, 1986) as:

$$\mathrm{DBI} = \left[\sum 1 \times \left(\%\ \textit{monounsaturated lipid species}\right) + 2 \times \left(\%\ \textit{diunsaturated lipid species}\right) \ldots\right] / \left[100 \times \left(\textit{number of acyl chains in lipid}\right)\right]$$

To facilitate comparisons across different lipids classes with different number of acyl chains (TAG has 3, phospholipids PC, PE, PS and PI all have 2, and SM has only 1 acyl chain in the molecule) the formula reports the double bond contents per single acyl chain (i.e., fatty acid).

Statistical Analyses

CO_2 production was used as proxy of metabolic rate, and studied with a generalized linear mixed model using the normal distribution and an identity link. The CO_2 data was $\log_{10}$-transformed due to heavy left-skewness, divided by mass in g and then used as dependent variable. As factorial explanatory variables species (CPB, MB, and AB) and diapause phase (initiation, maintenance, and termination) were added. While preliminary observations suggested beetles moved very little during the measurement, we added the arbitrary activity metric as continuous covariate to correct for slight movement. To investigate how lipid stores varied among the species and diapause phase a generalized linear model with the normal distribution and an identity link was again used. The relative storage lipid amount was used as dependent variable in a model where species and diapause phase were added as factorial explanatory variables. The TAG and membrane lipid viscosity related indexes were analyzed with generalized linear models with the normal distribution and an identity link was again used. Lipid viscosity traits were used as dependent variable in individual models and species and diapause phase as factorial explanatory variables. Non-significant interactions were removed from the final model (Sokal and Rohlf, 2003), whose improvement was also tracked using the Akaike Information Criterion. For significant interactions, the main level effects were *post hoc* tested with univariate F-tests and pair-wise tests on group estimated marginal means with Bonferroni multiple-comparison corrections. Significant main effects were subjected to the same pairwise testing procedure. For analyzing CO_2 production, storage lipid content and viscosity indexes the IBM SPSS statistics 25.0 (IBM SPSS Inc., Chicago, IL, United States) statistical software package was used. Finally, for overall description of lipid species dynamics, the molar percentages of individual lipid species were divided by 100, ArcSin transformed, block-normalized and standardized, after which they were subjected to PCA (Sirius 8.0, Pattern Recognition Systems AS). The last step involved forcing standard deviations to be equal, while allowing means to fluctuate. Thus, the common lipid species do not dominate the patterns, potentially obscuring important changes in relative abundance of less common lipid species. Statistical differences among groups in main components were investigated using SIMCA (Wold and Sjöström, 1977) with an alpha level of 0.05. The PCA analysis and subsequent SIMCA was run separately for storage and phospholipid species.

RESULTS

Metabolic Suppression

Three diapause phases were investigated, of which the first (0 months) represented diapause initiation still at relatively high temperature (15°C), and the subsequent represented diapause maintenance (2 months) and diapause termination (4 months) at a lower temperature (5°C). Note that the measurements were performed at a standardized temperature of 15°C. Respiratory patterns varied dramatically among species (**Figure 1**). The CPB displayed cyclic and DGC and only very few cases of continuous gas exchange. The MB displayed all the three respiratory patterns, and the AB only displayed continuous or cyclic respiration. For the CPB the proportion of DGC decreased as diapause progressed. In the MB the proportion displaying

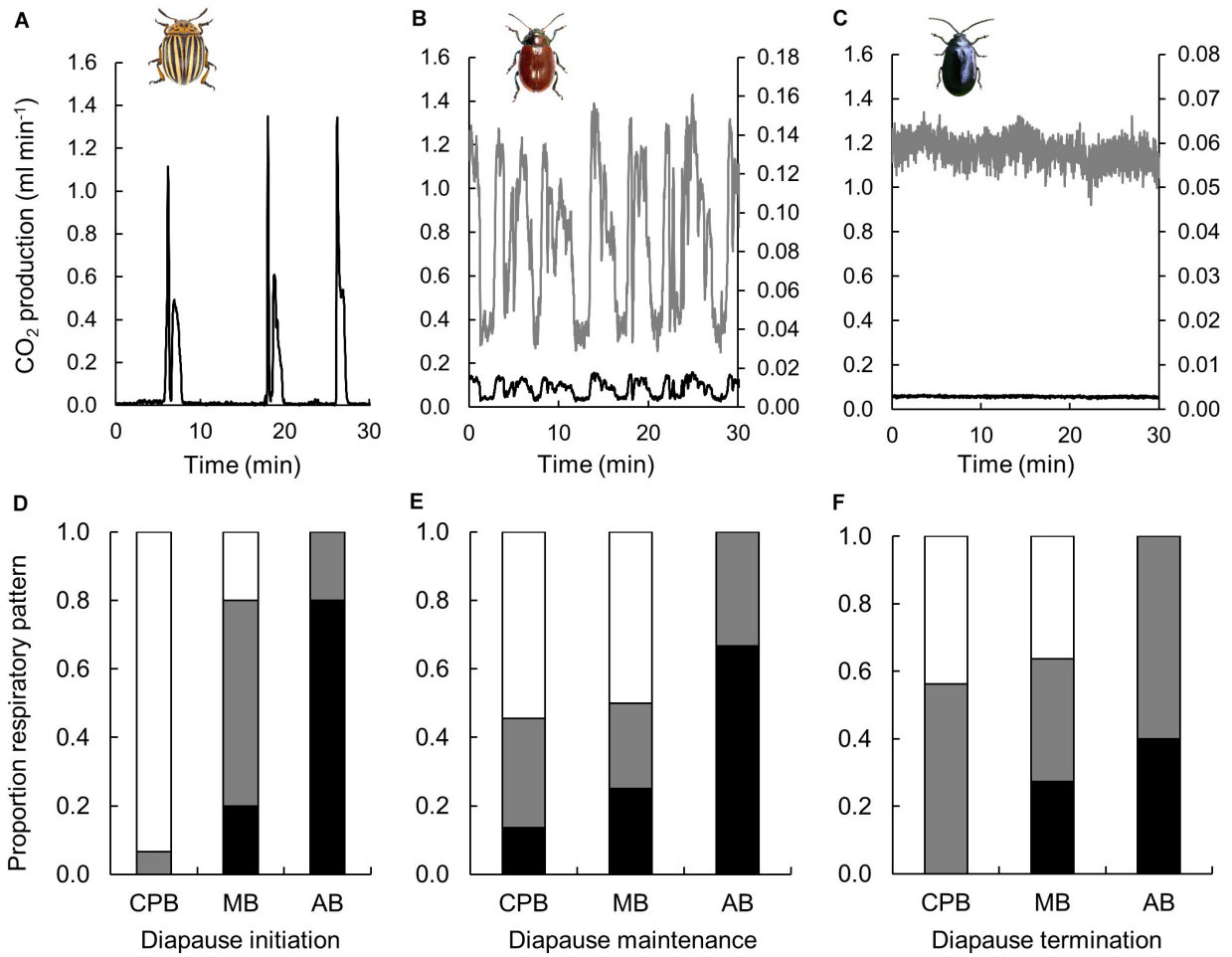

FIGURE 1 | Respiratory patterns varied during winter in three high-latitude chrysomelid beetle species. Panels **(A–C)** show examples of discontinuous gas exchange in a CPB **(A)**, of cyclic gas exchange in a MB **(B)** and continuous gas exchange in an AB **(C)**. The black line shows CO_2 production on an equal scale, while the gray trace in **(B,C)** shows the same traces scaled for clarity (secondary *y*-axis). These traces are all from stationary individuals, of which a sample image is shown in the inserts. Panels **(D–F)** show proportions of CPB, MB and AB showing discontinuous (white), cyclic (gray) or continuous (black) gas exchange during diapause initiation **(D)**, diapause maintenance **(E)** and diapause termination **(F)**. Insert beetle figures by (a) U. Schmidt, (b) www.ukbeetles.co.uk, and (c) Trevor and Dilys Pendleton/www.eakringbirds.com.

continuous gas exchange was quite static (around 0.2) but the proportion showing DGC increased with time in diapause. The proportion of AB displaying cyclic gas exchange increased as diapause progressed.

Additional signs of metabolic suppression were investigated by measuring the CO_2 production of the beetles. Overall, the three species showed relatively similar average CO_2 production values (**Table 1A**), especially at later diapause phases. However, CO_2 production profiles differed between the species. The CPB showed a consistent increase in CO_2 production as diapause progressed. In contrast, the MB showed a consistent decrease in CO_2 production. In the AB, the CO_2 production first increased between diapause initiation and maintenance, and then decreased as beetles transitioned from diapause maintenance to termination (**Figure 2A**). While the difference for both the CPB and the MB between diapause initiation and termination were significant, overall absolute differences among species within diapause phases were relatively minor.

Lipid Classes and Overall Lipid Species Composition

The quantitatively most important structural lipid classes of membranes were PC, SM, PE, PS+PI, and free sterols, including cholesterol (Ster) (**Supplementary Figure S2**). The quantitatively most important storage lipids were TAG, DAG, and SE (**Supplementary Figure S2**). In all beetle species TAGs dominated the lipid profile and made up 50–60% of the total lipid present. Removing the storage lipid classes revealed underlying dynamics in structural lipid classes that otherwise was obscured. The SM, PS+PI and Ster showed variation with time in diapause. These changes were, however, limited to the MB and AB (**Supplementary Table S6**). In the CPB, no significant

TABLE 1 | Final generalized linear models describing how **(A)** CO_2 production and **(B)** storage lipid content changed during diapause in three high-latitude Chrysomelid beetles.

Effect	Wald chi-square	df	Significance
(A) CO_2 production			
Intercept	1.521	1	0.217
Activity	6.534	1	0.011
Species	13.941	2	0.001
Diapause phase	4.585	2	0.101
Species × diapause phase	21.225	4	<0.001
(B) Total storage lipid content			
Intercept	1260.200	1	<0.001
Species	0.730	2	0.694
Diapause phase	8.098	2	0.017

changes occurred in any structural lipid class as a function of time in diapause, and there was overall much variation among individuals.

The PCA of TAG species profiles showed two main axes of variation that together explained 51% of the variation in TAG data (**Figure 3A**). PC1 (explaining 31% of variation) likely reflects the difference between the invading species and the two native species, while PC2 (explaining 20% of variation) separates both the MB from the AB, and all diapause initiation samples of CPB and AB from their later diapause phases. PC3 (explaining 11% of variation) is required to separate the diapause initiation samples of the MB from the later diapause phases in that species (**Figure 3B**). SIMCA comparisons of two sample groups at a time (above **Figure 3A**) showed that in all the three beetle species the TAG lipid species composition shifts dramatically from diapause initiation toward diapause maintenance but then remains relatively similar until termination (above **Figure 3A**). The individual TAG species affecting the separation most strongly are the highly unsaturated species, enriched in initiation samples, and several species with 0–2 double bonds, which associate with the later phases of diapause (**Figure 3**). The detailed TAG species profile was largely changed in all three beetle species (**Figure 3** and **Supplementary Figure S3**).

The PCA of phospholipid species profiles showed three main axes of variation that together explained 61% of variation in phospholipid data (**Figure 3C**). PC1 (explaining 30% of variation) likely reflects the difference between the invading species and the two native species, while PC2 (explaining 16% of variation) seems to separate the MB from both the AB and CPB, and finally PC3 (explaining 15% of variation) seems to describe the progression from early diapause to later diapause phases. The phospholipid species with highest loadings for PC1 are either polyunsaturated species, which were found in higher amounts in the AB and MB, or those with 1–3 double bonds, which were more common in CPB that in the other beetle species. The separation along PC2 was largely driven by different degree of unsaturation of SM species; more monounsaturated SM species in MB and more saturated SM species in the other beetle species. For PC3, the major drivers seem to be the acidic PI and PS species, and highly unsaturated PC and PE species, all

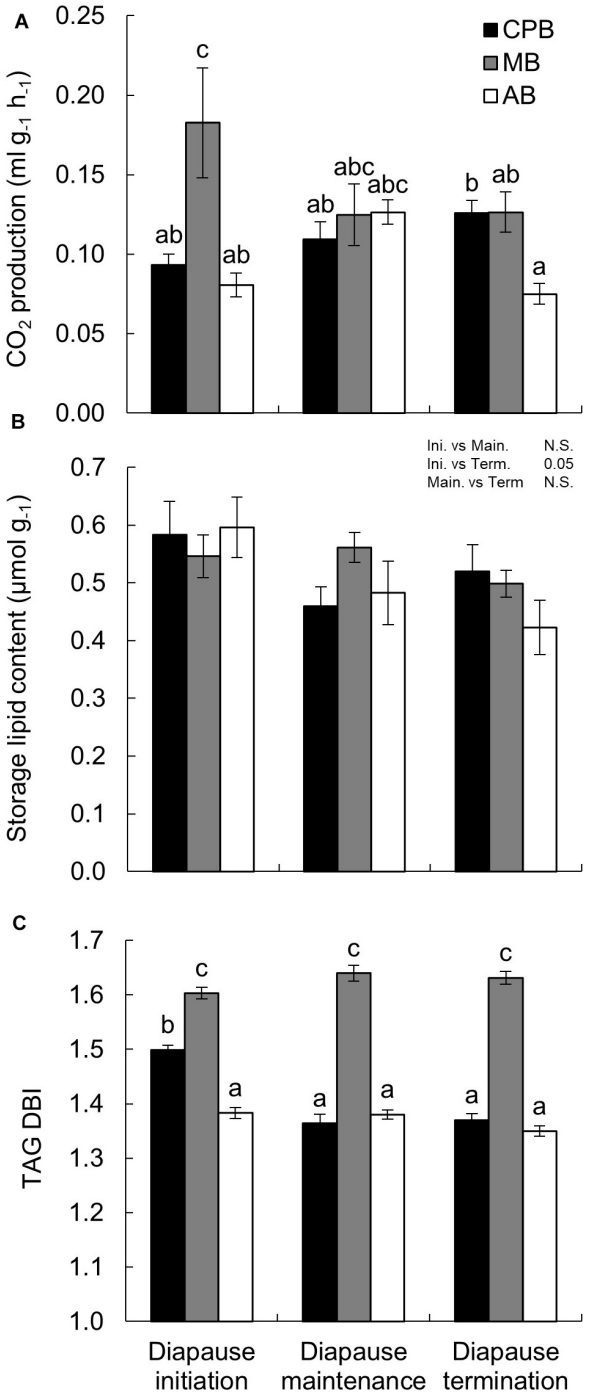

FIGURE 2 | Winter energetics and phospholipid viscosity in three high-latitude chrysomelid beetle species. **(A)** CO_2 production as a function of diapause phase. Note that while mass-specific CO_2 production is shown on the *y*-axis, the statistical model used mass as covariate. **(B)** Mass-corrected total storage lipid content as a function of time in diapause. **(C)** Double bond index (DBI) of triacylglycerol (TAG) calculated per acyl chain (three-fold for intact TAG molecule). Bonferroni corrected pairwise comparisons are shown in each panel. Comparisons between main effects are shown above the panel. **(A,C)** Letters show comparisons for the interaction between main effects. No common letters denotes $P < 0.05$. All numbers are expressed as mean ± standard error of mean.

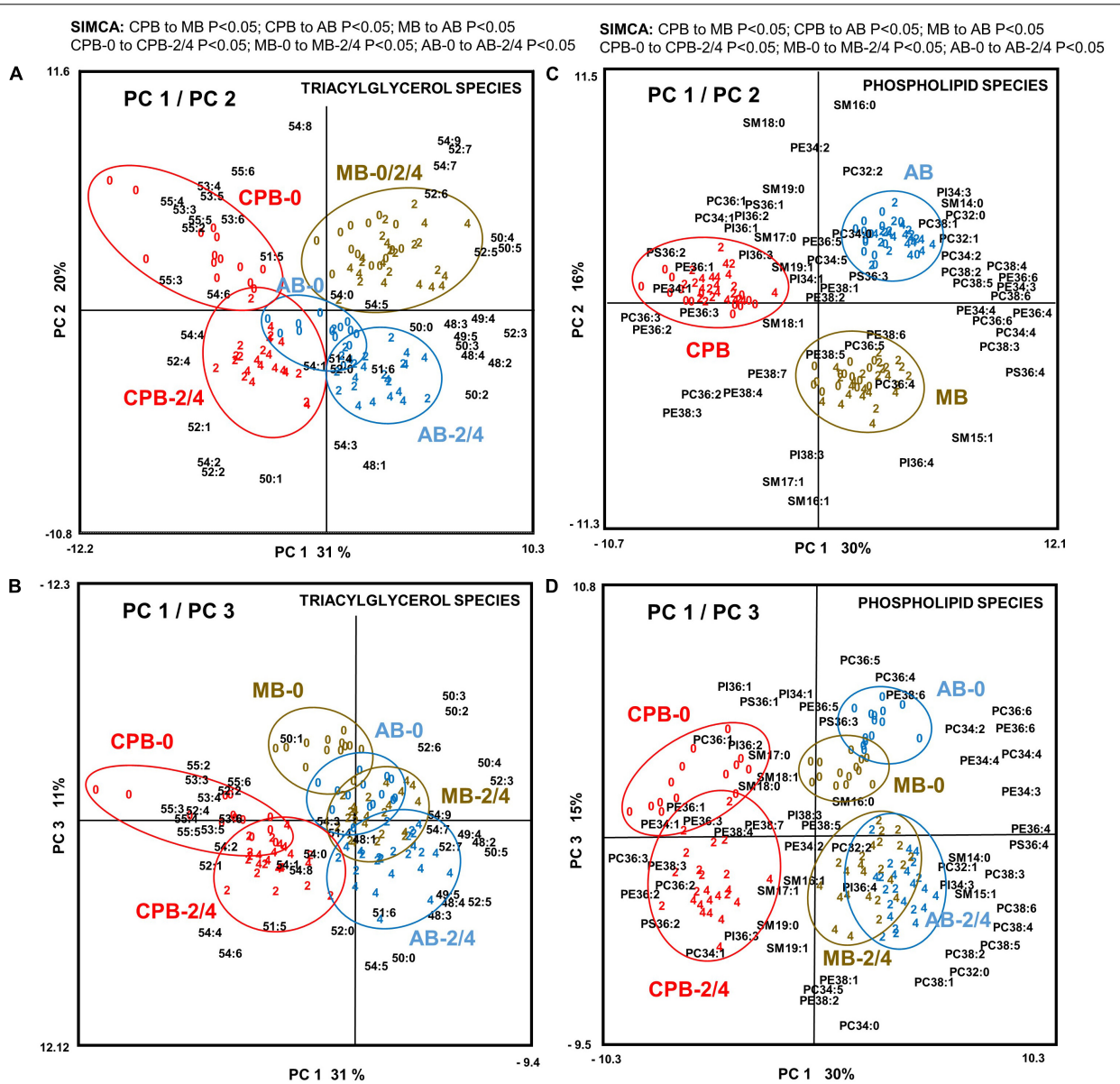

FIGURE 3 | Principal component analysis of all **(A,B)** 42 triacylglycerol (TAG) species and **(C,D)** 58 phospholipid species in the three investigated beetles (*N* = 114) showing **(A,C)** PC1 and PC2 and **(B,D)** PC1 and PC3. For TAG species, these three axes explained 31, 20, and 11% of variation, respectively (i.e., over 60% together). Plotting the data with the coordinates PC1 and PC3 gave further separation related to the phase of the diapause. For phospholipid species, these three axes explained 30, 16, and 15% of variation, respectively (i.e., over 60% together). The data consisted of relative molar percentage (%) values for each lipid species within its lipid class, which was ArcSin-transformed and Block-normalized before analysis. Beetles have been color-coded so that red symbols represent CPB, brown are MB, and blue are AB individuals. Individual beetles are marked by a number referring to diapause phase (0 = diapause initiation, 2 = diapause maintenance at 2-month time-point, 4 = diapause termination at 4-month time-point). The results of pair-wise tests using soft independent modeling of class analogies (SIMCA) ($P < 0.05$) are listed on top of panels **A** and **C**.

promoting cellular metabolism, and are associated with diapause initiation (**Figure 3D**). Further, the PC3 axis demonstrates that in later diapause phases the overall degree of unsaturation seems to decrease and the relative proportions of several SM species increase.

The species profiles were also compared separately in each lipid class. Such comparisons in one diapause phase at a time resulted in statistically significantly different profiles for all the beetle species pairs and all the major lipid classes TAG, PC, SM, and PE (as the only exception, MB and AB had similar PC profiles at the initiation phase of diapause). In general, the beetle species comparisons at certain time points resulted statistically significant differences more often than the time point comparisons in one species (**Table 2**). The class specific lipid species profiles that were tested are also shown as bar-plots (**Supplementary Figures S3–S8**).

TABLE 2 | Statistically significantly different species profiles when each lipid class was studied separately during the initiation, maintenance and termination phase of diapause in three high latitude Chrysomelid beetles.

(A)	Diapause initiation (0)			Diapause maintenance (2)			Diapause termination (4)		
	CPB-MB	CPB-AB	MB-AB	CPB-MB	CPB-AB	MB-AB	CPB-MB	CPB-AB	MB-AB
TAG	*	*	*	*	*	*	*	*	*
PC	*	*	*	*	*	*	*	*	*
SM	*	*	*	*	*	*	*	*	*
PE	*	*	*	*	*	*	*	*	*
PS	NS	NS	NS	*	NS	NS	*	NS	NS
PI	NS	*	*	*	*	*	*	*	*
(B)	**CPB**			**MB**			**AB**		
	0–2	**0–4**	**2–4**	**0–2**	**0–4**	**2–4**	**0–2**	**0–4**	**2–4**
TAG	*	*	NS	*	*	NS	*	*	NS
PC	NS	*	NS	*	*	NS	*	*	NS
SM	*	NS	NS	NS	NS	NS	*	*	NS
PE	NS	NS	NS	*	*	NS	*	*	NS
PS	NS	NS	NS	NS	NS	NS	NS	NS	NS
PI	NS	NS	NS	NS	NS	NS	*	NS	NS

*Displayed are pairwise comparisons using SIMCA, where *means $P < 0.05$ for the specific comparison, and NS means a non-significant result.* ***(A)*** *shows differences among species within diapause time-points, while* ***(B)*** *shows differences within species, among time-points (0 = diapause initiation, 2 = diapause maintenance, 4 = diapause termination). The species profiles in each lipid class and time-point of the beetle species are presented in* ***Supplementary Figures S3–S8****. TAG, triacylglycerol; PC, phosphatidylcholine; SM, sphingomyelin; PE, phosphatidylethanolamine; PS, phosphatidylserine; PI, phosphatidylinositol.*

Lipid Store Size and Utilization

Storage lipid content was analyzed as the sum of TAG+DAG+SE (together amounting to over 70% of lipid present). The relative lipid amount accumulated before diapause was very similar in the three species (**Figure 2B**) and did not differ significantly between the species in any of the diapause phases (**Table 1B**). In all species, however, did lipid stores decrease as diapause progressed (**Figure 2B**), non-significantly between diapause initiation and maintenance, but significantly between these two phases and diapause termination (**Figure 2B** and **Table 1B**).

Homeoviscous Adaptation in Storage Lipids

While the three species shared an overall decrease in lipid stores size, the composition and viscosity of the main storage lipid, TAG, differed in a more complex manner. The CPB had a moderate TAG DBI which decreased as diapause progressed and then stabilized (**Figure 2C** and **Table 3A**). The MB had an overall high TAG DBI which did not change during diapause. The AB had an overall low TAG DBI which did not change during diapause.

Homeoviscous Adaptation in Structural Lipids

Two metrics of phospholipid viscosity were calculated, the ratio of PE to PC and the unsaturation degree of fatty acids in the main phospholipids (PC, SM, PI, PS, and PE), expressed as DBI. For easy comparison the DBI values were calculated per acyl chain, despite that the lipids studied have 1–3 acyl chains in the molecule. There were several clear differences among species and diapause phases in these indexes (**Table 3**), and since the species × diapause phase interactions was significant only for PE DBI, the models suggested relatively straightforward shifts for most of the traits. The PE/PC ratio was highest in the AB, similar in the MB and CPB and did not change statistically significantly with diapause phase in any beetle species (**Figure 4A**). Still, the AB had slight decreasing and CPB slight increasing tendency in their PE/PC ratio as diapause progressed. The PC DBI was lower in the CPB than the two native beetles, and decreased significantly as diapause progressed in all species (**Figure 4B**) albeit the effects were relatively minor. The SM DBI stayed relatively unchanged during diapause, and when the beetle species are compared, the MB had a much higher SM DBI than the other two species, which did not differ from each other (**Figure 4C**). The PE DBI was high and stable in both the MB and AB during diapause, while the CPB displayed both a lower overall PE DBI, which also decreased with time in diapause (**Figure 4D**). The PS showed similar DBI patterns as PE with little dynamics during diapause, and the AB and MB having an overall higher degrees of DBI than the CPB (**Figure 4E**). The PI DBI increased significantly as diapause progressed in all species, and also differed among the species so that the MB again had the overall highest DBI (**Figure 4F**).

DISCUSSION

The present study investigates how a recently invaded beetle compares to two native beetle species, from the same latitudinal origin, in several traits related to two key stressors that insects need to overcome during diapause, energetic stress and cold stress. Failure to cope with these could lead to mortality or

TABLE 3 | Final generalized linear models describing how **(A)** TAG DBI, **(B)** PE/PC ratio and **(C–G)** DBI of major phospholipid classes changed during diapause in three high-latitude Chrysomelid beetles.

Effect	Wald chi-square	df	Significance
(A) TAG DBI			
Intercept	166481.843	1	<0.001
Species	960.600	2	<0.001
Diapause phase	29.021	2	<0.001
Species × diapause phase	88.677	4	<0.001
(B) PE/PC ratio			
Intercept	6020.654	1	<0.001
Species	370.862	2	<0.001
Diapause phase	0.866	2	0.649
(C) PC DBI			
Intercept	22957.731	1	<0.001
Species	68.801	2	<0.001
Diapause phase	20.402	2	<0.001
(D) SM DBI			
Intercept	24047.125	1	<0.001
Species	1625.385	2	<0.001
Diapause phase	2.280	2	0.320
(E) PE DBI			
Intercept	119853.795	1	<0.001
Species	296.708	2	<0.001
Diapause phase	1.874	2	0.392
Species × diapause phase	13.253	4	0.010
(F) PS DBI			
Intercept	141945.875	1	<0.001
Species	289.818	2	<0.001
Diapause phase	1.150	2	0.563
(G) PI DBI			
Intercept	57383.026	1	<0.001
Species	58.653	2	<0.001
Diapause phase	21.840	2	<0.001

otherwise reduced fitness and act as an expansion barrier for species shifting range into habitats with harsher winters. Understanding how native beetles cope with these challenges, and characterizing their physiological toolbox, can therefore provide valuable insight into the mechanisms behind high-latitude seasonal adaptations. Overall, the data suggest that the invasive species is comparable or even superior to the native beetles in terms of managing energetic stress, but shows an overall more varied and less canalized diapause lipidome, suggesting less evolved capacity to manage cold stress. This latter finding is in agreement with findings of a previous study of the same three beetles, that showed the invasive species had an overall poorer tolerance against direct cold shocks, and less well canalized metabolome, than the native species (Lehmann et al., 2015a). The main findings are summarized in **Table 4** and discussed in detail below, in a trait-by-trait manner. Together these studies suggest that the CPB shows a diapause phenotype less well adapted to high-latitude conditions than native relatives, which might potentially be one reason for the retardation of expansion to higher latitudes observed globally over the last decades. It is even possible that the buffering effect of their microhabitats has constrained selection to act on diapause-related physiology and allowed the CPB to spread into harsh winter climates primarily due to its behavioral plasticity (Izzo et al., 2014; Lehmann et al., 2014a). It would therefore be important to systematically investigate the influence of overwintering microhabitat and field conditions (Yocum et al., 2011b) on energy fluxes and cold tolerance in the three species in future experiments. Also, studies should compare these traits among populations, to see if selection already is acting on these traits within the European range of the CPB (Lyytinen et al., 2012; Lehmann et al., 2015c). It should also be noted that even though we maintained a large and outbred laboratory population of the CPB, and have no reason to suspect laboratory selection and drift, a future study should compare the species when collected straight from the field, or after being kept for similar periods in the laboratory for more direct comparison.

Metabolic Suppression

The three beetle species investigated in the present study all showed signs of suppressed metabolism. Comparing CO_2 production values of CPB during diapause initiation (i.e., at 15°C) to non-diapause individuals (Lehmann et al., 2014a) suggests that CO_2 production, and thus metabolic rate, is suppressed to about 10% of non-diapause values. The extent of suppression is more difficult to assess for AB and MB as no beetles have been measured during summer using a similar setup. For AB, metabolism appears fully reversibly suppressed to about 5% of normal resting metabolic rate when they are subjected to acute hypoxia (Kölsch et al., 2002), which might be a naturally occurring condition during diapause (Große and Schröder, 1984). These numbers reflect what has been reported in other insects (Williams et al., 2015; Lehmann et al., 2016), and suggest metabolic suppression to be a good phenotypic marker of diapause maintenance in these species. Overall, the results suggest that the invasive CPB has similar or even stronger capacity to suppress metabolism, when compared to the native species.

The beetle species showed large differences in respiratory patterns. For CPB and MB, most individuals, especially in the later diapause phases, showed DGC. This is in general agreement with previous data on diapausing insects, including for instance beetles (Lehmann et al., 2015b; Ploomi et al., 2018), bumblebees (Beekman and Stratum, 1999), stinkbugs (Ciancio, 2018) and butterflies (Schneiderman and Williams, 1953; Jõgar et al., 2004; Stålhandske et al., 2015). It is commonly seen during periods of stress or during periods of suppressed metabolism (Lighton, 2008). Since diapause constitutes both, DGC would be expected, especially given that the three investigated species all spend winter burrowed into the soil, thus potentially facing hypercapnic environments. DGC as protective mechanism against hypercapnia has been suggested as one putative reason why it has evolved, and why it is common in fossorial insects (Lighton, 1998). Since the theory is relatively clear about the benefits entailed by DGC (Chown et al., 2006; Matthews and White, 2011), it is interesting why the AB did not display any DGC. One potential explanation is that the AB has a different overwintering microhabitat, in wet soil, and

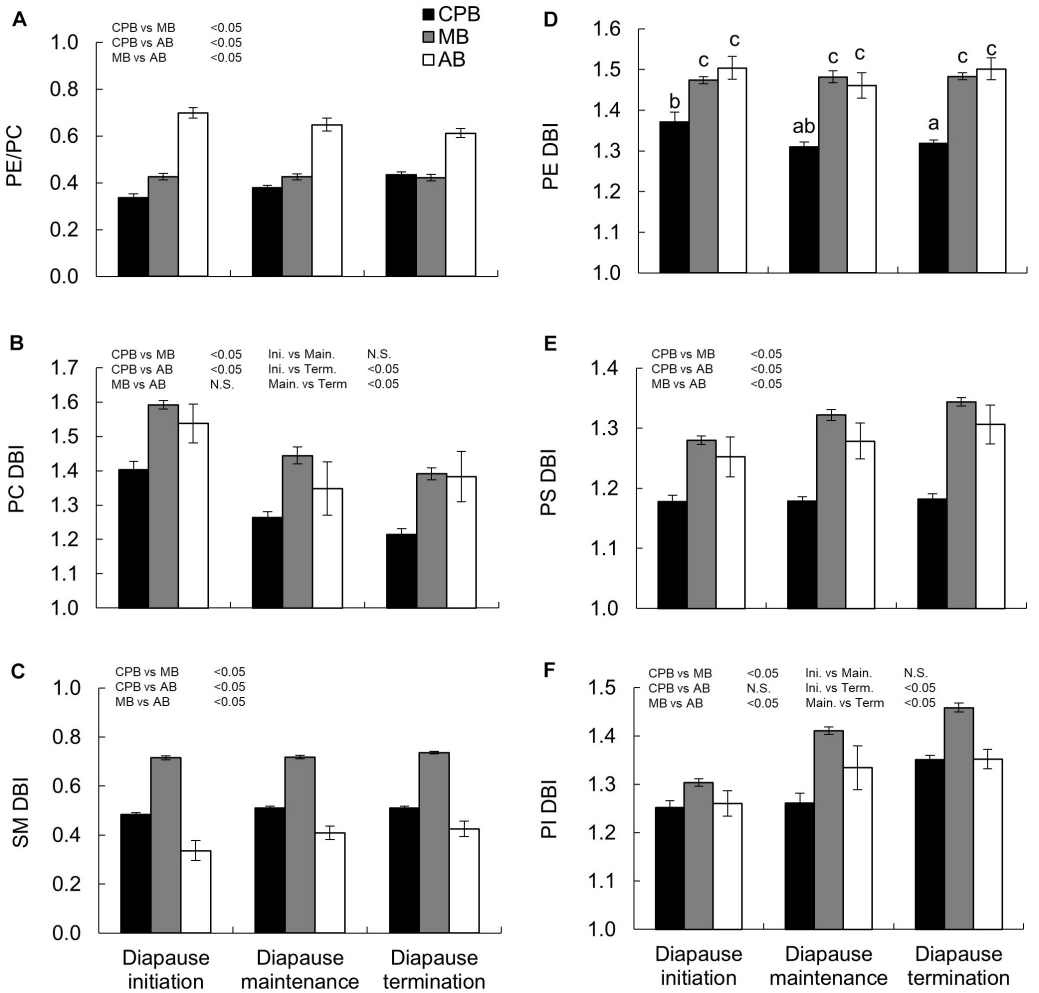

FIGURE 4 | Winter energetics and phospholipid viscosity in three high-latitude chrysomelid beetle species. **(A)** Ratio of PE to PC phospholipids, **(B–F)** unsaturation indexes (double bond index, DBI) calculated for all phospholipid classes studied, and expressed per acyl chain for easy comparison between lipids classes with 1 (SM), 2 (PC, PE, PS, PI), or 3 (TAG in **Figure 2C**) acyl chains. Bonferroni corrected pairwise comparisons are shown in each panel. Comparisons between main effects are shown above the panel. For **(D)** letters show comparisons for the interaction between main effects. No common letters denotes $P < 0.05$. All numbers are expressed as mean ± standard error of mean. Lipid abbreviations are: PE, phosphatidylethanolamine; PC, phosphatidylcholine; SM, sphingomyelin; PS, phosphatidylserine; PI, phosphatidylinositol; TAG, triacylglycerol. For calculation of PE/PC ratio, the diacyl species of PE and PC (no ether species) were used.

thus could display a different eco-physiological strategy than the MB and CPB (but see Hodek, 2012). This environment may be water-loaded and thus potentially frozen (Große and Schröder, 1984; Kölsch et al., 2002; Lehmann et al., 2015a). If the AB overwinter in frozen microhabitats then metabolic restrictions should be different. First, moist and frozen soils are expected to have higher thermal conductivity than dry soils (Lal, 2017), and therefore the AB might experience overall colder overwintering conditions than the MB and CPB. If this is the case, then metabolism should be inherently more suppressed as a consequence of lower ambient temperature. Further, water-loaded or frozen soils might become hypoxic to a higher degree than dry soils and thus AB would face oxygen limitation that likely would act to suppress metabolism (Guppy and Wither, 1999). While it is tempting to suggest that overwintering in frozen microhabitats might indicate that the AB themselves might be frozen (which should act to heavily suppress metabolism), previous studies on the AB suggest this is not the case, even partially (Lehmann et al., 2015a). It can be noted that the CPB prefers to overwinter in porous soils with medium water loading, if given a choice, and this behavior might be explained to some degree by hypoxia avoidance (Ushatinskaya, 1977; Noronha and Cloutier, 1998). Monitoring the abiotic conditions in actual overwintering microhabitats of the AB and MB would be important in future studies.

Lipid Store Size, Utilization and Homeoviscous Adaptation of Storage Lipids

The three species gathered large lipid stores prior to winter. The proportion of TAG, which represents the main storage

TABLE 4 | Summary of the results related to oxidative energy metabolism and membrane properties during different phases of diapause in three high-latitude Chrysomelid beetles, including potential implications of results with regard to further range expansion and climate change in local overwintering habitats.

	CPB	MB	AB
Oxidative energy metabolism traits:			
Gas exchange pattern	Discontinuous	Cycling	Continuous
Metabolic suppression	High	High	High
Relative lipid store size	Large	Large	Large
Lipid store utilization	Stable → slight decrease	Stable → slight decrease	Decrease
Storage TAG unsaturation (DBI)	Average, decrease	High, no change	Average, no change
Membrane properties:			
PE/PC ratio and its change (head-group restructuring)	Low, little change	Average, no change	High, little change
PC unsaturation (DBI)	Average, decrease	High, decrease	High, decrease
SM unsaturation (DBI)	Average, no change	High, no change	Low, no change
PE unsaturation (DBI)	Average, slight decrease	High, no change	High, no change
PS+PI (acidic phospholipid classes) unsaturation (DBI)	Low, increase in PI	Average → high, increase	Average → high, increase
Possible implications:			
Range expansion	Need for profound restructuring of membrane lipids may limit northward expansion.	Wide current range reflected by strong winter energetic and cold stress adaptations.	Adapted to high latitude conditions, expanding south not likely.
Climate change	Discontinuous respiration and stable lipid stores indicate buffering capacity against warming winters. Further, milder winter temperatures could require less membrane restructuring, thus facilitating expansion.	Cyclic respiration and stable lipid stores suggest buffering capacity against warming winters exist.	Continuous respiration and decreasing lipid stores suggests poor capacity to handle warming winters.

Note that the degree of unsaturation in each lipid class refers to the average double bond content per acyl chain, and even if the average degree of unsaturation is not changed, numerous alterations in the proportions of individual lipid species may occur.

form of lipid, was about 50–60% of total lipid in all species. The amount stored per unit of body mass was very similar in the three species during diapause initiation, and while the interaction effect between species and diapause was non-significant, some differences between the species seem likely. While there was an overall decrease in all species between the early and later phases in diapause, an analysis on the data split by species (not shown) suggests that the effect of diapause phase is only significant in the AB, which thus seems contribute the most to the overall decrease in lipid stores. This could again be related to the overwintering microhabitat of the AB. If it normally experiences lower winter temperatures than the other species, it might be less-well equipped for handling the relatively high diapause maintenance temperatures used here (5°C) (e.g., due to lack of DGC). Such a pattern would coincide with the much higher cold tolerance found in the AB compared to the other two species previously (Lehmann et al., 2015a). In any case, the results suggest that the invasive CPB gathers similar amounts of lipid and utilizes them at a rate comparable to, or even more economical than, the two native beetle species.

With progressing diapause, the PCA of TAG species in the three species, but especially the CPB, showed a strong decrease in the relative abundance of TAGs containing PUFAs, a response mirrored by the decrease in TAG DBI in the CPB. In mammals it has been shown that TAG species harboring polyunsaturated acyl chains are most rapidly hydrolyzed, due to their higher hydrophilicity, which exposes them to cytosolic lipases (Raclot, 2003). Thus, even though total storage lipids only show a moderate decrease, these findings lend support to the notion of lipid oxidization for energy production during diapause, especially in the CPB. While lipids likely are used for energy production in all three species, overall rate of lipid consumption was low (in terms of decreasing storage lipid size). This is reflective of patterns found also in other studies (Irwin and Lee, 2003; Williams et al., 2012; Fründ et al., 2013; Lehmann et al., 2016) and probably highlights the effect of metabolic suppression (Sinclair, 2015). It is of course also possible that other substrates are used for energy production than lipid, even though lipid seems most commonly used (Hahn and Denlinger, 2007; Toprak et al., 2020). In the CPB it has for instance been shown that large quantities of a storage protein called Diapause Protein 1 is sequestered prior to diapause (Lehmann et al., 2014b). While primarily consumed after diapause (Lefevere et al., 1989; De Kort and Koopmanschap, 1994) it could provide energy throughout diapause at low rate. It would therefore be important in future studies to directly assess lipid and energy utilization in a more direct manner, by for instance measuring respiratory quotient (RQ) (Schmidt-Nielsen, 1990) or using metabolic tracers (Williams et al., 2016), in order to more firmly establish energy substrate. Finally we note that the MB showed a much higher TAG DBI than the other two species from the outset. This could be due to the very high 18:3n-3 contents of mint leaves (Rao and Lakshminarayana, 1988; Xu et al., 2020) consumed by the MB,

which likely explained the high proportions of the TAG species 54:9 (3 × 18:3) and consequently, the high overall TAG DBI.

Homeoviscous Adaptation of Structural Lipids

For cold stress, the present paper investigates a core mechanism of membrane homeostasis – HVA (Sinensky, 1974; Lewis et al., 1989; Hazel, 1995), and finds results that support it, and details that seem to refute it. Most importantly, the adaptive modifications of lipids were clearly species-specific, and did not follow one simple "beetle pattern." For lipid classes, two results that refuted generally expected HVA responses stood out. In no species was there a marked increase in the molar ratio of PE to PC when they entered diapause. An increase in this ratio would be expected, since it would lead to impaired molecular packing and thus increased membrane fluidity (Šlachta et al., 2002; Koštál, 2010; Rozsypal et al., 2013). Thus, this mechanism does not seem to be employed in the seasonal acclimatization process of the studied beetle species but apparently played a role in their evolutionary temperature adaptation. As a sign of this, the AB had a relatively high baseline PE/PC ratio, in line with the fact that this species overwinters in the coldest microhabitats of the three species (close to the surface, potentially close to frozen water) (Hiiesaar et al., 2018). However, the present experiments were performed under common-garden conditions, and thus it is unclear whether the species would have shown similar responses if acclimated to natural overwintering microhabitats. Another result refuting the HVA is the general increase in molar percentage of SM, as an increase in this lipid class is expected to increase structural integrity in lipid membranes. Still, as will be described below, there were changes in the lipid species composition of SM that do lend support to HVA. It would be interesting to further explore even lower temperatures than 5°C, since this temperature, at least for the AB, is higher than what the beetles normally face. Indeed, we might partly be observing high-temperature-related stress responses in this species.

Overall, the changes in the phospholipid species profiles found between the different diapause phases were complex, and the differences nuanced between the three Chrysomelid beetles. Indeed, the three species showed distinct phospholipid species profiles, albeit that the AB and MB grouped closer together on the PC1-axis than the CPB. The null-hypothesis in the current experiment was that phospholipid species composition would show little dynamics during diapause. This would indicate that the lipidome is formed prior to winter and then kept static during diapause (Lehmann et al., 2016), which could be explained by metabolic and biochemical costs of membrane remodeling during low-temperature and potentially hypoxic conditions (Bhat and Block, 1992). Since all three species showed large dynamism during the transition from diapause initiation to diapause maintenance, the original null-hypothesis could be rejected. This dynamism then decreased, because only small differences in the later diapause phases were observed. Since the transition from diapause initiation to diapause maintenance in the current experiment is associated with a temperature decrease from 15 to 5°C, the data strongly suggest that we are observing a plastic temperature-dependent acclimation response, even though other factors, including endogenous diapause development, are likely also important. These data therefore do lend support to the notion of a relatively static lipidome during diapause maintenance (Koštál et al., 2013; Lehmann et al., 2016), putting it in contrast to the dynamism seen in the metabolome and transcriptome of these and other species during the maintenance phase (Lehmann et al., 2015a, 2018; Ragland et al., 2015; Koštál et al., 2017).

The main qualitative change in phospholipid dynamics as beetles transitioned from diapause initiation to maintenance in all species was a shift of PC species profile toward a higher diversity in the length of acyl chains. After entering diapause, in this lipid class, the species with short (32- and 34-carbon) and long (38-carbon) acyl chains were favored, at the expense of the species with mid-length (36-carbon) acyl chains. These data suggest that the PC species profile becomes more complex as diapause progresses. The confirmatory fatty acid analyses conducted for each of the species by gas chromatography indicated that the lipids included only six quantitatively important fatty acids: 16:0, 16:1n-7, 18:0, 18:1n-9, 18:2n-6 and 18:3n-3, and several minor ones. Thus the pairs for 32-carbon phospholipid species are mainly comprised of two 16-carbon fatty acids (but see Lehmann et al., 2012). For 34-carbon species, the pair consisted of 16- and 18-carbon fatty acids, while for the lesser 38-carbon species the pair consisted of 18- and 20-carbon fatty acids. The change to a more diverse fatty acid chain length composition in lipid species has been suggested by Lewis et al. to be one hallmark of DPB (Lewis et al., 1989). In their study, they were focused on PE-species, but in our study the phenomenon was clearer for PC-species. For PE species, all beetle species showed relatively little dynamics related to the phase of the diapause, but still differed in their compositions. Both the MB and AB had a large proportion of unsaturated lipid species already during diapause initiation (the PC species 36:4, 36:5 and 36:6, and the PE species 36:5, 36:6 and 38:6). Arranging the beetle species according to their overall degree of PE unsaturation showed that the CPB had clearly lower double bond content of PE than the MB and AB, congruent with HVA-expectations. Later in diapause, the increase in long PE-species (PE 38:1 and PE 38:2) likely enhanced the DPB influence in all the species. Although PE DBI seems to be set high in MB and AB and low in CPB, the PE profile in all three species reacted little to the progression of diapause, in fact, the only temporal trend was a slight decrease in the PE DBI for the CPB, bringing it even further from that of the other species.

A feature that was common to all three beetle species was a decrease in the proportions of PS+PI between diapause initiation and the later diapause phases. These decreases support the idea of regulated metabolic suppression since both PI and PS with their derivatives have important roles in metabolism in the inner leaflets of biological membranes (Corbalán-García and Gómez-Fernández, 2014; Kay and Fairn, 2019). Apparently, the membrane lipidome changes contribute to down-regulation of metabolism. Comparing the PS and PI species profiles between diapause initiation and especially diapause termination further shows that unsaturation overall is increasing in these lipid classes, when PI species that primarily are monounsaturated

early in diapause, become polyunsaturated later (**Supplementary Figures S7, S8**). This finding is in clear agreement with the expectations of the HVA-hypothesis but at the same time the polyunsaturated species are the preferred precursors for the production of signaling derivatives (Vrablik and Watts, 2013). For SM species the data suggested interesting differences between the species. First, the AB had an overall low SM DBI. Increasing the DBI of SM occurs primarily through conversion of saturated to monounsaturated fatty acids via transcriptionally activated Δ9-desaturase (Ballweg and Ernst, 2017). Since this process is oxygen dependent (Bai et al., 2015) the AB, which might face periods in hypoxia or even anoxia during diapause, might be challenged to achieve unsaturation this way, and might instead be more dependent on dietary PUFA-containing lipids. In the CPB, which seems more aerobic during diapause, there was a small increase in the DBI of this lipid class as winter progressed, while the MB instead had a high SM DBI from the outset.

CONCLUSION

Overall, our results show that the invasive CPB has a powerful capacity of metabolic suppression and while it utilizes part of its lipid stores during diapause, as do the native cold-adapted MB and AB, lipid stores diminish only modestly. As pertains to the original hypotheses, for the energetic traits investigated, the invasive CPB shows comparable or better capacity for energy management during diapause, than the native species. However, since the CPB has a less canalized diapause lipidome, with overall large inter-individual variability than the native species, the current study suggests a diapause phenotype that is less well adapted to high-latitude conditions than native relatives. This could potentially be one reason for the retardation of expansion to higher latitudes observed globally over the last decades. Still, the data presented here shows that several relevant energy metabolism and cold-tolerance related mechanism are in place and likely could be targets for future selection also in the CPB, and further studies should target different populations across the CPB-range to see whether selection already is acting to improve cold tolerance in this important pest species. At least the metabolic diversity of the CPB, larger than what was detected in the MB and AB, could suggest capacity for evolutionary adaptation through natural selection. With warmer future winters, and provided that the phenotypes of the native MB and AB show little plasticity, they even risk facing metabolic and thermal stress during winter if diapause is shortened, food resources do not increase, and the biochemical properties of membrane lipids and proteins do not adapt fast enough.

DATA AVAILABILITY STATEMENT

All datasets analysed in this study can be found in the article/**Supplementary Material**.

AUTHOR CONTRIBUTIONS

PL and LL designed the study and collected samples. PL performed respirometry analyses while MW, PT, and RK performed lipid analyses in the HiLIPID/HiLIFE facility. PL wrote the first draft which all authors co-edited and approved.

FUNDING

This work was financed by the Academy of Finland (projects 118456, 128888) and the Finnish Centre of Excellence in Biological Interactions Research (252411).

ACKNOWLEDGMENTS

The authors wish to thank Aigi Margus for help with rearing the beetles used in the study. The Colorado potato beetle is a quarantine species in Finland, and therefore this experiment was carried out with permissions (Evira 8787/0614/2011 and Evira 2758/544/2006).

SUPPLEMENTARY MATERIAL

The Supplementary Material for this article can be found online at: https://www.frontiersin.org/articles/10.3389/fphys.2020.576617/full#supplementary-material

REFERENCES

Alyokhin, A. (2009). Colorado potato beetle management on potatoes: current challenges and future prospects. *Fruit Veg. Cereal Sci. Biotechnol.* 3, 10–19.

Arrese, E. L., and Soulages, J. L. (2010). Insect fat body: energy, metabolism, and regulation. *Annu. Rev. Entomol.* 55, 207–225. doi: 10.1146/annurev-ento-112408-085356

Athenstaedt, K., and Daum, G. (2006). The life cycle of neutral lipids: synthesis, storage and degradation. *Cell. Mol. Life Sci.* 63, 1355–1369. doi: 10.1007/s00018-006-6016-8

Bai, Y., McCoy, J. G., Levin, E. J., Sobrado, P., Rajashankar, K. R., Fox, B. G., et al. (2015). X-ray structure of a mammalian stearoyl-CoA desaturase. *Nature* 524, 252–256. doi: 10.1038/nature14549

Bale, J. S., and Hayward, S. A. L. (2010). Insect overwintering in a changing climate. *J. Exp. Biol.* 213, 980–994. doi: 10.1242/jeb.037911

Ballweg, S., and Ernst, R. (2017). Control of membrane fluidity: the OLE pathway in focus. *Biol. Chem.* 398, 215–228. doi: 10.1515/hsz-2016-0277

Beekman, M., and Stratum, P. (1999). Respiration in bumblebee queens: effect of life phase on the discontinuous ventilation cycle. *Entomol. Exp. Appl.* 92, 295–298. doi: 10.1046/j.1570-7458.1999.00550.x

Bhat, G. B., and Block, E. R. (1992). Effect of hypoxia on phospholipid metabolism in porcine pulmonary artery endothelial cells. *Am. J. Physiol. Lung. Cell. Mol. Physiol.* 262, L606–L613. doi: 10.1152/ajplung.1992.262.5.L606

Boiteau, G., and Coleman, W. (1996). Cold tolerance in the Colorado potato beetle (Leptinotarsa decemlineata) (Say) (Coleoptera: Chrysomelidea). *Can. Entomol.* 128, 1087–1099. doi: 10.4039/Ent1281087-6

Brügger, B., Erben, G., Sandhoff, R., Wieland, F. T., and Lehmann, W. D. (1997). Quantitative analysis of biological membrane lipids at the low picomole level by nano-electrospray ionization tandem mass spectrometry. *Proc. Natl. Acad. Sci. U.S.A.* 94, 2339–2344. doi: 10.1073/pnas.94.6.2339

Chown, S. L., Gibbs, A. G., Hetz, S. K., Klok, C. J., Lighton, J. R. B., and Marais, E. (2006). Discontinuous gas exchange in insects: a clarification of hypotheses and approaches. *Physiol. Biochem. Zool.* 79, 333–343. doi: 10.1086/499992

Ciancio, J. (2018). Overwintering Biology of the Brown Marmorated Stink Bug, Halyomorpha halys (Hemiptera: Pentatomidae). Available online at: https://ir.lib.uwo.ca/etd/5813 (accessed August 20, 2020).

Corbalán-García, S., and Gómez-Fernández, J. C. (2014). Classical protein kinases C are regulated by concerted interaction with lipids: the importance of phosphatidylinositol-4,5-bisphosphate. *Biophys. Rev.* 6, 3–14. doi: 10.1007/s12551-013-0125-z

Danks, H. V. (1987). *Insect Dormancy: An Ecological Perspective*. Ottawa: Biological Survey of Canada.

De Kort, C. A. D., and Koopmanschap, A. B. (1994). Nucleotide and deduced amino acid sequence of a cDNA clone encoding diapause protein 1, an arylphorin-type storage hexamer of the Colorado potato beetle. *J. Insect Physiol.* 40, 527–535. doi: 10.1016/0022-1910(94)90126-0

Denlinger, D. L., and Lee, R. E. J. (2010). *Low Temperature Biology of Insects*. Cambridge: Cambridge University Press.

Dingle, H. (ed.) (1978). *Evolution of Insect Migration and Diapause*. Berlin: Springer.

EPPO (2006). *Data sheets on quarantine pests - Leptinotarsa decemlineata*. Paris: EPPO.

Folch, J. M., Lees, M., and Sloane-Stanley, G. H. (1957). A simple method for the isolation and purification of total lipides from animal tissue. *J. Biol. Sci.* 497–509.

Fründ, J., Zieger, S. L., and Tscharntke, T. (2013). Response diversity of wild bees to overwintering temperatures. *Oecologia* 173, 1639–1648. doi: 10.1007/s00442-013-2729-1

Große, W., and Schröder, P. (1984). Oxygen supply of roots by gas transport in alder-trees. *Z. Naturforsch. C* 39, 1186–1188. doi: 10.1515/znc-1984-11-1234

Guppy, M., and Wither, P. (1999). Metabolic depression in animals: physiological perspectives and biochemical generealizations. *Biol. Rev.* 74, 1–40. doi: 10.1111/j.1469-185x.1999.tb00180.x

Hahn, D. A., and Denlinger, D. L. (2007). Meeting the energetic demands of insect diapause: Nutrient storage and utilization. *J. Insect Physiol.* 53, 760–773. doi: 10.1016/j.jinsphys.2007.03.018

Hahn, D. A., and Denlinger, D. L. (2011). Energetics of insect diapause. *Annu. Rev. Entomol.* 56, 103–121. doi: 10.1146/annurev-ento-112408-085436

Haimi, P., Uphoff, A., Hermansson, M., and Somerharju, P. (2006). Software tools for analysis of mass spectrometric lipidome data. *Anal. Chem.* 78, 8324–8331. doi: 10.1021/ac061390w

Hazel, J. R. (1995). Thermal adaptation in biological membranes: Is homeoviscous adaptation the explanation? *Annu. Rev. Physiol.* 57, 19–42. doi: 10.1146/annurev.ph.57.030195.000315

Hiiesaar, K., Kaart, T., Williams, I. H., Luik, A., Metspalu, L., Ploomi, A., et al. (2018). Dynamics of Supercooling Ability and Cold Tolerance of the Alder Beetle (Coleoptera: Chrysomelidae). *Environ. Entomol.* 47, 1024–1029. doi: 10.1093/ee/nvy075

Hodek, I. (2012). Adult Diapause in Coleoptera. *Psyche* 2012, 1–10. doi: 10.1155/2012/249081

Irwin, J. T., and Lee, R. E. J. (2003). Cold winter microenvironments conserve energy and improve overwintering survival and potential fecundity of the goldenrod gall fly, Eurosta solidaginis. *Oikos* 100, 71–78. doi: 10.1034/j.1600-0706.2003.11738.x

Izzo, V. M., Hawthorne, D. J., and Chen, Y. H. (2014). Geographic variation in winter hardiness of a common agricultural pest, Leptinotarsa decemlineata, the Colorado potato beetle. *Evol. Ecol.* 28, 505–520. doi: 10.1007/s10682-013-9681-8

Jõgar, K., Kuusik, A., Metspalu, L., Hiiesaar, K., Luik, A., Mänd, M., et al. (2004). The relations between the patterns of gas exchange and water loss in diapausing pupae of large white butterfly Pieris brassicae (Lepidoptera: Pieridae). *Eur. J. Entomol.* 101, 467–472. doi: 10.14411/eje.2004.066

Johnson, C. G. (1967). International dispersal of insects and insect-borne viruses. *Neth. J. Plant Pathol.* 73, 21–43. doi: 10.1007/BF01974421

Kates, M. (1986). *Techniques of Lipidology*. Amsterdam: Elsevier.

Kay, J. G., and Fairn, G. D. (2019). Distribution, dynamics and functional roles of phosphatidylserine within the cell. *Cell Commun. Signal.* 17:126. doi: 10.1186/s12964-019-0438-z

Kölsch, G., Jakobi, K., Wegener, G., and Braune, H. J. (2002). Energy metabolism and metabolic rate of the alder leaf beetle *Agelastica alni* (L.) (Coleoptera, Chrysomelidae) under aerobic and anaerobic conditions: a microcalorimetric study. *J. Insect Physiol.* 48, 143–151. doi: 10.1016/S0022-1910(01)00158-5

Kort, C. A. D. (1990). Thirty-five years of diapause research with the Colorado potato beetle. *Entomol. Exp. Appl.* 56, 1–13. doi: 10.1111/j.1570-7458.1990.tb01376.x

Koštál, V. (2006). Eco-physiological phases of insect diapause. *J. Insect Physiol* 113–127. doi: 10.1016/j.jinsphys.2005.09.008

Koštál, V. (2010). "Cell structural modifications in insects at low temperatures," in *Low Temperature Biology of Insects*, eds D. L. Denlinger and R. E. J. Lee (Cambridge: Cambridge University Press), 116–132. doi: 10.1017/cbo9780511675997.006

Koštál, V., Štìtina, T., Poupardin, R., Korbelová, J., and Bruce, A. W. (2017). Conceptual framework of the eco-physiological phases of insect diapause development justified by transcriptomic profiling. *Proc. Natl. Acad. Sci. U.S.A.* 114, 8532–8537. doi: 10.1073/pnas.1707281114

Koštál, V., Urban, T., Øimnáèová, L., Berková, P., and Šimek, P. (2013). Seasonal changes in minor membrane phospholipid classes, sterols and tocopherols in overwintering insect, *Pyrrhocoris apterus*. *J. Insect Physiol.* 59, 934–941. doi: 10.1016/j.jinsphys.2013.06.008

Lal, R. (ed.) (2017). *Encyclopedia of Soil Science*. Boca Raton, FL: CRC Press.

Leather, S. R. (1993). *The Ecology of Insect Overwintering*. Cambridge: Cambridge University Press.

Lefevere, K. S., and De Kort, C. A. D. (1989). Adult diapause in the Colorado potato beetle, Leptinotarsa decemlineata: effects of external factors on maintenance, termination and post-diapause development. *Physiol. Entomol.* 14, 299–308. doi: 10.1111/j.1365-3032.1989.tb01097.x

Lefevere, K. S., Koopmanschap, A. B., and De Kort, C. A. D. (1989). Changes in the concentrations of metabolites in haemolymph during and after diapause in female Colorado potato beetle, Leptinotarsa decemlineata. *J. Insect Physiol.* 35, 121–128. doi: 10.1016/0022-1910(89)90045-0

Lehmann, P., Lyytinen, A., Sinisalo, T., and Lindström, L. (2012). Population dependent effects of photoperiod on diapause related physiological traits in an invasive beetle (Leptinotarsa decemlineata). *J. Insect Physiol.* 58, 1146–1158. doi: 10.1016/j.jinsphys.2012.06.003

Lehmann, P. (2013). *Eco-physiological Aspects of Adaptation to Seasonal Environments: The Latitudinal Range Expansion of the Colorado potato beetle Across Europe*. Available online at: http://urn.fi/URN:ISBN:978-951-39-5364-5 (accessed August 15, 2020).

Lehmann, P., Lyytinen, A., Piiroinen, S., and Lindström, L. (2014a). Northward range expansion requires synchronization of both overwintering behavior and physiology with photoperiod in the invasive Colorado potato beetle (Leptinotarsa decemlineata). *Oecologia* 176, 57–68. doi: 10.1007/s00442-014-3009-4

Lehmann, P., Piiroinen, S., Kankare, M., Lyytinen, A., Paljakka, M., and Lindström, L. (2014b). Photoperiodic effects on diapause-associated gene expression trajectories in European *Leptinotarsa decemlineata* populations. *Insect Mol. Biol.* 23, 566–578. doi: 10.1111/imb.12104

Lehmann, P., Kaunisto, S., Koštál, V., Margus, A., Zahradníèková, H., and Lindström, L. (2015a). Comparative ecophysiology of cold-tolerance-related traits: assessing range expansion potential for an invasive insect at high latitude. *Physiol. Biochem. Zool.* 3, 254–265. doi: 10.1086/680384

Lehmann, P., Piiroinen, S., Lyytinen, A., and Lindström, L. (2015b). Responses in metabolic rate to changes in temperature in diapausing Colorado potato beetle *Leptinotarsa decemlineata* from three European populations. *Physiol. Entomol.* 40, 123–130. doi: 10.1111/phen.12095

Lehmann, P., Lyytinen, A., Piiroinen, S., and Lindström, L. (2015c). Latitudinal differences in diapause related photoperiodic responses of European Colorado potato beetles (*Leptinotarsa decemlineata*). *Evol. Ecol.* 29, 269–282. doi: 10.1007/s10682-015-9755-x.

Lehmann, P., Pruisscher, P., Posledovich, D., Carlsson, M., Käkelä, R., Tang, P., et al. (2016). Energy and lipid metabolism during direct and diapause development in a pierid butterfly. *J. Exp. Biol.* 219, 3049–3060.

Lehmann, P., Pruisscher, P., Koštál, V., Moos, M., Šimek, P., Nylin, S., et al. (2018). Metabolome dynamics of diapause in the butterfly *Pieris napi*: distinguishing maintenance, termination and post-diapause phases. *J. Exp. Biol.* 221:jeb169508.

Lehmann, P., Ammunét, T., Barton, M., Battisti, A., Eigenbrode, S. D., Jepsen, J. U., et al. (2020). Complex responses of global insect pests to climate warming. *Front. Ecol. Environ.* 18, 141–150. doi: 10.1002/fee.2160

Lewis, R. N. A. H., Mannock, D. A., McElhaney, R. N., Turner, D. C., and Gruner, S. M. (1989). Effect of fatty acyl chain length and structure on the lamellar gel to liquid-crystalline and lamellar to reversed hexagonal phase transitions of aqueous phosphatidylethanolamine dispersions. *Biochemistry* 28, 541–548. doi: 10.1021/bi00428a020

Lighton, J. B. R. (2008). *Measuring Metabolic Rates: A Manual for Scientists*. New York, NY: Oxford University Press.

Lighton, J. R. B. (1998). Notes from underground: Towards ultimate hypotheses of cyclic, discontinuous gas-exchange in tracheate arthropods. *Am. Zool.* 38, 483–491. doi: 10.1093/icb/38.3.483

Lindestad, O., Schmalensee, L., Lehmann, P., and Gotthard, K. (2020). Variation in butterfly diapause duration in relation to voltinism suggests adaptation to autumn warmth, not winter cold. *Funct. Ecol.* 34, 1029–1040. doi: 10.1111/1365-2435.13525

Lindström, L., and Lehmann, P. (2015). "Climate change effects on agricultural insect pests in Europe," in *Climate Change and Insect Pests*, eds C. Björkman and P. Niemelä (Wallingford: CABI), 136–153. doi: 10.1079/9781780643786.0136

Lyytinen, A., Mappes, J., and Lindström, L. (2012). Variation in Hsp70 levels after cold shock: signs of evolutionary responses to thermal selection among *Leptinotarsa decemlineata* populations. *PLoS ONE* 7:e31446. doi: 10.1371/journal.pone.0031446

Marèelja, S. (1976). Lipid-mediated protein interaction in membranes. *Biochim. Biophys. Acta* 455, 1–7.

Matthews, P. G. D., and White, C. R. (2011). Discontinuous gas exchange in insects: Is it all in their heads? *Am. Nat.* 177, 130–134. doi: 10.1086/657619

May, M. L. (1989). Oxygen consumption by adult Colorado potato beetles, Leptinotarsa decemlineata (Say) (Coleoptera: Chrysomelidae). *J. Insect Physiol.* 35, 797–804. doi: 10.1016/0022-1910(89)90138-8

Murphy, R. C., James, P. F., McAnoy, A. M., Krank, J., Duchoslav, E., and Barkley, R. M. (2007). Detection of the abundance of diacylglycerol and triacylglycerol molecular species in cells using neutral loss mass spectrometry. *Anal. Biochem.* 366, 59–70. doi: 10.1016/j.ab.2007.03.012

Nickels, J. D., Smith, M. D., Alsop, R. J., Himbert, S., Yahya, A., Cordner, D., et al. (2019). Lipid rafts: buffers of cell membrane physical properties. *J. Phys. Chem. B* 123, 2050–2056. doi: 10.1021/acs.jpcb.8b12126

Noronha, C., and Cloutier, C. (1998). Effects of soil conditions and body size on digging by prediapause Colorado potato beetles. *Can. J. Zool.* 76, 1705–1713.

Piiroinen, S., Ketola, T., Lyytinen, A., and Lindström, L. (2011). Energy use, diapause behaviour and northern range expansion potential in the invasive Colorado potato beetle: Energy use and diapause behaviour. *Funct. Ecol.* 25, 527–536. doi: 10.1111/j.1365-2435.2010.01804.x

Ploomi, A., Kuusik, A., Jõgar, K., Metspalu, L., Hiiesaar, K., Karise, R., et al. (2018). Variability in metabolic rate and gas exchange patterns of the Colorado potato beetle of winter and prolonged diapauses: gas exchange patterns of Colorado potato beetle. *Physiol. Entomol.* 43, 251–258. doi: 10.1111/phen.12254

Raclot, T. (2003). Selective mobilization of fatty acids from adipose tissue triacylglycerols. *Prog. Lipid Res.* 42, 257–288. doi: 10.1016/S0163-7827(02)00066-8

Raclot, T., Holm, C., and Langin, D. (2001). Fatty acid speci?city of hormone-sensitive lipase: implication in the selective hydrolysis of triacylglycerols. *J. Lipid Res.* 2049–2057.

Ragland, G. J., Almskaar, K., Vertacnik, K. L., Gough, H. M., Feder, J. L., Hahn, D. A., et al. (2015). Differences in performance and transcriptome-wide gene expression associated with Rhagoletis (Diptera: Tephritidae) larvae feeding in alternate host fruit environments. *Mol. Ecol.* 24, 2759–2776.

Rao, K., and Lakshminarayana, G. (1988). Lipid class and fatty acid composition of edible tissues of *Peucedanim graveolens*, *Mentha arvensis*, and *Colocasia esculenta* plants. *J. Agric. Food Chem.* 36, 475–578. doi: 10.1021/jf00081a017

Rozsypal, J., Koštál, V., Berková, P., Zahradníèková, H., and Šimek, P. (2014). Seasonal changes in the composition of storage and membrane lipids in overwintering larvae of the codling moth, *Cydia pomonella*. *J. Therm. Biol.* 45, 124–133. doi: 10.1016/j.jtherbio.2014.08.011

Rozsypal, J., Koštál, V., Zahradníèková, H., and Šimek, P. (2013). Overwintering strategy and mechanisms of cold tolerance in the codling moth (*Cydia pomonella*). *PLoS One* 8:e61745. doi: 10.1371/journal.pone.0061745

Schmidt-Nielsen, K. (1990). *Animal Physiology: Adaptation and Environment*. Cambridge: Cambridge University Press.

Schneiderman, H., and Williams, C. (1953). The physiology of insect diapause. VII. The respiratory metabolism of the Cecropia silkworm during diapause and development. *Biol. Bull.* 105, 320–334.

Silfverberg, H. (2011). Enumeratio renovata Coleopterorum Fennoscandiae, Daniae et Baltiae. *Sahlbergia* 16, 1–144.

Sinclair, B. J. (2015). Linking energetics and overwintering in temperate insects. *J. Therm. Biol.* 54, 5–11. doi: 10.1016/j.jtherbio.2014.07.007

Sinensky, M. (1974). Homeoviscous adaptation: a homeostatic process that regulates the viscosity of membrane lipids in *Escherichia coli*. *Proc. Natl. Acad. Sci. U.S.A.* 71, 522–525. doi: 10.1073/pnas.71.2.522

Šlachta, M., Berková, P., Vambera, J., and Koštál, V. (2002). Physiology of cold-acclimation in non-diapausing adults of *Pyrrhocoris apterus* (Heteroptera). *Eur. J. Entomol.* 99, 181–187. doi: 10.14411/eje.2002.026

Sokal, R. R., and Rohlf, F. J. (2003). *Biometry: The Principles and Practice of Statistics in Biological Research*. New York, NY: W.H. Freeman and Company.

Stålhandske, S., Lehmann, P., Pruisscher, P., and Leimar, O. (2015). Effect of winter cold duration on spring phenology of the orange tip butterfly. Anthocharis cardamines. *Ecol. Evol.* 5, 5509–5520.

Tauber, M. J., Tauber, C. A., and Masaki, S. (1986). *Seasonal Adaptations of Insects*. Oxford: Oxford University Press.

Toprak, U., Hegedus, D., Doðan, C., and Güney, G. (2020). A journey into the world of insect lipid metabolism. *Arch. Insect Biochem. Physiol.* 104, 1–67. doi: 10.1002/arch.21682

Tougeron, K. (2019). Diapause research in insects: historical review and recent work perspectives. *Entomol. Exp. Appl.* 167, 27–36. doi: 10.1111/eea.12753

Toxopeus, J., and Sinclair, B. J. (2018). Mechanisms underlying insect freeze tolerance. *Biol. Rev.* 93, 1891–1914. doi: 10.1111/brv.12425

Urbanski, J., Mogi, M., O'Donnell, D., DeCotiis, M., Toma, T., and Armbruster, P. (2012). Rapid adaptive evolution of photoperiodic response during invasion and range expansion across a climatic gradient. *Am. Nat.* 179, 490–500.

Ushatinskaya, R. S. (1977). Seasonal migration of the imago of the Colorado potato beetle (Leptinotarsa decemlineata Say) in different types of soil and the physiological variations of specimens in hibernating populations. *Ecol. Bull.* 25, 526–529.

Vrablik, T. L., and Watts, J. L. (2013). Polyunsaturated fatty acid derived signaling in reproduction and development: insights from *Caenorhabditis elegans* and *Drosophila melanogaster*. *Mol. Reprod. Dev.* 80, 244–259. doi: 10.1002/mrd.22167

Williams, C., Hellmann, J., and Sinclair, B. (2012). Lepidopteran species differ in susceptibility to winter warming. *Clim. Res.* 53, 119–130. doi: 10.3354/cr01100

Williams, C. M., Chick, W. D., and Sinclair, B. J. (2015). A cross-seasonal perspective on local adaptation: metabolic plasticity mediates responses to winter in a thermal-generalist moth. *Funct. Ecol.* 29, 549–561. doi: 10.1111/1365-2435.12360

Williams, C. M., Henry, H. A. L., and Sinclair, B. J. (2014). Cold truths: How winter drives responses of terrestrial organisms to climate change. *Biol. Rev.* 90, 214–235.

Williams, C. M., McCue, M. D., Sunny, N. E., Szejner-Sigal, A., Morgan, T. J., Allison, D. B., et al. (2016). Cold adaptation increases rates of nutrient flow and metabolic plasticity during cold exposure in Drosophila melanogaster. *Proc. Biol. Sci.* 283:20161317.

Wodtke, E. (1981). Temperature adaptation of biological membranes. *Biochim. Biophys. Acta* 640, 710–720.

Wold, S., and Sjöström, M. (1977). "SIMCA: a method for analyzing chemical data in terms of similarity and analogy," in *Chemometrics: Theory and Application,* ed. B. R. Kowalski (Washington, DC: American Chemical Society).

Xu, X., Akbar, S., Shrestha, P., Venugoban, L., Devilla, R., Hussain, D., et al. (2020). A synergistic genetic engineering strategy induced triacylglycerol accumulation in potato (*Solanum tuberosum*) leaf. *Front. Plant Sci.* 11:215. doi: 10.3389/fpls.2020.00215.

Yocum, G. D., Buckner, J. S., and Fatland, C. L. (2011a). A comparison of internal and external lipids of nondiapausing and diapause initiation phase adult Colorado potato beetles, Leptinotarsa decemlineata. *Comp. Biochem. Physiol. B Biochem. Mol. Biol.* 159, 163–170. doi: 10.1016/j.cbpb.2011.03.007

Yocum, G. D., Rinehart, J. P., and Larson, M. L. (2011b). Monitoring diapause development in the Colorado potato beetle, Leptinotarsa decemlineata, under field conditions using molecular biomarkers. *J. Insect Physiol.* 57, 645–652.

Zehmer, J. K. (2005). Thermally induced changes in lipid composition of raft and non-raft regions of hepatocyte plasma membranes of rainbow trout. *J. Exp. Biol.* 208, 4283–4290. doi: 10.1242/jeb.01899

Conflict of Interest: The authors declare that the research was conducted in the absence of any commercial or financial relationships that could be construed as a potential conflict of interest.

frontiers in Physiology

REVIEW
published: 29 September 2020
doi: 10.3389/fphys.2020.577717

Physiological and Pathological Regulation of Peripheral Metabolism by Gut-Peptide Hormones in *Drosophila*

*Xiaoya Zhou[1,2], Guangming Ding[1,2], Jiaying Li[1,2], Xiaoxiang Xiang[1,2], Elisabeth Rushworth[1,2] and Wei Song[1,2]**

[1]*Department of Oncology, Renmin Hospital of Wuhan University, Wuhan, China,* [2]*Frontier Science Center for Immunology and Metabolism, Medical Research Institute, Wuhan University, Wuhan, China*

The gastrointestinal (GI) tract in both vertebrates and invertebrates is now recognized as a major source of signals modulating, *via* gut-peptide hormones, the metabolic activities of peripheral organs, and carbo-lipid balance. Key advances in the understanding of metabolic functions of gut-peptide hormones and their mediated interorgan communication have been made using *Drosophila* as a model organism, given its powerful genetic tools and conserved metabolic regulation. Here, we summarize recent studies exploring peptide hormones that are involved in the communication between the midgut and other peripheral organs/tissues during feeding conditions. We also highlight the emerging impacts of fly gut-peptide hormones on stress sensing and carbo-lipid metabolism in various disease models, such as energy overload, pathogen infection, and tumor progression. Due to the functional similarity of intestine and its derived peptide hormones between *Drosophila* and mammals, it can be anticipated that findings obtained in the fly system will have important implications for the understanding of human physiology and pathology.

Keywords: gut hormone, *Drosophila*, metabolism and endocrinology, disease model, nutrient sensing, gut bacteria, tumor-induced wasting, stress sensing

OPEN ACCESS

Edited by:
Kai Lu,
Fujian Agriculture and Forestry University, China

Reviewed by:
Erjun Ling,
Shanghai Institutes for Biological Sciences (CAS), China
Christian Wegener,
Julius Maximilian University of Würzburg, Germany

****Correspondence:***
Wei Song
songw@whu.edu.cn

Specialty section:
This article was submitted to Invertebrate Physiology, a section of the journal Frontiers in Physiology

Received: *29 June 2020*
Accepted: *07 September 2020*
Published: *29 September 2020*

Citation:
Zhou X, Ding G, Li J, Xiang X, Rushworth E and Song W (2020) Physiological and Pathological Regulation of Peripheral Metabolism by Gut-Peptide Hormones in Drosophila. Front. Physiol. 11:577717. doi: 10.3389/fphys.2020.577717

INTRODUCTION

More than 100 bioactive gut-peptide hormones are produced by enteroendocrine cells (EEs) in the gastrointestinal (GI) tract, which is thus considered as the biggest endocrine organ in vertebrates (Sun et al., 2018). Emerging therapies, which are based on gut-peptide hormones and have been proven to be efficient in the treatment of metabolic disorders (Alexiadou et al., 2019), have drawn increasing attention to the gut-peptide-hormone modulation of systemic energy balance, including carbo-lipid metabolism in the liver, adipose tissue, muscle, heart, kidney, pancreas, bone, immune cells, as well as brain (Martin et al., 2019). The *Drosophila* intestine exhibits high similarities with the mammalian GI tract, not only in structure and physiology (**Figure 1**), but also in the production of gut-peptide hormones and its impact on metabolism homeostasis (Miguel-Aliaga et al., 2018). Research using the *Drosophila* system has addressed several fundamental issues regarding the function and regulation of gut-peptide hormones. In this review, we will summarize the types, metabolic impacts, stress sensing, and

participating signaling pathways of adult fly gut-peptide hormones under both physiological and pathological conditions.

TYPES AND FUNCTIONS OF *DROSOPHILA* GUT-PEPTIDE HORMONES

The luminal surface of the *Drosophila* adult intestine comprises four cell types (**Figure 1B**): intestinal stem cells (ISCs), enteroblasts (EBs), enterocytes (ECs), and enterendocrine cells (EEs). The epithelium is covered and protected by a peritrophic membrane (PM), equivalent to human mucus, from intestinal microbes. The epithelial monolayer is aligned on its basal side on the basement membrane (BM). There are visceral muscles (VMs) that drive peristaltic movements, trachea that provide oxygen, and innervated neurons, underneath the BM (Miguel-Aliaga et al., 2018). Similar to that of vertebrates, the majority of gut-peptide hormones are produced by the fly EEs to target distal organs (Reiher et al., 2011; Liu and Jin, 2017). Interestingly, growing evidence indicates that other cell types, like ECs and VMs, also produce bioactive peptides in response to extracellular stresses, many of which have shown systemic metabolic influences and are considered as novel gut-peptide hormones (**Figure 1C**).

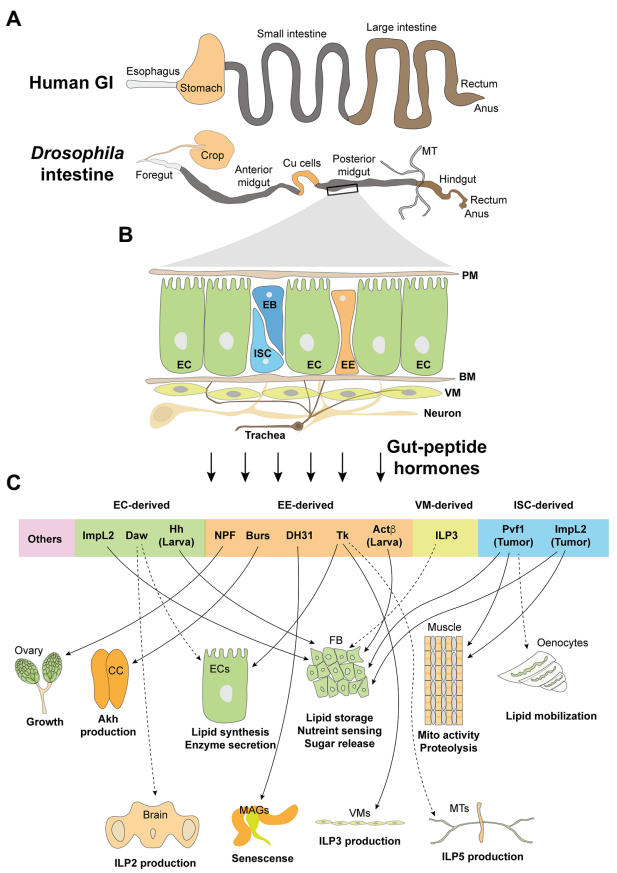

FIGURE 1 | The adult intestine and its cell types and derived peptide hormones. **(A)** Human and *Drosophila* adult intestines share high similarities in the esophagus/foregut, small intestine/midgut, large intestine/hindgut, rectum, as well as anus. Differences include the presence of *Drosophila* Malpighian tubules (MT) that functions as human kidney. Moreover, crop and Cu cells function as storage digestive organs, respectively, to partially mimic the stomach. **(B)** General composition and cell types of adult midgut: PM, peritrophic membrane; EC, enterocyte; ISC, intestinal stem cell; EB, enteroblast; EE, enteroendocrine cell; BM, basement membrane; VM, visceral muscle; neuron and trachea. **(C)** Gut hormones, which are derived by different cell types, target various organs and modulate their metabolic activities. CC, corpora cardiaca; FB, fat body; MAGs, male accessory glands.

EE-Derived-Peptide Hormones

A few established proproteins, like allatostatin A (AstA), AstB/Mip, AstC, neuropeptide F (NPF), short neuropeptide F (sNPF), tachykinin (TK), diuretic hormone 31 (DH31), and CCHamides 1 (CCHa1) and CCHa2, which can be processed into over 20 mature peptides, are produced by both larval and adult EEs as shown using antibody detection and proteomic analysis (Veenstra et al., 2008; Veenstra, 2009; Reiher et al., 2011). The protein maturation of the prohormones into multiple bioactive peptides in EEs is processed by a conserved prohormone convertase Amon and, probably, other putative enzyme homologs, like dCPD, Phm, and Pal1/2 (Reiher et al., 2011). Emerging single-cell RNAseq (scRNAseq) technologies have identified additional gut-peptide hormones in the EEs (Guo et al., 2019; Hung et al., 2020; **Table 1**). Even though several gut-peptide hormones such as DH31 and Tk were previously shown by *in vitro* assays to stimulate gut mobility and possible nutrient delivery decades ago (Siviter et al., 2000; LaJeunesse et al., 2010), the investigation of their physiological roles is largely hampered due to lack of genetic tools. As most Gal4 lines for genes that encode gut-peptide hormones in EEs also target those neurons expressing the same genes in the brain, it is very difficult to distinguish their roles in the gut and brain.

We have established a *Tk-g-Gal4*, that is predominantly expressed in all Tk$^+$ EEs, the most abundant one accounting for ~40% EEs in the midgut (Song et al., 2014), and a very small portion of Tk$^+$ neurons in the brain. Using this *Tk-g-Gal4*, we are able to ablate Tk$^+$ EEs and diminish Tk production in the gut with rarely affecting its expression in the brain, thus revealing *in vivo* metabolic roles of gut Tk in intestinal and systemic lipid metabolism. Mature gut-peptides Tk1–Tk5, which are processed from the pro-Tk, target the G-protein coupled receptor (GPCR) TkR99D in the ECs and triggers cAMP/PKA signaling to suppress the activity of Sterol regulatory-element binding protein (SREBP) and lipogenic programs in the gut, leading to decreased lipid production in the ECs and reduced lipid storage in the whole body. In addition, gut Tk6, another pro-Tk-derived mature peptide, activates another GPCR TkR86C in the VMs and increases ILP3 production to modulate both local and systemic insulin signaling and lipid homeostasis (Poels et al., 2009; Amcheslavsky et al., 2014; Kamareddine et al., 2018). Tk has been reported to activate Malpighian tubules (MTs; Soderberg et al., 2011), as well as ILP-producing cells (IPCs) in the brain (Birse et al., 2011), *via* TkR99D to regulate ILPs secretion and nutrient-deprivation response as well. Thus, it is believed that gut-derived Tk targets multiple tissues/organs to collectively regulate systemic energy homeostasis.

TABLE 1 | Summary of metabolic impacts of gut-peptide hormones in *Drosophila*.

Cell types	Gut hormones	Metabolic impacts	Targeted organs
EC	Daw	Decrease EC enzyme production and increase ILP2 production in IPCs (Chng et al., 2014; Ghosh and O'Connor, 2014)	ECs, IPCs
	ImpL2	Decrease lipid storage (Hang et al., 2014)	ECs, FB
	Hh (larva)	Increase lipid mobilization (Rodenfels et al., 2014; Zhang et al., 2020)	FB
	Tk	Increase lipid production in ECs and ILP3 release in VMs (Song et al., 2014; Kamareddine et al., 2018)	ECs, VMs
	NPF	Unknown (Ameku et al., 2018)	Ovary
EE	DH31	Unknown (Takeda et al., 2018)	MAGs
	Burs	Increase Akh release and lipid mobilization (Scopelliti et al., 2019)	Neuron
	Actβ (larva)	Increase Akh response (Song et al., 2017)	FB
ISC/tumor	ImpL2	Increase lipid loss, glycemic level, and muscle wasting (Kwon et al., 2015)	Multiple
	Pvf1	Increase lipid loss and muscle wasting (Ghosh et al., 2019; Song et al., 2019)	FB, muscle, oenocytes
VM	ILP3	Increase systemic insulin signaling and lipid storage (Kamareddine et al., 2018)	Multiple

Single-cell RNAseq and biochemical analysis indicate that Tk$^+$ EEs also produce DH31, Burs, NPF, Gpb5, and Nplp2, in different regions of the midgut (Chen et al., 2016a; Guo et al., 2019; Hung et al., 2020). Another study using the *Tk-g-Gal4* revealed that gut NPF non-autonomously controls mating-induced proliferation of germline stem cells *via* ovarian NPF receptor (NPFR; Ameku et al., 2018). Like TkR99D, NPFR is also expressed in MTs and is highly associated with nutrient-deprivation response (Chintapalli et al., 2012). It will be interesting to determine whether gut NPF regulates systemic metabolic homeostasis together with Tk.

Pros-Gal4, a driver that specifically targets all EEs in the midgut and a few neuroendocrine cells (Scopelliti et al., 2019), has recently been used for characterizing the functions of gut-peptide hormones in *Drosophila*. Even though the gut-peptide hormone Burs is produced by a small subset of Tk$^+$ EEs (Chen et al., 2016a), a group has characterized its opposite role to that of Tk in lipid metabolic control by knocking down its expression in EEs with *Pros-Gal4* (Scopelliti et al., 2019). They demonstrated that Burs remotely activates the GPCR DLgr2 in a specialized type of neurons and subsequently inhibits the activity of neighbor neuroendocrine cells that produce adipokinectic hormone (Akh) in the corpora cardiaca (CC). Akh is the key hormone modulating lipid mobilization and carbohydrate release in the fat body *via* AkhR/cAMP/PKA cascade and promoting food seeking through a subset of neurons in the brain (Kim and Rulifson, 2004; Gronke et al., 2007; Huang et al., 2020). Gut-derived Burs, therefore, impairs Akh-associated triglyceride (TAG) breakdown and promotes systemic lipid accumulation.

Using *Pros-Gal4* to eliminate the expression of DH31 in the midgut, another group revealed that gut-derived DH31 remotely regulates the senescent responses of male accessory glands (MAGs; Takeda et al., 2018), suggesting the hormonal effects of this gut peptide. Since DH31 has been reported to target MTs *via* the GPCR Dh31-R (Coast et al., 2001; Johnson et al., 2005), it could be anticipated that gut-derived DH31 also modulates MTs function, like water flux as well as systemic metabolic homeostasis.

Earlier studies indicated that AstC$^+$ EEs, another large subpopulation of EEs in the midgut, also produce multiple gut peptides, such as AstA, AstB/Mip, CCHa1, and CCHa2 (Chen et al., 2016a; Guo et al., 2019). CCHa2 deficiency is associated with impaired ILPs production in larval brain (Ren et al., 2015; Sano et al., 2015). Even though, at least, fat-body-produced CCHa2 is shown to contribute to the regulation of ILP2 secretion (Sano et al., 2015), the origins of bioactive CCHa2 are still controversial. Using different drivers to examine whether brain- or gut-derived CCHa2 also targets adult IPCs in the brain and modulate systemic energy balance will help address this puzzle in the future (Ren et al., 2015; Sano et al., 2015).

Global *AstA* removal results in disruption of systemic lipid homeostasis and appetite control (Hergarden et al., 2012; Chen et al., 2016b). It is considered as a direct regulation of Akh and insulin releases by AstA, as the GPCR of AstA, AstA-R2, is highly expressed in both Akh- and insulin-producing cells (Hentze et al., 2015). However, these studies failed to distinguish the differential functions between gut- and brain-derived AstA. Another group used *Pros-Gal4* to knock down AstA expression in the midgut and revealed its systemic role as a peptide hormone in longevity modulation (Takeda et al., 2018). Therefore, it is possible that gut AstA modulates release of Akh or insulin to affect energy homeostasis, but further genetic validation is required.

Remarkably, flies lacking all EEs are relatively normal in terms of food intake and carbo-lipid metabolism but are shorter-lived (Amcheslavsky et al., 2014), indicating anticipated counter-regulatory impacts between distinct gut-peptide hormones on energy balance. We speculate that flies might execute differential metabolic impacts *via* certain gut-peptide hormones in the context of various stress responses.

In addition to adult EEs, larval EEs produce peptide hormones to regulate systemic metabolism as well. We have recently characterized Activin-β (Actβ) as an important EE-derived peptide hormone in the larval midgut (Song et al., 2017). Using *Actβ-Gal4*, *Tk-g-Gal4*, as well as *Pros-Gal4*, we uncovered that gut-derived Actβ remotely activates Babo/Smox signaling in the fat body and enhances its Akh response, leading to carbohydrate breakdown and elevation of glycemic level.

EC-Derived-Peptide Hormones

Enterocyte is the biggest cell population in both larval and adult midguts and also produces multiple peptide hormones that regulate systemic energy homeostasis (**Figure 1C** and **Table 1**). ImpL2, an established hormone robustly blocking circulating ILP bioavailabilities and downregulating systemic insulin signaling (Honegger et al., 2008), is majorly expressed in the adult ECs (Hung et al., 2020) and is associated with the impairment of lipid metabolism caused by gut bacteria (Hang et al., 2014). Adult ECs also produce the TGF-beta/activin ligand, Dawdle (Daw), into the hemolymph to impair systemic carbo-lipid homeostasis. Possible mechanisms include that Babo/Smox signaling modulates the expression of carbohydrases and insulin secretion in the ECs and brain IPCs, respectively (Chng et al., 2014; Ghosh and O'Connor, 2014). In addition, larval ECs secret Hedgehog (Hh), a conserved ligand that regulates metabolism and development across species (Teperino et al., 2014), *via* lipoprotein particles into the hemolymph to directly activate Ci/Bmm-axis and lipolysis in the fat body, resulting in systemic lipid loss (Rodenfels et al., 2014; Zhang et al., 2020).

There are a few cytokines, like Upd3 and Dpp (Jiang et al., 2009; Tian and Jiang, 2017), produced by ECs to maintain local tissue homeostasis. ECs also secret bioactive enzymes, including multiple trypsins for food digestion and peptidoglycan recognition proteins (PGRPs) that degrade gut-bacteria-derived peptidoglycans (PGNs) and blunt inflammatory responses (Guo et al., 2014; Charroux et al., 2018), to affect systemic carbo-lipid metabolism. It will be interesting to investigate whether they function as circulating hormones and directly affect metabolic activities of other organs in the future.

Peptide Hormones Derived by Other Intestinal Cell Types

Other gut cell types also produce peptide hormones that execute important metabolic roles (**Figure 1C** and **Table 1**). VM-secreted ILP3, which was previously characterized to maintain local insulin signaling and ISC activity in the gut (O'Brien et al., 2011), is currently found to contribute to insulin signaling in the whole fly (Kamareddine et al., 2018). ISCs that bear an active oncogene *yki* proliferate as malignant tumors and produce large amounts of bioactive peptide hormones, like ImpL2 and Pvf1, to impair lipid metabolism in the fat body (Kwon et al., 2015; Song et al., 2019). Despite the peptide hormones mentioned above, other cytokines/peptides, such as Delta (Dl) in ISCs (Ohlstein and Spradling, 2007), vein (vn) in VMs (Biteau and Jasper, 2011), PDF in neurons (Talsma et al., 2012), as well as Dpp in gut-associated trachea and hemocytes (Li et al., 2013; Ayyaz et al., 2015; **Table 2**), that influence ISC activity and local gut homeostasis have shown very limited impacts on metabolic activities of distal organs. Thus, we will not discuss them further in this review.

DIETARY REGULATION OF GUT-PEPTIDE-HORMONE PRODUCTION

Gut-peptide hormones act in concert to modulate the physiologies of both GI itself and other distal organs to ensure nutrient absorption, delivery, mobilization, as well as storage, after a meal. Note that, the production and release of gut-peptide hormones are directly controlled by the digested food in a

TABLE 2 | Summary of gut-produced cytokines/peptides in *Drosophila*.

Cell types	Gut peptides
ISC/EB	Dl, ILP6, egr, Hh, spi, wg, Upd1, and Upd2 (Ohlstein and Spradling, 2007; Jiang et al., 2009; Karpowicz et al., 2010; Osman et al., 2012; Tian et al., 2015, 2016; Doupe et al., 2018)
EC	Hh, Dpp, Gbb, Krn, PGRP-SA, PGRP-SB1, PGRP-SC1a, PGRP-SC1b, PGRP-SC2, PGRP-SD, PGRP-LB, Upd1, Upd2, and Upd3 (Werner et al., 2000; Bischoff et al., 2006; Jiang et al., 2009, 2011; Osman et al., 2012; Guo et al., 2014; Tian and Jiang, 2014, 2017; Lee et al., 2015; Iatsenko et al., 2016)
EE	AstA, AstC, AstB/Mip, CCHa1, CCHa2, sli, Orcokinin B, CCAP, Nplp2, Gbp5, and ITP (Veenstra et al., 2008; Biteau and Jasper, 2014; Veenstra and Ida, 2014; Ren et al., 2015; Chen et al., 2016a; Benguettat et al., 2018; Rommelaere et al., 2019; Hung et al., 2020)
Hemyocyte	Dpp (Ayyaz et al., 2015)
Neuron	sNPF, DH44, PDF, and AstA (Talsma et al., 2012; Dus et al., 2015; Chen et al., 2016b; Shen et al., 2016)
Trachea	Dpp (Li et al., 2013)
VM	Vn, wg, and Dpp (Jiang and Edgar, 2009; Tian et al., 2016; Tian and Jiang, 2017)

feedback loop. For example, Tk production in the midgut is suppressed (Song et al., 2014), while Burs production is enhanced (Scopelliti et al., 2019), under the feeding condition. On the other hand, chronic high-caloric diets also perturb the production of gut-peptide hormones and systemic metabolic balance. Advanced imaging tools in *Drosophila* have demonstrated and visualized the *in vivo* nutrient sensing, which is associated with the production of gut peptides, in the midgut in response to individual component(s) in the food.

Amino Acids

A recent study using the cytoplasmic calcium reporter CaLexA has indicated that dietary amino acids like casein peptone and lysine directly activate intracellular Ca^{2+} cascade, an increase in which is associated with peptide release in multiple endocrine cells (Dus et al., 2015; Benguettat et al., 2018; Oh et al., 2019), in Tk^{+} and $DH31^{+}$ EEs (Park et al., 2016). Consistently, the protein level and release of Tk peptides in EEs are increased in starved flies and other insects to control gut mobility and EC lipogenesis (Winther and Nassel, 2001; Song et al., 2014), while refeeding flies only yeast that contains plenty of amino acids, but not sucrose or coconut oil, blunts the increase in Tk peptide level (Song et al., 2014). Several transporters or receptors that sense distinct amino acids and trigger the downstream signaling pathways have been characterized in *Drosophila* (Maniere et al., 2020). However, their roles in EEs are not fully identified yet.

Carbohydrates

Nutrient deprivation reduces release of Burs from EEs into the hemolymph and causes intestinal Burs accumulation. Either sucrose refeeding or diminishing the expression of Glut1, a glucose transporter, in the EEs, alleviates Burs accumulation (Scopelliti et al., 2019), confirming the control of Burs release by dietary glucose or sucrose. In addition, starvation suppresses, while yeast refeeding restores, global larval CCHa2 mRNA levels (Sano et al., 2015). Interesting, the researchers found that glucose, but not amino acids, contained in yeast paste results in CCHa2 transcriptional suppression and further uncovered fat body TOR signaling as the sensor (Sano et al., 2015). It is possible that CCHa2 transcription in the EEs is similarly regulated by nutrients as well, but more biochemical and genetic evidence are required for further validation. In addition to hormone production and release, dietary carbohydrates also influence EE mass in the larval midgut. We have uncovered that chronic high-sucrose diet perturbs larval gut homeostasis and promotes EE differentiation with unknown mechanism(s), resulting in excessive Actβ production, enhanced Akh response in the fat body, and hyperglycemia (Song et al., 2017).

Lipids

The absorption of fatty acids in fly intestine has not been carefully studied, even though homologs of fatty acid transport proteins (FATPs), fatty acid translocase FAT (CD36), and fatty-acid-binding proteins (FABPs) that regulate fatty acid binding and transport are all present in *Drosophila* (Adams et al., 2000). So far, there is no clear evidence suggesting a direct regulation of gut-peptide hormone release by dietary lipids in *Drosophila*. However, a group demonstrated that adult EE numbers are decreased by lipid-deleted food, while increased by high-cholesterol food (Obniski et al., 2018). They also revealed that dietary cholesterol, absorption of which is regulated by the Hr96/NPC2b axis in the intestine, influences endomembrane lipid composition and the subcellular localization, trafficking, as well as turnover, of the Delta/Notch complex in the ISCs. These changes further suppress Notch signaling in the EBs and promote EE differentiation and subsequent production of EE-derived peptide hormones (Obniski et al., 2018).

Non-nutrient Components

An interesting study reported that 10 gustatory receptors are expressed in the EEs (Park and Kwon, 2011). These gustatory receptors can be activated by diverse dietary chemicals, such as caffeine, bitter compounds, and carbohydrates (Hanlon and Andrew, 2015; **Table 3**). Even though the ligand/receptor action in the gut is not characterized yet, it raises the hypothesis that diet might regulate gut-peptide hormone release and subsequent systemic metabolism *via* taste components in addition to nutrients. On the other hand, a recent study demonstrated that yeast particles trigger mechanical stress in the midgut and activate ISC proliferation (Li et al., 2018a). Several mechanical sensors, including TrpA1 and Piezo that activate Ca^{2+} cascade, are reported to be expressed in the adult EEs (Du et al., 2016; He et al., 2018), it will be likely that food containing indigestible particles or fibers would perturb the production and release of gut-peptide hormones independent of nutrients.

GUT MICROBIOTA AND PEPTIDE-HORMONE PRODUCTION

The gut microbiota emerges as a neglected metabolic organ based on a number of important discoveries of its products, including short-chain fatty acids (SCFAs), amino acids, and bacteriocin, that regulate host immunity and metabolism (Depetris-Chauvin et al., 2017; Li et al., 2018b; Qiao et al., 2019). The simpler microbiota and signaling systems of the *Drosophila* have provided researchers with a unique opportunity to study the impact of either commensal or pathogenic intestinal microbes on host feeding behavior and energy balance in a more controlled and targeted fashion (Capo et al., 2019). Several studies further

TABLE 3 | Gustatory receptor expression in adult EEs (Park and Kwon, 2011; Hanlon and Andrew, 2015).

Gustatory receptors	Producing cells	Putative ligands
Gr28a, Gr28b, Gr33a, Gr93a	Tk/NPF^{+} EEs	Caffeine
Gr36c, Gr59a	Tk/NPF^{+} EEs	Bitter compounds
Gr39a	Tk/NPF^{+} EEs	Mating pheromone
Gr43a, Gr64a	Tk/NPF^{+} EEs	Carbohydrates
Gr58c	NPF^{-} EEs	Unknown

illustrated gut-peptide hormones as key regulators mediating host immune response and carbo-lipid metabolism in response to diverse gut microbiota.

Commensal Bacteria

Different groups have shown that axenic adult flies exhibit a delayed development, lipid and glycogen accumulation, and hyperglycemia (Shin et al., 2011; Wong et al., 2014). Impairment of systemic insulin signaling, which is associated with the dominant gut commensal microbiota (*Lactobacillus plantarum* and *Acetobacter pomorum*), is considered as a major regulator. *L. plantarum* produces branched-chain amino acids to directly activate host TOR and insulin signaling (Storelli et al., 2011), while SCFAs like acetate produced by *A. pomorum* modulate systemic insulin signaling *via* gut-peptide hormone production (Kamareddine et al., 2018). As we mentioned, both mRNA and peptide levels of gut Tk, which promotes ILP3 production in VMs *via* TkR99D activation to modulate systemic insulin signaling and energy balance (Poels et al., 2009), are increased by intestinal acetate (Kamareddine et al., 2018). Even though the receptors sensing acetate are not yet identified in *Drosophila*, researchers indicated that intestinal microbial acetate activates immune responses *via* PGRP-LC/Rel signaling to increase Tk$^+$ EEs mass and Tk synthesis in the gut (**Figure 2**). Note that, acetate-activated Rel signaling is observed not only in Tk$^+$ EEs but also in AstC$^+$ EEs, ISCs, and ECs (Kamareddine et al., 2018). EC-derived ImpL2 is previously reported to be suppressed by intestinal acetate content (Hang et al., 2014). Further, other hormones, like AstA and CCHa2 produced in AstC$^+$ EEs, are probably associated with ILP2 production and systemic insulin response as well (Hentze et al., 2015; Ren et al., 2015). Therefore, it is quite likely that intestinal acetate modulates differential gut-peptide hormone production in multiple cell types *via* Rel activation and orchestrates their influences on insulin signaling and host metabolism (**Figure 2**).

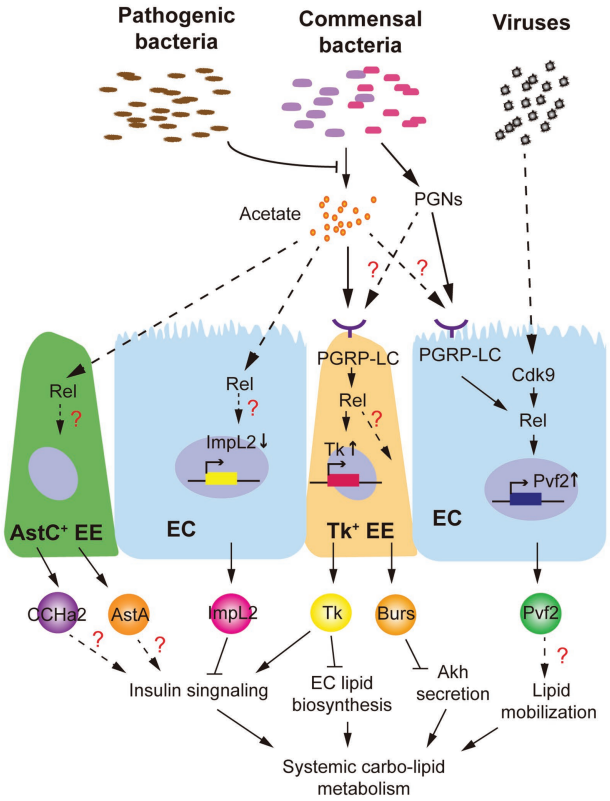

FIGURE 2 | *Drosophila* intestinal microbiota influence production of gut-peptide hormones. Commensal bacteria-derived acetate, which is suppressed by *Vibrio cholerae*, a pathogenic bacterium, promotes Tk production in enterocytes (ECs) *via* activation of PGPR-LC/Rel signaling and modulates systemic insulin signaling and lipid homeostasis. Production of other gut hormones such as ImpL2, CCHamides 2 (CCHa2), allatostatin A (AstA), and Burs regarding systemic energy balance is probably regulated by similar mechanism(s). Viral infection and commensal bacteria-derived peptidoglycans (PGNs) activate Cdk9/Rel and PGRP-LC/Rel cascades, respectively, to increase production of Pvf2, which is associated with Pvr activation in the fat body and lipid loss.

Pathogenic Bacteria

A few studies have demonstrated that pathogenic bacteria also perturb host metabolism through gut-peptide hormones. Oral infection of *Vibrio cholerae*, a life-threatening bacterium for both human and *Drosophila*, does not influence the gut microbiota or the epithelial barrier but reprograms acetate metabolism in the gut through acetate metabolic genes, *CrbR* and *CrbS* (Hang et al., 2014). In response to intestinal microbial acetate switch, production of ImpL2 and Tk is affected to impair systemic insulin signaling (Hang et al., 2014; Kamareddine et al., 2018). Dietary acetate supplementation further successfully alleviates *Vibrio cholerae*-disrupted host insulin signaling and metabolism. Note that, PGRP-LC/Rel signaling, which is shown to regulate Tk production, could be modulated by various PGNs derived by non-commensal bacteria as well (Royet and Charroux, 2013). Another group recently showed that septic, but not oral, infection of bacterial pathogen *Photorhabdus luminescens*, *Photorhabdus asymbiotica*, or non-pathogenic *Escherichia coli* modulate gut Tk production without affecting gut microbiota homeostasis, resulting in lipid accumulation in the gut and whole body (Harsh et al., 2019). This evidence indicates that gut-peptide hormone could be regulated by the circulating PGNs derived from non-commensal bacteria. Given the vast products such as virulence factors, secreted peptides, and metabolites produced by both commensal and non-commensal bacteria in the fly intestine, it will be necessary to dissect their impacts on gut-peptide hormones in terms of receptors sensing them and the signaling pathways they regulate.

Viruses

Drosophila C virus (DCV), a natural RNA virus for *Drosophila*, has recently been found to cause severe mortality as well as depleted stores of triglycerides and glycogen in adult flies (Arnold et al., 2013; Chtarbanova et al., 2014). The morphology and structure of midgut in DCV-infected flies are severely impaired. Importantly, the production of Pvf2, a peptide homolog of human platelet-derived growth factor (PDGF) and vascular endothelial

growth factor (VEGF), is dramatically upregulated in the ECs by the Cdk9/Rel pathway in response to viral infection (Sansone et al., 2015). Although in this study Pvf2 is shown to mediate intestinal antiviral immunity, its metabolic impact is not investigated yet. Interestingly, activation of Pvr, the receptor of Pvf2, in the fat body and oenocytes results in systemic lipid loss (Zheng et al., 2017; Ghosh et al., 2019; Song et al., 2019), phenocopying the DCV infection and suggesting a Pvf2/Pvr axis in the gut-to-fat-body communication. Infection of other RNA viruses like Flock House virus (FHV) also leads to the decline of systemic lipid accumulation (Chtarbanova et al., 2014), whether gut-peptide hormone is involved in FHV-associated metabolic disruption is an interesting question to address in the future.

GUT TUMORS AND PEPTIDE-HORMONE PRODUCTION

Tumor-bearing guts have recently been characterized as a differentiated endocrine organ that remotely impairs systemic metabolic homeostasis and causes a cachexia-like phenotype. Induction of an active oncogene *yki*, the homolog of human Yap1, in the ISCs leads to malignant tumorigenesis in the gut and subsequent wasting of host organs, including ovary degeneration, lipid loss, muscle dysfunction, hyperglycemia, as well as mortality (Kwon et al., 2015; Song et al., 2019). Because the affected flies eat normally, it is less likely that yki-gut tumors impair nutrient absorption in the gut. Integrating transcriptome analysis and RNAi screening, we have uncovered that yki-gut tumors produce various peptide hormones to disrupt the balance of systemic anabolism and catabolism (**Figure 3**).

First, yki-gut tumors release large amounts of ImpL2 to suppress IGF/insulin signaling and its associated anabolism in multiple host organs. As a consequence, ovary size and storages of lipid and glycogen in the fat body are decreased. The flies climb poorly, as the mitochondrial integrity and activity are both impaired in the skeletal muscles (Kwon et al., 2015). Second, yki-gut tumors produce excessive Pvf1, another hormone homologous to mammalian VEGF and PDGF, to extensively activate Pvr/MEK cascade and promote catabolism in the host organs, including lipid and carbohydrate breakdown in the fat body and muscular protein degradation. Small-molecule inhibitors against MEK/ERK strongly alleviate the wasting effects in yki-tumor-bearing flies, as well as C26-tumor cell models, providing pharmaceutical opportunities in prevention and treatment of cancer-associated cachexia (Song et al., 2019). Third, other potential tumor-derived peptide hormones have also been characterized using RNAi screening to regulate host wasting with unknown mechanisms (Song et al., 2019; **Figure 3**).

How yki activation in ISCs modulates production of cachectic peptide hormones is currently unknown. Possible mechanisms could include yki-induced direct transcriptional regulation of certain peptides and yki-associated ISC proliferation that enlarges the mass of peptide-producing cells. However, the transcriptional levels of these cachectic peptide hormones are increased far more than ISC marker genes and yki-target genes, like *diap1* and *Ex*, in the yki-gut tumors (Song et al., 2019). We, therefore, speculate

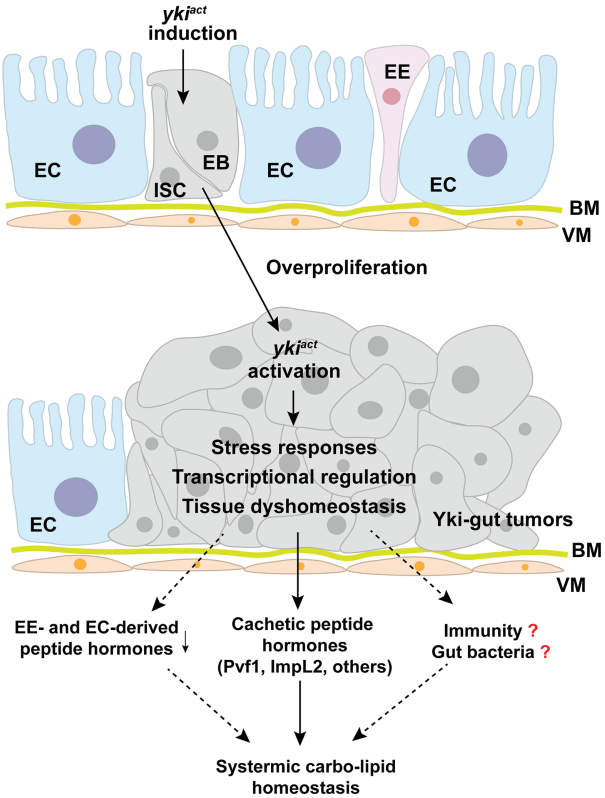

FIGURE 3 | Yki-tumor-bearing gut produces cachectic peptide hormones. Induction of an active *yki* in the intestinal stem cells (ISCs) results in malignant tumor-cell growth in the midgut and production of large amounts of cachectic peptide hormones, including ImpL2, Pvf1, and others. Potential molecular mechanisms include *yki*-associated transcriptional regulation, stress responses, tissue dyshomeostasis, and subsequent immune regulation. EC, enterocyte; ISC, intestinal stem cell; EB, enteroblast; EE, enteroendocrine cell; BM, basement membrane; VM, visceral muscle.

that yki-activation might also trigger unknown intracellular stress responses to increase peptide-hormone production in a cascade-amplification fashion (**Figure 3**).

Nevertheless, we also noticed that yki-gut tumors perturb midgut homeostasis by increasing the mass of ISCs but decreasing that of ECs and EEs. As expected, most of the endogenous immune-associated enzymes and peptide hormones that are produced by ECs and EEs are suppressed (Song et al., 2019; **Figure 3**). Whether these endogenous enzymes, which maintain intestinal bacteria balance and systemic immune response, and peptide hormones contribute to host wasting is another insightful question to be addressed.

OTHER PATHOLOGICAL CONDITIONS AND GUT-PEPTIDE HORMONES

Drosophila model has also indicated high associations between systemic metabolism and other pathological conditions. For instance, aged flies exhibit less intestinal and systemic TAG storages (Karpac et al., 2013), while either diet restriction or

impaired insulin signaling significantly extends lifespan and increases systemic TAG accumulation (Song et al., 2010; Luis et al., 2016). Recent studies have uncovered important clues regarding participation of gut-peptide hormones, including increased EE mass and bacterial load that are associated with gut-peptide production in aged adult midgut (Ayyaz and Jasper, 2013; He et al., 2018). Moreover, removal of gut-derived AstA and DH31 modulate fly longevity in an opposite manner (Takeda et al., 2018). It will be essential to examine whether gut-peptide hormones are involved in the regulation of aging and carbo-lipid metabolic homeostasis.

Another example is sleep deprivation, a well-established condition that disrupts systemic metabolic balance (Stahl et al., 2017). Researchers have revealed that an EC-derived amino acid, D-serine, is essential for sleep control (Dai et al., 2019), indicating a participating role of fly gut. Strikingly, a recent study further demonstrated that sleep deprivation results in accumulation of reactive oxygen species (ROS) and triggers consequent oxidative stress specifically in the gut, whereas diminishment of ROS accumulation in the gut improves survival without sleep in flies (Vaccaro et al., 2020). Given the fact that ROS regulates diverse metabolic signaling pathways, as well as tissue homeostasis and commensal bacterial control, in the gut (Ha et al., 2005; Ayyaz and Jasper, 2013; Xu et al., 2017), we speculate that ROS-associated production and release of gut-peptide hormone might function as a nexus between sleep and metabolic homeostasis and beyond.

CONCLUSION AND OUTLOOK

In this review, we have summarized the gut-hormone regulation of systemic metabolism and its essential impacts on physiological and pathogenic outputs, focusing on their genetic characterization, stress-sensing, as well as the mechanisms of act, in *Drosophila*. Despite the gained knowledge and ongoing functional validation of gut-peptide hormones, several fundamental questions in this field still remain unaddressed (**Figure 4**). In particular, the stress-sensing of intestinal cells regarding peptide production in response to multiple internal and external stimuli is largely unknown. Growing findings of novel stress responses, such as mechanical stress induced by different components in the food (He et al., 2018; Li et al., 2018a), local hypoxic response caused by bacterial infection (Valzania et al., 2018; Krejcova et al., 2019), immune response triggered by intestinal microbial metabolites (Kamareddine et al., 2018), as well as the newly-identified oxidative stress associated with sleep loss (Vaccaro et al., 2020), keep shaping our current understanding of intestinal phenomena. Therefore, integrating multi-reporter system, long-term live imaging (Martin et al., 2018), and scRNAseq to monitor diverse stress responses and study whether and how gut-peptide-hormone production is affected by them will add new dimensions for exploiting gut physiology and metabolic homeostasis (**Figure 4A**). This strategy will also help illustrate the compositional change

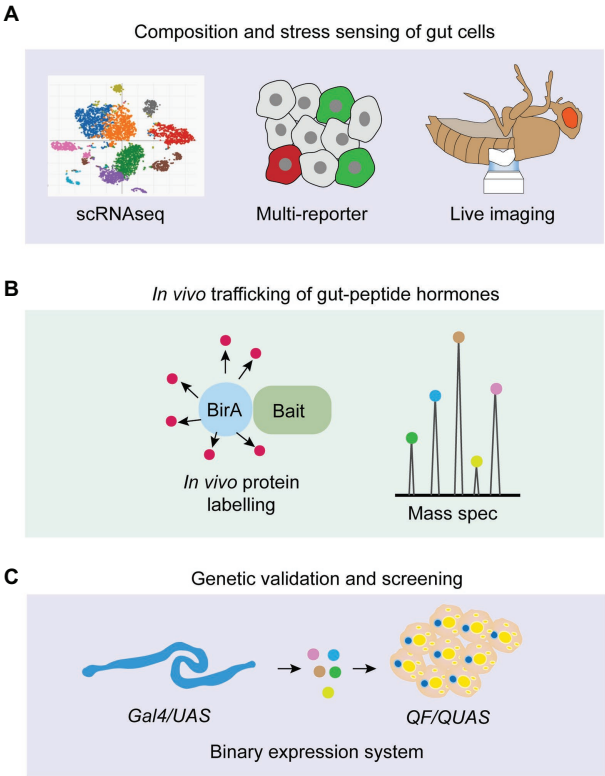

FIGURE 4 | Strategic options for future gut-peptide hormone research in *Drosophila*. **(A)** Single-cell RNAseq (scRNAseq), multi-reporter system, and live imaging can be used to monitor homeostatic composition of intestinal cells and various stress responses that trigger gut-peptide hormone production under different physiological conditions. **(B)** BirA-induced biotin labeling of endogenous protein can be applied to identify novel gut-peptide hormones, investigate their *in-vivo* trafficking, and characterize their targeted organs. **(C)** Binary expression system and genetic screening in *Drosophila* offer us a unique opportunity to investigate peptide-hormone-induced gut-to-other-organ axis and metabolic modulation at the genetic level.

of different gut cells that produce distinct hormones and the orchestrating impacts on systemic metabolism under chronic conditions, like tumor progression and high-caloric diet (**Figure 4A**). *In vivo* trafficking of hormones is difficult to achieve due to limited genetic tools. Recent studies, which engineered a promiscuous biotin ligase, BirA, to specifically label secreted proteins including peptide prohormones (Stevens et al., 2019; Droujinine et al., 2020), are very promising to address the limitation (**Figure 4B**). They used a fused BirA to biotinylate all proteins in the muscle ER and detected biotin-labeled proteins in the blood to identify potential myokines. Moreover, they further detected biotin-labeled proteins in the other organs to characterize *in vivo* trafficking of these myokines from skeletal muscle to the fat body (Droujinine et al., 2020). Genetic validation is required to confirm the physiological outputs of gut-peptide hormone-induced interorgan communication. The binary expression systems such as LexA/LexAop (Kockel et al., 2016) and QF/QUAS (Riabinina and Potter, 2016) together with Gal4/UAS

offer us a unique opportunity. For instance, we could increase the release of a gut-peptide hormone using the *LexA/LexAop* system and simultaneously block its receptor or downstream signaling pathways in the receiving organ using the *Gal4/UAS* system to evaluate the physiological regulation of the particular gut-peptide hormone under study. Conversely, we can also use the *QF/QUAS* system to set up reliable readouts (e.g., Ca^{2+} signaling in Akh-producing cells induced by Burs) and screen for the potential stress pathways and trafficking regulators of the matched hormones (e.g., Burs) with the *Gal4/UAS* system (**Figure 4C**).

Taken together, the *Drosophila* organism with the accessibility of genetic tools, the simplicity of its genome, and the feasibility for disease modeling, will serve as a powerful system for the future research of gut-peptide hormones. Some of the metabolic regulations that are found in *Drosophila* have recently been shown to be similar in mammals. For example, similar to fly Tk regulation of ILP3/5 secretion, mammalian Substance P and neurokinin A also promote insulin release (Schmidt et al., 2000). Mammalian galanin inhibits insulin secretion as fly AstA does (Tang et al., 2012). Like fly Pvf1, VEGFs are also produced in malignant colon tumors and found to promote lipid mobilization (Sun et al., 2012; Bendardaf et al., 2017). These evidence might, therefore, become relevant in the context of human physiology and pathologies such as diet-induced obesity and diabetes, infectious diseases, and cancer cachexia.

AUTHOR CONTRIBUTIONS

XZ wrote the part of bacteria-induced gut hormone production. GD wrote the section of gut hormone types. JL wrote the section of tumor-induced gut hormone production. XX wrote the part of dietary regulation. ER wrote the section of other conditions. WS discussed and organized the whole manuscript. All authors contributed to the article and approved the submitted version.

FUNDING

WS is funded by Chinese National Natural Science Foundation (91957118, 31971079, and 31800999) and the Fundamental Research Funds for the Central Universities.

ACKNOWLEDGMENTS

We thank Richard Binari and Charles Xu for the insightful discussion for this manuscript.

REFERENCES

Adams, M. D., Celniker, S. E., Holt, R. A., Evans, C. A., Gocayne, J. D., Amanatides, P. G., et al. (2000). The genome sequence of *Drosophila melanogaster*. *Science* 287, 2185–2195. doi: 10.1126/science.287.5461.2185

Alexiadou, K., Anyiam, O., and Tan, T. (2019). Cracking the combination: gut hormones for the treatment of obesity and diabetes. *J. Neuroendocrinol.* 31:e12664. doi: 10.1111/jne.12664

Amcheslavsky, A., Song, W., Li, Q., Nie, Y., Bragatto, I., Ferrandon, D., et al. (2014). Enteroendocrine cells support intestinal stem-cell-mediated homeostasis in *Drosophila*. *Cell Rep.* 9, 32–39. doi: 10.1016/j.celrep.2014.08.052

Ameku, T., Yoshinari, Y., Texada, M. J., Kondo, S., Amezawa, K., Yoshizaki, G., et al. (2018). Midgut-derived neuropeptide F controls germline stem cell proliferation in a mating-dependent manner. *PLoS Biol.* 16:e2005004. doi: 10.1371/journal.pbio.2005004

Arnold, P. A., Johnson, K. N., and White, C. R. (2013). Physiological and metabolic consequences of viral infection in *Drosophila melanogaster*. *J. Exp. Biol.* 216, 3350–3357. doi: 10.1242/jeb.088138

Ayyaz, A., and Jasper, H. (2013). Intestinal inflammation and stem cell homeostasis in aging *Drosophila melanogaster*. *Front. Cell. Infect. Microbiol.* 3:98. doi: 10.3389/fcimb.2013.00098

Ayyaz, A., Li, H., and Jasper, H. (2015). Haemocytes control stem cell activity in the *Drosophila* intestine. *Nat. Cell Biol.* 17, 736–748. doi: 10.1038/ncb3174

Bendardaf, R., El-Serafi, A., Syrjanen, K., Collan, Y., and Pyrhonen, S. (2017). The effect of vascular endothelial growth factor-1 expression on survival of advanced colorectal cancer patients. *Libyan J. Med.* 12:1290741. doi: 10.1080/19932820.2017.1290741

Benguettat, O., Jneid, R., Soltys, J., Loudhaief, R., Brun-Barale, A., Osman, D., et al. (2018). The DH31/CGRP enteroendocrine peptide triggers intestinal contractions favoring the elimination of opportunistic bacteria. *PLoS Pathog.* 14:e1007279. doi: 10.1371/journal.ppat.1007279

Birse, R. T., Soderberg, J. A., Luo, J., Winther, A. M., and Nassel, D. R. (2011). Regulation of insulin-producing cells in the adult *Drosophila* brain via the tachykinin peptide receptor DTKR. *J. Exp. Biol.* 214, 4201–4208. doi: 10.1242/jeb.062091

Bischoff, V., Vignal, C., Duvic, B., Boneca, I. G., Hoffmann, J. A., and Royet, J. (2006). Downregulation of the *Drosophila* immune response by peptidoglycan-recognition proteins SC1 and SC2. *PLoS Pathog.* 2:e14. doi: 10.1371/journal.ppat.0020014

Biteau, B., and Jasper, H. (2011). EGF signaling regulates the proliferation of intestinal stem cells in *Drosophila*. *Development* 138, 1045–1055. doi: 10.1242/dev.056671

Biteau, B., and Jasper, H. (2014). Slit/Robo signaling regulates cell fate decisions in the intestinal stem cell lineage of *Drosophila*. *Cell Rep.* 7, 1867–1875. doi: 10.1016/j.celrep.2014.05.024

Capo, F., Wilson, A., and Di Cara, F. (2019). The intestine of *Drosophila melanogaster*: an emerging versatile model system to study intestinal epithelial homeostasis and host-microbial interactions in humans. *Microorganisms* 7:336. doi: 10.3390/microorganisms7090336

Charroux, B., Capo, F., Kurz, C. L., Peslier, S., Chaduli, D., Viallat-Lieutaud, A., et al. (2018). Cytosolic and secreted peptidoglycan-degrading enzymes in *Drosophila* respectively control local and systemic immune responses to microbiota. *Cell Host Microbe* 23, 215.e214–228.e214. doi: 10.1016/j.chom.2017.12.007

Chen, J., Kim, S. M., and Kwon, J. Y. (2016a). A systematic analysis of *Drosophila* regulatory peptide expression in enteroendocrine cells. *Mol. Cell* 39, 358–366. doi: 10.14348/molcells.2016.0014

Chen, J., Reiher, W., Hermann-Luibl, C., Sellami, A., Cognigni, P., Kondo, S., et al. (2016b). Allatostatin A signalling in *Drosophila* regulates feeding and sleep and is modulated by PDF. *PLoS Genet.* 12:e1006346. doi: 10.1371/journal.pgen.1006346

Chintapalli, V. R., Terhzaz, S., Wang, J., Al Bratty, M., Watson, D. G., Herzyk, P., et al. (2012). Functional correlates of positional and gender-specific renal asymmetry in *Drosophila*. *PLoS One* 7:e32577. doi: 10.1371/journal.pone.0032577

Chng, W. B., Bou Sleiman, M. S., Schupfer, F., and Lemaitre, B. (2014). Transforming growth factor beta/activin signaling functions as a sugar-sensing feedback loop to regulate digestive enzyme expression. *Cell Rep.* 9, 336–348. doi: 10.1016/j.celrep.2014.08.064

Chtarbanova, S., Lamiable, O., Lee, K. Z., Galiana, D., Troxler, L., Meignin, C., et al. (2014). *Drosophila* C virus systemic infection leads to intestinal obstruction. *J. Virol.* 88, 14057–14069. doi: 10.1128/JVI.02320-14

Coast, G. M., Webster, S. G., Schegg, K. M., Tobe, S. S., and Schooley, D. A. (2001). The *Drosophila melanogaster* homologue of an insect calcitonin-like

diuretic peptide stimulates V-ATPase activity in fruit fly Malpighian tubules. *J. Exp. Biol.* 204, 1795–1804.

Dai, X., Zhou, E., Yang, W., Zhang, X., Zhang, W., and Rao, Y. (2019). D-serine made by serine racemase in *Drosophila* intestine plays a physiological role in sleep. *Nat. Commun.* 10:1986. doi: 10.1038/s41467-019-09544-9

Depetris-Chauvin, A., Galagovsky, D., Chevalier, C., Maniere, G., and Grosjean, Y. (2017). Olfactory detection of a bacterial short-chain fatty acid acts as an orexigenic signal in *Drosophila melanogaster* larvae. *Sci. Rep.* 7:14230. doi: 10.1038/s41598-017-14589-1

Doupe, D. P., Marshall, O. J., Dayton, H., Brand, A. H., and Perrimon, N. (2018). *Drosophila* intestinal stem and progenitor cells are major sources and regulators of homeostatic niche signals. *Proc. Natl. Acad. Sci. U. S. A.* 115, 12218–12223. doi: 10.1073/pnas.1719169115

Droujinine, I. A., Wang, D., Hu, Y., Udeshi, D., Mu, L., Svinkina, T., et al. (2020). Proteomics of protein trafficking by *in vivo* tissue-specific labeling. bioRxiv [Preprint]. doi: 10.1101/2020.04.15.039933

Du, E. J., Ahn, T. J., Kwon, I., Lee, J. H., Park, J. H., Park, S. H., et al. (2016). TrpA1 regulates defecation of food-borne pathogens under the control of the Duox pathway. *PLoS Genet.* 12:e1005773. doi: 10.1371/journal.pgen.1005773

Dus, M., Lai, J. S., Gunapala, K. M., Min, S., Tayler, T. D., Hergarden, A. C., et al. (2015). Nutrient sensor in the brain directs the action of the brain-gut axis in *Drosophila*. *Neuron* 87, 139–151. doi: 10.1016/j.neuron.2015.05.032

Ghosh, A. C., and O'Connor, M. B. (2014). Systemic Activin signaling independently regulates sugar homeostasis, cellular metabolism, and pH balance in *Drosophila melanogaster*. *Proc. Natl. Acad. Sci. U. S. A.* 111, 5729–5734. doi: 10.1073/pnas.1319116111

Ghosh, A., Tattikota, S., Liu, Y., Comjean, A., Hu, Y., Barrera, V., et al. (2019). Drosophila PDGF/VEGF signaling from muscles to hepatocyte-like cells protects against obesity. bioRxiv [Preprint]. doi: 10.1101/2019.12.23.887059

Gronke, S., Muller, G., Hirsch, J., Fellert, S., Andreou, A., Haase, T., et al. (2007). Dual lipolytic control of body fat storage and mobilization in *Drosophila*. *PLoS Biol.* 5:e137. doi: 10.1371/journal.pbio.0050137

Guo, L., Karpac, J., Tran, S. L., and Jasper, H. (2014). PGRP-SC2 promotes gut immune homeostasis to limit commensal dysbiosis and extend lifespan. *Cell* 156, 109–122. doi: 10.1016/j.cell.2013.12.018

Guo, X., Yin, C., Yang, F., Zhang, Y., Huang, H., Wang, J., et al. (2019). The cellular diversity and transcription factor code of *Drosophila* enteroendocrine cells. *Cell Rep.* 29, 4172.e4175–4185.e4175. doi: 10.1016/j.celrep.2019.11.048

Ha, E. M., Oh, C. T., Bae, Y. S., and Lee, W. J. (2005). A direct role for dual oxidase in *Drosophila* gut immunity. *Science* 310, 847–850. doi: 10.1126/science.1117311

Hang, S., Purdy, A. E., Robins, W. P., Wang, Z., Mandal, M., Chang, S., et al. (2014). The acetate switch of an intestinal pathogen disrupts host insulin signaling and lipid metabolism. *Cell Host Microbe* 16, 592–604. doi: 10.1016/j.chom.2014.10.006

Hanlon, C. D., and Andrew, D. J. (2015). Outside-in signaling—a brief review of GPCR signaling with a focus on the *Drosophila* GPCR family. *J. Cell Sci.* 128, 3533–3542. doi: 10.1242/jcs.175158

Harsh, S., Heryanto, C., and Eleftherianos, I. (2019). Intestinal lipid droplets as novel mediators of host-pathogen interaction in *Drosophila*. *Biol. Open* 8:bio039040. doi: 10.1242/bio.039040

He, L., Si, G., Huang, J., Samuel, A. D. T., and Perrimon, N. (2018). Mechanical regulation of stem-cell differentiation by the stretch-activated Piezo channel. *Nature* 555, 103–106. doi: 10.1038/nature25744

Hentze, J. L., Carlsson, M. A., Kondo, S., Nassel, D. R., and Rewitz, K. F. (2015). The neuropeptide allatostatin A regulates metabolism and feeding decisions in *Drosophila*. *Sci. Rep.* 5:11680. doi: 10.1038/srep11680

Hergarden, A. C., Tayler, T. D., and Anderson, D. J. (2012). Allatostatin-A neurons inhibit feeding behavior in adult *Drosophila*. *Proc. Natl. Acad. Sci. U. S. A.* 109, 3967–3972. doi: 10.1073/pnas.1200778109

Honegger, B., Galic, M., Kohler, K., Wittwer, F., Brogiolo, W., Hafen, E., et al. (2008). Imp-L2, a putative homolog of vertebrate IGF-binding protein 7, counteracts insulin signaling in *Drosophila* and is essential for starvation resistance. *J. Biol.* 7:10. doi: 10.1186/jbiol72

Huang, R., Song, T., Su, H., Lai, Z., Qin, W., Tian, Y., et al. (2020). High-fat diet enhances starvation-induced hyperactivity via sensitizing hunger-sensing neurons in *Drosophila*. *eLife* 9:e53103. doi: 10.7554/eLife.53103

Hung, R. J., Hu, Y., Kirchner, R., Liu, Y., Xu, C., Comjean, A., et al. (2020). A cell atlas of the adult *Drosophila* midgut. *Proc. Natl. Acad. Sci. U. S. A.* 117, 1514–1523. doi: 10.1073/pnas.1916820117

Iatsenko, I., Kondo, S., Mengin-Lecreulx, D., and Lemaitre, B. (2016). PGRP-SD, an extracellular pattern-recognition receptor, enhances peptidoglycan-mediated activation of the *Drosophila* Imd pathway. *Immunity* 45, 1013–1023. doi: 10.1016/j.immuni.2016.10.029

Jiang, H., and Edgar, B. A. (2009). EGFR signaling regulates the proliferation of *Drosophila* adult midgut progenitors. *Development* 136, 483–493. doi: 10.1242/dev.026955

Jiang, H., Grenley, M. O., Bravo, M. J., Blumhagen, R. Z., and Edgar, B. A. (2011). EGFR/Ras/MAPK signaling mediates adult midgut epithelial homeostasis and regeneration in *Drosophila*. *Cell Stem Cell* 8, 84–95. doi: 10.1016/j.stem.2010.11.026

Jiang, H., Patel, P. H., Kohlmaier, A., Grenley, M. O., McEwen, D. G., and Edgar, B. A. (2009). Cytokine/Jak/Stat signaling mediates regeneration and homeostasis in the *Drosophila* midgut. *Cell* 137, 1343–1355. doi: 10.1016/j.cell.2009.05.014

Johnson, E. C., Shafer, O. T., Trigg, J. S., Park, J., Schooley, D. A., Dow, J. A., et al. (2005). A novel diuretic hormone receptor in *Drosophila*: evidence for conservation of CGRP signaling. *J. Exp. Biol.* 208, 1239–1246. doi: 10.1242/jeb.01529

Kamareddine, L., Robins, W. P., Berkey, C. D., Mekalanos, J. J., and Watnick, P. I. (2018). The *Drosophila* immune deficiency pathway modulates enteroendocrine function and host metabolism. *Cell Metab.* 28, 449.e445–462.e445. doi: 10.1016/j.cmet.2018.05.026

Karpac, J., Biteau, B., and Jasper, H. (2013). Misregulation of an adaptive metabolic response contributes to the age-related disruption of lipid homeostasis in *Drosophila*. *Cell Rep.* 4, 1250–1261. doi: 10.1016/j.celrep.2013.08.004

Karpowicz, P., Perez, J., and Perrimon, N. (2010). The Hippo tumor suppressor pathway regulates intestinal stem cell regeneration. *Development* 137, 4135–4145. doi: 10.1242/dev.060483

Kim, S. K., and Rulifson, E. J. (2004). Conserved mechanisms of glucose sensing and regulation by *Drosophila* corpora cardiaca cells. *Nature* 431, 316–320. doi: 10.1038/nature02897

Kockel, L., Huq, L. M., Ayyar, A., Herold, E., MacAlpine, E., Logan, M., et al. (2016). A *Drosophila* LexA enhancer-trap resource for developmental biology and neuroendocrine research. *G3* 6, 3017–3026. doi: 10.1534/g3.116.031229

Krejcova, G., Danielova, A., Nedbalova, P., Kazek, M., Strych, L., Chawla, G., et al. (2019). *Drosophila macrophages* switch to aerobic glycolysis to mount effective antibacterial defense. *eLife* 8:e50414. doi: 10.7554/eLife.50414

Kwon, Y., Song, W., Droujinine, I. A., Hu, Y., Asara, J. M., and Perrimon, N. (2015). Systemic organ wasting induced by localized expression of the secreted insulin/IGF antagonist ImpL2. *Dev. Cell* 33, 36–46. doi: 10.1016/j.devcel.2015.02.012

LaJeunesse, D. R., Johnson, B., Presnell, J. S., Catignas, K. K., and Zapotoczny, G. (2010). Peristalsis in the junction region of the *Drosophila* larval midgut is modulated by DH31 expressing enteroendocrine cells. *BMC Physiol.* 10:14. doi: 10.1186/1472-6793-10-14

Lee, K. A., Kim, B., Bhin, J., Kim, D. H., You, H., Kim, E. K., et al. (2015). Bacterial uracil modulates *Drosophila* DUOX-dependent gut immunity via hedgehog-induced signaling endosomes. *Cell Host Microbe* 17, 191–204. doi: 10.1016/j.chom.2014.12.012

Li, Q., Nirala, N. K., Nie, Y., Chen, H. J., Ostroff, G., Mao, J., et al. (2018a). Ingestion of food particles regulates the Mechanosensing Misshapen-Yorkie Pathway in *Drosophila* intestinal growth. *Dev. Cell* 45, 433.e436–449.e436. doi: 10.1016/j.devcel.2018.04.014

Li, Z., Quan, G., Jiang, X., Yang, Y., Ding, X., Zhang, D., et al. (2018b). Effects of metabolites derived from gut microbiota and hosts on pathogens. *Front. Cell. Infect. Microbiol.* 8:314. doi: 10.3389/fcimb.2018.00314

Li, Z., Zhang, Y., Han, L., Shi, L., and Lin, X. (2013). Trachea-derived dpp controls adult midgut homeostasis in *Drosophila*. *Dev. Cell* 24, 133–143. doi: 10.1016/j.devcel.2012.12.010

Liu, Q., and Jin, L. H. (2017). Organ-to-organ communication: a *Drosophila* gastrointestinal tract perspective. *Front. Cell Dev. Biol.* 5:29. doi: 10.3389/fcell.2017.00029

Luis, N. M., Wang, L., Ortega, M., Deng, H., Katewa, S. D., Li, P. W., et al. (2016). Intestinal IRE1 is required for increased triglyceride metabolism and longer lifespan under dietary restriction. *Cell Rep.* 17, 1207–1216. doi: 10.1016/j.celrep.2016.10.003

Maniere, G., Alves, G., Berthelot-Grosjean, M., and Grosjean, Y. (2020). Growth regulation by amino acid transporters in *Drosophila* larvae. *Cell. Mol. Life Sci.* doi: 10.1007/s00018-020-03535-6 [Epub ahead of print]

Martin, J. L., Sanders, E. N., Moreno-Roman, P., Jaramillo Koyama, L. A., Balachandra, S., Du, X., et al. (2018). Long-term live imaging of the *Drosophila* adult midgut reveals real-time dynamics of division, differentiation and loss. *eLife* 7:e36248. doi: 10.7554/eLife.36248

Martin, A. M., Sun, E. W., and Keating, D. J. (2019). Mechanisms controlling hormone secretion in human gut and its relevance to metabolism. *J. Endocrinol.* 244, R1–R15. doi: 10.1530/JOE-19-0399

Miguel-Aliaga, I., Jasper, H., and Lemaitre, B. (2018). Anatomy and physiology of the digestive tract of *Drosophila melanogaster*. *Genetics* 210, 357–396. doi: 10.1534/genetics.118.300224

Obniski, R., Sieber, M., and Spradling, A. C. (2018). Dietary lipids modulate notch signaling and influence adult intestinal development and metabolism in *Drosophila*. *Dev. Cell* 47, 98.e115–111.e115. doi: 10.1016/j.devcel.2018.08.013

O'Brien, L. E., Soliman, S. S., Li, X., and Bilder, D. (2011). Altered modes of stem cell division drive adaptive intestinal growth. *Cell* 147, 603–614. doi: 10.1016/j.cell.2011.08.048

Oh, Y., Lai, J. S., Mills, H. J., Erdjument-Bromage, H., Giammarinaro, B., Saadipour, K., et al. (2019). A glucose-sensing neuron pair regulates insulin and glucagon in *Drosophila*. *Nature* 574, 559–564. doi: 10.1038/s41586-019-1675-4

Ohlstein, B., and Spradling, A. (2007). Multipotent *Drosophila* intestinal stem cells specify daughter cell fates by differential notch signaling. *Science* 315, 988–992. doi: 10.1126/science.1136606

Osman, D., Buchon, N., Chakrabarti, S., Huang, Y. T., Su, W. C., Poidevin, M., et al. (2012). Autocrine and paracrine unpaired signaling regulate intestinal stem cell maintenance and division. *J. Cell Sci.* 125, 5944–5949. doi: 10.1242/jcs.113100

Park, J. H., Chen, J., Jang, S., Ahn, T. J., Kang, K., Choi, M. S., et al. (2016). A subset of enteroendocrine cells is activated by amino acids in the *Drosophila* midgut. *FEBS Lett.* 590, 493–500. doi: 10.1002/1873-3468.12073

Park, J. H., and Kwon, J. Y. (2011). Heterogeneous expression of *Drosophila* gustatory receptors in enteroendocrine cells. *PLoS One* 6:e29022. doi: 10.1371/journal.pone.0029022

Poels, J., Birse, R. T., Nachman, R. J., Fichna, J., Janecka, A., Vanden Broeck, J., et al. (2009). Characterization and distribution of NKD, a receptor for *Drosophila* tachykinin-related peptide 6. *Peptides* 30, 545–556. doi: 10.1016/j.peptides.2008.10.012

Qiao, H., Keesey, I. W., Hansson, B. S., and Knaden, M. (2019). Gut microbiota affects development and olfactory behavior in *Drosophila melanogaster*. *J. Exp. Biol.* 222:jeb192500. doi: 10.1242/jeb.192500

Reiher, W., Shirras, C., Kahnt, J., Baumeister, S., Isaac, R. E., and Wegener, C. (2011). Peptidomics and peptide hormone processing in the *Drosophila* midgut. *J. Proteome Res.* 10, 1881–1892. doi: 10.1021/pr101116g

Ren, G. R., Hauser, F., Rewitz, K. F., Kondo, S., Engelbrecht, A. F., Didriksen, A. K., et al. (2015). CCHamide-2 is an orexigenic brain-gut peptide in *Drosophila*. *PLoS One* 10:e0133017. doi: 10.1371/journal.pone.0133017

Riabinina, O., and Potter, C. J. (2016). The Q-system: a versatile expression system for *Drosophila*. *Methods Mol. Biol.* 1478, 53–78. doi: 10.1007/978-1-4939-6371-3_3

Rodenfels, J., Lavrynenko, O., Ayciriex, S., Sampaio, J. L., Carvalho, M., Shevchenko, A., et al. (2014). Production of systemically circulating hedgehog by the intestine couples nutrition to growth and development. *Genes Dev.* 28, 2636–2651. doi: 10.1101/gad.249763.114

Rommelaere, S., Boquete, J. P., Piton, J., Kondo, S., and Lemaitre, B. (2019). The exchangeable apolipoprotein Nplp2 sustains lipid flow and heat acclimation in *Drosophila*. *Cell Rep.* 27, 886.e886–899.e886. doi: 10.1016/j.celrep.2019.03.074

Royet, J., and Charroux, B. (2013). Mechanisms and consequence of bacteria detection by the *Drosophila* gut epithelium. *Gut Microbes* 4, 259–263. doi: 10.4161/gmic.24386

Sano, H., Nakamura, A., Texada, M. J., Truman, J. W., Ishimoto, H., Kamikouchi, A., et al. (2015). The nutrient-responsive hormone CCHamide-2 controls growth by regulating insulin-like peptides in the brain of *Drosophila melanogaster*. *PLoS Genet.* 11:e1005209. doi: 10.1371/journal.pgen.1005209

Sansone, C. L., Cohen, J., Yasunaga, A., Xu, J., Osborn, G., Subramanian, H., et al. (2015). Microbiota-dependent priming of antiviral intestinal immunity in *Drosophila*. *Cell Host Microbe* 18, 571–581. doi: 10.1016/j.chom.2015.10.010

Schmidt, P. T., Tornoe, K., Poulsen, S. S., Rasmussen, T. N., and Holst, J. J. (2000). Tachykinins in the porcine pancreas: potent exocrine and endocrine effects via NK-1 receptors. *Pancreas* 20, 241–247. doi: 10.1097/00006676-200004000-00004

Scopelliti, A., Bauer, C., Yu, Y., Zhang, T., Kruspig, B., Murphy, D. J., et al. (2019). A neuronal relay mediates a nutrient responsive gut/fat body axis regulating energy homeostasis in adult *Drosophila*. *Cell Metab.* 29:269.e210–284.e210. doi: 10.1016/j.cmet.2018.09.021

Shen, R., Wang, B., Giribaldi, M. G., Ayres, J., Thomas, J. B., and Montminy, M. (2016). Neuronal energy-sensing pathway promotes energy balance by modulating disease tolerance. *Proc. Natl. Acad. Sci. U. S. A.* 113, E3307–E3314. doi: 10.1073/pnas.1606106113

Shin, S. C., Kim, S. H., You, H., Kim, B., Kim, A. C., Lee, K. A., et al. (2011). *Drosophila* microbiome modulates host developmental and metabolic homeostasis via insulin signaling. *Science* 334, 670–674. doi: 10.1126/science.1212782

Siviter, R. J., Coast, G. M., Winther, A. M., Nachman, R. J., Taylor, C. A., Shirras, A. D., et al. (2000). Expression and functional characterization of a *Drosophila* neuropeptide precursor with homology to mammalian preprotachykinin A. *J. Biol. Chem.* 275, 23273–23280. doi: 10.1074/jbc.M002875200

Soderberg, J. A., Birse, R. T., and Nassel, D. R. (2011). Insulin production and signaling in renal tubules of *Drosophila* is under control of tachykinin-related peptide and regulates stress resistance. *PLoS One* 6:e19866. doi: 10.1371/journal.pone.0019866

Song, W., Cheng, D., Hong, S., Sappe, B., Hu, Y., Wei, N., et al. (2017). Midgut-derived activin regulates glucagon-like action in the fat body and glycemic control. *Cell Metab.* 25, 386–399. doi: 10.1016/j.cmet.2017.01.002

Song, W., Kir, S., Hong, S., Hu, Y., Wang, X., Binari, R., et al. (2019). Tumor-derived ligands trigger tumor growth and host wasting via differential MEK activation. *Dev. Cell* 48, 277.e6–286.e6. doi: 10.1016/j.devcel.2018.12.003

Song, W., Ren, D., Li, W., Jiang, L., Cho, K. W., Huang, P., et al. (2010). SH2B regulation of growth, metabolism, and longevity in both insects and mammals. *Cell Metab.* 11, 427–437. doi: 10.1016/j.cmet.2010.04.002

Song, W., Veenstra, J. A., and Perrimon, N. (2014). Control of lipid metabolism by tachykinin in *Drosophila*. *Cell Rep.* 9, 40–47. doi: 10.1016/j.celrep.2014.08.060

Stahl, B. A., Slocumb, M. E., Chaitin, H., DiAngelo, J. R., and Keene, A. C. (2017). Sleep-dependent modulation of metabolic rate in *Drosophila*. *Sleep* 40:zsx084. doi: 10.1093/sleep/zsx084

Stevens, L. M., Zhang, Y., Volnov, Y., Chen, G., and Stein, D. S. (2019). Isolation of secreted proteins from *Drosophila* ovaries and embryos through in vivo BirA-mediated biotinylation. *PLoS One* 14:e0219878. doi: 10.1371/journal.pone.0219878

Storelli, G., Defaye, A., Erkosar, B., Hols, P., Royet, J., and Leulier, F. (2011). *Lactobacillus plantarum* promotes *Drosophila* systemic growth by modulating hormonal signals through TOR-dependent nutrient sensing. *Cell Metab.* 14, 403–414. doi: 10.1016/j.cmet.2011.07.012

Sun, E. W. L., Martin, A. M., Young, R. L., and Keating, D. J. (2018). The regulation of peripheral metabolism by gut-derived hormones. *Front. Endocrinol.* 9:754. doi: 10.3389/fendo.2018.00754

Sun, K., Wernstedt Asterholm, I., Kusminski, C. M., Bueno, A. C., Wang, Z. V., Pollard, J. W., et al. (2012). Dichotomous effects of VEGF-A on adipose tissue dysfunction. *Proc. Natl. Acad. Sci. U. S. A.* 109, 5874–5879. doi: 10.1073/pnas.1200447109

Takeda, K., Okumura, T., Terahata, M., Yamaguchi, M., Taniguchi, K., and Adachi-Yamada, T. (2018). *Drosophila* peptide hormones allatostatin A and diuretic hormone 31 exhibiting complementary gradient distribution in posterior midgut antagonistically regulate midgut senescence and adult lifespan. *Zool. Sci.* 35, 75–85. doi: 10.2108/zs160210

Talsma, A. D., Christov, C. P., Terriente-Felix, A., Linneweber, G. A., Perea, D., Wayland, M., et al. (2012). Remote control of renal physiology by the intestinal neuropeptide pigment-dispersing factor in *Drosophila*. *Proc. Natl. Acad. Sci. U. S. A.* 109, 12177–12182. doi: 10.1073/pnas.1200247109

Tang, G., Wang, Y., Park, S., Bajpayee, N. S., Vi, D., Nagaoka, Y., et al. (2012). Go2 G protein mediates galanin inhibitory effects on insulin release from pancreatic beta cells. *Proc. Natl. Acad. Sci. U. S. A.* 109, 2636–2641. doi: 10.1073/pnas.1200100109

Teperino, R., Aberger, F., Esterbauer, H., Riobo, N., and Pospisilik, J. A. (2014). Canonical and non-canonical Hedgehog signalling and the control of metabolism. *Semin. Cell Dev. Biol.* 33, 81–92. doi: 10.1016/j.semcdb.2014.05.007

Tian, A., Benchabane, H., Wang, Z., and Ahmed, Y. (2016). Regulation of stem cell proliferation and cell fate specification by Wingless/Wnt signaling gradients enriched at adult intestinal compartment boundaries. *PLoS Genet.* 12:e1005822. doi: 10.1371/journal.pgen.1005822

Tian, A., and Jiang, J. (2014). Intestinal epithelium-derived BMP controls stem cell self-renewal in *Drosophila* adult midgut. *eLife* 3:e01857. doi: 10.7554/eLife.01857

Tian, A., and Jiang, J. (2017). Dual role of BMP signaling in the regulation of *Drosophila* intestinal stem cell self-renewal. *Fly* 11, 297–302. doi: 10.1080/19336934.2017.1384104

Tian, A., Shi, Q., Jiang, A., Li, S., Wang, B., and Jiang, J. (2015). Injury-stimulated hedgehog signaling promotes regenerative proliferation of *Drosophila* intestinal stem cells. *J. Cell Biol.* 208, 807–819. doi: 10.1083/jcb.201409025

Vaccaro, A., Kaplan Dor, Y., Nambara, K., Pollina, E. A., Lin, C., Greenberg, M. E., et al. (2020). Sleep loss can cause death through accumulation of reactive oxygen species in the gut. *Cell* 181, 1307.e1315–1328.e1315. doi: 10.1016/j.cell.2020.04.049

Valzania, L., Coon, K. L., Vogel, K. J., Brown, M. R., and Strand, M. R. (2018). Hypoxia-induced transcription factor signaling is essential for larval growth of the mosquito *Aedes aegypti*. *Proc. Natl. Acad. Sci. U. S. A.* 115, 457–465. doi: 10.1073/pnas.1719063115

Veenstra, J. A. (2009). Peptidergic paracrine and endocrine cells in the midgut of the fruit fly maggot. *Cell Tissue Res.* 336, 309–323. doi: 10.1007/s00441-009-0769-y

Veenstra, J. A., Agricola, H. J., and Sellami, A. (2008). Regulatory peptides in fruit fly midgut. *Cell Tissue Res.* 334, 499–516. doi: 10.1007/s00441-008-0708-3

Veenstra, J. A., and Ida, T. (2014). More *Drosophila* enteroendocrine peptides: Orcokinin B and the CCHamides 1 and 2. *Cell Tissue Res.* 357, 607–621. doi: 10.1007/s00441-014-1880-2

Werner, T., Liu, G., Kang, D., Ekengren, S., Steiner, H., and Hultmark, D. (2000). A family of peptidoglycan recognition proteins in the fruit fly *Drosophila melanogaster*. *Proc. Natl. Acad. Sci. U. S. A.* 97, 13772–13777. doi: 10.1073/pnas.97.25.13772

Winther, A. M., and Nassel, D. R. (2001). Intestinal peptides as circulating hormones: release of tachykinin-related peptide from the locust and cockroach midgut. *J. Exp. Biol.* 204, 1269–1280.

Wong, A. C., Dobson, A. J., and Douglas, A. E. (2014). Gut microbiota dictates the metabolic response of *Drosophila* to diet. *J. Exp. Biol.* 217, 1894–1901. doi: 10.1242/jeb.101725

Xu, C., Luo, J., He, L., Montell, C., and Perrimon, N. (2017). Oxidative stress induces stem cell proliferation via TRPA1/RyR-mediated Ca(2+) signaling in the *Drosophila* midgut. *eLife* 6:e22441. doi: 10.7554/eLife.22441

Zhang, J., Liu, Y., Jiang, K., and Jia, J. (2020). Hedgehog signaling promotes lipolysis in adipose tissue through directly regulating Bmm/ATGL lipase. *Dev. Biol.* 457, 128–139. doi: 10.1016/j.ydbio.2019.09.009

Zheng, H., Wang, X., Guo, P., Ge, W., Yan, Q., Gao, W., et al. (2017). Premature remodeling of fat body and fat mobilization triggered by platelet-derived growth factor/VEGF receptor in *Drosophila*. *FASEB J.* 31, 1964–1975. doi: 10.1096/fj.201601127R

Conflict of Interest: The authors declare that the research was conducted in the absence of any commercial or financial relationships that could be construed as a potential conflict of interest.

frontiers in Physiology

MINI REVIEW
published: 22 October 2020
doi: 10.3389/fphys.2020.580687

The Role of Muscle in Insect Energy Homeostasis

*Heidi Bretscher and Michael B. O'Connor**

Department of Genetics, Cell Biology and Development, University of Minnesota, Minneapolis, MN, United States

Maintaining energy homeostasis is critical for ensuring proper growth and maximizing survival potential of all organisms. Here we review the role of somatic muscle in regulating energy homeostasis in insects. The muscle is not only a large consumer of energy, it also plays a crucial role in regulating metabolic signaling pathways and energy stores of the organism. We examine the metabolic pathways required to supply the muscle with energy, as well as muscle-derived signals that regulate metabolic energy homeostasis.

Keywords: insect, muscle, energy, homeostasis, glycogen, lipids, signaling

OPEN ACCESS

Edited by:
Oleh Lushchak,
Vasyl Stefanyk Precarpathian National University, Ukraine

Reviewed by:
Julia Cordero,
University of Glasgow, United Kingdom
Aram Megighian,
University of Padua, Italy

***Correspondence:**
Michael B. O'Connor
moconnor@umn.edu

Specialty section:
This article was submitted to Invertebrate Physiology, a section of the journal Frontiers in Physiology

Received: *06 July 2020*
Accepted: *09 September 2020*
Published: *22 October 2020*

Citation:
Bretscher H and O'Connor MB (2020) The Role of Muscle in Insect Energy Homeostasis. Front. Physiol. 11:580687. doi: 10.3389/fphys.2020.580687

INTRODUCTION

Regulating energy utilization and storage is essential for proper development and environmental adaptation. A constant supply of diet derived energy is required to sustain healthy cellular functions. Organisms must also maintain energy stores for times when nutrients are scarce as well as to fuel periods of high-energy expenditure, such as movement or flight. While energy stores are vital to survival, they must be tightly regulated as excessive or insufficient energy reserves are deleterious to survival and organismal health. In fact, excess energy stores are associated with many human metabolic diseases, obesity, cardiovascular disease and diabetes making the study of energy homeostasis of great interest to human health.

Energy homeostasis requires coordination of multiple organ systems, which communicate through many well-characterized cell signaling pathways. For example, in mammals insulin and glucagon are two well-conserved pathways that are crucial to energy homeostasis. Under nutrient rich conditions the hormone insulin is secreted from pancreatic beta cells. Insulin signals through the insulin receptor resulting in activation of two important pathways: the Mitogen-activated Protein Kinase (MAP-Kinase) and the Phosphatidylinositol-3-Kinase (PI3K). Activation of the MAP-kinase pathway results in cell mass increase through transcriptional upregulation of cell growth genes. The PI3K pathway has several functions, the most important being to signal glucose uptake as well as energy storage. Energy is stored in two main forms: glycogen and lipids. Glycogen is composed of long branched chains of glucose and is stored primarily in the liver and skeletal muscle. Lipids are synthesized from nutrient-derived carbons and stored primarily in adipose tissue as chains of varying lengths connected by a glycerol backbone. These energy stores become important under limited nutrient conditions or periods of increased energy demand. During these periods, insulin secretion decreases and secretion of a second hormone, glucagon, from pancreatic alpha cells increases. Glucagon signals through a G protein coupled receptor (GPCR) leading to mobilization of stored glycogen and lipids in a form that can fuel ongoing energy needs. These two signaling pathways are key to maintaining energy homeostasis of the whole organism and are conserved from mammals to insects.

In recent years *Drosophila melanogaster* has emerged as a model for studying metabolic homeostasis. Like many organisms, Drosophila relies on insulin and glucagon signaling to maintain energy balance. In this species, insulin like peptides (dILPs) are secreted from several sources, most importantly the Insulin Producing Cells (IPCs) in the brain. Upon secretion, dILPs bind the insulin receptor (InR) activating the MAP-kinase and PI3K pathways with similar downstream targets to mammals (Nässel et al., 2013; Mattila and Hietakangas, 2017). Conversely, in times of limited nutrients adipokinetic hormone (Akh), a functional glucagon homolog, signals through its corresponding GPCR (AkhR) and leads to energy mobilization (Grönke et al., 2007; Bharucha et al., 2008; Gáliková et al., 2015). Like mammals, *Drosophila* store energy in the form of lipids and glycogen. Lipids are found primarily in the fat body, which is analogous to mammalian adipose tissue and liver, while glycogen is found in skeletal muscles as well as fat body and the central nervous system. Again, analogous to mammals, these energy reserves are essential not only for times when nutrients are scarce, but also for times of increased energy demand such as movement or flight. The high degree of genetic conservation between mammalian and *Drosophila* metabolic pathways, the extensive genetic tool kit available in *Drosophila* and short generation time, makes *Drosophila* an ideal model to study regulators of metabolic and energy homeostasis. In addition, *D. melanogaster* are generalists and can thus be raised on a flexible diet enabling study of gene-diet interactions. *Drosophila* have emerged as a model for studying genetic and dietary forms of Type 2 Diabetes (Musselman et al., 2011) as well as glycogen storage diseases (Zirin et al., 2013).

In most triploblastic organisms, muscle is the largest organ by weight and can account for up to 50% of the adult mass. The major function of muscle is to enable movement to find food, escape predation, and initiate courtship behavior. As a consequence, it is the largest consumer of energy. Insect flight is a one of the most metabolically demanding processes in the animal kingdom. During flight, oxygen consumption increases one-hundred fold (Eanes et al., 2006). Thus, it is not surprising that somatic muscle plays an important role in regulating energy stores as well. Here we review the role of *Drosophila* skeletal muscle as an energy consumer and as an organ that regulates energy storage, and modulates insulin signaling.

THE SKELETAL MUSCLE IS A LARGE CONSUMER OF ENERGY

Insect flight is a truly incredible process and has been a source of fascination and study for more than seven decades. Adult flight is powered by direct flight muscles (DFMs) and indirect flight muscle (IFMs), which are found in the thorax. IFMs are capable of producing a mechanical force of just under 80 W kg^{-1} during flight (Lehmann and Dickinson, 1997). A separate set of muscles, known as jump muscles, are located in the legs and give the animal the ability to walk and jump. Adult body wall muscle is similar in structure to vertebrate counterparts, being tubular in shape. However, unlike the adult, larval body wall muscles are largely two-dimensional one cell thick thin sheets. Most larval muscles are histolyzed during metamorphosis and replaced by adult muscles that are derived from adult muscle founder cells (Gunage et al., 2017). A more detailed description of *Drosophila* muscle types and function has been thoroughly reviewed previously (Bernstein et al., 1993). Despite being among the most metabolically demanding processes in the animal kingdom, 1 week old *Drosophila* can sustain flight for an average of 278 min (Wigglesworth, 1949). Upon flight initiation, glucose is consumed in approximately 2 min (Sacktor and Worbber-Shavit, 1966). While this is associated with a temporary dip in glucose levels, they soon return to a steady state, which is maintained during flight (Sacktor and Worbber-Shavit, 1966). The main source of glucose used to power flight is glycogen, and glycogen stores are readily mobilized during flight and almost depleted in flies flown to exhaustion (Wigglesworth, 1949). Upon exhaustion, supplying flies with a glucose solution allows a return to flight within 30–45 s, whereas other carbohydrates, such as lactose and xylose, require longer time intervals to take effect, suggesting that glucose is the main fuel source for the muscle (Wigglesworth, 1949). In addition to glucose, muscles also readily utilize trehalose, an insect specific carbohydrate that is synthesized in the fat body (Sacktor and Worbber-Shavit, 1966). Trehalose is composed of two glucose molecules linked by a glucoside linkage and can be transported into skeletal muscle and cleaved into two glucose molecules (Shukla et al., 2015). Trehalose is also a vital fuel source during eclosion, as flies unable to synthesize trehalose die during the eclosion process (Matsuda et al., 2015). Thus, glucose, and trehalose are vital sources of energy for muscles. Despite the fact that the original research on glucose and glycogen consumption during flight was conducted over 70 years ago, (Wigglesworth, 1949) the signals required for glycogen mobilization upon flight initiation remain ill-defined. Furthermore, the role of lipids in powering flight in *Drosophila* is an area that requires further study.

In several insect species, including cockroaches and migratory locusts (*Locusta migratoria*), Akh is released upon flight initiation (Gäde et al., 1997). This results in mobilization of fat body glycogen stores, leading to increased hemolymph trehalose levels needed to supply increased energy demands by muscle. While some insects, including flies and cockroaches, rely primarily on carbohydrates to fuel flight, stored lipids are an important fuel source for locusts (Gäde et al., 1997). In locusts, Akh release results in fat body lipid mobilization and increases the lipid carrying capacity of the hemolymph by activating lipoproteins (Gäde et al., 1997; Van Der Horst, 2003). Fatty acids derived from hemolymph lipids can be oxidized by muscles of locusts and used for energy (Van Der Horst, 2003). Interestingly, in *Drosophila*, Akh appears to be dispensable for flight performance and climbing ability (Gáliková et al., 2015). In fact, the Akh receptor, AkhR, is expressed mainly in fat body and gustatory neurons and not muscle (Yoshida et al., 2016). Additionally, Akh is dispensable for the mobilization of glycogen and lipids during development. However, Akh does play a role in carbohydrate homeostasis as both larvae (Lee and Park, 2004) and adult (Gáliková et al., 2015) Akh mutants have lower levels of hemolymph trehalose (Lee and Park, 2004; Gáliková et al., 2015).

In light of the role of Akh in mobilizing energy for flight in other insects, as well as its role in maintaining trehalose levels in *Drosophila,* it is interesting that Akh does not appear to affect *Drosophila* flight performance.

In *Drosophila* and other related insects, muscles rely primarily on aerobic glycolysis to convert glucose and other carbohydrates into energy. Glycolysis occurs in the cytoplasm of muscle cells and consists of a series of enzymatic reactions that convert glucose into two molecules of pyruvate and two ATP molecules per molecule of glucose (**Figure 1**). The majority of energy is derived from the TCA/Krebs Cycle, which occurs in the matrix of the mitochondria (Sacktor and Worbber-Shavit, 1966). Pyruvate enters the mitochondria and is converted to Acetyl-CoA (**Figure 1**). Acetyl-CoA is oxidized in a series of chemical reactions generating CO_2, ATP and a pool of NADH and $FADH_2$ (**Figure 1**). NADH and $FADH_2$ are then oxidized in a process known as oxidative phosphorylation. The majority of energy from this process is stored as an electrochemical gradient and used to power ATP synthase (**Figure 1**). ATP is then supplied to the myosin ATPase enabling muscle contraction. Disrupting this process in muscle can affect the ability of muscle to function optimally (Wojtas et al., 1997).

Glycolysis is necessary for maximal wing beat frequency as inhibition of glycolysis reduces wing beat rate (Eanes et al., 2006). Most glycolytic enzymes, with the exception of hexokinase and phosphoglycerate mutase (PGM) (**Figure 1**) are present in excess, as reductions in enzymatic expression levels do not alter wing beat frequency (Eanes et al., 2006). Glycolytic enzymes in muscle are located in distinct patterns enabling resulting ATP to be supplied to the myosin ATPase. Incorrect localization of enzymes results in decreased flight ability (Wojtas et al., 1997) highlighting the importance of aerobic glycolysis in powering flight.

Aerobic glycolysis is not limited to adult flies, but is also required for proper larval development. During larval stages, animals increase in size roughly two hundred fold in a matter of days, and body wall muscle must increase in size rapidly in order to power larval locomotion. Again aerobic glycolysis is required to sustain the energetically expensive process of growth. Larvae mutant for proteins important for stabilizing the glycolytic enzymes aldolase and PGM show decreased glycolytic flux resulting in decreased amino acid pools and decreased ATP levels (Bawa et al., 2020). This results in small degenerated muscles, thus underscoring the importance of this process in fueling proper development and growth (Bawa et al., 2020). Similarly, lack of the glycolytic enzyme phosphoglycerate mutase 2 (pgam2) results in abnormally thin muscles (Tixier et al., 2013).

Unlike mammals, flies do not typically rely on anaerobic respiration, a process by which pyruvate is converted to lactate in the cytoplasm (Feala et al., 2007; **Figure 1**). Interestingly, this makes flies remarkably resistant to hypoxic and even anoxic conditions. While humans can survive for only minutes in anoxia, flies can survive for up to 4 h (Feala et al., 2007). Increased survival time for flies is due to lack of lactate build up. Rather than converting pyruvate to lactate, flies covert pyruvate to alanine and acetate, which are less acidic and more energetically favorable than lactate (Feala et al., 2007). In addition, levels of proline and glutamine decrease indicating that amino acids are being broken down and entering the Krebs cycle (Sacktor and Worbber-Shavit, 1966; Feala et al., 2007). These findings suggest that rather than relying on cytoplasmic lactate production, flies utilize the mitochondria and the Krebs cycle to power muscle movement in times of hypoxic stress.

Given the importance of the Krebs cycle in energy production in the muscle, it is no surprise that mitochondria are also central to maintaining energy homeostasis. In larvae, disrupting mitochondrial activity results in decreased oxygen consumption, decreased ATP production, and smaller muscles (Song et al., 2017). During the first 7 days of adulthood, muscle mitochondrial area increases, which is correlated with maximal flight performance (Sohal, 1975). Mitochondria are very dynamic structures and undergo fission and fusion, which are necessary for both quality control and energy production. During the first 7 days of adulthood, mitochondria increase size by growth as well as fusion (Wigglesworth, 1949). As flies age, total area occupied by mitochondria remains steady, but fission occurs resulting in smaller mitochondria. Decreased mitochondrial size is enhanced in dewinged flies (Sohal, 1975). This observation suggests that exercise may be required to maintain mitochondrial structure in older adults, however, the relationship between exercise and mitochondrial function remains a notable area for further study.

Mitochondrial fission and fusion require expression of nuclear encoded genes, which are regulated by the nuclear encoded transcription factor Ewg (mammalian NRF1 homolog). Loss of Ewg results in decreased expression of Optic atrophy 1 (Opa1), which is required for inner membrane fusion (Rai et al., 2014), resulting in smaller rounded mitochondria that co-localize with the lysosome suggesting that they are undergoing mitophagy. The smaller mitochondrial structure leads to abnormal muscle development during pupation. As adults, animals mutant for Ewg, and therefore expressing lower levels of Opa1, show a decreased number of IFMs and disorganized DLMs (Rai et al., 2014). Taken together these findings demonstrate that muscle mitochondrial fission and fusion is required for proper pupal development and adult muscle function.

The inner mitochondrial membrane contains many cristae, or folds, that maximize surface area, allowing for efficient electron chain transfer and ATP production. Cristae structure is maintained by the mitochondrial contact site and cristate organizing system (MICOS) (Yoon et al., 2019). MICOS is activated by the ATPase YME1 like ATPase (YME1L), and YME1L in turn is activated by the serine/threonine kinase aarF domain containing kinase (dADCK1). Thus, loss of dADCK1 results in lack of YME1L 1 and MICOS activation. dADCK1 mutant animals are delayed in development and are small in size demonstrating the importance of mitochondria in fueling the growth process (Yoon et al., 2019). While dADCK1 mutants are lethal, depleting dADCK1 specifically in the muscle results in viable adults with abnormal mitochondrial structure, decreased mitochondrial surface area and decreased mitochondrial membrane potential resulting in decreased ATP pools. Lack of sufficient ATP leads to decreased wing movement and abnormal wing posture, demonstrating the importance of

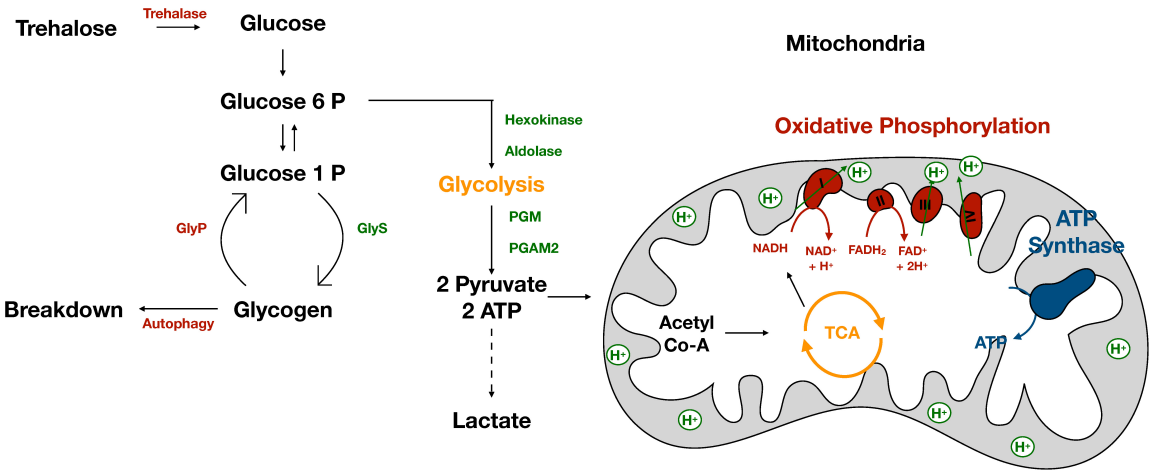

FIGURE 1 | The muscle stores and consumes energy. The muscle stores energy in the form of glycogen. Glycogen consists of long chains of glucose and is synthesized by GlyS. Glycogen can be broken down by GlyP or via autophagy to provide the muscle with energy in times of need. When energy is needed glucose enters glycolysis, a series of enzymatic reactions which occur in the cytoplasm to form two molecules of pyruvate and ATP. The majority of pyruvate enters the inner matrix of the mitochondria where it is converted to Acetyl-CoA and oxidized in the TCA cycle producing NADH and $FADH_2$. NADH and $FADH_2$ power oxidative phosphorylation which creates an electrochemical gradient used to power ATP synthase producing ATP.

mitochondrial cristae in providing the muscles with energy to power wing movement and flight (Yoon et al., 2019).

Mitochondria also play an important role in maintaining energy homeostasis when responding to different nutrient sources. Specifically, mitochondria are flexible as to the substrates that enter the electron transfer chain based on availability. However, metabolic overload can overwhelm mitochondria and reduce this flexibility (Cormier et al., 2019). For example, animals fed on a high fat diet (HFD), become reliant on a single mitochondrial membrane complex for entry into the electron transfer chain (Cormier et al., 2019) and are limited in the types of substrates that can be oxidized. Metabolic overload and lack of mitochondrial flexibility ultimately brings about decreased ATP in the thoracic muscle as well as decreased climbing ability and a decreased lifespan. In addition to lower ATP, muscles were found to have decreased levels of stored energy, likely contributing to decreased muscle performance (Cormier et al., 2019). This demonstrates that muscles are not only active consumers of energy but also must store some of their own energy to mobilize in times of need. Given the ease of diet manipulation, it is surprising that more studies have not investigated the relationship between specific diet components and locomotor behavior in larvae or adults.

SKELETAL MUSCLES AS A SOURCE OF STORED ENERGY

Given the intense energy demands of insect muscle, it is no surprise that muscles are also an important source of stored energy in the form of glycogen (Yamada et al., 2018, 2019; **Figure 1**). Glycogen consists of long branched chains of glucose synthesized by the enzyme glycogen synthase (GlyS) (**Figure 1**). Synthesis of glycogen from dietary glucose in the fat body requires insulin signaling (Yamada et al., 2018) and animals lacking dILP1 (Liao et al., 2020), dILP2, or dILP5 have lower whole body glycogen levels (Post et al., 2018). However, the relationship between insulin signaling and glycogen storage in the muscle has not been studied. Insulin resistance resulting from a high sugar diet leads to lower glycogen levels despite elevated hemolymph sugars in both larvae (Musselman et al., 2011) and adults (Morris et al., 2012), but again whether this difference is limited to just fat body glycogen levels or also affects muscle glycogen levels is unknown.

Glycogen is broken down by glycogen phosphatase (GlyP) (**Figure 1**) to liberate free glucose molecules used to power movement and flight. GlyP is negatively regulated by insulin signaling, specifically by dILP2 (Post et al., 2018). In many insects, Akh is important for activating GlyP upon flight initiation (van Marrewijk et al., 1986; Van Der Horst, 2003). During times of high demand, GlyP works at near saturation as small alterations in GlyP levels results in decreased wing beat frequency (Eanes et al., 2006). However, the signal that activates GlyP in *Drosophila* upon flight initiation is unlikely to be Akh (Grönke et al., 2007; Bharucha et al., 2008; Gáliková et al., 2015) and its identity is an important goal that remains to be determined.

Glycogen is an important fuel source throughout development. Most animals lacking GlyS, and thus unable to synthesize glycogen, die as larvae; however, a few make it to adulthood. Larval survival of GlyS mutants can be increased by a high yeast, high glucose diet, but many of these animals die during metamorphosis (Yamada et al., 2019). In larvae, glycogen is primarily stored in body wall muscles, but is also found in the fat body and CNS. Lack of GlyS in the muscles results in a significant decrease in survival rate, similar to that of a GlyS mutant, while loss of GlyS in the fat body does not affect survival (Yamada et al., 2018). While not required for survival, fat body stores of glycogen can fuel the animal through brief periods of

starvation and has thus been termed a "metabolic safeguard" (Yamada et al., 2018). In the fat body, glycogen can be either converted directly to glucose, or used to synthesize trehalose. Trehalose is secreted from the fat body, and can be used by other tissues, such as the muscle. Once in the muscle, trehalase breaks down trehalose into glucose which can be used as an energy source (Yoshida et al., 2016). In the fat body glycogen breakdown occurs mostly by GlyP (Zirin et al., 2013). However, starvation induced glycogen breakdown in the muscle can occur either through GlyP or autophagy. Inhibiting either process alone does not prevent starvation induced glycogen breakdown, however, inhibiting both simultaneously prevents starvation induced glycogen breakdown in the muscle (Zirin et al., 2013). In the fat body, starvation induced autophagy requires inhibition of the Tor kinase pathway. While the link between Tor activity and insulin signaling in muscle has not been fully explored, it is tempting to speculate that it is reduced insulin signaling upon starvation that inhibits Tor activity. Inhibition of both GlyP and autophagy also results in reduced crawling speeds following periods of starvation underscoring the importance of glycogen as a fuel source for the muscle in sustaining movement (Zirin et al., 2013). It would be interesting to know whether Tor activity modulates the activity of GlyP, or just starvation induced autophagy.

In addition to being important for larval survival and larval locomotion, glycogen is a key source of stored energy in adult muscle. In adults, glycogen is also stored in the fat body, halteres, proventriculus and midgut (Wigglesworth, 1949). Glycogen stores peak at 1 week in age, which is correlated with maximal flight performance (Wigglesworth, 1949). Decreased flight performance and climbing speeds are seen in animals lacking GlyS or GlyP highlighting the importance of glycogen in physical fitness (Yamada et al., 2019). However, these animals can still climb and fly indicating that some level of compensation for lack of glycogen stores must be occurring. Due to changes in levels of glucogenic amino acids in GlyS and GlyP mutants, it has been speculated that these mutants have altered amino acid metabolism (Yamada et al., 2019). Loss of both GlyS and GlyP also results in decreased trehalose levels since glycogen is often used to synthesize trehalose (Yamada et al., 2019). Trehalose is an important fuel source for muscles, and animals hypomorphic for trehalose-6-phosphate synthase (Tps1), which is required for trehalose synthesis, also demonstrate reduced flight and climbing performance (Matsuda et al., 2015).

While enzymes involved directly in carbohydrate metabolism have clear roles in maintaining carbohydrate homeostasis, homeostasis is also affected by other factors. In order to synthesize glycogen, animals must digest dietary carbohydrates to form glucose. Digestion begins in the midgut where amylases are secreted into the gut lumen. Expression of these amylases is tightly regulated and is controlled in part by the nuclear receptor DHR38 (Ruaud et al., 2011). Animals lacking DHR38 have reduced expression levels of two digestive amylases as well as phosphoglycomutase that result in reduced glycogen stores in the muscle highlighting the importance of these enzymes in maintaining glycogen homeostasis (Ruaud et al., 2011). On the flip side, amylases are inhibited by high dietary sugar via the transcription factor Sugarbabe (Mattila et al., 2015). Metabolic overload, such as a high sugar diet, leads to reduced glycogen stores (Musselman et al., 2011; Morris et al., 2012), further emphasizing the importance of nutrition in maintaining energy homeostasis. The transcription factor missing oocyte (Mio) (ChREBP homolog) also regulates the expression of genes required for utilization of diet derived fuel sources. In the muscle, Mio is important for glycogen utilization since animals lacking Mio in the muscle have increased glycogen levels (Polak et al., 2015). Loss of Mio in the muscle also leads to small and disorganized myofibrils with irregular spaces filled with glycogen granules. As a result, increased glycogen granules and abnormal muscle structure contribute to decreased flight performance as observed in animals lacking Mio expression in the muscle (Polak et al., 2015). Given the importance of glycogen stores for muscle function, it seems likely that additional genes beside dILP2 (Post et al., 2018), DHR38 (Ruaud et al., 2011), and Mio (Polak et al., 2015) are required to modulate levels of muscle glycogen stores and screens to identify them should prove fruitful.

THE ROLE OF MUSCLE IN MAINTAINING LIPID HOMEOSTASIS

Under normal conditions, lipids/triacylglycerol (TAG) are not found in muscle but are stored mainly in fat body and oenocytes (Heier and Kühnlein, 2018). Ectopic fat accumulation in muscle is associated with insulin resistance, muscle weakness and structural abnormalities and is seen with dietary or genetically induced obesity (Villanueva et al., 2019). Obese animals also have disorganized myofibrils and mitochondrial damage leading to an accelerated age related decrease in climbing rate. Interestingly, accumulation of lipid droplets in the muscle of obese flies can be rescued by time restricted feeding (Villanueva et al., 2019). In addition to obesity, age is also associated with lipid droplet accumulation in muscles, especially jump muscles (Yan et al., 2017). Increased lipid droplets in aged flies are a result of an increase in Perilipin 2 (PLIN2), which has been shown to protect lipid droplets. In young flies, PLIN2 levels are modulated through the activity of histone deacetylase 6 (HDAC6) and the chaperone Heat shock 70 kDA protein cognate 4 (Hsc4) that mediate ubiquitin-proteasomal and lysosomal degradation of native and/or misfolded proteins. HDAC6 expression decreases with age, thereby effecting an increase in PLIN2 and subsequent lipid droplet accumulation in muscle (Yan et al., 2017). Increased insulin signaling in the muscle also results in the presence of TAGs in the muscle of adult flies, while decreasing TAGs elsewhere (Zhao and Karpac, 2017). Insulin signaling typically represses the transcription factor forkhead box subgroup O (FoxO). Loss of FoxO in the thoracic skeletal muscle results in the appearance of lipids in the muscle and upregulation of the cytokine unpaired 2 (upd2). This in turn leads to increased Akh secretion, mobilization of lipid, and decreased TAGs in the fat body and gut, despite having ectopic lipid accumulation in the muscle (Zhao and Karpac, 2017). This demonstrates that while lipids are usually absent in the muscle, the muscle can be an important regulator of lipid levels. It is interesting that

both insulin resistance and increased insulin signaling in muscle result in ectopic lipid accumulation, suggesting that a very precise level of insulin signaling is needed in muscle to suppress muscle TAG accumulation.

While muscles do not typically store lipids, myokines serve as important regulators of organismal lipid stores. Lipid stores in the fat body of adults are regulated in response to muscle derived Wingless (Wg), the expression of which requires muscle Med13, part of the complex that regulates interactions between RNA Pol II and transcription factors (Lee et al., 2014). Lack of either Med13 or Wg in muscle produces increased TAGs in fat body, increased lipid droplet size and starvation resistance. Interestingly, loss of Med13 or Wg in either the skeletal muscle or cardiac muscle is sufficient to increase TAG levels (**Figure 2**). A second myokine that has been shown to suppress obesity is the PDGF/VEGF ligand Pvf1. However, unlike Wg that signals to the fat body, Pvf1 signals to the oenocytes, a specialized hepatocyte like cell. Oenocytes express the Pvf1 receptor PvR, and activation of PvR in oenocytes results in activation of mTOR which in turn leads to increased PI3K and Akt. This Pvf1-mTOR-Akt signaling cascade from muscle to oenocytes slows the rate of lipid synthesis without affecting the rate of lipid mobilization (Ghosh et al., 2020; **Figure 2**). The rate of lipid synthesis is very rapid in young flies, and Pvf1 expression levels are found to be very low at the time of eclosion. Overexpression of Pvf1 in young flies results in inhibition of developmentally programmed TAG synthesis (Ghosh et al., 2020). Future studies will be needed to elucidate the signal between oenocytes and fat body in response to muscle derived Pvf1.

While loss of Wg signaling or Pvf1 in muscle increases TAG levels, loss of cytokine activated Janus Kinase/signal transducer and activator of transcription (JAK/Stat) signaling in muscle decreases TAGs (Kierdorf et al., 2020; **Figure 2**). This dynamic is mediated through increased p-AKT levels and thereby increased insulin signaling. In addition to decreasing TAGs, loss of JAK/Stat and the consequent increased insulin signaling leads to TAG presence in the muscle and decreased total glucose and glycogen levels in the organism, likely resulting from an increased metabolic rate (Kierdorf et al., 2020). This result is similar to what was seen with loss of FoxO, a negative regulator of insulin signaling, which also results in ectopic lipid accumulation in muscle (Zhao and Karpac, 2017). Interestingly, this report also found an upregulation of the JAK/Stat ligand Upd2 in the muscle of animals with increased insulin signaling. It would be interesting to know whether Upd2 may be able to signal back to the muscle to reduce insulin signaling. Finally, in larvae, increased expression of the Transforming growth factor-beta (TGF-β) ligand Activin-β in the muscle generates increased free fatty acids, organismal TAGs and TAG storage in the fat body (**Figure 2**). Activin-β signals through a heterodimeric receptor composed of Baboon and Punt, which are found in the fat body, increasing TAG storage (Song et al., 2017).

Despite the fact that TAGs are not stored in muscle, the muscle is still important in regulating TAG homeostasis as can be seen under conditions of dietary restriction. Dietary restriction has been shown to increase lifespan in many models, including *Drosophila*. In *Drosophila* dietary restriction is not associated

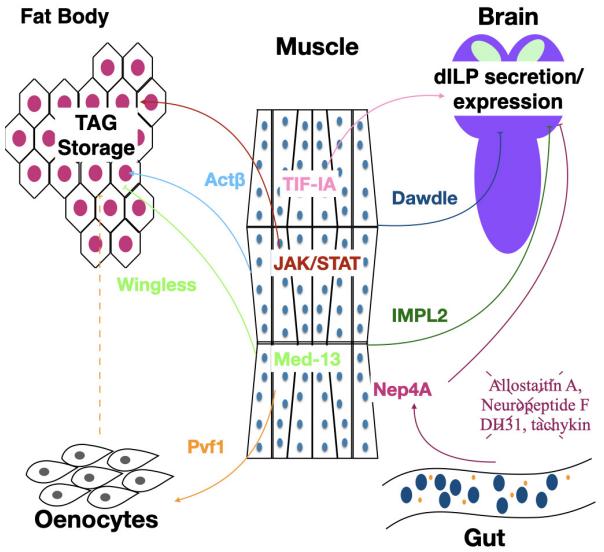

FIGURE 2 | The muscle regulates TAG storage and insulin signaling. Signaling pathways from and to the muscles affect metabolic homeostasis. Actβ and Dawdle are Activin-like members of the TGFβ superfamily of signaling factors. JAK/STAT factors are signal transduction components that act downstream of insect Unpaired ligands. TIF-IA is a transcription factor that connects RNA polymerase I with the UBF/SL-1 complex to initiate the transcription of pre-ribosomal RNA. Med13 is a member of the Mediator Complex a transcriptional coactivator complex. Pvf1 is an insect PDGF/VDGF homolog. IMPL2 is an insect insulin binding protein. Nep4A is a muscle localized Neprilysin that likely is responsible for cleavage of the several neuroendocrine peptides including DH31, Allatostatin A, tachykinin, and Neuropeptide F are derived from the gut that regulate insulin secretion from the brain.

with a decrease in total TAG levels, but conversely an increase in both total body TAG stores and lipid droplet size as well as the rate of both lipogenesis and lipolysis. The molecular mechanism by which lipolysis is increased is not known. It would be interesting to see whether dietary restriction changes the length or saturation level of stored TAGs, as this has been shown in other systems to alter the lipolysis rates (Benito-Gallo et al., 2015). In addition to increased TAG turnover, animals fed a restricted diet also demonstrate increased physical activity and improved muscle function (Katewa et al., 2012). These phenotypes are dependent on the enzyme Acetyl-CoA carboxylase (ACC). Interestingly, ACC in the fat body, the tissue where the majority of TAGs are stored, is not required to increase life span, but instead ACC in the muscle, a tissue that does not typically store TAGs is required for increased lifespan resulting from dietary restriction (Katewa et al., 2012). Why ACC expression would be required in the muscle and not the fat body remains to be determined. The muscle is clearly key to mediating the effects of dietary restriction as genome wide loss of ACC results in decreased expression of muscle structure and function genes. Furthermore, inhibiting physical activity of flies by ablating or clipping wings significantly reduced the effects of dietary restriction on increased lifespan (Katewa et al., 2012). These results demonstrate that the muscle is a key tissue for responding to dietary restriction, but do not

address the question of what specific role ACC might play in muscle. Since dietary restrictions results in increased TAG turnover (Katewa et al., 2012), it would be interesting to see if TAGs transport to muscles is required for the increased lipolysis. Furthermore, this study looked only at TAG levels in response to dietary restriction and did not consider glycogen, another important form of stored energy. It would be interesting to see whether glycogen stores in muscle and or fat body are altered by dietary restriction.

THE SKELETAL MUSCLE MODULATES INSULIN SIGNALING

Proper growth of muscles is dependent on insulin signaling. Lack of insulin signaling in muscle results in smaller muscle size and decreased nuclear ploidy (Demontis and Perrimon, 2009). Decreased size is due to lack of insulin dependent inhibition of the transcription factor FoxO. Increased FoxO activity results in inhibition of dMyc expression, which is required for muscles to reach normal size and nuclear ploidy (Demontis and Perrimon, 2009). FoxO dependent regulation of myc is also important in response to low nutrient conditions. In the muscle, inhibition of myc by FoxO results in decreased protein translation, presumably to conserve energy (Teleman et al., 2008). Insulin signaling in larval muscles is regulated by other signaling pathways including the TFG-β/Activin signaling pathway ligand Activin-β. Activin-β positively regulates insulin signaling and is required for proper muscle geometry and sarcomere protein level (Kim and O'Connor, 2020). While these studies show the importance of insulin signaling in proper muscle size and structure, whether insulin signaling in the muscle alters levels of stored glycogen locally or globally is unknown. This is surprising given the importance of insulin signaling in maintaining carbohydrate homeostasis.

The JAK/Stat and insulin signaling pathway cooperate in larval muscle to mount an immune response. Fighting infections is an energetically expensive process. Following parasitic wasp infection hemocyte derived Upd2 and Upd3 activate JAK/Stat signaling in muscle, which in turn increases insulin signaling (Yang and Hultmark, 2017). This process is fueled by glycogen stored in muscle. Thus, animals lacking sufficient muscle glycogen stores are more susceptible to infection (Yang and Hultmark, 2017). This is one of the only reports that clearly links muscle glycogen stores to a distinct function in larvae. Another report found that glycogen muscle stores were needed for optimal locomotor function under starvation conditions (Zirin et al., 2013). Interestingly, in adults, JAK/Stat signaling is required to prevent high levels of insulin signaling. JAK/Stat ligands Upd1, 2, 3 are supplied by plasmocytes and activate JAK/Stat signaling in muscle. Suppression of JAK/Stat signaling in adult muscle results in increased insulin signaling in muscle, which shortens life span and decreases climbing ability (Kierdorf et al., 2020). This may simply be a difference between larvae and adults, however, it may also suggest that both low and high levels of JAK/Stat signaling in the muscle can result in increased insulin signaling. It has been demonstrated that increased insulin signaling in muscle results in muscle upregulation of Upd2 (Zhao and Karpac, 2017). Whether Upd2 signals back to the muscle, and if so, does it positively or negatively regulate insulin signaling remains unclear.

As described above, insulin signaling to the muscle plays an important role in proper muscle growth and function. In addition to being a receiver of insulin signaling, the muscle modulates insulin signaling in the whole animal. During larval development, insulin signaling is coupled to the availability of nutrients via the TOR pathway, which is required for growth (Colombani et al., 2003). One way it does this is by increasing mRNA and protein levels of Transcription initiation factor-IA (TIF-IA), a transcription factor required for ribosomal synthesis (Ghosh et al., 2014). In addition to promoting muscle growth, TIF-IA also affects the level of insulin signaling. Loss of TIF-IA in the muscle results in decreased dILP3 and dILP5 mRNA levels, increased retention of dILP2 in the IPCs as well as increased expression of Imaginal morphogenesis protein-Late 2 (IMPL2), a negative regulator of insulin signaling (**Figure 2**). It remains unclear the mechanism by which TIF-IA in muscle affects transcription levels of dILPs or dILP release. It is worth mentioning that when TIF-IA expression was decreased in muscle using RNAi, resulting in the decrease in dILP transcription levels, the driver used (mef2 gal4) is not specific to the muscle, and also shows some expression in the CNS. Testing with additional specific-muscle only drivers seems warranted.

Overexpression of the transcription factor FoxO in muscle, which is negatively regulated by insulin signaling, results in repression of the TGF-β ligand Dawdle. Dawdle signals cell-autonomously to muscle through the TGF-β receptor Baboon, which activates the transcription factor Smox (Bai et al., 2013). Low insulin signaling therefore results in lower Smox activation and transcriptional upregulation of autophagic genes preserving muscle function and structure in older animals. In addition to affecting the muscle, increased Dawdle expression from the muscle gives rise to decreased dILP2 secretion and decreased insulin signaling (**Figure 2**). The combination of increased autophagic genes in the muscle and decreased insulin signaling in the whole animal results in an extended lifespan (Bai et al., 2013). However, a more recent study suggests that the role of muscle TGFβ signaling in regulating lifespan is more complicated since overexpression of either Dawdle or a second ligand Myoglianin in adult muscle appears to extend lifespan, in part, through enhanced production of the 26S proteasome (Langerak et al., 2018). Increased lifespan as a result of decreased insulin signaling can also be achieved through mild mitochondrial perturbation in larval muscle, which results in upregulation of IMPL2 in adults, which then binds to and inhibits dILPs (Owusu-Ansah et al., 2013; **Figure 2**).

Another way in which muscle is thought to modulate insulin signaling is via expression of the neprilysin Neprilysin4A (Nep4A), which can cleave and inactivate regulatory peptides. Overexpression of Nep4A in larval body wall muscle results in several phenotypes indicative of decreased insulin signaling including reduced body size, decreased food intake and increased glucose levels (Hallier et al., 2016). Indeed, overexpression of Nep4A in muscle reduces expression of dILPs 1,2,3, and 5. Given that Nep4 is found localized to the membrane of muscle

cells suggests that Nep4A may cleave peptides that positively regulate insulin signaling. *In vitro* experiments found that Nep4A cleaves several peptides involved in dILP synthesis and/or feeding behavior including Allatostatin A, Neuropeptide F, DH31 and tachykinins 1,2,4, and 5 (Hallier et al., 2016). These peptides are produced in the CNS as well as by enteroendocrine cells in the midgut, leading the authors to speculate that Nep4A on muscle may cleave gut derived peptides as they travel through the hemolymph from the gut, thereby preventing them from reaching the IPCs (**Figure 2**). It is worth noting that Nep4A is also expressed in the CNS and is found localized to the membrane of IPCs. While neural or glial knockdown of Nep4A does not alter feeding behavior or body size, it is not clear if CNS expression of Nep4A may be important for cleavage of insulin promoting peptides, derived either from the gut or the CNS (Hallier et al., 2016).

CONCLUDING REMARKS

While it has been appreciated for over half a century that insect muscle is a large consumer of energy (Wigglesworth, 1949; Sacktor and Worbber-Shavit, 1966), more recently the focus has shifted to the role of muscle in maintaining energy homeostasis (Katewa et al., 2012; Lee et al., 2014; Hallier et al., 2016; Song et al., 2017; Zhao and Karpac, 2017) and numerous avenues of investigation remain to be explored. One curious observation is that, while Akh signaling is required in several insects for maximal flight performance (Gäde et al., 1997; Van Der Horst, 2003), Akh seems to be dispensable for flight performance in *Drosophila* (Gáliková et al., 2015). What serves as the signal to the muscle that additional energy is needed upon flight initiation? It has been shown that muscle glycogen stores are necessary for maximal flight performance (Yamada et al., 2019). However, the signals that initiate breakdown of muscle glycogen stores during flight remain unknown. Furthermore, while several studies have focused on signals that regulate storage of fats in muscle and elsewhere, how glycogen storage is regulated in muscle and fat body remains largely unexplored.

Several reports have focused on how the muscle regulates insulin and Akh signaling at the organismal level (Hallier et al., 2016; Yan et al., 2017; Bawa et al., 2020). However, little is known about the effect of insulin and Akh signaling on energy storage in the muscle itself. While, it has been demonstrated that increased insulin signaling in the muscle can lead to ectopic lipid accumulation (Zhao and Karpac, 2017), the question of if and how insulin signaling regulates muscle glycogen stores remains to be determined.

One exciting new avenue that is being developed is the use of *Drosophila* as an exercise model. Worldwide, obesity rates are increasing and causing an increase in diseases associated with obesity, such as Type II diabetes, cardiovascular disease and kidney disease to name a few. One of the most prescribed treatments for obesity is increased physical exercise, yet the genetics behind the response to exercise remains largely unknown. Given that *Drosophila* has served as an excellent model for better understanding energy homeostasis, there has been a recent push to develop an exercise model for *Drosophila*. Thus far, a *Drosophila* Treadwheel (Lowman et al., 2018) has been developed as well as rotational exercise quantification system (Watanabe and Riddle, 2017). These new tools should enable exciting future work exploring how exercise affects muscle and the effects this has on organismal energy homeostasis.

AUTHOR CONTRIBUTIONS

HB conceived and wrote the manuscript. MO'C edited the manuscript and provided funding. All authors contributed to the article and approved the submitted version.

FUNDING

This work was supported by a grant from the National Institutes of Health grant 1R35GM118029 to MO'C and an IRACDA fellowship from NIH supported training grant K12 GM119955 to HB.

ACKNOWLEDGMENTS

The authors thank Myung-Jun Kim and MaryJane Shimell for critical review of the manuscript.

REFERENCES

Bai, H., Kang, P., Hernandez, A. M., and Tatar, M. (2013). Activin signaling targeted by Insulin/dFOXO regulates aging and muscle proteostasis in *Drosophila*. *PLoS Genet.* 9:e1003941. doi: 10.1371/journal.pgen.1003941

Bawa, S., Brooks, D. S., Neville, K. E., Tipping, M., Sagar, M. A., Kollhoff, J. A., et al. (2020). *Drosophila* TRIM32 cooperates with glycolytic enzymes to promote cell growth. *eLife* 9:e52358. doi: 10.7554/eLife.52358.sa2

Benito-Gallo, P., Franceschetto, A., Wong, J. C. M., Marlow, M., Zann, V., Scholes, P., et al. (2015). Chain length affects pancreatic lipase activity and the extent and pH-time profile of triglyceride lipolysis. *Eur. J. Pharm. Biopharm.* 93, 353–362. doi: 10.1016/j.ejpb.2015.04.027

Bernstein, S. I., O'Donnell, P. T., and Cripps, R. M. (1993). Molecular genetic analysis of muscle development, structure, and function in *Drosophila*. *Int. Rev. Cytol.* 143, 63–152. doi: 10.1016/s0074-7696(08)61874-4

Bharucha, K. N., Tarr, P., and Zipursky, S. L. (2008). A glucagon-like endocrine pathway in *Drosophila* modulates both lipid and carbohydrate homeostasis. *J. Exp. Biol.* 211, 3103–3110. doi: 10.1242/jeb.016451

Colombani, J., Raisin, S., Pantalacci, S., Radimerski, T., Montagne, J., and Léopold, P. (2003). A nutrient sensor mechanism controls *Drosophila* growth. *Cell* 114, 739–749. doi: 10.1016/s0092-8674(03)00713-x

Cormier, R. P. J., Champigny, C. M., Simard, C. J., St-Coeur, P. D., and Pichaud, N. (2019). Dynamic mitochondrial responses to a high-fat diet in *Drosophila* melanogaster. *Sci. Rep.* 9, 1–11. doi: 10.1038/s41598-018-36060-5

Demontis, F., and Perrimon, N. (2009). Integration of Insulin receptor/Foxo signaling and dMyc activity during muscle growth regulates body size in *Drosophila*. *Development* 118, 401–415. doi: 10.1242/dev.027466

Eanes, W. F., Merritt, T. J. S., Flowers, J. M., Kumagai, S., Sezgin, E., and Zhu, C. T. (2006). Flux control and excess capacity in the enzymes of glycolysis and their relationship to flight metabolism in *Drosophila* melanogaster. *Proc. Natl. Acad. Sci. U.S.A.* 103, 19413–19418. doi: 10.1073/pnas.0607095104

Feala, J. D., Coquin, L., McCulloch, A. D., and Paternostro, G. (2007). Flexibility in energy metabolism supports hypoxia tolerance in *Drosophila* flight muscle: metabolomic and computational systems analysis. *Mol. Syst. Biol.* 3:99. doi: 10.1038/msb4100139

Gäde, G., Hoffmann, K. H., and Spring, J. H. (1997). Hormonal regulation in insects: facts, gaps, and future directions. *Physiol. Rev.* 77, 963–1032. doi: 10.1152/physrev.1997.77.4.963

Gáliková, M., Diesner, M., Klepsatel, P., Hehlert, P., Xu, Y., Bickmeyer, I., et al. (2015). Energy homeostasis control in *Drosophila* adipokinetic hormone mutants. *Genet. Investig* 201, 665–683. doi: 10.1534/genetics.115.178897

Ghosh, A., Rideout, E. J., and Grewal, S. S. (2014). TIF-IA-dependent regulation of ribosome synthesis in *Drosophila* muscle is required to maintain systemic insulin signaling and larval growth. *PLoS Genet.* 10:e1004750. doi: 10.1371/journal.pgen.1004750

Ghosh, A. C., Tattikota, S. G., Liu, Y., Comjean, A., Hu, Y., Barrera, V., et al. (2020). *Drosophila* PDGF/VEGF signaling from muscles to hepatocyte-like cells protects against obesity. *bioRxiv* [Preprint]. doi: 10.1101/2019.12.23.887059

Grönke, S., Müller, G., Hirsch, J., Fellert, S., Andreou, A., Haase, T., et al. (2007). Dual lipolytic control of body fat storage and mobilization in *Drosophila*. *PLoS Biol.* 5:e137. doi: /10.1371/journal.pbio.0050137

Gunage, R. D., Dhanyasi, N., Reichert, H., and VijayRaghavan, K. (2017). *Drosophila* adult muscle development and regeneration. *Semin. Cell Dev. Biol.* 72, 56–66. doi: 10.1016/j.semcdb.2017.11.017

Hallier, B., Schiemann, R., Cordes, E., Vitos-Faleato, J., Walter, S., Heinisch, J. J., et al. (2016). *Drosophila* neprilysins control insulin signaling and food intake via cleavage of regulatory peptides. *eLife* 5:e19430. doi: 10.7554/eLife.19430.019

Heier, C., and Kühnlein, R. P. (2018). Triacylglycerol metabolism in *drosophila* melanogaster. *Genetics* 210, 1163–1184. doi: 10.1534/genetics.118.301583

Katewa, S. D., Demontis, F., Kolipinski, M., Hubbard, A., Gill, M. S., Perrimon, N., et al. (2012). Intramyocellular fatty-acid metabolism plays a critical role in mediating responses to dietary restriction in *drosophila* melanogaster. *Cell Metab.* 16, 97–103. doi: 10.1016/j.cmet.2012.06.005

Kierdorf, K., Hersperger, F., Sharrock, J., Vincent, C. M., Ustaoglu, P., Dou, J., et al. (2020). Muscle function and homeostasis require cytokine inhibition of AKT activity in *drosophila*. *eLife* 9:e51595. doi: 10.7554/eLife.51595

Kim, M.-J., and O'Connor, M. B. (2020). *Drosophila* Activin signaling promotes muscle growth through InR/dTORC1 dependent and independent processes. *bioRxiv* [preprint]. doi: 10.1101/2020.03.23.003756

Langerak, S., Kim, M. J., Lamberg, H., Godinez, M., Main, M., Winslow, L., et al. (2018). The *Drosophila* TGF-beta/Activin-like ligands Dawdle and Myoglianin appear to modulate adult lifespan through regulation of 26S proteasome function in adult muscle. *Biol. Open* 7:bio029454. doi: 10.1242/bio.029454

Lee, G., and Park, J. H. (2004). Hemolymph sugar homeostasis and starvation-induced hyperactivity affected by genetic manipulations of the adipokinetic hormone-encoding gene in *Drosophila* melanogaster. *Genetics* 167, 311–323. doi: 10.1534/genetics.167.1.311

Lee, J. H., Bassel-Duby, R., and Olson, E. N. (2014). Heart- and muscle-derived signaling system dependent on MED13 and Wingless controls obesity in *Drosophila*. *Proc. Natl. Acad. Sci. U.S.A.* 111, 9491–9496. doi: 10.1073/pnas.1409427111

Lehmann, F. O., and Dickinson, M. H. (1997). The changes in power requirements and muscle efficiency during elevated force production in the fruit fly *Drosophila* melanogaster. *J. Exp. Biol.* 200(Pt 7), 1133–1143.

Liao, S., Post, S., Lehmann, P., Veenstra, J. A., Tatar, M., and Nässel, D. R. (2020). Regulatory roles of *Drosophila* insulin-like peptide 1 (DILP1) in metabolism differ in pupal and adult stages. *Front. Endocrinol.* 11:180. doi: 10.3389/fendo.2020.00180

Lowman, K. E., Wyatt, B. J., Cunneely, O. P., and Reed, L. K. (2018). The treadwheel: interval training protocol for gently induced exercise in *Drosophila* melanogaster. *J. Vis. Exp.* 2018:57788. doi: 10.3791/57788

Matsuda, H., Yamada, T., Yoshida, M., and Nishimura, T. (2015). Flies without trehalose. *J. Biol. Chem.* 290, 1244–1255. doi: 10.1074/jbc.m114.619411

Mattila, J., Havula, E., Ripatti, S., Sandmann, T., Hietakangas, V., Suominen, E., et al. (2015). Mondo-Mlx mediates organismal sugar sensing through the gli-similar transcription factor sugarbabe. *Cell Rep.* 13, 350–364. doi: 10.1016/j.celrep.2015.08.081

Mattila, J., and Hietakangas, V. (2017). Regulation of carbohydrate energy metabolism in *Drosophila* melanogaster. *Genetics* 207, 1231–1253.

Morris, S. N. S., Coogan, C., Chamseddin, K., Fernandez-Kim, S. O., Kolli, S., Keller, J. N., et al. (2012). Development of diet-induced insulin resistance in adult *Drosophila* melanogaster. *Biochim. Biophys. Acta Mol. Basis Dis.* 1822, 1230–1237. doi: 10.1016/j.bbadis.2012.04.012

Musselman, L. P., Fink, J. L., Narzinski, K., Ramachandran, P. V., Hathiramani, S. S., Cagan, R. L., et al. (2011). A high-sugar diet produces obesity and insulin resistance in wild-type *Drosophila*. *DMM Dis. Model. Mech.* 4, 842–849. doi: 10.1242/dmm.007948

Nässel, D. R., Kubrak, O. I., Liu, Y., Luo, J., and Lushchak, O. V. (2013). Factors that regulate insulin producing cells and their output in *Drosophila*. *Front. Physiol.* 4:252. doi: 0.3389/fphys.2013.00252

Owusu-Ansah, E., Song, W., and Perrimon, N. (2013). Muscle mitohormesis promotes longevity via systemic repression of insulin signaling. *Cell* 155, 699–712. doi: 10.1016/j.cell.2013.09.021

Polak, G. L., Pasqualino, A., Docherty, J. E. B., Beck, S. J., and Di Angelo, J. R. (2015). The regulation of muscle structure and metabolism by Mio/dChREBP in *Drosophila*. *PLoS One* 10:e0136504. doi: 10.1371/journal.pone.0136504

Post, S., Karashchuk, G., Wade, J. D., Sajid, W., De Meyts, P., and Tatar, M. (2018). *Drosophila* insulin-like peptides DILP2 and DILP5 differentially stimulate cell signaling and glycogen phosphorylase to regulate longevity. *Front. Endocrinol.* 9:245. doi: 10.3389/fendo.2018.00245

Rai, M., Katti, P., and Nongthomba, U. (2014). *Drosophila* Erect wing (Ewg) controls mitochondrial fusion during muscle growth and maintenance by regulation of the Opa1-like gene. *J. Cell Sci.* 127, 191–203. doi: 10.1242/jcs.135525

Ruaud, A.-F., Lam, G., and Thummel, C. S. (2011). The *Drosophila* NR4A nuclear receptor dhr38 regulates carbohydrate metabolism and glycogen storage. *Mol. Endocrinol.* 25, 83–91. doi: 10.1210/me.2010-0337

Sacktor, B., and Worbber-Shavit, E. (1966*). Regulation of metabolism in working muscle in viva i. Concentrations of some glycolytic, tricarboxylic acid cycle, and amino acid intermediates in i?u'sect flight muscle during flight. *J. Biol. Chem.Istry* 241, 624–631.

Shukla, E., Thorat, L. J., Nath, B. B., and Gaikwad, S. M. (2015). Insect trehalase: physiological significance and potential applications. *Glycobiology* 25, 357–367. doi: 10.1093/glycob/cwu125

Sohal, R. S. (1975). Mitochondrial changes in flight muscles of normal and flightless *Drosophila* melanogaster with age. *J. Morphol.* 145, 337–353. doi: 10.1002/jmor.1051450307

Song, W., Owusu-Ansah, E., Hu, Y., Cheng, D., Ni, X., Zirin, J., et al. (2017). Activin signaling mediates muscle-to-adipose communication in a mitochondria dysfunction-associated obesity model. *Proc. Natl. Acad. Sci. U.S.A.* 114, 8596–8601. doi: 10.1073/pnas.1708037114

Teleman, A. A., Hietakangas, V., Sayadian, A. C., and Cohen, S. M. (2008). Nutritional control of protein biosynthetic capacity by Insulin via Myc in *Drosophila*. *Cell Metab.* 7, 21–32. doi: 10.1016/j.cmet.2007.11.010

Tixier, V., Bataille, L., Etard, C., Jagla, T., Weger, M., DaPonte, J. P., et al. (2013). Glycolysis supports embryonic muscle growth by promoting myoblast fusion. *Proc. Natl. Acad. Sci. U.S.A.* 110, 18982–18987. doi: 10.1073/pnas.1301262110

Van Der Horst, D. J. (2003). Insect adipokinetic hormones: release and integration of flight energy metabolism. *Comp. Biochem. Physiol. B Biochem. Mol. Biol.* 136, 217–226. doi: 10.1016/s1096-4959(03)00151-9

van Marrewijk, W. J. A., van den Broek, A. T. M., and Beenakkers, A. M. T. (1986). Hormonal control of fat-body glycogen mobilization for locust flight. *Gen. Comp. Endocrinol.* 64, 136–142. doi: 10.1016/0016-6480(86)90039-0

Villanueva, J. E., Livelo, C., Trujillo, A. S., Chandran, S., Woodworth, B., Andrade, L., et al. (2019). Time-restricted feeding restores muscle function in *Drosophila* models of obesity and circadian-rhythm disruption. *Nat. Commun.* 10, 1–17. doi: 10.1038/s41467-019-10563-9

Watanabe, L. P., and Riddle, N. C. (2017). Characterization of the rotating exercise quantification system (REQS), a novel *Drosophila* exercise quantification apparatus. *PLoS One* 12:e0185090. doi: 10.1371/journal.pone.0185090

Wigglesworth, V. B. (1949). The utilization of reserve substances in *Drosophila* during flight. *J. Exp. Biol.* 26, 150–163.

Wojtas, K., Slepecky, N., von Kalm, L., and Sullivan, D. (1997). Flight muscle function in *Drosophila* requires colocalization of glycolytic enzymes. *Mol. Biol. Cell* 8, 1665–1675. doi: 10.1091/mbc.8.9.1665

Yamada, T., Habara, O., Kubo, H., and Nishimura, T. (2018). Fat body glycogen serves as a metabolic safeguard for the maintenance of sugar levels in <em>*Drosophila*</em&gt. *Development* 145:dev158865. doi: 10.1242/dev.158865

Yamada, T., Habara, O., Yoshii, Y., Matsushita, R., Kubo, H., Nojima, Y., et al. (2019). The role of glycogen in development and adult fitness in *Drosophila*. *Development* 146:dev176149. doi: 10.1242/dev.176149

Yan, Y., Wang, H., Hu, M., Jiang, L., Wang, Y., Liu, P., et al. (2017). HDAC6 suppresses age-dependent ectopic fat accumulation by maintaining the proteostasis of PLIN2 in *Drosophila*. *Dev. Cell* 43, 99.e5–111.e5. doi: 10.1016/j.devcel.2017.09.001

Yang, H., and Hultmark, D. (2017). *Drosophila* muscles regulate the immune response against wasp infection via carbohydrate metabolism. *Sci. Rep* 7:15713. doi: 10.1038/s41598-017-15940-2

Yoon, W., Hwang, S.-H., Lee, S.-H., and Chung, J. (2019). *Drosophila* ADCK1 is critical for maintaining mitochondrial structures and functions in the muscle. *PLoS Genet.* 15:e1008184. doi: 10.1371/journal.pgen.1008184

Yoshida, M., Matsuda, H., Kubo, H., and Nishimura, T. (2016). Molecular characterization of Tps1 and Treh genes in *Drosophila* and their role in body water homeostasis. *Sci. Rep.* 6, 1–12. doi: 10.1038/srep30582

Zhao, X., and Karpac, J. (2017). Muscle directs diurnal energy homeostasis through a myokine-dependent hormone module in *Drosophila*. *Curr. Biol.* 27, 1941.e6–1955.e6.

Zirin, J., Nieuwenhuis, J., and Perrimon, N. (2013). Role of autophagy in glycogen breakdown and its relevance to chloroquine myopathy. *PLoS Biol.* 11:e1001708. doi: 10.1371/journal.pbio.1001708

Conflict of Interest: The authors declare that the research was conducted in the absence of any commercial or financial relationships that could be construed as a potential conflict of interest.

frontiers in Physiology

ORIGINAL RESEARCH
published: 29 October 2020
doi: 10.3389/fphys.2020.580618

Regulation of Metabolism by an Ensemble of Different Ion Channel Types: Excitation-Secretion Coupling Mechanisms of Adipokinetic Hormone Producing Cells in *Drosophila*

*Rebecca J. Perry, Cecil J. Saunders, Jonathan M. Nelson, Michael J. Rizzo, Jason T. Braco and Erik C. Johnson**

Department of Biology, Wake Forest University, Winston-Salem, NC, United States

OPEN ACCESS

Edited by:
Oleh Lushchak, Vasyl Stefanyk Precarpathian National University, Ukraine

Reviewed by:
Christian Wegener, Julius Maximilian University of Würzburg, Germany
Dalibor Kodrík, Academy of Sciences of the Czech Republic, Czechia

***Correspondence:**
Erik C. Johnson
johnsoec@wfu.edu

Specialty section:
This article was submitted to Invertebrate Physiology, a section of the journal Frontiers in Physiology

Received: *06 July 2020*
Accepted: *07 October 2020*
Published: *29 October 2020*

Citation:
Perry RJ, Saunders CJ, Nelson JM, Rizzo MJ, Braco JT and Johnson EC (2020) Regulation of Metabolism by an Ensemble of Different Ion Channel Types: Excitation-Secretion Coupling Mechanisms of Adipokinetic Hormone Producing Cells in Drosophila. Front. Physiol. 11:580618. doi: 10.3389/fphys.2020.580618

Adipokinetic Hormone (AKH) is the primary insect hormone that mobilizes stored energy and is functional equivalent to mammalian glucagon. While most studies have focused on exploring the functional roles of AKH, relatively little is known about how AKH secretion is regulated. We assessed the AKH cell transcriptome and mined the data set for specific insight into the identities of different ion channels expressed in this cell lineage. We found reliable expression of multiple ion channel genes with multiple members for each ionic species. Specifically, we found significant signals for 39 of the either known or suspected ion channel genes within the *Drosophila* genome. We next performed a targeted RNAi screen aimed to identify the functional contribution of these different ion channels that may participate in excitation-secretion coupling in AKH producing cells (APCs). We assessed starvation survival, because changes in AKH signaling have previously been shown to impact starvation sensitivity. Genetic knockdown of three genes (*Ca-Beta*, *Sur*, and *sei*), in AKH producing cells caused highly significant changes ($P < 0.001$) in both male and female lifespan, and knockdown of six other genes (*Shaw*, *cac*, *Ih*, *NaCP60E*, *stj*, and *TASK6*) caused significant changes ($P < 0.05$) in only female lifespan. Specifically, the genetic knockdown of *Ca-Beta* and *Sur* led to increases in starvation lifespan, whereas the knockdown of *sei* decreased starvation survivorship. Focusing on these three strongest candidates from the behavioral screen, we assessed other AKH-dependent phenotypes. The AKH hormone is required for starvation-induced hyperactivity, and we found that these three ion channel gene knockdowns changed activity profiles and further suggest a modulatory role of these channels in AKH release. We eliminated the possibility that these genetic elements caused AKH cell lethality, and using independent methods, we verified expression of these genes in AKH cells. Collectively, these results suggest a model of AKH-cell excitability and establish an experimental framework for evaluating intrinsic mechanisms of AKH release.

Keywords: ion channel, transcriptome, metabolism, starvation, endocrine

INTRODUCTION

In excitable tissues, changes in membrane potential are paramount in mediating specific aspects of cell physiology, including muscle contraction and hormonal secretion. A major molecular component that alters membrane potential are ion channels. Ion channels display considerable variation in their activation kinetics, their gating mechanisms, the specific ionic species that can pass (Hille, 2001). However, it is thought that the specific biophysics and biochemistry of the exact ion channels ultimately bestow the cell with its excitable properties. These channels shape the regular contraction cycles of cardiac muscle and determine the probabilities of formation of action potentials. In this study, we aimed to determine the ion channels present in an endocrine gland in *Drosophila*, which is paramount in regulating metabolism.

In insects, the Adipokinetic hormone (AKH) is the functional equivalent of mammalian glucagon, as it is the primary hormone that facilitates the mobilization of stored energy (Gäde and Auerswald, 2003). During periods of low circulating energy, AKH is secreted from a discrete subset of neuroendocrine cells and binds to its specific receptor (AKHR) (Park et al., 2002; Staubli et al., 2002). AKHR is expressed in the insect fat body (Grönke et al., 2007), which is the principal organ involved in fat and carbohydrate stores. AKHR activation leads to increased glycogen phosphorylase activity as well as the mobilization of stored lipids through lipase activity (Van Der Horst, 2003; Grönke et al., 2007). In *Drosophila*, AKHR is also expressed in a small subset of central neurons, where is thought to facilitate gustatory sensitivity (Inagaki et al., 2014; Jourjine et al., 2016; Yu et al., 2016), as well as in other tissues in other insects (e.g., Jedlička et al., 2016).

In *Drosophila*, targeted ablation or blockade of hormonal release of AKH-expressing neuroendocrine cells cause increased survival during starvation (Lee and Park, 2004; Isabel et al., 2005). The underlying mechanism thought to lead to lifespan extension is the accumulation of energy stores and a loss of starvation-induced hyperactivity (Lee and Park, 2004; Isabel et al., 2005). These phenotypes are also exhibited in strains that lack either the AKH hormone or its specific receptor (Bharucha et al., 2008; Braco et al., 2012; Gáliková et al., 2015) and implicate the AKH hormone as being a critical regulator of normal responses to starvation. Despite the importance of AKH as a metabolic regulator, little work has explored the physiology of AKH cells with specific regards to the mechanisms that couple nutrient sensing to changes in AKH cell excitability.

AKH expressing cells are intrinsically sensitive to changes in hemolymph sugar levels and show elevated calcium levels when trehalose levels decrease (Kim and Rulifson, 2004; Braco et al., 2012). We previously identified that the AMP-activated protein kinase (AMPK) is critical for heightened AKH secretion during low energy conditions, and the mechanism of action is the modulation of AKH cell excitability (Braco et al., 2012). Additionally, AMPK has been shown to alter the function of several different ion channel species (Evans et al., 2009). Furthermore, AKH cells are electrically excitable, display spontaneous electrical activity (Bloemen and de Vlieger, 1985), and introduction of a potassium leak channel mirrors AKH loss of function phenotypes suggesting an electrical silencing of AKH release (Kim and Rulifson, 2004; Braco et al., 2012).

Thus, we suspect that AKH release is modulated at the level of excitation-secretion coupling and hormone secretion is ultimately dependent on the specific biochemistries and biophysics of the cohort of ion channels expressed in this cell type. To investigate the potential mechanisms gating AKH secretion, we first evaluated the specific AKH cell transcriptome using a single cell RNA sequencing platform. We identified varying but consistent levels of expression of 39 different ion channel genes present in the *Drosophila* genome. We then performed a screen to identify ion channels regulating AKH release and employed RNAi elements that targeted these different ion channels genes identified in the transcriptome. Using starvation lifespan as a behavioral readout, we identify a cohort of ion channels that we suspect are critical for regulating AKH cell excitability. Paramount in this process, are the channels encoded by the *seizure*, *Ca-Beta*, and *Sur* genes. These results implicate these channels as important factors that mediate AKH hormonal release and suggest a model of AKH-cell excitation-secretion coupling.

RESULTS

AKH Cells Express Multiple Ion Channel Types

To gain insight into the regulatory mechanisms that underlie AKH cell excitability and AKH hormonal release, we assessed the AKH cell transcriptome. Individual AKH cells were identified by introducing a GFP reporter prior to microdissection and RNA sequenced. The transcriptome was assessed from five replicate individuals each that had experienced 24 h of starvation and compared to animals that were fed *ad libitum*. An initial analysis of the RNA sequencing of 13 billion nucleotides corresponding to 11,456 transcripts showed no significant effects of the starvation experiments on the normalized levels of ion channel encoding genes, and consequently all replicates were pooled for further analysis.

Of the 47 genes that are either known or suspected to encode ion channel genes (Littleton and Ganetzky, 2000), we found reliable and consistent expression of 39 of them (**Figure 1**). We found expression of all the calcium channel members present in *Drosophila*, as well as every known sodium channel. Multiple potassium channel and chloride channel types were also found, and other suspected but as of yet, not molecularly determined ion channel genes. While multiple channel types were found, the relative abundance of each channel type was far from uniform, with only a handful of ion channels being highly expressed (as defined by two standard deviations from the mean expression level), and the vast majority having a consistently low level of expression. Given the molecular stability of ion channel proteins, low levels of transcript expression are expected and consistent

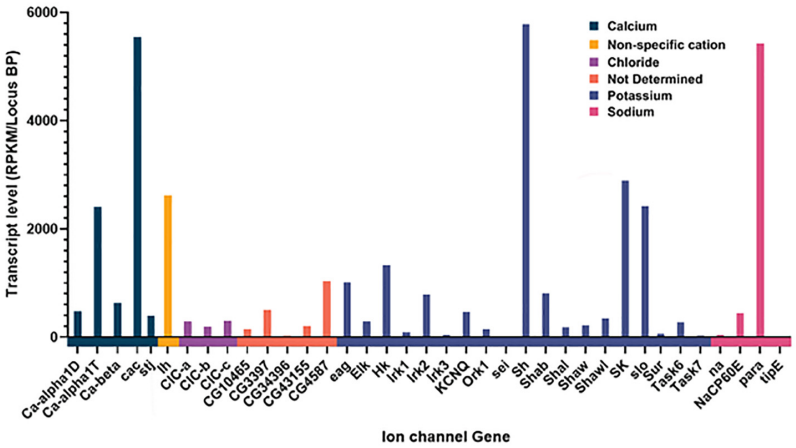

FIGURE 1 | Expression of Ion channel genes in AKH cells through sc-RNAseq. Channels are grouped together by specificity and the normalized amount of transcript is plotted for each ion channel gene. Normalization was the total number of reads per kB mapped and normalized for transcript length.

with other transcriptome analyses in *Drosophila* (Allen et al., 2020) and other animals (Fuzik et al., 2016).

RNAi Knockdown of Specific Ion Channels Leads to Starvation Phenotypes

Based on the transcriptome data, we next wanted to evaluate the functional significance of this ensemble of different ion channels in mediating AKH cell excitability. Ideally, direct measurements of AKH cell membrane potential would be revealing, but the anatomy of adult AKH cells makes this infeasible if not impossible with current electrophysiological techniques. We employed a genetic behavioral screen to specifically evaluate the potential contributions of different ion channel genes in modulating AKH cell physiology. This behavioral screen was based on previous observations that the genetic ablation of AKH cells or loss of function variants of the hormone and receptor all produce animals that are long-lived under a starvation paradigm (Lee and Park, 2004; Isabel et al., 2005; Bharucha et al., 2008; Gáliková et al., 2015). Furthermore, we have previously used starvation lifespan to gauge the contribution of the AMP-activated protein kinase (AMPK) as an intrinsic AKH nutrient sensor (Braco et al., 2012). We used a specific GAL4 to limit expression of a DS-RNA targeting a specific ion channel gene to only AKH-expressing cells and assessed survivorship during starvation (Lee and Park, 2004). The RNAi elements were purchased from Bloomington Stock Center and were derived from the Transgenic RNAi Project (TRiP) and has the benefit of all the elements sharing a genomic insertion site and genetic background (Perkins et al., 2015). At the time of these experiments, we were able to get and test RNAi lines for each ion channel expressed in AKH cells (**Figure 1**), with the exception of *Clc-A* and *Irk1*.

We evaluated starvation longevity in progeny of the crosses introducing an RNAi element to AKH cells. Introduction of RNAi elements targeting the *Calcium Beta* (*Ca-Beta*) and the *Sulfonylurea receptor* (*Sur*) gene caused a highly significant (ANOVA, $p < 0.001$) increase in lifespan during starvation. Conversely, expression of an RNAi element targeting the *seizure (sei)* gene caused a highly significant reduction in starvation lifespan in both males and females as compared to control animals (AKH-GFP) ($P < 0.001$) (**Figure 2**). Notably, this GFP control line shares the same transgene insertion site as all of the RNAi elements, making it the ideal genetic control. In females, we found six other genes that significantly ($P < 0.05$) deviated from our control line and include *cac*, *stj*, *NaCP60E*, *Ih*, *TASK6*, and *Shaw* (**Figure 2A**). We also included a long-lived control (AKH-rpr), in which AKH cells are genetically ablated through the introduction of the pro-apoptotic gene, *reaper*, for the sake of comparison. We found that all lines were statistically different than this control variant, apart from the *Ca-beta* and *Sur* knockdowns, and this was similarly independent of sex. We independently repeated the screen with a subset of lines including all the candidates and three lines that did not differ from our AKH-GFP control line and found the same rank order of starvation sensitivity. Given that the screen yielded three candidates that were the same in both males and females, and showed the most robust differences between control lines, we focused on these three candidates. To further validate these three candidates, we obtained independently derived RNAi lines targeting these three ion channel encoding genes. We tested these lines for starvation lifespan and did not find any statistical difference between the two lines for each candidate ($P = 0.86$, *T*-Test).

Another AKH-dependent phenotype is the requirement of this hormone for starvation-induced hyperactivity (Lee and Park, 2004; Isabel et al., 2005; Bharucha et al., 2008; Braco et al., 2012; Gáliková et al., 2015). Specifically, the loss of the AKH receptor, the AKH hormone, or AKH expressing cells all cause the absence of heightened activity that accompanies starvation in normal flies. This behavior is thought to facilitate heightened foraging (Johnson, 2017). Consequently, we hypothesized that if these three ion channel genes are altering the excitability of AKH cells,

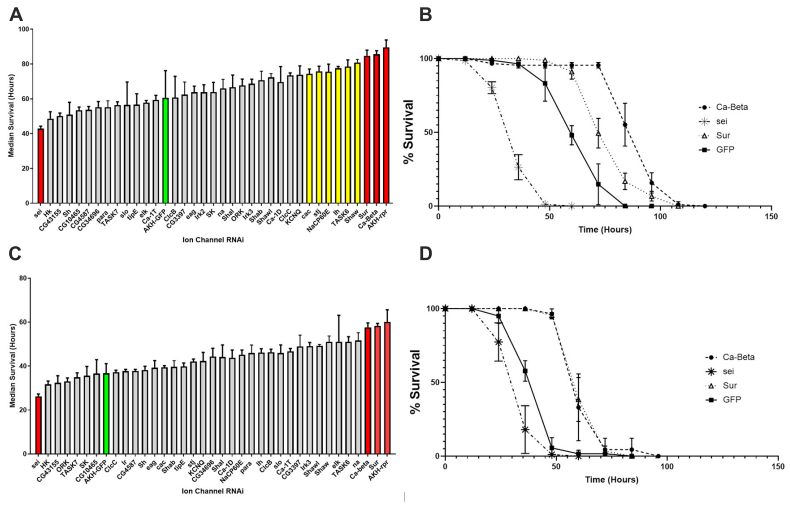

FIGURE 2 | Starvation lifespan in strains with AKH-cell specific genetic knockdowns of different ion channel genes. The mean median survival was derived from three replicate vials of 30 individuals for each sex and was assessed during starvation conditions every 12 h. Mean median survival was determined for each genotype and is shown ± SEM. Bars in red denote significance levels at $P < 0.01$ and yellow bars denote significance levels at $P < 0.05$ from a One Way ANOVA and a Tukey *post-hoc* test comparing mean survival to the AKH-GFP controls (green). **(A)** Female starvation results are shown in the top panel and male starvation results are shown in the bottom panel **(B)**. Starvation lifespan curves are plotted for the three strongest candidates (Sur, Ca-Beta, and sei) with control (AKH-GFP-RNAi) for females **(C)** and males **(D)**.

then these genetic manipulations should manifest as changes in locomotor activity profiles. We found that locomotor activity under replete conditions was heightened in animals expressing any of these three ion channel RNAi elements in both males and females ($P < 0.001$) (**Figure 3**). Next, we asked whether locomotor profiles change in response to starvation in animals with altered ion channel function? In males, we found that RNAi knockdown of *Sur* and *Ca-Beta* led to significantly reduced changes in starvation-locomotion compared to wildtype. We excluded the *sei* RNAi males, because a significant number of males would have died during our window of analysis. In females, we found that there was no increase in locomotion in wildtype and *Sur* RNAi females. Knockdown of *seizure* and *Ca-beta* caused elevated locomotor responses to starvation (**Figure 3**).

One potential explanation for the behavioral phenotypes is that these RNAi elements may adversely affect AKH cell viability or impair hormone synthesis. To evaluate potential AKH cell pathology associated with RNAi element expression, we employed a specific antibody against AKH to assess cell survival and hormone expression. We found that in all genotypes, AKH cell viability and minimally, synthesis of the AKH precursor were unaffected (**Figure 4**). These results indicate that the behavioral phenotypes are not likely to be caused by developmental defects, AKH cell lethality, or the lack of AKH hormone expression caused by RNAi introduction. We next sought to confirm the transcriptome and behavioral data and independently assessed whether these ion channel genes are expressed in this cell lineage. We employed single-cell RT-PCR on AKH cells and were able to specifically amplify all three of these genes. Amplicons were detected from AKH, Ca-Beta, sei, and Sur transcripts and were of the correct size and were sequence verified (data not shown).

DISCUSSION

Here, we present evidence that multiple ion channel genes are expressed in the neuroendocrine cells that release the Adipokinetic Hormone. Multiple ion channel transcripts were identified through an analysis of the AKH-cell specific transcriptome. We then employed a genetic approach to determine the overall contribution of these ion channels in modulating AKH secretion through the examination of AKH related starvation phenotypes. We identified that the genetic knockdown of three ion channel encoding genes strongly impacted starvation survival and found several other genes whose impacts were significant but modest in comparison. We also examined locomotor activity from animals expressing an RNAi targeting each of these three ion channel genes whose AKH cell specific knockdown highly impacted starvation survival. In each case, changes in locomotor activity were present either in the replete or starvation state. Lastly, we verified the knockdown of these genes did not cause AKH cell lethality, and we employed independent measures to confirm the AKH cell specific expression of these genes.

One question that arises from our transcriptome results: Why are there so many different channels? We note that most of the ion channel genes within the *Drosophila* genome are expressed in this secretory tissue. However, we note that single cell (sc) transcriptomes of individual neurons also show a diversity of ion channels present (Fuzik et al., 2016; Northcutt et al., 2019). While many of these sc-RNA studies attempt to elucidate potential genetic heterogeneity of either a brain area or groups of neurons that share a transmitter phenotype, it is clear that a meta- analysis of sc-transcriptomes from mammalian and invertebrate neuronal tissue show multiple

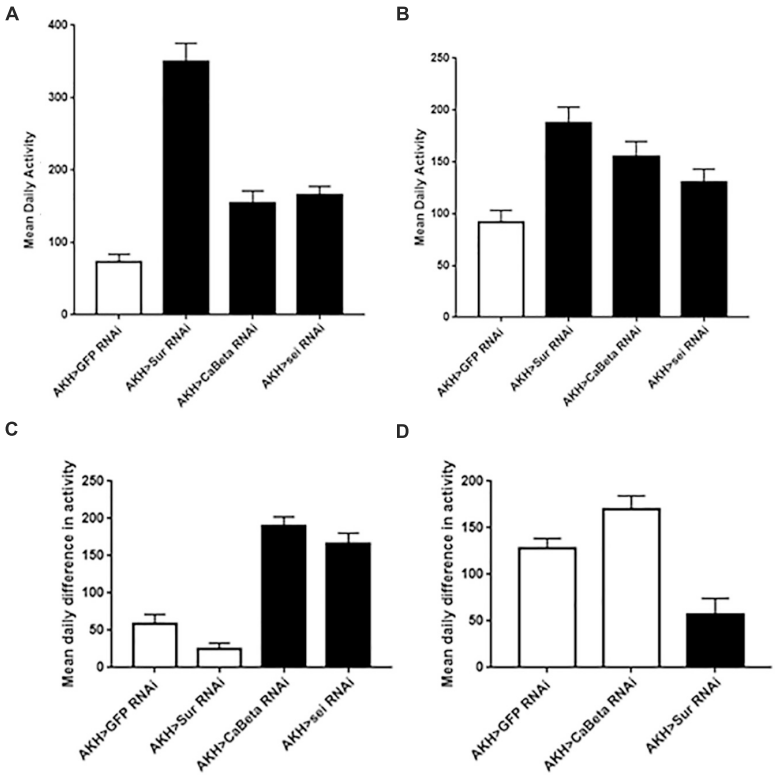

FIGURE 3 | Locomotor activity in animals expressing the Sur-RNAi, sei-RNAi, and Ca-beta RNAi elements under replete and starvation conditions. Locomotor activity was monitored for 3 days with *ad libitum* food and mean daily activity (beam breaks for 24 h) was assessed for females **(A)** and males **(C)**. Black bars denote significant differences ($P < 0.05$) from control animals (One Way ANOVA). Locomotor activity during starvation conditions was also assessed in females **(B)** and in males **(D)**. The hypersensitivity of sei-RNAi to starvation precluded measuring daily activity during starvation). Black bars denote significant differences ($P < 0.05$) from control animals (One Way ANOVA).

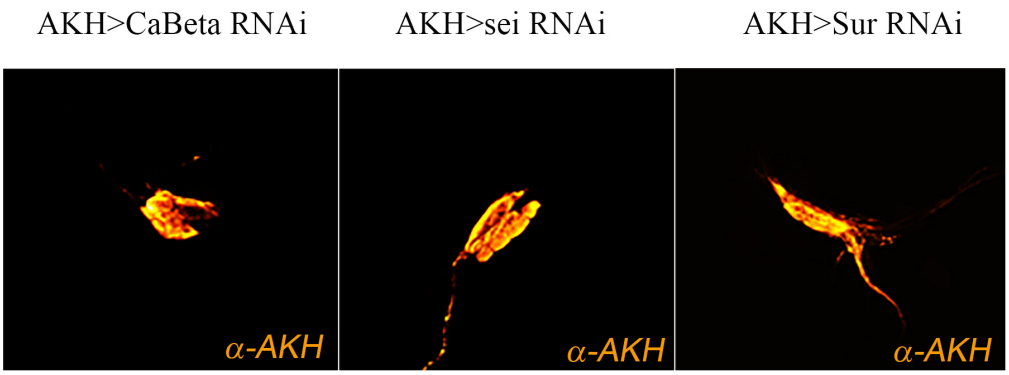

FIGURE 4 | Expression of ion channel RNAi elements do not change AKH cell viability. Expression of ion channel RNAi's does not impair cell viability or AKH synthesis. Representative images of adult AKH cells expressing Ca-Beta-RNAi **(left)**, sei-RNAi **(middle)**, and Sur-RNAi **(right)** counterstained with α-AKH.

channel types present in an individual neuron. We also cannot rule out the possibility that some of our transcriptome samples stem from synaptic terminals projecting to AKH cells that may express a diversity of ion channels. Nonetheless, our transcriptome analysis represents a first requisite step in gauging the complement of genes expressed in APCs and is consistent with other neuronal sc-transcriptomes (Fuzik et al., 2016; Northcutt et al., 2019) and mammalian pancreatic sc-transcriptomes (Muraro et al., 2016).

Following our transcriptome analysis, we performed a targeted RNAi screen using AKH-dependent behavioral phenotype and identified three genes (*Ca-Beta, Sur*, and *seizure*) that are strong candidates in the regulation excitation-secretion coupling in this cell lineage (**Figure 5**). As in the case of any

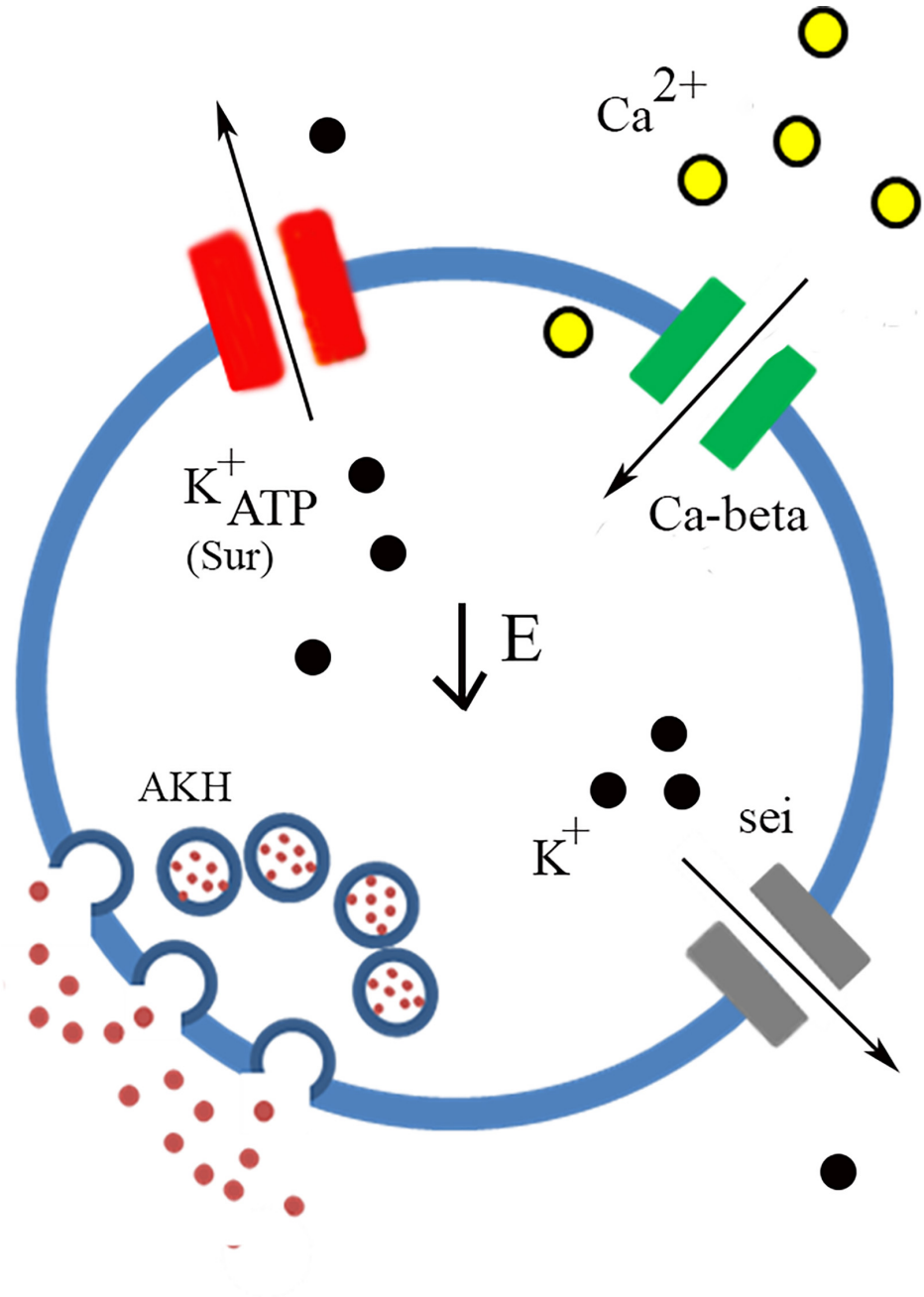

FIGURE 5 | Model of AKH cell excitability. Low Energy (center) is the trigger that facilitates AKH release. Nutrient sensing is likely to occur through the ATP gating of K^+_{ATP} channels of which *Sur* is an essential component. Calcium enters through the cell through calcium channels and the *Ca-beta* subunit is likely a critical component of functional calcium channels present in AKH cells. Potassium channels, likely containing *sei* subunits, also participate in the regulation of AKH cell excitability and the subsequent secretion of the hormone.

behavioral screen, negatives are not necessarily informative, although we maintain that some of the reasons that we failed to identify other strong candidates may reflect biological vs. technical reasons. Unfortunately, the technical limitations of the single-cell RT PCR and the expense of performing a transcriptome on each genetic variant make quantification of transcript levels of the target genes infeasible. However, we do note that all these lines share a genetic insertion site (Perkins et al., 2015), suggesting that if there are differences in the lines, those difference map to the specific DS-RNA species. Ion channels are known to form heteromultimeric complexes that often consist of different subunits (Cai, 2008), and multimeric assembly of ion channels potentially explains both the observation of many different channel types present via

the transcriptome analysis and that relatively few manipulations lead to AKH phenotypes. Furthermore, the fact that there are many different ion channels that pass the same ion suggests that there could be considerable functional redundancy. For example, it is interesting that we found a strong starvation phenotype from knockdown of a regulatory subunit of a calcium channel (*Ca-Beta*) and despite the observation of all known pore-forming calcium channel genes being present in AKH cells via the transcriptome, knockdown of those produced largely no effect. We do note that the knockdown of *cac,* which is a pore forming calcium channel subunit (Smith et al., 1998) produced a significant effect on starvation, albeit weaker in comparison to the Ca-Beta knockdowns. We speculate that this observation may reflect the presence of multiple different functional calcium channel types in AKH cells, and that *Ca-beta*, being the sole regulatory subunit, is a critical component that regulates disparate calcium channels. Its worthy to note that, in mammals, Ca-Beta subunits show diverse functions including channel trafficking, activation/inactivation kinetics, and setting voltage dependence (Buraei and Yang, 2013). We also note that our transcriptome showed a wide variation in ion channel expression levels, and we note that the most robust phenotypes targeted ion channel genes that were typically lower in expression levels, and that were novel subtypes. Furthermore, we did observe weaker starvation phenotypes in a number of different ion channel genes (*Shaw*, *cac*, *Ih*, *NaCP60E*, *stj*, and *TASK6*), but only in females. We suspect that the behavioral output (starvation lifespan) has greater resolution in females as they live considerably longer during this challenge, as opposed to an inherent dimorphism mapping to AKH cells.

An important result of the behavioral analysis is the further confirmation of the *Sur* gene as being a critical factor that regulates AKH secretion. Specifically, *Sur* is one component of the functional K^+_{ATP} channel (Nichols, 2006) and had been previously implicated in being expressed in larval AKH expressing cells (Kim and Rulifson, 2004). Notably, the other component of the K^+_{ATP} channel include an inward rectifying potassium channel, and in *Drosophila* there are three distinct genes that encode channels in this subfamily (Littleton and Ganetzky, 2000). None of these IRK channels produced a behavioral phenotype which suggests that these components of K^+_{ATP} channels are functionally redundant. The significance of this finding is that K^+_{ATP} channels are, eponymously, gated by intracellular energy stores, ATP. Consequently, this channel may function as a direct link to energy status and AKH release. Of further interest is the observation that this channel type appears to gate glucagon and insulin release from pancreatic alpha and beta cells, respectively (Göpel et al., 2000; Rorsman et al., 2014). Pharmacological studies in *Drosophila* using a K^+_{ATP} agonist, tolbutamide, produced metabolic phenotypes that are consistent with previous studies and our genetic interdiction of K^+_{ATP} channel function (Kim and Rulifson, 2004). Mechanistically, we predict that the loss of *Sur* likely prevents AKH cells from coupling low extracellular energy to changes in membrane potential, leading to an overall reduction in AKH signaling. Of note, we previously identified that AMPK is critical for normal AKH cell function, and acts as an intrinsic nutrient sensor (Braco et al., 2012). We also determined that AMPK activation leads to enhanced AKH cell secretion and is most likely at the level of excitation-secretion coupling. Our results and those presented in the literature suggest that a key future experiment is to test whether these two nutrient sensors present in AKH cells act independently or in concert.

Mutations in *sei* have previously shown to lead to increased spontaneous depolarization in other tissues in a temperature sensitive manner (Zheng et al., 2014), consistent with the idea that the normal potassium conductance passed by this channel would lead to hyperpolarization. Genetic knockdown of *sei* showed a significant reduction in lifespan and increased locomotion under replete and starvation conditions. These phenotypes suggest an increased level of AKH secretion. Of interest, mammalian pancreatic alpha cells express hERG channels, a homolog of *sei*, which regulates resting membrane potential (Qiu et al., 2016), and acute pharmacologic blockade of ERG channels shows an overall reduction in glucagon secretion (Qiu et al., 2016). The finding of *seizure* channels as a regulator of AKH secretion suggests that there may be significant parallels in the regulatory components of glucagon secretion and AKH cells. Interestingly, many of the channels we found essential for AKH secretion are similar to the channels regulating glucagon secretion (Rorsman et al., 2014).

AKH cells are a critical locus for integrating sensory information regarding energy status and facilitating appropriate behavioral and physiological responses (Johnson, 2017). Specifically, these cells integrate intracellular status of energy within the context of other hormones to coordinate an appropriate behavioral and physiological response to nutrient depletion. An important component of these responses is that they are fundamentally graded (i.e., an hour of restricted food availability is different than 24 h of starvation). Inspection of AKH loss of function phenotypes clearly shows that AKH is required for starvation-induced hyperactivity, although the locomotor phenotypes we observed in AKH cell specific knockdown of these ion channels suggest a more complex role of AKH in determination of total locomotor activity. Indeed, AKH has been shown to impact different aspects of locomotion in a wide variety of insects that appear to be separate and distinct from nutrient limitations (e.g., Kodrík, 2008). Nonetheless, as we suspect that AKH secretion is being decoupled from nutrient sensing in these genetic variants targeted ion channel function, we observed changes in basal (replete) locomotion as we expected. The interaction between abnormal secretion events and starvation suggest a more complex role of AKH in these behaviors. We acknowledge that lifespan under starvation is influenced by multiple physiological setpoints and is a rather conservative measure to use to identify candidate molecules that regulate AKH cell physiology. Likewise, the profound impact on locomotor activity observed in variants that are complete loss of AKH functions, may not be expected to be observed in genetic manipulations that modulate AKH cell activity. Consequently, while the changes in locomotor activity in AKH deficient animals may lead to heightened starvation survival, the connections between starvation survival and locomotor activity are likely to be more complicated than anticipated.

Given these behavioral phenotypes, it is reasonable to ask whether these genetic perturbations of ion channel function negatively impact APC physiology vs. a specific secretion phenotype. We used immunohistochemistry to evaluate the general health of APCs and documented that they were present and, minimally expressing the AKH precursor. The next requisite step would be direct measurements of APC excitability using electrophysiological methods. Indirect measures of AKH concentrations, either in APCs or in the hemolymph clearly correlate with secretion profiles but are not solely measuring secretion. We, and others have previously used immunocytochemistry to evaluate AKH concentrations within APCs (Braco et al., 2012; Kim and Neufeld, 2015) or in the hemolymph (Oh et al., 2019). Cellular AKH levels are dependent on secretion rates, but also the degree to which the hormone is transcribed and processed. Circulating AKH levels are subject to peptidase degradation and receptor binding. We have used secretion reporters previously to document that AKH cell secretion is dependent upon AMPK activation, and while this direct measure of cellular secretion is preferable to indirect measures outlines above, such reporters are better suited to measure differentials (Levitan and Shakiryanova, 2010) and would not be useful in this study to measure changes in the predicted spontaneous peptide release as a consequence of altered APC excitability. We are attempting to measure parameters of APC excitability using electrophysiological methods as such information will provide critical insight into the precise mechanisms of altered APC function.

Nonetheless, we maintain that there is most probable an ensemble of ion channels that regulate excitation-secretion of this metabolic hormone and any other potential cotransmitters, and that we have identified a select few channels, whose functional importance is larger than others. Consequently, our screen informs future studies that directly assess AKH cell excitability and has the potential to establish parallel mechanisms of nutrient sensing to hormone release across wide phylogenetic distances. For example, our screen informs experiments aimed at direct electrophysiological assessment of APCs, which will be able to resolve the specific details regarding APC excitability and hormonal release.

TABLE 1 | List of ion channel RNAi elements used in this study.

Gene name	Bloomington stock number(s)	Ion selectivity
Ca-alpha 1D	33413	Calcium
Ca-alpha 1T	39029	Calcium
Ca-beta	29575, 43292	Calcium
cacophony (cac)	27244	Calcium
CG10465	26002	Suspected potassium
CG3397	44115	Suspected anion
CG34696	26011	Suspected potassium
CG43155	27033	Suspected potassium
CG4587	25893	Suspected anion
Clc-B	25826	Chloride
Clc-C	27034	Chloride
eag	31675	Potassium
elk	25821	Potassium
Hk	28330	Potassium
Irk2	41981	Potassium
Irk3	26720	Potassium
KCNQ	27252	Potassium
Ih	29574	Cation
na	25808	Sodium
NaCp60E	26012	Sodium
Ork1	25885	Potassium
para	31471	Sodium
sei	31681, 31682	Potassium
Sh	31680	Potassium
Shab	41999	Potassium
Shal	31879	Potassium
Shaw	28346	Potassium
Shawl	25819	Potassium
SK	27238	Calcium-activated Potassium
slo	26247	Calcium-activated potassium
stj	25807	Potassium
Sur	36087, 67246	Potassium
TASK6	28015	Potassium
TASK7	27264	Potassium
tipE	26249	Sodium
AKH-GAL4	25864	NA
UAS-GFP	35786	NA
UAS-rpr	5823	NA

Each ion channel gene name along with the corresponding Bloomington Stock number and the suspected or predicted ion channel selectivity is listed. Ion channel selectivity information is based on Littleton and Ganetzky (2000).

MATERIALS AND METHODS

Drosophila Stock and Husbandry

All flies were maintained in an incubator maintained at 25°C and under a 12:12 LD cycle. Flies were cultured on a standard molasses-malt-cornmeal-agar-yeast medium and housed in uncrowded conditions. All stocks were purchased from Bloomington stock center and are listed in **Table 1**.

RNA Sequencing

AKH cells expressing GFP under the AKH promoter (12 per animal) were microdissected in HL-3 solution containing Triton X 100 (Braco et al., 2012) and aspirated into a glass pipette, which was placed in a PCR tube and flash frozen in an ethanol-dry ice bath. The tubes were stored at −80°C for no longer than 3 weeks while 10 samples were prepared from 5 fed and 5 starved female flies aged 3–10 days. On the day of RNA amplification, the contents of the pcr tubes were centrifuged and the RNA from these samples was amplified in parallel with the Arcturus RiboAmp HS PLUS Kit by following the manufacturers protocol (KIT0505, Thermo Fisher Scientific). RNA libraries were then prepared using the Kapa Stranded mRNA-Seq library prep kit and 50 bp single end sequencing was performed on an Illumina HiSeq 4000 at Duke Center for Genomic and Computational Biology (Durham, NC). This data is available at the NCBI Sequence Read Archive under project number PRJNA642982.

The raw reads were filtered using Trimmomatic v0.36 to remove Illumina adaptors, leading or trailing bases below a quality score of 3, 4-base sliding window average quality below 15 and reads less than 36 bp long. Filtered reads were aligned to *Drosophila melanogaster* genome BDGP6.22 using star v2.5 (Dobin et al., 2013) and a count table generated from coordinate sorted BAM files using summarize overlaps from the biocondutor package GenomicAlignments (Lawrence et al., 2013). We identified genes differentially expressed by starvation using the Bioconductor package DESeq2 (Love et al., 2014) but no ion channels were differentially expressed under starvation conditions (adjusted $p > 0.05$). The source code for this analysis is available at github (Saunders, 2020).

Lifespan Measurements

We placed 30, 3–5 day old mated flies (males and females housed separately) in vials with a two percent agar solution to starve the animals (Zhao et al., 2010). We assessed percent survival of at least three replicate vials twice daily. For each vial, we assessed the median survival for the treatment and data were pooled to estimate a mean median survival and then employed a one-way ANOVA with *post-hoc* Tukey's comparison for differences between genotypes.

Locomotor Measurements

Locomotor activity was monitored with a TriKinetics Locomotor Population Monitor (Waltham, MA) on the aggregate population of 30, 3–5 day old flies (Zhao et al., 2010). Each vial was considered a replicate and 3–4 replicates per condition were run. Flies were housed in a 12:12 LD cycle for 3 days prior to the experiments. Flies were transferred to a vial containing starvation or normal medium at ZT0. Total beam counts were monitored continuously through an automated system for 48 h. We determined the amount of activity during starvation relative to the activity of fed conditions for the same time period (Zhao et al., 2010; Braco et al., 2012).

AKH Cell Imaging and Immunocytochemistry

Adult progeny from flies carrying the *AKH-GAL4* transgene crossed to the UAS-RNAi lines were dissected. Brains were fixed in a 4% Paraformaldehyde/7% picric acid fixative for 1 h at room temperature and washed six times with phosphate buffered saline (PBS) containing Triton-X 100. A 1:1,000 dilution of polyclonal anti-AKH (Brown and Lea, 1988) was incubated overnight at 4°C. Brains were washed and a Cy-3 conjugated anti-rabbit secondary antibody was applied overnight at 1:1,000 dilution. Tissues were then mounted and viewed on a Zeiss 710 confocal microscope. Images were collected using a 40X 0.95NA objective and 561 laser line, Z stack images were taken and collapsed using maximum intensity projections. Microscope settings were constant between images and adjusted post imaging for contrast and brightness.

Single Cell RT-PCR

Individual AKH cells expressing GFP were microdissected and stored in Trizol. A Single-cell RT- PCR kit from Qiagen was used to make cDNA and amplify using gene specific primers, and methods are described in detail in Braco et al. (2012). The primers were designed to flank intronic sequences and were as follows:

CaBeta: (forward): ATACAATCAATCATCCGTCACAAC
(reverse): TTGATCAAACGCTGTAAAACCTTA
Sur : (forward) TTCAAAAGTTCTACAGGTGCTCAG
(reverse): AAGGATTTCGGTGAATCTAGTCTG
sei: (forward): AGGATCCCAATGACATGATTACTT
(reverse): AATTGGATCGGAGTTGATGTATTT

DATA AVAILABILITY STATEMENT

The datasets generated for this study can be found in the online repositories. The names of the repository/repositories and accession number(s) can be found below: https://www.ncbi.nlm.nih.gov/, PRJNA642982.

AUTHOR CONTRIBUTIONS

CS and EJ: design of experiments and analyzing data. CS, RP, JN, MR, and JB: performing experiments. EJ: drafting the manuscript. All authors contributed to the article and approved the submitted version.

FUNDING

This work was supported by the NSF IOS1355097 and a Center for Molecular Signaling grant to EJ.

ACKNOWLEDGMENTS

We thank the Bloomington Stock Center for fly stocks and acknowledge the Distributed Environment for Academic Computing (DEAC) at Wake Forest University for providing HPC resources that have contributed to the research results reported within this manuscript (https://is.wfu.edu/deac).

REFERENCES

Allen, A. M., Neville, M. C., Birtles, S., Croset, V., Treiber, C. D., Waddell, S., et al. (2020). A single-cell transcriptomic atlas of the adult *Drosophila* ventral nerve cord. *eLife* 9:e54074. doi: 10.7554/eLife.54074

Bharucha, K. N., Tarr, P., and Zipursky, S. L. (2008). A glucagon-like endocrine pathway in *Drosophila* modulates both lipid and carbohydrate homeostasis. *J. Exper. Biol.* 211, 3103–3110. doi: 10.1242/jeb.016451

Bloemen, R. E. B., and de Vlieger, T. A. (1985). Spontaneous electrical activity recorded extracellularly from the glandular lobe of the corpus cardiacum of *Locusta migratoria*. *Comp. Biochem. Physiol. A* 82, 627–633. doi: 10.1016/0300-9629(85)90444-X

Braco, J. T., Gillespie, E. L., Alberto, G. E., Brenman, J. E., and Johnson, E. C. (2012). Energy-dependent modulation of glucagon-like signaling in *Drosophila* via the AMP-activated protein kinase. *Genetics* 192, 457–466. doi: 10.1534/genetics.112.143610

Brown, M. R., and Lea, A. O. (1988). FMRFamide- and adipokinetic hormone-like immunoreactivity in the nervous system of the mosquito, *Aedes aegypti*. *J. Compar. Neurol.* 270, 606–614. doi: 10.1002/cne.902700413

Buraei, Z., and Yang, J. (2013). Structure and function of the β subunit of voltage-gated Ca2+ channels. *Biochim. Biophys. Acta Biomembr.* 1828, 1530–1540. doi: 10.1016/j.bbamem.2012.08.028

Cai, X. (2008). Subunit stoichiometry and channel pore structure of ion channels: all for one, or one for one? *J. Physiol.* 586, 925–926. doi: 10.1113/jphysiol.2007.149153

Dobin, A., Davis, C. A., Schlesinger, F., Drenkow, J., Zaleski, C., Jha, S., et al. (2013). STAR: ultrafast universal RNA-seq aligner. *Bioinformatics* 29, 15–21. doi: 10.1093/bioinformatics/bts635

Evans, A. M., Hardie, D. G., Peers, C., Wyatt, C. N., Viollet, B., Kumar, P., et al. (2009). Ion channel regulation by AMPK. *Ann. N. Y. Acad. Sci.* 1177, 89–100. doi: 10.1111/j.1749-6632.2009.05041.x

Fuzik, J., Zeisel, A., Máté, Z., Calvigioni, D., Yanagawa, Y., Szabó, G., et al. (2016). Integration of electrophysiological recordings with single-cell RNA-seq data identifies novel neuronal subtypes. *Nat. Biotechnol.* 34, 175–183. doi: 10.1038/nbt.3443

Gäde, G., and Auerswald, L. (2003). Mode of action of neuropeptides from the adipokinetic hormone family. *Gen. Comp. Endocrinol.* 132, 10–20. doi: 10.1016/S0016-6480(03)00159-X

Gáliková, M., Diesner, M., Klepsatel, P., Hehlert, P., Xu, Y., Bickmeyer, I., et al. (2015). Energy homeostasis control in *Drosophila* adipokinetic hormone mutants. *Genetics* 201, 665–683. doi: 10.1534/genetics.115.178897

Göpel, S. O., Kanno, T., Barg, S., Weng, X.-G., Gromada, J., and Rorsman, P. (2000). Regulation of glucagon release in mouse α-cells by KATP channels and inactivation of TTX-sensitive Na+ channels. *J. Physiol.* 528, 509–520. doi: 10.1111/j.1469-7793.2000.00509.x

Grönke, S., Müller, G., Hirsch, J., Fellert, S., Andreou, A., Haase, T., et al. (2007). Dual lipolytic control of body fat storage and mobilization in *Drosophila*. *PLoS Biol.* 5:e050137. doi: 10.1371/journal.pbio.0050137

Hille, B. (2001). *Ion Channels of Excitable Membranes*, 3rd Edn, Sunderland, MA: Sinauer Press.

Inagaki, H. K., Panse, K. M., and Anderson, D. J. (2014). Independent, reciprocal neuromodulatory control of sweet and bitter taste sensitivity during starvation in *Drosophila*. *Neuron* 84, 806–820. doi: 10.1016/j.neuron.2014.09.032

Isabel, G., Martin, J.-R., Chidami, S., Veenstra, J. A., and Rosay, P. (2005). AKH-producing neuroendocrine cell ablation decreases trehalose and induces behavioral changes in *Drosophila*. *Am. J. Physiol. Regul. Integrat. Compar. Physiol.* 288, R531–R538. doi: 10.1152/ajpregu.00158.2004

Jedlièka, P., Ernst, U. R., Votavová, A., Hanus, R., and Valterová, I. (2016). Gene expression dynamics in major endocrine regulatory pathways along the transition from solitary to social life in a bumblebee, *Bombus terrestris*. *Front. Physiol.* 7:574. doi: 10.3389/fphys.2016.00574

Johnson, E. C. (2017). "Stressed-out insects II. Physiology, behavior and neuroendocrine circuits mediating stress responses," in *Hormones, Brain and Behavior*, eds D. Pfaff and M. Joels (Oxford: Academic Press), 465–481. doi: 10.1016/b978-0-12-803592-4.00038-9

Jourjine, N., Mullaney, B. C., Mann, K., and Scott, K. (2016). Coupled sensing of hunger and thirst signals balances sugar and water consumption. *Cell* 166, 855–866. doi: 10.1016/j.cell.2016.06.046

Kim, J., and Neufeld, T. P. (2015). Dietary sugar promotes systemic TOR activation in *Drosophila* through AKH-dependent selective secretion of Dilp3. *Nat. Commun.* 6:6846.

Kim, S. K., and Rulifson, E. J. (2004). Conserved mechanisms of glucose sensing and regulation by *Drosophila* corpora cardiaca cells. *Nature* 431, 316–320. doi: 10.1038/nature02897

Kodrík, D. (2008). Adipokinetic hormone functions are not associated with insect flight. *Physiol. Entomol.* 33, 171–180. doi: 10.1111/j.1365-3032.2008.00625.x

Lawrence, M., Huber, W., Pagès, H., Aboyoun, P., Carlson, M., Gentleman, R., et al. (2013). Software for computing and annotating genomic ranges. *PLoS Computat. Biol.* 9:e1003118. doi: 10.1371/journal.pcbi.1003118

Lee, G., and Park, J. H. (2004). Hemolymph sugar homeostasis and starvation-induced hyperactivity affected by genetic manipulations of the adipokinetic hormone-encoding gene in *drosophila* melanogaster. *Genetics* 167, 311–323. doi: 10.1534/genetics.167.1.311

Levitan, E. S., and Shakiryanova, D. (2010). Imaging neuropeptide release in the *Drosophila* neuromuscular junction (NMJ). *Cold Spring Harb. Protoc.* 2010:pdb.rot5529.

Littleton, J. T., and Ganetzky, B. (2000). Ion channels and synaptic organization: analysis of the *drosophila* genome. *Neuron* 26, 35–43. doi: 10.1016/S0896-6273(00)81135-6

Love, M. I., Huber, W., and Anders, S. (2014). Moderated estimation of fold change and dispersion for RNA-seq data with DESeq2. *Genome Biol.* 15:550. doi: 10.1186/s13059-014-0550-8

Muraro, M. J., Dharmadhikari, G., Grün, D., Groen, N., Dielen, T., Jansen, E., et al. (2016). A single-cell transcriptome atlas of the human pancreas. *Cell Syst.* 3, 385–394. doi: 10.1016/j.cels.2016.09.002

Nichols, C. G. (2006). KATP channels as molecular sensors of cellular metabolism. *Nature* 440, 470–476. doi: 10.1038/nature04711

Northcutt, A. J., Kick, D. R., Otopalik, A. G., Goetz, B. M., Harris, R. M., Santin, J. M., et al. (2019). Molecular profiling of single neurons of known identity in two ganglia from the crab Cancer borealis. *Proc. Natl. Acad. Sci. U.S.A.* 116, 26980–26990. doi: 10.1073/pnas.1911413116

Oh, Y., Lai, J. S., Mills, H. J., Erdjument-Bromage, H., Giammarinaro, B., Saadipour, K., et al. (2019). A glucose-sensing neuron pair regulates insulin and glucagon in *Drosophila*. *Nature* 574, 559–564. doi: 10.1038/s41586-019-1675-4

Park, Y., Kim, Y.-J., and Adams, M. E. (2002). Identification of G protein-coupled receptors for *Drosophila* PRXamide peptides, CCAP, corazonin, and AKH supports a theory of ligand-receptor coevolution. *Proc. Natl. Acad. Sci. U.S.A.* 99, 11423–11428. doi: 10.1073/pnas.162276199

Perkins, L. A., Holderbaum, L., Tao, R., Hu, Y., Sopko, R., McCall, K., et al. (2015). The transgenic RNAi project at harvard medical school: resources and validation. *Genetics* 201, 843–852. doi: 10.1534/genetics.115.180208

Qiu, H.-Y., Yuan, S.-S., Yang, F.-Y., Shi, T.-T., and Yang, J.-K. (2016). HERG protein plays a role in moxifloxacin-induced hypoglycemia. *J. Diabetes Res.* 2016, 1–6. doi: 10.1155/2016/6741745

Rorsman, P., Ramracheya, R., Rorsman, N. J. G., and Zhang, Q. (2014). ATP-regulated potassium channels and voltage-gated calcium channels in pancreatic alpha and beta cells: similar functions but reciprocal effects on secretion. *Diabetologia* 57, 1749–1761. doi: 10.1007/s00125-014-3279-8

Saunders, C. J. (2020). *JakeSaunders/Dmel_AKHcell_RNA-seq v1.0.1*. Genève: Zenodo.

Smith, L. A., Peixoto, A. A., Kramer, E. M., Villella, A., and Hall, J. C. (1998). Courtship and visual defects of cacophony mutants reveal functional complexity of a calcium-channel alpha1 subunit in *Drosophila*. *Genetics* 149, 1407–1426.

Staubli, F., Jørgensen, T. J. D., Cazzamali, G., Williamson, M., Lenz, C., Søndergaard, L., et al. (2002). Molecular identification of the insect adipokinetic hormone receptors. *Proc. Natl. Acad. Sci. U.S.A.* 99, 3446–3451. doi: 10.1073/pnas.052556499

Van Der Horst, D. J. (2003). Adipokinetic hormones of insect: release, signal transduction, and responses. *Comp. Biochem. Physiol. B* 136, 217–226. doi: 10.1016/S1096-4959(03)00151-9

Yu, Y., Huang, R., Ye, J., Zhang, V., Wu, C., Cheng, G., et al. (2016). Regulation of starvation-induced hyperactivity by insulin and glucagon signaling in adult *Drosophila*. *eLife* 5:e15693. doi: 10.7554/eLife.15693

Zhao, Y., Bretz, C. A., Hawksworth, S. A., Hirsh, J., and Johnson, E. C. (2010). Corazonin neurons function in sexually dimorphic circuitry that shape behavioral responses to stress in *Drosophila*. *PLoS One* 5:e9141. doi: 10.1371/journal.pone.0009141

Zheng, X., Valakh, V., DiAntonio, A., and Ben-Shahar, Y. (2014). Natural antisense transcripts regulate the neuronal stress response and excitability. *eLife* 3:e01849. doi: 10.7554/eLife.01849

Conflict of Interest: The authors declare that the research was conducted in the absence of any commercial or financial relationships that could be construed as a potential conflict of interest.

frontiers in Physiology

ORIGINAL RESEARCH
published: 19 November 2020
doi: 10.3389/fphys.2020.594845

Genome Mining and Expression Analysis of Carboxylesterase and Glutathione S-Transferase Genes Involved in Insecticide Resistance in Eggplant Shoot and Fruit Borer, *Leucinodes orbonalis* (Lepidoptera: Crambidae)

*B. Kariyanna[1,2], A. Prabhuraj[1], R. Asokan[3], A. Agrawal[2], R. Gandhi Gracy[2], P. Jyoti[2], T. Venkatesan[2], M. Bheemanna[1], B. Kalmath[1], J. R. Diwan[4], Y. Pampanna[5] and M. Mohan[2]**

[1] Department of Agricultural Entomology, University of Agricultural Sciences, Raichur, India, [2] ICAR-National Bureau of Agricultural Insect Resources, Bengaluru, India, [3] ICAR-Indian Institute of Horticultural Research, Bengaluru, India, [4] Department of Genetics and Breeding, University of Agricultural Sciences, Raichur, India, [5] Department of Horticulture, University of Agricultural Sciences, Raichur, India

The shoot and fruit borer, *Leucinodes orbonalis* (Lepidoptera: Crambidae) is the major cause of low productivity in eggplant and insecticides being the mainstay of management of *L. orbonalis*. However, field control failures are widespread due to the evolution of insecticide resistance. Taking advantage of the whole genome sequence information, the present study investigated the level of insecticide resistance and the expression pattern of individual carboxylesterase (CE) and glutathione S-transferases (GSTs) genes in various field collected populations of *L. orbonalis*. Dose-mortality bioassays revealed a very high level of resistance development against fenvalerate (48.2–160-fold), phosalone (94-534.6-fold), emamectin benzoate (7.2–55-fold), thiodicarb (9.64–22.7-fold), flubendiamide (187.4–303.0-fold), and chlorantraniliprole (1.6–8.6-fold) in field populations as compared to laboratory-reared susceptible iso-female colony (Lo-S). Over-production of detoxification enzymes *viz.*, CE and GST were evident upon enzyme assays. Mining of the draft genome of *L. orbonalis* yielded large number of genes potentially belonging to the CE and GST gene families with known history of insecticide resistance in other insects. Subsequent RT-qPCR studies on relative contribution of individual genes revealed over-expression of numerous GSTs and few CEs in field populations, indicating their possible involvement of metabolic enzymes in insecticide resistance. The genomic information will facilitate the development of novel resistance management strategies against this pest.

Keywords: ***Leucinodes orbonalis*, insecticide resistance, genome, arboxylesterase, gene expression, glutathione S-transferase, carboxylesterase**

OPEN ACCESS

Edited by:
Kai Lu,
Fujian Agriculture and Forestry University, China

Reviewed by:
Wei Dou,
Southwest University, China
Yuji Yasukochi,
National Agriculture and Food Research Organization (NARO), Japan

***Correspondence:**
M. Mohan
Mohan.M@icar.gov.in

Specialty section:
This article was submitted to Invertebrate Physiology, a section of the journal Frontiers in Physiology

Received: *14 August 2020*
Accepted: *22 October 2020*
Published: *19 November 2020*

Citation:
Kariyanna B, Prabhuraj A, Asokan R, Agrawal A, Gandhi Gracy R, Jyoti P, Venkatesan T, Bheemanna M, Kalmath B, Diwan JR, Pampanna Y and Mohan M (2020) Genome Mining and Expression Analysis of Carboxylesterase and Glutathione S-Transferase Genes Involved in Insecticide Resistance in Eggplant Shoot and Fruit Borer, Leucinodes orbonalis (Lepidoptera: Crambidae). Front. Physiol. 11:594845. doi: 10.3389/fphys.2020.594845

HIGHLIGHTS

- High levels of multiple insecticide resistance in field collected *Leucinodes orbonalis* populations.
- Enhanced midgut activities of carboxylesterase and glutathione S-transferase enzymes.
- Qualitative changes in esterase banding pattern in resistant populations.
- Mining and retrieval of 94 carboxylesterase and 33 glutathione S-transferase full length gene sequences from draft assembled genome and transcriptome of *L. orbonalis*.
- Over-expression of large number of glutathione S-transferase and few carboxylesterase genes in resistant field collected populations.

INTRODUCTION

Eggplant or aubergine (*Solanum melongena*), also called as brinjal, is one of the most popular vegetable crops in south-east Asia especially India, China, and Bangladesh. The most important limiting factor in brinjal cultivation is the damage caused by shoot and fruit borer, *Leucinodes orbonalis* Guenee (Lepidoptera: Crambidae). It was first described from India and now it is distributed all over Asia, Africa, and in few parts of Europe (Mally et al., 2015). In India and Bangladesh, it causes severe yield losses up to 93% despite best management practices (Kodandaram et al., 2017; Prodhan et al., 2018). Surveys in India and Bangladesh indicated that farmers spray chemical insecticides up to 84 times during a 6–7 month cropping season. A very high level of pesticide load at a concentration 40–450 times higher than the maximum residue limit (MRL) in marketed brinjal fruits poses major health concerns (Srinivasan, 2008; Latif et al., 2010; Kariyanna et al., 2020b). It is also considered as a pest of quarantine significance to the number of countries outside its native range. *L. orbonalis* has high reproductive potential with overlapping generations. Studies reporting high level of insecticide resistance development in *L. orbonalis* might be attributed to the long-term indiscriminate use of various insecticides on eggplant (Kodandaram et al., 2017; Shirale et al., 2017).

Resistant insects overcome the toxic effect of insecticide molecules by adopting one or more mechanisms ranging from cuticular thickening, nerve impenetration, altered production of metabolic enzymes, target site insensitivity, enhanced excretion through ABC transporters as well as by gut symbionts (Mohan et al., 2015). The enhanced detoxification of insecticides by metabolic enzymes *viz.*, carboxylesterases (CE) and glutathione S-transferases (GSTs) are commonly reported in resistant populations of many insect species and mites (Ranson et al., 2002; Enayati et al., 2005; Oakeshott et al., 2005; Perry et al., 2011; Das and Dutta, 2014; Akıner and Ekşi, 2015; Benoit et al., 2015). The resistant individuals metabolize the insecticides faster due to higher catalytic rate or enhanced production of the enzyme as a consequence of increased transcription or gene duplication (Panini et al., 2016; Kariyanna et al., 2020a). The GSTs are phase II metabolic enzymes and are distributed in most of the animals (Hayes and Pulford, 1995). Among several subclasses of GST, the enzymes which are frequently associated with the insecticide resistance are Delta and Epsilon classes (Friedman, 2011; Lumjuan et al., 2011). Similarly, enhanced metabolism of organophosphates, carbamates, and pyrethroids are frequently associated with CEs through gene amplification, upregulation, mutations by coding sequence, or a combination of all these mechanisms (Zhang et al., 2012; Cui et al., 2015).

Considering the economic and social impact of *L. orbonalis*, genetically modified eggplant expressing insecticidal *cry1Ac* gene from *Bacillus thuringiensis* has been developed (Shelton et al., 2018), but, a moratorium on its commercialization was imposed by Indian Government due to public concern. Though *Bt* eggplant is commercialized in Bangladesh way back in 2014, yet the area under cultivation is <2500 Ha (Shelton et al., 2018) due to various reasons. Baring *Bt* brinjal, the insecticides remain the sole method of controlling *L. orbonalis* in all the eggplant growing countries. With the availability of genome sequence, the present study investigated the level of insecticide and the expression pattern of CE and GST genes from field collected insecticide resistant *L. orbonalis* populations, to pinpoint the key metabolic genes involved in insecticide degradation.

MATERIALS AND METHODS

Insect Collection and Maintenance

The field populations of *L. orbonalis* larvae were collected during 2017–2018 from intensive eggplant growing regions of India *viz.*, Raichur (16.2120° N, 77.3439° E), Dharmapuri (12.0933° N, 78.2020° E), Bhubaneshwar (20.2961° N, 85.8245° E), Pune (18.5204° N, 73.8567° E), and Varanasi (25.3176° N, 82.9739° E). All the field populations were reared under laboratory conditions at 27 ± 2°C, 60–70% relative humidity (RH), and a photoperiod of 14:10 h (L:D) on a natural diet and the F_1 individuals were used for bioassay and biochemical studies. The insecticide susceptible iso-female line (National Accession number: NBAIR-IS-CRA-01A), designated as Lo-S (65th generation) was originally derived from *L. orbonalis* collected near Bengaluru (12.9716° N, 77.5946° E) and maintained at insect genomic resources laboratory at ICAR-NBAIR.

Insecticide Resistance Bioassays

Insecticides fenvalarate (20% EC), emamectin benzoate (5% EC), phosalone (35%), thiodicarb (75%), flubendiamide (20%), and chlorantraniliprole (18.5%) were selected for conducting dose-mortality bioassays based on their usage history on brinjal by farmers. Filter paper residue assay (Cheng et al., 2010) with essential modifications was used for insecticide resistance bioassays on early second instar larvae of *L. orbonalis*. Five to seven appropriate concentrations of each of the selected insecticides were prepared based on the dose bracketing technique. The filter paper discs (4.5 cm diameter) were dipped in the appropriate dilutions and dried vertically under shade for 1 h. Then, the discs were placed individually in plastic containers (5 cm diameter) and 10 larvae were released in each container. Moistened filter paper discs without insecticide

TABLE 1 | Primer details for carboxylesterase (CE) genes.

Sl. No	Sequence		Primer sequence 5′→3′	Length	GC (%)	Tm (°C)	Sequence length	Product size	E (%)
1.	Contig8459-0.14	F	GTGTCAAACGTGTTCAGAATC	21	43	54	2796	100	91.43
		R	TACCCAGGAAAGTAGTGTAGT	21	43	54			
2.	Contig12636-0.8	F	CTTGCACTCTGTTCACTAACT	21	43	54	2712	95	88.17
		R	TCTGTCGTCGTTGTTGTATTC	21	43	54			
3.	Contig11486-0.8	F	TCACATGAGACTGGGTAGAA	20	48	55	3936	95	103.22
		R	CTCTGTAGTGTCTGTCGTAGA	21	45	54			
4.	Contig4177-0.23	F	AACCTGTTCTCACAAGCTATC	21	48	55	1146	95	98.05
		R	AGTCTAGTACCTCTCAGGATTG	22	45	55			
5.	Contig5480-0.2	F	TCCCTCACACTAACGAAAGA	20	45	55	6498	95	98.12
		R	TCCAGGTATTCAGGAGTGATAG	22	45	55			
6.	Contig11205-0.1	F	AACGTGGAACCTTACTTCAC	20	45	54	597	100	97.60
		R	CACCTTCGTCTTCGTTGTAA	20	45	54			
7.	Contig4653-0.41	F	TGCAAGTGACTGTGAACGAAG	21	48	58	2417	179	101.88
		R	AGCGTTACCAGGGATGTCTTT	21	48	58			
8.	Contig132-0.69	F	ATCCCTCTGGAACCTCAAAAA	21	43	54	3375	179	88.81
		R	GGGAACATTCTGAAAGGGAAG	21	48	54			
9.	Contig3761-0.1	F	TGTGGGCTAACTTCGCTAAAA	21	43	55	681	233	90.70
		R	TTCGATTTTTCTCACCACACC	21	43	56			
10.	Contig3761-0.2	F	CCTGGCTCTGAAACTGACTTG	21	52	55	1251	150	99.31
		R	TTGATAGGAGGAGCAGCGTAA	21	43	55			
11.	Contig9545-0.25	F	CAAAGAACTTCAACTTCACT	20	35	49	555	193	101.67
		R	TTTTTCGTCAGGTTTGTGAGG	21	43	55			
12.	Contig9545-0.26	F	TCCTTCATTCCTGCAAAGAGA	21	43	55	804	167	100.15
		R	AGTAGTCACCCACCACGTCAG	21	57	60			
13.	Contig11588-0.37	F	CTGGTAACGCTGGTATCAAA	20	45	54	1269	111	97.11
		R	CAGCTGATTGACCGAAGATAG	21	48	55			
14.	Contig5480-0.52	F	ACCAATCAGACGACTCACACC	21	52	59	1863	157	90.48
		R	GCGATGTTCACCAGTTTTGAT	21	43	55			
15.	Contig5480-0.3	F	GGTCCTGTGAAAGGTTACAA	20	45	55	663	94	92.15
		R	TGTATTTGTCAGCACCAGTAG	21	43	55			
16.	Contig11205-0.4	F	GAAGGTGAAATCGTGAACAAC	21	43	54	225	165	97.11
		R	TTGGTATGATGATGAACCGTGT	22	41	56			

were used in control. After 24 h, the larvae were transferred to untreated natural diet. All the assays were replicated and repeated at least thrice on alternate days. The mortality of the larvae was assessed after 48 h. The pooled larval mortality data were subjected to probit analysis using the software POLO (LeOra, 1987) and the lethal concentration to kill 50% of the test larvae (LC_{50}) was calculated for each population. Resistance ratios (RRs) were calculated with the following formula: LC_{50} of field population/LC_{50} of insecticide susceptible Lo-S population.

Preparation of Midgut Homogenate

The starved late second instar larvae were used for the preparation of midgut homogenate. Midguts were dissected and homogenized with homogenization buffer (0.1 M sodium phosphate buffer pH 7.8 containing 1 mM each of DTT, EDTA, PTU, and PMSF). The content was centrifuged at 12,000 rpm for 20 min and the clear supernatant was used as a enzyme source for estimating the titers of carboxylesterase and GST. The total protein content of the preparations was assessed by Coomassie brilliant blue G-250 dye-binding method using bovine serum albumin (BSA) as the standard (Bradford, 1976).

Assays on Carboxylesterase and Glutathione S-Transferase

The activity of carboxylesterase was determined using the method described by van Asperen (1962) with essential modifications and α-naphthyl acetate as a substrate. The assay mixture in a 96 well microplate (iMark, Biorad microplate reader) consisted of an appropriate amount of midgut homogenate, 0.1 M sodium phosphate buffer pH 7.8 and 800 µl of 3 mM α-naphthyl acetate containing 0.3 mM eserine. The mixture was incubated at 30°C for 30 min. Finally, 200 µl of 0.1% tetrazotized o-dianisidine (Fast blue B) in 3.5% sodium dodecyl sulfate was added and incubated for 20 min at room temperature in dark. The α-naphthol formation was measured at 590 nm and the enzyme activity was computed from α-naphthol standard curve.

Glutathione S-transferase activity was determined using 1-chloro-2,4-dinitrobenzene (CDNB) as a substrate (Kao et al.,

TABLE 2 | Primer details for glutathione S-transferase (GST) genes.

Sl. No	Sequence		Primer sequence 5′→3′	Length	GC%	Tm (°C)	Sequence length	Product size	E (%)
1.	Contig7206-0.56	F	GCCTCAAGACTGCATGAAAAG	21	48	56	600	223	98.59
		R	GTCAGCCAGAGTGATTTCGTC	21	52	58			
2.	Contig2323-0.22	F	TTCACCTCCTTGCAGATCAGT	21	48	58	375	160	87.80
		R	GAAGTCACCGTCTTTCAGCAG	21	52	58			
3.	Contig8855-0.81	F	ACGACATCCTGAACACTCTGC	21	52	59	657	165	98.93
		R	TTCTCCATTGTCTCACCCAAG	21	48	57			
4.	Contig2841-0.35	F	CGCTATGAGATTCTGCCCTTAC	22	50	57	762	120	104.58
		R	GAGAAGTCGAACAGCCATTCA	21	48	57			
5.	Contig2596-0	F	TGCTACCTGGTGGACAAATTC	21	48	57	639	236	92.92
		R	CCCATTTAGTGTCGTTCAGGA	21	48	56			
6.	Contig14202-0.24	F	TATCCTGGCTCTGAACGCTAA	21	48	58	717	171	105.55
		R	TCGTCCAGGTATTCCACAGTC	21	52	59			
7.	Contig1970-0.34	F	GACGCTCTGAGACTGTTCGAC	21	57	60	564	190	96.96
		R	CTTCGTAACCAGGAGCAGTTG	21	52	58			
8.	Contig1510-0.48	F	ATCGGTTGGCTGAACACTATG	21	48	57	726	227	95.00
		R	AAAGTAGCCAGCATTTGAGCA	21	43	57			
9.	Contig2478-0.25	F	TCTGGGACTCACACGCTATCT	21	52	56	654	208	100.59
		R	ATTTGAGCCAGGTTTTCAGGT	21	43	60			
10.	Contig3755-0.39	F	CGCTATCATGCAATACGTGTG	21	48	56	654	183	102.61
		R	AGACCCAGAGGAGTTCTTTCG	21	52	59			
11.	Contig3537-0.3	F	ACAAATTCAACCTGCTGCCTA	21	43	56	423	227	96.58
		R	CAGTTTACCAGCGAAGTGACC	21	52	58			
12.	Contig10769-0.3	F	TCACTGGCTATCGCTAGATACA	22	45	57	621	116	98.89
		R	CGTTTGACCAGAAGTCGAAGAT	22	45	57			
13.	Contig1010-1.18	F	GACGCTCTGAGACTGTTCGAC	21	57	60	648	190	98.00
		R	CTTCGTAACCAGGAGCAGTTG	21	52	58			
14.	Contig9166-0.22	F	ACAAATCAGTGGCTGCTAAA	20	40	54	345	97	95.31
		R	GGCAGGTAGTACAGTTTGATAG	22	45	54			
15.	Contig6423-0.33	F	TGCTACCTGGTGGACAAATTC	21	48	57	645	236	89.22
		R	CCCATTTAGTGTCGTTCAGGA	21	48	56			
16.	Contig199-0.91	F	TGTGAAAGCTCTGGGTGAATC	21	48	57	567	233	99.14
		R	GAAGTCCACGTTCATGTCGAT	21	48	57			
17.	Contig8048-0.1	F	TCAATCGAAGAAGACCTGGAA	21	43	55	486	150	98.83
		R	CAGCAGTTGAGGGTACACGTT	21	52	60			
18.	Contig11878-0.11	F	TGCTACCTGGTGGACAAATTC	21	48	57	540	236	98.55
		R	CCCATTTAGTGTCGTTCAGGA	21	48	56			
19.	Contig7006-0	F	CGCTAGATACCTGGCTAACAAA	22	45	56	606	98	92.55
		R	CCCAGAAGTCGTAGATGTTCAG	22	50	57			
20.	Contig3023-0.16	F	GCTGCTTACGAAGGTAGAATG	21	48	55	618	173	99.14
		R	GCAGGGAAGTGTTCTTTAGGG	21	52	58			
21.	Contig2596-0	F	TGCTACCTGGTGGACAAATTC	21	48	57	639	235	101.31
		R	CCCATTTAGTGTCGTTCAGGA	21	48	56			
22.	Contig2478-0.15	F	CATCACACGCTATCACTACTT	21	43	54	456	102	97.25
		R	GCAGTCTTTGGTCGATTCT	19	47	54			
23.	Contig3291-0.7	F	TATCGTGTCAGGTATCCAAC	20	45	53	402	179	92.16
		R	GTCAGCCAGAGTCAGTTGGTC	21	57	60			
24.	Contig4841-1.1	F	TGGACGACACTAGACCTAAA	20	45	54	327	81	93.78
		R	GTTGGATACCTGACACGATAG	21	48	54			
25.	Contig2323-0.23	F	CTCACACGCTATCACTACTTAC	22	45	54	645	101	95.56
		R	GCAGTCTTTGGTCGATTCT	19	47	54			

1989). The assay mixture composed of 50 mM each of CDNB and L-glutathione reduced and 10 µl gut homogenate. The change in absorbance was measured at 340 nm for 5 min and the enzyme activity in terms of nmoles of CDNB conjugated per minute per mg protein using the molar extinction coefficient of 5.3 mM^{-1} (optimized for the path length: 0.55 cm).

TABLE 3 | Resistance pattern of field populations of *L. orbonalis* against various insecticides.

Insecticide	Population	LC50 (ppm)	Slope ± SE	Fiducial limits		χ^2 heterogeneity (DF)	Resistance ratio
				Lower	Upper		
Fenvalerate	Bhubaneswar	259.2	2.6 ± 0.52	125.61	623.8	7.01 (3)	160
	Raichur	93.2	3.1 ± 0.2 2	56.1	125.8	3.92 (3)	57.5
	Dharmapuri	78.4	2.5 ± 0.23	53.2	145	2.81 (3)	48.3
	Pune	5.9	2.1 ± 0.11	2.51	16.32	2.91 (3)	3.6
	Varanasi	153.2	1.6 ± 0.23	75.2	432.4	3.37 (4)	94.6
	Bengaluru (Lo-S)	1.62	2.2 ± 0.42	0.85	3.57	2.62 (4)	–
Phosalone	Bhubaneswar	641.5	2.61 ± 0.22	283.51	2564.6	6.90 (3)	534.6
	Raichur	190.2	1.9 ± 0.2 1	110.1	280.5	3.90(3)	158.5
	Dharmapuri	113	3.3 ± 0.56	56.4	203.2	0.89 (3)	94.2
	Pune	8.81	1.7 ± 0.08	4.34	24.81	3.48 (3)	7.3
	Varanasi	435.8	1.9 ± 0.21	210.5	1202.8	1.37 (3)	363.2
	Bengaluru (Lo-S)	1.2	1.2 ± 0.21	0.521	2.42	1.91 (3)	–
Emamectin benzoate	Bhubaneswar	0.072	1.4 ± 0.09	0.291	0.204	3.4 (3)	7.2
	Raichur	0.1	1.1 ± 0.10	0.07	0.2	1.19 (3)	10
	Dharmapuri	0.07	1.5 ± 0.31	0.03	0.1	2.66 (3)	7
	Pune	0.012	1.8 ± 0.09	0.005	0.045	1.07 (3)	1.2
	Varanasi	0.55	1.2 ± 0.28	0.231	1.821	6.89 (4)	55
	Bengaluru (Lo-S)	0.01	1.4 ± 0.07	0.004	0.051	3.17 (3)	–
Thiodicarb	Bhubaneswar	211.6	1.71 ± 0.83	116.23	621.78	1.91 (3)	18.2
	Raichur	263.2	2.1 ± 0.21	121.3	467.9	2.3 (3)	22.7
	Dharmapuri	161.9	2.05 ± 0.30	83.82	341.7	7.2 (3)	13.9
	Pune	23.6	2.0 ± 0.12	32.01	184.8	1.3 (3)	2.03
	Varanasi	112	2.2 ± 0.18	56.82	456.8	1.7 (4)	9.6
	Bengaluru (Lo-S)	11.61	1.73 ± 0.32	5.462	23.56	4.7 (3)	–
Flubendiamide	Bhubaneswar	69.7	1.20 ± 0.08	36.34	173.35	3.7 (3)	303.0
	Raichur	43.1	1.72 ± 0.10	22.39	93.72	2.9 (3)	187.4
	Dharmapuri	61.5	1.3 ± 0.13	35.65	129.39	7.2 (3)	267.4
	Pune	6.79	1.10 ± 01.0	3.02	17.93	14.6 (4)	29.5
	Varanasi	61.3	1.79 ± 0.08	20.32	173.8	17.5 (4)	266.5
	Bengaluru (Lo-S)	0.23	–	–	–	–	–
Chlorantraniliprole	Bhubaneswar	2.29	0.66 ± 0.16	0.28	6.4	4.08 (3)	6.9
	Raichur	0.80	0.59 ± 0.16	0.02	2.9	2.80 (3)	2.4
	Dharmapuri	2.84	0.63 ± 0.15	0.41	7.94	4.92 (3)	8.6
	Pune	1.76	0.6 ± 0.16	0.12	5.59	3.08 (3)	5.3
	Varanasi	0.60	0.47 ± 0.15	0.002	3.2	5.68 (3)	1.6
	Bengaluru (Lo-S)	0.33	0.81 ± 0.26	0.003	1.24	1.55 (3)	–

TABLE 4 | Metabolic enzymes activities in the midgut of *L. orbonalis* populations.

L. orbonalis population	Glutathione -S- transferase		Carboxylesterase	
	Specific activity (nMoles/min/mg protein)	Fold variation as compared to Lo-S	Specific activity (μMoles/mg/min)	Fold variation as compared to Lo-S
Bhubaneswar	70.5 ± 3.6*	5.6	6.02 ± 0.21*	2.8
Raichur	73.0 ± 3.6*	5.8	6.83 ± 0.21*	3.2
Dharmapuri	112.3 ± 11.2*	8.9	5.78 ± 0.33*	2.7
Varanasi	51.8 ± 2.8*	4.1	3.52 ± 3.4	1.7
Pune	103.4 ± 9.5*	8.2	3.28 ± 0.33	1.5
Bengaluru (Lo-S)	12.62 ± 1.3	–	2.12 ± 0.13	–

**Indicates significant differences by Mann–Whiteney U-test ($p < 0.05$) as compared to Lo-S population.*

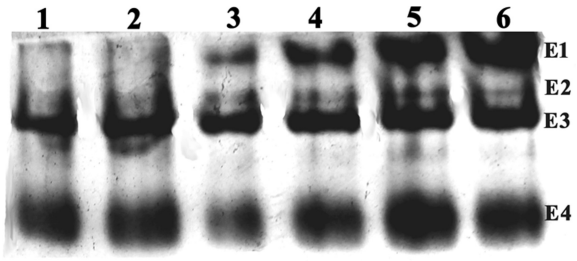

FIGURE 1 | The Native PAGE of the esterase isozyme pattern of *L. orbonalis* (1. Lo-S, 2. Pune, 3. Varanasi, 4. Raichur, 5. Bhubaneswar, 6. Dharmapuri).

Esterase Isozyme Studies

The native polyacrylamide gel electrophoresis (PAGE) with 10% resolving gel was performed as per Davis (1964) to visualize the esterase isozymes from the 2nd instar midgut larval homogenates of the *L. orbonalis* populations tested. Midgut homogenates with 20 μg protein were loaded onto the native PAGE and run at a constant voltage of 70 for 1.5 h. Gel was briefly stained with freshly prepared 0.05% (w/v) α-naphthyl acetate and 0.1% (w/v) fast blue B in 50 mM phosphate buffer pH 7.8.

Genome Mining and Phylogenetic Analysis

The draft assembled genome (NCBI Bioproject ID: PRJNA377400) of *L. orbonalis* was used as query for extracting the gene sequences of glutathione S-transferases (GSTs) and carboxylesterases (CEs). The hmm model for carboxylesterase and GST (CE-PF00135, PF02230, and GST-C PF00043, GST-N PF02798, GST-PF13417, PF14497, PF17171, PF17172)

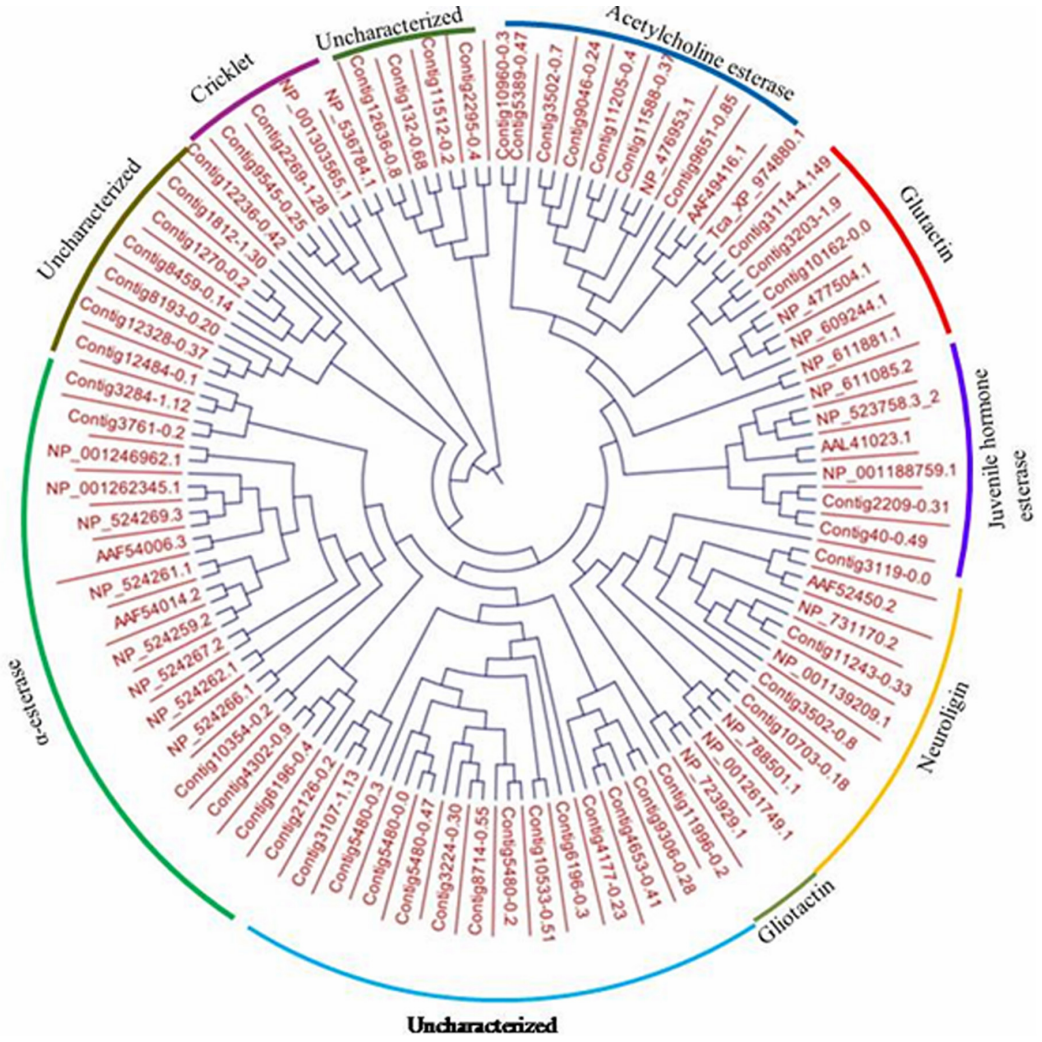

FIGURE 2 | Phylogenetic relationships of 94 CE proteins of *L. orbonalis* with selected *D. melanogaster* protein representative of seven characterized carboxylesterase classes. Putative CE proteins in *L. orbonalis* were identified using hmmsearch against PFAM CE families (CE PF00135). The Maximum likelihood tree was constructed using CLC workbench.

were obtained from PFAM database[1]. A total of 94 and 33 putative CE and GST sequences were mined using hmm search with HMMER3 software package[2]. Among them, the genes with known history of involvement in insecticide resistance in other insects were selected and further confirmed with NCBI BLASTX. The GST and CE protein sequences of *Drosophila melanogaster* was downloaded from its genome database (Marygold et al., 2013), GenBank[3] and Uniprot[4]. We combined these putative GST protein sequences with *D. melanogaster*'s annotated protein sequences for each of the six subclasses of GST (Epsilon, Sigma, Omega, Delta, Zeta, and Theta). The sequences were multiple aligned using CLUSTALW and a maximum likelihood tree with 1000 bootstrap value was constructed using MEGA7[5] and TreeDyn online server[6] was used to visualize the tree. Similarly, 94 CE protein sequences under seven subclasses (α-esterases, gliotactin, glutactin, neurolignin, juvenile hormone esterases, acetylcholinesterases, and cricklet) were combined, multiple aligned using MAFFT online server using conserved domain feature and phylogenetic tree of CE genes from *L. orbonalis* using *D. melanogaster* as a reference were constructed with the help of CLC workbench (QIAGEN Bioinformatics[7]) using maximum likelihood approach.

[1]http://pfam.xfam.org

[2]http://hmmer.janelia.org

[3]http://www.ncbi.nlm.nih.gov/

[4]http://www.uniprot.org/

[5]http://www.megasoftware.net

[6]www.treedyn.org

[7]https://www.qiagenbioinformatics.comproductsclc-main-workbench

Quantitative Real-Time PCR

The late 2nd instar larvae were used for RNA extraction (ISOLATE II RNA mini kit) by following the manufacturer's guidelines (Bioline). Purity and concentration of total RNA were measured in a spectrophotometer (NanoDrop Lite, Thermo Fisher Scientific) and denatured agarose gel (Masek et al., 2005). RNA samples with an A260/A280 ratio ranging from 1.8 to 2.0 and A260/A230 ratio >2.0 were used for cDNA preparation. First strand of complementary DNA was synthesized from 4 μg of total RNA using Revert AID first strand cDNA synthesis kit (Thermo Fisher Scientific™, Lithuania) following the suppliers guidelines and stored at −80°C till further use.

qPCR primers for 25 GST and 16 CE gene sequences were designed using Primer 3.0 software. The detailed information of the primers used in the current study is listed in **Tables 1**, **2**. To remove the primer dimer and confirm the efficiency, OligoEvaluator™ sequence analysis tool (accessed on July 2018[8]) was used. Primer specificity analysis was observed by single peak in the melting curve and single band from the agarose gel of the all candidate genes of CE and GST ranged from 90.36 to 104.58% (**Tables 1**, **2**). Quantitative real-time PCR (RT-qPCR) amplifications were performed in 20 μL reaction consisted of 10 μL 2×SYBR® Premix EX TaqTM II (Tli RNaseH Plus, TAKARA®, Japan), 1 μl cDNA and gene specific primer pair. The parameters used for RT-qPCR are: One cycle of 95°C for 3 min; 35 cycles of 95°C for 30 s, 53°C for 45 s, and 72°C for 1 min; a final cycle of 72°C for 10 min using Roche 480II machine. All the samples including control (no template)

[8]http://www.sigmaaldrich.com/life-science/custom-oligos/custom-dna/learning-center/calculator.html

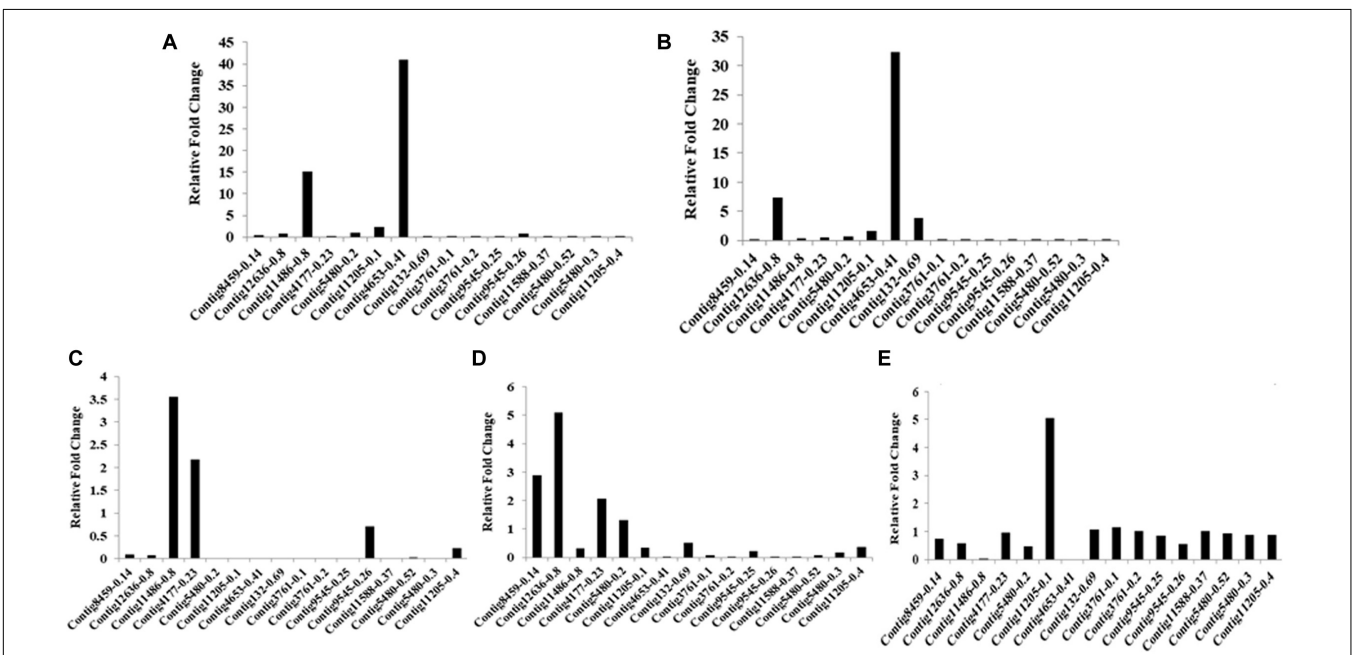

FIGURE 3 | Transcription profiling of carboxylesterase genes in field collected populations of *L. orbonalis* depicted as fold change over the susceptible Lo-S colony. **(A)** Bhubaneswar, **(B)** Dharmapuri, **(C)** Pune, **(D)** Raichur, **(E)** Varanasi.

and internal control were performed in triplicates. The PCR products were electrophoresed on 2.0% agarose gel in a 1.0×TAE buffer. Relative expression levels for the CE and GST genes were calculated by $2^{-\Delta\Delta CT}$ method. The 28SR3 (28S ribosomal protein S3 mitochondrial) (Kariyanna et al., 2019) gene was used as an internal control to normalize the expression of target genes.

RESULTS

Insecticide Resistance Monitoring

The LC_{50} values against fenvalerate, phosalone, thiodicarb, emamectin benzoate, flubendiamide and chlorantraniliprole indicated that there is a large shift in susceptibility of field-populations of *L. orbonalis* as compared to the laboratory reared susceptible iso-female colony (Lo-S). The field collected populations exhibited 3.6–160-fold resistance against fenvalerate, 7.3–534.6-fold resistance against phosalone, 7.0–55.0-fold resistance against emamectin benzoate, 2.0–22.7-fold resistance against thiodicarb, 29.5–303.0-fold resistance against flubendiamide, and 1.6–8.6-fold resistance against chlorantraniliprole. However, the susceptibility level of all the field populations and the Lo-S did not vary significantly against chlorantraniliprole based on the overlapping fiducial limit values. High level of resistance development against phosalone and flubendiamide was observed in *L. orbonalis* collected from Varanasi whereas other field populations, the RRs were non-significant as compared to Lo-S. *L. orbonalis* populations from Bhubaneswar showed a significantly very high levels of resistance against fenvalerate, phosalone and flubendiamide as compared to Lo-S. The population of *L. orbonalis* collected from high hills near Pune recorded less RR and the susceptibility status was almost on par with Lo-S population (**Table 3**).

Activities of Detoxification Enzymes

Quantitative differences in the titer of GST and CE were determined using α-naphthyl acetate and 1-chloro-2,4-dinitrobenzene (CDNB) as substrates, respectively. Significant level of elevated GST activities (4.1–8.9-fold) was observed in field collected *L. orbonalis* as compared to susceptible Lo-S population. However, the overproduction of CE has not pronounced much (1.5–3.2-fold), but there was a significant level of overproduction in two field populations based on Mann–Whiteney U-test. The results indicated that GST activity was altered more profoundly than the CE (**Table 4**).

The qualitative differences in carboxylesterase isozymes were visualized under native PAGE after incubation of the gels in the α-naphthyl acetate as a substrate. Among the four major esterase activity bands (E_1 to E_4), the high molecular weight E_1 and E_2 bands were absent in Lo-S and Pune populations and faint in case of Varanasi population. However, the E_1 band was very prominent and intense in other field populations indicating its over-production nature (**Figure 1**).

Differential Expression of CE Genes

Ninety-four CE genes were identified from the genome and transcriptome sequences of *L. orbonalis*. They were classified under seven subfamilies *viz.*, α-esterases, gliotactin, glutactin, neurolignin, juvenile hormone esterases, acetylcholinesterases, and cricklet like orthologs (**Figure 2**). The length of the gene sequences ranged from 225 to 6498 bp. Expression profiling of 16 genes (homologous to resistant genes in other insects with ≥90% query coverage) was examined from the mRNA samples derived from late second instar larvae of five field-collected *L. orbonalis* populations by RT-qPCR. The CE genes contig11486-0.8 and contig4653-0.41 were over-expressed more than 10-fold as compared to susceptible Lo-S population (**Figures 3**, **4**).

Differential Expression of Glutathione S-Transferase Genes

Mining of genome and transcriptome data of *L. orbonalis* yielded 33 unigenes codings for GSTs. Lengths of the identified GST unigene sequences ranged from 370 to 5,048 bp. The phylogenetic analysis revealed that the predicted GST genes are represented under all six classes of GST *viz.,* Epsilon (10 genes), Sigma (6 genes), Omega (5 genes), Delta (8 genes), Zeta (3 genes), and Theta (1 gene) (**Figure 5**). RT-qPCR analysis of 25 GST genes (homologous to other insects resistant genes) revealed that many of them were over-expressed in larvae collected from the field. The GST genes named contig2323-0.22, contig14202-0.24, contig3755-0.39, contig3537-0.3, contig199-0.91, contig3023-0.16, contig3291-0.7, contig4841-1.1, and contig2323-0.23 were

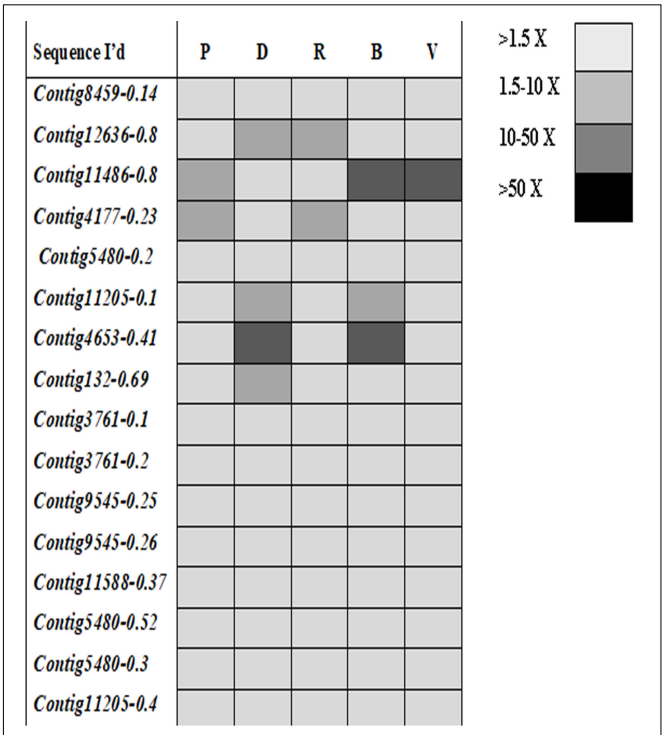

FIGURE 4 | Expression profiles (fold changes over Lo-S population) of carboxylesterase genes across field collected *L. orbonalis* populations (P, Pune; D, Dharmapuri; R, Raichur; B, Bhubaneswar; V, Varanasi). The fold changes are indicated in different shades indicate significant difference as per Mann–Whiteney U-test p-value < 0.05.

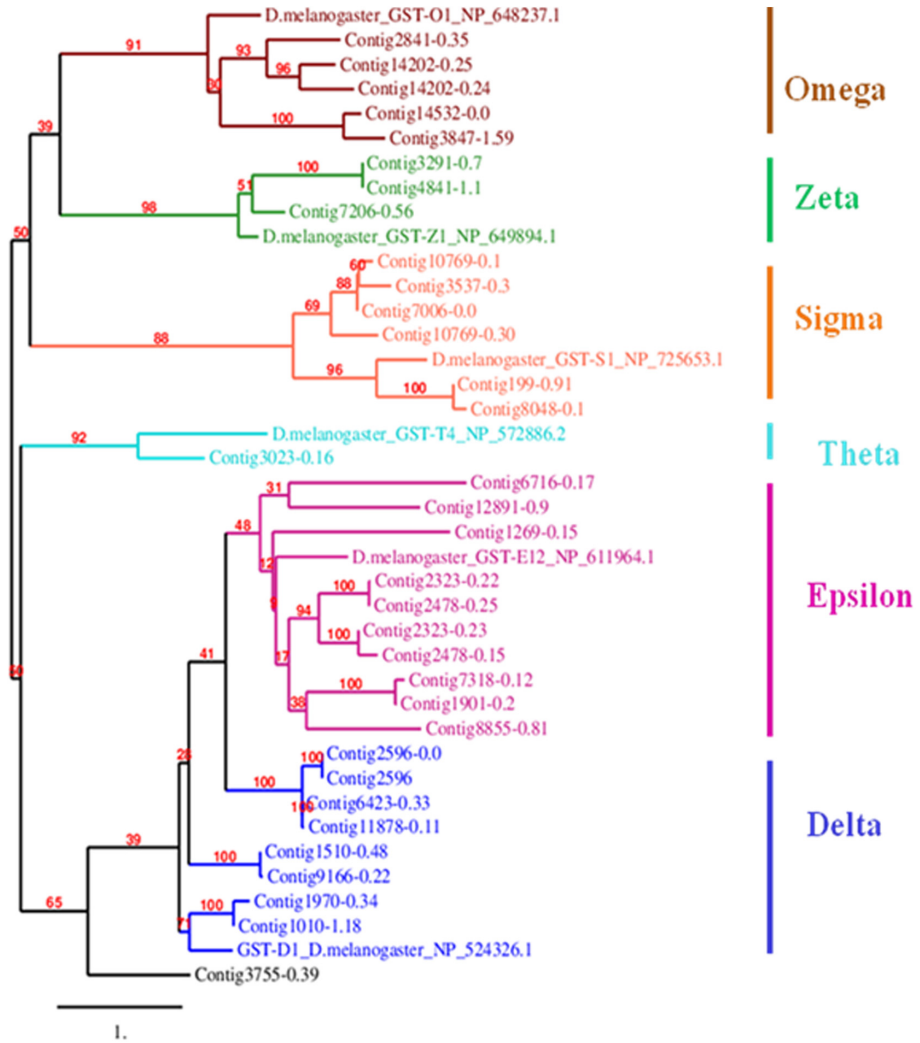

FIGURE 5 | Phylogenetic tree of 34 predicted *L. orbonalis* glutathione S-transferase proteins with *D. melanogaster* genes representative of the six characterized GST classes. Putative GST proteins in *L. orbonalis* were identified using hmmsearch against PFAM GST families (GST-C PF00043, GST-N PF02798), the Maximum Likelihood tree with 1000 bootstraps was constructed using MEGA7 and TreeDyn online server was used to visualize the tree. Number on each node is bootstrap values in percent. Scale = 1 amino acid substitution per site.

very highly expressed (>50-fold) in one or more resistant field-collected *L. orbonalis* populations (**Figures 6**, **7**) over the susceptible Lo-S population.

DISCUSSION

Damage caused by *L. orbonalis* is the major limiting factor in realizing maximum productivity of eggplant in many Asian countries including India, China, and Bangladesh. The high reproductive potential and shorter life cycle of the pest coupled with the evolution of multiple insecticide resistance pose a major challenge in profitable cultivation of eggplant (Prodhan et al., 2018). The insecticide resistance levels detected in the field collected populations ranged from low (>10-fold) to moderate (10–100-fold) and high (>100-fold) against fenvalerate (48.2–160-fold), phosalone (94–534.58-fold), emamectin benzoate (7–55-fold), thiodicarb (9.64–22.67-fold), and flubendiamide (29.51–363.91-fold). The resistance levels reflect the occurrence of differential selection pressure associated with long term history of insecticide use against *L. orbonalis*. However, the response to chlorantraniliprole was similar among the resistant field collected populations with RRs below 10-fold. The efficacy of chlorantraniliprole has been reported earlier (Kodandaram et al., 2013; Munje et al., 2015). The chlorantraniliprole and flubendiamide are anthranilic and phthalic diamides, respectively, are the newer insecticides with little or no cross-resistance among them and also with other classes of insecticides. They are the activators of the ryanodine receptor.

Insect employs various mechanisms to nullify the toxic effect of xenobiotic compounds. Insect metabolic enzymes play a major

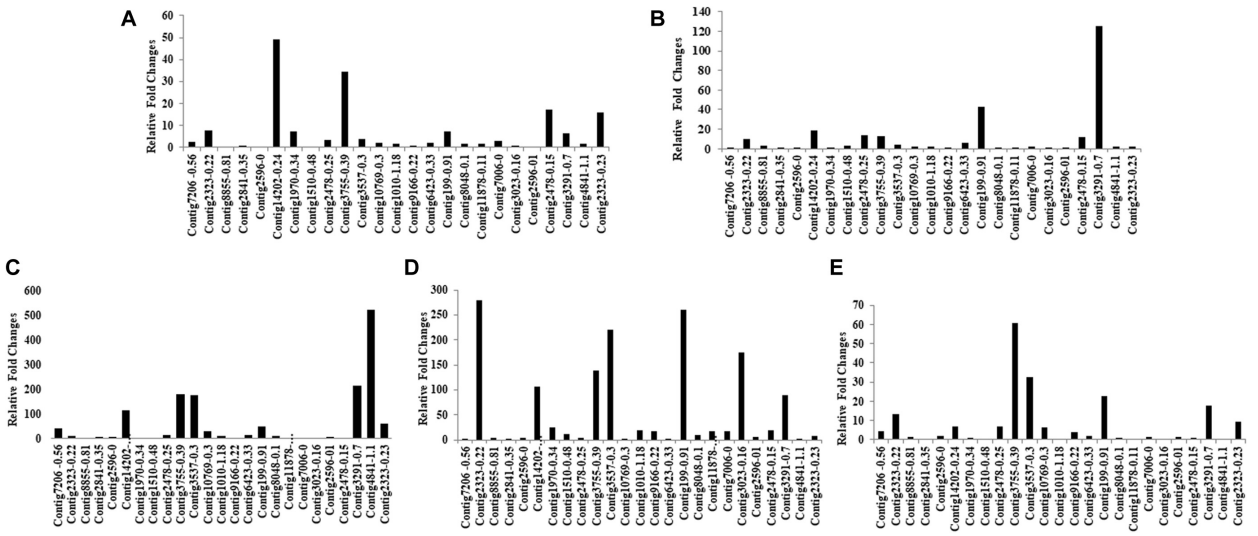

FIGURE 6 | Transcription profiling of glutathione -S- transferase genes in field collected populations of *L. orbonalis* depicted as fold change over the susceptible Lo-S colony. **(A)** Bhubaneswar, **(B)** Dharmapuri, **(C)** Pune, **(D)** Raichur, **(E)** Varanasi.

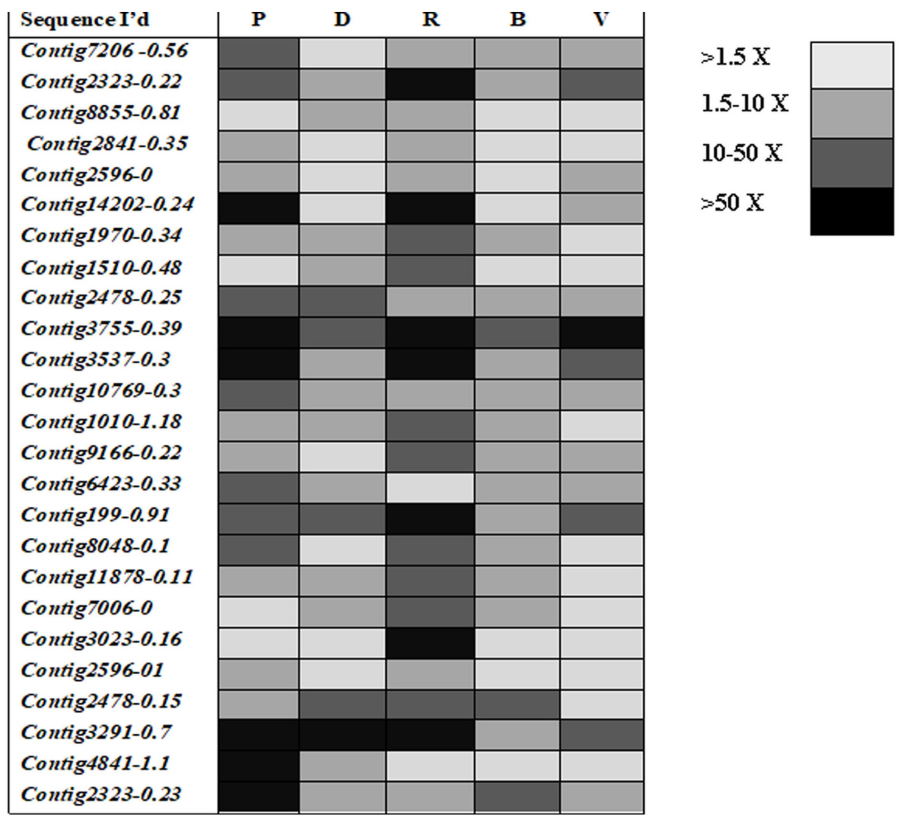

FIGURE 7 | Expression profiles (fold changes over Lo-S population) of glutathione -S- transferase genes across field collected *L. orbonalis* populations (P, Pune; D, Dharmapuri; R, Raichur; B, Bhubaneswar; V, Varanasi). The fold changes are indicated in different shades indicate significant difference as per Mann–Whiteney U-test p-value < 0.05.

role in detoxification of plant allelochemicals and pesticidal compounds in addition to other physiological roles. Insect pests have evolved large reservoirs of various detoxification enzymes. Glutathione S-transferases mediated detoxification can be direct or by the metabolism of secondary products generated from other detoxification enzymes. The insecticides are metabolized rapidly into readily excretable water-soluble metabolites by reductive dehydrochlorination or by conjugation with reduced glutathione (Pavlidi et al., 2018). The carboxylesterase is a phase-1 detoxification enzyme that mainly hydrolyses organophosphates, carbamates, and synthetic pyrethroids.

The quantitative mechanisms underlying metabolic resistance is characterized by over-production due to gene amplification or transcriptional upregulation (Mohan et al., 2015; Feyereisen, 2015; Pavlidi et al., 2018). A qualitative mechanism occurs as a result of changes in the enzymatic characteristics. The present investigation on the enhanced metabolism of insecticides in resistant populations of *L. orbonalis* resistance is very prominent as inferred by elevated GST (1.2–2.6-fold) and carboxylesterases (6.3–13.1-fold) titers. The involvement of CEs and GSTs in insecticide resistance is commonly reported in many other insect species (Mohan et al., 2015; Pavlidi et al., 2018).

With the advent of genome and transcriptome information, multiple GSTs and carboxylesterases encoding genes have been characterized from insects and mites such as *Plutella xylostella, Culex* spp., *Tribolium castaneum, Bombyx mori, Leptinotarsa decemlineata, Tetranychus cinnabarinus, Musca domestica* and in many other insect species (Yang and Liu, 2011; Wang et al., 2014; Cui et al., 2015; Meisel and Scott, 2018; Pavlidi et al., 2018). *L. orbonalis* genome has large expansion of CE and GST genes which is comparable to many other insects. However, the GSTs have prominent role in insecticide resistance as compared to CEs. mRNA level of at least nine GSTs were over-expressed >50-fold where as none of the CEs showed very high levels of expression in the field collected resistant populations. The over-expression of few CE genes in field populations, especially from Varanasi, Raichur, and Bhubaneswar, also aligned with additional high molecular weight esterase band (E1) probably contributed to overall resistance. A similar high molecular weight esterase band associated with B-esterase type was reported from diamondback moth (Mohan and Gujar, 2003). In addition to qualitative changes in esterase banding pattern, there is a significant increase in the production of the CEs in at least three field populations. The over-production and appearance of new esterase isozymes might be the consequence of increased transcription or gene duplication events (Malathi et al., 2015; Panini et al., 2016).

Most of the GST gene expansions are from epsilon and delta subclasses together accounting for 18 genes (54.5%) out of 33 genes identified from the draft genome of *L. orbonalis*. These two GST subclasses are insect-specific, widely expanded in many other insect species whereas other classes have wider taxonomic distribution (Friedman, 2011). There were at least nine GSTs over-expressed >50-fold in one or more of the field-collected resistant populations of *L. orbonalis*. In *Anopheles gambiae, Apis mellifera, B. mori, D. melanogaster, Nasonia vitripennis,* and *T. castaneum* respectively 28, 8, 23, 37, 19, 35 GSTs and 51, 24, 76, 35, 41, 49 CEs were identified (Yu et al., 2008, 2009; Oakeshott et al., 2010). Similarly, the gene expansion of cytochromoe p450 monooxygenases (CYP) and their role in insecticide resistance in *L. orbonalis* were recently documented (Kariyanna, 2019; Kariyanna et al., 2020a). Together with the results of present and earlier studies it is very much evident that multiple metabolic enzymes contribute toward overall insecticide resistance in *L. orbonalis*. However, in many insect species including *L. orbonalis*, it is difficult to distinguish whether the expansion of these metabolic genes and their involvement in insecticide detoxification are driven from ancestry or adaptation to stress or both.

CONCLUSION

In conclusion, the present study provides the first genomic level information on GST and CE gene families of *L. orbonalis* and their role in insecticide resistance. The information further supports insect resistance management through use of reduced risk pesticides including biologicals.

DATA AVAILABILITY STATEMENT

The datasets presented in this study can be found in online repositories. The names of the repository/repositories and accession number(s) can be found in the article/**Supplementary Material**.

AUTHOR CONTRIBUTIONS

BKr: conducted the experiment, analysis, manuscript writing, materials and methods, and hypothesis. AP: analysis, material methods, and corrections. RA: analysis and technical suggestion, manuscript correction, and resource supply. AA and PJ: bioinformatics and analysis. RG and BKl: resources supply and, technical guidance and suggestions. TV: resources supply, technical guidance and suggestions, and reviews and literatures. MB and JD: analysis, technical guidance and suggestions, and reviews and literatures. MM: designing experiment, resources supply, manuscript corrections, analysis, material and methods, technical guiding, and suggestions. YP: technical guidance and suggestions, and reviews and literatures. All authors contributed to the article and approved the submitted version.

ACKNOWLEDGMENTS

The authors profusely thank Indian Council of Agricultural Research for generous funding under ICAR-CRP Genomics project. The first author acknowledges the award of DST-Inspire fellowship (2016/IF160900) and UAS Raichur for

necessary support. Authors are thankful to Director, ICAR-NBFGR for timely release of fund. The facilities extended by Director, ICAR-NBAIR, and Director, ICAR-IIHR, Bengaluru are gratefully acknowledged.

SUPPLEMENTARY MATERIAL

The Supplementary Material for this article can be found online at: https://www.frontiersin.org/articles/10.3389/fphys.2020.594845/full#supplementary-material

Supplementary Table 1 | Highlights of the research.

Supplementary Table 2 | Sequence information GST and CE from *L. orbonalis*.

Supplementary Table 3 | Resistance genes of GST and CE from *L. orbonalis*.

Supplementary Table 4 | Detailed sequence information of CE from *L. orbonalis*.

Supplementary Table 5 | Detailed sequence information of GST from *L. orbonalis*.

Supplementary Table 6 | NCBI ID and description for the Reference protein taken in GST and CE phylogeny.

Supplementary Table 7 | Comparative characterization *L. orbonalis* CE genes with other group based on the nr hit.

Supplementary Table 8 | Descriptive information of the *L. orbonalis* CE sequences.

Supplementary Presentation 1 | Graphical representation of the manuscript.

REFERENCES

Akıner, M. M., and Ekşi, E. (2015). Evaluation of insecticide resistance and biochemical mechanisms of *Culex pipiens* L. in four localities of east and middle mediterranean basin in Turkey. *Int. J. Mosq. Res.* 2, 39–44.

Benoit, J., Adelman, B. Z. N., Reinhardt, K., Dolan, A., Poelchau, M., Jennings, E. C., et al. (2015). Unique features of the bed bug, a global human ectoparasite, identified through genome sequencing. *Nat. Commun.* 7:10165. doi: 10.1038/ncomms10165

Bradford, M. M. (1976). Rapid and sensitive method for the quantitation of microgram quantities of protein utilizing the principle of protein-dye binding. *Anal. Biochem.* 72, 248–254. doi: 10.1016/0003-2697(76)90527-3

Cheng, X., Chang, C., and Daia, S.-M. (2010). Responses of striped stem borer, Chilo suppressalis (*Lepidoptera*: *Pyralidae*), from Taiwan to a range of insecticides. *Pest Manag. Sci.* 66, 762–766. doi: 10.1002/ps.1939

Cui, F., Li, M. X., Chang, H. J., Mao, Y., Zhang, H. Y., Lu, L. X., et al. (2015). Carboxylesterase-mediated insecticide resistance: quantitative increase induces broader metabolic resistance than qualitative change. *Pestic. Biochem. Physiol.* 121, 88–96. doi: 10.1016/j.pestbp.2014.12.016

Das, M., and Dutta, P. (2014). Status of insecticide resistance and detoxifying enzyme activity of *Aedes albopictus* population in Sonitpur district of Assam. India. *Int. J. Mosq. Res.* 1, 35–41.

Davis, B. J. (1964). Disc electrophoresis II. Method and application to human serum proteins. *Ann. N.Y. Acad. Sci.* 121, 404–427. doi: 10.1111/j.1749-6632.1964.tb14213.x

Enayati, A. A., Ranson, H., and Hemingway, J. (2005). Insect glutathione transferases and insecticide resistance. *Insect Molec. Biol.* 14, 3–8. doi: 10.1111/j.1365-2583.2004.00529.x

Feyereisen, R. (2015). Insect P450 inhibitors and insecticides: challenges and opportunities. *Pest Manag. Sci.* 71, 793–800. doi: 10.1002/ps.3895

Friedman, R. (2011). Genomic organization of the glutathione S-transferase family in insects. *Molec. Phylogenet. Evol.* 61, 924–932. doi: 10.1016/j.ympev.2011.08.027

Hayes, J. D., and Pulford, D. J. (1995). The glutathione S-transferase supergene family: regulation of GST and the contribution of the isoenzymes to cancer chemoprotection and drug resistance. *Crit. Rev. Biochem. Molec. Biol.* 30, 445–600. doi: 10.3109/10409239509083491

Kao, C. H., Hung, C. F., and Sun, C. N. (1989). Parathion and methyl parathion resistance in diamondback moth (*Lepidoptera*: *Plutellidae*) larvae. *J. Econ. Entomol.* 82, 1299–1304. doi: 10.1093/jee/82.5.1299

Kariyanna, B. (2019). *Identification and Functional Analysis of Genes Involved in Insecticide Resistance in Leucinodes orbonalis Guenee (Lepidoptera: Crambidae)*. PhD thesis, University of Agricultural Sciences, Raichur, Karnataka, 1–199.

Kariyanna, B., Prabhuraj, A., Asokan, R., Babu, P., Jalali, S. K., Venkatesan, T., et al. (2019). Identification of suitable reference genes for normalization of RT-qPCR data in eggplant fruit and shoot borer (*Leucinodes orbonalis* Guenée). *Biologia* 75, 289–297. doi: 10.2478/s11756-019-00346-4

Kariyanna, B., Prabhuraj, A., Asokan, R., Ramkumar, G., Venkatesan, T., Gracy, R. G., et al. (2020a). Genomewide analysis and expression patterns of cytochrome P450 genes involved in insecticide resistance in *Leucinodes orbonalis* (*Lepidoptera*: *Crambidae*). *Biotechnol. Appl. Biochem.* 1–12. doi: 10.1002/bab.1997

Kariyanna, B., Prabhuraj, A., Bheemanna, M., Kalmat, B., Pamapanna, Y., Mohan, M., et al. (2020b). Insecticide usage pattern and evolution of resistance in brinjal shoot and fruit borer, *Leucinodes orbonalis* (*Lepidoptera*: *Crambidae*) in India. *Plant Arch.* 20(Suppl. 2), 1255–1261.

Kodandaram, M. H., Rai, A. B., Sharma, S. K., and Singh, B. (2017). Shift in the level of susceptibility and relative resistance of brinjal shoot and fruit borer *Leucinodes orbonalis* (Guen) to diamide insecticides. *Phytoparasitica* 45, 151–154. doi: 10.1007/s12600-017-0584-z

Kodandaram, M. H., Sujoy Saha, A. B. R., and Prakash, S. N. (2013). *Compendium on Pesticide use in Vegetables*. Extension Bulletin No. 50. Varanasi: Indian Institute of Vegetable Research, 133.

Latif, M. A., Rahman, M. M., and Alam, M. Z. (2010). Efficacy of nine insecticides against shoot and fruit borer, *Leucinodes orbonalis* Guenee (*Lepidoptera*: *Pyralidae*) in eggplant. *J. Pest Sci.* 83, 391–397. doi: 10.1007/s10340-010-0309-2

LeOra, S. (1987). *). Polo-Plus, POLO for Windows*. Petaluma, CA: LeOra Software.

Lumjuan, N., Rajatileka, S., Changsom, D., Wicheer, J., Leelapat, P., Prapanthadara, L. A., et al. (2011). The role of the *Aedes aegypti* Epsilon glutathione transferases in conferring resistance to DDT and pyrethroid insecticides. *Insect Biochem. Molec. Biol.* 41, 203–209. doi: 10.1016/j.ibmb.2010.12.005

Malathi, V. M., Jalali, S. K., Gowda, D. K., Mohan, M., and Venkatesan, T. (2015). Establishing the role of detoxifying enzymes in field-evolved resistance to various insecticides in the brown planthopper (*Nilaparvata lugens*) in South India. *Insect Sci.* 24, 35–46. doi: 10.1111/1744-7917.12254

Mally, R., Korycinska, A., Agassiz, D. J. L., Hall, J., Hodgetts, J., and Nuss, M. (2015). Discovery of an unknown diversity of *Leucinodes* species damaging Solanaceae fruits in sub-Saharan Africa and moving in trade (*Insecta*. *Lepidoptera*, *Pyraloidea*). *Zookeys* 472, 117–162. doi: 10.3897/zookeys.472.8781

Marygold, S. J., Leyland, P. C., Seal, R. L., Goodman, J. L., Thurmond, J., Strelets, V. B., et al. (2013). FlyBase: improvements to the bibliography. *Nucleic Acids Res.* 41, D751–D757.

Masek, T., Vopalensky, V., Suchomelovam, P., and Pospisek, M. (2005). Denaturing RNA electrophoresis in TAE agarose gels. *Anal. Biochem.* 336, 46–50. doi: 10.1016/j.ab.2004.09.010

Meisel, R. P., and Scott, J. G. (2018). Using genomic data to study insecticide resistance in the house fly. *Musca domestica*. *Pestic. Biochem. Physiol.* 151, 76–81. doi: 10.1016/j.pestbp.2018.01.001

Mohan, M., and Gujar, G. T. (2003). Local variation in susceptibility of the diamondback moth, *Plutella xylostella* (Linnaeus) to insecticides and role of detoxification enzymes. *Crop Prot.* 22, 495–504. doi: 10.1016/s0261-2194(02)00201-6

Mohan, M., Venkatesan, T., Sivakumar, G., Yandigeri, M. S., and Verghese, A. (2015). *Fighting Pesticide Resistance in Arthropods*. New Delhi: Westville Publishers.

Munje, S. S., Salunke, P. B., and Botre, B. S. (2015). Toxicity of newer insecticides against *Leucinodes orbonalis* (Guen.). *Asian J. Biol. Sci.* 10, 106–109. doi: 10.15740/has/ajbs/10.1/106-109

Oakeshott, J. G., Claudianos, C., Campbell, P. M., Newcomb, R. D., and Russell, R. J. (2005). "Biochemical genetics and genomics of insect esterases," in *Comprehensive Molecular Insect Science-Pharmacology*, Vol. 5, eds L. I. Gilbert, K. Latrou, and S. S. Gill (Oxford: Elsevier), 309–381. doi: 10.1016/b0-44-451924-6/00073-9

Oakeshott, J. G., Johnson, R. M., Berenbaum, M. R., Ranson, H., Cristino, A. S., and Claudianos, C. (2010). Metabolic enzymes associated with xenobiotic and chemosensory responses in *Nasonia vitripennis*. *Insect Biochem. Molec. Biol.* 19, 147–163. doi: 10.1111/j.1365-2583.2009.00961.x

Panini, M., Manicardi, G. C., Moores, G., and Mazzoni, E. (2016). An overview of the main pathways of metabolic resistance in insects. *Invertebrate Surviv. J.* 13, 326–335.

Pavlidi, N., Vontas, J., and Leeuwen, T. V. (2018). The role of glutathione S-transferases (GSTs) in insecticide resistance in crop pests and disease vectors. *Curr. Opi. Insect Sci.* 27, 97–102. doi: 10.1016/j.cois.2018.04.007

Perry, T., Batterham, P., and Daborn, P. J. (2011). The biology of insecticidal activity and resistance. *Insect Biochem. Molec. Biol.* 41, 411–422. doi: 10.1016/j.ibmb.2011.03.003

Prodhan, M. Z., Hasan, H. M. T., Chowdhury, M. M. I., Alam, M. S., Rahman, M. L., Azad, A. K., et al. (2018). *Bt* eggplant (*Solanum melongena* L.) in Bangladesh: fruit production and control of eggplant fruit and shoot borer (*Leucinodes orbonalis* Guenee), effects on non-target arthropods and economic returns. *PLoS One* 13:e0205713. doi: 10.1371/journal.pone.0205713

Ranson, H., Claudianos, C., Ortelli, F., Abgrall, C., Hemingway, J., Sharakhova, M. V., et al. (2002). Evolution of supergene families associated with insecticide resistance. *Science* 298, 179–181. doi: 10.1126/science.1076781

Shelton, A. M., Hossain, M. J., Paranjape, V., Azad, A. K., Rahman, M. L., Khan, A. S. M. M. R., et al. (2018). *Bt* eggplant project in bangladesh: history, present status, and future direction. *Front. Bioeng. Biotechnol.* 6:106. doi: 10.3389/fbioe.2018.00106

Shirale, D., Patil, M., and Parimi, S. (2017). Insecticide resistance in field populations of *Leucinodes orbonalis* (*Lepidoptera*: *Crambidae*) in India. *Can. Entomol.* 149, 399–407. doi: 10.4039/tce.2017.3

Srinivasan, R. (2008). Integrated pest management for eggplant fruit and shoot borer (*Leucinodes orbonalis*) in south and southeast Asia: past, present and future. *J. Biopesticides.* 1, 105–112.

van Asperen, K. (1962). A study of house fly esterase by means of a sensitive colorimetric method. *J. Insect Physiol.* 8, 401–416. doi: 10.1016/0022-1910(62)90074-4

Wang, Y., Zhao, S., Shi, L., Xu, Z., and He, L. (2014). Resistance selection and Biochemical mechanism of resistance against cyflumetofen in *Tetranychus cinnabarinus* (Boisduval). *Pestic. Biochem. Physiol.* 111, 24–30. doi: 10.1016/j.pestbp.2014.04.004

Yang, T., and Liu, N. (2011). Genome analysis of cytochrome P450s and their expression profiles in insecticide resistant mosquitoes. *Culex quinquefasciatus*. *PLoS One* 6:e29418. doi: 10.1371/journal.pone.0029418

Yu, Q., Lu, C., Li, B., Fang, S., Zuo, W., Dai, F., et al. (2008). Identification, genomic organization and expression pattern of glutathione S-transferase in the silkworm, *Bombyx mori*. *Insect Biochem. Molec. Biol.* 38, 1158–1164. doi: 10.1016/j.ibmb.2008.08.002

Yu, Q. Y., Lu, C., Li, W. L., Xiang, Z. H., and Zhang, Z. (2009). Annotation and expression of carboxylesterases in the silkworm, *Bombyx mori*. *BMC Genomics* 10:553. doi: 10.1186/1471-2164-10-553

Zhang, Y., Wang, L., Guo, H., Li, G., Zhang, Z., and Xie, L. (2012). A transcriptome-based screen of carboxylesterase-like genes that are involved in chlorpyrifos resistance in *Laodelphax striatellus* (Fallen). *Pestic. Biochem. Physiol.* 104, 224–228. doi: 10.1016/j.pestbp.2012.08.006

Conflict of Interest: The authors declare that the research was conducted in the absence of any commercial or financial relationships that could be construed as a potential conflict of interest.

frontiers in Physiology

ORIGINAL RESEARCH
published: 19 November 2020
doi: 10.3389/fphys.2020.575718

Molecular and Functional Characterization of Trehalase in the Mosquito *Anopheles stephensi*

*Sanjay Tevatiya[1], Seena Kumari[1], Punita Sharma[1], Jyoti Rani[1], Charu Chauhan[1], Tanwee Das De[1], Kailash C. Pandey[1], Veena Pande[2] and Rajnikant Dixit[1]**

[1] *Laboratory of Host-Parasite Interaction Studies, ICMR-National Institute of Malaria Research, New Delhi, India,*
[2] *Department of Biotechnology, Kumaun University, Nainital, India*

Like other insects, in blood-feeding mosquitoes, trehalase (TRE; EC 3.2.1.28), an enzyme that metabolizes trehalose, may influence a wide array of functions including flight, survival, reproduction, and vectorial capacity, but its role has not been investigated in detail. Here, we characterized a 1,839-bp-long transcript, encoding a 555-aa-long trehalase-2 homolog protein from the mosquito *Anopheles stephensi*. With a conserved insect homology, and in *silico* predicted membrane-bound protein, we tested whether trehalase (*As-TreH*) also plays a role in mosquito physiologies. Constitutive expression during aquatic development or adult mosquito tissues, and a consistent upregulation until 42 h of starvation, which was restored to basal levels after sugar supply, together indicated that *As-TreH* may have a key role in stress tolerance. A multifold enrichment in the midgut ($p < 0.001819$) and salivary glands ($p < 4.37E-05$) of the *Plasmodium vivax*-infected mosquitoes indicated that *As-TreH* may favor parasite development and survival in the mosquito host. However, surprisingly, after the blood meal, a consistent upregulation until 24 h in the fat body, and 48 h in the ovary, prompted to test its possible functional correlation in the reproductive physiology of the adult female mosquitoes. A functional knockdown by dsRNA-mediated silencing confers *As-TreH* ability to alter reproductive potential, causing a significant loss in the egg numbers ($p < 0.001$), possibly by impairing energy metabolism in the developing oocytes. Conclusively, our data provide initial evidence that *As-TreH* regulates multiple physiologies and may serve as a suitable target for designing novel strategies for vector control.

Keywords: mosquito, migdut, trehalase (E.C 3.2.1.28), energy metabolism, reproduction, Plasmodium vivax

OPEN ACCESS

Edited by:
Oleh Lushchak,
Vasyl Stefanyk Precarpathian National University, Ukraine

Reviewed by:
Leena Thorat,
York University, Canada
Gustavo Bueno Rivas,
Texas A&M University, United States

****Correspondence:***
Rajnikant Dixit
dixitrk@mrcindia.org;
dixit2k@yahoo.com

Specialty section:
This article was submitted to Invertebrate Physiology, a section of the journal Frontiers in Physiology

Received: *24 June 2020*
Accepted: *20 October 2020*
Published: *19 November 2020*

Citation:
Tevatiya S, Kumari S, Sharma P, Rani J, Chauhan C, Das De T, Pandey KC, Pande V and Dixit R (2020) Molecular and Functional Characterization of Trehalase in the Mosquito Anopheles stephensi. Front. Physiol. 11:575718. doi: 10.3389/fphys.2020.575718

INTRODUCTION

In nature, both adult male and female mosquitoes met their energy requirements from nectar sugar. However, adult female mosquitoes need a blood meal from a vertebrate host to nourish its eggs for reproductive success. Sugar metabolism in the adult mosquito influences the wide array of behavior including flight, survival, reproduction, and vectorial capacity. Like other insects, also in mosquitoes principal circulating sugar includes the non-reducing disaccharide trehalose (also known as hemolymph sugar), which is synthesized by the absorbed glucose in the fat body. However, trehalose exists in a wide variety of organisms, including nematodes, crustacean's algae, plants, fungi, bacteria, and yeast, but lack in vertebrates. Trehalose performs multiple roles

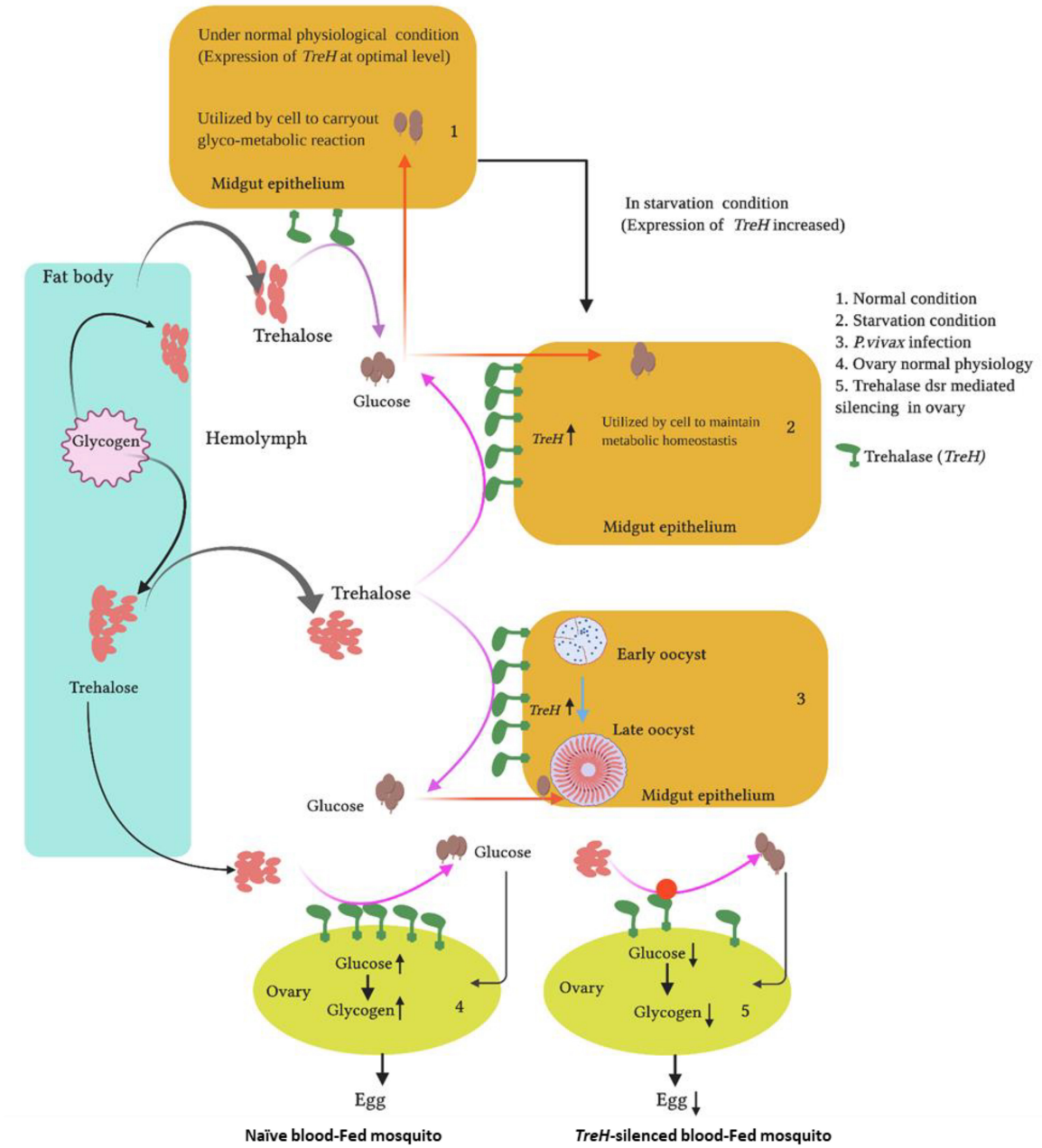

GRAPHICAL ABSTRACT | Proposed functions of trehalase in mosquito tissues in response to altered pathophysiological conditions: Starvation, *Plasmodium vivax* infection, and reproduction.

in these organisms, such as a structural component of cell walls in bacteria, fungi, and plants (Shimakata and Minatogawa, 2000; Müller et al., 2001; Wingler, 2002; Tang et al., 2018). In insects, it serves as a key source of energy to deal with abiotic stress and metabolic physiologies (McDougall and Steele, 1988; Shi Z. K. et al., 2017).

Structurally, trehalose is a disaccharide molecule consisting of two glucose units generated with the help of two enzymes, trehalose-6-phosphate synthase (TPS; EC 2.4.1.15) and trehalose-6-phosphate phosphatase (TPP; EC 3.1.3.12), in the fat body of the mosquitoes/insects. TPS catalyzes the formation of trehalose-6-phosphate (T-6-P) by transferring glucose from UDP-glucose to glucose-6-phosphate (Shukla et al., 2015). TPP then undergoes de-phosphorylation catalyzed by TPP, which removes the phosphate group from T-6-P to form trehalose, which is then released in the hemolymph for utilization (Shukla et al., 2016; Vanaporn et al., 2017).

Trehalase has been identified and characterized from bacteria to insects and shown to play an important role in desiccation and dehydration stress, thermal stress tolerance, asexual development, and virulence of insect mycopathogens (Shukla et al., 2016; Vanaporn et al., 2017; Hagan et al., 2018; Qiu et al., 2020). Trehalase has also been described as a potential virulence-associated gene in bacteria, as it is present in pathogenic bacteria but is missing in nonpathogenic bacteria (Shukla et al., 2016).

Insects encode two variants of the trehalase enzyme-soluble form (TRE-1) and membrane-bound form (TRE-2). Tre-1 is located inside the cell and hydrolyzes intracellular trehalose, whereas Tre-2 is a transmembrane enzyme facing the outside of the enzyme and hydrolyzing the extracellular trehalose (Chen et al., 2010; Zhao et al., 2016). In insects, the activity of trehalase varies widely over various stages of development and is highly affected by nutritional and environmental conditions such as modulation in activity of trehalase which plays a vital role in physiological adaptation to the cooling process in *Harmonia axyridis* (Shi Z. et al., 2016; Shi et al., 2019). Recently, Shukla et al. (2018) identify a new variant of trehalase from the insect oriental aquatic midge *Chironomus ramosus*.

The role of trehalase in energy metabolism under multiple physiologies has been investigated in various insects (Thompson, 2003; Mariano et al., 2009). Although identifiable in the genome, the direct function of trehalase has not been established in any mosquito species, until recent demonstration that RNA interference of trehalase causes reduced phenotypes associated with hydration level such as blood-feeding in *Culex pipiens* (Hagan et al., 2018). Earlier, knockdown of the trehalose transporter gene, *AgTreT1*, has been shown to affect stress adaptation and malaria pathogen development in the mosquito *An. gambiae* (Liu et al., 2013), while studies on RNA interference of the juvenile hormone III (JH) receptor methoprene-tolerant (Met) and 20E receptor, i.e., ecdysone receptor (EcR) suggested a regulatory switching role in the coordination of carbohydrate metabolism and female mosquito reproductive cycle maintenance, in the mosquito *Aedes aegypti* (Hou et al., 2015). Since trehalase is the only glucosidase that irreversibly hydrolyzes trehalose into glucose units to utilize it in cellular energy metabolism and that makes the trehalase enzyme an attractive molecular target, here we evaluated the transcriptional regulation of membrane-bound trehalase under distinct pathophysiological conditions in *Anopheles stephensi*, an important human malarial vector, in urban India. Using functional genomic approaches, we established a functional correlation of trehalase in reproduction, affecting egg-laying capacity (fertility) and survival of mosquitoes.

MATERIALS AND METHODS

Mosquito Rearing and Maintenance

The Indian strain of mosquito *An. stephensi* was reared and maintained in the insectary at a temperature of 28 ± 2°C, with a relative humidity of ∼80% with a 12-h light–dark cycle, as mentioned previously (Sharma et al., 2015; Thomas et al., 2016). Adult mosquitoes were fed daily on sterile sugar solution (10%) using a cotton swab throughout the experiment. All protocols for rearing and mosquito infection to *Plasmodium vivax* were approved by the Institute Ethics Committee (ECR/NIMR/EC/2012/41).

Sample Collection, RNA Extraction, and Infectivity Assay

Experimentally required tissues were dissected and pooled from the cold anesthetized adult female mosquitoes under different physiological conditions. To examine the tissue-specific expression of target genes, selected tissues such as hemocyte, spermatheca, and salivary gland and male reproductive tissues were dissected from 3- to 4-day-old naïve sugar-fed mosquitoes. Further, to check the effect of starvation on the mosquito survival and trehalase expression, we collected the midgut sample at different time points (24, 48, and 72 h) post starvation. To examine the molecular response under nutritional and reproductive physiological conditions, we collected ∼25 post blood-fed mosquito ovaries (4, 24, 48, and 72 h) and fat body (8, 16, 24, and 48 h). Midguts were dissected from 25 mosquitoes fed on rabbit blood and collected at different time points (3, 24, 48, 72 h, 10, and 14 days). For the collection of midgut infected with *P. vivax* sporozoites, 3–4-days-old *An. stephensi* mosquitoes were fed on the blood of *P. vivax*-infected patients (∼2% gametocytaemia) through a pre-optimized artificial membrane feeding assay as described earlier (Sharma, 2020). The confirmation of the *P. vivax* infection was done by staining the midgut with 5% mercurochrome to visualize the oocysts after 4 days of infection (DPI), as described earlier (Sharma, 2020). After confirmation, ∼20–25 mosquito tissues, i.e., midgut and salivary glands, were dissected at selected time points. Total RNA from the salivary gland, midgut, and other tissues was isolated using the standard Trizol method as described previously.

cDNA Preparation and Gene Expression Analysis

Approximately 1 μg total RNA was utilized for the synthesis of first-strand cDNA synthesis using a mixture of oligo-dT and random hexamer primers and Superscript II reverse transcriptase as per the described protocol (Verso cDNA synthesis Kit, Cat#AB-1453/A, EU, Lithuania; Sharma et al., 2015; Thomas et al., 2016). For differential gene expression analysis, routine RT-PCR and agarose gel electrophoresis protocols were used. Approximately 25 ng of cDNA was used in 10-μL real-time PCR reactions. The relative abundance of the gene of interest was assessed using the SYBR Green qPCR master mix (Thermo Fisher Scientific), using the Bio-Rad CFX96 PCR machine. PCR cycle parameters involved an initial denaturation at 95°C for 15 min, 40 cycles of 10 s at 95°C, 15 s at 52°C, and 22 s at 72°C. After the final extension step, the melting curve was derived and examined for quality control. Each experiment was performed in three independent biological replicates. The relative quantification results were normalized with an internal control (actin) and analyzed by the $2^{-\Delta\Delta Ct}$ method and statistical

analysis was performed using Origin 8.1 software. Differences between test samples and their respective controls were evaluated by the Student's "*t*"-test.

dsRNA-Mediated Gene Silencing Assays

For the knockdown of *As-TreH*, dsRNA primers carrying T7 overhang were synthesized as listed in **Supplementary Table 2**. The amplified PCR products were examined by agarose gel electrophoresis, purified (Thermo Fisher Scientific Gene JET PCR Purification Kit #K0701), quantified, and subjected to double-stranded RNA synthesis using Transcript Aid T7 high-yield transcription kit (Cat# K044, Ambion, United States), while the *dsrLacZ* gene of bacterial origin was used as a control. Approximately, ∼69 nl (3 μg/μL) of purified *dsRNA* product was injected into the thorax of a cold anesthetized 1–2-day-old female mosquito using a nano-injector (Drummond Scientific, CA, United States) as described earlier (Kumari et al., 2020). The silencing of the respective gene was confirmed by quantitative RT-PCR after 3–4 days of dsRNA injection.

Starvation and Survival Assay

In the starvation assay, 2–3-day-old (∼230 adult female) mosquitoes were securely emerged in a cotton cage and kept in the insectary at the temperature of 28 ± 2°C and relative humidity of ∼80% with a 12 h light–dark cycle. The control mosquito group was kept on sugar meal (sugar+water), while the starved mosquito group was deprived of both sugar and water until the end of the experiment. All the test assays were performed in a non-crowded condition, and the number of living mosquitoes was tracked until all had died. In the survival time assay, the live mosquitoes were moved into new cages every alternate day, and the numbers of dead mosquitoes were counted daily basis. Gehan-Breslow-Wilcoxon test was used for statistical analysis of data using Prism 8.0 software (GraphPad Software Inc, CA).

In silico Bioinformatic Analysis

Phylogenetic trees were prepared with selected trehalase protein sequences by the maximum likelihood (ML) method in MEGA X program as described previously (Kumar et al., 2018). We aligned all selected insects and other putative trehalase protein sequences using the ClustalW algorithm, where the reliability of the branching was tested by 1,000 bootstrap value of the replicates. The processed phylogenetic tree was examined based on clusters and nodes formed.

RESULTS

Identification, Annotation, and Phylogenomics Analysis of *As-TreH*

Our recent RNA-Seq study demonstrates that early (3–6-days) *P. vivax* infection significantly alters the metabolic machinery of the mosquitoes midgut (Tevatiya et al., 2019). Identification of a unique transcript, encoding the trehalase homolog protein, from the *P. vivax*-infected gut-RNAseq library, prompted further investigation of its possible role in mosquito physiology. The initial BLASTX analysis of the selected 1,839 bp long *TreH* transcript showed 91.61% identity with the *TreH* homolog of *Anopheles gambiae* (AGAP012053-PA), having a conserved trehalase domain (**Figure 1A**). The *AsTreH* transcript showed 53.2% identity with the *TreH* homolog of *Tribolium castaneum* (Coleoptera) and 52% identity with *Apis florea* (Hymenoptera) showed a less conserved region. Additionally, six copies of the trehalase gene in *Tribolium castaneum* (Coleoptera) and three copies of the trehalase gene in *Apis florea* (Hymenoptera) compared to only two copies in the Diptera reflect functional diversification of the trehalase enzyme during the course of evolution. For example, the existence of several copies of the trehalase gene in Coleoptera may be described as an adaptation to a trehalose-rich diet of insectivorous, detritivorous, and mycophagous species, as trehalose sugar is present in high concentrations in fungi (Nardelli et al., 2019).

A homology search against *An. stephensi* database further verified that the identified *As-TreH* is a 1,839 bp full-length (ASTEI06114-RA), a single-copy gene, which encodes a protein of 555 amino acids. Multiple-sequence alignment with other trehalase members, originating from Hymenoptera and Diptera orders, showed the highest identity and conservation with Anopheles mosquitoes (**Figures 1B,C**). Phylogenetic analysis showed the formation of two independent clades, where each clade defines a separate lineage for trehalase, which is further divided into specific subclades.

Developmental and Tissue-Specific Transcriptional Response of *As-TreH*

To monitor the developmental regulation of trehalase, we performed real-time PCR-based transcriptional profiling. Though *As-TreH* showed constitutive expression throughout the aquatic developmental stages (**Figure 2A**), we observed a higher abundance during egg (active embryogenesis) and pupae stages ($p < 0.01716$) than other larval stages. We also observed that the relative expression of trehalase was higher ($p < 0.01476$) in adult males than in female mosquitoes (**Figure 2A**). Tissue-specific transcriptional profiling also showed a dominant expression of trehalase in the midgut ($p < 0.000291$), spermatheca ($p < 0.033$) of the adult female, and testis of adult male mosquitoes (**Figure 2B**). Together, we hypothesize that *As-TreH* may function in the maintenance of gut-nutritional homeostasis and reproductive physiology.

As-TreH Influences Nutritional Homeostasis and Reproductive Physiology

To test the above hypothesis, first, we evaluated the molecular correlation between sugar/water deprivation and mosquito survival. A 42-h-long deprivation of sugar and water not only caused significant mortality ($p < 0.000239$) but also elevated the expression of trehalase in surviving mosquitoes (**Supplementary Table 1**). However, rapid downregulation in response to re-supply of sugar indicated that *As-TreH* may have a role in the maintenance of nutritional physiology (**Figure 3A**). Next, to test the possible role in reproductive physiology, we examined the spatial and temporal expression of

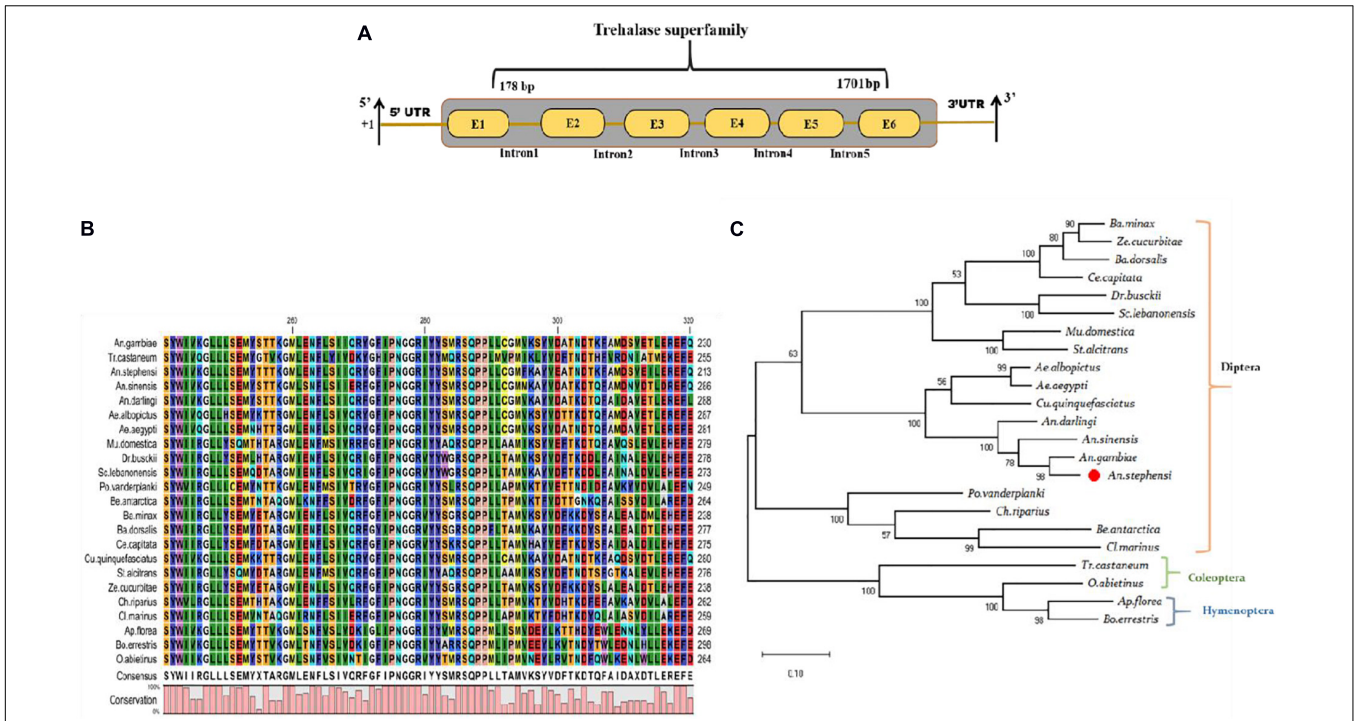

FIGURE 1 | Genomic organization and molecular characterization of *An. stephensi As-TreH*: **(A)** Schematic representation of the genomic architecture of trehalase: Six brown color boxes (E1–E6) represent exons, and +1 indicates translation initiation site. A 50-bp UTR region is present on both the 5' and 3' ends of the transcript and one conserved trehalase superfamily domain present (1178–1701 bp). **(B)** Multiple-sequence alignment of mosquitoes and other insect-encoded trehalase homolog protein showing strong conservation among Anopheline mosquitoes. **(C)** Phylogenetic relationship of *As-TreH* proteins within the insect's community. The red circle represents *Anopheles stephensi* in Diptera and the relationship of identified putative *As-TreH* with other Coleoptera, Hymenoptera showing a distance relationship with dipteran trehalase.

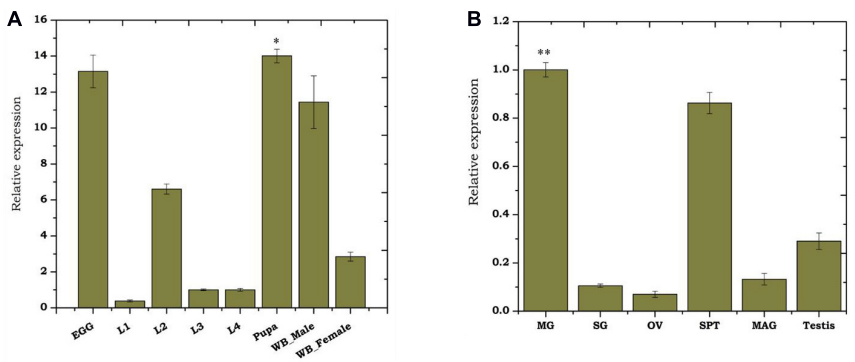

FIGURE 2 | Transcriptional profiling of *As-TreH*: **(A)** Relative gene expression of *As-TreH* during developmental stages of *An. stephensi* mosquito i.e., L1 (instar larval stage 1), L2 (instar larval stage 2), L3 (instar larval stage 3), L4 (instar larval stage 4), pupa ($p < 0.01716$), and whole body in male ($p < 0.01476$) and female ($p < 0.004148$); the L3 stage was considered as controls for each test sample. **(B)** Tissue-specific expression kinetics of *As-TreH* in male and female mosquitoes. SG: salivary glands; MG: midgut ($p < 0.000292$); OV: ovary; SP: Spermatheca ($p < 0.033$); MAG: male accessory gland; testis. SG was considered as control for each test sample. Three independent biological replicates were considered for statistical analysis, viz. *$p < 0.05$; **$p < 0.005$; and ***$p < 0.0005$, using the Student's *t*-test.

As-TreH in the midgut, fat body, and ovary of the blood-fed adult female mosquitoes. *As-TreH* showed a gradual enrichment until 24 h in the fat body ($p < 6.03E-06$) and 48 h in the ovary ($p < 0.032802$) (**Figures 3B,C**), indicating a unique role in egg development in the mosquito. Finally, to establish a functional correlation, we performed dsRNA-mediated gene silencing in virgin 3–4-day-old male as well as female mosquitoes. However, after silencing we did not observe any significant behavioral changes either in virgin or in mated mosquitoes (data not shown); surprisingly, we noticed a 50% reduction ($p < 0.03288$) in the egg-laying of the *As-TreH* silenced blood-fed female mosquitoes (**Figures 3D,E**), indicating that

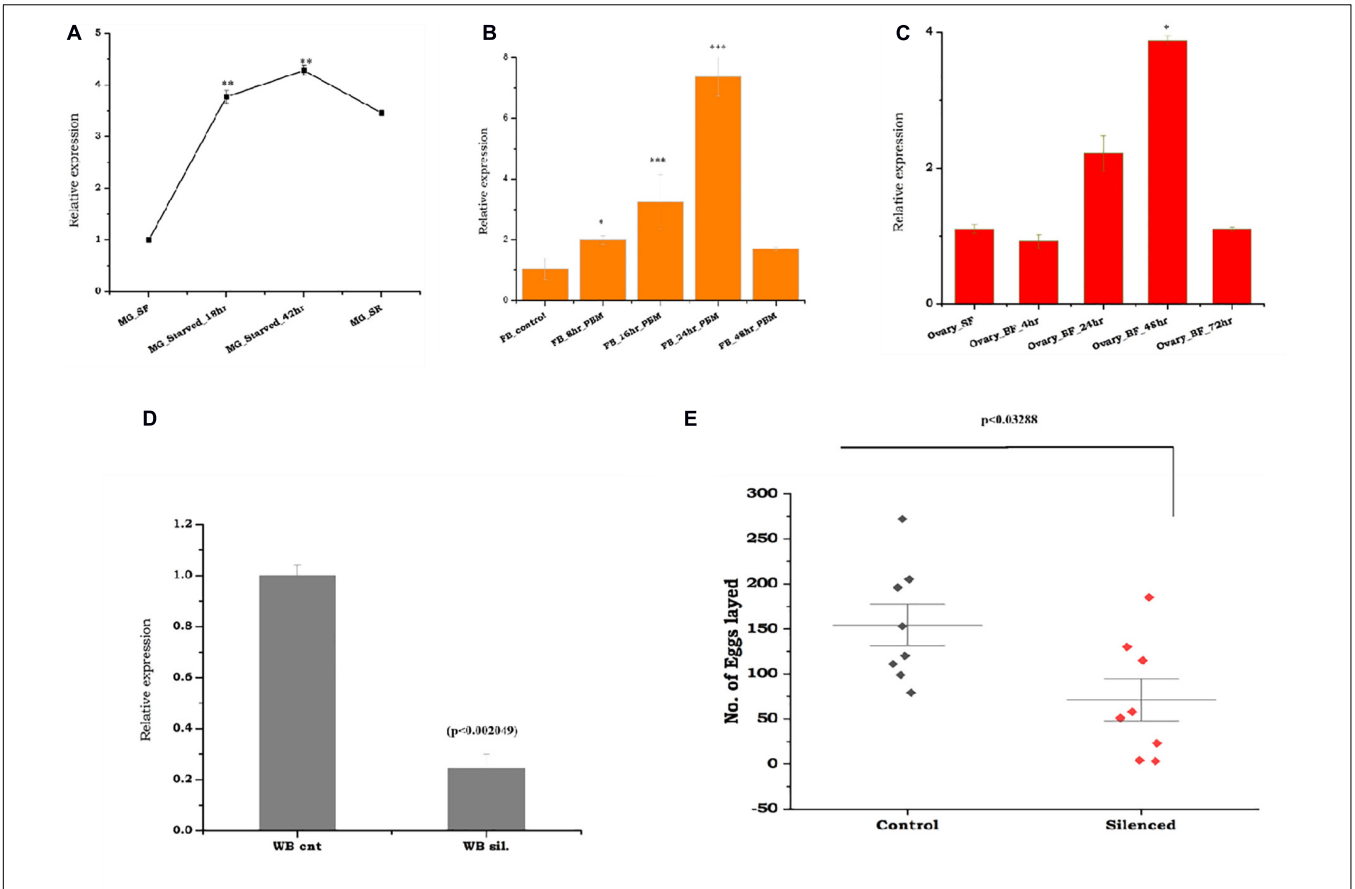

FIGURE 3 | Comparative transcriptional profiling of the *As-TreH* genes in response to starvation, blood-feeding, and trehalase silencing effects on female fertility: **(A)** Temporal expression of mosquito trehalase in the starved mosquito midgut tissues (MG_starved 18 h ($p < 0.000607$), 42 h ($p < 0.000239$), and starved recovered mosquitoes (MG_SR/($p < 0.014342$). **(B)** Relative expression profiling of *As-TreH* in a blood meal time-series experiment; the fat body (FB) was collected from naive sugar-fed adult female mosquitoes, and blood meal time-series expression is represented as 8 h ($p < 2.06E-06$), 16 h ($p < 0.000388$), 24 h ($p < 6.03E-06$), and 48 h. **(C)** Relative expression profiling of *As-TreH* in a blood meal time-series experiment; ovaries were collected from naive sugar-fed and blood-fed adult female mosquito, and the expression is represented as 4 h ($p < 0.4253$), 24 h ($p < 0.07693$), 48 h ($p < 0.082802$), and 72 h ($p < 0.498118$). **(D)** *As-TreH* silencing exhibited a >70% reduction in mRNA reduction as compared to control levels ($p < 0.002049$) tested in the whole body. Three independent biological replicates were considered for statistical analysis, viz. $p < 0.05$, $p < 0.005$, and $p < 0.0005$ using the Student's *t*-test. **(E)** After mating with age-matched healthy male mosquitoes, *As-TreH*-silenced female mosquito lays reduced number of the eggs ($p < 0.03288$) than the control mosquito group. A minimum of three biological replicates was performed, and the females were allowed to lay eggs between the 3rd and 4th days (median with range; $n = 3–5$, 15–25 females/trial) and ($p < 0.03288$, Mann–Whitney *U*-test).

trehalase plays a key role in the regulation of mosquito reproductive physiology.

P. vivax Infection Alters *As-TreH* Expression in the Midgut and Salivary Gland

Previous studies have shown that the depletion of hemolymph trehalose sugar in *Plasmodium*-infected mosquitoes is likely due to rapid consumption by the fast-developing parasite, to meet their energy requirements (Mack and Vanderberg, 1978; Mack et al., 1979). Being a disaccharide, trehalose could not be utilized directly by the parasite, and also we retrieved a hexose transporter transcript of *Plasmodium* from RNAseq results; we opined that trehalase may have a role to convert trehalose to a sugar molecule. To test this, we tracked the trehalase expression during the development of oocyst in the gut, and sporozoite invaded salivary glands of *P. vivax*-infected female mosquitoes. A multifold enriched expression during early to late-stage oocysts in the gut as well as salivary glands (**Figures 4A,B**) suggests that trehalase may significantly contribute to hydrolyzes of the trehalose to provide glucose for the rapid proliferation of parasites and generation of new biomass.

DISCUSSION

Here, we demonstrated that insect homolog trehalase may play a significant role in maintaining the nutritional homeostasis and reproductive physiology of the mosquito tissues. We characterized an 1,839-bp-long unique transcript, encoding 555-aa-long trehalase-2, originally identified from the

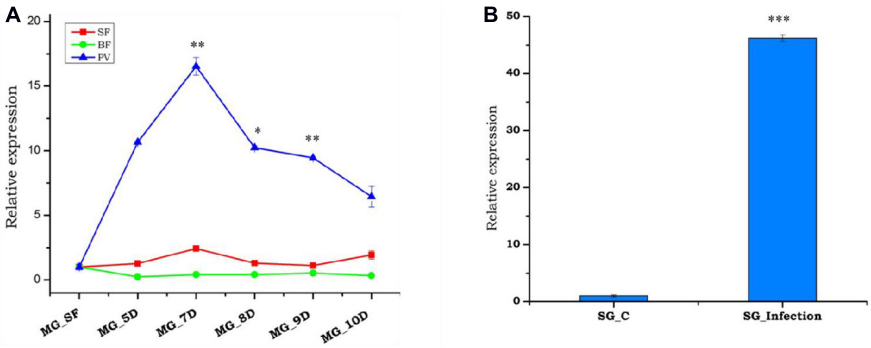

FIGURE 4 | Relative expression profiling of trehalase under different conditions, i.e., sugar-fed, blood meal, and *Plasmodium vivax* infection in mosquito tissues. **(A)** Relative expression profiling of trehalase in a blood meal time-series experiment; midgut (MG) was collected from naive sugar-fed, blood-fed, and *P. vivax*-infected adult female mosquitoes, and significant modulation of expression in response to *P. vivax* is represented as time points 5D ($p < 0.001148$), 7D ($p < 0.001819$), 8D (0.00056), 9D ($p < 0.002828$), and 10D ($p < 0.000289$). D repentants number of days after blood-meal or *P. vivax* infection. **(B)** Transcriptional profiling of trehalase in response to post *P. vivax* infected (time point 12–14 D) SG glands ($p < 4.37E-05$) and age-matched normal blood-fed SG as a control. Three independent biological replicates were considered for statistical analysis, viz. $*p < 0.05$, $**p < 0.005$, and $***p < 0.0005$ using the Student's *t*-test.

P. vivax-infected gut and salivary gland RNAseq database of mosquito *An. stephensi* (Tevatiya et al., 2019). We noticed that putative *TreH* is a membrane-bound protein, with conservation among insects and mosquito species, and may have a similar function in nutritional physiology (Shukla et al., 2015). Previous studies suggest that except vertebrate trehalase, which is required for metabolization of ingested trehalose, in other animals including insects, trehalase is involved in the recovery from diverse stress conditions, and regulation of energy metabolism and nutritional physiological homeostasis (Shukla et al., 2016; Shi J.F. et al., 2017; Vanaporn et al., 2017; Karpova et al., 2019).

Our observation of an enriched expression of *As-TerH* in developing eggs and pupae correlates its active role in the trehalose metabolization, to fulfill the nutritional sugar supply demand for highly metamorphic development stages (Gu et al., 2009; Shi J.F. et al., 2016). Consistent with previous studies, an abundant expression in the age-matched adult male than in female mosquitoes indicated a hyper-metabolic energy status of males, which may likely meet sexual behavioral activities (Hou et al., 2015). However, we also observed that sugar and water deprivation for a longer duration (∼42 h) reduces the survival rate of the mosquitoes, but a parallel upregulation of trehalase transcript after starvation, and restoration upon sugar re-supplementation, in the gut of surviving mosquitoes further corroborate previous studies that trehalose metabolization is crucial to stress tolerance and nutritional homeostasis maintenance (Liu et al., 2013). In their recent study, Hou et al. (2015) showed a dynamic expression regulation of trehalose metabolizing enzymes TPS, TPP, and trehalase transcripts, i.e., post eclosion, a sharp downregulation, and increased expression in the mosquito *Ae. Aegypti* within 36 h after blood-feeding (Hou et al., 2015). A direct functional role for any of these enzymes is yet to unravel; however, RNA interference studies have demonstrated that JH and 20E are key to regulating the coordination of carbohydrate metabolism during the mosquito reproduction cycle (Hou et al., 2015). 20E, JH, and insulin-like peptide (ILP) signaling pathways also seem to regulate the transcription of trehalase genes in the *Colorado potato* beetle (Shi Z. K. et al., 2017). We observed that blood-feeding boosts the gradual upregulation of trehalase until 24 h in the fat body and 48 h in the ovary; we tested whether trehalase influences the reproductive physiology. Functional knockdown experiments showed a 50% reduction of eggs laid by the trehalase gene silenced mosquitoes, than the control mosquito group. As oocytes synthesize and accumulate glycogen, trehalose from the hemolymph could be the main source for this synthesis; our data strengthen the hypothesis that a membrane-bound trehalase may play a crucial role in meeting the high nutritional requirement for oocytes development (Santos et al., 2008; Kuang et al., 2018).

Emerging studies have also demonstrated that *Plasmodium* infection imbalances glucose/trehalose metabolism, where gut microbiota likely plays a key role in the regulation of malaria parasite development in the mosquitoes (Wang et al., 2020). After traversing the midgut, a single ookinete with no reserved food (glycogen or lipid) transforms into an oocyst that produces thousands of haploid sporozoites. The parasite must scavenge nutrients from the host. Owing to the membrane-bound nature, we tested how fast-developing *P. vivax* oocysts or sporozoites influence trehalase expression in the gut or salivary glands of mosquitoes. We noticed that *P. vivax* infection may severely affect the energy metabolism of its vector, by modulating the trehalase expression in both tissues. Since the molecular nature of salivary sporozoites is different from circulatory sporozoites in the hemolymph (Tevatiya et al., 2019) and only attains its maturity or virulence through high energy requirements from its host, the tissue-specific altered expression of trehalase may likely favor *Plasmodium* development, survival, or transmission.

CONCLUSION

In summary, we provide evidence that insect homolog membrane-bound trehalase plays a crucial role in the maintenance of nutritional homeostasis and reproductive

physiology of the mosquito *An. stephensi*. An altered expression in response to *P. vivax* infection further supports the hypothesis that sugar metabolism-related enzymes, such as trehalase, may serve as a unique target for the design of vector control strategy.

DATA AVAILABILITY STATEMENT

All datasets generated for this study are included in the article/**Supplementary Material**.

ETHICS STATEMENT

The studies involving human participants were reviewed and approved by the ECR/NIMR/EC/2012/41. The patients/participants provided their written informed consent to participate in this study.

AUTHOR CONTRIBUTIONS

ST and RD conceived the scientific hypothesis and designed the experiments. SK, CC, JR, TD, and PS were responsible for the technical support for tissue dissection, collection, and gene profiling, data review, and presentation. RD and KP contributed to the reagents, materials, and analysis tools, and edited the manuscript. All authors read and approved the final manuscript.

FUNDING

Work in the laboratory was supported by the Department of Biotechnology (DBT), Government of India (BT/HRD/35/02/01/2009), Indian Council of Medical Research (ICMR), Government of India. ST was the recipient of the UGC Research Fellowship [22/12/2013(II)EU-V].

ACKNOWLEDGMENTS

We would like to thank all the technical staff members of the central insectary for mosquito rearing and Kunwarjeet Singh for lab assistance. We are grateful to the patients of the malaria clinic, who contributed to the study. Finally, we thank Xcelris Genomics, Ahmedabad, for NGS sequencing.

SUPPLEMENTARY MATERIAL

The Supplementary Material for this article can be found online at: https://www.frontiersin.org/articles/10.3389/fphys.2020.575718/full#supplementary-material

REFERENCES

Chen, J., Tang, B., Chen, H., Yao, Q., Huang, X., Chen, J., et al. (2010). Different functions of the insect soluble and membrane-bound trehalase genes in chitin biosynthesis revealed by rna interference. *PLoS One* 5:e10133. doi: 10.1371/journal.pone.0010133

Gu, J., Shao, Y., Zhang, C., Liu, Z., and Zhang, Y. (2009). Characterization of putative soluble and membrane-bound trehalases in a hemipteran insect, Nilaparvata lugens. *J. Insect. Physiol.* 55, 997–1002. doi: 10.1016/j.jinsphys.2009.07.003

Hagan, R. W., Didion, E. M., Rosselot, A. E., Holmes, C. J., Siler, S. C., Rosendale, A. J., et al. (2018). Dehydration prompts increased activity and blood feeding by mosquitoes. *Sci. Rep.* 8:6804. doi: 10.1038/s41598-018-24893-z

Hou, Y., Wang, X. L., Saha, T. T., Roy, S., Zhao, B., Raikhel, A. S., et al. (2015). Temporal coordination of carbohydrate metabolism during mosquito reproduction. *PLoS Genet.* 11:e1005309. doi: 10.1371/journal.pgen.1005309

Karpova, E. K., Eremina, M. A., Pirozhkova, D. S., and Gruntenko, N. E. (2019). Stress-related hormones affect carbohydrate metabolism in *Drosophila* females. *Arch. Insect. Biochem. Physiol.* 101:e21540. doi: 10.1002/arch.21540

Kuang, H., Yang, F., Zhang, Y., Wang, T., and Chen, G. (2018). The impact of egg nutrient composition and its consumption on cholesterol homeostasis. *Cholesterol* 2018:22. doi: 10.1155/2018/6303810

Kumar, S., Stecher, G., Li, M., Knyaz, C., and Tamura, K. (2018). MEGA X: molecular evolutionary genetics analysis across computing platforms. *Mol. Biol. Evol.* 35, 1547–1549. doi: 10.1093/molbev/msy096

Kumari, S., De Das, T., Chauhan, C., Rani, J., and Tevatiya, S. (2020). Salivary AsHPX12 influence pre-blood meal associated behavioral properties in the mosquito *Anopheles stephensi*. *bioRxiv* doi: 10.1101/2020.06.12.147959

Liu, K., Dong, Y., Huang, Y., Rasgon, J. L., and Agre, P. (2013). Impact of trehalose transporter knockdown on *Anopheles gambiae* stress adaptation and susceptibility to Plasmodium falciparum infection. *Proc. Natl. Acad. Sci. U.S.A.* 110, 17504–17509. doi: 10.1073/pnas.1316709110

Mack, S. R., Foley, D. A., and Vanderberg, J. P. (1979). Hemolymph volume of noninfected and Plasmodium berghei-infected *Anopheles stephensi*. *J. Invertebr. Pathol.* 34, 105–109. doi: 10.1016/0022-2011(79)90088-0

Mack, S. R., and Vanderberg, J. P. (1978). Hemolymph of *Anopheles stephensi* from noninfected and plasmodium berghei-infected mosquitoes. 1. Collection procedure and physical characteristics. *J. Parasitol.* 64, 918–923. doi: 10.2307/3279531

Mariano, A. C., Santos, R., Gonzalez, M. S., Feder, D., Machado, E. A., Pascarelli, B., et al. (2009). Synthesis and mobilization of glycogen and trehalose in adult male *Rhodnius prolixus*. *Arch. Insect. Biochem. Physiol.* 72, 1–15. doi: 10.1002/arch.20319

McDougall, G. E., and Steele, J. E. (1988). Free fatty acids as a source of energy for trehalose synthesis in the fat body of the American cockroach (Periplaneta americana). *Insect. Biochem.* 18, 591–597. doi: 10.1016/0020-1790(88)90011-X

Müller, J., Aeschbacher, R. A., Wingler, A., Boller, T., and Wiemken, A. (2001). Trehalose and trehalase in *Arabidopsis*. *Plant Physiol.* 125, 1086–1093. doi: 10.1104/pp.125.2.1086

Nardelli, A., Vecchi, M., Mandrioli, M., and Manicardi, G. C. (2019). The evolutionary history and functional divergence of trehalase (treh) genes in insects. *Front. Physiol.* 10:62. doi: 10.3389/fphys.2019.00062

Qiu, L., Wei, X. Y., Wang, S. J., and Wang, J. J. (2020). Characterization of trehalose-6-phosphate phosphatase in trehalose biosynthesis, asexual development, stress resistance and virulence of an insect mycopathogen. *Pestic. Biochem. Physiol.* 163, 185–192. doi: 10.1016/j.pestbp.2019.11.016

Santos, R., Mariano, A. C., Rosas-Oliveira, R., Pascarelli, B., Machado, E. A., Meyer-Fernandes, J. R., et al. (2008). Carbohydrate accumulation and utilization by oocytes of *Rhodnius prolixus*. *Arch. Insect. Biochem. Physiol.* 67, 55–62. doi: 10.1002/arch.20217

Sharma, P. (2020). Altered gut microbiota and immunity defines *Plasmodium vivax* survival in *Anopheles stephensi*. *Front. Immunol.* 11:609. doi: 10.3389/fimmu.2020.00609

Sharma, P., Sharma, S., Mishra, A. K., Thomas, T., De, Das, T., et al. (2015). Unraveling dual feeding associated molecular complexity of salivary glands in the mosquito *Anopheles culicifacies*. *Biol. Open* 4, 1002–1015. doi: 10.1242/bio.012294

Shi, J. F., Sun, Q. K., Mu, L. L., Guo, W. C., and Li, G. Q. (2017). Transcription response of three putative trehalase genes to hormonal stimulation in the Colorado potato beetle, Leptinotarsa decemlineata (Coleoptera: Chrysomelidae). *Appl. Entomol. Zool.* 52, 37–49. doi: 10.1007/s13355-016-0451-2

Shi, Z. K., Wang, S., Wang, S. G., Zhang, L., Xu, Y. X., Guo, X. J., et al. (2017). Effects of starvation on the carbohydrate metabolism in *Harmonia axyridis* (Pallas). *Biol. Open* 6, 1096–1103. doi: 10.1242/bio.025189

Shi, J. F., Xu, Q. Y., Sun, Q. K., Meng, Q. W., Mu, L. L., Guo, W. C., et al. (2016). Physiological roles of trehalose in Leptinotarsa larvae revealed by RNA interference of trehalose-6-phosphate synthase and trehalase genes. *Insect. Biochem. Mol. Biol.* 77, 52–68. doi: 10.1016/j.ibmb.2016.07.012

Shi, Z., Liu, X., Xu, Q., Qin, Z., Wang, S., Zhang, F., et al. (2016). Two novel soluble trehalase genes cloned from *Harmonia axyridis* and regulation of the enzyme in a rapid changing temperature. *Comp. Biochem. Physiol. Part B Biochem. Mol. Biol.* 198, 10–18. doi: 10.1016/j.cbpb.2016.03.002

Shi, Z. K., Wang, S. G., Zhang, T., Cao, Y., Li, Y., and Li, C. (2019). Three novel trehalase genes from *Harmonia axyridis* (Coleoptera: Coccinellidae): cloning and regulation in response to rapid cold and re-warming. *3 Biotech* 9:321. doi: 10.1007/s13205-019-1839-9

Shimakata, T., and Minatogawa, Y. (2000). Essential role of trehalose in the synthesis and subsequent metabolism of corynomycolic acid in *Corynebacterium matruchotii*. *Arch. Biochem. Biophys.* 380, 331–338. doi: 10.1006/abbi.2000.1924

Shukla, E., Thorat, L., Bendre, A. D., Jadhav, S., Pal, J. K., Nath, B. B., et al. (2018). Cloning and characterization of trehalase: a conserved glycosidase from oriental midge, *Chironomus ramosus*. *3 Biotech* 8:352. doi: 10.1007/s13205-018-1376-y

Shukla, E., Thorat, L., Bhavnani, V., Bendre, A. D., Pal, J. K., Nath, B. B., et al. (2016). Molecular cloning and in silico studies of physiologically significant trehalase from *Drosophila melanogaster*. *Int. J. Biol. Macromol.* 92, 282–292. doi: 10.1016/j.ijbiomac.2016.06.097

Shukla, E., Thorat, L. J., Nath, B. B., and Gaikwad, S. M. (2015). Insect trehalase: physiological significance and potential applications. *Glycobiology* 25, 357–367. doi: 10.1093/glycob/cwu125

Tang, B., Zhang, L., Xiong, X., Wang, H., and Wang, S. (2018). Advances in trehalose metabolism and its regulation of insect chitin synthesis. *Sci. Agric. Sin.* 51, 697–707. doi: 10.3864/j.issn.0578-1752.2018.04.009

Tevatiya, S., Kumari, S., Chauhan, C., Singla, D., De Das, T., Sharma, P., et al. (2019). Genetic changes of *P. vivax* tempers host tissue-specific responses in *Anopheles stephensi*. *bioRxiv* doi: 10.1101/774166

Thomas, T., De Td, Sharma, P., Lata, S., Saraswat, P., Pandey, K. C., et al. (2016). Hemocytome: deep sequencing analysis of mosquito blood cells in Indian malarial vector *Anopheles stephensi*. *Gene* 585, 177–190. doi: 10.1016/j.gene.2016.02.031

Thompson, S. N. (2003). Trehalose - the insect "Blood" sugar. *Adv. Insect. Phys.* 31, 205–285. doi: 10.1016/S0065-2806(03)31004-5

Vanaporn, M., Sarkar-Tyson, M., Kovacs-Simon, A., Ireland, P. M., Pumirat, P., Korbsrisate, S., et al. (2017). Trehalase plays a role in macrophage colonization and virulence of *Burkholderia pseudomallei* in insect and mammalian hosts. *Virulence* 8, 30–40. doi: 10.1080/21505594.2016.1199316

Wang, M., An, Y., Dong, S., Feng, Y., Gao, L., Wang, P., et al. (2020). Glucose-mediated expansion of a gut commensal bacterium promotes Plasmodium infection through alkalizing mosquito midgut. *bioRxiv* [preprint] doi: 10.1101/2020.02.27.967315

Wingler, A. (2002). The function of trehalose biosynthesis in plants. *Phytochemistry* 144, 3–5. doi: 10.1016/S0031-9422(02)00137-1

Zhao, L., Yang, M., Shen, Q., Liu, X., Shi, Z., Wang, S., et al. (2016). Functional characterization of three trehalase genes regulating the chitin metabolism pathway in rice brown planthopper using RNA interference. *Sci. Rep.* 6:27841. doi: 10.1038/srep27841

Conflict of Interest: The authors declare that the research was conducted in the absence of any commercial or financial relationships that could be construed as a potential conflict of interest.

frontiers in Physiology

ORIGINAL RESEARCH
published: 25 November 2020
doi: 10.3389/fphys.2020.518876

Regulatory Functions of *Nilaparvata lugens* GSK-3 in Energy and Chitin Metabolism

*Yan-Juan Ding[1,2], Guo-Yong Li[1], Cai-Di Xu[2], Yan Wu[1], Zhong-Shi Zhou[1], Shi-Gui Wang[2] and Can Li[1]**

[1] *Guizhou Provincial Key Laboratory for Rare Animal and Economic Insect of the Mountainous Region, Guizhou Provincial Engineering Research Center for Biological Resources Protection and Efficient Utilization of the Mountainous Region, College of Biology and Environmental Engineering, Guiyang University, Guiyang, China,* [2] *College of Life and Environmental Sciences, Hangzhou Normal University, Hangzhou, China*

Glucose metabolism is a biologically important metabolic process. Glycogen synthase kinase (GSK-3) is a key enzyme located in the middle of the sugar metabolism pathway that can regulate the energy metabolism process in the body through insulin signaling. This paper mainly explores the regulatory effect of glycogen synthase kinase on the metabolism of glycogen and trehalose in the brown planthopper (*Nilaparvata lugens*) by RNA interference. In this paper, microinjection of the target double-stranded GSK-3 (ds*GSK-3*) effectively inhibited the expression of target genes in *N. lugens*. *GSK-3* gene silencing can effectively inhibit the expression of target genes (glycogen phosphorylase gene, glycogen synthase gene, trehalose-6-phosphate synthase 1 gene, and trehalose-6-phosphate synthase 2 gene) in *N. lugens* and trehalase activity, thereby reducing glycogen and glucose content, increasing trehalose content, and regulating insect trehalose balance. *GSK-3* can regulate the genes chitin synthase gene and glucose-6-phosphate isomerase gene involved in the chitin biosynthetic pathway of *N. lugens*. *GSK-3* gene silencing can inhibit the synthesis of chitin *N. lugens*, resulting in abnormal phenotypes and increased mortality. These results indicated that a low expression of *GSK*-3 in *N. lugens* can regulate the metabolism of glycogen and trehalose through the insulin signal pathway and energy metabolism pathway, and can regulate the biosynthesis of chitin, which affects molting and wing formation. The relevant research results will help us to more comprehensively explore the molecular mechanism of the regulation of energy and chitin metabolism of insect glycogen synthase kinases in species such as *N. lugens*.

Keywords: ***Nilaparvata lugens*, RNA interference, glycogen synthase kinase 3, glycogen and trehalose metabolism, chitin metabolism**

OPEN ACCESS

Edited by:
Kai Lu,
Fujian Agriculture and Forestry University, China

Reviewed by:
Rui Pang,
Guangdong Academy of Sciences, China
Leena Thorat,
York University, Canada

****Correspondence:***
Can Li
lican790108@163.com

Specialty section:
This article was submitted to Invertebrate Physiology, a section of the journal Frontiers in Physiology

Received: *10 December 2019*
Accepted: *20 October 2020*
Published: *25 November 2020*

Citation:
Ding Y-J, Li G-Y, Xu C-D, Wu Y, Zhou Z-S, Wang S-G and Li C (2020) Regulatory Functions of Nilaparvata lugens GSK-3 in Energy and Chitin Metabolism. Front. Physiol. 11:518876. doi: 10.3389/fphys.2020.518876

INTRODUCTION

Rice is one of the most important food crops grown in large quantities in Southeast Asian countries (Kang et al., 2019). However, rice is threatened by hundreds of pests throughout many stages, from planting to storage (Ghaffar et al., 2011). *Delphacidae* are one of the most serious rice pests, with the family including insects such as *Laodelphgax striatellus*, *Sogatella furcifera,* and *Nilaparvata lugens*. Since *N. lugens* has a single feeding habit feeding on rice, and is also a carrier of rice rough stunt

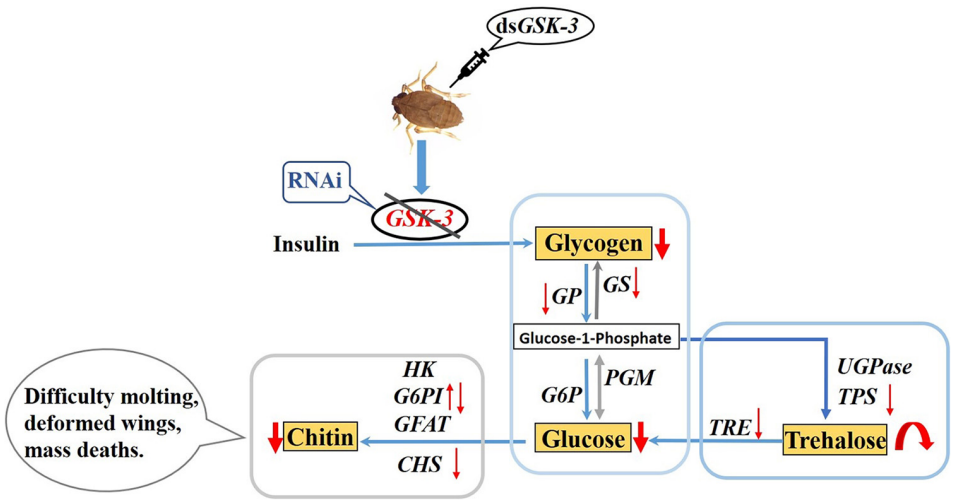

GRAPHICAL ABSTRACT | Regulation of *GSK-3* on energy and chitin metabolism of *Nilaparvata lugens*.

virus (RRSV) and grass stunt virus (Zhu et al., 2017), it has become the most serious type of *Delphacidae* (Jing et al., 2017; Zhang et al., 2018). At present, most of the chemical pesticides are used to control *N. lugens*, but because of its resistance to a large number of insecticides, the control effect is not satisfactory. In addition, the use of chemical pesticides poses a strong threat to the ecological environment (Diptaningsari et al., 2019).

Glucose metabolism is an important energy metabolism process in living organisms, supplying energy for life activities such as the growth and development of organisms (Carlson et al., 2018). Glycogen is the main form of glucose stored in insects and supplies energy according to the needs of different tissues (Prats et al., 2018). In animals, glucose can be converted to glycogen under the catalysis of glycogen synthase (Klotz and Forchhammer, 2017; Chang et al., 2018), and glycogen degradation requires the action of glycogen phosphorylase (Yamada et al., 2018). Glycogen is mainly stored in the fat bodies of insects and is converted to glucose or trehalose if necessary (Duran et al., 2012; Tang et al., 2012). In insects, glycogen is not a major energy substance, but it is used together with trehalose as a spare sugar to maintain glucose availability (Santiago-Martínez et al., 2016; Prats et al., 2018).

Trehalose is a non-reducing disaccharide unique to insects because it forms the main hemolymph sugar, also known as the "blood sugar" of insects (Zhang et al., 2017b). In fact, trehalose is synthesized by glucose under the catalysis of trehalose-6-phosphate synthase (Matsuda et al., 2015). In addition to providing energy and functioning as a carbon source, trehalose also has bio-protective properties that protects cells and proteins in extreme environments such as cold, oxidation, hypoxia, and dryness (Matsuda et al., 2015; Wen et al., 2016). The degradation of trehalose occurs mainly during the production of glucose under the catalysis of trehalase, which provides energy for life activities such as insect flight. There are two forms of trehalase in insects, soluble trehalase and membrane-bound trehalase (Tang et al., 2017). The synthetic substrates of trehalose, uridine diphosphate glucose and phosphate-6-glucose, can be derived from the decomposition of glycogen (Mitsumasu et al., 2010). Therefore, glycogen metabolism in insects is closely related to the formation and utilization of trehalose.

Trehalase can regulate chitin synthesis in insects (Zhang et al., 2017a). Chitin is the main structural material that constitutes the complex exoskeleton of insects and is found in many insects and arthropods (Zhu et al., 2016). In addition to trehalase, the chitin biosynthetic pathway also includes hexokinase (HK), glucose-6-phosphate isomerase, and glutamine; fructose 6-phosphate transaminase (GFAT), glucosamine-6-phosphate N-acetyltransferase (GNPNA), phosphor acetylglucosamine mutase (PAGM), UDP-N-acetylglucosamine pyrophosphorylase (UAP), and chitin synthase are essential for insect growth and development (Merzendorfer, 2006; Guo et al., 2019). Chitin is the main component of the peritrophic membrane (PM) in the midgut of insects. PM is the natural immune barrier of insects, which can resist the invasion of bacteria, viruses, and other pathogens (Wang and Granados, 2010). Studies on insects such as *Drosophila*, *Bombyx mori*, and *Locust* have found that the obstruction of chitin synthesis can lead to abnormal phenomena such as insect molting, increased mortality, and ovarian hypoplasia (Yang et al., 2015; Xu et al., 2017; Liu and Klein, 2018). Tang et al. (2016) and Chen et al. (2018) found that after RNA interference inhibited the expression of the *N. lugens* trehalase gene and trehalose synthase gene, the chitin content was significantly reduced, and high mortality and difficulty in molting were observed. However, there are few studies on the metabolism of chitin in insects with respect to the Glycogen synthase kinase (*GSK-3*) gene.

In recent years, there have been more and more studies on insect energy metabolism. In addition, various metabolic pathways of insects have become increasingly clear (Arrese and Soulages, 2010; Yang et al., 2014). Glycogen synthase kinase 3 is a key enzyme located in the middle of the sugar metabolism pathway (Mury et al., 2016). Woodgett et al. (1993) isolated

and purified two subtypes from skeletal muscle, GSK-3α and GSK-3β, which are encoded by two different genes and are widely expressed in different tissues and cells (Maqbool et al., 2016). *GSK-3* is involved in the regulation of various signaling pathways, such as insulin, Wnt/β-catenin, Hedgehog, and Notch signaling pathways, which play important roles in regulating cell differentiation, metabolism, apoptosis, and gene expression (Wei and Wei, 2015; Khan et al., 2017; Sato and Shibuya, 2018). In insects, *GSK-3* can inactivate glycogen synthase by phosphorylating glycogen synthase, inhibit the final step of glycogen synthesis, and also block the transmission of the insulin signaling pathway to inhibit glycogen synthesis (Frame and Cohen, 2001; Contreras et al., 2016). The conversion between glycogen and trehalose is inseparable, so the expression of *GSK-3* has an important influence on the anabolism of glycogen and trehalose.

The main purpose of this study was to microinject double-stranded RNA into *N. lugens*, thereby silencing the expression of the corresponding gene and achieving RNA interference. This method has been widely used in insect gene research in species such as *N. lugens* (Yu et al., 2013; Qiu et al., 2016; Shi et al., 2016). Once the expression of *GSK-3* in insects is abnormal, the process of glucose metabolism in the body will be unbalanced, and the development of insects, molting, and other life activities will be abnormal (Avonce et al., 2006; Mitsumasu et al., 2010; Shukla et al., 2015). Therefore, this study aimed to investigate the regulation of glycogen synthase kinase on energy metabolism and the chitin synthesis pathway in *N. lugens*. It provides a theoretical basis for pest control through energy and chitin metabolism.

MATERIALS AND METHODS

Insects

All the *N. lugens* used in this study were collected from the China Rice Research Institute and were kept in our laboratory. Rice varieties were insect-resistant rice TN1 (Taichung Native 1). Before rice planting, we first immersed rice seeds in warm water at about 70°C for about 10 min to break dormancy; then, seeds were soaked in tap water and placed in a 30°C artificial climate incubator for 24 h. Then, we washed the seeds several times with tap water, wrapped the seeds with wet gauze, and then placed them in a 30°C artificial climate incubator for 24–48 h. Seeds were germinated and sown in plastic pots, and appropriate fertilization promoted seedling growth. After the rice seedlings grew to about 10 cm, they were planted in the field. At the middle of the tillering stage, rice was moved to the insect cage, and rice was replaced every 2−3 days. The conditions for feeding *N. lugens* were as follows: temperature 26°C ± 1°C, photoperiod 16 h/8 h, and relative humidity of 70%.

Total RNA Extraction and cDNA Synthesis

Total RNA from *N. lugens* was extracted according to the Trizol kit instructions (Invitrogen, Carlsbad, CA, United States). After extraction, the mass of total RNA was detected by 1% agarose gel electrophoresis, and then the concentration and purity of RNA were measured using a NanoDrop 2000 spectrophotometer (Thermo Fisher Scientific, Waltham, MA, United States). The Prime Link® RT Reagent Kit (NARISHIGE, Japan) with gDNA Eraser Kit was used to configure the system and synthesize the first strand of cDNA.

Synthesis of dsRNA

We designed and synthesized specific primers based on *GSK-3* dsRNA specific fragments. Then, PCR amplification was performed, and the amplified product was subjected to T cloning. The cross-PCR reaction was then carried out using a primer with a T7 promoter. Related primer sequences are shown in **Table 1**. The synthesis of ds*GSK-3* was performed according to the instructions of the T7 RiboMAX^{TM} Express RNAi System kit (Promega Corporation, Madison, United States), and the concentration of ds*GSK-3* was determined by a NanoDrop^{TM} 2000 spectrophotometer. The same method was used to synthesize *GFP* dsRNA as a control group (Tang et al., 2010; Zhao et al., 2014). In addition, a trehalose solution and a glucose solution at a concentration equal to dsRNA were prepared.

Microinjection of *N. lugens*

The injection group of this experiment included the ds*GSK-3* only injection group, the ds*GSK-3* and glucose mixed injection group, the ds*GSK-3* and trehalose (Sigma-Aldrich, Saint Louis, MO 63103, United States) mixed injection group, and the ds*GFP* injection group as a control. For the mixed injection group, ds*GSK-3* was mixed in equal volume with an equal concentration of trehalose or glucose solution before injection. The dsRNA was injected into a standard capillary to determine the volume that the microinjector (NARISHIGE, Japan) pumped each time. Then, we adjusted the volume of the pumped dsRNA by nitrogen pressure so that the pumped volume was in accordance with the amount required for injection. Fifth instar *N. lugens* was anesthetized with CO_2, and then placed in a disposable culture dish with an agar plate on the abdomen. The injection site was the softer part of the first pair of feet in the middle of the foot. The

TABLE 1 | Primers used for the synthesis of dsRNA for *GFP* and *GSK3* genes.

Gene	Application type	Primer set	Forward primer (5′–3′)	Reverse primer (5′–3′)
Nl*GSK-3*	dsRNA synthesis	dsNl*GSK-3* dsNl*GSK-3*-T7	CTGCGACAGCGGCGAAATG T7-CTGCGACAGCGGCGAAATG	CGGTGACAGATGCCCAGCGAGT T7-CGGTGACAGATGCCCAGCGAGT
GFP	dsRNA synthesis	dsNl*GFP* dsNl*GFP*-T7	AAGGGCGAGGAGCTGTTCACCG T7-AAGGGCGAGGAGCTGTTCACCG	CAGCAGGACCATGTGATCGCGC T7-CAGCAGGACCATGTGATCGCGC
T7	dsRNA synthesis		GGATCCTAATACGACTCACTATAGG	

injection volume of each *N. lugens* was 200 ng, with 100 injections per treatment group. The samples were taken at 48 and 72 h after injection for determination of trehalose, glucose, glycogen content, and trehalase activity and the expression of related genes (Tang et al., 2017).

Expression Studies of Key Genes After *GSK*-3 RNAi

The expressions of key genes in the energy metabolism pathway, insulin signaling pathway, and chitin synthesis pathway were detected by qRT-PCR at 48 and 72 h after injection of *N. lugens*. Parallel sampling was taken; three tubes per treatment group, five *N. lugens* per tube, and three tubes of parallel cDNA were obtained for each sample and were stored in a −80°C refrigerator. During the experiment, three samples of cDNA per tube were obtained, and nine data points were obtained from three tubes of parallel cDNA. Each sample was presented as the average ± standard error to ensure the reliability of the data. The qRT-PCR reaction system (Bio-Rad Laboratories Inc.) (10 μL) was as follows: 5 μL SYBR Premix Ex Taq (SYBR Green Premix Ex Taq, Takara, Japan); 0.4 μL upstream/downstream primer; 1 μL cDNA; and 3.2 μL sterile ultrapure water. Quantitative primers are shown in **Table 2**, with 18S as the internal control gene. The reaction procedure was as follows: pre-denaturation at 95°C for 10 s, melting at 95°C for 5 s, annealing at 59°C for 30 s, 40 cycles (Zhang et al., 2017b).

Determination of Trehalose, Glucose, Total Glycogen Content, and Trehalase Activity

Each treatment and control material was added, after which 100 μL of phosphate buffered saline (PBS) was added, ground, and then added to 100 μL of PBS; sonication was performed until to no blocky structure was observed, after which the samples were crushed, added to 800 μL of PBS, and centrifuged at 1,000 *g* for 20 min at 4°C. Then, 350 μL of supernatant was collected and ultracentrifuged for 60 min at 4°C, 20,800 *g*. The 1,000 *g* centrifugation supernatant was used for determination of the protein concentration, glycogen concentration, and trehalose concentration. The supernatant after ultracentrifugation was used for the determination of the glucose content (supernatant), soluble trehalase activity (TRE1), and protein (Pr1). In addition, the pellet was suspended in PBS and used for the determination of the glucose content (suspension), membrane-bound trehalase (TRE2), and protein (Pr2). The specific steps are described in the kit instructions. In short, 75 μL of 40 mM trehalose (Sigma-Aldrich, Saint Louis, Mo 63103 United States) and 165 μL PBS (pH 7.0) were added into 60 μL 1,000 *g* supernatant. The

TABLE 2 | Primers used for qRT-PCR measurements of metabolism key genes.

Gene name	Genebank number	Forward primer (5′–3′)	Reverse primer (5′–3′)
QNI18S	JN662398.1	CGCTACTACCGATTGAA	GGAAACCTTGTTACGACTT
QNI*GSK-3*	XM_022340458	GGAAAGTTGAATCAAAGTGCTCG	AGGCTTTTGCCAGGGATG
QNI*PGM1*	KU556839.1	TTCTCGGTTGGTGGTGC	CCTTCAGCCTGGGACAT
QNI*PGM2*	KU556840.1	CGTTACAGGCTACGGAAGT	GACCCAAAGCAGTCAAA
QNI*GP*	KU556838.1	GCTGCCTATGGCTATGGTATTC	TCTGAGTGTTGACCCACTTCTTG
QNI*GS*	KU556837.1	GCTCCAAAGCCTATGTTTCTACTG	TGGTAACCCCTGTCCCTCA
QNI*UGPase*	KU556842.1	ATACAAGATGGCGGCTAA	TTGTGGCAGTTGATAGAGC
QNI*TPS1*	GQ397450	AAGACTGAGGCGAATGGT	AAGGTGGAAATGGAATGTG
QNI*TPS2*	KU556826	AGAGTGGACCGCAACAACA	TCAACGCCGAGAATGACTT
QNI*TPS3*	KU556827	GTGATGCGTCGGTGGCTAT	CCGTTCATCATTGGGCATAGT
QNI*TRE1-1*	FJ790319	GCCATTGTGGACAGGGTG	CGGTATGAACGAATAGAGCC
QNI*TRE1-2*	KU556829	GATCGCACGGATGTTTA	AATGGCGTTCAAGTCAA
QNI*TRE2*	GQ397451	TCACGGTTGTCCAAGTCT	TGTTTCGTTTCGGCTGT
QNI*HK*	KU556830	GGTGCGAGAAGAAGTGAAG	GTGAAACCCATTGGTAGAGT
QNI*GFAT*	KU556833	CCTCCCAGTTCATCTCGC	CCAAGTTCTTCAAACCCTTTAT
QNI*G6Pase*	KU556841.1	AGACCCTGGCAGTAGAATAG	GGGAAGTGAGCCGAAAT
QNI*G6PI1*	KU556832.1	GTTCACGGTCGTCTGGAAAG	TGACTGCTCCGTTTCACTCT
QNI*G6PI2*	KU556831.1	AACAAGGCGACATGGAATCG	ACCATTTGTTCCTGGTTCGC
QNI*CHS1*	AEL88648	CCGCAAACGATTCCTACAGA	AGGTCCTTGACGCTCATTCC
QNI*CHS1a*	JQ040014	TGTTCTTGCTACAACTCAATAAA	ACACCAATCCGATAGGCTC
QNI*CHS1b*	JQ040013	GCTGTCTTTGCTTTCTTCAT	ACACCAATCCGATAGGCTC
QNIInR1	KF974333	GAGTGCAACCCGGAGTATGT	TCTTGACGGCACACTTCTTG
QNI*InR2*	KF974334	CTCTTGCCGAACAGCCTTAC	GGGTCGTTTAGTGGGTCTGA
QNI*Ilp1*	KF974340	AACGATGCTGACTTGCAGATT	CGTACACGCGGAATAAATCA
QNI*Ilp2*	KF974341	TTCTCAGCCGCTCTAGCAAT	CAGACGAAGGATCAGGGAA G
QNI*Ilp3*	KF974342	ATACTGCGGCCAATAGCAAG	TCTCAATCCCCAAAATCAGC
QNI*Ilp4*	KF974343	TCCCGGACAGTTCTCACTTT	TTGTATTCTCCGGAGGCAAG

mixture was immersed in water for 60 min at 37°C and 5 min at 100°C. TRE activity was measured with glucose detection kit (Sigma-Aldrich) using supernatant (50 μL). The protein content in 1,000 *g* supernatant, ultracentrifugation supernatant, and suspension was determined by BCA Protein Assay Kit (Beyotime, China). Trehalose content was measured by anthrone method, and 30 μL 1% H_2SO_4 was added to 30 μL samples. The mixture was bathed in water at 90°C for 10 min and in ice for 3 min. After 30 μL 30% KOH was added, the mixture was again bathed in water at 90°C for 10 min and in ice for 3 min. Then, 600 μL developer (0.02 g fluorenone + 100 ml 80% H_2SO_4) was added, water bathed at 90°C for 10 min, and cooled in an ice bath. The absorbance of the sample was measured at 630 nm with a microplate reader. One hundred sixty microliter of the supernatant was obtained after centrifugation of 1,000 *g* for the determination of glycogen content. Six hundred microliter of anthrone sulfate reagent was added to the sample, placed in a water bath at 90°C for 10 min, and then cooled in an ice bath. The absorbance of the sample was measured at 625 nm with a microplate reader. The Glucose Assay Kit (SIGMA) was used to determine the glucose content in the supernatant and pellet suspension obtained after centrifugation at 20,800 *g*. 150 μL of the sample was placed into an EP (Eppendorf), and then 30 μL of 2N H_2SO_4 was added to stop the reaction after 30 min in a 37°C water bath, and the absorbance of the sample at 540 nm was then measured using a microplate reader.

Chitin Analysis

The detection method of the proportion of chitin in the brown planthopper refers to the "Insect Biochemical and Molecular Biology Experimental Technology" compiled by Cao and Gao (2009), with appropriate modifications. Two glass tubes were connected to both ends of a rubber tube, about 30–50 cm long. Another test tube with a rubber plug with holes was taken and the glass tube was inserted at one end of the rubber tube into the rubber plug, and the other end was passed into the water to prevent the lye from splashing out. 40 *N. lugens* was taken, three groups were paralleled, and then dried in an oven at 50°C. The *N. lugens* dried to a constant weight was weighed and recorded as W1. The dried insect body was poured into a test tube, 5 mL saturated potassium hydroxide solution was added, and it was heated in a glycerin bath at 160°C until the insect body developed a transparent film. The residue was filtered, rinsed carefully with water, dried in an oven at 50°C, weighed, and counted as W2. The relative content of chitin (%) = (W2 / W1) × 1.26 × 100 (%), where 1.26 is the ratio of relative molecular mass of acetylglucosamine to glucosamine.

Statistical Analyses

The average CT value of the three replicate wells was used for calculation, and the final data were the mean ± standard error. Then, the $2^{-\Delta\Delta CT}$ formula was used to calculate the CT value of the ds*GFP* group injected into *N. lugens*. The $2^{-\Delta\Delta CT}$ calculation formula is as follows:

$$2^{-\Delta\Delta CT} = 2^{-[(\text{CT of experimental group} - \text{CT of experiment 18S}) - (\text{CT of control group} - \text{CT of control 18S})]}.$$

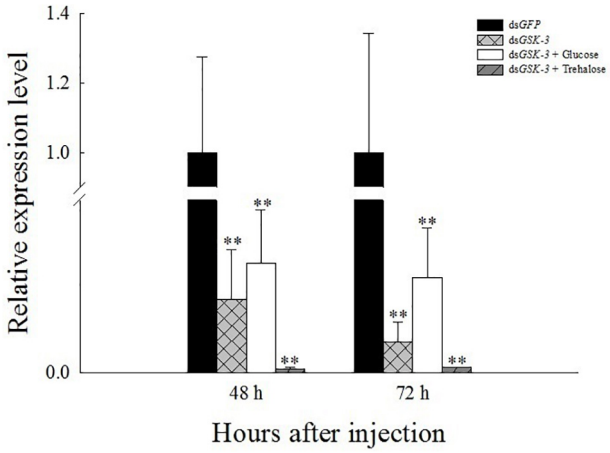

FIGURE 1 | Relative expression level of *N. lugens GSK-3* 48 and 72 h after RNA interference. **Indicates significant differences at $P < 0.01$. Error bars is the standard error.

Charts were drawn using Excel software, statistical analysis was performed using STATISTICA 8.0 and SigmaPlot 10.0, and the significance difference test was performed using one-way ANOVA (* indicates $P < 0.05$, the difference is significant; ** indicates $P < 0.01$, the difference is extremely significant).

RESULTS

Expression of *GSK*-3 After RNAi

Compared with the injection of the ds*GFP* group, the expression levels of *GSK-3* mRNA in the three treatment groups were significantly decreased at 48 and 72 h after injection. Among them, the ds*GSK-3* and trehalose mixed injection group decreased most obviously ($P < 0.01$) (**Figure 1**). This result indicates that the injection of ds*GSK-3*, a mixture of ds*GSK-3* and glucose, a mixture of ds*GSK-3,* and trehalose can significantly reduce the expression of *GSK-3*.

Effects of *GSK*-3 RNAi on Glycogen, Glucose, and Trehalose Contents

Compared with the injection of the ds*GFP* group, glycogen and glucose levels were extremely significantly decreased or significantly decreased 48 h after injection (**Figures 2A,B**), and the trehalose content increased extremely significantly 48 h after ds*GSK-3* injection ($P < 0.01$) (**Figure 2C**). The glycogen, glucose, and trehalose contents were significantly decreased or extremely significantly decreased 72 h after ds*GSK-3* injection (**Figure 2**); the glucose and glycogen contents were significantly increased after injection of a mixture of ds*GSK-3* and glucose ($P < 0.05$) (**Figures 2A,B**), and the glycogen and glucose contents were restored to a level similar to that observed in the control group after injection of a mixture of ds*GSK-3* and trehalose (**Figures 2A,B**). In the two mixed injection groups, the change in the trehalose content was not significant (**Figure 2C**).

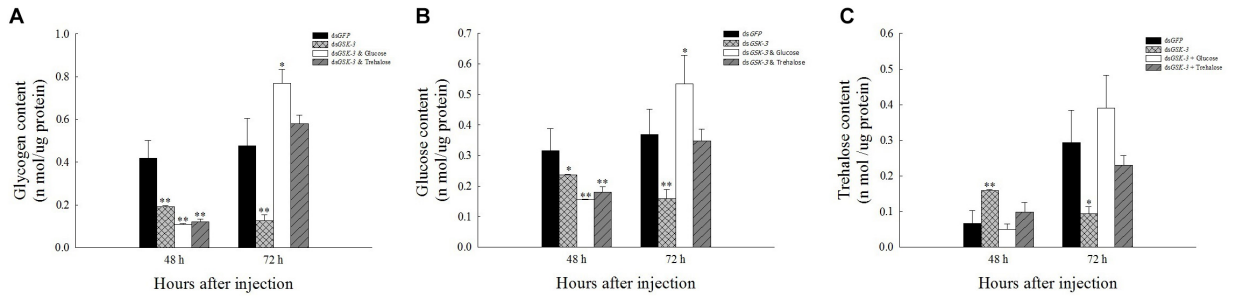

FIGURE 2 | Effect of *GSK-3* RNA interference on glycogen, glucose, and trehalase contents of *N. lugens*. Changes in glycogen **(A)**, glucose **(B)**, and trehalose **(C)** contents in *N. lugens* were observed at 48 and 72 h after injection in each treatment group. *Indicates significant differences at $P < 0.05$ and **indicates significant differences at $P < 0.01$. Error bars is the standard error.

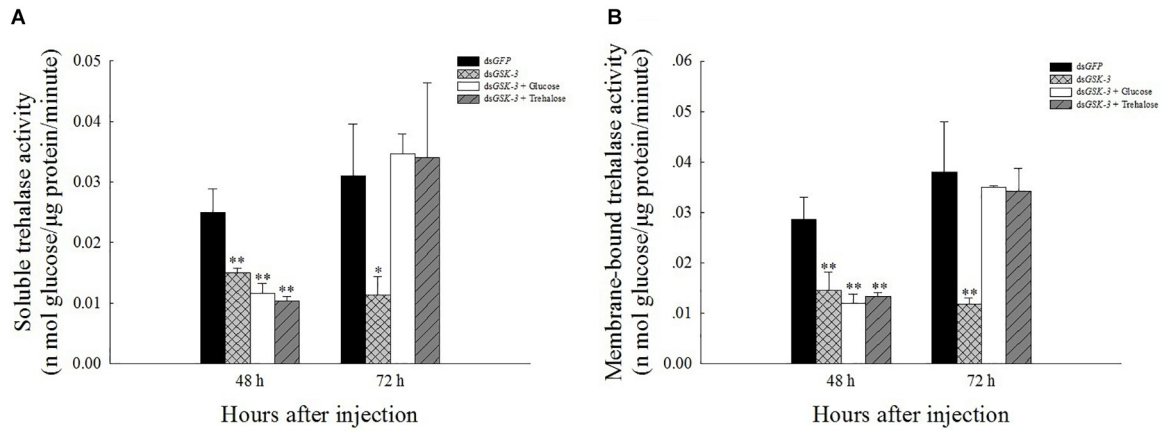

FIGURE 3 | Effect of *GSK-3* RNA interference on trehalase activity of *N. lugens*. The soluble trehalase **(A)** and membrane-bound trehalase **(B)** activities of *N. lugens* were observed 48 h and 72 h after injection in each treatment group. *Indicates significant differences at $P < 0.05$ and **indicates significant differences at $P < 0.01$. Error bars is the standard error.

Effects of *GSK*-3 RNAi on Two Kinds of Trehalase in *N.lugens*

The results of the trehalase activity assay showed that the soluble trehalase and membrane-bound trehalase activities of the three treatment groups were extremely significantly decreased 48 h after injection ($P < 0.01$) (**Figures 3A,B**). The two trehalase activities were significantly reduced 72 h after ds*GSK-3* injection ($P < 0.01$) (**Figures 3B,C**), and the trehalase activity of the two mixed injection groups returned to a level similar to the control group (**Figure 3**).

Expression of Chitin Synthesis Pathway-Related Genes After *GSK*-3 RNAi

The expression of *TRE1*-1 and *TRE2* decreased or decreased significantly compared with the injection of ds*GFP* after RNAi inhibited the expression of *N. lugens GSK*-3. The expression of *TRE1*-2 increased significantly 48 h after injection of a mixture of ds*GSK-3* and trehalose ($P < 0.01$) and decreased slightly 72 h after injection, and the expression of *TRE1*-2 also increased significantly after injection of a mixture of ds*GSK-3* and glucose ($P < 0.01$, **Figure 4A**). There was no significant change in the expression of *GFAT* and *HK* genes after ds*GSK-3* and a mixture of ds*GSK-3* and glucose injection (**Figure 4B**). After inhibition, the expression level of *G6PI* showed a trend of increasing first and then decreasing (**Figure 4C**). The expression of *CHS1a* was extremely significantly increased 48 h after ds*GSK-3* injection ($P < 0.01$), the expression of *CHS1b* was extremely significantly decreased after injection ($P < 0.01$), and the expression of *CHS* was not significantly changed 48 h after injection of a mixture of ds*GSK-3* and glucose. Injection of a mixture of ds*GSK-3* and trehalose showed significant inhibition of *CHS* expression ($P < 0.05$). The expression levels of *CHS* in each treatment group decreased or decreased extremely significantly 72 h after injection (**Figure 4D**).

Expression of Genes Involved in the Energy Metabolism Pathway After *GSK-3* RNAi

Compared with the control group ds*GFP*, the expression levels of *TPS1* and *TPS2* were extremely significantly decreased after treatment. The expression of *TPS3* increased but was not

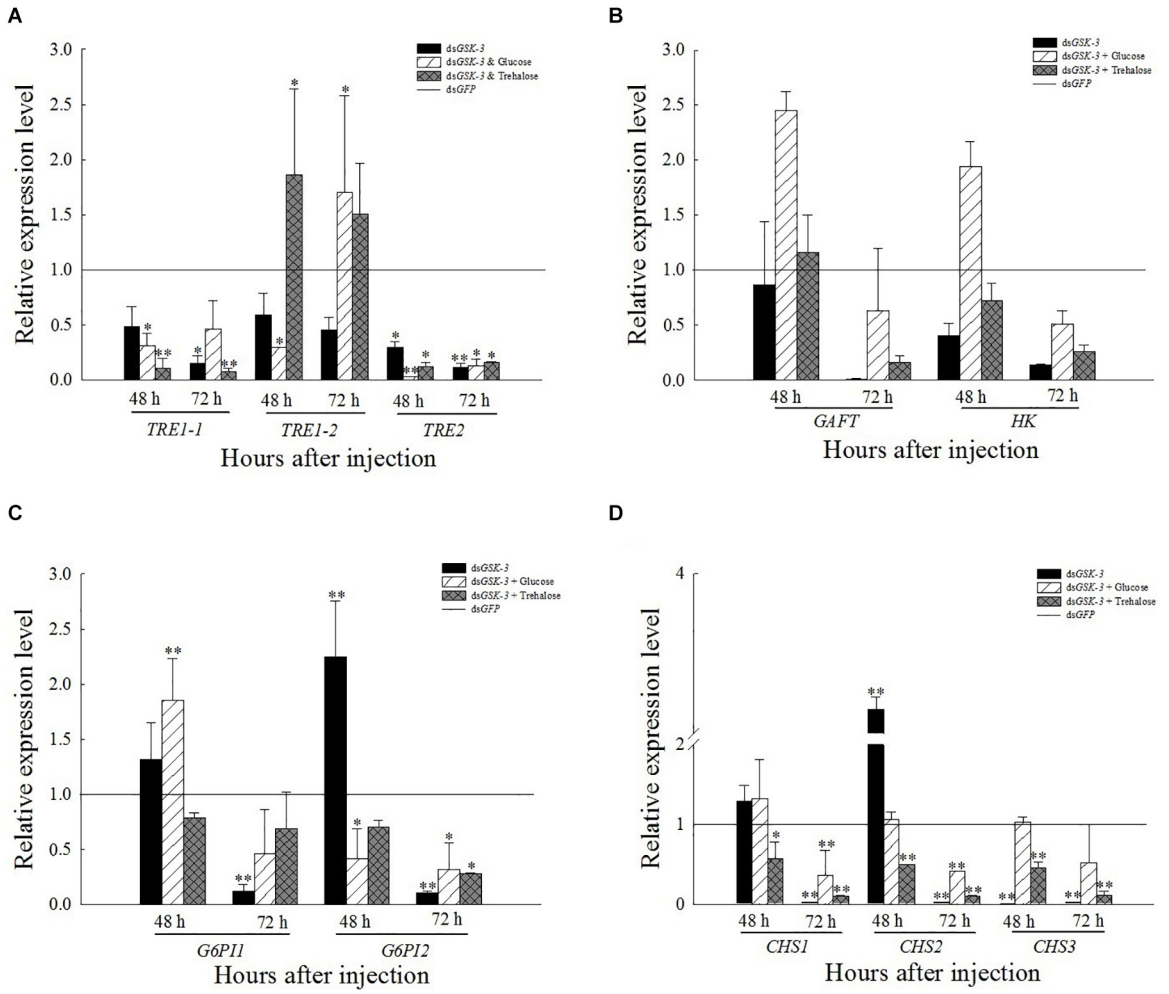

FIGURE 4 | Expression levels of regulated genes in the chitin synthesis pathway after *GSK-3* RNA interference. The relative expression levels of three *TRE* genes **(A)**, *GFAT* and *HK* genes **(B)**, *G6PI* genes **(C)**, and *CHS* **(D)** genes after dsRNA injection compared with the control ds*GFP*. *Indicates significant differences at $P < 0.05$ and **indicates significant differences at $P < 0.01$. Error bars is the standard error.

significant 48 h after injection of ds*GSK-3* and a mixture of ds*GSK-3* and glucose (**Figure 5A**). The expression of *PGM1* was extremely significantly increased 72 h after ds*GSK-3* and a mixture of ds*GSK-3* and glucose injection, and there was no significant change in *PGM2* expression (**Figure 5B**). The expression of *GS* and *GP* decreased extremely significantly after injection in each treatment group (**Figure 5D**). The expression of *G6P* increased significantly 48 h after ds*GSK-3* injection and decreased after 72 h. The expression of *UGPase* and *PFK* did not change significantly (**Figure 5B**).

Expression of Insulin Signaling Pathway-Related Genes After *GSK-3* RNAi

After RNAi inhibited the expression of *GSK*-3, the expression levels of *InR*, *Ilp1,* and *Ilp2* were extremely significantly lower than those of ds*GFP* ($P < 0.01$) (**Figure 6**). The expression of *Ilp3* and *Ilp4* was significantly or extremely significantly decreased 48 h after injection, and increased extremely significantly 72 h after the injection of a mixture of ds*GSK-3* and glucose. The expression of *Ilp4* increased extremely significantly 72 h after ds*GSK-3* injection (**Figure 6B**).

Analysis of Phenotype, Malformation Rate, Mortality, and Chitin Content After *GSK-3* RNAi

After injection of dsRNA, the death rate of *N. lugens* increased, and various abnormal phenotypes appeared. Compared with the control group injected with ds*GFP*, the mortality rate was significantly increased at 48 h after mixed injection of ds*GSK-3* and trehalose and 72 h after the interference of ds*GSK-3* ($P < 0.05$) (**Figure 7A**). *N. lugens* in each treatment group showed abnormal phenotypes, including molting deformities and wing deformities (**Figure 7D**); the deformity rate of the mixed injection group was higher than that of the ds*GSK-3* alone injection group (**Figure 7B**).

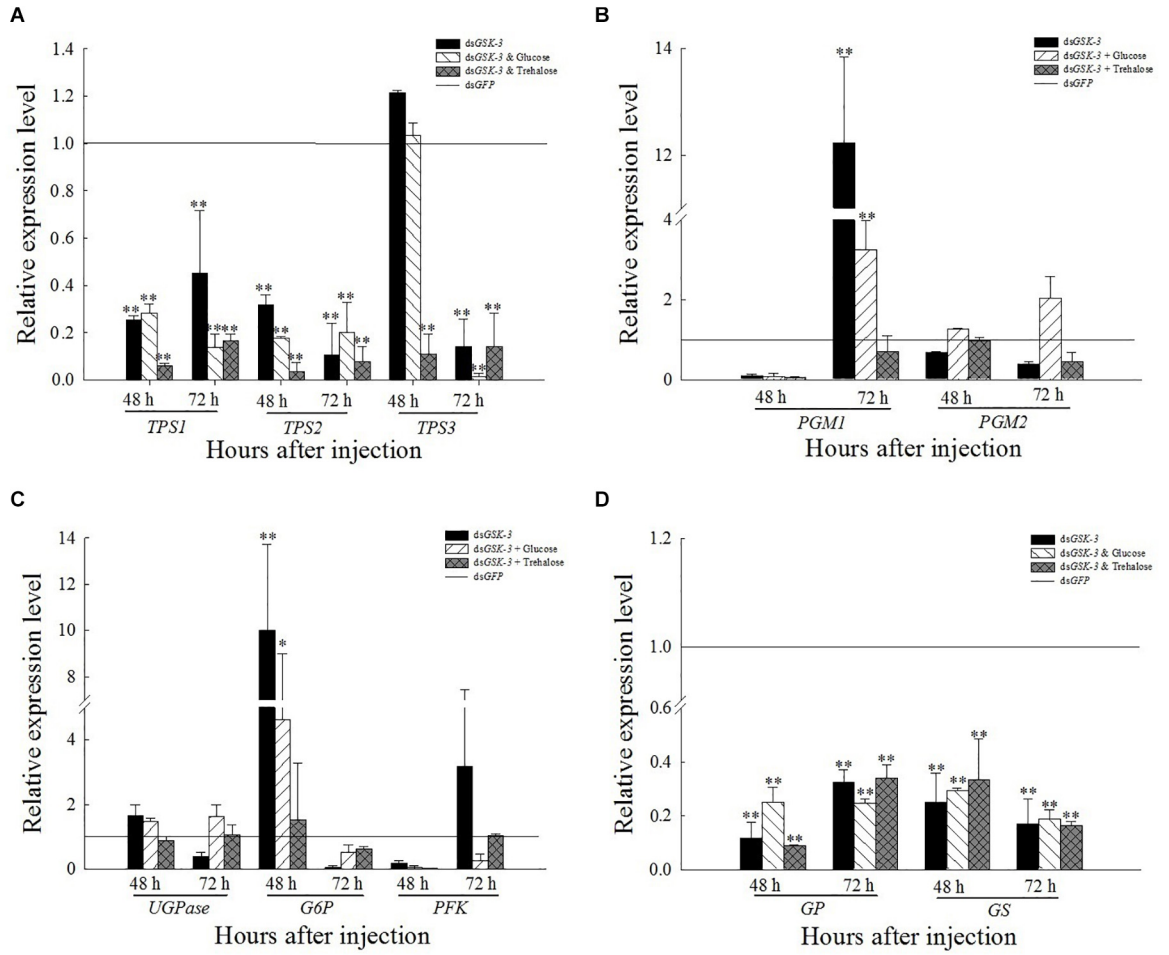

FIGURE 5 | Expression levels of regulated genes in the energy metabolism pathway after *GSK-3* RNA interference. The relative expression levels of *TPS* genes **(A)**, *PGM* genes **(B)**, *UGPase*, *G6P,* and *PFK* genes **(C)**, and *GP* and *GS* genes **(D)** were compared with the control ds*GFP* after injection in each treatment group. *Indicates significant differences at $P < 0.05$ and **indicates significant differences at $P < 0.01$. Error bars is the standard error.

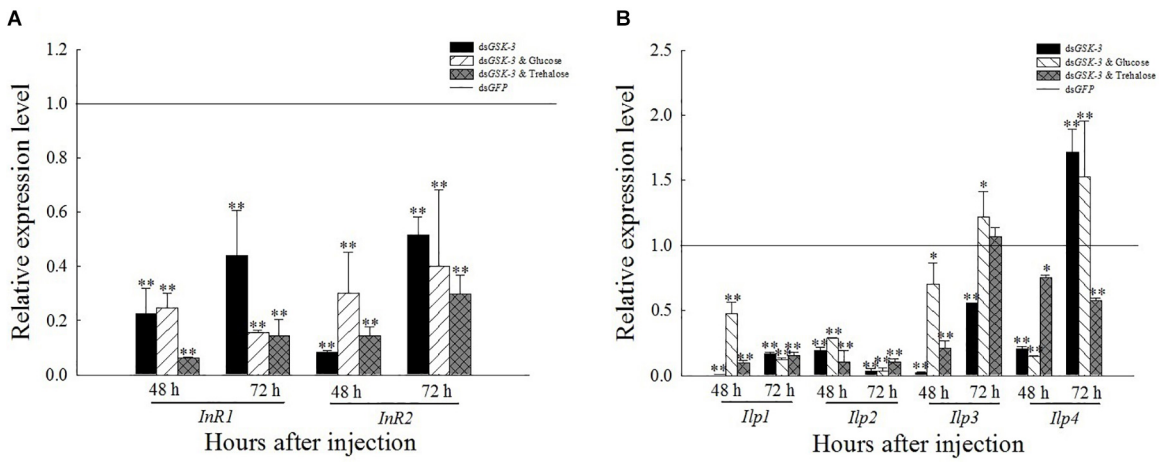

FIGURE 6 | Expression levels of regulated genes in the insulin signaling pathway after GSK-3 RNA interference. The relative expression levels of *InR* genes **(A)** and *Ilp* genes **(B)** were compared with the control dsGFP after injection in each treatment group. *Indicates significant differences at $P < 0.05$ and **indicates significant differences at $P < 0.01$. Error bars is the standard error.

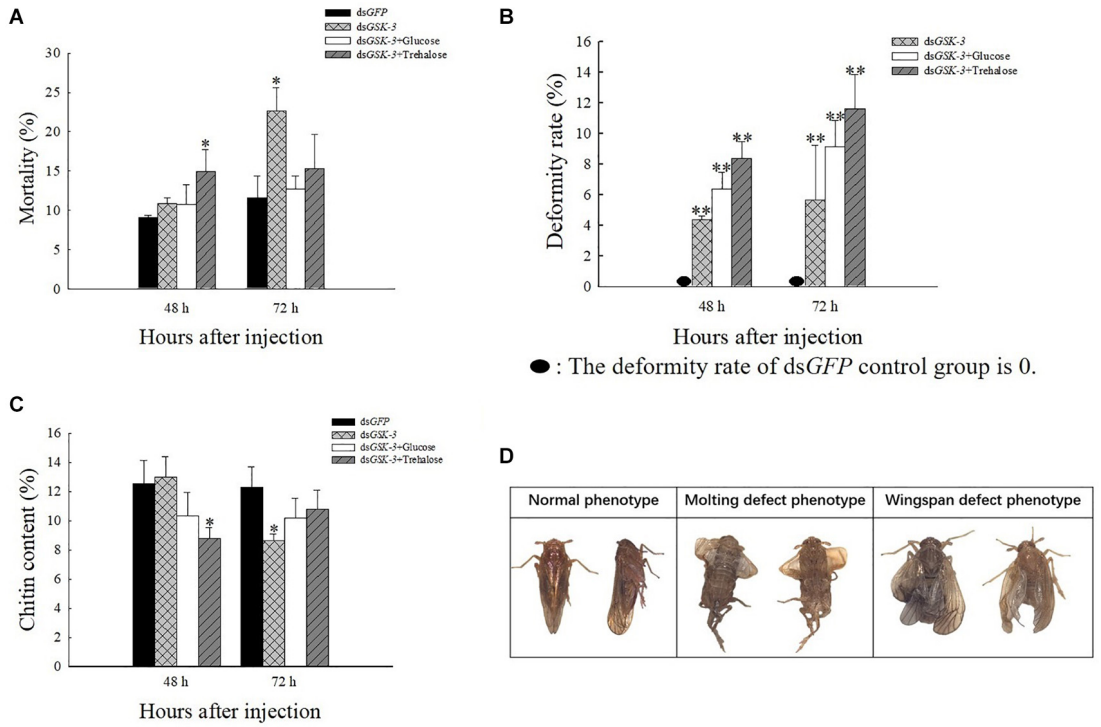

FIGURE 7 | The effect of *GSK-3* gene silencing on the chitin content and phenotype of *N. lugens*. Mortality rate **(A)**, deformity rate **(B)**, chitin content **(C)**, and Normal and abnormal phenotypes of *N. lugens* **(D)** were compared with the control dsGFP after injection in each treatment group. *Indicates significant differences at $P < 0.05$ and **indicates significant differences at $P < 0.01$. Error bars is the standard error.

After RNAi treatment, the relative content of chitin in *N. lugens* changed. 48 h after the injection, except for the ds*GSK-3* and trehalose mixed injection group, there was a significant decrease ($P < 0.05$), and the other injection groups had no significant changes. 72 h after ds*GSK-3* injection, the content of chitin in *N. lugens* significantly decreased ($P < 0.05$), while the other injection groups did not decrease significantly (**Figure 7C**). These results indicate that *GSK-3* gene silencing affects the metabolism of chitin and the formation of wings in *N. lugens*.

DISCUSSION

RNA interference has great potential for studying insect gene function, mainly by microinjecting dsRNA or siRNA into insects to inhibit gene expression (Xi et al., 2015; Li et al., 2017) or synthesized *in vitro* and topically applied to crops (Murphy et al., 2016). In this study, the expression levels of the *GSK-3* gene were extremely significantly decreased after injection in each treatment group of *N. lugens*, indicating that the RNA interference effect is obvious, and the interference effect can last up to 72 h (**Figure 1**). Previous studies have found that *GSK-3* is involved in a variety of signaling pathways and plays an important regulatory role in cells (Liu et al., 2018). *GSK-3* acts on the Ser332 site of insulin receptor substrate-1 (IRS-1) to block the insulin-signaling pathway, thereby regulating glycogen synthesis (Liberman and Eldar-Finkelman, 2005). After insulin enters the insect, it activates *Ilp* and *InR* and then activates phosphatidylinositol kinase (PI3K). Activated PI3K catalyzes phosphorylation of phosphatidylinositol, which in turn causes phosphorylation of the effector Akt, which prevents phosphorylation of glycogen synthase (GSK-3), thereby promoting glycogen synthesis (Woodgett et al., 1993; Nagy et al., 2018). The effect of *Ilp* on glucose metabolism cannot only promote glycogen synthesis but also inhibit gluconeogenesis and conversion of excess sugar into lipids in specific tissues (Semaniuk et al., 2018; Kawabe et al., 2019). The results of this study showed that the expressions of insulin signaling pathway-related genes *InR*, *Ilp1*, *Ilp2*, and *Ilp3* were extremely significantly decreased 48 and 72 h after ds*GSK-3* injection (**Figure 6**). Only the expression of *Ilp4* increased extremely significantly 72 h after injection (**Figure 6B**), presumably related to its regulation of the reproduction of *N. lugens* (Lu et al., 2018). At the same time, the glycogen and glucose contents of *N. lugens* were significantly or extremely significantly decreased (**Figures 2A,B**), indicating that *N. lugens GSK*-3 can regulate glycogen and glucose synthesis through the insulin signaling pathway (McManus et al., 2005).

Trehalose can act as an energy reserve for the life activities of insects under stress, such as starvation and dryness (Yasugi et al., 2017). Under various stresses, trehalose accumulation occurs in insects (Fountain et al., 2016; Tamang et al., 2017; Paithankar et al., 2018). This study found that the trehalose content increased extremely significantly 48 h after ds*GSK-3* injection (**Figure 2C**), and the two trehalase activities decreased extremely

significantly (**Figures 3A,B**), showing consistency. However, the trehalose content decreased extremely significantly (**Figure 2C**) and trehalase activity remained significantly decreased 72 h after injection (**Figures 3A,B**). TPS can affect the energy supply, growth and development, stress recovery, chitin synthesis, and other biological processes of *N. lugens* (Tang et al., 2018). When the expression of *TPS* and *TRE* in the trehalose metabolism pathway of the *N. lugens* was inhibited, the glycogen content decreased (Zhang et al., 2017b). In this study, the expressions of *TPS1*, *TPS2,* and *TRE* were down-regulated after *GSK-3* interference (**Figures 4A**, **5A**), that is, the accumulation of trehalose in *N. lugens* led to an increase in its content 48 h after GSK-3 RAN interference, but due to the resistance of trehalose synthesis, the content of trehalose decreased 72 h after injection. The expression of *TPS3* increased 48 h after *GSK-3* interference, probably because the structure of *TPS3* is different from that of *TPS1* and *TPS2*, so their functions are also different. Al Baki MA et al. found that the chyme content of *Alpaki* was increased after *Ilp* and *InR* RNAi (Al Baki et al., 2019), which is consistent with the results of this study (**Figures 6A,B**), that is, glycogen and glucose are converted into trehalose after ds*GSK-3* injection, which leads to an increase in glucose metabolism and maintains the balance of glucose metabolism in insects, which is consistent with previous studies (Mitsumasu et al., 2010; Tang et al., 2012).

The metabolism of glycogen requires a combination of enzymes, mainly regulated by glycogen synthase (GS) and glycogen phosphorylase (GP) (Zhang et al., 2017b). *GSK-3* can phosphorylate glycogen synthase to inhibit glycogen synthesis (Contreras et al., 2016). In our study, the expression of *GS* and *GP* was extremely significantly decreased 48 and 72 h after ds*GSK-3* injection (**Figure 5D**). In animals, glycogen plays a role in different tissues, and hepatic glycogen can be decomposed into glucose during hypoglycemia to control blood sugar stability; glycogen can also supply energy to organisms through the glycolysis pathway (Roach et al., 2012; Falkowska et al., 2015). In this study, the expression of the *PGM1* gene in the energy metabolism pathway decreased slightly 48 h after injection but increased extremely significantly 72 h after injection (**Figure 5B**). In addition, the expression of *G6P* associated with glycogen degradation returned to a level similar to that of the ds*GFP* group after a significant increase after injection (**Figure 5C**; Klotz and Forchhammer, 2017). That is, the expression of *GSK-3* can inhibit the metabolism of carbohydrates.

The reasonable intake of dietary sugar is essential for the growth and development of insects, while the trehalose of insects is mostly synthesized by the intake of glucose (Thompson et al., 2003; Mattila and Hietakangas, 2017). Under a high-sugar diet, the glucose content in *Drosophila* increased, while the expression of adiponectin (*Akh*) was down-regulated, and the glycogen content was reduced (Gáliková et al., 2015; Hemphill et al., 2018). Our results showed that the glycogen and glucose levels of two mixed injection groups showed extremely significant decreases compared with the control group 48 h after injection; the glycogen and glucose levels increased significantly 72 h after injection of a mixture of ds*GSK-3* and glucose, and the mixed injection group of ds*GSK-3* and trehalose returned to a level similar to the control group (**Figures 2A,B**). In contrast, the two mixed injection groups had no significant effect on the trehalose content (**Figure 2C**), but both types of trehalase activity decreased significantly 48 h after injection and rose to a level similar to the control group 72 h after injection (**Figures 3A,B**). *TRE1* mainly exists in the midgut of *N. lugens* and regulates the decomposition of endogenous trehalose; *TRE2* mainly absorbs and assimilates exogenous trehalose (Tang et al., 2016). Therefore, the expression level of *TRE1-2* was significantly increased 48 h after a mixture of ds*GSK-3* and glucose injection and 72 h after a mixture of ds*GSK-3* and trehalose injection (**Figure 4A**). *HK* catalyzes the conversion of glucose to glucose-6-phosphate, and *GFAT* decomposes fructose-6-phosphate. The expression of *GFAT*, *HK*, and *G6PI1* in the chitin pathway increased or significantly increased 48 h after injection of a mixture of ds*GSK-3* and glucose (**Figures 4B,C**). *In vitro* injection of glucose or trehalose can compensate for the interference of ds*GSK-3* in the energy metabolism and chitin synthesis of *N. lugens*, but it seems that *N. lugens* is more sensitive to changes in the glucose content (Masumura et al., 2000; Ugrankar et al., 2015).

The growth and development of insects are closely related to the biosynthesis of chitin (Merzendorfer and Zimoch, 2003; Muthukrishnan et al., 2018). Trehalose is the first gene in the chitin biosynthesis pathway of insects, which regulates chitin synthase (Zhao et al., 2016; Tang et al., 2017). Previous studies have shown that the inhibition of *CHS* gene expression will lead to a decrease in the content of chitin, abnormal phenotypes and an increase in mortality of *N. lugens* (Yang et al., 2017; Li et al., 2017; Pan et al., 2019). Our results showed a decrease or a significant decrease in *TRE* expression after ds*GSK-3* injection (**Figure 4A**). At the same time, compared with the ds*GFP* group, the expression of *CHS1* was similar 48 h after ds*GSK-3* injection; the expression of *CHS1a* was extremely significantly increased, the expression of *CHS1b* was extremely significantly decreased, and the expression of three *CHS* genes was significantly decreased 72 h after injection (**Figure 4D**). At the same time, the content of chitin was significantly reduced 48 h after ds*GSK-3* and trehalose injection and 72 h after ds*GSK-3* injection (**Figure 7C**). This suggests that ds*GSK-3* has different regulatory effects on different chitin synthase genes, but ultimately inhibits their expression, which may be related to the functional specificity of chitin synthase (Arakane et al., 2009; Merzendorfer, 2011). Our research also found that *N. lugens* had difficulty molting, deformed wings, and increased mortality after ds*GSK-3* injection (**Figures 7A,B,D**). In addition, the expression of *G6PI* also increased 48 h after ds*GSK-3* injection and decreased after 72 h (**Figure 4C**). The interference of *GSK-3* has an effect on the expression of genes involved in the chitin biosynthesis pathway of *N. lugens*.

CONCLUSION

GSK-3 RNAi can effectively inhibit the expression of target genes in *N. lugens*; *GSK-3* can down-regulate the expression of energy metabolism pathway-related genes and trehalase activity, thereby reducing the glycogen and glucose content, increasing the trehalose content, and regulating insect trehalose balance; *GSK-3* can regulate genes involved in the chitin biosynthesis pathway

of *N. lugens*, affecting its chitin synthesis, leading to phenotypic abnormalities and even death.

DATA AVAILABILITY STATEMENT

All datasets generated for this study are included in the article/supplementary material.

AUTHOR CONTRIBUTIONS

Y-JD, G-YL, and CL conceived and manuscript structure design. C-DX, YW, and S-GW performed the current articles collection and related metabolic genes' analysis. Y-JD, Z-SZ, and CL wrote the manuscript. All authors contributed to the article and approved the submitted version.

FUNDING

We thank the Regional First-class Discipline Construction of Guizhou Province [No. (2017)85], the scientific research funds of Guiyang University [No. GYU-KY-(2021)], the Provincial Key and Special Subject of Guizhou Province-Ecology [No. ZDXK(2015)11], Training Project for High-Level Innovative Talents in Guizhou Province [No. 2016 (4020)], and the Program for Academician Workstation in Guiyang University (20195605) for financial support.

REFERENCES

Al Baki, M. A., Lee, D. W., Jung, J. K., and Kim, Y. (2019). Insulin-like peptides of the legume pod borer, *Maruca vitrata*, and their mediation effects on hemolymph trehalose level, larval development, and adult reproduction. *Arch. Insect. Biochem. Physiol.* 100:e21524. doi: 10.1002/arch.21524

Arakane, Y., Dixit, R., Begum, K., Park, Y., Specht, C. A., Merzendorfer, H., et al. (2009). Analysis of functions of the chitin deacetylase gene family in *Tribolium castaneum*. *Insect. Biochem. Mol. Biol.* 39, 355–365. doi: 10.1016/j.ibmb.2009.02.002

Arrese, E. L., and Soulages, J. L. (2010). Insect fat body: energy, metabolism, and regulation. *Annu. Rev. Entomol.* 55, 207–225. doi: 10.1146/annurev-ento-112408-085356

Avonce, N., Mendoza-Vargas, A., Morett, E., and Iturriaga, G. (2006). Insights on the evolution of trehalose biosynthesis. *BMC Evol. Biol.* 6:109. doi: 10.1186/1471-2148-6-109

Cao, C. W., and Gao, C. Q. (2009). *Experimental Techniques of Insect Biochemistry and Molecular Biology*. Harbin: Northeast Forestry University Press, 24–26.

Carlson, G. M., Dienel, G. A., and Colbran, R. J. (2018). Introduction to the thematic minireview series: brain glycogen metabolism. *J. Biol. Chem.* 293, 7087–7088. doi: 10.1074/jbc.TM118.002642

Chang, C. H., Huang, J. J., Yeh, C. Y., Tang, C. H., Hwang, L. Y., and Lee, T. H. (2018). Salinity effects on strategies of glycogen utilization in livers of Euryhaline Milkfish (*Chanos chanos*) under hypothermal stress. *Front. Physiol.* 9:81. doi: 10.3389/fphys.2018.00081

Chen, Q. W., Jin, S., Zhang, L., Shen, Q. D., Wei, P., Wei, Z. M., et al. (2018). Regulatory functions of trehalose-6-phosphate synthase in the chitin biosynthesis pathway in *Tribolium castaneum* (Coleoptera: Tenebrionidae) revealed by RNA interference. *Bull. Entomol. Res.* 108, 388–399. doi: 10.1017/S000748531700089X

Contreras, C. J., Segvich, D. M., Mahalingan, K., Chikwana, V. M., Kirley, T. L., Hurley, T. D., et al. (2016). Incorporation of phosphate into glycogen by glycogen synthase. *Arch. Biochem Biophys.* 597, 21–29. doi: 10.1016/j.abb.2016.03.020

Diptaningsari, D., Trisyono, Y. A., Purwantoro, A., and Wijonarko, A. (2019). Inheritance and realized heritability of resistance to imidacloprid in the Brown Planthopper, *Nilaparvata lugens* (Hemiptera: Delphacidae), from Indonesia. *J. Econ. Entomol.* 112, 1831–1837. doi: 10.1093/jee/toz090

Duran, J., Tevy, M. F., Garcia-Rocha, M., Calbó, J., Milán, M., and Guinovart, J. J. (2012). Deleterious effects of neuronal accumulation of glycogen in flies and mice. *EMBO Mol. Med.* 4, 719–729. doi: 10.1002/emmm.201200241

Falkowska, A., Gutowska, I., Goschorska, M., Nowacki, P., Chlubek, D., and Baranowska-Bosiacka, I. (2015). Energy metabolism of the brain, including the cooperation between astrocytes and neurons, especially in the context of glycogen metabolism. *Int. J. Mol. Sci.* 16, 25959–25981. doi: 10.3390/ijms161125939

Fountain, T., Melvin, R. G., Ikonen, S., Ruokolainen, A., Woestmann, L., Hietakangas, V., et al. (2016). Oxygen and energy availability interact to determine flight performance in the Glanville fritillary butterfly. *J. Exp. Biol.* 219, 1488–1494. doi: 10.1242/jeb.138180

Frame, S., and Cohen, P. (2001). GSK3 takes centre stage more than 20 years after its discovery. *Biochem. J.* 359, 1–16.

Gáliková, M., Diesner, M., Klepsatel, P., Hehlert, P., Xu, Y., Bickmeyer, I., et al. (2015). Energy homeostasis control in *Drosophila* adipokinetic hormone mutants. *Genetics* 201, 665–683. doi: 10.1534/genetics.115.178897

Ghaffar, M. B., Pritchard, J., and Ford-Lloyd, B. (2011). Brown planthopper (*N. lugens Stål*) feeding behaviour on rice germplasm as an indicator of resistance. *PLoS One* 6:e22137. doi: 10.1371/journal.pone.0022137

Guo, J., Xu, Y., Yang, X. S., Sun, X. H., Sun, Y., and Zhou, D. (2019). TRE1 and CHS1 contribute to deltamethrin resistance in *Culex pipiens pallens*. *Arch. Insect. Biochem. Physiol.* 100:e21538. doi: 10.1002/arch.21538

Hemphill, W., Rivera, O., and Talbert, M. (2018). RNA-sequencing of *Drosophila melanogaster* head tissue on high-sugar and high-fat diets. *G3* 8, 279–290. doi: 10.1534/g3.117.300397

Jing, S. L., Zhao, Y., Du, B., Chen, R. Z., Zhu, L. L., and He, G. C. (2017). Corrigendum to "Genomics of interaction between the brown planthopper and rice" [Curr. Opin. Insect Sci. 19 (2017) 82-87]. *Curr. Opin. Insect. Sci.* 27:118. doi: 10.1016/j.cois.2018.01.002

Kang, K., Yue, L., Xia, X., Liu, K., and Zhang, W. (2019). Comparative metabolomics analysis of different resistant rice varieties in response to the brown planthopper *Nilaparvata lugens* Hemiptera: Delphacidae. *Metabolomics* 15:62. doi: 10.1007/s11306-019-1523-4

Kawabe, Y., Waterson, H., and Mizoguchi, A. (2019). Bombyxin (Bombyx Insulin-Like Peptide) increases the respiration rate through facilitation of carbohydrate catabolism in *Bombyx mori*. *Front. Endocrinol.* 10:150. doi: 10.3389/fendo.2019.00150

Khan, I., Tantray, M. A., Alam, M. S., and Hamid, H. (2017). Natural and synthetic bioactive inhibitors of glycogen synthase kinase. *Eur. J. Med. Chem.* 125, 464–477. doi: 10.1016/j.ejmech.2016.09.058

Klotz, A., and Forchhammer, K. (2017). Glycogen, a major player for bacterial survival and awakening from dormancy. *Future Microbiol.* 12, 101–104. doi: 10.2217/fmb-2016-0218

Li, T. C., Chen, J., Fan, X. B., Chen, W. W., and Zhang, W. Q. (2017). MicroRNA and dsRNA targeting chitin synthase A reveal a great potential for pest management of the hemipteran insect *Nilaparvata lugens*. *Pest. Manag. Sci.* 73, 1529–1537. doi: 10.1002/ps.4492

Liberman, Z., and Eldar-Finkelman, H. (2005). Serine 332 phosphorylation of insulin receptor substrate-1 by glycogen synthase kinase-3 attenuates insulin signaling. *J. Biol. Chem.* 280, 4422–4428. doi: 10.1074/jbc.M410610200

Liu, X., and Klein, P. S. (2018). Glycogen synthase kinase-3 and alternative splicing. *Wiley Interdiscip. Rev. RNA* 9:e1501. doi: 10.1002/wrna.1501

Liu, X. J., Sun, Y. W., Li, D. Q., Li, S., Ma, E. B., and Zhang, J. Z. (2018). Identification of LmUAP1 as a 20-hydroxyecdysone response gene in the chitin biosynthesis pathway from the migratory locust, *Locusta migratoria*. *Insect Sci.* 25, 211–221. doi: 10.1111/1744-7917.12406

Lu, K., Chen, X., Li, W. R., Li, Y., Zhang, Z. C., and Zhou, Q. (2018). Insulin-like peptides and DNA/tRNA methyltransferases are involved in the nutritional

regulation of female reproduction in *Nilaparvata lugens* (Stål). *Gene* 639, 96–105. doi: 10.1016/j.gene.2017.10.011

Maqbool, M., Mobashir, M., and Hoda, N. (2016). Pivotal role of glycogen synthase kinase-3: a therapeutic target for Alzheimer's disease. *Eur. J. Med. Chem.* 107, 63–81. doi: 10.1016/j.ejmech.2015.10.018

Masumura, M., Satake, S., Saegusa, H., and Mizoguchi, A. (2000). Glucose stimulates the release of bombyxin, an insulin-related peptide of the silkworm *Bombyx mori*. *Gen. Comp. Endocrinol.* 118, 393–399. doi: 10.1006/gcen.1999.7438

Matsuda, H., Yamada, T., Yoshida, M., and Nishimura, T. (2015). Flies without trehalose. *J. Biol. Chem.* 290, 1244–1255. doi: 10.1074/jbc.M114.619411

Mattila, J., and Hietakangas, V. (2017). Regulation of carbohydrate energy metabolism in *Drosophila melanogaster*. *Genetics* 207, 1231–1253. doi: 10.1534/genetics.117.199885

McManus, E. J., Sakamoto, K., Armit, L. J., Ronaldson, L., Shpiro, N., Marquez, R., et al. (2005). Role that phosphorylation of GSK3 plays in insulin and Wnt signalling defined by knockin analysis. *Embo J.* 24, 1571–1583. doi: 10.1038/sj.emboj.7600633

Merzendorfer, H. (2006). Insect chitin synthases: a review. *J. Comp. Physiol. B* 176, 1–15. doi: 10.1007/s00360-005-0005-3

Merzendorfer, H. (2011). The cellular basis of chitin synthesis in fungi and insects: common principles and differences. *Eur. J. Cell Biol.* 90, 759–769. doi: 10.1016/j.ejcb.2011.04.014

Merzendorfer, H., and Zimoch, L. (2003). Chitin metabolism in insects: structure, function and regulation of chitin synthases and chitinases. *J. Exp. Biol.* 206, 4393–4412. doi: 10.1242/jeb.00709

Mitsumasu, K., Kanamori, Y., Fujita, M., Iwata, K., Tanaka, D., Kikuta, S., et al. (2010). Enzymatic control of anhydrobiosis-related accumulation of trehalose in the sleeping chironomid, *Polypedilum vanderplanki*. *FEBS J.* 277, 4215–4228. doi: 10.1111/j.1742-4658.2010.07811.x

Murphy, K. A., Tabuloc, C. A., Cervantes, K. R., and Chiu, J. C. (2016). Ingestion of genetically modified yeast symbiont reduces fitness of an insect pest via RNA interference. *Sci. Rep.* 6:22587. doi: 10.1038/srep22587

Mury, F. B., Lugon, M. D., Da Fonseca, R. N., Silva, J. R., Berni, M., Araujo, H. M., et al. (2016). Glycogen Synthase Kinase-3 is involved in glycogen metabolism control and embryogenesis of *Rhodnius prolixus*. *Parasitology* 143, 1569–1579. doi: 10.1017/S0031182016001487

Muthukrishnan, S., Arakane, Y., Yang, Q., Zhang, C. X., Zhang, J., Zhang, W., et al. (2018). Future questions in insect chitin biology: a microreview. *Arch. Insect. Biochem. Physiol.* 98:e21454. doi: 10.1002/arch.21454

Nagy, L., Márton, J., Vida, A., Kis, G., Bokor, É, Kun, S., et al. (2018). Glycogen phosphorylase inhibition improves beta cell function. *Br. J. Pharmacol.* 175, 301–319. doi: 10.1111/bph.13819

Paithankar, J. G., Raghu, S. V., and Patil, R. K. (2018). Concomitant changes in radiation resistance and trehalose levels during life stages of *Drosophila melanogaster* suggest radio-protective function of trehalose. *Int. J. Radiat. Biol.* 94, 576–589. doi: 10.1080/09553002.2018.1460499

Pan, B. Y., Li, G. Y., Wu, Y., Zhou, Z. S., Zhou, M., and Li, C. (2019). Glucose utilization in the regulation of chitin synthesis in brown planthopper. *J. Insect Sci.* 19:3. doi: 10.1093/jisesa/iez081

Prats, C., Graham, T. E., and Shearer, J. (2018). The dynamic life of the glycogen granule. *J. Biol. Chem.* 293, 7089–7098. doi: 10.1074/jbc.R117.802843

Qiu, J., He, Y., Zhang, J., Kang, K., Li, T., and Zhang, W. (2016). Discovery and functional identification of fecundity-related genes in the brown planthopper by large-scale RNA interference. *Insect. Mol. Biol.* 25, 724–733. doi: 10.1111/imb.12257

Roach, P. J., Depaoli-Roach, A. A., Hurley, T. D., and Tagliabracci, V. S. (2012). Glycogen and its metabolism: some new developments and old themes. *Biochem. J.* 441, 763–787. doi: 10.1042/BJ20111416

Santiago-Martínez, M. G., Encalada, R., Lira-Silva, E., Pineda, E., Gallardo-Pérez, J. C., Reyes-García, M. A., et al. (2016). The nutritional status of *Methanosarcina acetivorans* regulates glycogen metabolism and gluconeogenesis and glycolysis fluxes. *FEBS J.* 283, 1979–1999. doi: 10.1111/febs.13717

Sato, A., and Shibuya, H. (2018). Glycogen synthase kinase 3ß functions as a positive effector in the WNK signaling pathway. *PLoS One* 13:e0193204. doi: 10.1371/journal.pone.0193204

Semaniuk, U. V., Gospodaryov, D. V., Feden'ko, K. M., Yurkevych, I. S., Vaiserman, A. M., Storey, K. B., et al. (2018). Insulin-like peptides regulate feeding preference and metabolism in *Drosophila*. *Front. Physiol.* 9:1083. doi: 10.3389/fphys.2018.01083

Shi, J. F., Mu, L. L., Chen, X., Guo, W. C., and Li, G. Q. (2016). RNA interference of chitin synthase genes inhibits chitin biosynthesis and affects larval performance in *Leptinotarsa decemlineata* (Say). *Int. J. Biol. Sci.* 12, 1319–1331. doi: 10.7150/ijbs.14464

Shukla, E., Thorat, L. J., Nath, B. B., and Gaikwad, S. M. (2015). Insect trehalase: physiological significance and potential applications. *Glycobiology* 25, 357–367. doi: 10.1093/glycob/cwu125

Tamang, A. M., Kalra, B., and Parkash, R. (2017). Cold and desiccation stress induced changes in the accumulation and utilization of proline and trehalose in seasonal populations of *Drosophila immigrans*. *Comp. Biochem. Physiol. A Mol. Integr. Physiol.* 203, 304–313. doi: 10.1016/j.cbpa.2016

Tang, B., Chen, J., Yao, Q., Pan, Z. Q., Xu, W. H., Wang, S. G., et al. (2010). Characterization of a trehalose-6-phosphate synthase gene from *Spodoptera exigua* and its function identification through RNA interference. *J. Insect. Physiol.* 56, 813–821. doi: 10.1016/j.jinsphys.2010.02.009

Tang, B., Wang, S., Wang, S. G., Wang, H. J., Zhang, J. Y., and Cui, S. Y. (2018). Invertebrate trehalose-6-phosphate synthase gene: genetic architecture, biochemistry, physiological function, and potential applications. *Front. Physiol.* 9:30. doi: 10.3389/fphys.2018.00030

Tang, B., Wei, C. J., Wang, S. G., and Zhang, W. Q. (2012). Progress in gene features and functions of insect trehalases. *Acta Entomol. Sin.* 55, 1315–1321. doi: 10.16380/j.kcxb.2012.11.008

Tang, B., Wei, P., Zhao, L. N., Shi, Z. K., Shen, Q. D., Yang, M. M., et al. (2016). Knockdown of five trehalase genes using RNA interference regulates the gene expression of the chitin biosynthesis pathway in *Tribolium castaneum*. *BMC Biotechnol.* 16:67. doi: 10.1186/s12896-016-0297-2

Tang, B., Yang, M. M., Shen, Q. D., Xu, Y. X., Wang, H. J., and Wang, S. G. (2017). Suppressing the activity of trehalase with validamycin disrupts the trehalose and chitin biosynthesis pathways in the rice brown planthopper, *Nilaparvata lugens*. *Pestic. Biochem. Physiol.* 137, 81–90. doi: 10.1016/j.pestbp.2016.10.003

Thompson, S. N., Borchardt, D. B., and Wang, L. W. (2003). Dietary nutrient levels regulate protein and carbohydrate intake, gluconeogenic/glycolytic flux and blood trehalose level in the insect *Manduca sexta L. J. Comp. Physiol. B* 173, 149–163. doi: 10.1007/s00360-002-0322-8

Ugrankar, R., Berglund, E., Akdemir, F., Tran, C., Kim, M. S., Noh, J., et al. (2015). *Drosophila* glucome screening identifies Ck1alpha as a regulator of mammalian glucose metabolism. *Nat. Commun.* 6:7102. doi: 10.1038/ncomms8102

Wang, P., and Granados, R. R. (2010). Molecular structure of the peritrophic membrane (PM): identification of potential PM target sites for insect control (p 110-118). *Arch. Insect. Biochem. Physiol.* 2, 110–118. doi: 10.1002/arch.1041

Wei, C., and Wei, H. X. (2015). Expression analysis of GSK-3β in diapause pupal brains in the cotton bollworm. *Helicoverpa armigera*. *Insect Sci.* 22, 597–605. doi: 10.1111/1744-7917.12215

Wen, X., Wang, S., Duman, J. G., Arifin, J. F., Juwita, V., Goddard, W. A., et al. (2016). Antifreeze proteins govern the precipitation of trehalose in a freezing-avoiding insect at low temperature. *Proc. Natl. Acad. Sci. U.S.A.* 113, 6683–6688. doi: 10.1073/pnas.1601519113

Woodgett, J. R., Plyte, S. E., Pulverer, B. J., Mitchell, J. A., and Hughes, K. (1993). Roles of glycogen synthase kinase-3 in signal transduction. *Biochem. Soc. Trans.* 21, 905–907. doi: 10.1042/bst0210905

Xi, Y., Pan, P. L., Ye, Y. X., Yu, B., Xu, H. J., and Zhang, C. X. (2015). Chitinase-like gene family in the brown planthopper, *Nilaparvata lugens*. *Insect. Mol. Biol.* 24, 29–40. doi: 10.1111/imb.12133

Xu, G. F., Zhang, J., Lyu, H., Liu, J., Ding, Y., Feng, Q., et al. (2017). BmCHSA-2b, a Lepidoptera specific alternative splicing variant of epidermal chitin synthase, is required for pupal wing development in *Bombyx mori*. *Insect. Biochem. Mol. Biol.* 87, 117–126. doi: 10.1016/j.ibmb.2017

Yamada, T., Habara, O., Kubo, H., and Nishimura, T. (2018). Correction: fat body glycogen serves as a metabolic safeguard for the maintenance of sugar levels in *Drosophila*. *Development* 145:dev165910. doi: 10.1242/dev.165910

Yang, M. M., Zhao, L. N., Shen, Q. D., Xie, G. Q., Wang, S. G., and Tang, B. (2017). Knockdown of two trehalose-6-phosphate synthases severely affects chitin metabolism gene expression in the brown planthopper *Nilaparvata lugens*. *Pest. Manag. Sci.* 73, 206–216. doi: 10.1002/ps.4287

Yang, W. J., Wu, Y. B., Chen, L., Xu, K. K., Xie, Y. F., and Wang, J. J. (2015). Two chitin biosynthesis pathway genes in *Bactrocera dorsalis* (Diptera:

Tephritidae): molecular characteristics, expression patterns, and roles in Larval-Pupal transition. *J. Econ. Entomol.* 108, 2433–2442. doi: 10.1093/jee/tov186

Yang, Y. X., Xu, S. X., Xu, J. X., Guo, Y., and Yang, G. (2014). Adaptive evolution of mitochondrial energy metabolism genes associated with increased energy demand in flying insects. *PLoS One* 9:e99120. doi: 10.1371/journal.pone.0099120

Yasugi, T., Yamada, T., and Nishimura, T. (2017). Adaptation to dietary conditions by trehalose metabolism in *Drosophila*. *Sci. Rep.* 7:1619. doi: 10.1038/s41598-017-01754-9

Yu, N., Christiaens, O., Liu, J., Niu, J., Cappelle, K., Caccia, S., et al. (2013). Delivery of dsRNA for RNAi in insects: an overview and future directions. *Insect Sci.* 20, 4–14. doi: 10.1111/j.1744-7917.2012.01534

Zhang, J. L., Yuan, X. B., Chen, S. J., Chen, H. H., Xu, N., Xue, W. H., et al. (2018). The histone deacetylase NlHDAC1 regulates both female and male fertility in the brown planthopper, *Nilaparvata lugens*. *Open Biol.* 8:180158. doi: 10.1098/rsob.180158

Zhang, L., Qiu, L. Y., Yang, H. L., Wang, H. J., Zhou, M., Wang, S. G., et al. (2017a). Study on the effect of wing bud chitin metabolism and its developmental network genes in the Brown Planthopper, *Nilaparvata lugens,* by knockdown of *TRE* gene. *Front. Physiol.* 8:750. doi: 10.3389/fphys.2017.00750

Zhang, L., Wang, H. J., Chen, J. Y., Shen, Q. D., Wang, S. G., Xu, H. X., et al. (2017b). Glycogen phosphorylase and glycogen synthase: gene cloning and expression analysis reveal their role in trehalose metabolism in the Brown Planthopper, *Nilaparvata lugens Stål* (Hemiptera: Delphacidae). *J. Insect. Sci.* 17:42. doi: 10.1093/jisesa/iex015

Zhao, L. N., Wei, P., Guo, H. S., Wang, S. G., and Tang, B. (2014). Suppressing the expression of a forkhead transcription factor disrupts the chitin biosynthesis pathway in Spodoptera exigua. *Arch. Insect. Biochem. Physiol.* 86, 4–18. doi: 10.1002/arch.21145

Zhao, L. N., Yang, M. M., Shen, Q. D., Liu, X. J., Shi, Z. K., Wang, S. G., et al. (2016). Functional characterization of three trehalase genes regulating the chitin metabolism pathway in rice brown planthopper using RNA interference. *Sci. Rep.* 6:27841. doi: 10.1038/srep27841

Zhu, J. J., Jiang, F., Wang, X. H., Yang, P. C., Bao, Y. Y., Zhao, W., et al. (2017). Genome sequence of the small brown planthopper, *Laodelphax striatellus*. *GigaScience* 6, 1–12. doi: 10.1093/gigascience/gix109

Zhu, K. Y., Merzendorfer, H., Zhang, W., Zhang, J., and Muthukrishnan, S. (2016). Biosynthesis, turnover, and functions of chitin in insects. *Annu. Rev. Entomol.* 61, 177–196. doi: 10.1146/annurev-ento-010715-023933

Conflict of Interest: The authors declare that the research was conducted in the absence of any commercial or financial relationships that could be construed as a potential conflict of interest.

frontiers in Physiology

ORIGINAL RESEARCH
published: 16 December 2020
doi: 10.3389/fphys.2020.596729

Anise Hyssop *Agastache foeniculum* Increases Lifespan, Stress Resistance, and Metabolism by Affecting Free Radical Processes in *Drosophila*

*Olha M. Strilbytska[1], Alina Zayachkivska[1], Alexander Koliada[2], Fabio Galeotti[3], Nicola Volpi[3], Kenneth B. Storey[4], Alexander Vaiserman[2] and Oleh Lushchak[1]**

[1] Department of Biochemistry and Biotechnology, Vasyl Stefanyk Precarpathian National University, Ivano-Frankivsk, Ukraine, [2] D.F. Chebotarev Institute of Gerontology, National Academy of Medical Sciences (NAMS), Kyiv, Ukraine, [3] Department of Life Sciences, University of Modena and Reggio Emilia, Modena, Italy, [4] Department of Biology, Carleton University, Ottawa, ON, Canada

Anise hyssop, *Agastache foeniculum*, is a widely used medicinal herb with known antioxidant properties. We studied how dietary supplementation with dried *A. foeniculum* leaf powder affected physiological and metabolic traits as well as activities of antioxidant enzymes and markers of oxidative stress in *Drosophila melanogaster*. Dietary hyssop extended the lifespan in a sex and genotype independent manner over a broad range of concentrations up to 30 mg/ml. Dietary supplementation with the herb significantly increased fecundity, resistance to oxidative stress and starvation. Higher transcript levels of *Drosophila* insulin-like peptide (*dilp2*) and decreased *dilp3* and *dilp6* transcripts together with increased levels of glycogen and triacylglycerols support an alteration of insulin signaling by the plant extract. Increased enzymatic activities of superoxide dismutase and aconitase as well as elevated protein and low molecular mass thiols also supported an alteration of free radical process in flies treated with dietary *A. foeniculum* leaf powder. Thus, physiological and metabolic traits as well as free radical processed may be affected by active compounds detected in extracts of anise hyssop leaves and contribute to the increased lifespan and reproductive (egg-laying) activity observed.

Keywords: ***Agastache foeniculum*, lifespan, metabolism, oxidative stress, *Drosophila***

OPEN ACCESS

Edited by:
Elzbieta M. Pyza, Jagiellonian University, Poland

Reviewed by:
Jean-René Martin, UMR 9197 Institut des Neurosciences Paris Saclay (Neuro-PSI), France
Pamela Menegazzi, Julius Maximilian University of Würzburg, Germany

****Correspondence:***
Oleh Lushchak
oleh.lushchak@pnu.edu.ua

Specialty section:
This article was submitted to Invertebrate Physiology, a section of the journal Frontiers in Physiology

Received: *20 August 2020*
Accepted: *26 November 2020*
Published: *16 December 2020*

Citation:
Strilbytska OM, Zayachkivska A, Koliada A, Galeotti F, Volpi N, Storey KB, Vaiserman A and Lushchak O (2020) Anise Hyssop Agastache foeniculum Increases Lifespan, Stress Resistance, and Metabolism by Affecting Free Radical Processes in Drosophila. Front. Physiol. 11:596729. doi: 10.3389/fphys.2020.596729

INTRODUCTION

Anti-aging pharmacology is an extremely promising field as it could allow humans to substantially increase lifespan and healthspan (Vaiserman and Lushchak, 2017; Piskovatska et al., 2019). Aging is a normal physiological process that is regulated by a set of genes and signaling pathways that are evolutionarily conserved in eukaryotes. Recent research has concentrated on the influence of different naturally occurring compounds on the lifespan of model organisms. Pathways controlling lifespan and aging are partially conserved in a wide range of species, from yeast to humans (Bitto et al., 2015; Fontana and Partridge, 2015). *Drosophila melanogaster* is emerging as an important model to study anti-aging medications. Since *D. melanogaster* can be easily manipulated genetically and experimentally, it has served as a good model for examining the anti-aging properties of

resveratrol (Bass et al., 2007; Wang et al., 2013), 4-phenylbutyrate (Kang et al., 2002), caffeine (Nikitin et al., 2008), curcumin (Lee et al., 2010), statin (Spindler et al., 2012), *Rhodiola rosea* (Gospodaryov et al., 2013), *Rosa damascena* (Schriner et al., 2012), blueberry extract (Peng et al., 2012), and many other natural compounds.

Longevity can be modulated by preventing age-related diseases, including cardiovascular disease, type 2 diabetes, cancer and Alzheimer's disease. It is well-known that dietary antioxidants play potential roles in the prevention of age-related diseases (Meydani, 2001). Numerous studies have shown that plant extracts from *R. rosea* or *Ludwigia octovalvis* can extend lifespan of more than one model organism. In *Drosophila, R. rosea* delayed an age-related decline of locomotor activity and increased stress resistance (Gospodaryov et al., 2013), whereas *Theobroma cacao* increased lifespan in *D. melanogaster* due to its antioxidant properties (Bahadorani and Hilliker, 2008). Being known for its powerful antioxidant activity, antibacterial and hepatoprotective properties, rosemary extract (*Rosmarinus officinalis* L.) produced a longevity phenotype in *Drosophila* that was associated with increased superoxide dismutase and catalase activities (Wang et al., 2017). Extended lifespan was also observed when fruit flies were fed *L. octovalvis* that is a rich in antioxidants including polyphenolic compounds, phytosterols, and squalene in either regular or high-calorie diets (Lin et al., 2014).

Among herbs and spices, *Agastache foeniculum* (AF), known as anise hyssop, has been given much attention in particular for its high antioxidant activity and is often used for the production of essential oils. Traditional medicine applies AF for acute respiratory diseases, functional disorders of the gastrointestinal tract, and inflammatory diseases of the urinary system (Marcel et al., 2013). Three groups of compounds were identified in the essential oil of AF: monoterpenes (sylvestrene and 1-octen-3-ol acetate), phenylpropenes (methyl chavicol, eugenol, and methyl isoeugenol), and sesquiterpenes (β-caryophyllene, spathulenol, and caryophyllene oxide) (Ivanov et al., 2019). Studies have investigated the antimicrobial and antioxidant activity of hyssop essential oil (Ivanov et al., 2019), as well as antimutagenic, anti-nociceptive, anti-inflammatory and cytotoxic activity with cancer cell lines (Zielińska and Matkowski, 2014). Individual parts of the plant are used for different purposes but leaves are the most useful ones. Indeed, the leaves of hyssop can be used in herbal tea or added fresh in small quantities to a salad with other greens. The dried leaves can be used for medicinal purposes to treat coughs, fevers, wounds, and diarrhea. In this regard, we decided to evaluate the effect of AF on physiology, metabolism and free radical processes in *D. melanogaster*. We found that extracts of plant leaves are full of flavonoids and active compounds.

The results revealed that the lifespan of both sexes and two fly lines (*Canton S* and w^{1118}) was extended significantly by dietary supplementation with different concentrations of AF dry leaves. Furthermore, AF significantly increased fertility, climbing ability, and resistance to oxidative stress and starvation of *Canton S* flies. Enzymatic activities of aconitase and catalase were also significantly increased when *A. foeniculum* was consumed and *Canton S* flies fed diets with AF added displayed lower body glucose content, but, higher levels of stored glycogen and triglycerides.

MATERIALS AND METHODS

Analysis of Extracts by HPLC/MS

The composition of herbal extracts was analyzed using high-performance liquid chromatography (HPLC) with subsequent mass spectrometry. The high-performance liquid chromatography equipment was from Jasco (Tokyo, Japan) and included a pump (model PU-1580), UV detector (UV-1570), Rheodyne injector equipped with a 20 μL loop, and Jasco-Borwin software (rel. 1.5). Samples were separated using a 250 × 4.6-mm stainless-steel column Discovery-C18 4 μm 80 Ä (from Sigma-Aldrich). The eluates were (A) 0.5% acetic acid and (B) acetonitrile. Separations were performed at room temperature by solvent gradient elution from 0 min at 50% A/50% B to 60 min at 100% B at a flow rate of 0.8 mL/min. A UV detector set at 260 nm was also used on-line with the HPLC equipment. An Agilent 1100 VL series mass spectrometer (Agilent Technologies, Inc., Santa Clara, CA, United States) was further used on-line with the HPLC equipment. The electrospray interface was set in negative ionization mode with a capillary voltage of 3,500 V and a temperature source of 350°C in full scan spectra (200–2,200 Da, 10 full scans/s). Nitrogen was used as a drying (9 L/min) anebulizing gas (11 p.s.i.). Software versions were 4.0 LC/MSD trap control 4.2 and Data Analysis 2.2 (Agilent Technologies, Inc.).

Antioxidant Properties

Dry crushed leaves of *Agastache foeniculum* were purchased from a local store in Ivano-Frankivsk (Ukraine). Leaves were ground to a powder and an aqueous extraction was performed by adding the powder to hot water (85–90°C) in concentrations of 2.5, 5, 10, or 30 mg/ml. Liquid extracts were filtered and kept at 4°C for 24 h. Extracts were used the next day for experiments. This protocol of extraction was used because it closely matched the conditions for preparing food for fly experiments in which leaf powder was added into hot fly food (85–90°C) that was then poured into vials and kept at 4°C before use. To assess the antioxidant of ability, plant extracts were assessed for their ability to scavenge $ABTS^{+}$ radical cations or reduce ferric ions were determined as described previously (Bayliak et al., 2016).

Resistance to Starvation and Oxidative Stress

Flies of *Canton S* strain were fed control or experimental food (5 or 10 mg/ml plant powder) for 30 days. Flies were separated under light CO_2 anesthesia and kept overnight for recovery. Starvation resistance was measured in flies given only 1% agar as a food source. To study resistance to oxidative stress 25–30 flies of each experimental cohort were transferred into empty vials for 2 h for starvation. After starvation, flies were transferred into vials containing folded and rammed strips (2.4 × 12 cm) of 4-layer cellulose filter paper soaked with 0.8 ml of 20 mM menadione in 5% sucrose solution (Lushchak et al., 2014). Dead flies were

counted at 9 a.m., 3 p.m., and 9 p.m. Stress resistance was expressed as the percentage of flies that survived over the time.

Enzyme Activities

Flies, fed control or herb-supplemented diet for 30 days were fixed by freezing in liquid nitrogen and kept at −80°C before use. For analysis were homogenized using a Potter-Elvejhem glass homogenizer (1:10 w:v) in cold 50 mM potassium phosphate buffer, pH 7.5, containing 0.5 mM EDTA and 1 mM phenylmethylsulfonyl fluoride. Centrifugation was performed at 16,000 g for 15 min at 4°C in an Eppendorf 5415R centrifuge (Germany). The supernatants were collected and used for the determination of enzyme activities.

The activities of superoxide dismutase (SOD) and catalase were measured as described previously (Lozinsky et al., 2012). Briefly, SOD activity was assayed at 406 nm by inhibition of quercetin oxidation by superoxide anion. One unit of SOD activity was defined as the amount of soluble protein that inhibited the maximum rate of quercetin oxidation by 50%. Catalase activity was determined by the rate of hydrogen peroxide decomposition at 240 nm. Enzyme activity was calculated using an extinction coefficient for hydrogen peroxide of 39.4 M^{-1} cm^{-1}.

Aconitase activity was measured as a decrease in substrate concentration as described earlier (Lozinsky et al., 2013). Briefly, the decrease in absorbance at 240 nm was followed for 2 min and the extinction coefficient used for calculations was 3.701 M^{-1} cm^{-1} for cis-aconitate.

All reactions were started by addition of enzyme supernatant. Activities were measured at 25°C and expressed per milligram of soluble protein in the supernatant.

Protein and Low Molecular Mass Thiols

The content of free thiols was determined by the Ellman's method using DTNB, as described previously (Lushchak et al., 2011). The content of protein thiols groups was calculated as the difference between total and low molecular mass thiols. The content of protein thiols was expressed as μmol per mg protein and low molecular weight thiols as mg per mg of wet weight.

Fly Stocks and Rearing

Fruit flies of *Canton S* (BDRC #64349) and w^{1118} (BDRC #3605) strains were obtained from Bloomington Stock Center (Bloomington, IN, United States). The flies were cultured in a standard molasses medium (7.5% molasses, 5% yeast, 6% corn, 1% agar, 0.18% methylparaben) in uncrowded (70–100 eggs/vial) conditions at 25°C, 60% humidity and photoperiod 12 L:12 D. *Canton S* flies were used throughout this study whereas flies of the w^{1118} strain were used only for lifespan assay.

Lifespan

Newly eclosed flies were transferred into fresh food and kept for 3 days for mating. Then flies were separated by sex under light CO_2 anesthesia and kept for another day for recovery. About 150 flies of each strain and sex were gently transferred to 1.5 L demographic cages with an attached plastic vial filled with 5 ml control food or experimental food supplemented with different concentrations of anise hyssop (*A. foeniculum*) dry crushed leaves. The standard medium consisted of 5% of dry yeast, 5% of sucrose, 1.2% agar, and 0.18% methylparaben. Herbal powder was directly added to the experimental food (t = 70°C) in different concentrations (2.5, 5, 10, or 30 mg/ml). Food was changed every second day, and dead flies were removed and recorded. The experiment was run in two biological replicates. To study the effects of different yeast concentrations, diet with 5% yeast was defined as 1×. Yeast content was changed to 0.25% to obtain 0.05× diet, 1% to obtain 0.2× diet and 20% to get 4× diet. All experimental diets were supplemented with 5 or 10 mg/ml of herb powder.

Fecundity

To determine the impact of anise hyssop on fruit fly fecundity 20 female flies were placed into demographic cage supplemented with food vial. Amount of laid eggs was counted 24 h after fresh food was applied. The measurements were repeated every 3 days up to day 30. Four groups of flies were tested per condition.

Negative Geotaxis and Heat Shock Resistance

Flies were fed control or herb supplemented diet for 30 days. Negative geotaxis, sensitivity and recovery after heat shock were measured as described in Lushchak et al. (2012).

Glucose, Trehalose, Glycogen, and TAG

Flies were fed experimental diets for 30 days and that used for measurements of metabolites. Flies were decapitated and centrifuged 5 min at 3,000 g to extract hemolymph (Perkhulyn et al., 2015). Pre-weighted whole flies were homogenized in 50 mM sodium phosphate buffer pH 6.5 (1:10 w/v) and centrifuged. Resulted supernatants were used for the determination of glucose, glycogen and trehalose contents. Measurements were performed using a glucose assay kit (Liquick Cor-Glucose diagnostic kit, Cormay, Poland). Glycogen was converted into glucose by incubation with amyloglucosidase from *Aspergillus niger* at 25°C for 4 h followed by measuring glucose. Trehalose was determined in samples after incubation with porcine trehalase to digest trehalose into glucose. For TAG estimation weighed flies were homogenized in 200 mM PBST (phosphate buffered saline containing 0.05% Triton X100), boiled and centrifuged for 10 min at 13,000 g (Rovenko et al., 2015). TAG levels were measured using a diagnostic kit Liquick Cor-TG (PZ 290 Cormay S.A., Łomianki, Poland) following the manufacturer's instructions. TAG levels were expressed as milligrams per gram of wet weight (mg/gww).

Gene Expression

Total RNA from heads or whole flies was extracted using an RNeasy Plus Mini Kit (Qiagen), concentration was measured, and 2 μg of total RNA were into converted cDNA with QuantiTect Reverse Transcription Kit (Qiagen). Expression of genes of interest was measured using an ABI Prism 7000 instrument (Applied Biosystems), a SensiFAST SYBR Hi-ROX Kit, and a

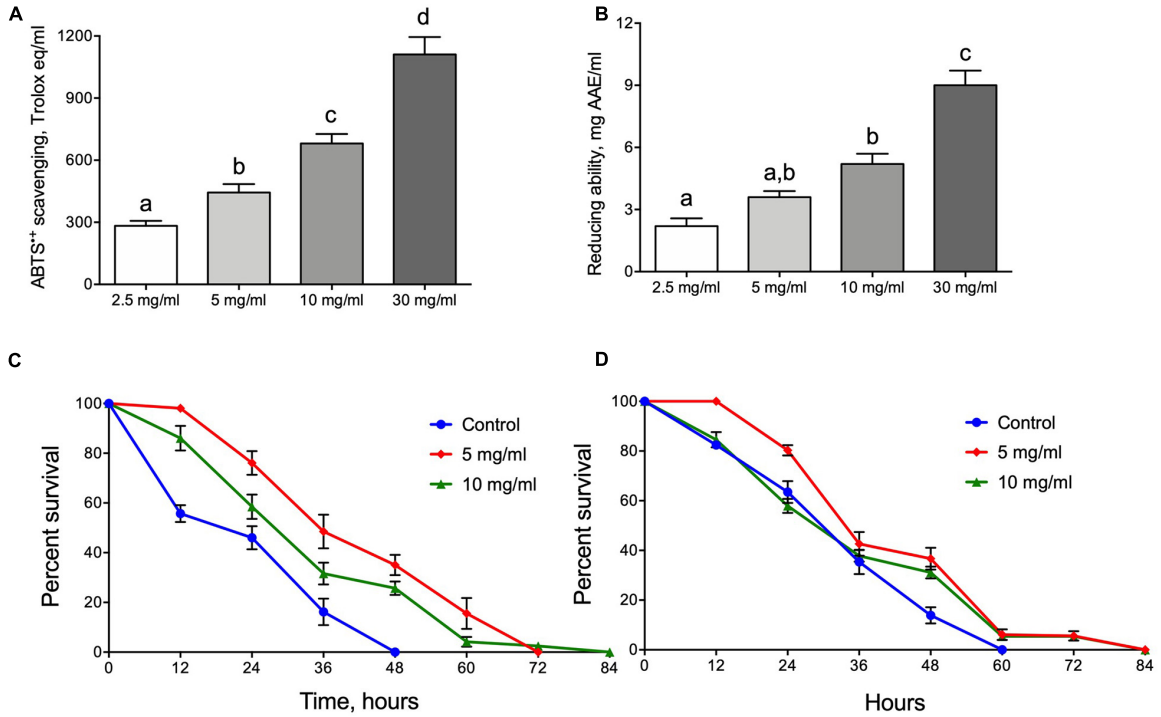

FIGURE 1 | Antioxidant and protective properties of Hyssop extracts. ABTS^{+} radical scavenging activity **(A)** and ability to reduce ferric ions **(B)**. Resistance of male **(C)** and female **(D)** flies to oxidative stress induced by menadione. Data shown in **(A,B)** represent mean ± SEM for four independent extractions. Different letters on **(A,B)** represent groups significantly different from each other ($p < 0.05$).

QuantiTect SYBR Green PCR Kit (Qiagen) under conditions recommended by the manufacturer. Levels of mRNA were measured in heads (*dilp2, 3,* and *5*) or whole flies (*dilp6, akh, 4ebp, tobi, pepck, bmm*). Each analytical and standard reaction was performed in three technical replicates. The ΔΔCt method was used with rp49 as the reference gene. All primers were as described earlier (Lushchak et al., 2015).

Statistical Analysis

Fly lifespans and survival under starvation or oxidative stress were compared by a Log Rank test. Activities of antioxidant enzymes, markers of oxidative stress and levels of metabolites were analyzed by a two-way ANOVA followed by a Dunnett's multiple comparison test. Levels of specific mRNAs were compared by a Student's *t*-test. Significant differences between groups were accepted by a *p*-value < 0.05. Statistical analysis was performed in Prism Graphpad 5 (GraphPad Software, San Diego, CA, United States).

RESULTS

Active Compounds in Extract of *Agastache foeniculum*

Analysis of *A. foeniculum* extract with HPLC-MS identified the presence of many bioactive species previously described to possess beneficial properties. We detected acacetin, apigenin, 3-O-caffeoylquinic acid, calycosin, caffeic acid, 6,7-Dimethoxyquercetin 3-O-glucopyranoside, genistein, kaempferol 3-O-glucoside, rosmarinic acid, tilianin, ursolic acid, and β-sitosterol in significant amounts (**Supplementary Table S1**). These active compounds have been previously shown to increase the life- and healthspan of different model organisms including *Drosophila*. Moreover, varied additional benefits were described in relation to protection against oxidative stress.

Antioxidant Properties of *A. foeniculum* Extract and Fly Resistance to Oxidative Stress

The antioxidant properties of water extracts of *A. foeniculum* leaves were tested for their ability to scavenge ABTS^{+} radical cations or reduce ferric ions. An extract made of the herb at a concentration of 2.5 mg/ml had scavenging activity of ∼300 Trolox equivalents (**Figure 1A**). A further increase in herb concentration during extraction did not linearly increase the ability to scavenge ABTS cation. The activity was about 50% higher for the 5 mg/ml extract. Further increases of herb content to 10 and 30 mg/ml increased scavenging ability by approximately 2.2- and 3.3-fold (**Figure 1A**). A similar tendency was observed when the extracts were tested for the ability to reduce ferric ions (**Figure 1B**). Reducing ability was about 2.5 mg AAE/ml for the extract made with 2.5 mg/ml herb powder, whereas a 12-fold increase in herb content (30 mg/ml) increased the reduction ability by about 4-fold.

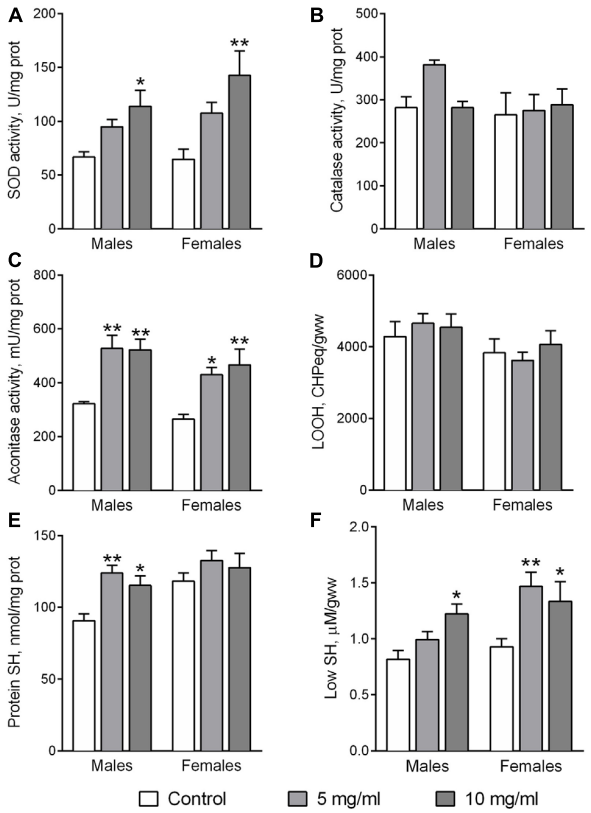

FIGURE 2 | Activities of antioxidant enzymes SOD **(A)**, catalase **(B)**, aconitase **(C)**, and the levels of lipid peroxides **(D)**, protein **(E)**, and low molecular weight thiols **(F)** in flies consuming control diet or diet supplemented with 5 or 10 mg/ml *A. foeniculum*. Results are presented as mean ± SEM of four replicates per group. Group comparisons were performed using Dunnett's test. Asterisks indicate significant difference from the control flies ($p < 0.05$).

Since the AF extracts were identified as having significant antioxidant activities it was logical to predict that flies fed diets supplemented with AF powder would be more resistant to oxidative stress induced by the redox cycling agent menadione. **Figure 1C** (male) and **Figure 1D** (female) show that flies fed diets with AF leaf powder were lived longer under oxidative stress exposure. Male flies fed diets with 5 or 10 mg/ml of AF powder were more resistant by 40 and 75%, respectively (Log Rank test, $p < 0.0001$) (**Figure 1C** and **Supplementary Table S2**). AF powder in concentration of 5 mg/ml increased female resistance by 20% as compared to control (Log Rank test, $p < 0.0001$) (**Figure 1D** and **Supplementary Table S2**).

Antioxidant Enzymes, Aconitase, and Markers of Oxidative Stress

The antioxidant enzymes superoxide dismutase (SOD) and catalase are involved in the detoxification of the reactive oxygen species (ROS) superoxide anion and hydrogen peroxide, respectively. The activity of SOD was affected by food supplementation with AF powder (**Figure 2A**). Fly treatment with AF supplemented food for 30 days at a concentration of 10 mg/ml significantly increased SOD activity in flies by 1.71-fold in males (Dunnett's test, $p = 0.014$) and 2.21-fold in females (Dunnett's test, $p = 0.010$). However, dietary AF did not influence the activity of catalase (**Figure 2B**).

Increased ROS production and/or a decrease of the detoxification potential can induce oxidative stress (Lushchak, 2014). This may be reflected by specific markers such as the activity of the ROS-sensitive enzyme aconitase, protein carbonyl groups, lipid peroxides, protein and low molecular mass thiol groups (Lushchak et al., 2011). A higher activity of aconitase was observed in flies of both sexes fed by diets supplemented with 5 or 10 mg/ml AF powder (**Figure 2C**). Activity increased by about 1.62-fold (Dunnett's test, $p = 0.003$) and 1.63-fold (Dunnett's test, $p = 0.03$) in male and female flies, respectively. Interestingly, fly feeding with an AF supplemented diet did not affect the contents of lipid peroxides (LOOH) (**Figure 2D**) and protein carbonyl groups (not shown). However, the antioxidant properties of AF in flies were reflected in reduced protein and low molecular weight thiol (Low SH) groups (**Figures 2E,F**). Higher contents of protein SH groups were observed in male flies fed diets with AF in concentrations of 5 mg/ml (Dunnett's test, $p = 0.005$) and 10 mg/ml ($p = 0.024$). Low SH contents, that are mostly represented by glutathione and cysteine, were significantly higher in flies fed diets with AF (**Figure 2F**). Diet supplementation with AF increased Low SH by 50% (Dunnett's test, $p = 0.011$) and 45% ($p = 0.05$) in male and female flies, respectively (**Figure 2F**).

Lifespan of Different Strains

Identification of nutritional supplements that can delay aging and extend lifespan is one of the most promising ways to improve the quality of life. To directly test whether *A. foeniculum* elicits beneficial effects on lifespan, we raised fruit flies on diets supplemented with of dried crushed leaves added to the food medium at different concentrations. The median lifespan control group of male *Canton S* flies lived approximately 34 days. Lifespan was significantly increased by 15% in male *Drosophila* line *Canton S* fed diets with 5, 10 mg/ml of AF powder or by 32% at 30 mg/ml (Log Rank test, $p < 0.03$) (**Figure 3A** and **Supplementary Table S3**). Female flies of the *Canton S* strain lived longer by 37, 33, 37, and 37% when fed diet with 2.5, 5, 10, and 30 mg/ml AF powder, respectively (Log Rank test, $p < 0.02$) (**Figure 3B** and **Supplementary Table S3**).

Dietary supplementation with *A. foeniculum* herb also extended the lifespan of male and female flies of another *Drosophila* strain, w^{1118} flies. Male flies that consumed foods with 2.5, 5, 10, or 30 mg/ml AF powder lived longer as compared to controls (Log Rank test, $p < 0.05$) (**Figure 3C** and **Supplementary Table S3**). We also observed longer lifespan in females, when the herb was added to the food at concentrations of 10 mg/ml (by 40%), 30 mg/ml (by 49%) (Log Rank test, $p < 0.0001$) (**Figure 3D** and **Supplementary Table S3**).

Lifespan on Diets With Different Yeast Contents

Dietary protein content is an important determinant of aging and lifespan that is mostly regulated by activity of TOR signaling

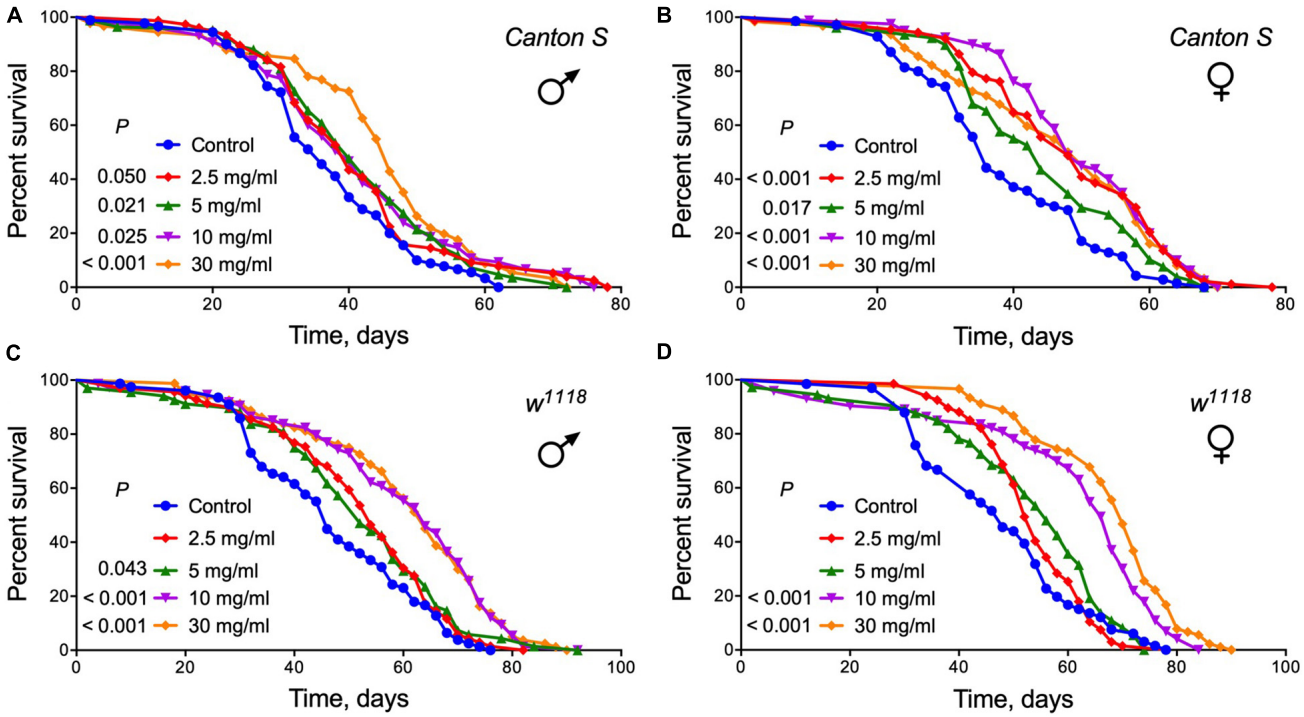

FIGURE 3 | Survival curves for flies of two different lines fed control diet vs. diets supplemented with *A. foeniculum* extract at four different concentrations. **(A)** males of *Canton S*; **(B)** females of *Canton S*; **(C)** males of w^{1118}; **(D)** females of w^{1118}. Each curve represents the percentage of alive flies within respect time. The cohorts were compared using a Log rank test (see **Supplementary Table S2** for complete statistics).

pathway (Kapahi et al., 2004, 2017; Soultoukis and Partridge, 2016; Lushchak et al., 2017, 2019). We observed higher survival of flies of both sexes when reared on media with 0.05× yeast content and AF powder at both 5 or 10 mg/ml concentrations (Log Rank test, $p \leq 0.0001$) (**Figures 4A,B** and **Supplementary Table S4**). Males and females also lived longer on 0.2× yeast (1%) containing medium with *A. foeniculum* (Log Rank test, $p < 0.02$) (**Figures 4C,D** and **Supplementary Table S4**). However, at a very high yeast content (4× or 20%) in conjunction with *A. foeniculum* survival was substantially lower compared with controls (Log Rank test, $p < 0.04$) (**Figures 4E,F** and **Supplementary Table S4**). Consequently, we detected the highest mean lifespan of both sexes at 10 mg/ml of *A. foeniculum* under 0.05×, 0.2×, and 1× yeast concentrations in the diet but the lowest mean lifespan occurred under 4× yeast content (**Figures 4G,H**).

Fecundity and Negative Geotaxis

Fertility and negative geotaxis are very important life history traits and are excellent indicators of overall health (Flatt, 2020). Early after eclosion, egg production rose in all three groups of adult flies tested (control, 5 and 10 mg/ml) with highest levels after about 12–15 days and a subsequent gradual decrease thereafter (**Figure 5A**). Flies fed with diets containing *A. foeniculum* (both 5 and 10 mg/ml) had significantly higher daily egg production on day 6 than controls but thereafter fecundity of the 10 mg/ml diet group dropped back by 21 days to at or below control levels. However, fecundity of flies on the 5 mg/ml diet remained significantly higher than controls from day 6 to 27. Consequently, AF has a positive impact on reproduction rate with more obvious effects at moderate concentration (5 mg/ml).

We observed that AF supplementation improved negative geotaxis response only in male flies (**Figure 5B**). Males that consumed a diet with 5 mg/ml *A. foeniculum* showed approximately 60% higher performance as compared to the control group (Dunnett's test, $p = 0.008$).

Resistance to Starvation and Heat Stress

To further explore beneficial effects of *A. foeniculum* on lifespan, we assessed effects of this supplement on stress resistance by examining responses of flies to experimental starvation conditions and high temperature. Flies fed diets with AF powder for 30 days demonstrated a longer lifespan under complete starvation conditions with significantly higher survival of male flies fed diets with of 5 mg/ml and 10 mg/ml AF concentrations (Log Rank test, $p \leq 0.0005$) (**Figure 5C**). Moreover, *A. foeniculum* supplementation to the medium led to higher starvation resistance in females fed by 10 mg/ml by 37% as compared to control (Log Rank test, $p = 0.003$) (**Figure 5D**). These data may suggest high nutritional value of the *A. foeniculum*.

We also examined the effect of *A. foeniculum* on the fly resistance to high temperature. Males, that consumed media supplemented with AF powder resisted heat shock significantly longer as compared to controls (**Figure 5E**). Moreover, the

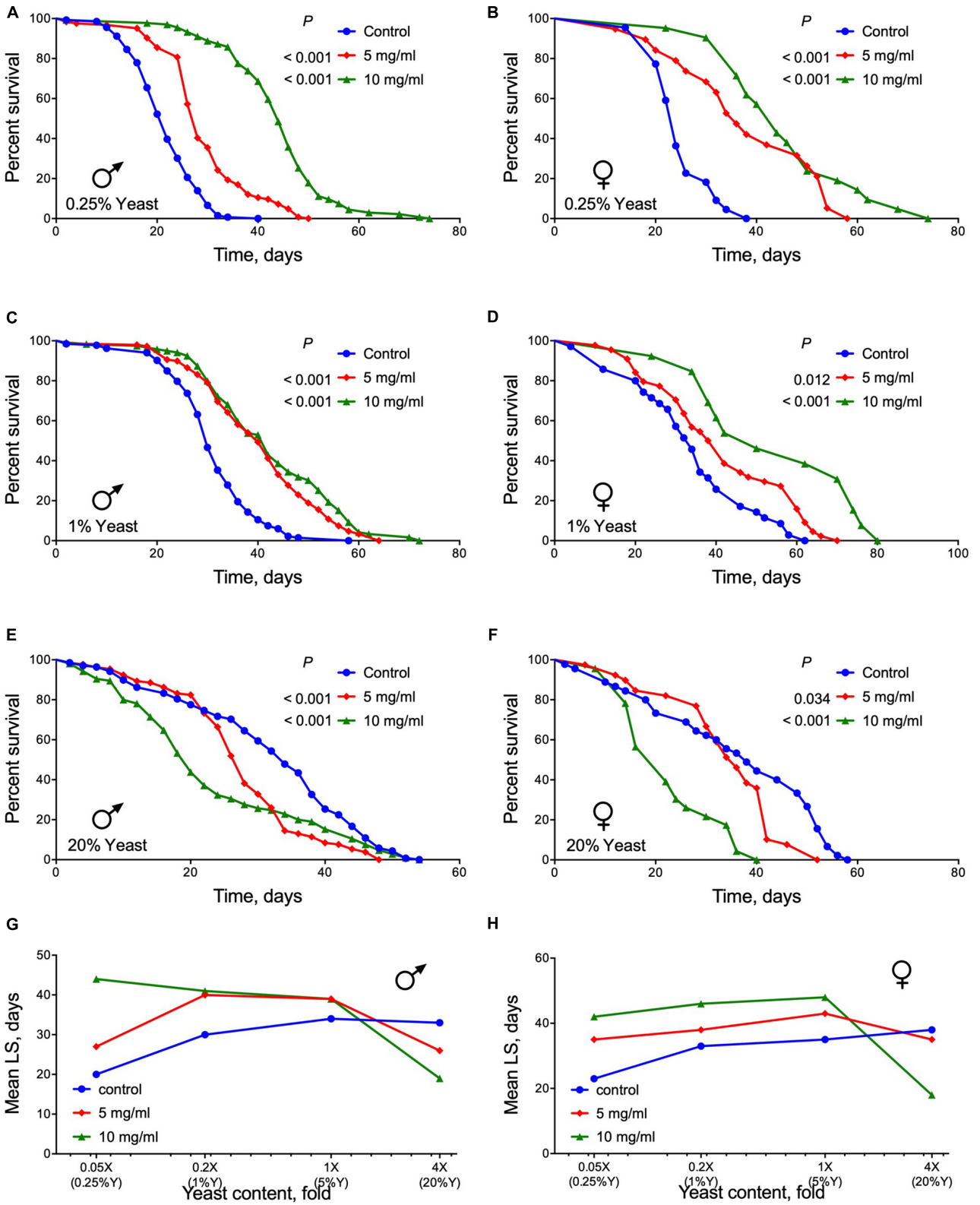

FIGURE 4 | Lifespan of flies fed diets with different concentrations of yeast and supplemented with AF in concentrations of 5 or 10 mg/ml. **(A,B)** show data for yeast concentration 0.05×, **(C,D)** 0.2×, **(E,F)** 4×. Data for male flies are shown in **(A,C,E)** and females in **(B,D,F)**. **(G,H)** show mean lifespan values for male and female flies, respectively.

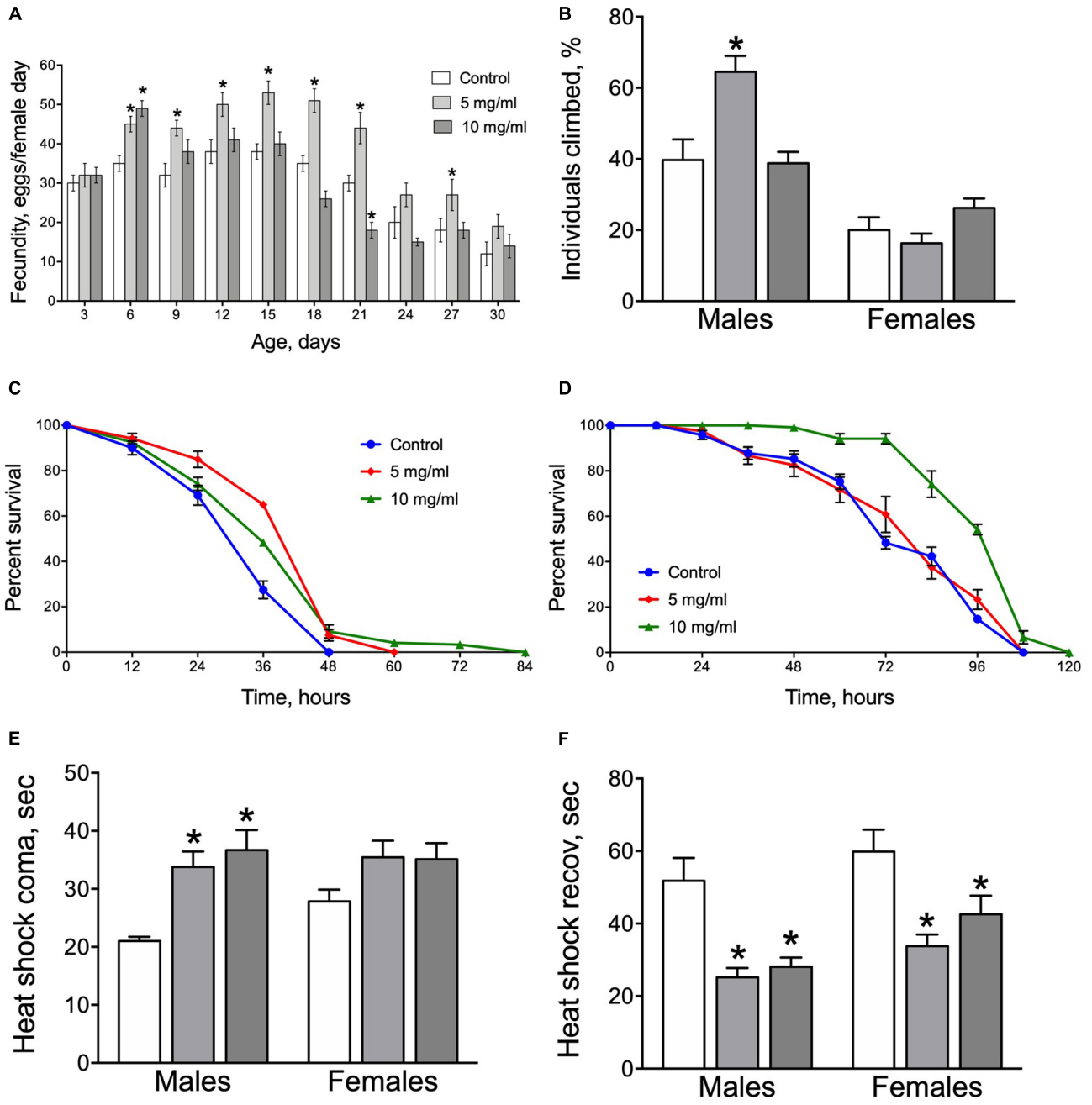

FIGURE 5 | Fecundity **(A)**, negative geotaxis **(B)**, resistance to starvation **(C,D)** and resistance to heat stress **(E)** and recovery **(F)** in flies fed diets supplemented with *A. foeniculum* leaf powder. Data are presented as mean ± SEM with 10 flies tested per cohort. Group comparisons were performed using Dunnett's test. Asterisks indicates a significant difference from control flies ($p < 0.05$). Color coding for figures **(B,E,F)** as on **(A)**.

recovery time of flies of both sexes was shorter for the AF consuming groups (**Figure 5F**). Consequently, *A. foeniculum* in the diet enhances *Drosophila* resistance to the heat stress.

Metabolites

Glucose, trehalose, glycogen, and TAGs are parameters extensively used for analysis of carbohydrate and fat metabolism in *Drosophila* (Tennessen et al., 2014). We found that consumption of food with 10 mg/ml AF powder decreased the amount of body glucose in males by 17% (Dunnett's test, $p = 0.037$), but had no impact on females (**Figure 6A**). Glycogen levels in flies that consumed food with AF in concentrations of 5 and 10 mg/ml was higher by 25 and 30% in males and by 21 and 29% in females, respectively (**Figure 6C**). TAG concentration was 43% higher in males (at 10 mg/ml AF supplementation) and by 63 and 55% in females fed diets with 5 and 10 mg/ml

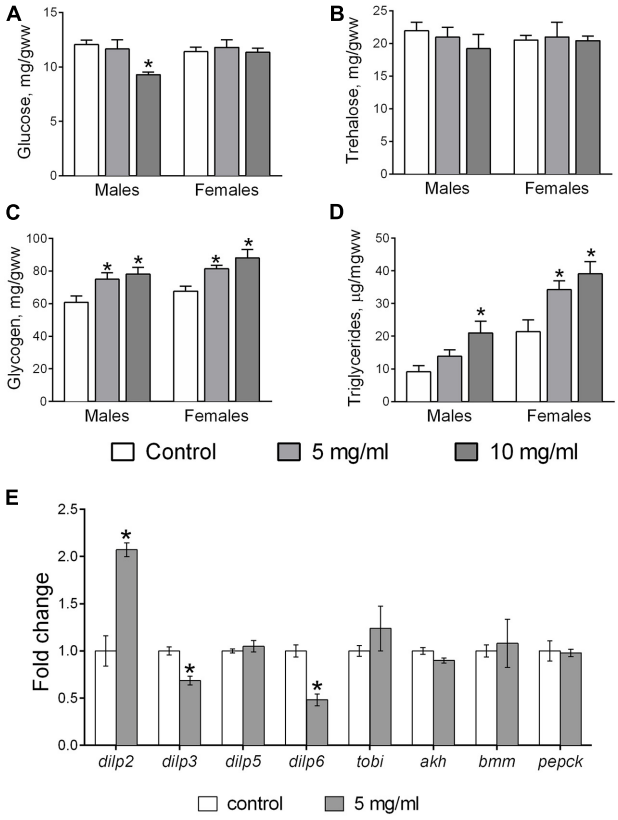

FIGURE 6 | Content of metabolites and mRNA levels for genes involved in regulation of metabolism. Whole body glucose **(A)**, trehalose **(B)**, glycogen **(C)**, TAG **(D)**, and mRNA levels for eight metabolic genes **(E)** in flies treated with AF. Results are mean ± SEM of 4–5 replicates per group. Group comparisons were performed using Dunnett's test for metabolites and Student's *t*-test for mRNA. Asterisk indicates significant difference from the control flies with $p < 0.05$.

AF, respectively (**Figure 6D**). AF supplementation did not affect body trehalose levels of either sex (**Figure 6B**).

Gene Expression

We measured the relative expression of eight genes involved in the regulation of intermediary metabolism. The *Drosophila* insulin-like proteins, *dilp2, 3,* and *5,* are co-expressed in insulin producing cells (IPCs) of the brain and hence, their transcript levels were measured in fly heads. *Dilp6* is primarily expressed by fat body cells and its expression and the mRNA levels of adipokinetic hormone (*akh*), target of brain insulin (*tobi*), phosphoenolcarboxykinase (*pepck*), and Brummer, a triglyceride lipase (*bmm*) were measured in whole fly body. Flies that consumed food supplemented with 5 mg/ml AF powder had significantly higher levels of *dilp2* transcripts by about 2-fold in fly heads (**Figure 6E**; Student's *t*-test, $p = 0.004$). Moreover, we observed a decrease of mRNA levels for *dilp3* (by 30%; Student's *t*-test, $p = 0.005$) and *dilp6* (by 50%; Student's *t*-test, $p = 0.003$) in flies that consumed diet with *A. foeniculum* powder. No changes were observed in the mRNA levels of *dilp5, akh, tobi, pepck*, and *bmm*.

DISCUSSION

Plant-derived active compounds can be used successfully to treat age-related diseases and extend life- and healthspan (Vaiserman and Lushchak, 2017). Most of the detected components in AF leaf extracts were flavonoids that are intensively studied natural compounds with antioxidant, antineoplastic, antihyperglycemic, cardioprotective, or neuroprotective properties. The HPLC-MS analysis revealed the presence of 24 bioactive compounds as shown in **Supplementary Table S1**. For example, 2,5-dihydroxycinnamic acid was previously shown to induce apoptosis and may impair autophagic flux in RCC4 renal cancer cells (Selka et al., 2019), whereas 3-O-caffeoylquinic acid acts as a metformin mimetic in extending *Drosophila* lifespan (Liu et al., 2013) and is also widely known for its anti-hyperlipidemic effect (Liu et al., 2013). 6,7-Dimethoxyquercetin 3-O-glucopyranoside has antiradical activity (de Amorim et al., 2013). The flavonoid, acacetin, is a potent inhibitory constituent and affects eclosion rate, feeding, climbing and lifespan in *Drosophila* (Wang et al., 2015). It is often used in humans for Alzheimer's disease treatments. Flies that were reared on apigenin in their diet showed an increase in lifespan, glutathione, and dopamine content, as well as reduced oxidative stress and apoptosis in a transgenic *Drosophila* model of Parkinson's disease (Siddique and Jyoti, 2017). Treatment with caffeic acid alleviates oxidative stress induced neurotoxicity in cells and *Drosophila* models (Wu et al., 2017). The naturally occurring calycosin is a known antioxidant that prevents redox imbalance in organisms. It also promotes lifespan in the nematode, *Caenorhabditis elegans*, because of its antioxidant action as well as its ability to enhance stress resistance and reduce ROS through insulin signaling pathway inhibition (Lu et al., 2017). The possible lifespan-extending effects of genistein were previously investigated using *C. elegans* (Lee et al., 2015). Protocatechuic acid similarly extended lifespan in *C. elegans* and increased stress resistance associated with its antioxidant properties (Kim et al., 2014). Caffeic acid was shown to increase antioxidant capacity *in vivo* and, by means of a lipofuscin assay, reduce oxidative damage in nematodes, which resulted in increased lifespan (Pietsch et al., 2011). Ursolic acid (UA) is a naturally occurring triterpenoid exhibiting potential antimicrobial, anti-inflammatory and antiobesity activity and it was shown that dietary UA improved health span and lifespan in male *D. melanogaster* (Staats et al., 2019). β-Sitosterol is capable of extending lifespan, likely via activating AMP-activated protein kinase (AMPK) (Lin et al., 2014). Consequently, all the components detected in *A. foeniculum* extracts have been shown to have lifespan extending effects in various animal models.

We supplemented fly food with crushed dried leaves of *A. foeniculum* (AF) at different concentrations and fed *Drosophila* of two lines (*Canton S* and w^{1118}). We found strong prolongevity activity that was independent of genotype. In addition, AF considerably enhanced the survival rate of flies under both menadione-induced oxidative stress and starvation conditions.

Since there is a clear correlation between lifespan-extension and stress resistance (Kenyon, 2010), the protective action against stress may be a positive factor in AF-mediated lifespan extension.

It is also important that factors extending the lifespan have no negative effects on reproduction that reflect healthspan. In this study, we found a higher fecundity rate in AF-fed flies. Although we detected an increase in reproductive ability of flies, previous studies suggested that phytoestrogen exposure negatively affects reproductive health (Jefferson et al., 2012). We also studied functional aging using a locomotion assay. Interestingly, *Agastache* significantly enhanced the mobility of male flies indicating that this herb provides beneficial effects on healthspan as well as lifespan.

The health- and lifespan of *D. melanogaster* are determined by metabolic rate, stress responses and the expression of metabolic genes (Staats et al., 2019). Our results indicate that the health-promoting effects of AF may be caused by changes in metabolism. Indeed, we observed that the prolongevity phenotype is associated with decrease in body glucose levels and increase in stored glycogen and TAG content. The level of circulating and stored metabolites is regulated by DILPs and the glucagon-like peptide AKH (Bharucha et al., 2008). Notably, a significant reduction of mRNA levels for *dilp3* and *dilp6* and increase *dilp2* were observed in response to dietary supplementation with *Agastache*.

To uncover the mechanisms of how *Agastache* protects against oxidative stress, we analyzed antioxidant enzyme activities using fly homogenates from different treatment groups. Our results show that activities of both aconitase and catalase (in males) were significantly increased by AF in the diet, implicating an attenuation of oxidative stress. Additionally, AF-treated flies may also be more resistant to oxidative stress in part because of the various other phenolic compounds in the plant extract that exhibit antioxidant activity.

Low molecular weight (L-SH) and protein thiols are reliable markers of oxidative stress. Flies, fed with AF showed higher antioxidant potential as demonstrated by higher levels of L-SH in females and protein thiols in males, as well as higher aconitase and catalase activities. We suggest that combined together these changes could be responsible for the lower levels of oxidative damage in AF fed flies. The higher pool of L-SH in females might also be associated with a more extensive biosynthetic metabolism related to the need for egg production (Perkhulyn et al., 2017).

In conclusion, our study revealed lifespan extending effects of *Agastache* in *D. melanogaster* linked in part to elevated antioxidant activity and increased stress resistance. The health benefits of polyphenols found in *Agastache* extract are linked to their capacity to directly scavenge free radicals and other nitrogen species (Halliwell, 2007). However, whether dietary supplementation with AF will be beneficial to mammals and ultimately to humans will require further studies.

DATA AVAILABILITY STATEMENT

The authors acknowledge that the data presented in this study must be deposited and made publicly available in an acceptable repository, prior to publication. Frontiers cannot accept a manuscript that does not adhere to our open data policies.

AUTHOR CONTRIBUTIONS

OS: study design, experimental part, data analysis, and writing of drafts. AZ, AK, FG, NV, and AV: experiments and data analysis. KS: initial draft and critical analysis. OL: idea, study design, data analysis, manuscript preparation, and project management. All authors contributed to the article and approved the submitted version.

FUNDING

This work was partially supported by a grant from the National Science Foundation of Ukraine (#2020.02/0118) and a Discovery grant from the Natural Sciences and Engineering Research Council of Canada (#6793) to KS.

SUPPLEMENTARY MATERIAL

The Supplementary Material for this article can be found online at: https://www.frontiersin.org/articles/10.3389/fphys.2020.596729/full#supplementary-material

REFERENCES

Bahadorani, S., and Hilliker, A. J. (2008). Cocoa confers life span extension in *Drosophila melanogaster*. *Nutr. Res.* 28, 377–382. doi: 10.1016/j.nutres.2008.03.018

Bass, T. M., Weinkove, D., Houthoofd, K., Gems, D., and Partridge, L. (2007). Effects of resveratrol on lifespan in *Drosophila melanogaster* and *Caenorhabditis elegans*. *Mech. Ageing Dev.* 128, 546–552. doi: 10.1016/j.mad.2007.07.007

Bayliak, M. M., Shmihel, H. V., Lylyk, M. P., Storey, K. B., and Lushchak, V. I. (2016). Alpha-ketoglutarate reduces ethanol toxicity in *Drosophila melanogaster* by enhancing alcohol dehydrogenase activity and antioxidant capacity. *Alcohol* 55, 23–33. doi: 10.1016/j.alcohol.2016.07.009

Bharucha, K. N., Tarr, P., and Zipursky, S. L. (2008). A glucagon-like endocrine pathway in *Drosophila* modulates both lipid and carbohydrate homeostasis. *J. Exp. Biol.* 211, 3103–3110. doi: 10.1242/jeb.016451

Bitto, A., Wang, A. M., Bennett, C. F., and Kaeberlein, M. (2015). Biochemical genetic pathways that modulate aging in multiple species. *Cold Spring Harb. Perspect. Med.* 5:a025114. doi: 10.1101/cshperspect.a025114

de Amorim, M. R., Rinaldo, D., do Amaral, F. R., Magenta, M., Vilegas, W., and Santos, L. (2013). HPLC-DAD method for quantification of the flavonoids with antiradicalar activity in the hydroethanolic extract from *Tonina fluviatilis* aubl. *Planta Medica* 79:1348737. doi: 10.1055/s-0033-1348737

Flatt, T. (2020). Life-History Evolution and the Genetics of Fitness Components in *Drosophila melanogaster*. *Genetics* 214, 3–48. doi: 10.1534/genetics.119.300160

Fontana, L., and Partridge, L. (2015). Promoting health and longevity through diet: from model organisms to humans. *Cell* 161, 106–118. doi: 10.1016/j.cell.2015.02.020

Gospodaryov, D. V., Yurkevych, I. S., Jafari, M., Lushchak, V. I., and Lushchak, V. (2013). Lifespan extension and delay of age-related functional decline caused by *Rhodiola rosea* depends on dietary macronutrient balance. *Longev. Healthspan* 2:5. doi: 10.1186/2046-2395-2-5

Halliwell, B. (2007). Dietary polyphenols: good, bad, or indifferent for your health? *Cardiovasc. Res.* 73, 341–347. doi: 10.1016/j.cardiores.2006.10.004

Ivanov, I., Vrancheva, R., Traycheva Petkova, N., Tumbarski, Y., Nedyalkova Dincheva, I., and Badjakov, I. (2019). Phytochemical compounds of anise hyssop (*Agastache foeniculum*) and antibacterial, antioxidant, and acetylcholinesterase inhibitory properties of its essential oil. *J. Appl. Pharmaceut. Sci.* 9, 72–78. doi: 10.7324/JAPS.2019.90210

Jefferson, W. N., Patisaul, H. B., and Williams, C. J. (2012). Reproductive consequences of developmental phytoestrogen exposure. *Reproduction* 143, 247–260. doi: 10.1530/REP-11-0369

Kang, H. L., Benzer, S., and Min, K. T. (2002). Life extension in *Drosophila* by feeding a drug. *Proc. Natl. Acad. Sci. U S A.* 99, 838–843. doi: 10.1073/pnas.022631999

Kapahi, P., Kaeberlein, M., and Hansen, M. (2017). Dietary restriction and lifespan: Lessons from invertebrate models. *Ageing Res. Rev.* 39, 3–14. doi: 10.1016/j.arr.2016.12.005

Kapahi, P., Zid, B. M., Harper, T., Koslover, D., Sapin, V., and Benzer, S. (2004). Regulation of lifespan in Drosophila by modulation of genes in the TOR signaling pathway. *Curr. Biol.* 14, 885–890. doi: 10.1016/j.cub.2004.03.059

Kenyon, C. J. (2010). The genetics of ageing. *Nature* 464, 504–512. doi: 10.1038/nature08980

Kim, Y. S., Seo, H. W., Lee, M. H., Kim, D. K., Jeon, H., and Cha, D. S. (2014). Protocatechuic acid extends lifespan and increases stress resistance in *Caenorhabditis elegans*. *Arch. Pharm. Res.* 37, 245–252. doi: 10.1007/s12272-013-0183-6

Lee, E. B., Ahn, D., Kim, B. J., Lee, S. Y., Seo, H. W., Cha, Y. S., et al. (2015). Genistein from *Vigna angularis* extends lifespan in *Caenorhabditis elegans*. *Biomol. Ther.* 23, 77–83. doi: 10.4062/biomolther.2014.075

Lee, K. S., Lee, B. S., Semnani, S., Avanesian, A., Um, C.-Y., Jeon, H. J., et al. (2010). Curcumin extends life span, improves health span, and modulates the expression of age-associated aging genes in *Drosophila melanogaster*. *Rejuvenation Res.* 13, 561–570. doi: 10.1089/rej.2010.1031

Lin, W. S., Chen, J. Y., Wang, J. C., Chen, L. Y., Lin, C. H., Hsieh, T. R., et al. (2014). The anti-aging effects of *Ludwigia octovalvis* on *Drosophila melanogaster* and SAMP8 mice. *Age* 36, 689–703. doi: 10.1007/s11357-013-9606-z

Liu, H., Zhang, X., Wu, C., Wu, H., Guo, P., and Xu, X. (2013). Anti-hyperlipidemic caffeoylquinic acids from the fruits of *Pandanus tectorius* Soland. *J. Appl. Pharmaceut. Sci.* 3, 16–19. doi: 10.7324/JAPS.2013.3803

Lozinsky, O. V., Lushchak, O. V., Kryshchuk, N. I., Shchypanska, N. Y., Riabkina, A. H., Skarbek, S. V., et al. (2013). S-nitrosoglutathione-induced toxicity in *Drosophila melanogaster*: Delayed pupation and induced mild oxidative/nitrosative stress in eclosed flies. *Comp. Biochem. Physiol. A Mol. Integr. Physiol.* 164, 162–170. doi: 10.1016/j.cbpa.2012.08.006

Lozinsky, O. V., Lushchak, O. V., Storey, J. M., Storey, K. B., and Lushchak, V. I. (2012). Sodium nitroprusside toxicity in *Drosophila melanogaster*: delayed pupation, reduced adult emergence, and induced oxidative/nitrosative stress in eclosed flies. *Arch. Insect Biochem. Physiol.* 80, 166–185. doi: 10.1002/arch.21033

Lu, L., Zhao, X., Zhang, J., Li, M., Qi, Y., and Zhou, L. (2017). Calycosin promotes lifespan in *Caenorhabditis elegans* through insulin signaling pathway via daf-16, age-1 and daf-2. *J. Biosci. Bioeng.* 124, 1–7. doi: 10.1016/j.jbiosc.2017.02.021

Lushchak, O. V., Carlsson, M. A., and Nässel, D. R. (2015). Food odours trigger an endocrine response that affects food ingestion and metabolism. *Cell Mol. Life Sci.* 72, 3143–3155. doi: 10.1007/s00018-015-1884-4

Lushchak, O. V., Gospodaryov, D. V., Rovenko, B. M., Glovyak, A. D., Yurkevych, I. S., Klyuba, V. P., et al. (2012). Balance between macronutrients affects life span and functional senescence in fruit fly *Drosophila melanogaster*. *J. Gerontol. A Biol. Sci. Med. Sci.* 67, 118–125. doi: 10.1093/gerona/glr184

Lushchak, O., Piroddi, M., Galli, F., and Lushchak, V. I. (2014). Aconitase post-translational modification as a key in linkage between Krebs cycle, iron homeostasis, redox signaling, and metabolism of reactive oxygen species. *Redox Rep.* 19, 8–15. doi: 10.1179/1351000213Y.0000000073

Lushchak, O., Rovenko, B., Gospodaryov, D., and Lushchak, V. (2011). *Drosophila melanogaster* larvae fed by glucose and fructose demonstrate difference in oxidative stress markers and antioxidant enzymes of adult flies. *Comp. Biochem. Physiol. A Mol. Integr. Physiol.* 160, 27–34. doi: 10.1016/j.cbpa.2011.04.019

Lushchak, O., Strilbytska, O. M., Yurkevych, I., Vaiserman, A. M., and Storey, K. B. (2019). Implications of amino acid sensing and dietary protein to the aging process. *Exp. Gerontol.* 115, 69–78. doi: 10.1016/j.exger.2018.11.021

Lushchak, O., Strilbytska, O., Piskovatska, V., Storey, K. B., Koliada, A., and Vaiserman, A. (2017). The role of the TOR pathway in mediating the link between nutrition and longevity. *Mech. Ageing Dev.* 164, 127–138. doi: 10.1016/j.mad.2017.03.005

Lushchak, V. (2014). Free radicals, reactive oxygen species, oxidative stress and its classification. *Chem. Biol. Interact.* 224, 164–175. doi: 10.1016/j.cbi.2014.10.016

Marcel, D. M., Vârban, D. I., Muntean, S., Moldovan, C., and Olar, M. (2013). Use of species *Agastache foeniculum* (Pursh) Kuntze. *Hop. Med. Plant* 2, 41–42.

Meydani, M. (2001). Nutrition interventions in aging and age-associated disease. *Ann. N Y. Acad. Sci.* 928, 226–235. doi: 10.1111/j.1749-6632.2001.tb05652.x

Nikitin, A. G., Navitskas, S., and Gordon, L. A. (2008). Effect of varying doses of caffeine on life span of *Drosophila melanogaster*. *J. Gerontol. A Biol. Sci. Med. Sci.* 63, 149–150. doi: 10.1093/gerona/63.2.149

Peng, C., Zuo, Y., Kwan, K. M., Liang, Y., Ma, K. Y., Chan, H. Y. E., et al. (2012). Blueberry extract prolongs lifespan of *Drosophila melanogaster*. *Exp. Gerontol.* 47, 170–178. doi: 10.1016/j.exger.2011.12.001

Perkhulyn, N. V., Rovenko, B. M., Lushchak, O. V., Storey, J. M., Storey, K. B., and Lushchak, V. I. (2017). Exposure to sodium molybdate results in mild oxidative stress in *Drosophila melanogaster*. *Redox Rep.* 22, 137–146. doi: 10.1080/13510002.2017.1295898

Perkhulyn, N. V., Rovenko, B. M., Zvarych, T. V., Lushchak, O. V., Storey, J. M., Storey, K. B., et al. (2015). Sodium chromate demonstrates some insulin-mimetic properties in the fruit fly *Drosophila melanogaster*. *Comp. Biochem. Physiol. C Toxicol. Pharmacol.* 167, 74–80. doi: 10.1016/j.cbpc.2014.08.007

Pietsch, K., Saul, N., Chakrabarti, S., Stürzenbaum, S. R., Menzel, R., and Steinberg, C. E. (2011). Hormetins, antioxidants and prooxidants: defining quercetin-, caffeic acid- and rosmarinic acid-mediated life extension in *C. elegans*. *Biogerontology* 12, 329–347. doi: 10.1007/s10522-011-9334-7

Piskovatska, V., Strilbytska, O., Koliada, A., Vaiserman, A., and Lushchak, O. (2019). Health Benefits of Anti-aging Drugs. *Subcell. Biochem.* 91, 339–392. doi: 10.1007/978-981-13-3681-2_13

Rovenko, B. M., Perkhulyn, N. V., Gospodaryov, D. V., Sanz, A., Lushchak, O. V., and Lushchak, V. I. (2015). High consumption of fructose rather than glucose promotes a diet-induced obese phenotype in *Drosophila melanogaster*. *Comp. Biochem. Physiol. A Mol. Integr. Physiol.* 180, 75–85. doi: 10.1016/j.cbpa.2014.11.008

Schriner, S. E., Katoozi, N. S., Pham, K. Q., Gazarian, M., Zarban, A., and Jafari, M. (2012). Extension of *Drosophila lifespan* by *Rosa damascena* associated with an increased sensitivity to heat. *Biogerontology* 13, 105–117. doi: 10.1007/s10522-011-9357-0

Selka, A., Doiron, J. A., Lyons, P., Dastous, S., Chiasson, A., Cormier, M., et al. (2019). Discovery of a novel 2,5-dihydroxycinnamic acid-based 5-lipoxygenase inhibitor that induces apoptosis and may impair autophagic flux in RCC4 renal cancer cells. *Eur. J. Med. Chem.* 179, 347–357. doi: 10.1016/j.ejmech.2019.06.060

Siddique, Y. H., and Jyoti, S. (2017). Alteration in biochemical parameters in the brain of transgenic *Drosophila melanogaster* model of Parkinson's disease exposed to apigenin. *Integr. Med. Res.* 6, 245–253. doi: 10.1016/j.imr.2017.04.003

Soultoukis, G. A., and Partridge, L. (2016). Dietary Protein. Metabolism, and Aging. *Annu. Rev. Biochem.* 2, 5–34. doi: 10.1146/annurev-biochem-060815-014422

Spindler, S. R., Li, R., Dhahbi, J. M., Yamakawa, A., Mote, P., Bodmer, R., et al. (2012). Statin treatment increases lifespan and improves cardiac health in *Drosophila* by decreasing specific protein prenylation. *PLoS One* 7:e39581. doi: 10.1371/journal.pone.0039581

Staats, S., Wagner, A. E., Lüersen, K., Künstner, A., Meyer, T., Kahns, A. K., et al. (2019). Dietary ursolic acid improves health span and life span in male *Drosophila melanogaster*. *Biofactors* 45, 169–186. doi: 10.1002/biof.1467

Tennessen, J. M., Barry, W. E., Cox, J., and Thummel, C. S. (2014). Methods for studying metabolism in *Drosophila*. *Methods* 68, 105–115. doi: 10.1016/j.ymeth.2014.02.034

Vaiserman, A., and Lushchak, O. (2017). Implementation of longevity-promoting supplements and medications in public health practice: achievements, challenges and future perspectives. *J. Transl. Med.* 15:160. doi: 10.1186/s12967-017-1259-8

Wang, C., Wheeler, C. T., Alberico, T., Sun, X., Seeberger, J., Laslo, M., et al. (2013). The effect of resveratrol on lifespan depends on both gender and dietary

nutrient composition in *Drosophila melanogaster*. *Age* 35, 69–81. doi: 10.1007/s11357-011-9332-3

Wang, H. L., Sun, Z. O., Rehman, R. U., Wang, H., Wang, Y. F., and Wang, H. (2017). Rosemary extract-mediated lifespan extension and attenuated oxidative damage in *Drosophila melanogaster* fed on high-fat diet. *J. Food Sci.* 82, 1006–1011. doi: 10.1111/1750-3841.13656

Wang, X., Perumalsamy, H., Kwon, H. W., Na, Y. E., and Ahn, Y. J. (2015). Effects and possible mechanisms of action of acacetin on the behavior and eye morphology of *Drosophila models* of Alzheimer's disease. *Sci. Rep.* 5:16127. doi: 10.1038/srep16127

Wu, Y. L., Chang, J. C., Lin, W. Y., Li, C. C., Hsieh, M., Chen, H. W., et al. (2017). Treatment with caffeic acid and resveratrol alleviates oxidative stress induced neurotoxicity in cell and *Drosophila* models of spinocerebellar ataxia type3. *Sci. Rep.* 7:11641. doi: 10.1038/s41598-017-11839-0

Zielińska, S., and Matkowski, A. (2014). Phytochemistry and bioactivity of aromatic and medicinal plants from the genus *Agastache* (Lamiaceae). *Phytochem. Rev.* 13, 391–416. doi: 10.1007/s11101-014-9349-1

Conflict of Interest: The authors declare that the research was conducted in the absence of any commercial or financial relationships that could be construed as a potential conflict of interest.

frontiers in Physiology

ORIGINAL RESEARCH
published: 17 December 2020
doi: 10.3389/fphys.2020.614552

Unique Members of the Adipokinetic Hormone Family in Butterflies and Moths (Insecta, Lepidoptera)

Heather G. Marco[1], Petr Šimek[2] and Gerd Gäde[1]**

[1] Department of Biological Sciences, University of Cape Town, Rondebosch, South Africa, [2] Biology Centre, Czech Academy of Sciences, České Budějovice, Czechia

Lepidoptera is amongst one of the four most speciose insect orders and ecologically very successful because of their ability to fly. Insect flight is always aerobic and exacts a high metabolic demand on the animal. A family of structurally related neuropeptides, generically referred to as adipokinetic hormones (AKHs), play a key role in triggering the release of readily utilizable fuel metabolites into the hemolymph from the storage forms in the fat body. We used mass spectrometry to elucidate AKH sequences from 34 species of Lepidoptera and searched the literature and publicly available databases to compile (in a phylogenetic context) a comprehensive list of all Lepidoptera sequences published/predicted from a total of 76 species. We then used the resulting set of 15 biochemically characterized AKHs in a physiological assay that measures lipid or carbohydrate mobilization in three different lepidopteran species to learn about the functional cross-activity (receptor-ligand interactions) amongst the different butterfly/moth families. Our results include novel peptide structures, demonstrate structural diversity, phylogenetic trends in peptide distribution and order-specificity of Lepidoptera AKHs. There is almost an equal occurrence of octa-, nona-, and decapeptides, with an unparalleled emphasis on nonapeptides than in any insect order. Primitive species make Peram-CAH-II, an octapeptide found also in other orders; the lepidopteran signature peptide is Manse-AKH. Not all of the 15 tested AKHs are active in *Pieris brassicae*; this provides insight into structure-activity specificity and could be useful for further investigations into possible biorational insecticide development.

Keywords: butterflies and moths, Lepidoptera, adipokinetic hormone, mass spectrometry, primary structure, neuropeptides, biological assays

OPEN ACCESS

Edited by:
Fernando Ariel Genta, Oswaldo Cruz Foundation (Fiocruz), Brazil

Reviewed by:
Klaus H. Hoffmann, University of Bayreuth, Germany
Natraj Krishnan, Mississippi State University, United States
Małgorzata Słociñska, Adam Mickiewicz University, Poland

****Correspondence:***
Petr Šimek
simek@bclab.eu
Gerd Gäde
gerd.gade@uct.ac.za

Specialty section:
This article was submitted to Invertebrate Physiology, a section of the journal Frontiers in Physiology

Received: *06 October 2020*
Accepted: *03 November 2020*
Published: *17 December 2020*

Citation:
Marco HG, Šimek P and Gäde G (2020) Unique Members of the Adipokinetic Hormone Family in Butterflies and Moths (Insecta, Lepidoptera). Front. Physiol. 11:614552. doi: 10.3389/fphys.2020.614552

INTRODUCTION

Butterflies are esthetically beautiful and, hence, not only collected by many laymen enthusiasts but are also displayed for the general public in "butterfly houses." The negative impact of certain Lepidoptera are also known, e.g., the larvae of the fall and African armyworms (*Spodoptera frugiperda* and *Spodoptera exempta*; superfamily: Noctuoidea) damage crops that are the main staple food sources of people (Baudron et al., 2019); the Indian meal moth larvae (*Plodia interpunctella*; superfamily: Pyraloidea) devour stored food products, and species of the genera *Tinea* and *Tineola* (superfamily: Tineoidea) feed on woolen textiles (Basuk and Behera, 2018). In addition, toxins and/or the hairs/bristles of larvae from certain lepidopteran species cause severe medical problems such as urticarial dermatitis, allergies, and asthma (Donato et al., 1998; Marzano et al., 2020).

There are, however, several other traits that are known of Lepidoptera to classify them as "beneficial" for humankind. Many species are known pollinators (even specialist pollinators) (Veerman and Van Zon, 1965; Aker and Udovic, 1981; Rader et al., 2016). Further beneficial traits of Lepidoptera are the following, to name a few that are relevant to South Africa: (i) economically important sericulture not only with the domesticated *Bombyx mori* (superfamily: Bombycoidea) but also wild silk production using the African wild silk moth *Gonometa postica* (superfamily: Lasiocampoidea) (Teshome et al., 2014). (ii) biological weed control, e.g., larvae of the cactus moth, *Cactoblastis cactorum* (superfamily: Pyraloidea), control invasive *Opuntia* species introduced to Australia and South Africa (Anneke and Moran, 1978). (iii) Larvae of various species are sought-after delicacies for human populations in several countries worldwide: the high demand for Mopane worm in southern Africa (Emperor moth *Gonimbrasia belina*; superfamily: Bombycoidea) drives a lucrative market for women who collect the larvae in a sustainable manner (Sekonya et al., 2020).

Lepidoptera is, thus, clearly a diverse order with "beneficial" and "pest" insect status. Linked to this is the high number of extant butterfly/moth species (almost 160,000 described species) that puts Lepidoptera amongst one of the four most speciose insect orders besides Coleoptera, Hymenoptera, and Diptera (Grimaldi and Engel, 2005; van Nieukerken et al., 2011). The importance of a robust phylogenetic treatment of Lepidoptera to provide a framework for interpreting and understanding behavioral, metabolic and environmental processes, for example, in an evolutionary context, has interested scientists for a long time (a few recent examples are: Kristensen et al., 2007; Regier et al., 2013; Mitter et al., 2017). The latest and most comprehensive phylogenomic study takes the transcriptome and genome of 186 species of 34 of the 43 superfamilies into account and interprets 2098 protein-coding genes (Kawahara et al., 2019). **Figure 1** is a simplified, condensed version of the phylogenetic tree of Lepidoptera as proposed by Mitter et al. (2017) and Kawahara et al. (2019) and is based on the superfamilies investigated in the current study, thus it serves as orientation. The afore-mentioned studies all find monophyly of Lepidoptera, and the order Trichoptera (caddisflies) is a sister group, thus the closest relative. The largest clade of the Lepidoptera is the Ditrysia comprising 98% of the order's species. The "non-ditrysian" Lepidoptera are identified as "primitive moths," whose adults have mandibulate mouthparts in place of a proboscis, and consist of 14 superfamilies with the Micropterigoidea, that feed on detritus and bryophytes, as sister group to the remaining Lepidoptera (**Figure 1**). Tineoidea (bagworm moth and clothes moths) and the sister group Yponomeutoidea (best known example is the pest diamond back moth *Plutella xylostella* from the family Plutellidae) are at the base of the Dytrisia clade within which the group Apodytrisia resides which consists, *inter alia*, of the species-rich superfamily Tortricoidea (leaf roller moths, such as the pest species codling moth *Cydia pomonella*). Within Apodytrisia the next large clade is the Obtectomera (**Figure 1**), harboring all butterflies (Papilionoidea) and also the Pyraloidea (snout moths such as the meal moth genus *Plodia* or the cactus moth *C. cactorum*). Within the Obtectomera the clade Macroheterocera has been coined, consisting of the well-known and species-rich superfamilies of Noctuoidea (the owlet moths such as the fall army worm *S. frugiperda* or the corn earworm moth *Helicoverpa zea*) at the base, Geometroidea and as most advanced superfamily, the Bombycoidea with hawk moth, emperor moth and silk moth (Mitter et al., 2017; Kawahara et al., 2019; see **Figure 1**).

Insects were the first to have evolved sustained powered flight; fast fliers and long distance fliers are found amongst lepidopteran species with skippers (superfamily: Hesperioidea) clocking speeds of about 60 km h^{-1} through the air[1] and migratory flights – an important strategy for survival and reproduction – observed and studied in tortricid and noctuid pest species (Schumacher et al., 1997; Jiang et al., 2011; Zheng et al., 2011; Stokstad, 2017; Guo et al., 2020), in nymphalids (superfamily: Papilionoidea) (Brattström et al., 2010; Stefanescu et al., 2013; Chapman et al., 2015; Agrawal, 2017), as well as in a number of sphinx moths (superfamily: Bombycoidea; Reinhardt and Harz, 1989). From an energetic point of view, flight is the most demanding activity of insects, always based on aerobic metabolism, and oxygen consumption can be elevated above resting values by more than 100-fold (Kammer and Heinrich, 1978; Gäde, 1992). The major storage site for metabolic fuel is the fat body – triacylglycerides and/or glycogen stores are mobilized by peptide neurohormones of the so-called adipokinetic hormone (AKH) family to replenish the fast diminishing fuels in the contracting flight muscles during wing beating (Gäde, 1992). Zebe (1954) measured a respiratory quotient (RQ) of 0.7–0.8 in most studied butterfly and moth species and deduced the usage of fat as flight substrate. This was corroborated by measuring maximal activities of specific enzymes of major energetic pathways (Beenakkers, 1969; Crabtree and Newsholme, 1972) or measuring the metabolic rate plus quantifying the metabolites (lipids, glycogen, and trehalose) in the fall army worm moth *S. frugiperda* (Nayar and van Handel, 1971; van Handel and Nayar, 1972). On the other hand, there are also reports on the participation of carbohydrates in flight metabolism of Lepidoptera. Whereas unfed adults of the tobacco hornworm moth *Manduca sexta* used almost exclusively fat for flights (Ziegler and Schulz, 1986b), carbohydrates play a role in the same species during the initial phase of pre-flight warm-up (Joos, 1987). In a diurnal nectar-feeding hawkmoth (*Amphion floridensis*) RQ measurements established that fed moths primarily oxidized carbohydrates, whereas starved moths burnt almost only fats (O'Brien, 1999). In a short-distance flyer like the nymphalid Glanville fritillary butterfly (*Melitaea cinxia*) that flies about 500 m in 2 h as median maximal flight distance (Ovaskainen et al., 2008), an RQ of about 1.0 has been measured for flights of 10 min, thus indicating that carbohydrates are exclusively used (Haag et al., 2005).

Peptides of the AKH family are responsible for regulating mobilization of stored metabolites especially during intense locomotory activity such as flight, swimming, or running in insects (Gäde, 1997; Marco and Gäde, 2020). These peptides

[1]https://www.nhm.ac.uk/discover/record-breaking-butterflies.html

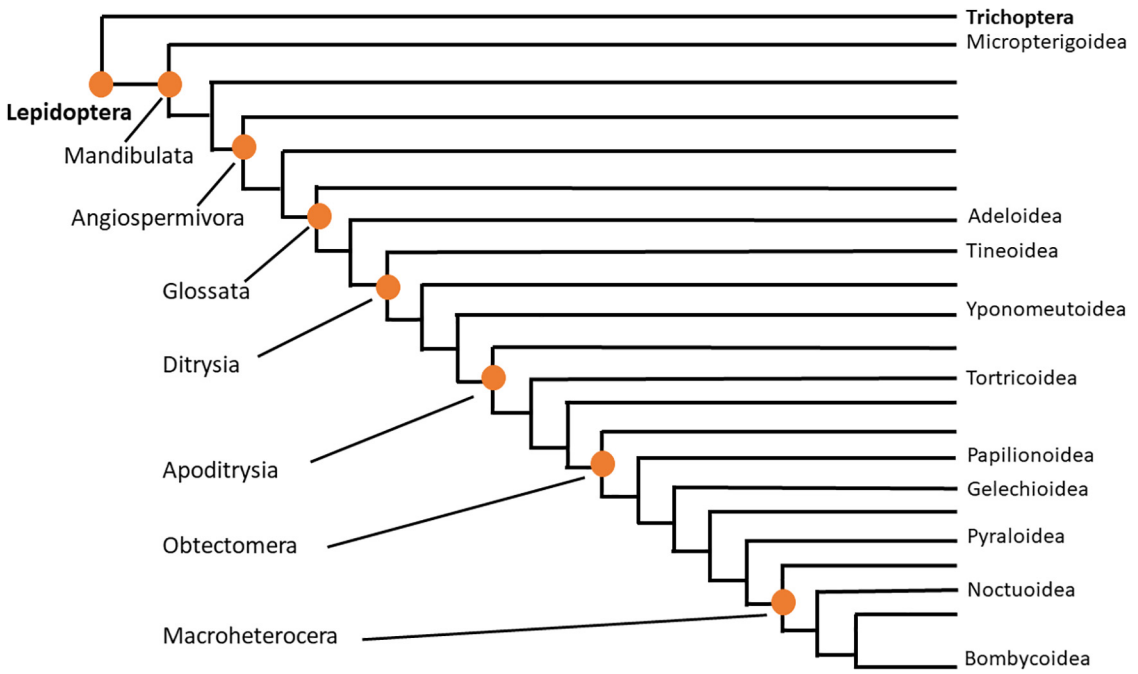

FIGURE 1 | Evolutionary tree of Lepidoptera. Adapted from Mitter et al. (2017) and Kawahara et al. (2019), this condensed tree reflects only the superfamilies that are dealt with in the current study. The two orders are indicated in bold letters; clades within the order Lepidoptera are indicated on the left; lepidopteran superfamilies covered in the current study are shown on the right.

are functionally comparable to vertebrate glucagon; structurally, however, AKH peptides and their cognate G-protein coupled receptors are related to the vertebrate gonadotropin releasing hormone (GnRH) system and together with two other insect neuropeptide systems, viz. corazonin (Cor) and its receptor, as well as AKH/corazonin-related peptide (ACP) and its receptor, comprise a large peptide superfamily (Hansen et al., 2010; Gäde et al., 2011; Roch et al., 2011). AKHs are synthesized and released from the neurohemal corpus cardiacum (CC). By primary structure the peptides are characterized by a chain length of 8–10 amino acid residues with post-translationally modified termini: a pyroglutamate residue at the N-terminus and a carboxy-amidation at the C-terminus, thus making the peptide insusceptible to digestion by exopeptidases. Other positions in the molecule show little variation when comparing multiple sequences: residue 2 from the N-terminus is either an aliphatic leucine, isoleucine, valine, or an aromatic phenylalanine or tyrosine; residue 3 is either threonine or asparagine, while residue 4 may be one of the two aromatic amino acids phenylalanine or tyrosine, and residue 5 may be either threonine or serine; a fair variety of amino acids can take up residues 6, 7, and 10, while residues 8 and 9 are always tryptophan and glycine, respectively (Gäde, 2009). More than 80 members of this peptide family are now known by sequence (Gäde, 2009; Marco and Gäde, 2020).

In Lepidoptera the first AKH that was completely structurally elucidated came from the CC of the tobacco hornworm moth, *M. sexta* (Family: Sphingidae) – the nonapeptide is called Manse-AKH (pELTFTSSWG amide; Ziegler et al., 1985), and it functions as a true adipokinetic, thus lipid-mobilizing, hormone in the adult moth and regulates carbohydrate metabolism in the larval stage (Ziegler et al., 1990). Since then, Manse-AKH was shown to be synthesized in the CC of a number of other butterflies and moths (for family and species details, see **Table 1**). The gene for Manse-AKH was also the first AKH gene that was cloned (Bradfield and Keeley, 1989). During the first separation attempts of biologically active AKH hormones in *M. sexta*, it became clear that activity was separated into two peaks (Ziegler and Gäde, 1984), one of which was the later identified Manse-AKH. It took, however, 28 years for the second *M. sexta* AKH peak to be sequenced by mass spectrometric methods as a decapeptide that was then found present in other sphingid moths as well (Manse-AKH-II, pELTFSSGWGQ amide; Weaver et al., 2012).

Next, a decapeptide that had some adipokinetic and pronounced trehalose-elevating activity in the cornear moth *Heliothis* (=*Helicoverpa*) *zea* (family: Noctuidae) was sequenced from the CC of this species and was, hence called a hypertrehalosemic hormone (Helze-HrTH, pELTFSSGWGN amide; Jaffe et al., 1988). It has since been found in other noctuids as well (see **Table 1**). In the common commercially exploited silk moth *B. mori* (family: Bombycidae) genomic and physiological information, as well as mass spectrometric measurements led to the identification of another decapeptide (Bommo-AKH: pELTFTPGWGQ amide) with lipid-mobilizing activity besides Manse-AKH (Liebrich and Gäde, 1995; Gäde et al., 2008; Roller et al., 2008). In the same year it was found by mass spectrometry that the CC of two owlet moths (family: Noctuidae), the bright-line brown-eye moth *Lacanobia oleracea* and the cabbage moth *Mamestra brassicae*, synthesized a third

TABLE 1 | The distribution of AKH peptides in the Lepidoptera, to date: primary sequence and calculated protonated mass.

Higher taxonomy	Family	Species	AKH name	AKH sequence*	$(M + H)^+$	References**
Glossata, Adeloidea	Adelidae	*Nemophora (=Nematopogon) pilella*	Peram-CAH-II	pELTFTPNWa	988.4887	T011091201
Ditrysia, Tineoidea	Psychidae	*Eumeta japonica*	NOVEL 1	pELTFTSNWGSa	1122.5214	GBP11607.1; Kono et al., 2019
Ditrysia, Yponomeutoidea	Pluttellidae	*Plutella xylostella*	Lacol-AKH Peram-CAH-II	pELTFTSSWGGa pELTFTPNWa	1065.5000 988.4887	XP_011565387.1 XP_011555237.1
Apoditrysia, Tortricoidea	Tortricidae	*Cryptophlebia peltastica*	Lacol-AKH Peram-CAH-II	pELTFTSSWGGa pELTFTPNWa	1065.5000 988.4887	This study
		Thaumatotibia leucotreta	Lacol-AKH	pELTFTSSWGGa	1065.5000	This study
		Cydia pomonella	Lacol-AKH Peram-CAH-II	pELTFTSSWGGa pELTFTPNWa	1065.5000 988.4887	This study; Garczynski et al., 2019
Obtectomera, Papilionoidea	Papilionidae	*Papilio machaon*	Manse-AKH	pELTFTSSWGa	1008.4785	KPJ15512.1
		Papilio xuthus	Manse-AKH	pELTFTSSWGa	1008.4785	KPI97662.1
		P. demodocus	Manse-AKH #(Vanca-AKH)	pELTFTSSWGa pELTFTSSWGGK-OH	1008.4785 1194.5790	This study
		Papilio polytes	Manse-AKH	pELTFTSSWGa	1008.4785	PpolytesGene0002562.mrna1
		Papilio glaucus	Manse-AKH	pELTFTSSWGa	1008.4785	Pgl722.20mrna
		P. memnon	Manse-AKH	pELTFTSSWGa	1008.4785	This study
		Parides arcas	Manse-AKH	pELTFTSSWGa	1008.4785	TO111202337
	Hesperiidae	*Lerema accius*	Manse-AKH	pELTFTSSWGa	1008.4785	Lac1208.8mRNA
	Pieridae	*Gonepteryx rhamni*	Manse-AKH	pELTFTSSWGa	1008.4785	This study
		Pieris napi	Manse-AKH	pELTFTSSWGa	1008.4785	PIENAPT00000010987
		Pieris rapae	Manse-AKH	pELTFTSSWGa	1008.4785	PIERAPT00000002073
		P. brassicae	Manse-AKH Piebr-AKH	pELTFTSSGWa pELTFSSGWa	1008.4785 907.4308	Marco and Gäde, 2017
		Leptidea sinapis	Manse-AKH	pELTFTSSWGa	1008.4785	VVC88225.1
		Phoebis sennae	Manse-AKH	pELTFTSSWGa	1008.4785	Pse4122.11
		Catopsilia florella	Manse-AKH	pELTFTSSWGa	1008.4785	This study
	Lycaenidae	*Polyommatus icarus*	Peram-CAH-II	pELTFTPNWa	988.4887	T011091239
		Calycopis cecrops	Manse-AKH	pELTFTSSWGa	1008.4785	Cce2042.16mRNA
	Nymphalidae	*Cethosia biblis*	Manse-AKH Piebr-AKH	pELTFTSSWGa pELTFSSGWa	1008.4785 907.4308	This study
		Heliconius melpomene	Manse-AKH Piebr-AKH	pELTFTSSWGa pELTFSSGWa	1008.4785 907.4308	This study; HMEL003881-PA
		H. hecale	Manse-AKH Piebr-AKH	pELTFTSSWGa pELTFSSGWa	1008.4785 907.4308	This study
		Dryas iulia	Manse-AKH Piebr-AKH	pELTFTSSWGa pELTFSSGWa	1008.4785 907.4308	This study
		Acraea horta	Manse-AKH Piebr-AKH Triin-AKH	pELTFTSSWGa pELTFSSGWa pELTFTPNWGa	1008.4785 907.4308 1045.5102	This study
		Parthenos sylvia	Manse-AKH Piebr-AKH	pELTFTSSWGa pELTFSSGWa	1008.4785 907.4308	This study
		Bicyclus anynana	Manse-AKH	pELTFTSSWGa	1008.4785	nBA.01-t08034-RA
		Caligo memnon	Manse-AKH	pELTFTSSWGa	1008.4785	This study
		Dira clytus clytus	Manse-AKH Dircl-AKH-I Dircl-AKH-II	pELTFTSSWGa pELTFSSGWGa pELTFSTGWa	1008.4785 964.4523 921.4465	This study
		Danaus plexippus	Manse-AKH	pELTFTSSWGa	1008.4785	This study; Köllisch et al. (2003) OWR54335.1
			Piebr-AKH	pELTFSSGWa	907.4308	This study; OWR54334.1

(Continued)

TABLE 1 | Continued

Higher taxonomy	Family	Species	AKH name	AKH sequence*	$(M + H)^+$	References**
		D. chrysippus	Manse-AKH	pELTFTSSWGa	1008.4785	This study
		Greta oto	Manse-AKH	pELTFTSSWGa	1008.4785	This study
			Piebr-AKH	pELTFSSWGa	907.4308	
		Idea leuconoe	Manse-AKH	pELTFTSSWGa	1008.4785	This study; OWR54335.1
		Melitaea cinxia	Manse-AKH	pELTFTSSWGa	1008.4785	This study; MCINX012977-PA
			Piebr-AKH	pELTFSSGWa	907.4308	This study
		Aglais io	Manse-AKH	pELTFTSSWGa	1008.4785	This study
		A. urticae	Manse-AKH	pELTFTSSWGa	1008.4785	This study; Köllisch et al., 2003
		Vanessa atalanta	Manse-AKH	pELTFTSSWGa	1008.4785	This study
		V. cardui	Manse-AKH	pELTFTSSWGa	1008.4785	Köllisch et al., 2000
		Junonia (=Precis) coenia	Manse-AKH	pELTFTSSWGa	1008.4785	Köllisch et al., 2003; JC_0008480-RA
Obtectomera, Gelechioidea	Stathmopodidae	*Atrijuglans hetaohei*	Manse-AKH	pELTFTSSWGa	1008.4785	AhAKH1 ID CL31877Contig1; Li et al., 2020
			Piebr-AKH	pELTFSSWGa	907.4308	AhAKH2 ID CL18765Contig1; Li et al., 2020
Obtectomera, Pyraloidea	Pyralidae	*Galleria mellonella*	Manse-AKH	pELTFTSSWGa	1008.4785	XP_026761256.1
		Plodia interpunctella	Manse-AKH	pELTFTSSWGa	1008.4785	Corzo et al., 2020
			Chipa-AKH	pELTFSTGWGNa	1092.5109	
		Amyelois transitella	Chipa-AKH	pELTFSTGWGNa	1092.5109	XP_013191035.1
	Crambidae	*Chilo partellus*	Manse-AKH	pELTFTSSWGa	1008.4785	This study
			Chipa-AKH	pELTFSTGWGNa	1092.5109	
		Chilo suppressalis	Manse-AKH	pELTFTSSWGa	1008.4785	ALM30296.1; Xu et al., 2016
			Chipa-AKH	pELTFSTGWGNa	1092.5109	ALM30297.1; Xu et al., 2016
		Ostrinia furnacalis	Manse-AKH	pELTFTSSWGa	1008.4785	XP_028164252
			NOVEL 2	pELTFSTGWGQa	1106.5265	XP_028164238
Macroheterocera, Noctuoidea	Noctuidae	*Helicoverpa (=Heliothis) zea*	Manse-AKH	pELTFTSSWGa	1008.4785	Jaffe et al., 1986; this study
			Helze-HrTH	pELTFSSGWGNa	1078.4952	Jaffe et al., 1988; this study
		Helicoverpa armigera	Manse-AKH	pELTFTSSWGa	1008.4785	AGH22544.1
			Helze-HrTH	pELTFSSGWGNa	1078.4952	AGH25545.1
		Spodoptera frugiperda	Manse-AKH	pELTFTSSWGa	1008.4785	Köllisch et al., 2003; Gäde et al., 2008; Abdel-Latief and Hoffmann, 2007; this study
			Helze-HrTH	pELTFSSGWGNa	1078.4952	
		Spodoptera littoralis	Manse-AKH	pELTFTSSWGa	1008.4785	Gäde et al., 2008
			Helze-HrTH	pELTFSSGWGNa	1078.4952	
		Spodoptera exigua	Manse-AKH	pELTFTSSWGa	1008.4785	AXY04229.1; Llopis-Giménez et al., 2019
			Helze-HrTH	pELTFSSGWGNa	1078.4952	AXY04230.1; Llopis-Giménez et al., 2019
		Lacanobia oleracea	Manse-AKH	pELTFTSSWGa	1008.4785	Gäde et al., 2008
			Helze-HrTH	pELTFSSGWGNa	1078.4952	
			Lacol-AKH	pELTFTSSWGGa	1065.5000	
		Mamestra brassicae	Manse-AKH	pELTFTSSWGa	1008.4785	Fónagy et al., 2008; Gäde et al., 2008; Gäde et al. (2008)
			Helze-HrTH	pELTFSSWGGNa	1078.4952	
			Lacol-AKH	pELTFTSSWGGa	1065.5000	Gäde et al. (2008)
		Hadena bicruris	Manse-AKH	pELTFTSSWGa	1008.4785	This study
			Helze-HrTH	pELTFSSGWGNa	1078.4952	
			Lacol-AKH	pELTFTSSWGGa	1065.5000	
		Agrotis ipsilon	Manse-AKH	pELTFTSSWGa	1008.4785	C0HL92; Interpretation of this study‡
			Helze-HrTH	pELTFSSGWGNa	1078.4952	Diesner et al., 2018
			Lacol-AKH	pELTFTSSWGGa	1065.5000	Diesner et al., 2018
		Mythimna separata	Lacol-AKH	pELTFTSSWGGa	1065.5000	ALX27200.1
			Helze-HrTH	pELTFSSGWGNa	1078.4952	APJ36628.1
		Trichoplusia ni	Manse-AKH	pELTFTSSWGa	1008.4785	XP_026731718.1

(Continued)

TABLE 1 | Continued

Higher taxonomy	Family	Species	AKH name	AKH sequence*	$(M + H)^+$	References**
	Erebidae	*Cyligramma latona*	Manse-AKH	pELTFTSSWGa	1008.4785	This study
			Helze-AKH	pELTFSSGWGNa	1078.4952	
		Arctia plantaginis	Manse-AKH	pELTFTSSWGa	1008.4785	CAB3233079.1
			Helze-HrTH	pELTFSSGWGNa	1078.4952	CAB3224801.1
Macroheterocera, Bombycoidea	Saturniidae	*Actias luna*	Manse-AKH	pELTFTSSWGa	1008.4785	This study
			Manse-AKH-II	pELTFSSGWGQa	1092.5109	
		Antherae yamamai	Manse-AKH	pELTFTSSWGa	1008.4785	This study
			Antya-AKH	pELTFSPGWGQa	1102.5316	
	Bombycidae	*Bombyx mori*	Manse-AKH	pELTFTSSWGa	1008.4785	Ishibashi et al., 1992; Gäde et al., 2008; NP_001104825.1
			Bommo-AKH	pELTFTPGWGQa	1116.5473	Gäde et al., 2008; NP_001124365.1
	Sphingidae	*Manduca sexta*	Manse-AKH	pELTFTSSWGa	1008.4785	Ziegler et al. (1985); Weaver et al. (2012)
			Manse-AKH-II	pELTFSSGWGQa	1092.5109	Weaver et al. (2012)
		Deilephila elpenor	Manse-AKH	pELTFTSSWGa	1008.4785	Weaver et al. (2012)
			Manse-AKH-II	pELTFSSGWGQa	1092.5109	
		Laothoe populi	Manse-AKH	pELTFTSSWGa	1008.4785	Weaver et al. (2012)
			Manse-AKH-II	pELTFSSGWGQa	1092.5109	
		Smerinthus ocellata	Manse-AKH	pELTFTSSWGa	1008.4785	Weaver et al. (2012)
		Acherontia atropos	Manse-AKH	pELTFTSSWGa	1008.4785	Weaver et al. (2012)
			Manse-AKH-II	pELTFSSGWGQa	1092.5109	
		Hyles lineata	Manse-AKH	pELTFTSSWGa	1008.4785	This study
			Manse-AKH-II	pELTFSSGWGQa	1092.5109	
		Agrius convolvuli	Manse-AKH	pELTFTSSWGa	1008.4785	This study
			Manse-AKH-II	pELTFSSGWGQa	1092.5109	
		Sphinx ligustri	Manse-AKH	pELTFTSSWGa	1008.4785	This study
			Manse-AKH-II	pELTFSSGWGQa	1092.5109	
		Daphnis nerii	Manse-AKH	pELTFTSSWGa	1008.4785	This study
			Manse-AKH-II	pELTFSSGWGQa	1092.5109	
		Hippotion eson	Manse-AKH-I	pELTFTSSWGa	1008.4785	Gäde et al., 2013
			Manse-AKH-II	pELTFSSGWGQa	1092.5109	
			Hipes-AKH-I	pELTFTSSWa	951.4571	
			Hipes-AKH-II	pELTFTSTWa	965.4727	
			Hipes-AKH-III	pELTFTSTWGa	1022.4942	
		Hippotion celerio	Manse-AKH	pELTFTSSWGa	1008.4785	Gäde et al., 2013
			Manse-AKH-II	pELTFSSGWGQa	1092.5109	
			Hipes-AKH-I	pELTFTSSWa	951.4571	
			Hipes-AKH-II	pELTFTSTWa	965.4727	
			Hipes-AKH-III	pELTFTSTWGa	1022.4942	

*The phylogenetic outline is as per Mitter et al. (2017) and Kawahara et al. (2019). *Mature peptide sequence: in the case of sequences derived from nucleotide databases, the post-translational modifications (i.e., blocked termini) are deduced from the characteristic features of previously sequenced AKHs. Note that the N-terminal pyroglutamic acid (pE) can arise from the cyclization of a glutamine (Q) or, more rarely, from a glutamate (E) residue. In the case of prepro-AKH sequences translated from mRNA, all have a glutamine amino acid residue at position 1 of the uncleaved AKH sequence. Novel peptide sequences deduced from data mining are consecutively numbered (1–2) – note that we have not confirmed the data experimentally. **Published work or database accession number. #Vanca-AKH is not considered a mature AKH peptide but an incompletely processed form of Manse-AKH. Although it occurs in many other Lepidoptera species, it is only indicated here. ‡Diesner et al. (2018) overlooked Manse-AKH in their interpretations of putative preprohormones identified from an A. ipsilon transcriptome and grouped the Manse-AKH precursor together with the Lacol-AKH precursor as "adipokinetic 1" [see data in* ***Table 2****, as well as mass spectrometry data in Figure 4B of Diesner et al. (2018), where the $(M + Na)^+$ adduct corresponding to Manse-AKH is shown].*

AKH peptide (besides Manse-AKH and Helze-HrTH); this was a decapeptide (Lacol-AKH, pELTFTSSWGG amide) which is near-identical to Manse-AKH save for an extra glycine residue (Gäde et al., 2008). A unique case of five different AKHs in the CC occurs in two species of the genus *Hippotion* (family: Sphingidae) – mass spectrometry unraveled the existence of three novel members of the AKH family: the octapeptides Hipes-AKH-I (pELTFTSSWamide) and Hipes-AKH-II (pELTFTSTW amide), as well as the nonapeptide Hipes-AKH-III (pELTFTFSTWG amide); Manse-AKH and Manse-AKH-II were also present (Gäde et al., 2013). All five peptides mobilize lipids after injection into *Hippotion eson* (Gäde et al., 2013), and quantitative studies showed that lipids are the main fuel during a 15 min flight of the sphingid moth, with only a small contribution by trehalose oxidation (Liebrich and Gäde, 1995). The latest addition to Lepidopteran AKHs is from the CC of the large

cabbage white butterfly *Pieris brassicae* (family: Pieridae) where a lipid-mobilizing peptide was mass spectrometrically sequenced as an octapeptide (Piebr-AKH, pELTFSSGW amide) which co-occurs with Manse-AKH and a biologically inactive, non-amidated peptide that resembles Manse-AKH and is code-named Vanca-AKH (Marco and Gäde, 2017). Vanca-AKH was first elucidated from the nymphalid painted lady butterfly, *Vanessa cardui* (pELTFTSSWGGK; Köllisch et al., 2000) and has since been identified in other Lepidoptera (**Table 1** shows Vanca-AKH only in the earliest known appearance, viz. in *Papilio demodocus*, family Papilionidae). Although Vanca-AKH had biological activity under certain conditions in *V. cardui* (Köllisch et al., 2000), it is not active in unmanipulated *P. brassicae* which reacted well to Manse-AKH and Piebr-AKH (Marco and Gäde, 2017), hence, Vanca-AKH is rather viewed as an incompletely processed peptide from the AKH-precursor. Such processing "mistakes"/intermediates are known from AKHs of other orders (Diptera, Coleoptera) as well (see, for example, Predel et al., 2004; Gäde and Marco, 2011).

It is evident from the above that, although there are about 160,000 extant species of Lepidoptera described, the number of investigated species with respect to AKH is small. Interestingly, all nine AKHs known so far by (bio)chemical sequencing methods are unique for this order, i.e., have not been found to be synthesized in the CC of any other insect order. This makes this group of peptides in Lepidoptera very interesting for further research to look for an order-specific control agent. The effort to find species-specific, biorational and biostable control agents (peptide mimetics that are based on the insect's own hormones), so-called "green" insecticides, is high on the agenda of basic research ventures to target and control pest insects of agriculture, horticulture and forestry, with little or no negative effect on beneficial insects, other organisms and the environment. So, for example, head-to-tail cyclic and other restricted conformation analogs of insect neuropeptides, such as AKH and diapause hormone, have been synthesized and tested in bioassays to study their active conformations and target selectivity (Zhang et al., 2011; Abdulganiyyu et al., 2020a). Amongst the diapause hormone mimetics both agonists and antagonists are identified (Zhang et al., 2011), while a cyclic AKH mimetic based on a locust peptide (Locmi-AKH-I) demonstrates selectivity in *in vitro* receptor assays, activating the AKH receptor of the desert locust but failing to activate the AKH receptor of the honeybee even at pharmacological concentrations (Abdulganiyyu et al., 2020a). Molecular dynamic analyses indicated that the cyclic mimetic failed to enter the binding pocket of the honeybee receptor 3D model during docking simulations (Abdulganiyyu et al., 2020a).

Whilst the above-mentioned mimetics are not yet in the field trial stage, such studies and the current investigation provide the groundwork for future "green" insecticides for, not surprisingly, several lepidopteran species also represent those insects that are a real threat to human food security, and with the general rise in resistance to chemical pesticides, the need for "green" insecticides as part of an integrated pest management strategy is becoming more urgent than ever. Before much effort and funds are invested in such a research area to make peptide mimetics based on a lepidopteran AKH, for example, one should first broaden the information base on the complement of AKHs in Lepidoptera.

The current study, therefore, had several objectives and is not hypothesis-driven:

1. To investigate more members of the order Lepidoptera and determine the structure of the respective AKH. Not only species from different superfamilies and families were analyzed but also from various regions of the world.
2. We are interested in the physiological function of AKHs and, therefore, checked for a few selected species whether the AKH is involved in lipid and/or carbohydrate regulation. In addition, we used *P. brassicae*, a recent introduced pest species in South Africa, as test case to ascertain whether all the known lepidopteran AKHs could successfully trigger the adipokinetic signaling system in a pest species. This information could be useful for further investigations into a possible order-specific control agent (lepidopteran-specific "green" insecticide).
3. As we had previously successfully implemented the use of the primary structure of AKHs in a few insect orders to verify certain phylogenetic trends and ancestral relationships (Gäde, 1989; Gäde and Marco, 2005, 2017; Gäde et al., 2020), we also wanted to use the structural information of the investigated AKHs to trace the general phylogeny of Lepidoptera and sketch a possible molecular evolution of the AKHs in this order.

MATERIALS AND METHODS

Insects

Corpora cardiaca were dissected from female and/or male adults. Specimens were either caught in the field by netting, were purchased from breeders or were received as a gift from a research institution or a commercial company. Some species were bred from eggs (*Actias luna*, *Catopsilia florella*, *P. brassicae*, and *Sphinx ligustri*). In total, 34 species of Lepidoptera were studied for their AKH complement; details of the species and the taxonomic affiliations are given below. For the latter, the phylogenetic outline given by Mitter et al. (2017) and Kawahara et al. (2019) were followed as explained in section "Introduction." **Figure 1** supplies a quick orientation to a much-simplified phylogenetic tree, showing the superfamilies investigated in the current study.

Superfamily Tortricoidea

Three species of leaf rollers (family: Tortricidae) were investigated. Pupae of the codling moth (*C. pomonella*; 20 CCs prepared), the litchi moth (*Cryptophlebia peltastica*; 20 CCs prepared) and the false codling moth [*Thaumatotibia* (=*Cryptophlebia*) *leucotreta*; 20 CCs prepared] were a gift of the River Bioscience Group (Port Elizabeth, South Africa). Larvae of these species are major pests to agricultural crops such as apples, pears and litchis.

Superfamily Papilionoidea

Nineteen species of butterflies were investigated. Two species belong to the swallowtails (family: Papillionidae): *P. demodocus*

(4 CCs prepared) were collected by netting in a private garden in Cape Town in the austral summer around a citrus tree, *Papilio memnon* (8 CCs prepared) was purchased as pupae from a commercial breeder in the United Kingdom.

Two species were of the whites (family: Pieridae): eggs of the African migrant (*C. florella*; 7 CCs prepared) were collected in a private garden in Cape Town from leaves of the monkey pod (*Cassia* ssp.) in March and reared to adult eclosion fed with those leaves. Adults of the brimstone (*Gonepteryx rhamni*; 4 CCs prepared) were caught by netting in a private garden in Bad Iburg (Germany) in April.

Fifteen species of the brush foots (family: Nymphalidae) from various subfamilies were investigated: pupae of the heliconid red lacewing (*Cethosia biblis*; 1 CC prepared), the postman (*Heliconius melpomene*; 6 CCs prepared), the tiger longwing (*Heliconius hecale*; 3 CCs prepared), the clipper (*Parthenos sylvia*; 5 CCs prepared) and the monarch butterfly (*Danaus plexippus*; 4 CCs prepared) came from a commercial breeder from the United Kingdom; adults of the giant owl (*Caligo memnon*; 2 CCs prepared), the glasswing butterfly (*Greta oto*; 10 CCs prepared), the Julia butterfly (*Dryas iulia*; 15 CCs prepared) and the paperkite butterfly (*Idea leuconoe*; 8 CCs prepared) were a gift from Butterfly World (Klapmuts, South Africa), CCs of the Glanville fritillary (*M. cinxia*; 67 CCs) were a gift from H. Fescemyer (The Pennsylvania State University, United States); adults of the Red Admiral (*Vanessa atalanta*; 4 CCs prepared), the European peacock (*Aglais io*; 4 CCs prepared) and the small tortoiseshell (*Aglais urticae*; 2 CCs prepared) were collected by netting in a private garden in Bad Iburg (Germany) on flowering *Buddleia*; adults of the garden Acraea (*Acraea horta*; 15 CCs prepared), the African Monarch (*Danaus chrysippus*; 3 CCs prepared) and the Cape autumn widow (*Dira clytus clytus*; 15 CCs prepared) were collected by netting in a private garden or at the grounds of the University of Cape Town in the austral summer.

Superfamily Pyraloidea

One species was investigated: pupae of the spotted stemborer (*Chilo partellus*; 20 CCs prepared) were a gift of Frank Chidawanyika (University of Bloemfontein, South Africa) and came originally from a culture held at the International Centre for Insect Physiology and Ecology (ICIPE) in Kenya. This species is especially damaging to staple food plants of maize and sorghum in eastern and southern Africa (Khadioli et al., 2014).

Superfamily Noctuoidea

Four species were investigated. CCs from adults of fall armyworm moths (*S. frugiperda*; 20 CC) and corn earworm moths (*H. zea*; 40 CC) were a gift from Howard W. Fescemyer (The Pennsylvania State University, United States), pupae of the Lychnis moth (*Hadena bicruris*; 11 CCs prepared) were a gift of Carmen Villacañas de Castro (University of Bremen, Germany) and adults of the cream striped owl moth (*Cyligramma latona*; 5 CCs prepared) were collected by netting at the grounds of the University of Namibia. Armyworm and earworm larvae have serious pest status with respect to a variety of food plants (Cunningham and Zalucki, 2014), while *H. bicruris* is a specialist nocturnal nursery pollinator of *Silene latifolia* (=*Melandrium album*) (Brantjes, 1976).

Superfamily Bombycoidea

Six species were investigated. The two species from the family Saturniidae were the luna moth (*Actias luna*; 7 CCs prepared) which were reared from eggs on walnut leaves (*Juglans regia*), and the Japanese oak silk moth (*Antheraea yamamai*; 4 CCs prepared) of which pupae were received as gift from Thomas Olthoff (University of Hamburg). Four species from the family Sphingidae were studied: the privet hawk moth (*S. ligustri*; 4 CCs prepared) which were reared from eggs on privet (*Ligustrum vulgare*), the Oleander hawkmoth (*Daphnis nerii*; 2 CCs prepared) of which the adults were collected in October near Heraklion (Greece) on a private property site, the convolvulus hawkmoth (*Agrius convolvuli*; 1 CC prepared) of which one adult was fortuitously netted in Windhoek (Namibia) and the white-lined sphinx moth (*Hyles lineata*; 4 CCs prepared) whose pupae were received as gift from Martin von Arx (University of Arizona, United States).

Biological Assays

Bioassays were performed with only a few species when adult specimens were available in sufficient numbers. *H. eson* and *P. brassicae* specimens were reared from eggs which were collected in a private garden in Cape Town, as described previously (Marco and Gäde, 2017, 2019); adults of both genders were used on the first or second day after eclosion. Individuals of *A. horta* used in bioassays were netted in a private garden in Cape Town; animals of unspecified age and both genders were used on the day of collection. Bioassay acceptor insects were kept individually under an up-ended funnel on moist tissue paper at ambient temperature (22.5 ± 1°C) in the laboratory for about 2 h for acclimatization and keeping them at rest. A first hemolymph sample of 0.5 μl was taken laterally from the metathorax or abdomen, or directly from the dorsal heart in the centerline of the abdomen, with a disposable glass microcapillary (Hirschmann Laborgeräte, Eberstadt, Germany), blown into a test tube of concentrated sulfuric assay and the animal was then injected ventrolaterally into the abdomen with 2 or 3 μl of either distilled water, a crude CC extract, or a synthetic peptide delivered in distilled water via a Hamilton fine-bore 10 μl syringe. After injection, the animal was returned to rest for 90 min after which a second hemolymph sample was taken from the same individual. The hemolymph samples in sulfuric acid were then measured for vanillin-positive material (=total lipids) or anthrone-positive material (=total carbohydrates) according to the phosphovanillin method (Zöllner and Kirsch, 1962) and anthrone method (Spik and Montreuil, 1964), respectively, as modified by Holwerda et al. (1977).

Student's paired *t*-test was used to compare the concentration of metabolites (lipids or carbohydrates) in the hemolymph before and after the injection of a test solution. Differences were considered significant at $p < 0.05$.

Dissection of Corpora Cardiaca, Peptide Extraction, and Separation, Mass Spectrometry and Sequence Analysis

The only source of AKH, the corpora cardiaca, were dissected from the heads of adult specimens of each of the 34 lepidopteran species under investigation with the aid of a stereomicroscope at 20 to 40-fold magnification. The neuroendocrine glands were placed into a microcentrifuge tube containing 80% v/v methanol, extracted as described previously (Gäde et al., 1984), and dried in a vacuum-centrifuge. Thereafter, extracts were dissolved in either distilled water for use in biological assays, or in 50 μl of aqueous formic acid for liquid chromatography tandem positive ion electrospray mass spectrometry (LC-ESI) on an LTQ XL linear ion trap instrument (Thermo Fisher Scientific, San Jose, CA, United States), as previously outlined in detail (Kodrík et al., 2010).

Exact mass and elemental composition were acquired by LC-ESI high-resolution mass spectrometry (HRMS) using the same Jupiter RP Proteo column and gradient elution, but a HRMS Orbitrap Q-Exactive Plus mass spectrometer (Thermo Fisher Scientific) equipped with a HESI-II ion source. Positive ESI mass spectra were scanned every 2.1 s and were acquired at resolution R = 70,000 with an internal lock mass m/z 622.02896 of hexakis(2,2-difluoroethoxy)phosphazene using the mass range of 450–1250 Da.

Synthetic Peptides

Synthetic peptides (see **Table 1** for full name and sequence) were used in biological assays and to confirm interpretations of mass spectrometric data. Peptides with the code-names Manse-AKH, Helze-AKH, Lacol-AKH and Peram-CAH-II were synthesized by Pepmic Co., Ltd. (Suzou, China); Bommo-AKH, Manse-AKH-II, Piebr-AKH, Hipes-AKH-I, -II, and -III were custom-synthesized by Kevin Clark (Department of Entomology, University of Georgia, Athens, Georgia), while the novel peptides of this study (Dircl-AKH-I and -II, Chipa-AKH, and Antya-AKH) were also made by Pepmic Co., Ltd.

Mining of AKH Sequences From Publicly Available Databases

We investigated AKH sequences from 34 lepidopteran species via MS in the current study. To gain greater insight into the distribution of AKHs in this speciose order we further tried to extend the knowledge base by using bioinformatic searches to identify Lepidoptera AKHs from protein, genomic and/or EST databases. Triant et al. (2018) provides a comprehensive list of Lepidoptera genomes and relevant databases. Some AKH sequences were retrieved directly from the 1KITE initiative (http://www.1kite.org/) and from Lepbase,[2] a useful hub for lepidopteran genomes that includes new genome assemblies and annotations (Challis et al., 2016). AKH sequences were accessed using BLAST (Basic Local Alignment Search Tool) search function with the nucleotide sequence of Manse-AKH or Bommo-AKH as query. Sequences were also retrieved via the National Center for Biotechnology Information[3].

RESULTS AND DISCUSSION

Presence of AKH Peptides in Select Lepidoptera Species and Physiological Action

Biological assays were performed with a few lepidopteran species to screen for hyperlipemic (and sometimes also) hypertrehalosemic activity embedded in the tested CC. Different permutations of a well-established *in vivo* biological assay system were used: (i) CC extracts were injected into adult *H. eson* – a well-characterized sphingid moth species with respect to metabolic assays and AKHs that elicit a hyperlipemic response (Gäde et al., 2013); (ii) CC extracts were injected into adult *A. horta* – a nymphalid butterfly species that is investigated here for the first time with respect to metabolic activity; and (iii) synthetic peptides of all biochemically known lepidopteran AKHs were injected into adult *P. brassicae* – a butterfly species that responds to AKHs with hyperlipemia (see Marco and Gäde, 2017); the latter dataset is presented and discussed below (see section "Adipokinetic Response of Lepidoptera AKH Family Bioanalogs: Potential for "Green" Insecticides?"). These acceptor species were selected based on availability of adult specimens in high enough numbers to provide statistically relevant data. From previously gained knowledge, *H. eson* and *P. brassicae* were only tested for an adipokinetic response, whereas *A. horta* (hitherto untested in metabolic assays) was investigated for an adipokinetic, as well as a hypertrehalosemic response. **Table 2A** shows that the circulating level of carbohydrates are much higher (more than double) in resting *A. horta* specimens than the lipid concentration, which we interpret as an indicator that trehalose is the preferred metabolic fuel of the garden *Acraea*. Interestingly, when half a pair of CC from *A. horta* was conspecifically injected, *A. horta* responded with a significant rise in the lipid concentration compared to water-injected animals, as well as a significant, pronounced increase in the carbohydrate concentration in the hemolymph (**Table 2A**). This butterfly, thus, utilizes both metabolites, and this was unequivocally corroborated following injection of AKH peptides that are identified as endogenous to the CC of *A. horta* (see section "Mass Spectrometric-Derived Results" below), viz. Manse-AKH, Piebr-AKH, and Triin-AKH: each peptide triggered the signal transduction cascade in *A. horta* to increase both the lipid and the carbohydrate concentration in the hemolymph – although the hypertrehalosemic effect is stronger than the adipokinetic effect, both metabolites are mobilized from the fat body in response to the respective endogenous AKH peptides when injected in synthetic form at a low concentration (**Table 2A**). Injection of half a pair of CC from the autumn brown butterfly, *Dira clytus clytus*, into *A. horta* significantly increased the carbohydrate concentration compared to water-injected controls (**Table 2A**) which indicated the presence of an AKH peptide in the CC of

[2]http://lepbase.org/

[3]https://blast.ncbi.nlm.nih.gov/

TABLE 2 | Bioassays for adipokinetic and hypertrehalosemic activity of crude methanolic extracts of butterfly corpora cardiaca (*Acraea horta*, *Dira clytus clytus*, and *Cyligramma latona*, and of synthetic peptides in two acceptor species: *A. horta* (butterfly) and *Hippotion eson* (moth).

Treatment	Hemolymph lipids (mg ml $^{-1}$)					Hemolymph carbohydrates (mg ml $^{-1}$)				
	n	0 min	90 min	Difference	*P**	*n*	0 min	90 min	Difference	*P**
A. Acceptor insect: *A. horta*										
Control (10 µl distilled water)	15	13.51 ± 4.37	13.21 ± 4.33	−0.30 ± 1.94	NS	13	49.60 ± 8.87	50.03 ± 8.91	0.43 ± 2.94	NS
A. horta CC extract (0.5 gland pair equivalent)	14	12.87 ± 6.36	16.93 ± 7.37	4.06 ± 2.55	0.00002	6	46.57 ± 1.26	51.57 ± 2.30	5.00 ± 2.04	0.0009
D. clytus clytus CC extract (0.5 gland pair equivalent)			**Not tested**			7	42.60 ± 5.90	54.45 ± 8.70	11.85 ± 4.02	0.00012
Manse-AKH (10 pmol)	6	13.41 ± 5.32	20.01 ± 4.72	6.60 ± 2.93	0.00002	6	50.96 ± 10.22	61.51 ± 9.99	10.55 ± 3.33	0.00029
Plebr-AKH (10 pmol)	10	10.13 ± 3.87	16.35 ± 5.18	6.21 ± 2.99	0.001	5	44.19 ± 3.64	53.06 ± 6.91	8.87 ± 4.01	0.0039
Triin-AKH (10 pmol)	6	15.98 ± 4.64	23.72 ± 6.31	7.74 ± 2.85	0.00058	6	30.59 ± 5.73	42.43 ± 14.97	11.84 ± 12.67	0.036
B. Acceptor insect: *H. eson*								**Not tested**		
Control (5 µl distilled water)	6	44.59 ± 10.21	47.61 ± 11.55	3.01 ± 9.1	NS					
C. latona CC extract (0.5 gland pair equivalent)	7	31.23 ± 10.57	59.50 ± 15.68	28.27 ± 13.67	0.001					
A. horta CC extract (0.5 gland pair equivalent)	5	38.78 ± 8.84	58.29 ± 17.84	19.51 ± 10.23	0.0065					
Lacol-AKH (10 pmol)	7	28.70 ± 21.23	57.27 ± 29.13	28.57 ± 9.15	0.00008					

*Data are presented as Mean ± SD. *Paired t-test was used to calculate the significance between pre- and post-injection. NS, not significant.*

autumn brown butterfly that interacted with the AKH receptor of *A. horta* to turn on the signal transduction cascade pathway. Due to insufficient numbers of *D. clytus clytus* we could not perform conspecific assays and did not have enough crude CC extract to test their lipid mobilizing effect in *A. horta*.

In heterologous bioassays with the sphingid moth *H. eson*, the injection of half a pair of CC from *A. horta* and of the noctuid moth *C. latona* resulted in a clear adipokinetic response when compared to the water-injected control group and was as high as or about 70% of the response to the decapeptide Lacol-AKH (**Table 2B**), which had previously been shown to have a full effect in *H. eson* (Marco and Gäde, 2015).

What can we conclude from these physiological experiments? The CC of all investigated species here synthesize one or more endogenous peptide that belongs to the AKH peptide family. In the case of heterologous injections, a positive adipokinetic or hypertrehalosemic response means that either the donor species contains exactly the same peptide(s) as the acceptor species or that the AKH receptor of the acceptor species recognizes a slightly modified peptide – this is not unusual for AKH receptors as, for example, structure activity studies with *H. eson* show (Marco and Gäde, 2019). In the case of *A. horta* this species has higher concentrations of carbohydrates than lipids in its hemolymph at rest which may be a hint that metabolism is carbohydrate-based since a correlation between the most abundant fuel substrate in an insect and the preferred utilization of a fuel was previously shown in insects (Gäde et al., 2004). Second, mobilization of stored fuels by a CC extract clearly pointed to a preference of carbohydrates versus lipids. Third, this hypertrehalosemic result could also be evoked by relatively low doses of all three synthetic AKHs that we find to be present in the CC of *A. horta* (see section "Mass Spectrometric-Derived Results" below). These results with *A. horta* are reminiscent of findings with the noctuid moth *H. zea*, where the endogenous decapeptide Helze-HrTH elicited an increase of both hemolymph metabolites, lipids and carbohydrates, but the hypertrehalosemic response was much more pronounced (Jaffe et al., 1988). In the sphingid moth *M. sexta*, the endogenous nonapeptide Manse-AKH is also responsible for the control of carbohydrate and lipid metabolism but this is stage-specific: in larvae the carbohydrate metabolic pathway is affected and in adults the lipids (Ziegler et al., 1990). Although not as rigorously investigated as in *M. sexta*, the bombycid *B. mori* appears to have the same type of regulation: in larvae AKH is involved in the homeostasis of the trehalose concentration in the hemolymph (Oda et al., 2000), whereas in adults CC injection and simulated flight increase hemolymph lipids (Liebrich and Gäde, 1995). For most other investigated lepidopteran species, it is only known that adults react with hyperlipemia (see, for example, Gäde et al., 2013; Marco and Gäde, 2017). The current results have shown quite clearly that AKH is involved in metabolic regulation, but it needs to be determined at a case to case event whether the endogenous AKH influences carbohydrate or lipid metabolism or both. Is there a link between flight distance and the metabolite fueling the intense aerobic activity? Lipids in the form of triglycerides are far less bulky to store in the fat body compared with glycogen, and triglycerides have a higher caloric content per unit of weight than

glycogen, hence, it comes as no surprise that lipid metabolism is prevalent in lepidopterans that engage in migratory (long distance) flights, such as sphingid moths (Liebrich and Gäde, 1995; Ziegler and Schulz, 1986a,b), cabbage moth and -butterfly (Fónagy et al., 2008; Marco and Gäde, 2017) and the nymphalid painted lady (Köllisch et al., 2000). In *Helicoverpa* moths, such as *H. zea* that practices short-range, long-range, and migratory movements,[4] both lipids and carbohydrates are mobilized (Jaffe et al., 1988). *A. horta* engages only in very short, flitting flights in the garden from one nectar source to the next, and this would fit with a mainly carbohydrate-based metabolism.

Isolation and Mass Spectral Analyses of Adipokinetic Hormones From Various Lepidoptera Species

Separation, detection, sequence assignment, and confirmation of AKHs from Lepidoptera species were carried out with mass spectrometry, as described below. Following on from this, we show and discuss the outcome of our search for AKH structures in all investigated lepidopteran species, including those where transcriptomic/genomic mining resulted in knowledge of AKH sequences.

Mass Spectrometric-Derived Results

Tortricoidea: Cydia pomonella

The methanolic CC extract of the codling moth *C. pomonella* was fractionated by reversed-phase liquid chromatography (LC), and the peptides detected by positive ion electrospray mass spectrometry (+ESI-MS). **Figure 2A** shows the base peak chromatogram, whereas **Figures 2B,C** depict extracted mass peaks of AKHs at 7.76 and 8.53 min, respectively, with the corresponding $(M + H)^+$ mass ions at *m/z* 1065.4 (**Figure 2D**) and *m/z* 988.4 (**Figure 2E**). The primary structure of these peak materials was deduced from the tandem MS^2 spectra obtained by collision-induced dissociation (CID) of the respective *m/z* ions. The spectrum of *m/z* 1065.5 (**Figure 3A**) with clearly defined b, y, b-H_2O, y-NH_3, and other product ions allowed an almost complete assignment of a typical decapeptide member of the AKH family under the assumption that the peptide has a characteristic pyroglutamate residue at the N-terminus (see schematic inset in **Figure 3A**). All other amino acids are assigned except at position two where the remaining mass of 113 can be accredited to one of the isomers: leucine or isoleucine. A peptide with the sequence pGlu-Leu-Thr-Phe-Thr-Ser-Ser-Trp-Gly-Gly amide, thus with the Leu^2 isomer, had previously been sequenced in certain noctuid moths and is called Lacol-AKH (see section "Introduction"). The second CID spectrum of the peptide at *m/z* 988.4 (**Figure 3B**) led to the interpretation of an octapeptide member of the AKH family with the sequence pGlu-Leu/Ile-Thr-Phe-Thr-Pro-Asn-Trp amide which, with Leu^2, is well-known under the name Peram-CAH-II as one of the two peptides found in the CC of blattid cockroaches (see Gäde, 2009). Since we had previously established that isobaric Leu^2/Ile^2 containing peptides have different LC retention times (Gäde et al., 2003, 2016) and since we had the synthetic peptides Lacol-AKH and Peram-CAH-II available, we could prove via co-elution experiments (**Supplementary Figures 1A–C**) that both assigned peptides of *C. pomonella* have Leu and not Ile as the second amino acid residue in the amino acid sequence and are, indeed, the peptides known as Lacol-AKH and Peram-CAH-II.

Papilionoidea: Dira clytus clytus

An extract from the CC of the Cape autumn widow *D. clytus clytus* gave information in LC-MS of four possible AKHs (**Figure 4A**): the first eluting peak with retention time of 5.40 min, displayed *m/z* 1194.7 (**Figure 4B**) with a primary sequence of pGlu-Leu-Thr-Phe-Thr-Ser-Ser-Trp-Gly-Gly-Lys-OH as interpreted from CID measurements (**Supplementary Figure 2A**). This amino acid sequence was shown to occur in the painted lady *V. cardui* and other nymphalids (see section "Introduction") and is the incompletely processed AKH known as Vanca-AKH which has biological activity only under certain (unnatural) bioassay conditions (Köllisch et al., 2000; Marco and Gäde, 2017). The other three peaks at retention times 7.91, 8.11, and 8.53 min (**Figure 4A**) each correspond to a mature AKH with a respective *m/z* of 964.5 (**Figure 4C**), 1008.5 (**Figure 4D**) and 921.5 (**Figure 4E**). CID (**Supplementary Figure 2B**) and co-elution experiments (**Supplementary Figures 2C–E**) proved that the peptide with $(M + H)^+$ 1008.5 is a nonapeptide with the sequence pGlu-Leu-Thr-Phe-Thr-Ser-Ser-Trp-Gly amide, well-known as Manse-AKH and found in *M. sexta* and a number of other butterflies and moths (see section "Introduction"). The other two peptides are novel and have not previously been found in any insect species. CID (**Figure 5A**) and co-elution (**Supplementary Figures 2F–H**) assigned the sequence for the peptide at *m/z* 964.5 as another nonapeptide: pGlu-Leu-Thr-Phe-Ser-Ser-Gly-Trp-Gly amide. We name it Dircl-AKH-I; it is identical to the first nine amino acid residues of Manse-AKH-II which is a decapeptide with a 10th residue, Gln (see **Table 1** for sequence). The last eluting peptide with *m/z* 921.5 was identified by CID (**Figure 5B**) and co-elution (**Supplementary Figures 2I–K**) as an octapeptide with the sequence pGlu-Leu-Thr-Phe-Ser-Thr-Gly-Trp amide and is named Dircl-AKH-II. It is identical to the first eight amino acids of the novel decapeptide found in *C. partellus*, Chipa-AKH (see below), which has the amino acid residues Gly and Asn in positions 9 and 10 to complete the decapeptide structure.

Papilionoidea: Acraea horta

The extracted base peak chromatograms of an extract from the CC of the garden Acraea *A. horta* exhibits four peaks representing AKHs at retention times of 5.18, 7.93, 8.08, and 8.16 min (**Supplementary Figures 3A–D**) corresponding, respectively, to $(M + H)^+$ mass ions at *m/z* 1194.6, 1008.5, 907.4, and 1045.5, respectively (**Supplementary Figures 3E–H**). In some cases also the $(M + NH_4)^+$ ion can be seen, at *m/z* 1025.4 and 1062.4 (**Supplementary Figures 3F,H**, respectively), corroborating the identified mass. The first two eluting peaks, i.e., *m/z* 1194.5 and 1008.5, were subjected to CID and co-elution experiments to determine the peptide sequence; the data revealed the same

[4]https://gd.eppo.int/download/doc/133_datasheet_HELIZE.pdf

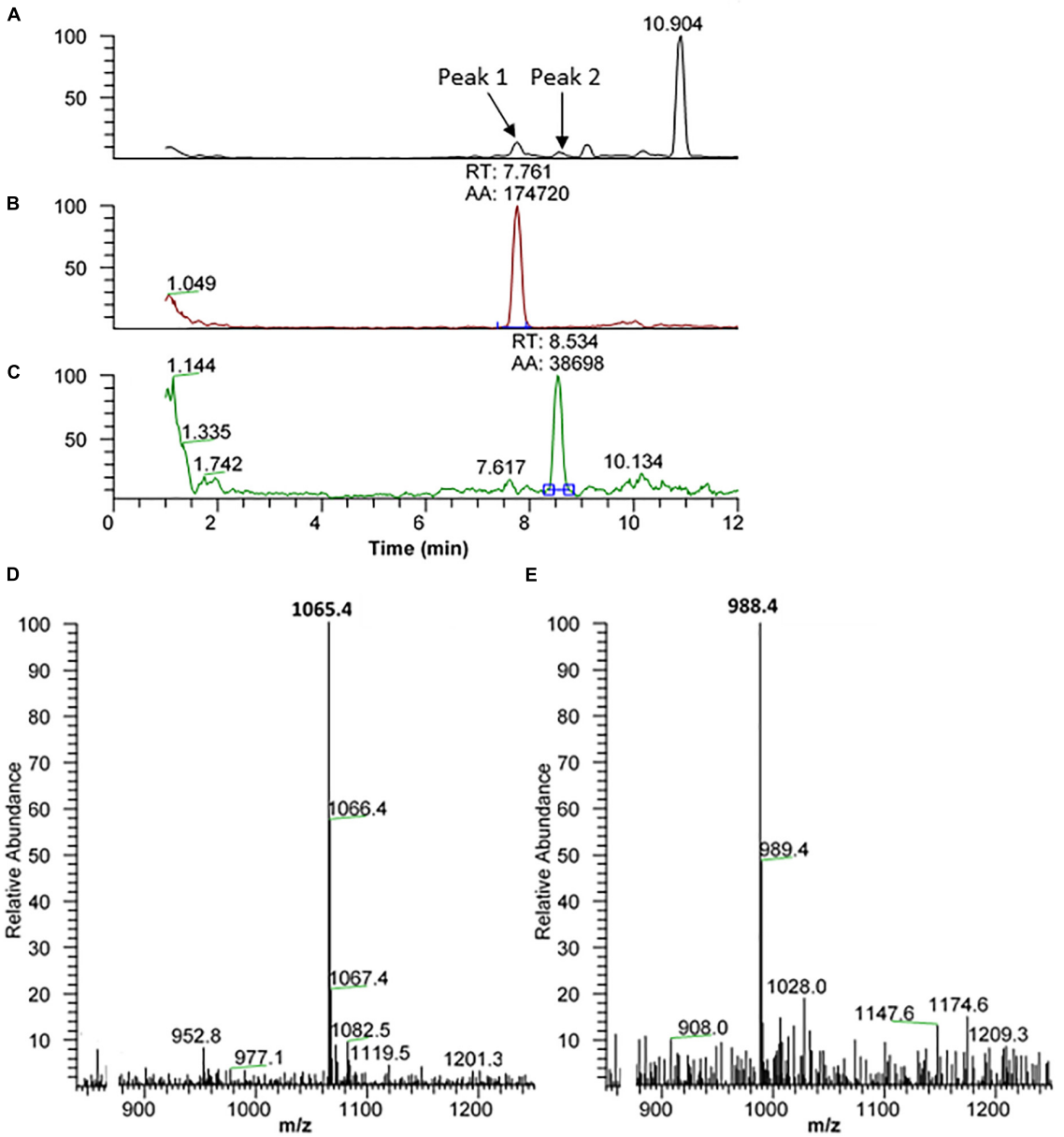

FIGURE 2 | Liquid chromatographic (LC) positive electrospray ionization (+ESI) mass spectrometric (MS) analysis of a methanolic extract from the corpus cardiacum of the codling moth *Cydia pomonella*. **(A)** Base peak chromatogram obtained by LC-MS analysis showing detection of two AKH peptides labeled peak 1 and peak 2 at 7.76 and 8.53 min, respectively. **(B)** The extracted LC-MS chromatogram of peak 1 at 7.76 min with $(M + H)^+$ at *m/z* 1065.5 (see **D**). **(C)** The extracted LC-MS chromatogram of peak 2 at 8.53 min with $(M + H)^+$ at *m/z* 988.4 (see **E**).

peptide sequences as found in the CC sample of *D. clytus clytus* (see above), viz. the incompletely processed AKH (*m/z* 1194.6, Vanca-AKH) and Manse-AKH (*m/z* 1008.5; **Supplementary Figure 3K** top panel). For the third eluting peptide from the CC of *A. horta*, the CID spectrum of *m/z* 907.5 assigned this peptide clearly as an octapeptide with the sequence pGlu-Leu/Ile-Thr-Phe-Ser-Ser-Gly-Trp amide (**Supplementary Figure 3I**), which, with a Leu^2 isomer, had previously been identified as Piebr-AKH (see section "Introduction" and **Table 1**). Co-elution with the synthetic peptide Piebr-AKH confirmed that *A. horta* contains this peptide (**Supplementary Figure 3K** middle panel). The last eluting AKH peptide of this extract at *m/z* 1045.5 was also easily identified from its CID spectrum (**Supplementary Figure 3J**). It is a nonapeptide with the sequence pGlu-Leu/Ile-Thr-Phe-Thr-Pro-Asn-Trp-Gly amide. Such a peptide, with Leu^2, had been shown to exist in the kissing bug *Triatoma infestans* and had, therefore, been named Triin-AKH (Marco et al., 2013). Co-elution of the *A. horta* extract with the synthetic Triin-AKH confirmed that this peptide also occurs in the garden Acraea (**Supplementary Figure 3K** bottom panel).

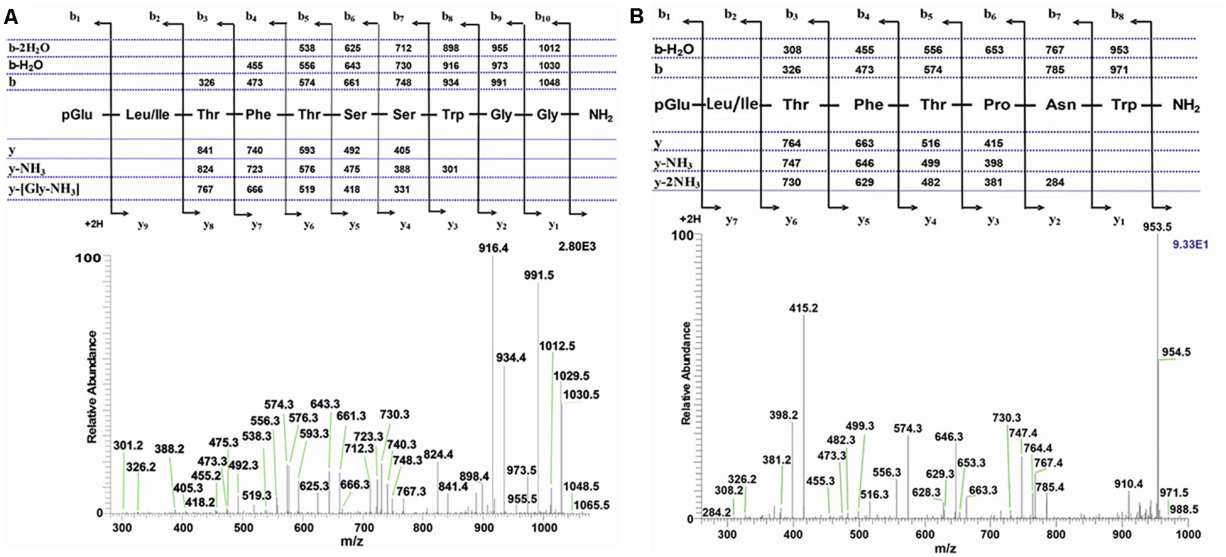

FIGURE 3 | Collision-induced dissociation (CID) tandem MS + ESI spectra. **(A)** The CID spectrum of the ion $(M + H)^+$ at *m/z* 1065.5 in **Figures 2B,D** from *C. pomonella*. **(B)** The CID spectrum of the ion $(M + H)^+$ at *m/z* 988.4 in **Figures 2C,E** from *C. pomonella*. The insets show the proposed peptide sequences together with diagnostic fragment ions observed in the MS^2 spectra.

Pyraloidea: Chilo partellus

The base peak chromatogram (**Supplementary Figure 4A**) of an extract from the CC of the spotted stem borer *C. partellus* shows two AKH peaks. The extracted mass peaks of those are at 7.62 and 8.01 min (**Supplementary Figures 4B,C**) with the corresponding $(M + H)^+$ mass ions at *m/z* 1092.5 (**Supplementary Figure 4D**, weak and embedded in other ions, see arrow) and *m/z* 1008.4 (**Supplementary Figure 4E**), respectively. The CID spectra gave clear product ions in both cases and led to the interpretation of a decapeptide AKH with the sequence pGlu-Leu/Ile-Thr-Phe-Ser-Thr-Gly-Trp-Gly-Asn amide (**Figure 6**) and a nonapeptide AKH with the sequence pGlu-Leu/Ile-Thr-Phe-Thr-Ser-Ser-Trp-Gly amide; the latter was shown to be the well-known Manse-AKH that occurs in the majority of Lepidoptera (see for example, **Supplementary Figure 2B** from *D. clytus clytus* CC; **Supplementary Figure 3K** from *A. horta* CC). By co-elution the Leu^2 isomer was established for both peptides (**Supplementary Figures 4F–H**). The decapeptide (*m/z* 1092.5) is novel and is given the name Chipa-AKH; it has the same sequence as the novel Dircl-AKH-II but is extended by Gly at position 9 and Asn at position 10. Chipa-AKH is structurally closely related to Helze-HrTH with a conservative Ser to Thr substitution at position 6 (see **Table 1**).

Bombycoidea: Actias luna

An extract from the CC of the luna moth *A. luna* of the family Saturniidae shows two ion peaks with retention time of 7.35 min and *m/z* 1092.5, and retention time of 8.03 min at *m/z* 1008.5 (**Supplementary Figures 5A–D**). In both cases further informative ions such as $(M + NH_4)^+$, $(M + Na)^+$, and $(M + NH_4 + Na)^+$ were detected as well. Although the masses are the same as what was found in the CCs of *C. partellus* (see above), CID and co-elution experiments clearly show that there is a different peptide behind the $(M + H)^+$ 1092.5 in *A. luna*: a sequence was assigned with two ambiguities due to isobaric amino acids at position 2 (Leu/Ile) and 10 (Gln/Lys; **Figure 7**). A peptide with the sequence pGlu-Leu-Thr-Phe-Ser-Ser-Gly-Trp-Gly-Gln amide, code-named Manse-AKH-II, is known to occur in several hawk moths (family: Sphingidae, see section "Introduction"); synthetic Manse-AKH-II was, therefore, used in a co-elution experiment and this clarified Leu at position 2 and Gln at position 10 of the *A. luna* peptide (**Supplementary Figure 5E**). Moreover, the elemental composition of a Gln residue is $C_5H_8N_2O_2$ = 128.0586 Da, while a Lys residue shows $C_6H_{12}N_2O$ = 128.0950 Da, thus, a difference of −0.0364 which is measurable by HRMS with Orbitrap mass spectrometry. Manse-AKH-II as an AKH in *A. luna* CC was corroborated when an exact mass of 1092.5109 was measured by HRMS with 0.8 ppm accuracy (n = 2); this corresponds to the elemental composition of $C_{50}H_{70}N_{13}O_{15}$ with Leu^2 and Gln^{10} assigned to the sequence in **Figure 7**. An alternative peptide with Leu^2 and Lys^{10} would have yielded MH^+ 1092.5473 that fits with the elemental composition of $C_{51}H_{74}N_{13}O_{14}$.

Collision-induced dissociation and coelution (**Supplementary Figure 5E**) of the $(M + H)^+$ ion at *m/z* 1008.5 led to the interpretation of pGlu-Leu-Thr-Phe-Thr-Ser-Ser-Trp-Gly amide as amino acid sequence, thus, Manse AKH is synthesized in *A. luna*.

Bombycoidea: Antheraea yamamai

An extract from the CC of the Japanese oak silk moth *A. yamamai* of the family Saturniidae shows two peaks with retention times of 7.64 and 7.95 min, respectively, which correspond with *m/z* 1102.5 and 1008.4, respectively (**Supplementary Figures 6A–C**). CID and co-elution experiments confirmed the well-known Manse-AKH for the latter (**Supplementary Figures 6D–F**)

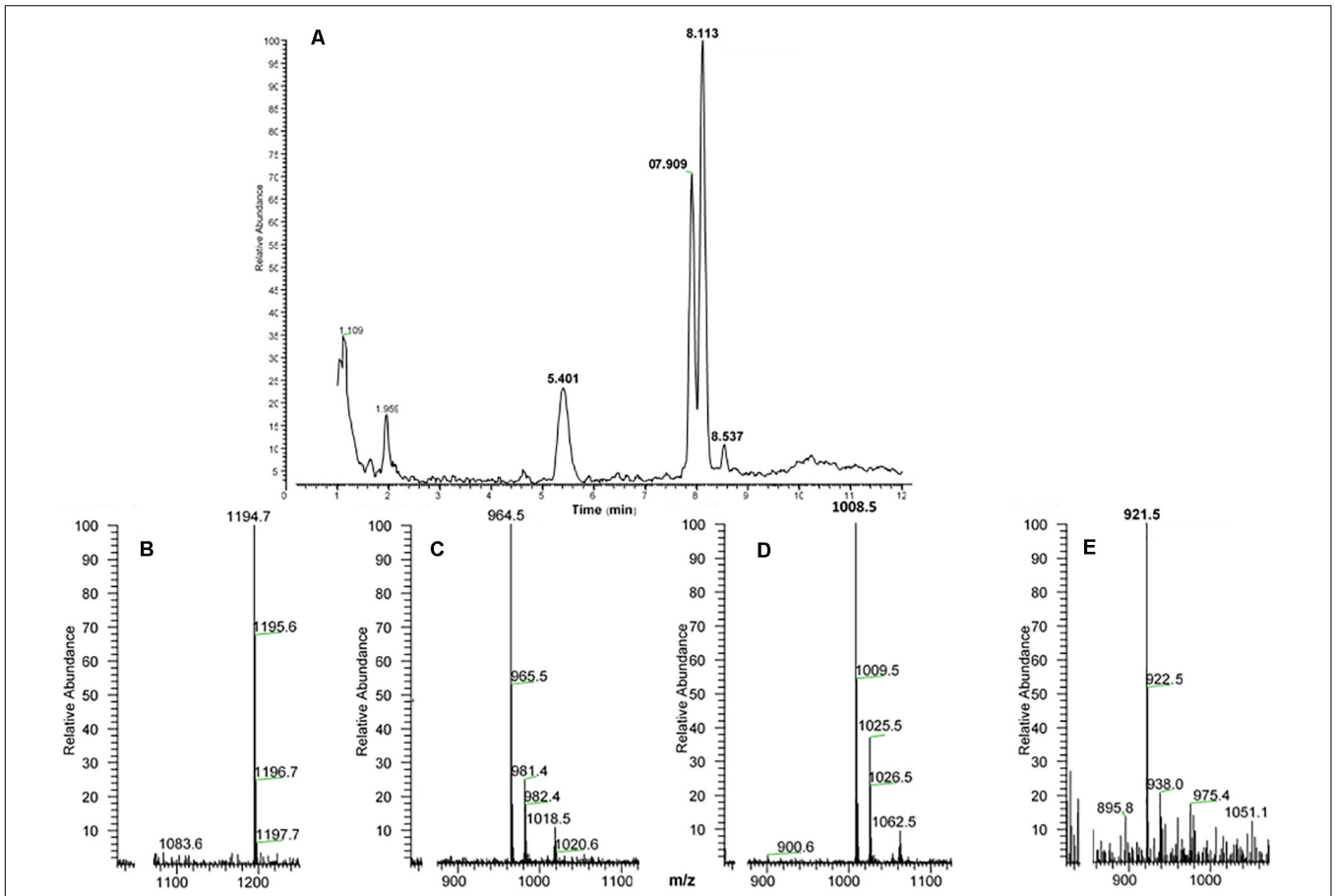

FIGURE 4 | LC-MS analysis of a methanolic extract from the corpus cardiacum of the Cape autumn widow *Dira clytus clytus*. **(A)** Base peak chromatogram obtained by LC-MS analysis showing detection of four AKH peptides labeled by retention times (RT) at 5.40, 7.91, 8.11, and 8.53 min, respectively. The background subtracted + ESI mass spectra are shown for **(B)** the ion at RT of 5.40 min and at *m/z* 1194.7; **(C)** the ion at RT 7.91 and at *m/z* 964.5; **(D)** the ion at RT of 8.11 and at *m/z* 1008.5; **(E)** the ion at RT of 8.53 and at *m/z* 921.5.

but the former led to the assignment of a novel decapeptide AKH for Lepidoptera. The CID assignment pointed to a peptide with two isobaric amino acids, a Leu or Ile residue at position 2 and a Gln or Lys residue at position 10 (**Figure 8**). A combination of co-elution with the synthetic compound having Leu^2 and Gln^{10} (**Supplementary Figures 6G–I**), as well as LC-HRMS measurement (MH^+ 1102.5316 in theory and 1102.5316 measured) led to the elemental composition of $C_{52}H_{72}N_{13}O_{14}$ and the sequence pGlu-Leu-Thr-Phe-Ser-Pro-Gly-Trp-Gly-Gln amide which we name Antya-AKH (**Figure 8**). This novel peptide is structurally most related to the decapeptide Bommo-AKH found in *B. mori*: a conservative Ser to Thr exchange has taken place at position 5.

AKHs of Lepidoptera Are (Almost) Exclusively Order-Specific

Extracts of CC from all other investigated Lepidoptera were treated the same as reported above, and the results of the assignment of their AKHs are collated in **Table 1**. By using ESI–MS methodology and comparison of various parameters of natural and synthetic peptide material, we have unequivocally identified the sequences of AKHs from 34 lepidopteran species of which the vast majority had not been investigated earlier. Four of these AKHs are novel and a further two have been found the first time in Lepidoptera but are known from other orders. Furthermore, we scanned databases for genomic/transcriptomic information on AKHs in Lepidoptera and have added those (predicted) AKH sequences, together with known lepidopteran AKHs from previously published reports (see section "Introduction") into **Table 1** to cover 76 lepidopteran species in total. Note that our efforts to scan genomes/transcriptomes did not always result in success, and such datasets, therefore, need to be taken with caution as it may be incomplete. Moreover, the interpretation of sequence processing from a gene/precursor does not take additional post-translational modifications of the peptide into account, other than cleavage from the precursor and amidation at the C-terminus. Cyclizing of the N-terminal Glu/Gln is inferred from sequence homology with biochemically sequenced AKHs, but there are several other post-translation modifications that are known to occur in AKHs – as gleaned from sequencing the mature peptides (e.g., hydroxprolination, C-mannosylation of Trp, modification

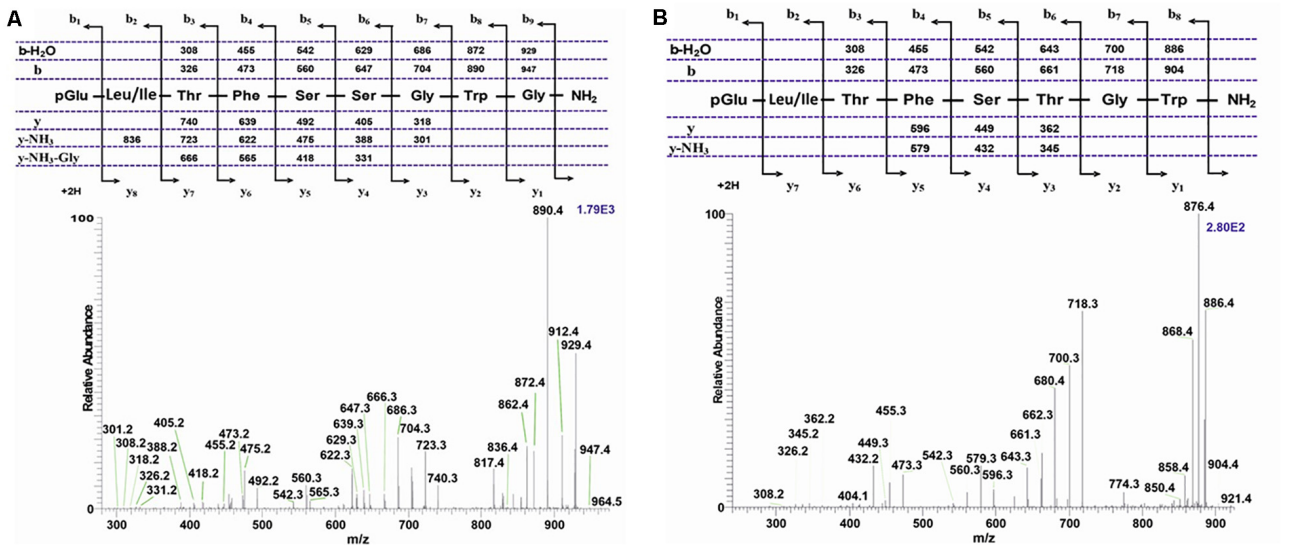

FIGURE 5 | CID tandem MS + ESI spectra. **(A)** The CID spectrum of the ion $(M + H)^+$ at *m/z* 964.5 in **Figure 4C** from *D. clytus clytus*. **(B)** The CID spectrum of the ion $(M + H)^+$ at *m/z* 921.5 in **Figure 4E** from *D. clytus clytus*. The insets show the proposed peptide sequences together with diagnostic fragment ions observed in the MS^2 spectra.

of Trp to kynurenine, sulfation, phosphorylation; see Marco and Gäde, 2020). Hence, predicted AKH sequences are just that: predictions and the sequence of the mature peptide remains to be confirmed by biochemical means; as such, we have given code names only to confirmed mature AKH sequences in the current study. Despite the shortcomings of only using bioinformatic searches, we have identified two more decapeptides that seem to be novel: in *Eumeta japonica* (superfamily: Tineoidea; pELTFTSNWGS amide) and in *Ostrinia furnacalis* (superfamily: Pyralidae; pELTFSTGWGQ amide). Once these putative AKHs have been shown, through mass spectrometry, to occur as mature peptides in the CC, they will be given their respective code names. Further, to orientate the reader, the data in **Table 1** are presented in a phylogenetic order (see Mitter et al., 2017; Kawahara et al., 2019; **Figure 1**).

When assessing this impressively large data set of 76 studied species in **Table 1**, we can reach a number of conclusions:

1. The maximal number of AKHs (five) expressed in the CC of the sphingid moth genus *Hippotion* (Gäde et al., 2013) is very likely a single evolutionary event. No other species investigated here has more than 2 or 3 AKHs (**Table 1**). Three AKHs are found in quite a few species of the family Noctuidae. Most other families have two AKHs. Interestingly, the most basal families of which we have data so far (from the superfamilies Adeloidea and Tineoidea) appear to have only one AKH, although it must be cautioned that this information was mined from genomic data which may have been incomplete or not completely accessible during our searches.
2. In total there are 15 different AKHs in Lepidoptera known to date from biochemical characterization – not counting the incompletely processed, inactive form of Manse-AKH (i.e., Vanca-AKH): six decapeptides, four nonapeptides and five octapeptides; a further two novel decapeptide sequences are predicted. This size distribution is quite different to what is seen in another speciose order, the Diptera, where 14 different AKHs are known to date – all are octapeptides, bar one (Gäde et al., 2020). Most interestingly, nonapeptides are a feature of Lepidoptera: the only other nonapeptide outside the Lepidoptera is found in the Hemiptera (a kissing bug; Marco et al., 2013); this same nonapeptide is identified in the current study in a nymphalid butterfly, *A. horta*.
3. Almost all lepidopteran species studied contain the nonapeptide Manse-AKH. This is certainly a signature peptide for the order Lepidoptera. It seems, however, to be absent in the more basal superfamilies represented in this study by Adeloidea, Tineoidea, Yponomeutoidea, and Tortricoidea and "emerges" with the Papilionoidea and is thereafter present in all phylogenetically "younger" superfamilies.
4. The basal superfamilies (mentioned above), on the other hand, all contain the octapeptide Peram-CAH-II, or the novel peptide predicted for *E. japonica* which differs from Peram-CAH-II at position 6 by a Ser instead of a Pro residue and in the chain length (octa- versus decapeptide). Peram-CAH-II is a peptide well-known from blattid cockroaches (order: Blattodea), from certain Caelifera (order: Orthoptera), Heteroptera (order: Hemiptera), and Chrysomeloidea (order: Coleoptera) (Gäde, 2009; Gäde et al., 2019) and recently, amplified and sequenced after data mining the codling moth transcriptome (Garczynski et al., 2019). From the superfamily Yponomeutoidea onward,

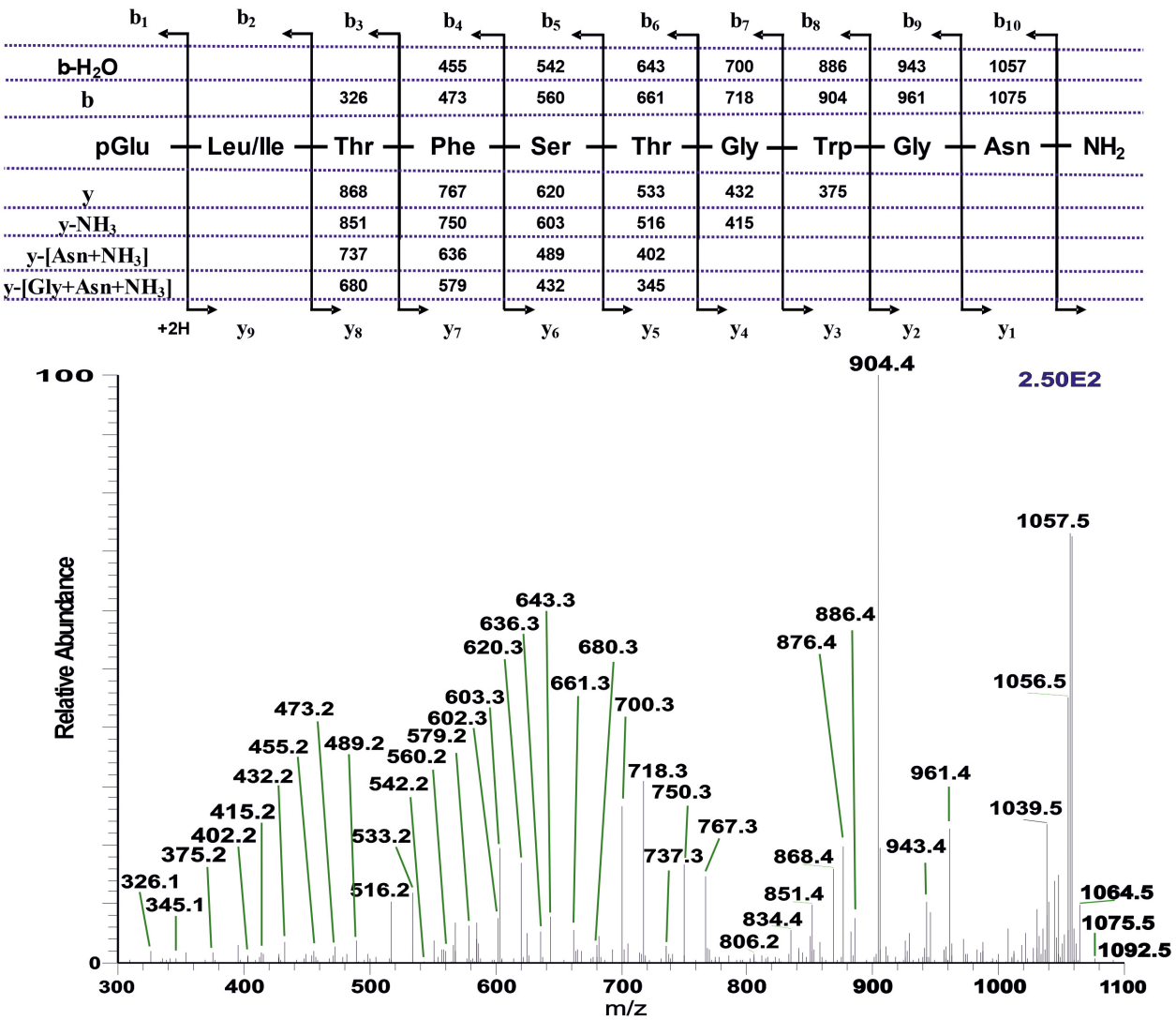

FIGURE 6 | The CID tandem MS + ESI spectrum of the ion $(M + H)^+$ at *m/z* 1092.5 (in **Supplementary Figure 4D**) from *Chilo partellus*. The inset shows the proposed peptide sequence together with diagnostic fragment ions observed in the MS^2 spectra.

including the superfamily Tortricoidea, we find also the decapeptide Lacol-AKH which then re-emerges in the superfamily Noctuoidea.

5. The octapeptide Piebr-AKH seems to be characteristic for the superfamily Papilionoidea (and also found in Gelechioidea) but has a scattered distribution in the various families: only one member of the Pieridae families and most species of the Nymphalidae produce Piebr-AKH together with Manse-AKH), whereas Papilionidae, Hesperiidae, and Lycaenidae do not. The latter families predominantly have Manse-AKH as sole AKH peptide, of those, four of the species were investigated by mass spectrometry and only Manse-AKH was detected and confirmed, while for the majority of species from these families, a bioinformatics search could only reveal Manse-AKH. Only two species of investigated Nymphalidae do not produce the common pair of AKHs (Manse-AKH + Piebr-AKH), or only Manse-AKH, viz. *D. clytus clytus* and *A. horta*. *D. clytus clytus* has a second nonapeptide – the novel Dircl-AKH-I – in addition to Manse-AKH, plus a novel octapeptide, Dircl-AKH-II, which differs from Piebr-AKH by a Ser/Thr exchange at position 5. *A. horta*, has, in addition to Manse-AKH and Piebr-AKH, also recruited a nonapeptide (Triin-AKH).
6. The one investigated species in the superfamily Gelechioidea, *Atrijuglans hetaohei*, produces Manse-AKH and Piebr-AKH (see Li et al., 2020). Apparently, there is still much controversy and discussion about the taxonomic status and the phylogenetic position of *A. hetaohei*: Chinese scholars have widely applied the proposal that *A. hetaohei* is a member of Heliodinidae (superfamily Yponomeutoidea) (see Wang et al., 2016).

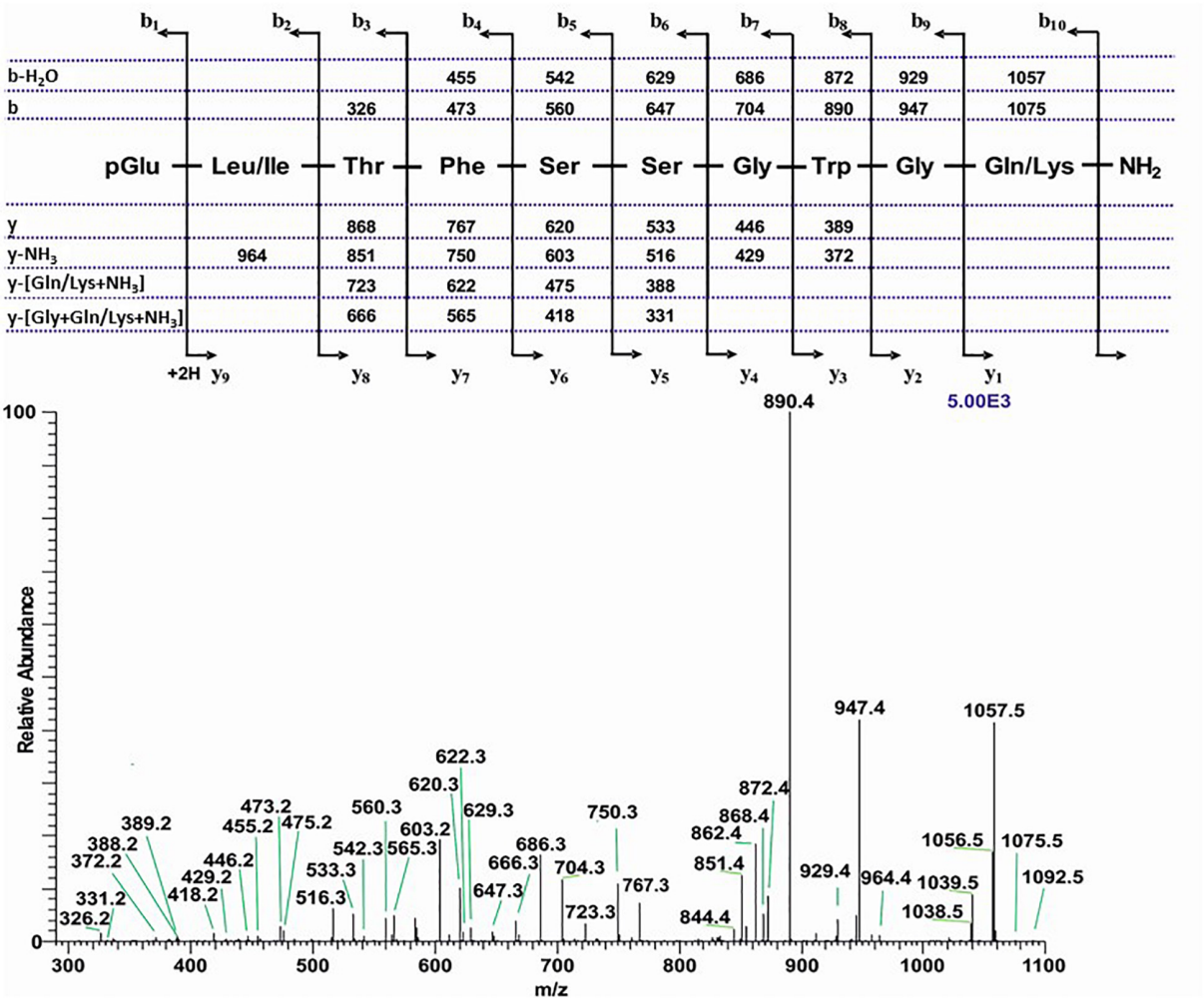

FIGURE 7 | The CID tandem MS + ESI spectrum of the ion $(M + H)^+$ at *m/z* 1092.5 (in **Supplementary Figure 5C**) from *Actias luna*. The inset shows the proposed peptide sequence together with diagnostic fragment ions observed in the MS^2 spectra.

This is, however, not the same conclusion drawn based on morphology and comparisons of mitochondrial genomes of Lepidoptera (Wang et al., 2016). Based on the predicted AKHs of *A. hetaohei* as deduced from transcriptome screening from heads of the moth (Li et al., 2020), we agree that *A. hetaohei* should be placed into family Stathmopodidae (superfamily Gelechioidea). Manse-AKH and Piebr-AKH both first appear in the superfamily Papillionoidea and cannot be reconciled to such an early appearance as in the superfamily Yponomeutoidea.

7. The superfamily Pyraloidea has as characteristic AKH the octapeptide Chipa-AKH (mostly in addition to the signature peptide Manse-AKH) or the novel peptide found in *O. furnacalis* which differs from Chipa-AKH only in residue 10 (a conservative Asn/Gln exchange).
8. The superfamily Noctuoidea contains always in addition to Manse-AKH the decapeptide Helze-HrTH, as shown previously (Jaffe et al., 1988). Thus, Helze-HrTH is certainly characteristic for this superfamily. Occasionally a third AKH can be found, Lacol-AKH (Gäde et al., 2008). Lacol-AKH, together with Helze-HrTH is also present in *Mythimna separata* (current study) and *Agrotis ipsilon* (Diesner et al., 2018). In studying the datasets of Diesner et al. (2018), we realize that the authors overlooked Manse-AKH in *A. ipsilon*: in their interpretation of putative preprohormones from transcriptomic information, the authors grouped the Manse-AKH precursor together with the Lacol-AKH precursor as "adipokinetic 1" (see data in Table 2 of Diesner et al., 2018). Evidence for the presence of Manse-AKH in CC tissue of *A. ipsilon* is shown (but not acknowledged/interpreted) in Figure 4B of Diesner et al. (2018) where the sodium adduct of Manse-AKH is clearly visible as mass ion 1030.47, along with the sodium adducts of Lacol-AKH (1087.49) and

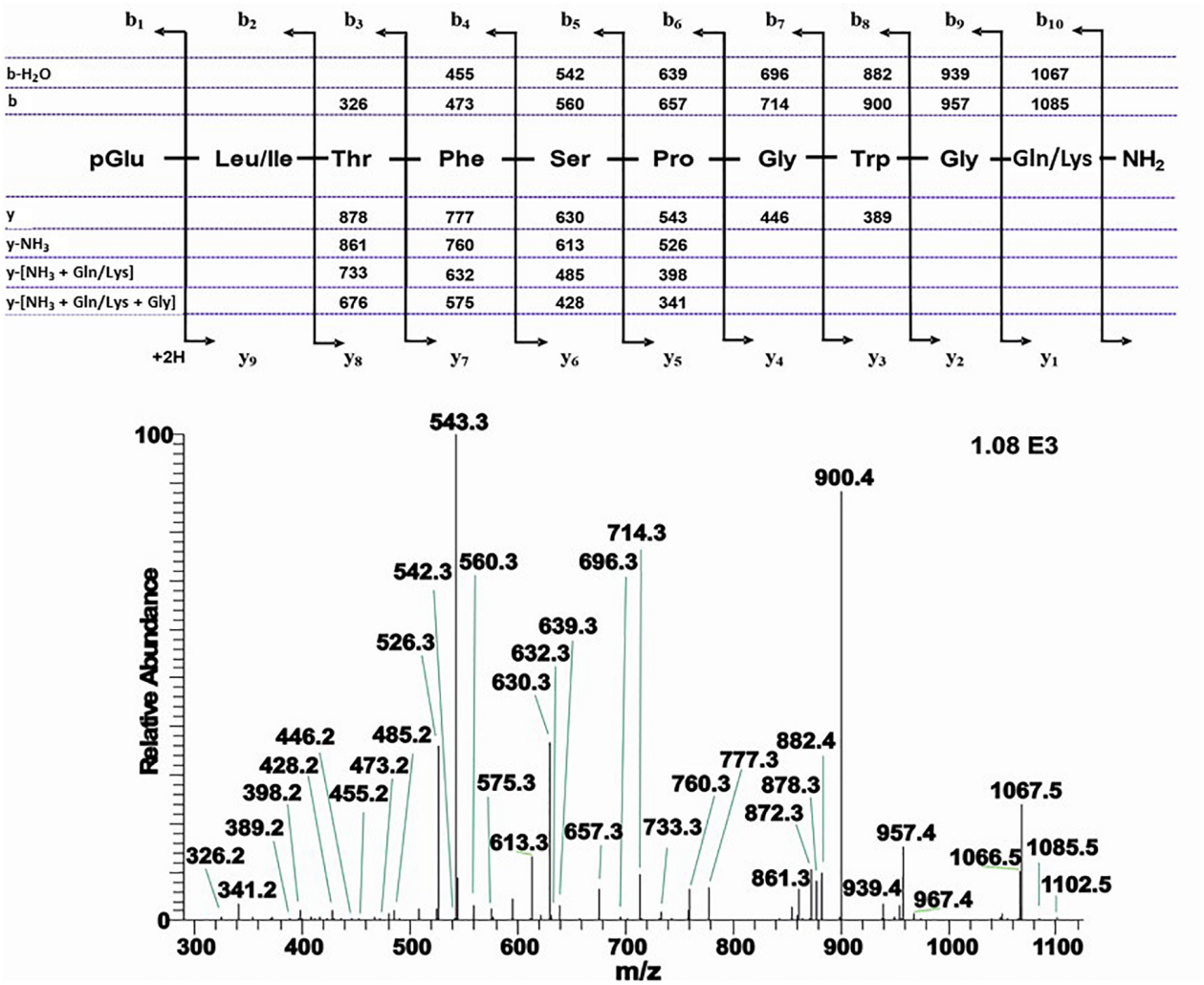

FIGURE 8 | The CID tandem MS + ESI spectrum of the ion $(M + H)^+$ at *m/z* 1102.5 (in **Supplementary Figure 6B**) from *A. yamamai*. The inset shows the proposed peptide sequence together with diagnostic fragment ions observed in the MS^2 spectra.

Helze-HrTH (1100.48). With our reinterpretation, thus, we have added Manse-AKH to the complement of AKHs in this noctuid moth species.

9. In the superfamily Bombycoidea, the three investigated families Saturniidae, Bombycidae, and Sphingidae contain besides the nonapeptide Manse-AKH, a decapeptide with the C-terminal tetrapeptide -GWGQ amide. Whereas Manse-AKH-II is found in all Sphingidae (except *Smerinthus ocellata*) and in one species of the Saturniidae, the other saturniid moth has the closely related Antya-AKH (Ser^6/Pro^6 exchange) and the bombycid moth has Bommo-AKH which differs from Antya-AKH by a Ser^5/Thr^5 substitution.
10. As a point of interest, one has to mention that no Val or Ile (normally at position 2) is found in any member of the AKHs of Lepidoptera, unlike in Diptera (Gäde et al., 2020).

Thus, we can conclude that the data as presented to date in **Table 1** point largely to an order-specificity and to some specificity in the superfamilies. In Nymphalidae where we have a relatively large data set with 19 studied species, no further differentiation between subfamilies can be made.

Adipokinetic Response of Lepidoptera AKH Family Bioanalogs: Potential for "Green" Insecticides?

We have already mentioned the dichotomous status of Lepidoptera as harmful (pest) and beneficial insects. Caterpillars of many lepidopteran species are assumed major agricultural pest species where they may be feeding mainly on flowers and reproductive structures of a single plant family or are polyphagous as a number of heliothine moths (Cunningham and Zalucki, 2014). The caterpillars may defoliate trees or whole

TABLE 3 | The difference in circulating lipid concentration following injection of distilled water or a synthetic Lepidoptera AKH peptide (10 pmol) into the cabbage white butterfly, *Pieris brassicae*.

Injectate/amino acid sequence	*n*	Difference (μg/μl)	*P*
Distilled water	10	−0.44 ± 2.87	NS
Peram-CAH-II: pELTFTPNWa	9	1.12 ± 2.57	NS
Bommo-AKH: pELTFTPGWGQa	6	0.94 ± 2.39	NS
Antya-AKH: pELTFSPGWGQa	8	1.80 ± 1.48	0.005
Dircl-AKH-II: pELTFSTGWa	10	3.60 ± 2.44	0.0006
Triin-AKH: pELTFTPNWGa	6	3.69 ± 1.71	0.002
Hipes-AKH-III: pELTFTSTWGa	9	3.77 ± 1.63	0.00006
Hipes-AKH-I: pELTFTSSWa	9	3.80 ± 1.58	0.00005
Manse-AKH-II: pELTFSSGWGQa	8	4.24 ± 1.18	0.00001
Helze-HrTH: pELTFSSGWGNa	7	4.56 ± 1.16	0.00002
Piebr-AKH: pELTFSSGWa	7	4.69 ± 2.05	0.0005
Manse-AKH: pELTFTSSWGa	6	4.70 ± 2.51	0.003
Dircl-AKH-I: pELTFSSGWGa	6	5.13 ± 1.77	0.0004
Lacol-AKH: pELTFTSSWGGa	7	5.18 ± 2.25	0.0004
Hipes-AKH-II: pELTFTSTWa	8	6.47 ± 1.63	0.00001
Chipa-AKH: pELTFSTGWGNa	7	8.28 ± 2.98	0.0002

Data arranged in increasing order of response.

forests or they can be devastating in destroying stored foods (see, Xu et al., 2016). Certain adult Lepidoptera (notably moths) are damaging too, by eating textiles (Basuk and Behera, 2018). Hence, it would be desirable to manage and fight such lepidopteran species/life stages specifically. Targeting insect neuropeptides and their cognate receptors (GPCRs) have been proposed as a good strategy for this task in integrated pest management (Audsley and Down, 2015; Verlinden et al., 2014). We assess here the potential of the AKH family of peptides. Whereas in a first step the complement of existing AKH peptides has to be determined, subsequent studies will aim to build a model of ligand-receptor binding, as has already been proposed for the AKH systems of the Malaria mosquito *Anopheles gambiae* (Mugumbate et al., 2013), the desert locust *Schistocerca gregaria* (Jackson et al., 2019) and the blowfly *Phormia terraenovae* (Abdulganiyyu et al., 2020b), as well as the red pigment-concentrating hormone system of the water flea, *Daphnia pulex* (Jackson et al., 2018). Thereafter, peptide mimetics will be tested (Altstein and Nässel, 2010) in a cellular receptor assay system (see, for example, in Caers et al., 2012; Abdulganiyyu et al., 2020a).

In the current study we have compiled a list of all the known Lepidoptera AKHs to date and went one step further to investigate ligand-receptor interaction of these AKH bioanalogs via a well-established *in vivo* bioassay in which the adipokinetic effect of an injected substance is measured in the hemolymph of a resting insect. The cabbage butterfly *P. brassicae* is the acceptor insect and all 15 biochemically confirmed, fully processed Lepidoptera AKH structures were tested (see **Table 3**). Previously, the incompletely processed AKH (Vanca-AKH) was tested in

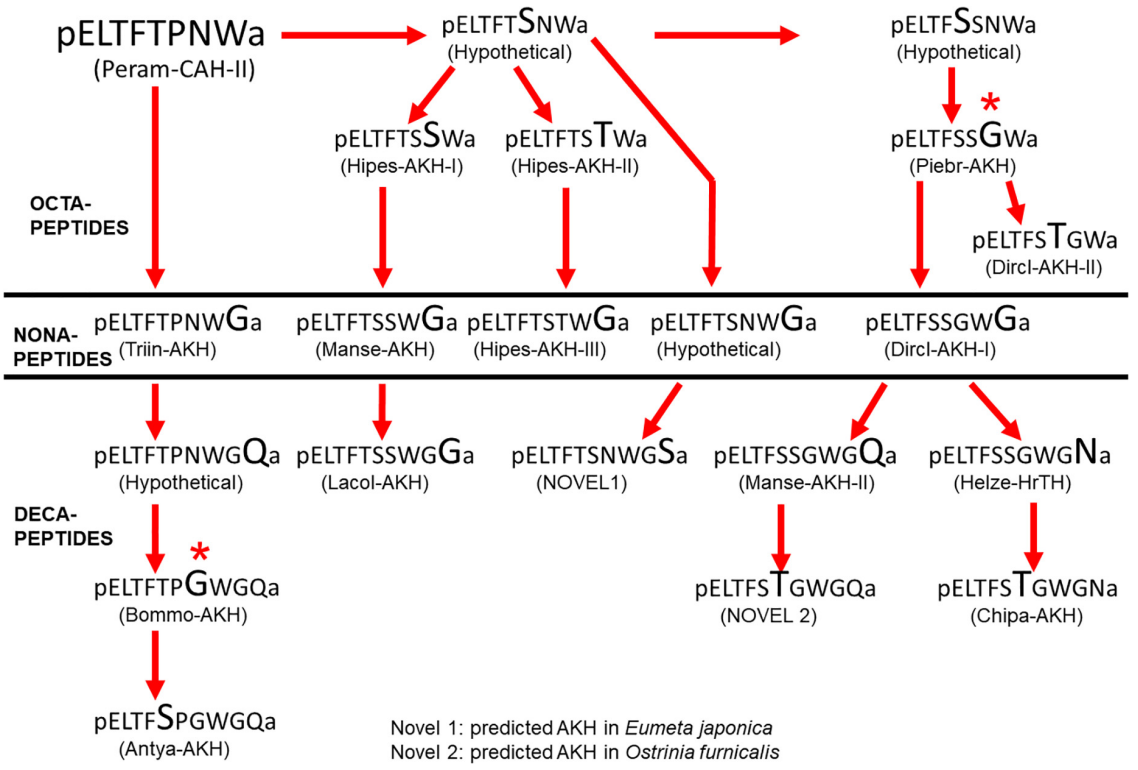

FIGURE 9 | Hypothetical molecular evolution of adipokinetic peptides in Lepidoptera. Peram-CAH-II is assumed here as ancestral peptide for this order. The amino acid substitution in each peptide is indicated in a larger font than in the peptide from which it is hypothetically derived. All substitutions are point mutations (except * for the proposed change from Asn to Gly) and four hypothetical peptide sequences are proposed to enable such a molecular evolution.

P. brassicae and found to have no adipokinetic activity (Marco and Gäde, 2017). The 15 chemically synthesized peptides were quantified via RP-HPLC and diluted in distilled water for injection, hence, distilled water served as a negative control substance to see that the solvent and handling of the animal did not artifactually increase the lipid concentration in the hemolymph. Both male and female test insects were used less than 48 h post-emergence and a mean lipid concentration of 22.22 ± 6.24 μg/μl (n = 123) was measured at the start of the experiment (**Supplementary Table 1**). A dose of 10 pmol peptide was injected as this previously gave unambiguous hyperlipemic results in *P. brassicae* (Marco and Gäde, 2017). The bioassay results are unequivocal (**Table 3** and **Supplementary Table 1**): distilled water and the handling/injection of butterflies do not elicit a stress (hyperlipemic) effect in the test insect, in fact, a slight dip in lipids (not significant) is recorded; two AKH bioanalogs fail to increase circulating lipids significantly in *P. brassicae* viz. Peram-CAH-II and Bommo-AKH, while Antya-AKH has a very small adipokinetic effect. One of the other low-performers is Triin-AKH; what these four peptides have in common is a Pro residue in position 6. One could speculate that Triin-AKH performed best in this group because it is a nonapeptide, which is a hallmark of Lepidoptera AKHs. Interestingly, when a Lacol-AKH analog was synthesized with Pro^6 and injected into *H. eson* adults in an earlier study (Marco and Gäde, 2015), the adipokinetic response was only slightly reduced to 94% of the possible maximal response. It may be too early to draw sound conclusions based only on experimentation with two species, but it seems as if the Pro^6 may differentially affect receptor-ligand interaction in AKH signaling in Lepidoptera. It can be predicted that *H. eson* would respond positively to the Pro-containing AKHs that performed poorly (or not at all) in *P. brassicae*. One could then speculate that a peptide mimetic based on a lead AKH peptide with Pro^6, may lend some specificity in its action amongst the Lepidoptera.

The remaining AKH bioanalogs tested currently in *P. brassicae* can be arbitrarily divided into different groups based on the resulting metabolic increase after injection. For example, in the lower-performing group are the octapeptides Dircl-AKH-II and Hipes-AKH-I, as well as the nonapeptide Hipes-AKH-III. None of these three peptides have a Pro residue; in the case of Hipes-AKH-I one could make two arguments (i) that peptide length is the decider on receptor interaction when the structure of Hipes-AKH-I is compared with that of one of the endogenous *P. brassicae* peptides (Manse-AKH): these peptides are near-identical save for the Gly^9 residue in Manse-AKH, and (ii) Hipes-AKH-I has two amino acid substitutions when compared with the endogenous octapeptide of *P. brassicae* Piebr-AKH, one of which is a Thr residue in position 5 instead of a Ser. The difference between Manse-AKH and Hipes-AKH-III also revolves around the seemingly simple, innocuous substitution of Ser and Thr in position 7, and the substitution of Ser and Thr is also involved between Piebr-AKH and Dircl-AKH-II but this time at position 6 (see **Table 3**). In all of these cases, the substituted Thr seems to be less-favored for endocrine signaling in the cabbage white butterfly, however the adipokinetic result with Chipa-AKH (a decapeptide with Thr^6) and Hipes-AKH-II (an octapeptide with Thr^7) are then enigmatic in that these peptides elicited the highest increase in lipid concentration after injection in the bioassay series. Chemical modeling of the AKH ligand-receptor interactions and NMR studies with the Lepidoptera ligands may shed light on the *in vivo* observations and explain the overall peptide conformation and how this affects interaction with the binding pocket of the different lepidopteran AKH receptor when amino acids are substituted in positions 5, 6, and/or 7.

The good adipokinetic response in *P. brassicae* achieved with the novel nonapeptide Dircl-AKH-I, and the decapeptides Lacol-AKH, Manse-AKH, Manse-AKH-II and Helze-HrTH are all consistent with the above observation that Ser^6Ser^7, and/or Ser^5Ser^6 seems to be preferred in the ligand for interaction with the *P. brassicae* AKH receptor. That such conservative exchanges of Thr/Ser at positions 5, 6, or 7 would influence the endocrine result is surprising because the chemical properties of the two amino acid residues are similar: both are polar amino acids, although Ser is more polar since Thr has an extra methyl group; Pro on the other hand is hydrophobic. *In vivo* bioassays with *H. eson* as test insect, however, also hinted that the AKH receptor has a slight preference for ligands with Ser^7 (Hipes-AKH-I, Manse-AKH, Lacol-AKH) or Gly^7 (Manse-AKH-II) over those with Thr^7 (Hipes-AKH-II and -III) (Gäde et al., 2013).

Can the current study provide useful pointers on the potential of the "green" insecticide concept with Lepidoptera AKHs? We see that Manse-AKH is a unique peptide present in almost all species of Lepidoptera but in no other order. It can be used as a lead peptide, and the chances that a final mimetic is specific only for Lepidoptera would then be high. Receptor binding studies have to be performed to ascertain whether further specificity is possible by making use of the various, superfamily specific, second AKHs. At first glance, the structures of these second AKHs seem not to be sufficiently different from Manse-AKH yet at the *in vivo* level, already small differences/trends can be seen in activity (current study). Previous receptor assay results with dipteran receptors and their endogenous AKHs (which are very similar in structure), also revealed subtle activation differences, giving hope that specificity on a case by case basis can be tested (Caers et al., 2012). Since a number of genomic studies on Lepidoptera have been carried out (Triant et al., 2018), which facilitates the cloning of more Lepidoptera AKH receptors, it is hoped that the modeling of ligand-receptor interaction and testing receptor activation may be achieved for some key lepidopteran species. It also remains to be seen whether Manse-AKH can function in the primitive Lepidoptera species where Peram-CAH-II is the endogenous AKH peptide.

Putative Molecular Evolution of Lepidopteran AKHs

A pre-requisite for the speculation of the molecular evolution of AKHs in Lepidoptera is the knowledge about a possible ancestral AKH of this order. This could probably be achieved by considering the structure of the AKH of the closest relatives to the Lepidoptera. Without doubt the caddisflies (Trichoptera) are assumed to be the sister group to Lepidoptera

(Kristensen et al., 2007; Mitter et al., 2017). Unfortunately, at present there is no published AKH structure from any member of the Trichoptera. Thus, our next best choice is to look at the AKH(s) present in the most basal lepidopteran superfamily, the Micropterigoidea, but we have neither collected any species nor have we mined any AKH sequence from this superfamily. As outlined in **Figure 1** we do, however, have data from a member of the family Adelidae (superfamily: Adeloidea) which has the octapeptide Peram-CAH-II predicted and a member of the family Psychidae (superfamily: Tineoidea) is predicted to have a very similar decapeptide (see **Table 1**). Since Peram-CAH-II has also been found in other orders and is the shorter of the two peptides, we assume here that this peptide is ancestral to Lepidoptera. As depicted in **Figure 9** one can construct a tree for the possible molecular evolution of the Lepidoptera AKHs, taking into account that we need (i) a few hypothetical peptides which may exist in the vast numbers of not-yet sequenced lepidopteran species, (ii) an elongation from octa- to nona- and then decapeptides, and (iii) in two cases, two nucleotides of the triplet (instead of just a single base change) were expected to have mutated to accommodate the change from an Asn to a Gly residue. Future work will confirm, refute or modify this hypothetical scheme.

DATA AVAILABILITY STATEMENT

The datasets presented in this study can be found in online repositories. The names of the repository/repositories and accession number(s) can be found in the article/**Supplementary Material**.

AUTHOR CONTRIBUTIONS

GG: concept and design of the study, acquisition of insect species and synthetic peptides, breeding of certain species from eggs, data acquisition (biological assays), interpretation and analysis of data, and writing the draft manuscript. HM: co-designed the study, data acquisition (biological assays, dissection of insect corpora cardiaca and preparation of extracts, and mining data bases for AKH sequences), interpretation and analyses of the data, and writing and refining the draft manuscript. PŠ: mass spectrometric analyses, data interpretation, and drafting of MS figures for the manuscript. All authors contributed to the article and approved the submitted version.

FUNDING

This work is based on the research supported in part by the National Research Foundation of South Africa: grant numbers 85768 (IFR13020116790) to GG and 109204 (IFR170221223270) to HM, and the University of Cape Town (Block Grants to GG and HM). PŠ was supported by the Czech Science Foundation, Project No. 17-22276S.

ACKNOWLEDGMENTS

The authors thank Pavla Kružberská for excellent technical support with MS measurements and all suppliers of insects mentioned in the main text.

SUPPLEMENTARY MATERIAL

The Supplementary Material for this article can be found online at: https://www.frontiersin.org/articles/10.3389/fphys.2020.614552/full#supplementary-material

REFERENCES

Abdel-Latief, M., and Hoffmann, K. H. (2007). The adipokinetic hormones in the fall armyworm, *Spodoptera frugiperda*: cDNA cloning, quantitative real time RT-PCR analysis, and gene specific localization. *Insect. Biochem. Mol. Biol.* 37, 999–1014. doi: 10.1016/j.ibmb.2007.05.007

Abdulganiyyu, I. A., Kaczmarek, K., Zabrocki, J., Nachman, R. J., Marchal, E., Schellens, S., et al. (2020a). Conformational analysis of a cyclic AKH neuropeptide analog that elicits selective activity on locust versus honeybee receptor. *Insect. Biochem. Mol. Biol.* 125:103362. doi: 10.1016/j.ibmb.2020.103362

Abdulganiyyu, I. A., Sani, M.-A., Separovic, F., Marco, H., and Jackson, G. E. (2020b). Phote-HrTH (*Phormia terraenovae* hypertrehalosaemic hormone), the metabolic hormone of the fruit fly: solution structure and receptor binding model. *Aust. J. Chem.* 73, 202–211. doi: 10.1071/CH19461

Agrawal, A. (2017). *Monarchs and Milkweed: A Migrating Butterfly, a Poisonous Plant, and their Remarkable Story of Coevolution*. Princeton: Princeton University Press.

Aker, C. L., and Udovic, D. (1981). Oviposition and pollination behavior of the Yucca moth, *Tegeticula maculata* (Lepidoptera: Prodoxidae), and its relation to the reproductive biology of *Yucca whipplei* (Agavaceae). *Oecologia* 49, 96–101. doi: 10.1007/bf00376905

Altstein, M., and Nässel, D. R. (2010). "Neuropeptide signalling in insects," in *Neuropeptide Systems as Targets for Parasite and Pest Control. Advances in Experimental Medicine and Biology*, eds T. G. Geary and A. G. Maule (Boston, MA: Springer).

Anneke, D. P., and Moran, V. C. (1978). Critical reviews on biological pest control in South Africa. 2. The prickly pear, *Opuntia ficus-indica* (L.) Miller. *J. Entomol. Soc. S. Afr.* 41, 161–188.

Audsley, N., and Down, R. E. (2015). G protein coupled receptors as targets for next generation pesticides. *Insect Biochem. Mol. Biol.* 67, 27–37. doi: 10.1016/j.ibmb.2015.07.014

Basuk, M., and Behera, J. (2018). A review on woollen cloth's moth and its remedies. *Banglad. Text. Today* 11, 68–77.

Baudron, F., Zaman-Allah, M. A., Chaipa, I., Chari, N., and Chinwada, P. (2019). Understanding the factors influencing fall armyworm (*Spodoptera frugiperda* J. E. Smith) damage in African smallholder maize fields and quantifying its impact on yield. A case study in Eastern Zimbabwe. *Crop Prot.* 120, 141–150. doi: 10.1016/j.cropro.2019.01.028

Beenakkers, A. M. T. (1969). Carbohydrate and fat as a fuel for insect flight. A comparative study. *J. Insect Physiol.* 15, 353–361. doi: 10.1016/0022-1910(69)90281-9

Bradfield, J. Y., and Keeley, L. L. (1989). Adipokinetic hormone gene sequence from *Manduca sexta*. *J. Biol. Chem.* 264, 12791–12793.

Brantjes, N. B. M. (1976). Riddles around the pollination of *Melandrium album* (Mill.) Garcke (Caryophyllaceae) during the oviposition by *Hadena bicruris* Hufn (Noctuidae, Lepidoptera) I. *Proc. Ser. C Biol. Med. Sci.* 79, 127–141.

Brattström, O., Bensch, S., Wassenaar, L. I., Hobson, K. A., and Åkesson, S. (2010). Understanding the migration ecology of European red admirals *Vanessa atalanta* using stable hydrogen isotopes. *Ecography* 33, 720–729. doi: 10.1111/j.1600-0587.2009.05748.x

Caers, J., Peeters, L., Janssen, T., De Haes, W., Gäde, G., and Schoofs, L. (2012). Structure-activity studies of *Drosophila* adipokinetic hormone (AKH) by a cellular expression system of dipteran AKH receptors. *Gen. Comp. Endocrinol.* 177, 332–337. doi: 10.1016/j.ygcen.2012.04.025

Challis, R. J., Kumar, S., Dasmahapatra, K. K., Jiggins, C. D., and Blaxter, M. (2016). Lepbase: the Lepidopteran genome database. *bioRxiv* [Preprint], doi: 10.1101/056994

Chapman, J. W., Reynolds, D. R., and Wilson, K. (2015). Long-range seasonal migration in insects: mechanisms, evolutionary drivers and ecological consequences. *Ecol. Lett.* 18, 287–302. doi: 10.1111/ele.12407

Corzo, F. L., Traverso, L., Sterkel, M., Benavente, A., Ajmat, M. T., and Ons, S. (2020). *Plodia interpunctella* (Lepidoptera: Pyralidae): intoxication with essential oils isolated from *Lippia turbinata* (Griseb.) and analysis of neuropeptides and neuropeptide receptors, putative targets for pest control. *Arch. Insect Biochem. Physiol.* 104:e21684. doi: 10.1002/arch.21684

Crabtree, B., and Newsholme, E. A. (1972). The activities of phosphorylase, hexokinase, phosphofructokinase, lactate dehydrogenase and the glycerol 3-phosphate dehydrogenase in muscles from vertebrates and invertebrates. *Biochem. J.* 126, 49–58. doi: 10.1042/bj1260049

Cunningham, J. P., and Zalucki, M. P. (2014). Understanding heliothine (Lepidoptera: Heliothinae) pests: what is a host plant? *J. Econ. Entomol.* 107, 881–896. doi: 10.1603/ec14036

Diesner, M., Gallot, A., Binz, H., Gaertner, C., Vitecek, S., Kahnt, J., et al. (2018). Mating-induced differential peptidomics of neuropeptides and protein hormones in *Agrotis ipsilon* moths. *J. Proteome Res.* 17, 1397–1414.

Donato, J. L., Moreno, R. A., Hyslop, S., Duarte, A., Antunes, E., Le Bonniec, B. F., et al. (1998). *Lonomia obliqua* caterpillar spicules trigger human blood coagulation via activation of factor x and prothrombin. *Thromb. Haemost.* 79, 539–542. doi: 10.1055/s-0037-1614940

Fónagy, A., Marco, H. G., König, S., and Gäde, G. (2008). Biological activity and identification of neuropeptides in the neurosecretory complexes of the cabbage pest insect, *Mamestra brassicae* (Noctuidae; Lepidoptera). *Acta Biol. Hung.* 59, 385–402. doi: 10.1556/abiol.59.2008.4.1

Gäde, G. (1989). The hypertrehalosaemic peptides of cockroaches: a phylogenetic study. *Gen. Comp. Endocrinol.* 75, 287–300. doi: 10.1016/0016-6480(89)90082-8

Gäde, G. (1992). The hormonal integration of insect flight metabolism. *Zool. JB Physiol.* 96, 211–225.

Gäde, G. (1997). "The explosion of structural information on insect neuropeptides," in *Progress in the Chemistry of Organic Natural Products*, Vol. 71, eds W. Herz, G. W. Kirby, R. E. Moore, W. Steglich, and C. H. Tamm (New York, NY: Springer), 1–128. doi: 10.1007/978-3-7091-6529-4_1

Gäde, G. (2009). "Peptides of the adipokinetic hormone/red pigment-concentrating hormone family - a new take on biodiversity," in *Trends in Comparative Endocrinology and Neurobiology. Annals of the New York Academy of Science*, Vol. 1163, eds H. Vaudry, E. W. Roubos, G. M. Coast, and M. Vallarino (Hoboken, NJ: Wiley-Blackwell), 125–136. doi: 10.1111/j.1749-6632.2008.03625.x

Gäde, G., Auerswald, L., Predel, R., and Marco, H. G. (2004). Substrate usage and its regulation during flight and swimming in the backswimmer, *Notonecta glauca*. *Physiol. Entomol.* 29, 84–93. doi: 10.1111/j.0307-6962.2004.0375.x

Gäde, G., Auerswald, L., Šimek, P., Marco, H. G., and Kodrík, D. (2003). Red pigment-concentrating hormone is not limited to crustaceans. *Biochem. Biophys. Res. Commun.* 309, 967–973. doi: 10.1016/j.bbrc.2003.08.107

Gäde, G., Goldsworthy, G. J., Kegel, G., and Keller, R. (1984). Single step purification of locust adipokinetic hormones I and II by reversed-phase high-performance liquid chromatography and the amino-acid composition of the hormone II. *Hoppe Seyler Z. Physiol. Chem.* 365, 393–398. doi: 10.1515/bchm2.1984.365.1.393

Gäde, G., and Marco, H. G. (2005). The adipokinetic hormones of Odonata: a phylogenetic approach. *J. Insect Physiol.* 51, 333–341. doi: 10.1016/j.jinsphys.2004.12.011

Gäde, G., and Marco, H. G. (2011). The adipokinetic hormone family in Chrysomeloidea: structural and functional considerations. *Zookeys* 157, 81–94. doi: 10.3897/zookeys.157.1433

Gäde, G., and Marco, H. G. (2017). The adipokinetic hormone of the coleopteran suborder Adephaga: structure, function, and comparison of distribution in other insects. *Arch. Insect Biochem. Physiol.* 95:e21399. doi: 10.1002/arch.21399

Gäde, G., Marco, H. G., Šimek, P., Audsley, N., Clark, K. D., and Weaver, R. J. (2008). Predicted versus expressed adipokinetic hormones, and other small peptides from the corpus cardiacum-corpus allatum: a case study with beetles and moths. *Peptides* 29, 1124–1139. doi: 10.1016/j.peptides.2008.03.002

Gäde, G., Šimek, P., Clark, K. D., and Marco, H. G. (2013). Five functional adipokinetic peptides expressed in the corpus cardiacum of the moth genus *Hippotion* (Lepidoptera, Sphingidae). *Regul. Pept.* 184, 85–95. doi: 10.1016/j.regpep.2013.03.029

Gäde, G., Šimek, P., and Marco, H. G. (2011). An invertebrate [hydroxyproline]-modified neuropeptide: further evidence for a close evolutionary relationship between insect adipokinetic hormone and mammalian gonadotropin hormone family. *Biochem. Biophys. Res. Commun.* 414, 592–597. doi: 10.1016/j.bbrc.2011.09.127

Gäde, G., Šimek, P., and Marco, H. G. (2016). Novel members of the adipokinetic hormone family in beetles of the superfamily *Scarabaeoidea*. *Amino Acids* 48, 2785–2798. doi: 10.1007/s00726-016-2314-0

Gäde, G., Šimek, P., and Marco, H. G. (2019). Structural diversity of adipokinetic hormones in the hyperdiverse coleopteran *Cucujiformia*. *Arch. Insect Biochem. Physiol.* 2019:e21611. doi: 10.1002/arch.21611

Gäde, G., Šimek, P., and Marco, H. G. (2020). The adipokinetic peptides in Diptera: structure, function, and evolutionary trends. *Front. Endocrinol.* 11:153. doi: 10.3389/fendo.2020.00153

Garczynski, S. F., Hendrickson, C. A., Harper, A., Unruh, T. R., Dhingra, A., Ahn, S.-J., et al. (2019). Neuropeptides and peptide hormones identified in codling moth, *Cydia pomonella* (Lepidoptera: Tortricidae). *Arch. Insect Biochem. Physiol.* 101:e21587. doi: 10.1002/arch.21587

Grimaldi, D. A., and Engel, M. S. (2005). *Evolution of the Insects*. Cambridge: Cambridge University Press.

Guo, J. L., Li, X. K., Shen, X. J., Wang, M. L., and Wu, K. M. (2020). Flight performance of *Mamestra brassicae* (Lepidoptera: Noctuidae) under different biotic and abiotic conditions. *Insect Sci.* 20, 1–9.

Haag, C. R., Saastamoinen, M., Marden, J. H., and Hanski, I. (2005). A candidate locus for variation in dispersal rate in a butterfly metapopulation. *Proc. R. Soc. B Biol. Sci.* 272, 2449–2456. doi: 10.1098/rspb.2005.3235

Hansen, K. K., Stafflinger, E., Schneider, M., Hauser, F., Cazzamali, G., Williamson, M., et al. (2010). Discovery of a novel insect neuropeptide signaling system closely related to the insect adipokinetic hormone and corazonin hormonal systems. *J. Biol. Chem.* 285, 10736–10747. doi: 10.1074/jbc.m109.045369

Holwerda, D. A., van Doorn, J., and Beenakkers, A. M. T. (1977). Characterization of the adipokinetic and hyperglycaemic substances from the locust corpus cardiacum. *Insect Biochem.* 7, 151–157. doi: 10.1016/0020-1790(77)90008-7

Ishibashi, J., Kataoka, H., Nagasawa, H., and Isogai, A. (1992). Isolation and identification of adipokinetic hormone of the silkworm, *Bombyx mori*. *Biosci. Biotech. Biochem.* 56, 66–70. doi: 10.1271/bbb.56.66

Jackson, G. E., Pavadai, E., Gäde, G., and Andersen, N. H. (2019). The adipokinetic hormones and their cognate receptor from the desert locust, *Schistocerca gregaria*: solution structure of endogenous peptides and models of their binding to the receptor. *PeerJ* 7:e7514. doi: 10.7717/peerj.7514

Jackson, G. E., Pavadai, E., Gäde, G., Timol, Z., and Andersen, N. H. (2018). Interaction of the red pigment-concentrating hormone of the crustacean *Daphnia pulex*, with its cognate receptor, Dappu-RPCHR: a nuclear magnetic resonance and modeling study. *Int. J. Biol. Macromol.* 106, 969–978. doi: 10.1016/j.ijbiomac.2017.08.103

Jaffe, H., Raina, A. K., Riley, C. T., Fraser, B. A., Bird, T. G., Tseng, C. M., et al. (1988). Isolation and primary structure of a neuropeptide hormone from *Heliothis zea* with hypertrehalosemic and adipokinetic activity. *Biochem. Biophys. Res. Commun.* 155, 344–350. doi: 10.1016/s0006-291x(88)81091-x

Jaffe, H., Raina, A. K., Riley, C. T., Fraser, B. A., Holman, G. M., Wagner, R. M., et al. (1986). Isolation and primary structure of a peptide from the corpora cardiaca of *Heliothis zea* with adipokinetic activity. *Biochem. Biophys. Res. Commun.* 135, 622–628. doi: 10.1016/0006-291x(86)90038-0

Jiang, X. F., Luo, L. Z., Zhang, L., Sappington, T. W., and Hu, Y. (2011). Regulation of migration in *Mythimna separata* (Walker) in China: a review integrating environmental, physiological, hormonal, genetic, and molecular factors. *Environ. Entomol.* 40, 516–533. doi: 10.1603/en10199

Joos, B. (1987). Carbohydrate use in the flight muscles of *Manduca sexta* during pre-flight warm-up. *J. Exp. Biol.* 133, 317–327.

Kammer, A. E., and Heinrich, B. (1978). Insect flight metabolism. *Adv. Insect Physiol.* 13, 133–228. doi: 10.1016/s0065-2806(08)60266-0

Kawahara, A. Y., Plotkin, D., Espeland, M., Meusemann, K., Toussaint, E. F. E., Donath, A., et al. (2019). Phylogenomics reveals the evolutionary timing and pattern of butterflies and moths. *Proc. Natl. Acad. Sci. U.S.A.* 116, 22657–22663. doi: 10.1073/pnas.1907847116

Khadioli, N., Tonnang, Z. E. H., Muchugu, E., Ong'amo, G., Achia, T., Kipchirchir, I., et al. (2014). Effect of temperature on the phenology of *Chilo partellus* (Swinhoe) (Lepidoptera: Crambidae), simulation and visualization of the potential future distribution of *C. partellus* in Africa under warmer temperatures through the development of life-table parameters. *Bull. Entomol. Res.* 104, 809–822. doi: 10.1017/s0007485314000601

Kodrík, D., Marco, H. G., Šimek, P., Socha, R., Štys, P., and Gäde, G. (2010). The adipokinetic hormones of Heteroptera: a comparative study. *Physiol. Entomol.* 35, 117–127. doi: 10.1111/j.1365-3032.2009.00717.x

Köllisch, G. V., Lorenz, M. W., Kellner, R., Verhaert, P. D., and Hoffmann, K. H. (2000). Structure elucidation and biological activity of an unusual adipokinetic hormone from corpora cardiaca of the butterfly, *Vanessa cardui*. *Eur. J. Biochem.* 267, 5502–5508. doi: 10.1046/j.1432-1327.2000.01611.x

Köllisch, G. V., Verhaert, P. D., and Hoffmann, K. H. (2003). *Vanessa cardui* adipokinetic hormone (Vanca-AKH) in butterflies and a moth. *Comp. Biochem. Physiol. Part A* 135, 303–308. doi: 10.1016/s1095-6433(03)00074-6

Kono, N., Nakamura, H., Ohtoshi, R., Tomita, M., Numata, K., and Arakawa, K. (2019). The bagworm genome reveals a unique fibroin gene that provides high tensile strength. *Commun. Biol.* 2:148. doi: 10.1038/s42003-019-0412-8

Kristensen, N. P., Scoble, M. J., and Karsholt, O. (2007). Lepidoptera phylogeny and systematics: the state of inventorying moth and butterfly diversity. *Zootaxa* 1668, 699–747. doi: 10.11646/zootaxa.1668.1.30

Li, F., Zhao, X., Zhu, S., Wang, T., Li, T., Tracy Woolfley, T., et al. (2020). Identification and expression profiling of neuropeptides and neuropeptide receptor genes in *Atrijuglans hetaohei*. *Gene* 743:144605. doi: 10.1016/j.gene.2020.144605

Liebrich, W., and Gäde, G. (1995). Adipokinetic neuropeptides and flight metabolism in three moth species of the families Sphingidae, Saturnidae and Bombycidae. *Z. Naturforsch.* 50c, 425–434. doi: 10.1515/znc-1995-5-614

Llopis-Giménez, A., Han, Y., Kim, Y., Ros, V. I. D., and Herrero, S. (2019). Identification and expression analysis of the *Spodoptera exigua* neuropeptidome under different physiological conditions. *Insect Mol. Biol.* 28, 161–175. doi: 10.1111/imb.12535

Marco, H. G., and Gäde, G. (2015). Structure-activity relationship of adipokinetic hormone analogs in the striped hawk moth, *Hippotion eson*. *Peptides* 68, 205–210. doi: 10.1016/j.peptides.2015.01.007

Marco, H. G., and Gäde, G. (2017). Structure and function of adipokinetic hormones of the large white butterfly *Pieris brassicae*. *Physiol. Entomol.* 42, 103–112. doi: 10.1111/phen.12175

Marco, H. G., and Gäde, G. (2019). Five neuropeptide ligands meet one receptor: how does this tally? A structure-activity relationship study using adipokinetic bioassays with the sphingid moth, *Hippotion eson*. *Front. Endocrinol.* 10:231. doi: 10.3389/fendo.2020.00231

Marco, H. G., and Gäde, G. (2020). "Adipokinetic hormone: a hormone for all seasons?," in *Advances in Invertebrate (Neuro)Endocrinology: A Collection of Reviews in the Post- Genomic Era*, Vol. 2, eds S. Saleuddin, A. B. Lange, and I. Orchard (New Jersey: Apple Academic Press), 126–170.

Marco, H. G., Šimek, P., Clark, K. D., and Gäde, G. (2013). Novel adipokinetic hormones in the kissing bugs *Rhodnius prolixus*, *Triatoma infestans*, *Dipetalogaster maxima* and *Panstrongylus megistus*. *Peptides* 41, 21–30. doi: 10.1016/j.peptides.2012.09.032

Marzano, M., Ambrose-Oji, B., Hall, C., and Moseley, D. (2020). Pests in the city: managing public health risks and social values in response to oak processionary moth (*Thaumetopoea processionea*) in the United Kingdom. *Forests* 11:199. doi: 10.3390/f11020199

Mitter, C., Davis, D. R., and Cummings, M. P. (2017). Phylogeny and evolution of Lepidoptera. *Annu. Rev. Entomol.* 62, 265–283. doi: 10.1111/j.1420-9101.2003.00681.x

Mugumbate, G., Jackson, G. E., van der Spoel, D., Kövér, K. E., and Szilágyi, L. (2013). *Anopheles gambiae*, Anoga-HrTH hormone, free and bound structure - a nuclear magnetic resonance experiment. *Peptides* 41, 94–100. doi: 10.1016/j.peptides.2013.01.008

Nayar, J. K., and van Handel, E. (1971). Flight performance and metabolism of the moth *Spodoptera frugiperda*. *J. Insect Physiol.* 17, 2475–2479. doi: 10.1016/0022-1910(71)90095-3

O'Brien, D. M. (1999). Fuel use in flight and its dependence on nectar feeding in the hawkmoth *Amphion floridensis*. *J. Exp. Biol.* 202, 441–451.

Oda, Y., Uejuma, M., Iwami, M., and Sakurai, S. (2000). Involvement of adipokinetic hormone in the homeostatic control of hemolymph trehalose concentration in the larvae of *Bombyx mori*. *Arch. Insect Biochem. Physiol.* 45, 156–165. doi: 10.1002/1520-6327(200012)45:4<156::aid-arch3>3.0.co;2-e

Ovaskainen, O., Smith, A. D., Osborne, J. L., Reynolds, D. R., Carreck, N. L., Martin, A. P., et al. (2008). Tracking butterfly movements with harmonic radar reveals an effect of population age on movement distance. *Proc. Natl. Acad. Sci. U.S.A.* 105, 19090–19095. doi: 10.1073/pnas.0802066105

Predel, R., Wegener, C., Russel, W. K., Tichy, S. E., Russel, D. H., and Nachman, R. J. (2004). Peptidomics of CNS-associated neurohemal systems of adult *Drosophila melanogaster*: a mass spectrometric survey of peptides from individual flies. *J. Comp. Neurol.* 474, 379–392. doi: 10.1002/cne.20145

Rader, R., Bartomeus, I., Garibaldi, L. A., Garratt, M. P. D., Howlett, B. G., Winfree, R., et al. (2016). Non-bee insects are important contributors to global crop pollination. *Proc. Natl. Acad. Sci. U.S.A.* 113, 146–151.

Regier, J. C., Mitter, C., Zwick, A., Bazinet, A. L., Cummings, M. P., Kawahara, A. Y., et al. (2013). A large-scale, higher-level, molecular phylogenetic study of the insect order Lepidoptera (moths and butterflies). *PLoS One* 8:e58568. doi: 10.1371/journal.pone.0058568

Reinhardt, R., and Harz, K. (1989). *Wandernde Schwärmerarten - Die Neue Brehm Bücherei*. Wittenberg: Ziemsen Verlag.

Roch, G. J., Busby, E. R., and Sherwood, N. M. (2011). Evolution of GnRH: diving deeper. *Gen. Comp. Endocrinol.* 171, 1–16. doi: 10.1016/j.ygcen.2010.12.014

Roller, L., Yamanaka, N., Watanabe, K., Daubnerova, I., Zitnan, D., Kataoka, H., et al. (2008). The unique evolution of neuropeptide genes in the silkworm *Bombyx mori*. *Insect Biochem. Mol. Biol.* 38, 1147–1157. doi: 10.1016/j.ibmb.2008.04.009

Schumacher, P., Weyeneth, A., Weber, D. C., and Dorn, S. (1997). Long flights in *Cydia pomonella* L. (Lepidoptera: Tortricidae) measured by a flight mill: influence of sex, mated status and age. *Physiol. Entomol.* 22, 149–160. doi: 10.1111/j.1365-3032.1997.tb01152.x

Sekonya, J. G., McClure, N. J., and Wynberg, R. P. (2020). New pressures, old foodways: governance and access to edible mopane caterpillars, *Imbrasia* (= *Gonimbrasia*) *belina*, in the context of commercialization and environmental change in South Africa. *Intern. J. Commons* 14, 139–153. doi: 10.5334/ijc.978

Spik, G., and Montreuil, J. (1964). Deux causes d'erreur dans les dosages colorimetriques des oses neutres totaux. *Bull. Soc. Chim. Biol.* 46, 739–749.

Stefanescu, C., Páramo, F., Åkesson, S., Alarcón, M., Ávila, A., Brereton, T., et al. (2013). Multi-generational long-distance migration of insects: studying the painted lady butterfly in the Western Palaearctic. *Ecography* 36, 474–486. doi: 10.1111/j.1600-0587.2012.07738.x

Stokstad, E. (2017). New crop pest takes Africa at lightning speed. *Science* 356, 473–474. doi: 10.1126/science.356.6337.473

Teshome, A., Raina, S. K., and Vollrath, F. (2014). Structure and properties of silk from the African wild silkmoth *Gonometa postica* reared indoors. *J. Insect Sci.* 14:36.

Triant, D. A., Cinel, S. D., and Kawahara, A. Y. (2018). Lepidoptera genomes: current knowledge, gaps and future directions. *Curr. Opin. Insect Sci.* 25, 99–105. doi: 10.1016/j.cois.2017.12.004

van Handel, E., and Nayar, J. K. (1972). Turn-over of diglycerides during flight and rest in the moth *Spodoptera frugiperda*. *Insect Biochem.* 2, 8–12. doi: 10.1016/0020-1790(72)90061-3

van Nieukerken, E. J., Kaila, L., Kitching, I. J., Kristensen, N. P., Lees, D. C., Minet, J., et al. (2011). Order Lepidoptera, Linnaeus, 1758. *Zootaxa* 3148, 212–221.

Veerman, A., and Van Zon, J. C. J. (1965). Insect pollination of pansies (*Viola* spp.). *Entomol. Exp. Appl.* 8, 123–134. doi: 10.1111/j.1570-7458.1965.tb00847.x

Verlinden, H., Vleugels, R., Zels, S., Dillen, S., Lenaerts, C., Crabbé, K., et al. (2014). Receptors for neuronal or endocrine signalling molecules as potential targets for the control of insect pests. *Adv In Insect Phys.* 46, 167–303. doi: 10.1016/B978-0-12-417010-0.00003-3

Wang, Q., Zhang, Z., and Tang, G. (2016). The mitochondrial genome of *Atrijuglans hetaohei* Yang (Lepidoptera: Gelechioidea) and related phylogenetic analyses. *Gene* 581, 66–74. doi: 10.1016/j.gene.2016.01.027

Weaver, R. J., Marco, H. G., Šimek, P., Audsley, N., Clark, K. D., and Gäde, G. (2012). Adipokinetic hormones (AKHs) of sphingid Lepidoptera, including the identification of a second *M. sexta* AKH. *Peptides* 34, 44–50. doi: 10.1016/j.peptides.2012.01.009

Xu, G., Gu, G.-X., Teng, Z.-W., Wu, S.-F., Huang, J., Song, Q.-S., et al. (2016). Identification and expression profiles of neuropeptides and their G protein-coupled receptors in the rice stem borer *Chilo suppressalis*. *Sci. Rep.* 6:28976.

Zebe, E. (1954). Über den Stoffwechsel der Lepidopteren. *Z. Vergl. Physiol.* 36, 290–317. doi: 10.1007/bf00298218

Zhang, Q., Nachman, R. J., Kaczmarek, K., Zabrocki, J., and Denlinger, D. L. (2011). Disruption of insect diapause using agonists and an antagonist of diapause hormone. *Proc. Natl. Acad. Sci. U.S.A.* 108, 16922–16926. doi: 10.1073/pnas.1113863108

Zheng, X. L., Cong, X. P., Wang, X. P., and Lei, C. L. (2011). A review of geographic distribution, overwintering and migration in *Spodopera exigua* Hübner (Lepidoptera: Noctuidae). *J. Entomol. Res. Soc.* 13, 39–48.

Ziegler, R., Eckart, K., and Law, J. H. (1990). Adipokinetic hormone controls lipid metabolism in adults and carbohydrate metabolism in larvae of *Manduca sexta*. *Peptides* 11, 1037–1040. doi: 10.1016/0196-9781(90)90030-9

Ziegler, R., Eckart, K., Schwarz, H., and Keller, R. (1985). Amino acid sequence of *Manduca sexta* adipokinetic hormone elucidated by combined fast atom bombardment (FAB)/tandem mass spectrometry. *Biochem. Biophys. Res. Commun.* 133, 337–342. doi: 10.1016/0006-291x(85)91880-7

Ziegler, R., and Gäde, G. (1984). Preliminary characterization of glycogen phosphorylase activating hormone and adipokinetic hormone from *Manduca sexta* corpora cardiaca. *Physiol. Entomol.* 9, 229–236. doi: 10.1111/j.1365-3032.1984.tb00702.x

Ziegler, R., and Schulz, M. (1986a). Regulation of carbohydrate metabolism during flight in *Manduca sexta*. *J. Insect Physiol.* 32, 997–1001. doi: 10.1016/0022-1910(86)90118-6

Ziegler, R., and Schulz, M. (1986b). Regulation of lipid metabolism during flight in *Manduca sexta*. *J. Insect Physiol.* 32, 903–908. doi: 10.1016/0022-1910(86)90106-x

Zöllner, N., and Kirsch, K. (1962). Über die quantitative Bestimmung von Lipoiden (Mikromethode) mittels der vielen natürlichen Lipoiden (allen bekannten Plasmalipoiden) gemeinsamen sulfophosphovanillin Reaktion. *Z. Ges. Exp. Medizin.* 135, 545–561. doi: 10.1007/bf02045455

Conflict of Interest: The authors declare that the research was conducted in the absence of any commercial or financial relationships that could be construed as a potential conflict of interest.

frontiers in Physiology

ORIGINAL RESEARCH
published: 18 December 2020
doi: 10.3389/fphys.2020.605145

Supplemental Sugar Is Required for Sex Pheromone Biosynthesis in *Mythimna separata*

Yaling Zhang[1†], Yuanchen Zhang[2†], Shuangyan Yao[1], Gaoping Wang[1], Jizhen Wei[1], Mengfang Du[1], Shiheng An[1] and Xinming Yin[1*]*

[1] Collaborative Innovation Center of Henan Grain Crops, College of Plant Protection, Henan Agricultural University, Zhengzhou, China, [2] College of Biology and Food Engineering, Innovation and Practice Base for Postdoctors, Anyang Institute of Technology, Anyang, China

Supplemental nutrients of adult moths maximize moth fitness and contribute to the pollination of many plants. Previous reports have revealed that sugar feeding promotes to sex pheromone biosynthesis by increasing the haemolymph trehalose concentration in mating moths. Here, *Mythimna separata* adults were employed as a model to investigate the effect of sugar feeding on sex pheromone biosynthesis. Results showed that in virgin females, sugar feeding markedly increased the concentrations of trehalose, pyruvic acid, and acyl-CoA in pheromone glands (PGs), which in turn led to an increase in sex pheromone titer, female ability to attract males and successfully mating frequency in sugar-fed females. Consistently, sugar-fed females laid more eggs than water-fed females. Furthermore, the refeeding of starved females also caused significantly increase in the concentrations of trehalose, pyruvic acid, and acyl-CoA in PGs, thus facilitating a significant increase in sex pheromone production. Most importantly, RNAi-mediated knockdown of trehalase (leading to PG starvation) resulted in an increase in trehalose content, and decrease in the concentrations of pyruvic acid, and acyl-CoA in PGs, which in turn led to a decrease of sex pheromone titer, female ability to attract males and successful mating efficacy. Altogether, results revealed a mechanism by which sugar feeding contributed to trehalose utilization in PGs, promoted to significantly increased sex pheromone precursor by increasing the concentrations of pyruvic acid and acyl-CoA, and facilitated to sex pheromone biosynthesis and successful mating.

Keywords: ***Mythimna separata*, sugar feeding, trehalase, sex pheromone biosynthesis, starve**

OPEN ACCESS

Edited by:
Bin Tang,
Hangzhou Normal University, China

Reviewed by:
Ya-Nan Zhang,
Huaibei Normal University, China
Liang Sun,
Chinese Academy of Agricultural Sciences (CAAS), China

***Correspondence:**
Jizhen Wei
weijizhen1986@163.com
Xinming Yin
xinmingyin@hotmail.com

† These authors have contributed equally to this work

Specialty section:
This article was submitted to Invertebrate Physiology, a section of the journal Frontiers in Physiology

Received: *11 September 2020*
Accepted: *03 December 2020*
Published: *18 December 2020*

Citation:
Zhang Y, Zhang Y, Yao S, Wang G, Wei J, Du M, An S and Yin X (2020) Supplemental Sugar Is Required for Sex Pheromone Biosynthesis in Mythimna separata. Front. Physiol. 11:605145. doi: 10.3389/fphys.2020.605145

INTRODUCTION

Insects are the most prosperous species on earth. Strong reproductive capacity is one of important factors for insect prosperity. Once the environment is suitable, insects produce a huge quantity of offspring, which causes the population to increase rapidly in a short period, finally leading to pest outbreak and considerable loss of crops. Like that of animals, the reproduction of most insects is sexual mating. Therefore, successful mating plays an important role in the process of insect reproduction. Unlike higher animals, insects, especially Lepidopteran moths, usually employ female sex pheromones as chemical signals for long-distance information exchange (Ando et al., 2004), which is the key factor for male moths to locate female moths.

Sex pheromone is a micro chemical synthesized and released by the female sex pheromone glands (PGs) located between the 8th and 9th abdominal segments (Tillman et al., 1999; Jurenka, 2003). Sex pheromone is comprised of multicomponent unsaturated fatty acids (10–18 straight chain hydrocarbons) with oxidized ends (alcohols, aldehydes, acetates, etc.) (Tillman et al., 1999). Sex pheromones were *de novo* synthesized from acetyl-CoA followed by chain shortening, desaturation and reduction (Tillman et al., 1999; Jurenka, 2003). Studies had confirmed that a neuropeptide, named as pheromone biosynthesis activating neuropeptide (PBAN), regulated female pheromone biosynthesis and release in Lepidoptera (Tillman et al., 1999). PBAN gene was first identified in *Bombyx mori* and *Helicoverpa zea* (Raina et al., 1989; Kitamura et al., 1990), and then in other Lepidoptera species (Davis et al., 1992; Ma et al., 1994; Xu et al., 1995; Kochansky et al., 1997; Jacquin-Joly et al., 1998; Tillman et al., 1999; Iglesias et al., 2002; Rafaeli, 2002; Ando et al., 2004; Xu and Denlinger, 2004; Lee and Boo, 2005; Jing et al., 2007). Sequence analysis found that PBAN consists of 33 amino acid residues with a conserved amidated C-terminal (Kochansky et al., 1997). PBAN receptor was also identified in *H. Zea* and *B. mori* (Choi et al., 2003; Hull et al., 2004). Studies confirmed that PBAN receptor was a kind of conserved G protein receptor (Choi et al., 2003). The finding of PBAN receptor was a groundbreaking contribution to the deciphering of signal transduction cascade mechanism following the ligand PBAN binding to its respective PBAN receptor in the PG. PBAN signal cascades were well documented in subsequent studies. In *H. armigera*, after binding with its receptor located at the plasma membrane of PG cells, PBAN employed Ca^{2+} and cAMP as second messages. On the one hand, Ca^{2+} - calmodulin complexes activate calcineurin, which in turn activate acetyl-CoA carboxylase through dephosphorylation at ser92 site (Acetyl-CoA carboxylase is the critical enzyme in fatty acid biosynthesis, which catalyzes carboxylation of acetyl-CoA to yield malonyl-CoA), finally leading to sex pheromone biosynthesis and release (Du et al., 2017). On the other hand, the cAMP/PKA signal suppresses the AMPK activity, which is an upstream kinase of acetyl-CoA carboxylase, thus ensuring the calcineurin activation of acetyl-CoA carboxylase (Du et al., 2017). In *B. mori*, PBAN was found to use Ca^{2+} as a second message. Ca^{2+} first activated calcineurin (a protein phosphatase) and calmodulin-dependent kinase II (CamKII). And then calcineurin in turn mediated fatty acyl reductase, while CamKII activated lipid storage droplet protein-1 by phosphorylation, thereby leading to lipolytic release of stored pheromone precursors (Ohnishi et al., 2011). These results well deciphered the detailed mechanism of PBAN signal transduction.

PBAN functions as an endogenous regulator of sex pheromone biosynthesis and release in moths. In fact, the biosynthesis and release of sex pheromone are also affected by other endogenous factors. Studies found that in *H. zea*, a pheromonostaitc peptide secreted from male accessory glands could strongly inhibit sex pheromone biosynthesis (Kingan et al., 1995). In *Drosophila melanogaster*, a sex peptide (SP) generated from the male accessory glands caused strong suppression of female receptivity, leading to a few mating of females with males (Ottiger et al., 2000). Most interestingly, this SP from *D. melanogaster* also promoted juvenile hormone synthesis and eventually caused a decrease in sex pheromone production in *H. armigera* (Fan et al., 2000). In addition, some exogenous factors also affect sex pheromone biosynthesis. In *H. virescens*, sugar-feeding led to a significant increase in sex pheromone biosynthesis in mating females, further studies demonstrated that sugar-feeding contributed to the increase in hemolymph trehalose, a key material to generate acetyl-CoA *via* glycolysis and tricarboxylic acid cycle (Foster, 2009). Most importantly, 65% of sex pheromone production comes from a single adult feed, implying the importance of sugar feeding on sex pheromone biosynthesis (Foster and Anderson, 2015). These studies had considerably deepened the understanding on the supplemental nutrition of female adults. In the present study, *M. separata* was used as a model to investigate the effect of adult supplemental nutrition on female mating, especially on sex pheromone biosynthesis.

MATERIALS AND METHODS

Insects

M. separata larvae were collected from maize field in Jiyuan, Henan province, China. Larvae were maintained with an artificial diet at 28°C with 16 h light/8 h dark photoperiod. Pupae were distinguished by gender and stored in separate cages until emergence. Newly emerged adults in the 1st photophase were referred to as 1 day-old adults and were subjected to subsequent feeding experiment.

Chemicals

PBAN was biosynthesized from Sangon Biotech (Shanghai, China). Z11-hexadecenal (Z11–16Ald), sex pheromone component of *M. separata*, was obtained from Sigma (St. Louis, MO) and used to quantify sex pheromone in PG by gas chromatography/mass spectrometry (GC/MS).

The Determination of Trehalose, Pyruvic Acid, and Acyl-CoA Concentration in the PGs

Newly emerged females were collected and placed on a new cage with 5% sugar solution ($n \geq 24$). The corresponding control females were also placed on other new cage with water alone. PGs were collected at different time points after feeding with sugar (including 48, 72, and 96 h after feeding with sugar). For starving treatments, the $n \geq 20$ newly emerged females (for each treatment) were fed only water for 24, 48, and 72 h later, then refed with 5% sugar solution. PGs were collected 24 h (including one photophase and one night phase) after refeeding to keep the adults had enough time to feed sugar, and biosynthesize sex pheromone. The above harvested PGs were subjected to quantitative determination of the concentrations of trehalose, pyruvic acid, and acyl-CoA by using the concentration

determination kits (A149-1-1, A076-1-1, and A081 kit from Nanjing Jiancheng Bioengineering Institute, respectively). The detailed steps followed the manufacturer's suggestions[1] and the previous reports (Du et al., 2017; Jiang et al., 2020; Xu et al., 2020).

The Measurement of Sex Pheromone Production by GC/MS

Newly emerged females were collected and placed on 5% sugar solution ($n \geq 20$). The corresponding control females were on water alone. Three replicates were adopted. Prior to collecting PGs, 10 pmol of PBAN was injected into PGs, after 1 h waiting time, PGs were collected at different time points after feeding (including 48, 72, and 96 h after feeding). The harvested PGs were dissolved in hexane and then subjected to further GC/MS analysis as described above (Zhao et al., 2018).

For starving treatment, the $n \geq 20$ newly emerged females (for each treatment) were fed only water for 24, 48, and 72 h later, then refed with 5% sugar solution for 24 h, PGs were then collected as the above method, and sex pheromone productions were tested by GC/MS.

Female Ability to Attract Males

Olfactometer was employed to investigate the effect of sugar feeding on female ability to attract males (Zhang et al., 2018). 20 newly emerged females were fed with 5% sugar solution or water. 72 h later, two treated females (5% sugar or water) were placed in two capture chambers (28 cm height × 30 cm width × 30 cm length with a 6 cm diameter of hole), respectively. 100 males (2 day-old) were together placed in released chamber (32 cm height × 30 cm width × 60 cm length) on 10 p.m. After 12 h (20:00 p.m. to 8:00 a.m.) waiting time, the male numbers in two capture chambers were recorded.

Mating Behavior

Females (n = 30) with sugar feeding at different time points (48, 72, and 96 h after feeding) were place a new cage (40 cm × 40 cm × 40 cm) with same number of males for 24 h. Then, the females were dissected, the proportion of successful mating was determined according to the presence of spermatophore in the bursa copulatrix (Zhao et al., 2018). Three biological replicates of each treatment were done.

Fecundity

Newly emerged females ($n \geq 20$) were collected and placed on a new cage with same number of males. In addition, 5% sugar solution was placed on cage to meet the female need to sugar. The corresponding control females were on water alone. Egg numbers were recorded after 120 h feeding. Three biological replicates of each treatment were done.

Quantitative Real-time PCR

Total RNA was extracted from the collected PG samples using TRIzol reagent (Invitrogen, Carlsbad, CA, United States) according to the manufacturer's instructions. RT-PCR was performed on by using first-strand cDNA as template, which was obtained from 1 μg total RNA exacted from each PG sample using the PrimeScriptRT reagent kit with gDNA Eraser (Takara, Beijing, China). The relative expression of gene associated sex pheromone biosynthesis (Du et al., 2017), trehalose transporter (Trel-E) (GenBank: MT995929), fatty acid reductase (FAR) (GenBank: MT995931), acetyl CoA carboxylase (ACC) (GenBank: MW286766), △-11 desturase (GenBank: MW286764), hexokinase (HK) (GenBank: MT995930), pyruvate kinase (PK) (GenBank: MW286765), and trehalase (GenBank: MT995933) were tested. The primers used for RT-PCR analysis are listed in **Table 1**. *M. separata* ribosomal protein gene GAPDH (GenBank: MT995932) and β-actin (GenBank: GQ856238.1) genes were used as reference genes. Real-time SYBR Green Supermix (Takara, Beijing, China) was employed to run PCR on an Applied Biosystems 7,500 Fast Real-Time PCR system (ABI, Carlsbad, CA, United States) following the manufacturer's instructions. The thermal cycler conditions for RT-PCR were set as following: 95°C for 4 min, followed by 40 cycles of 95°C for 15 s and 60°C for 20 s. Melting curve analysis and agarose gel electrophoresis analysis were employed to analysis the specificity of the SYBR Green PCR signal. The reliability and reproducibility of RT-PCR results were ensured by employing three biological replicates of each sample. Melting curve analysis and the calculation method for expression level of the target genes was done according to the description in Liu et al. (2015) and Wei et al. (2019).

Double-Stranded RNA (dsRNA) Synthesis

The templates for dsRNA synthesis were amplified using gene-specific primers containing T7 polymerase sites following previously described methods (Du et al., 2012a,b). A 488 bp cDNA fragment of trehalase was PCR-amplified to

TABLE 1 | Primers used for Real-time PCR in this study.

Primer name	Strand orientation	Sequence (5′–3′)
GAPDH –RTF	Forward	AGAGGGTGGTGCCAAGAAG
GAPDH –RTR	Reverse	GTAGCGGTGGTAGCGTGTA
β-actin –RTF	Forward	ACGAACGATTCCGTTGCCCT
β-actin –RTR	Reverse	TCTGCATACGGTCGGCGATG
Trel-E-RTF	Forward	AGTTATGTATGCTGCCTTTG
Trel-E –RTR	Reverse	TATGCTGTTGAGTTCGGTAA
FAR-RTF	Forward	AGTATCCATCGTCTTCCAT
FAR-RTR	Reverse	TCAACACTTCGTAGTCAGG
ACC –RTF	Forward	CACCTTTATGCTGCTTATC
ACC –RTR	Reverse	GTCTGTTACTTCTTGTCCCT
△-11 desturase -RTF	Forward	ACGGGCTTTATCTGTGCTT
△-11 desturase -RTR	Reverse	CAGTCAATGGCGGAGTTTT
Hexokinase -RTF	Forward	ATCTCACGCAACTGAAGCA
Hexokinase -RTR	Reverse	GCCGTCCTCTGACAGCATC
PK-RTF	Forward	GTAAAGAAGCCTCGTCCCA
PK-RTR	Reverse	CGTTGAAGAGCTGCCTGTG
Trehalase-RTF	Forward	TACAGTTTAGTTCCGCTT
Trehalase-RTR	Reverse	CCGTTAGGGATGTGACCG

[1]http://www.njjcbio.com/

generate the template for *in vitro* dsRNA synthesis. The primers were forward primer (5′-GATCACTAATACGACTCACTATAGGGAGAAGCCACCTATGTTGACAGC-3′) and reverse primer (5′-GATCACTAATACGACTCACTATAGGGAGACAAATCTGAGGCTAACGCTG-3′). PCR product was purified and then used as the template for *in vitro* dsRNA synthesis. MEGAscript RNAi kit (Ambion, Vilnius, Lithuaria) was used to synthesized dsRNA following the manufacturer's instructions. Resulting synthesized dsRNA was first treated with DNase and RNase to remove template DNA and single-stranded RNA and then purified using MEGAclearTM columns (Ambion, Vilnius, Lithuaria). Resulting dsRNA was finally eluted in diethyl pyrocarbonate (DEPC)-treated nuclease-free water. The concentrations of dsRNA were measured using a biophotometer (Eppendorf). Correspondingly enhanced green fluorescent protein (EGFP) dsRNA was also generated according to the above mentioned method and was used as the control (Du et al., 2012a,b).

The Effect of Trehalase Knockdown on Sex Pheromone Biosynthesis and Mating

dsRNA (10 μg) was injected into the intersegment membrane between the 7th and 8th abdominal segments of newly emerged females. 48 h after injection, the PGs were harvested and subject to RT-PCR analysis to test the interference frequency of RNAi. Just as above mentioned, females injected with dsRNA were decapitated to remove endogenous PBAN. 48 h after dsRNA injection, 10 pmol of PBAN was injected into female body. After 1 h waiting time, PGs were collected and dissolved in 100 μL hexane and stored in −80°C followed by GC/MS analysis to measure sex pheromone production. Females injected with 10 μg dsEGFP RNA were used as the controls. Correspondingly, the concernations of trehalose, pyruvate and acetyl-CoA were measured according to above mentioned methods to analysis the effect of trehalose knockdown on the concernations of trehalose, pyruvate and acetyl-CoA.

As the above method, 20 newly emerged females were injected with 15 μg dsRNA (trehalase or EGFP). 72 h after dsRNA injection, Male choosing number were recorded 12 h later. 30 females injected with dsRNA (trehalase or EGFP) were place a new cage with same number of untreated males. After 72 h, the proportion of successful mating was determined according to the presence of spermatophore in the bursa copulatrix (Zhao et al., 2018). Three biological replicates of each treatment were done.

Statistical Analysis

Significant difference in each two different treatments was compared with Student's *t*-test. Statistically significant differences are denoted with * ($P < 0.05$), ** ($P < 0.01$), and *** ($P < 0.001$). A *Yate-corrected chi-square test* was employed to determine the difference between the frequencies of male choosing different females with $P < 0.001$ (Zhang et al., 2018).

RESULTS

Effect of Sugar Feeding on the Contents of Trehalose, Pyruvic Acid, and Acyl-CoA in PGs

The effect of sugar feeding on the contents of trehalose, pyruvic acid, and acyl-CoA were investigated. The results showed that sugar feeding contributed to a significant increase in trehalose, ($P < 0.01$, **Figure 1A**), pyruvic acid ($P < 0.05$, **Figure 1B**), and acyl-CoA ($P < 0.05$, **Figure 1C**) production in female PGs compared with water feeding, indicating that sugar feeding affects the production of trehalose, pyruvic acid, and acyl-CoA in PG tissues.

Effect of Sugar Feeding on Sex Pheromone Production, Female's Ability to Attract Males and Mating

The sugar-fed females released significantly more sex pheromone at 72 and 96 h than water-feeding females ($P < 0.01$, **Figure 2A**). This increased sex pheromone production significantly lured more males than those fed with water ($X^2 = 11.36$, $P < 0.001$, **Figure 2B**). Most importantly sugar feeding promoted to an increase in the proportion of females to mate at 72 and 96 h ($P < 0.01$ and $P < 0.001$, respectively, **Figure 2C**), indicating successful mating frequency in sugar-fed females. Consistently, the sugar-fed females laid more eggs than the water-fed females ($P < 0.001$, **Figure 2D**).

Effect of Sugar Re-feeding of Starved Female on Sex Pheromone Biosynthesis

Starved females re-fed with sugar demonstrated significantly more contents of trehalose, pyruvic acid, and acyl-CoA in PG tissues than starved females fed with water ($P < 0.01$, **Figures 3A–C**). Most importantly, sugar refeeding of starved females caused to a significant increase in sex pheromone production ($P < 0.01$, **Figure 3D**).

Effect of Sugar Feeding on the Relative Expression of Genes Associated With Sex Pheromone Biosynthesis

Sugar feeding led to a significant decrease in the transcripts of Trel-E, fatty acid reductase (FAR), ACC, deta-11 desturase, hexokinase (HK), pyruvate kinase (PK) and trehalase after 48, 72, and 96 h (**Figure 4**), indicating that these gene expression levels were negative response to sugar feeding.

Effect of Trehalase Knockdown on Sex Pheromone Biosynthesis, Female Ability to Attract Males and Mating

A double-strand RNA of trehalase was injected into newly emerged females. RT-PCR was employed to investigate the interference efficacy at 48 h after injection. The results demonstrated that the injection of trehalase dsRNA led to a significant decrease in the transcript level of trehalase ($P < 0.01$,

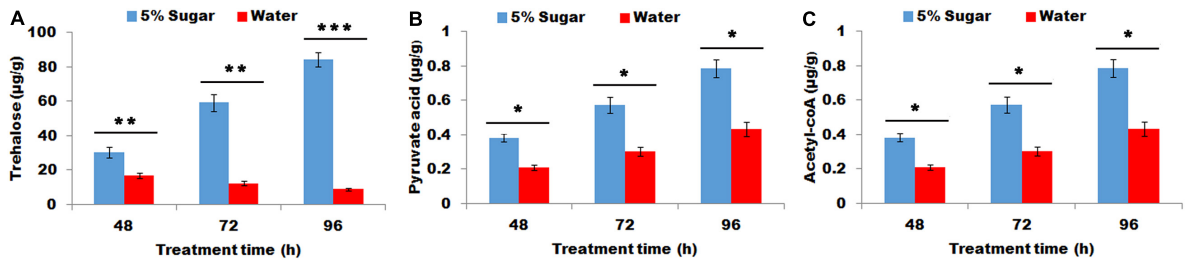

FIGURE 1 | Effect of sugar feeding on contents of trehalose **(A)**, pyruvic acid **(B)**, and acyl-CoA **(C)** in PGs. Each error bar represents the standard error of the mean from three replicates. Significant difference between 5% sugar feeding and water feeding was compared with Student's *t*-test. Asterisks showed significant differences, * ($P < 0.05$), ** ($P < 0.01$), and *** ($P < 0.001$) (Student's *t*-test).

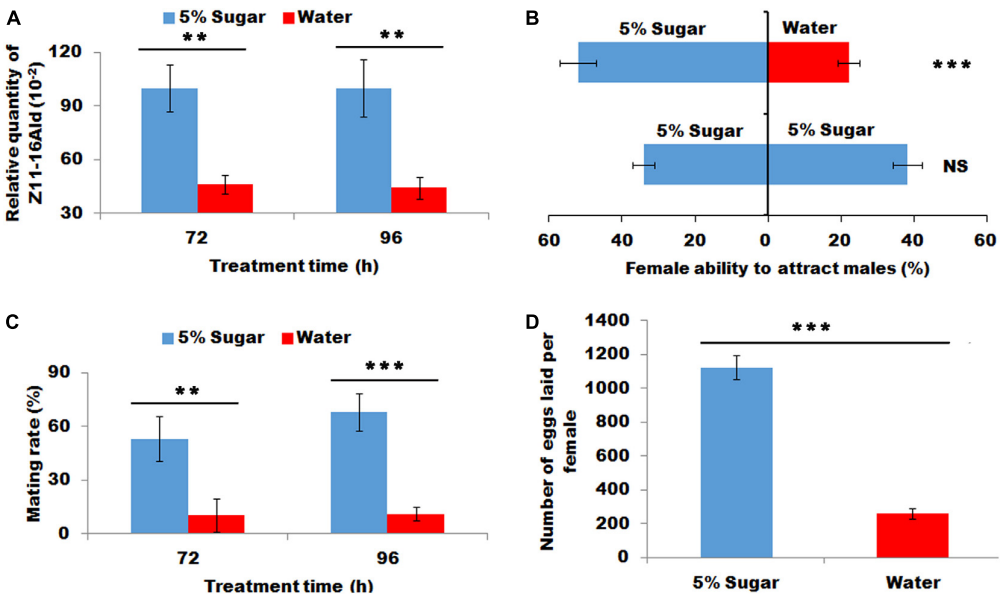

FIGURE 2 | Effect of sugar feeding on sex pheromone production **(A)**, female ability to attract males **(B)**, mating rate **(C)**, and fecundity **(D)**. Each error bar represents the standard error of the mean from three replicates. Significant differences between 5% sugar feeding and water feeding in sex pheromone production, mating rate and fecundity were compared with Student's *t*-test. The significant difference between 5% sugar feeding and water feeding in attractant rate was compared with *Yate-corrected chi-square test*. Asterisks showed significant differences, ** ($P < 0.01$) and *** ($P < 0.001$) (Student's *t*-test).

Figure 5A). After successful knockdown, the decrease in trehalase transcript caused a significant increase in trehalose in PGs ($P < 0.05$, **Figure 5B**). Consistently the RNAi-mediated knockdown of trehalase also resulted in a significant reduction in the contents of pyruvic acid and acytl-CoA ($P < 0.05$ and $P < 0.01$, respectively, **Figures 5C,D**). In addition, the females injected with trehalase dsRNA showed significantly decreased sex pheromone production, female ability to attract males and mating efficacy ($P < 0.05$, $X^2 = 9.47$, $P < 0.001$ and $P < 0.05$, respectively, **Figures 5E–G**), compared with the control females injected with EGFP dsRNA.

DISCUSSION

Insect larvae must feed its hosts that provided necessary nutrients to meet the needs of their growth and development (O'Brien et al., 2002). Therefore, feeding in larval stage was considered to be crucial for insect growth and development. As for adults, the food resources for the reproductions of most insects were thought to depend on larval feeding (Bradbury and Vehrencamp, 1998). However, most Lepidopteran species feed nectar that consists of water and sugar in the adult stage. Sugar feeding in the adult stage maximized the capacity of adult reproduction; however, it was generally thought to have a little effect on sex pheromone production (Bradbury and Vehrencamp, 1998). For example, in *Heliconius melpomene*, the male pheromone composition depends on larval feeding and is not associated with adult diet (Darragh et al., 2019), similarly a number of arctiid moth species produced their pheromones by using materials accumulated from larval feeding (Schulz et al., 1993; Edgar et al., 2007). These studies showed that adult moths seem to not use adult feeding to produce sex pheromone. However, a previous study revealed that the sugar feeding significantly increase sex pheromone

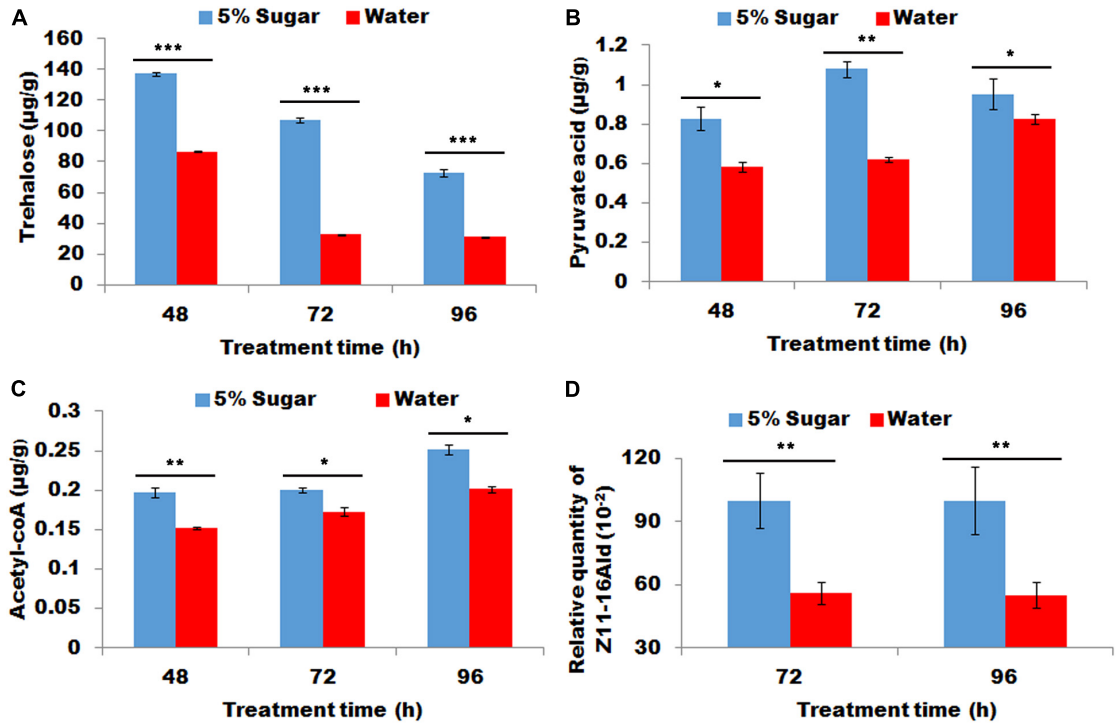

FIGURE 3 | Effect of sugar re-feeding of starved female on contents of trehalose **(A)**, pyruvic acid **(B)**, and acyl-CoA **(C)** and sex pheromone production **(D)**. As for 48 h treatment, newly-emerged females were first fed with water for 24 h and then refed with 5% sugar solution for 24 h (corresponding control females continue to feed with water for 24 h). As for 72 h treatment, newly-emerged females were first fed with water for 48 h and then re-fed with 5% sugar solution for 24 h (corresponding control females continue to feed with water for 24 h). As for 96 h treatment, newly-emerged females were first fed with water for 72 h and then re-fed with 5% sugar solution for 24 h (corresponding control females continue to feed with water for 24 h). Each error bar represents the standard error of the mean from three replicates. Significant difference between 5% sugar feeding and water feeding was compared with Student's *t*-test. Asterisks showed significant differences, * ($P < 0.05$), ** ($P < 0.01$), and *** ($P < 0.001$) (Student's *t*-test).

production in mated *H. virescens* (Foster, 2009). A subsequent study also revealed that even in virgin moths of *H. virescens*, adult feeding significantly increased sex pheromones, indicating that the starved stress in adults (sugar deficiency) led to a significant decrease in sex production on virgin or mated moths (Foster and Johnson, 2010). Most importantly, in *H. virescens* moths, only a single feeding (glucose) contributed to a maximum of 65% of *de novo* biosynthesized pheromone production (Foster and Anderson, 2015), indicating that sugar supplement in adult moths played a crucial role in sex pheromone biosynthesis. These results clarified the importance of supplemental sugar in sex pheromone biosynthesis. In the present study, sugar feeding significantly increased sex pheromone production and promoted to more proportion females to mate in *M. separata* (**Figures 1**–**3**). This finding was consistent with the result from *H. virescens* moths, that was, supplementary sugar played an important role in sex pheromone biosynthesis.

Sex pheromones were biosynthesized from precursor acetyl-CoA *via* fatty acid synthesis followed by desaturation, chain-shortening and reductive modification of carbonyl carbon (Tillman et al., 1999). As the precursor of sex pheromones, acetyl-CoA was produced *via* glycolysis and tricarboxylic acid cycle (Foster and Anderson, 2015). Most acetyl-CoAs for fatty acid biosynthesis originated from citrate, generated from pyruvate or fatty acid oxidation in the mitochondria. As for adult moth, carbohydrate was a supplementary sugar, which could be transformed to trehalose rapidly and easily. Trehalose serves as the main material to produce acetyl-CoA *via* glycolysis and tricarboxylic acid cycle (Foster and Anderson, 2015). In *H. virescens* moths, the deprivation of adult feeding caused a significant decrease in the trehalose concentration in adult haemolymph, finally leading to a reduction in sex pheromone production (Foster and Anderson, 2015). In *M. separata* adult, trehalose concentration in adult haemolymph was not detected in present study. Correspondingly, the trehalose concentration in PG tissues was investigated because trehalose in PG was better indicator for sex pheromone precursor than the trehalose in haemolymph. The results showed that sugar feeding increased trehalose concentration in PG tissues (**Figures 1A**, **3A**). Most importantly, the increase in the trehalose concentration in PG tissues in turn promoted an increase in pyruvate and subsequent acetyl-CoA production *via* glycolysis and tricarboxylic acid cycle, respectively (**Figures 1B,C**, **3B,C**), finally facilitating sex pheromone biosynthesis (**Figures 2B**, **3D**). Thus the trehalose in adult haemolymph contributed to sex pheromone biosynthesis and release in *M. separata* as shown by the trehalose, pyruvate and acetyl-CoA production in PG tissues. Given that mating leads to a great demand for sugar, sugar feeding in mated female

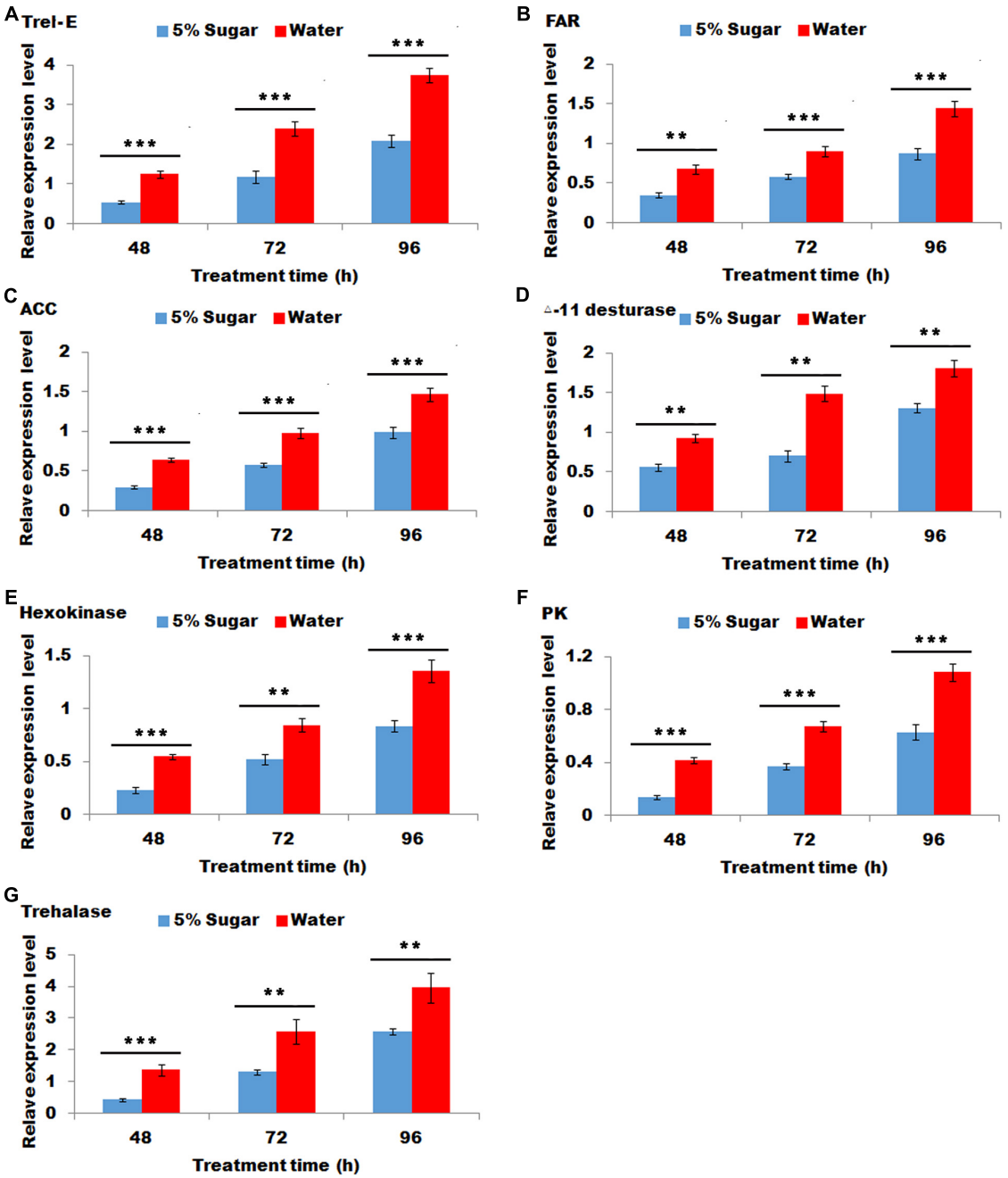

FIGURE 4 | Effect of sugar feeding on the relative expression levels of genes associated with sex pheromone biosynthesis. Each error bar represents the standard error of the mean from three replicates. Significant differences between 5% sugar feeding and water feeding in the expression of Trel-E **(A)**, fatty acid reductase (FAR) **(B)**, ACC **(C)**, △-11 desturase **(D)**, hexokinase (HK) **(E)**, pyruvate kinase (PK) **(F)**, and trehalase **(G)** were compared with Student's *t*-test. Asterisks showed significant differences, ** ($P < 0.01$) and *** ($P < 0.001$) (Student's *t*-test).

contributes to a significant increase in trehalose, pyruvate, acetyl-CoA and subsequent sex pheromones in *M. separata* moths. A similar phenomenon was also found in *H. virescens* adult, in which sugar feeding in mated female promoted an increase in sex pheromone. Interestingly, the early feeding of adult *H. virecence* (3 days before) had no effect on sex pheromone production, only adult feeding after 6 days showed a significant effect on sex pheromone biosynthesis (Foster and Johnson, 2010). However, in *M. separata* moths, only 2 days (48 h) feeding had a significant effect on sex pheromone biosynthesis, indicating the importance of sugar supplement for sex pheromone biosynthesis in this species (**Figure 1**). Different from *H. virescense*, *M. separata* moths have the habits of migration and gluttony, frequently leading to a large-area outbreak. The feeding amounts of

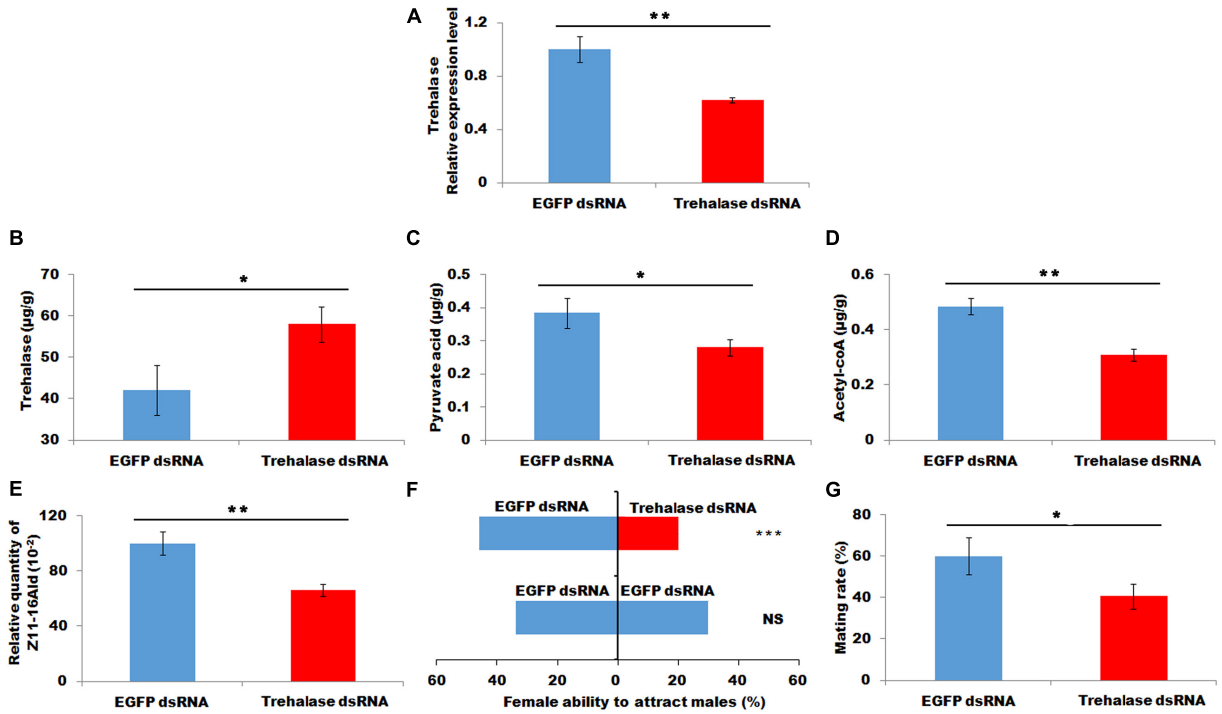

FIGURE 5 | Effect of trehalase knockdown on contents of trehalose **(B)**, pyruvic acid **(C)**, and acyl-CoA **(D)**, sex pheromone production **(E)**, attractant rate **(F)**, and mating rate **(G)**. **(A)**, the relative expression of trehalase. Each error bar represents the standard error of the mean from three replicates. Significant differences between injecting with trehalase RNA and dsEGFP RNA in expression level of trehalase, content of trehalose, pyruvic acid and acyl-CoA, sex pheromone production, attractant rate and mating rate were compared with Student's *t*-test. The significant difference in attractant rate was compared with *Yate-corrected chi-square test*. Asterisks showed significant differences, * ($P < 0.05$), ** ($P < 0.01$), and *** ($P < 0.001$) (Student's *t*-test).

M. separata moths were dozens of times higher than those of other Lepidopteran moths, indicating that the demands for supplementary nutrition were very high in *M. separata* moths. This finding possibly explained the reason why only 2 days (48 h) feeding significantly increased the sex pheromone production.

M. separata is a kind of gluttonous insect, thus investigating the effect of sugar supplement on sex pheromone in adult *M. separata* is ideal. However, some adult moths have no habits of supplementary nutrition. For example, after emergence, *B. mori* adults do not feed on anything and immediately produce sex pheromones and then mate (Matsumoto et al., 2010). Thus, no supplementary nutrition is available, females have to utilize the nutrition obtained by larvae to produce sex pheromone. In this kind of pattern, precursor fatty acids were generated from acetyl-CoA by larval feeding, and then stored in PGs in the form of triacylglycerols (TAGs). Evidences also revealed that lipid drops began to accumulate 3 days before emergence and rapidly increased 1 day before the emergence in PG tissues (Matsumoto et al., 2010). Once emergence, TAGs were available following PBAN release (Ohnishi et al., 2011). Correspondingly, PBAN stimulation led to a rapid decrease in the amount of lipid drops (Ohnishi et al., 2011). Therefore, as for this kind of patter, PBAN regulated the lipolysis of TAGs stored in PGs in advance by larval feeding biosynthesis (Ohnishi et al., 2011). Different to this pattern, the precursor fatty acids in TAGs were unavailable in many adult moths, such as *Ostrinia nubilalis*, although the much higher accumulation of TAGs in PGs, the stored TAGs in PGs were a dead end store and they did not serve as precursor acids for sex pheromone biosynthesis (Ohnishi et al., 2011). In *H. virescens*, the TAGs in PGs are similarly unavailable for sex pheromone biosynthesis (Foster et al., 2017). In these moths, TAGs in PGs act as a buffer for fatty acyl CoA. Given that these TAGs are not used as sex pheromone biosynthesis, the females have to *de novo* biosynthesize the fatty acid precursor for sex pheromone biosynthesis (Foster et al., 2017). In this kind of pattern, a rapid and convenient method is to employ the hemolymph trehalose to obtain the required precursor fatty acid for sex pheromone, indicating that adult feeding probably plays an important role in the rapid biosynthesis of precursor fatty acid. Foster (2004, 2009), Foster and Johnson (2010), and Foster and Anderson (2015) provided irrefutable facts that supplementary sugar is the main material for the precursor fatty acids of sex pheromones. Even a single feeding (glucose) contributed to a maximum of 65% of *de novo* biosynthesized pheromone production (Foster and Anderson, 2015). Correspondingly, different from the regulated pattern in *B. mori*, PBAN regulated the steps of fatty acid synthesis in these species (Matsumoto et al., 2010). For example, in *H. armigera*, PBAN mediated the activation of acetyl-CoA carboxylase, a speed-limited enzyme of fatty acid biosynthesis, and facilitated sex pheromone biosynthesis (Du et al., 2017). Thus, the differences in the habits of adult feeding were consistent with the differences in PBAN actions.

In the present study, sugar feeding promoted the increase in trehalose, pyruvate, and acetyl-CoA production in *M. separata* (**Figures 1**, **3**); and contributed to the increase in sex pheromone biosynthesis and the subsequent mating proportion of female moth (**Figures 2**, **3**). Trehalase was chosen as a readout of sugar metabolism to further investigate the effect of sugar supplement on sex pheromone biosynthesis. Trehalase is a key enzyme that catalyzes the hydrolysis of trehalose into two glucose molecules (Becker et al., 1996). Trehalase knockdown means although trehalose is sufficient, it does not normally transform to glucose (**Figure 5B**). In other word, as adults continued to feed, the females were still in the state of starvation. The results of the present study were well agreement with the previous prediction. RNAi-mediated knockdown of trehalase led to a significant accumulation of trehalose in the PGs (**Figure 5B**), and a significant decrease in pyruvate, acetyl-CoA concentration and sex pheromone production in PGs (**Figures 5C–E**), finally led to a decrease in the female ability to attract males and female mating frequency (**Figures 5F,G**). The results showed that *M. separata* adult adopted same strategies with those of *H. virescens* to produce sex pheromone (Foster, 2009; Foster and Johnson, 2010). Thus, adult feeding (sugar) contributed to the biosynthesis of pyruvate and acetyl-CoA from trehalose, and increased the sex pheromone biosynthesis and subsequent mating frequency.

In our study, the mating of *M. separate* can be significantly affected by feeding sugar. As an important migratory agricultural pest, *M. separata* must obtain supplemental sugar to reach target habitats and lay eggs (Guo et al., 2018). Therefore, reasonable planting and layout of nectar sources along the migratory pathway may help to cut the sugar supply, and finally leading to failure in mating and reproduction of *M. separate*.

DATA AVAILABILITY STATEMENT

The raw data supporting the conclusions of this article will be made available by the authors, without undue reservation.

AUTHOR CONTRIBUTIONS

XY, JW, GW, MD, and SA conceived and designed the experiments and wrote the manuscript. YaZ, YuZ, SY, XY, JW, and SA conducted the experiments and analyzed the data. All authors read and approved the manuscript.

FUNDING

This study was supported by the National Natural Science Foundation of China (Grant Nos. 31772536 and 31970472), the earmarked fund for China Agricultural Research system (Grant No. CARS-27), Henan Agriculture Research System (Grant No. S2014-11-G06), and the Key scientific and technological project of Henan Province (Grant No. 202102110073), the National Key R&D Program of China (Grant No. 2017YFD0301104), the Staring Foundation of Innovation and Practice Base for Postdoctors, Anyang Institute of Technology (Grant No. BHJ2020006), the Young Talents Promotion Project in Henan Province (Grant No. 2019HYTP014), the Educational Commission of Henan Province of China (Grant No. 18A210004), the Youth Innovation Foundation of Henan Agriculture University (Grant No. KJCX2018A14), and the Young Talents Foundation of Henan Agriculture University.

REFERENCES

Ando, T., Inomata, S. I., and Yamamoto, M. (2004). "Lepidopteran sex pheromones," in *The Chemistry of Pheromones and Other Semiochemicals I*, ed. S. Schulz (Berlin: Springer-Verlag), 51–96.

Becker, A., Schlöder, P., Steele, J. E., and Wegener, G. (1996). The regulation of trehalose metabolism in insects. *Experientia* 52, 433–439. doi: 10.1007/BF01919312

Bradbury, J. W., and Vehrencamp, S. L. (1998). *Principles of Animal Communication*. Sunderland, MA: Sinauaer Associates.

Choi, M. Y., Fuers, t E.J, Rafaeli, A., and Jurenka, R. A. (2003). Identification of a G protein-coupled receptor for pheromone biosynthesis activating neuropeptide from pheromone glands of the moth *Helicoverpa zea*. *Proc. Natl. Acad. Sci. U.S.A.* 100, 9721–9726. doi: 10.1073/pnas.1632485100

Darragh, K., Byers, K. J. R. P., Merrill, R. M., McMillan, W. O., Schulz, S., and Jiggins, C. D. (2019). Male pheromone composition depends on larval but not adult diet in *Heliconius melpomene*. *Ecol. Entomol.* 44, 397–405. doi: 10.1111/een.12716

Davis, M. T., Vakharia, V. N., Henry, J., Kempe, T. G., and Raina, A. K. (1992). Molecular cloning of the pheromone biosynthesis-activating neuropeptide in *Helicoverpa zea*. *Proc. Natl. Acad. Sci. U.S.A.* 89, 142–146. doi: 10.1073/pnas.89.1.142

Du, M., Liu, X., Ma, N., Liu, X., Wei, J., Yin, X., et al. (2017). Calcineurin-mediated dephosphorylation of acetyl-coA carboxylase is required for pheromone biosynthesis activating neuropeptide (PBAN)-induced sex pheromone biosynthesis in *Helicoverpa armigera*. *Mol. Cell. Proteomics* 16, 2138–2152. doi: 10.1074/mcp.RA117.000065

Du, M. F., Yin, X. M., Zhang, S. D., Zhu, B., Song, Q. S., and An, S. H. (2012a). Identification of lipases involved in PBAN-stimulated pheromone production in *Bombyx mori* using the DGE and RNAi approaches. *PLoS One* 7:e31045. doi: 10.1371/journal.pone.0031045

Du, M. F., Zhang, S. H., Zhu, B., Yin, X. M., and An, S. H. (2012b). Identification of a diacylglycerol acyltransferase 2 gene involved in pheromone biosynthesis activating neuropeptide stimulated pheromone production in *Bombyx mori*. *J. Insect. Physiol.* 58, 699–703. doi: 10.1016/j.jinsphys.2012.02.002

Edgar, J., Boppré, M., and Kaufmann, E. (2007). Insect-synthesised retronecine ester alkaloids: precursors of the common arctiine (Lepidoptera) pheromone hydroxydanaidal. *J. Chem. Ecol.* 33, 2266–2280. doi: 10.1007/s10886-007-9378-y

Fan, Y., Rafaeli, A., Moshitzky, P., Kubli, E., Choffat, Y., and Applebaum, S. W. (2000). Common functional elements of *Drosophila melanogaster* seminal peptides involved in reproduction of *Drosophila melanogaster* and *Helicoverpa armigera* females. *Insect Biochem. Mol. Biol.* 30, 805–812. doi: 10.1016/s0965-1748(00)00052-7

Foster, S. (2009). Sugar feeding via trehalose haemolymph concentration affects sex pheromone production in mated *Heliothis virescens* moths. *J. Exp. Biol.* 212, 2789–2794. doi: 10.1242/jeb.030676

Foster, S. P. (2004). Fatty acid and sex pheromone changes and the role of glandular lipids in the Z-strain of the European corn borer, *Ostrinia nubilalis* (Hübner). *Arch. Insect. Biochem.* 56, 73–83. doi: 10.1002/arch.10146

Foster, S. P., and Anderson, K. G. (2015). Sex pheromones in mate assessment: analysis of nutrient cost of sex pheromone production by females of the moth *Heliothis virescens*. *J. Exp. Biol.* 218, 1252–1258. doi: 10.1242/jeb.119883

Foster, S. P., Anderson, K. G., and Casas, J. (2017). Sex pheromone in the moth *Heliothis virescens* is produced as a mixture of two pools: de novo and *via*

precursor storage in glycerolipids. *Insect Biochem. Mol. Biol.* 87, 26–34. doi: 10.1016/j.ibmb.2017.06.004

Foster, S. P., and Johnson, C. P. (2010). Feeding and hemolymph trehalose concentration influence sex pheromone production in virgin *Heliothis virescens* moths. *J. Insect. Physiol.* 56, 1617–1623. doi: 10.1016/j.jinsphys.2010.06.002

Guo, P., Wang, G., Jin, L., Fan, X., He, H., Zhou, P., et al. (2018). Identification of summer nectar plants contributing to outbreaks of *Mythimna separata* (Walker) (Lepidoptera: Noctuidae) in North China. *JIA* 17, 1516–1526. doi: 10.1016/S2095-3119(17)61840-9

Hull, J. J., Ohnishi, A., Moto, K., Kawasaki, Y., Kurata, R., Suzuki, M. G., et al. (2004). Cloning and characterization of the pheromone biosynthesis activating neuropeptide receptor from the silkmoth, *Bombyx mori* significance of the carboxyl terminus in receptor internalization. *J. Biol. Chem.* 279, 51500–51507. doi: 10.1074/jbc.M408142200

Iglesias, F., Marco, P., Francois, M. C., Camps, F., Fabrias, G., and Jacquin-Joly, E. (2002). A new member of the PBAN family in *Spodoptera littoralis*: molecular cloning and immunovisualisation in scotophase hemolymph. *Insect Biochem. Mol. Biol.* 32, 901–908. doi: 10.1016/s0965-1748(01)00179-5

Jacquin-Joly, E., Burnet, M., Francois, M. C., Ammar, D., Meillour, P. N., and Descoins, C. (1998). cDNA cloning and sequence determination of the pheromone biosynthesis activating neuropeptide of *Mamestra brassicae*: a new member of the PBAN family. *Insect Biochem. Mol. Biol.* 28, 251–258. doi: 10.1016/s0965-1748(98)00017-4

Jiang, H., Zhang, N., Ji, C., Meng, X., Qian, Y., Zhang, Y., et al. (2020). Metabolic and transcriptome responses of RNAi-mediated AMPKα knockdown in *Tribolium castaneum*. *BMC Genomics* 21:655. doi: 10.1186/s12864-020-07070-3

Jing, T., Wang, Z., Qi, F., and Liu, K. (2007). Molecular characterization of diapause hormone and pheromone biosynthesis activating neuropeptide from the black-back prominent moth, *Clostera anastomosis* (L.) (Lepidoptera, Notodontidae). *Insect Biochem. Mol. Biol.* 37, 1262–1271. doi: 10.1016/j.ibmb.2007.07.012

Jurenka, R. A. (2003). "Biochemistry of female moth sex pheromones," in *Insect Pheromone Biochemistry and Molecular Biology-The Biosynthesis and Detection of Pheromones and Plant Volatiles*, eds G. J. Blomquist and R. G. Vogt (San Diego, CA: Elsevier Academic Press), 53–80.

Kingan, T. G., Bodnar, W. M., Raina, A. K., Shabanowitz, J., and Hunt, D. F. (1995). The loss of female sex pheromone after mating in the corn earworm moth *Helicoverpa zea*: identification of a male pheromonostatic peptide. *Proc. Natl. Acad. Sci. U.S.A.* 92, 5082–5086. doi: 10.1073/pnas.92.11.5082

Kitamura, A., Nagasawa, H., Kataoka, H., Ando, T., and Suzuki, A. (1990). Amino acid sequence of pheromone biosynthesis activating neuropeptide-II (PBAN-II) of the silkmoth, *Bombyx mori*. *Agricult. Biol. Chem.* 54, 2495–2497. doi: 10.1271/bbb1961.54.2495

Kochansky, J. P., Raina, A. K., and Kempe, T. G. (1997). Structure-activity relationships in C-terminal fragment analogs of pheromone biosynthesis activating neuropeptide in *Helicoverpa zea*. *Arch. Insect. Biochem.* 35, 315–322. doi: 10.1002/(SICI)1520-6327(199705)35:3<315::AID-ARCH5<3.0.CO;2-S

Lee, D. W., and Boo, K. S. (2005). Molecular characterization of pheromone biosynthesis activating neuropeptide from the diamondback moth, *Plutella xylostella* (L.). *Peptides* 26, 2404–2411. doi: 10.1016/j.peptides.2005.04.016

Liu, S., Wang, M., and Li, X. (2015). Over expression of Tyrosine hydroxylase and Dopa decarboxylase associated with pupal melanization in *Spodoptera exigua*. *Sci. Rep.* 5:11273. doi: 10.1038/srep11273

Ma, P. W., Knipple, D. C., and Roelofs, W. L. (1994). Structural organization of the *Helicoverpa zea* gene encoding the precursor protein for pheromone biosynthesis-activating neuropeptide and other neuropeptides. *Proc. Natl. Acad. Sci. U.S.A.* 91, 6506–6510. doi: 10.1073/pnas.91.14.6506

Matsumoto, S., Ohnishi, A., Lee, J. M., and Hull, J. J. (2010). Unraveling the pheromone biosynthesis activating neuropeptide (PBAN) signal transduction cascade that regulates sex pheromone production in moths. *Vitam. Horm. Adv. Res. Appl.* 83, 425–445. doi: 10.1016/S0083-6729(10)83018-3

O'Brien, D. M., Fogel, M. L., and Boggs, C. L. (2002). Renewable and nonrenewable resources: amino acid turnover and allocation to reproduction in Lepidoptera. *Proc. Natl. Acad. Sci. U.S.A.* 99, 4413–4418. doi: 10.1073/pnas.072346699

Ohnishi, A., Hull, J. J., Kaji, M., Hashimoto, K., Lee, J. M., Tsuneizumi, K., et al. (2011). Hormone signaling linked to silkmoth sex pheromone biosynthesis involves Ca2+/calmodulin-dependent protein kinase II-mediated phosphorylation of the insect PAT family protein *Bombyx mori* lipid storage droplet protein-1 (BmLsd1). *J. Biol. Chem.* 286, 24101–24112. doi: 10.1074/jbc.M111.250555

Ottiger, M., Soller, M., Stocker, R. F., and Kubli, E. (2000). Binding sites of *Drosophila melanogaster* sex peptide pheromones. *J. Neurobiol.* 44, 57–71. doi: 10.1002/1097-4695(200007)44:1<57::AID-NEU6<3.0.CO;2-Q

Rafaeli, A. (2002). Neuroendocrine control of pheromone biosynthesis in moths. *Int. Rev. Cytol.* 213, 49–91. doi: 10.1016/s0074-7696(02)13012-9

Raina, A., Jaffe, H., Kempe, T., Keim, P., Blacher, R. W., Fales, H. M., et al. (1989). Identification of a neuropeptide hormone that regulates sex pheromone production in female moths. *Science* 244, 796–798. doi: 10.1126/science.244.4906.796

Schulz, S., Francke, W., Boppré, M., Eisner, T., and Meinwald, J. (1993). Insect pheromone biosynthesis: stereochemical pathway of hydroxydanaidal production from alkaloidal precursors in *Creatonotus transiens* (Lepidoptera, Arctiidae). *Proc. Natl. Acad. Sci. U.S.A.* 90, 6834–6838. doi: 10.1073/pnas.90.14.6834

Tillman, J. A., Seybold, S. J., Jurenka, R. A., and Blomquist, G. J. (1999). Insect pheromones – an overview of biosynthesis and endocrine regulation. *Insect Biochem. Mol. Biol.* 29, 481–514. doi: 10.1016/s0965-1748(99)00016-8

Wei, J., Li, L., Yao, S., Zhou, S., Liu, X., Du, M., et al. (2019). Calcineurin-modulated antimicrobial peptide expression is required for the development of *Helicoverpa armigera*. *Front. Physiol.* 10:1312. doi: 10.3389/fphys.2019.01312

Xu, K., Pan, B., Wang, Y., Ren, Q., and Li, C. (2020). Roles of the PTP61F gene in regulating energy metabolism of *Tribolium castaneum* (Coleoptera: Tenebrionidae). *Front. Physiol.* 11:1071. doi: 10.3389/fphys.2020.01071

Xu, W. H., and Denlinger, D. L. (2004). Identification of a cDNA encoding DH, PBAN and other FXPRL neuropeptides from the tobacco hornworm, *Manduca sexta*, and expression associated with pupal diapause. *Peptides* 25, 1099–1106. doi: 10.1016/j.peptides.2004.03.021

Xu, W. H., Sato, Y., Ikeda, M., and Yamashita, O. (1995). Stage-dependent and temperature-controlled expression of the gene encoding the precursor protein of diapause hormone and pheromone biosynthesis activating neuropeptide in the silkworm, *Bombyx mori*. *J. Biol. Chem.* 270, 3804–3808. doi: 10.1074/jbc.270.8.3804

Zhang, H., Li, W., Luo, Q., Yang, L., Gong, D., Teng, X. H., et al. (2018). Fatal attraction: *Ricinus communis* provides an attractive but risky mating site for *Holotrichia parallela* beetles. *J. Chem. Ecol.* 44, 965–974. doi: 10.1007/s10886-018-0994-5

Zhao, W., Li, L., Zhang, Y., Liu, X., Wei, J., Xie, Y., et al. (2018). Calcineurin is required for male sex pheromone biosynthesis and female acceptance. *Insect Biochem. Mol. Biol.* 27, 373–382. doi: 10.1111/imb.12379

Conflict of Interest: The authors declare that the research was conducted in the absence of any commercial or financial relationships that could be construed as a potential conflict of interest.

frontiers in Physiology

ORIGINAL RESEARCH
published: 23 February 2021
doi: 10.3389/fphys.2021.619219

AKH Signaling in *D. melanogaster* Alters Larval Development in a Nutrient-Dependent Manner That Influences Adult Metabolism

Bryon N. Hughson[1], MaryJane Shimell[2] and Michael B. O'Connor[2]*

[1] Department of Ecology and Evolutionary Biology, University of Toronto, Toronto, ON, Canada, [2] Department of Genetics, Cell Biology and Development, University of Minnesota, Minneapolis, MN, United States

Metabolism, growth, and development are intrinsically linked, and their coordination is dependent upon inter-organ communication mediated by anabolic, catabolic, and steroid hormones. In *Drosophila melanogaster*, the corpora cardiaca (CC) influences metabolic homeostasis through adipokinetic hormone (AKH) signaling. AKH has glucagon-like properties and is evolutionarily conserved in mammals as the gonadotropin-releasing hormone, but its role in insect development is unknown. Here we report that AKH signaling alters larval development in a nutrient stress-dependent manner. This activity is regulated by the locus *dg2*, which encodes a cGMP-dependent protein kinase (PKG). CC-specific downregulation of *dg2* expression delayed the developmental transition from larval to pupal life, and altered adult metabolism and behavior. These developmental effects were AKH-dependent, and were observed only in flies that experienced low nutrient stress during larval development. Calcium-mediated vesicle exocytosis regulates ecdysteroid secretion from the prothoracic gland (PG), and we found that AKH signaling increased cytosolic free calcium levels in the PG. We identified a novel pathway through which PKG acts in the CC to communicate metabolic information to the PG via AKH signaling. AKH signaling provides a means whereby larval nutrient stress can alter developmental trajectories into adulthood.

Keywords: adipokinetic hormone, AKH, corpora cardiaca, prothoracic gland, metabolism, development, dg2, PKG

OPEN ACCESS

Edited by:
Kai Lu,
Fujian Agriculture and Forestry University, China

Reviewed by:
Christian Wegener,
Julius Maximilian University of Würzburg, Germany
Ryusuke Niwa,
University of Tsukuba, Japan
Dalibor Kodrík,
Institute of Entomology, Centre for Biology, Academy of Sciences of the Czech Republic, Czechia

****Correspondence:***
Bryon N. Hughson
bryon.n.hughson@gmail.com

Specialty section:
This article was submitted to Invertebrate Physiology, a section of the journal Frontiers in Physiology

Received: *19 October 2020*
Accepted: *11 January 2021*
Published: *23 February 2021*

Citation:
Hughson BN, Shimell M and O'Connor MB (2021) AKH Signaling in D. melanogaster Alters Larval Development in a Nutrient-Dependent Manner That Influences Adult Metabolism. Front. Physiol. 12:619219. doi: 10.3389/fphys.2021.619219

INTRODUCTION

Fundamental to all forms of life is the ability to maintain constancy of the internal milieu, or homeostasis, around precisely defined physiological setpoints (Bernard, 1854; Cannon, 1929). In *Drosophila melanogaster*, the stress-responsive neuroendocrine corpora cardiaca (CC) is ideally suited to this task (Vogt, 1946). The CC is the sole site of biosynthesis and secretion of the adipokinetic hormone (AKH), a glucagon-like peptide that mobilizes carbohydrate and lipid energy stores in response to starvation (Kim and Rulifson, 2004; Lee and Park, 2004; Isabel et al., 2005). The CC is functionally homologous to the mammalian pancreatic α cells. Perturbations in haemolymph glucose titers are detected by the CC through changes in the activity of evolutionarily conserved ATP-sensitive potassium (K_{ATP}) channels (Kim and Rulifson, 2004). In murine pancreatic α cells, a cGMP-dependent protein kinase (PKG, encoded by *cGK1* in mice) negatively regulates glucagon

secretion (Leiss et al., 2011). *cGK1* is evolutionarily conserved in *D. melanogaster* (*dg2*) and humans (*PRKG1*) (Kalderon and Rubin, 1989; Hofmann et al., 2006). From the murine literature, we hypothesized that *dg2* acts in the CC to negatively regulate AKH secretion.

dg2 was previously renamed *foraging* (Osborne et al., 1997). *for* was reported to encode naturally occurring allelic variants (rover, for^R, and sitter, for^s) that underlie a behavioral polymorphism (Sokolowski, 1980; de Belle et al., 1989). Precise excision of the P element 189Y altered sitter behavior morphs into rovers, and this was reported to identify a new for^s allele (i.e., for^{189Y}) (Osborne et al., 1997). Because 189Y was thought to be excised from the *dg2* locus, Osborne et al. (1997) reported that *dg2* is the *for* gene. However, 189Y was excised from the *lilliputian* (*lilli*) locus, which encodes a transcription factor (Flybase Id FBal0193987, FB2020_06; FlyBase Id FBgn0000721, FB2020_06; FlyBase Id FBti0007080, FB2020_06). Osborne et al. (1997) in fact identified *lilli* as the *for* gene, and their work remains the only molecular identification of *for* (Sokolowski, 2006; Wang et al., 2008). Consequently, it must be stated clearly that the present study examined the metabolic consequences of manipulating the PKG-encoding gene *dg2*.

A role for AKH in early development and sexual maturation was hypothesized but never identified (Owusu-Ansah and Perrimon, 2014; Gàlikovà et al., 2015). The possibility of such a role is suggested by the conservation of specific amino acids between AKH and the mammalian gonadotropin-releasing hormone (GnRH; Lindemans et al., 2009; Zandawala et al., 2017). GnRH acts in the hypothalamus-pituitary-gonadal (HPG) axis to signal the onset of puberty by stimulating increased steroid hormone biosynthesis and secretion. Support for the possibility that GnRH-like function may be conserved in AKH lies in the orthology between its receptor, AKHR, and the gonadotropin-releasing hormone receptor (GnRHR; Staubli et al., 2002). Phylogenetic analyses identified orthology between AKH and GnRH, and demonstrated that these peptides were ligands for orthologous receptors, AKHR and GnRHR (Jékely, 2013; Mirabeau and Joly, 2013).

The developmental transition between sexually immature larvae and mature adults in *D. melanogaster* also depends upon the precisely timed activity of steroid hormones (ecdysteroids) (Mirth and Riddiford, 2007). Ecdysteroid secretion at the end of the third larval instar permits pupariation and sexual maturation. Ecdysteroids are actively secreted from the prothoracic gland (PG) via calcium-mediated vesicle exocytosis (Yamanaka et al., 2015). The PG is an endocrine tissue adjacent to the CC. CC axons containing AKH project into the PG but their biological significance has never been identified (Kim and Rulifson, 2004). The possibility that these projections secrete AKH to target the PG is intriguing in light of the AKHR/GnRHR orthology. If AKH functions in a manner analogous to GnRH, then the steroid-producing PG is a logical target for its activity. The role of AKH as a nutrient stress signaling molecule makes it ideally suited for integrating metabolic information with developmental processes.

Here we report that reduced expression of *dg2* in the CC altered larval development, and that AKH signaling regulated these effects in a nutrient-dependent manner. Larvae reared in a low nutrient environment were developmentally delayed and showed increased lethality prior to pupariation. Flies that survived to adulthood were more starvation resistant, and had a greater proportion of whole body lipid content to body size than controls. AKH peptide abundance was reduced in the larval CC, and we identified the potential for paracrine secretion from the CC into the PG. We used *in vivo* calcium imaging techniques to show that AKH signaling in the PG increased cytosolic free calcium levels. These data identified an AKH-mediated signaling pathway that targeted the PG, either indirectly or directly via a novel CC-PG paracrine signaling pathway. This pathway might optimize the timing of developmental transitions in response to nutritional stress.

MATERIALS AND METHODS

Fly Stocks and Husbandry

Stocks used in the present study were: a *dg2* genetic background stock bore isogenic first, second, and third chromosomes (Allen et al., 2017), *akh*Gal4 (BDSC 25684), UAS-*Dcr2* (BDSC 24650), UAS-*dg2*-RNAi (Dason et al., 2019), UAS-*dg2*-RNAi (VDRC GD38320), UAS-*gfp*-RNAi^{142} (BDSC 44415), UAS-*dTrpA1.k* (BDSC 26263), UAS-*CD4:td= .Tom* (BDSC 35841), 10XUAS-IVS-*mCD8:gfp* (BDSC 32185), UAS-*nSyb-e.gfp* (BDSC 6922), UAS-*ANF-EMD* (BDSC 7001), UAS-*GCaMP6m* (Chen et al., 2013), *spok*-Gal4 (Shimell et al., 2018), UAS-*AkhR*-RNAi (KK109300 and BDSC 29577). In order to control for genetic background, transgenes were backcrossed for nine generations into chromosome 2, and six to nine generations into chromosome 3 of the *dg2* sitter stock. VDRC KK109300 and TRiP BDSC 29577 were not backcrossed. In all experiments, homozygous transgenic parental stocks were crossed to produce F1 that were heterozygous for the transgenes, and F1 heterozygous controls were generated from transgenic stocks crossed with *dg2* genetic background stock.

AKH^A, AKH^{AP} – loss of function mutants of AKH and AKH precursor-related peptide (APRP) – were generous gifts from Dr. R.P. Kühnlein (Gàlikovà et al., 2015). Third chromosome transgenes that were backcrossed into isogenic *dg2 background* for six to nine generations were backcrossed for two generations into AKH mutant third chromosomes. All AKH and AKHR mutant F1 used in experiments were homozygous for the mutant locus. $AKHR^1$ was a generous gift from Dr. S. Grönke (Grönke et al., 2007). The AKHR1 second chromosome was not backcrossed into *dg2* genetic background. All AKH and AKHR mutant F1 used in experiments were homozygous for the mutant locus.

Stocks were reared at 25°C and 60% RH. Transfer of adults between 18 and 30°C for the temporal and temperature manipulations took place within 1 h of eclosion. Rearing at 18 and 30°C was in 60% RH. A 12:12 L:D cycle was used in all rearing and experimental conditions.

Normal nutrient food consisted of 100 g sucrose, 50 g yeast, 13 g agar, 8 g potassium sodium tartrate tetrahydrate, 1 g potassium phosphate monobasic, 0.5 g sodium chloride, 0.5 g calcium chloride, 0.5 g magnesium chloride hexahydrate, 0.5 g

iron (III) sulfate hydrate, all dissolved in 1L of water. Five milliliter of propionic acid was added after boiling. Food was poured into standard fly vials, 10 mL of food per vial (Diamed, Cat #GEN32-120) at <40°C. Low nutrient food had 25% of the sucrose (25 g) and yeast (12.5 g) of normal nutrient food. Flies used in experiments were reared in a reduced agar (i.e., 9 g/L from 13 g/L) medium in order to reduce inter-vial variation in the ability of larvae to chew and ingest food.

Grape plates contained 2.0 g agar, 45 mL Welch's grape juice, 50 mL water with 2.5 mL acetic acid and 2.5 mL 95% ethanol added at <60°C. The grape juice-agar mixture was poured into lids taken from 35 mm × 10 mm petri dishes (Falcon, #351008) and allowed to set overnight. For egg-laying, parents were added to fly bottles (Fischer Scientific, #AS355) that were subsequently capped with the grape plate petri dish lid. A drop of liquid yeast paste was placed on the grape plate before capping. These bottles had a circular opening in their side plugged with a sponge to allow for air flow. Parents laid eggs for 2–3 h. Larvae were picked within 30 min of egg hatching.

Starvation Resistance Assay

As described in Hughson et al. (2018), starvation vials were made using standard fly vials (Diamed, Cat #GEN32-120) containing 10 mL of 1% agar and a cotton ball soaked with water. Virgin female flies were reared on standard food at 25°C in a 12:12-h light/dark cycle. Groups of 10 flies (n = 10; 7 ± 1 day old) were aspirated into each vial and the number of dead flies was counted every 6–8h. Starvation resistance was performed under specified rearing temperatures, light cycle and relative humidity.

Proboscis Extension Response (PER) Assay

As described in Hughson et al. (2018), proboscis extension response (PER) assays were modified from Shiraiwa and Carlson (2007). Virgin female flies (7 ± 1 day old) were aspirated into 100 mL pipette tips so that only the head and one foreleg extended from the opening. Foreleg tarsi were stimulated by contact (<1 s) with Kim wipe tissue "threads" soaked with either water or various sucrose solutions (0.1, 0.3, 1, 3, 10, or 30%, all w/v). Sucrose treatments were presented in randomized order, and water was presented before and after each sucrose stimulus. A positive result was recorded for every full extension of the proboscis. Flies that responded positively to water were eliminated from analysis, as they were no longer responding exclusively to feeding cues. The number of positive responses for each fly was summed to yield an individual sucrose response (SR) score. The mean SR score was then calculated for each strain-trea tment group. Flies were scored separately to yield an individual and strain-averaged SR score. Flies were treated as described above for fed, 24 and 48 h FD groups. All experiments were conducted between 1,300 and 1,700 h.

Triacylglyceride Quantification

Triacylglyceride (TAG) measurements were performed as described in Hughson et al. (2018). Feeding treatments were conducted as described above. Virgin females (n = 8; 7 ± 1 day old) were homogenized in 200 μL of 1× PBT with 0.5% TritonX (0.5% PBT-X). Another 800 μL of 0.5% PBT-X were added, the solution was vortexed, then heat inactivated at 70°C for 5 min. Samples were centrifuged at 5,000 rpm at 4°C for 1 min, the supernatant was removed and centrifuged again at 13,000 rpm for 3 min. Supernatant was removed and stored at −20°C for later use, or immediately pipetted into a Corning Falcon 96-well cell culture plate (VWR 351172): 50 μL of sample were added to each well, and three technical replicates were prepared for each sample. A blank reading of the plate was made at 562 nm using a BioTek Synergy HT spectrophotometer and Gen5 analytical software. Infinity TAG reagent (Thermo Scientific 796704) was preheated to 37°C and 200 μL were added to each well. The plate was incubated at 37°C for 15 min and read at 562 nm. Total TAG was determined using a standard curve made using a TAG standard (Trace DMA TR2291-030).

Pearce Bicinchoninic Acid (BCA) Assay

As described in Hughson et al. (2018), protein was quantified using the Pierce bicinchoninic acid (BCA) protein assay (Thermo Fisher Scientific 23225). Supernatants (50 μL, prepared as per the TAG assay) were loaded in triplicate into a Corning Falcon 96-well cell culture plate (VWR 351172). The plate was read at 562 nm for a blank reading. BCA solution (150 μL) was added to each well. The plate was incubated at 37°C for 30 min and read at 562 nm. The blank reading was subtracted from the final reading and total protein content was determined using a standard curve made from a protein standard (BCA kit).

Wing Measurements and Hair Counts

This method was adapted from Delcour and Lints (1967). The right wings of 7 ± 2 day old female adults were clipped and taped dorsal side up onto a slide. Relative wing size was measured by calculating the surface area within a polygonal region defined by the second costal break, the intersections of the lateral wing veins with the wing margin, and base of the aola. Images of wings were taken using a Zeiss epifluorescence microscope: wing area was quantified using FIJI and scaled using a micrometer slide; hair counts were made by hand from within a 100 μm × 100 μm area equidistant between the third and fourth lateral veins, and anterior to the posterior cross vein.

Larval Development Assay

Flies (n = 100 females, n = 50 males; 3–6 days old) were placed on grape plates and allowed to lay eggs for 2–6 h. About n = 30 newly hatched (<0.75 h after egg hatching, AEH) L1 were seeded per vial. Numbers of wandering, pupariating and eclosing larvae/flies in each vial were counted every 1 h.

Confocal Microscopy

A Leica TCS SP5 confocal laser-scanning microscope available through the University of Toronto Cell Systems Biology Imaging Facility was used for fluorescence imaging of all *ex vivo* immunohistochemistry and Nile red fat body staining, as well as *in vivo* calcium imaging.

Immunohistochemistry

Freshly dissected tissues were fixed in 4% paraformaldehyde on ice for 25 min, and at room temperature (RT) for 30 min with rocking. Tissues were washed 2 × 5 min in 0.5% PBT-X (phosphate-buffered saline, Triton-X); all washes used 0.5% PBT-X with rocking at RT. Tissues were washed 4 × 30 min, blocked (14 μL 5% bovine serum albumin, 35 μL normal goat serum, in 651 μL 0.5% PBT-X) for 2h at RT, and incubated with rocking overnight (∼15 h) at 4°C in primary antibody solution. Tissues were washed 2 × 5 min, washed 4 × 30 min, incubated for 2h in secondary antibody solution at RT (culture plate was wrapped in tinfoil), washed 4 × 30 min, and rinsed 2 × 5 min in 1× PBS. Tissues were mounted on glass slides (VWR CA48323-185) with Vectashield-DAPI mounting medium (Vector Laboratories H-1200). Stored at 4°C, tissues could be imaged for up to 3 months. Primary antibodies were made in blocking solution at concentrations of 1:500 for mouseαGFP (mouse anti-GFP; Life Technologies A-11120), rabbitαGFP (Life Technologies A6455s), chickenαGFP (Life Technologies A10262), mouseαRFP (Thermo Scientific MA5-15257), and 1:600 for rabbitαAKH. rαAKH was a generous gift from Dr. Jae Park. Secondary antibodies were made in blocking solution at concentrations of 1:500: goatαrabbit Alexa Fluor 488 (Life Technologies 11008), goatαrabbit Alexa Fluor 568 (Molecular Probes A11011), goatαrabbit Alexa Fluor 633 (Invitrogen A21071), goatαmouse Alexa Fluor 488 (Life Technologies A11005), and goatαchicken Alexa Fluor 488 (Life Technologies A11039).

Nile Red Fat Body Staining

Fat body staining was based upon Grönke et al. (2005). Briefly, freshly dissected fat body tissues were dissected and transferred to droplets of mounting medium on glass slides coated with 10% poly-L lysine. Mounting medium contained 50% glycerol and 0.5% PBT-X and 1:55,000 Nile red (Sigma, N3013-100MG) (stock solution of 10% Nile red in DMSO). Tissues were analyzed 6–12 h after mounting using a Leica SP5 confocal microscope.

Calcium Imaging

Central nervous system-ring gland tissues (CNS-RGs) were dissected from the cuticle in Schneider's insect medium (Sigma S0146) and transferred directly to imaging dishes containing a poly-L lysine-treated glass coverslip in 1,500 μL of haemolymph-like solution 6 (HL-6) with 4 mM calcium chloride; high trehalose concentration in HL-6 prolonged tissue survival, and reduced spontaneous calcium activity and AKH secretion (Macleod et al., 2002). Imaging dishes were constructed from 3.5 mm diameter culture dishes and thin (∼3 mm) sections cut from 2.5 mm diameter vials. The 2.5 mm vial sections were glued inside the 3.5 mm culture dishes to create the well in which the cover slip-tissue mounts were placed and imaged. Imaging was performed on a Leica TCS SP5 confocal laser-scanning microscope with a 63× water dipping objective (0.9 NA). Tissues were positioned on the coverslip and the objective focused on the PG. HL-6 (750 μL) was pipetted from the dish before the experiment started. At t = 5 min, 750 μL of HL-6 containing AKH peptide (Sigma Aqua peptide DAKH) was slowly pipetted into the dish over 1 min to a final concentration of 1 μM. Tetrodotoxin citrate (TTX, 100 nM; Abcam ab120055) was added with the HL-6/AKH solution in TTX experiments. CNS-RGs were scanned at 488 nm excitation at a speed of 1024 × 1024 every 5 s in 4 × 15 min blocks to permit refocusing as necessary. Total number of micro and macrospikes in each block was counted visually (Yamanaka et al., 2015).

Statistics

SigmaPlot Ver.12.5 statistical software was used for all statistical analyses. Larval development assay (LDA; **Figures 1**, **4E** and **Supplementary Figure 1**) two-way ANOVA (multiple pairwise comparisons, Bonferroni). Total number of pupae (**Figure 1B.II**) were analyzed with two-way ANOVA (multiple pairwise comparison, Dunn's). Immunoreactivity (**Figure 2C**) was analyzed with t-test (Mann–Whitney Rank Sum). Ecdysteroid titers (**Supplementary Figures 4A,B**) were analyzed with two-way ANOVA (multiple pairwise comparison, Holm-Sidak). Calcium spikes (**Figure 4D** and **Supplementary Figure 4C**) were quantified using FIJI[1] and analyzed using two-way ANOVA (all pairwise comparison, Holm-Sidak). Starvation resistance assay (SRA; **Figures 5A–C** and **Supplementary Figures 5A–E**) were analyzed with Kaplan–Meyer survival analysis (multiple pairwise comparisons, Holm-Sidak). PER (**Figure 5D**), lipid content (**Figure 5G**), protein content (**Supplementary Figure 5F**), and wing measurements (**Figures 5F,H**) were analyzed with one-way ANOVA (Holm-Sidak).

RESULTS

We investigated a putative role for *dg2* in the CC (i.e., CC-*dg2*) as a regulator of AKH secretion during early development using the GAL4-UAS binary system (Brand and Perrimon, 1993). We used a CC-specific driver, *akh*-GAL4 (Lee and Park, 2004), to silence *dg2* expression specifically in the CC using a *dg2*-RNAi transgene ($dg2^{COMa7}$-RNAi, Dason et al., 2019) in conjunction with UAS-*Dcr*. The reduction of *dg2* expression in the CC is hereafter referred to as *akh* > *Dcr*;*dg2*-RNAi. We focused this transgenic manipulation to the embryonic, larval and pupal stages by using temperature to manipulate GAL4-UAS activity (Yamamoto-Hino and Goto, 2013). GAL4 transcriptional activity is increased at high (30°C) temperatures relative to low (18°C) temperatures. We increased GAL4-UAS activity during embryonic, larval and pupal stages by rearing all flies at 30°C, and transferred newly eclosed adult flies to 18°C in order to reduce GAL4-UAS activity (Yamamoto-Hino and Goto, 2013).

From our hypothesis that *dg2* negatively regulates AKH secretion – and because AKH secretion increases in response to starvation – we predicted that the effect of *akh* > *Dcr*;*dg2*-RNAi would be apparent only under conditions of larval nutrient stress.

[1] https://fiji.sc/

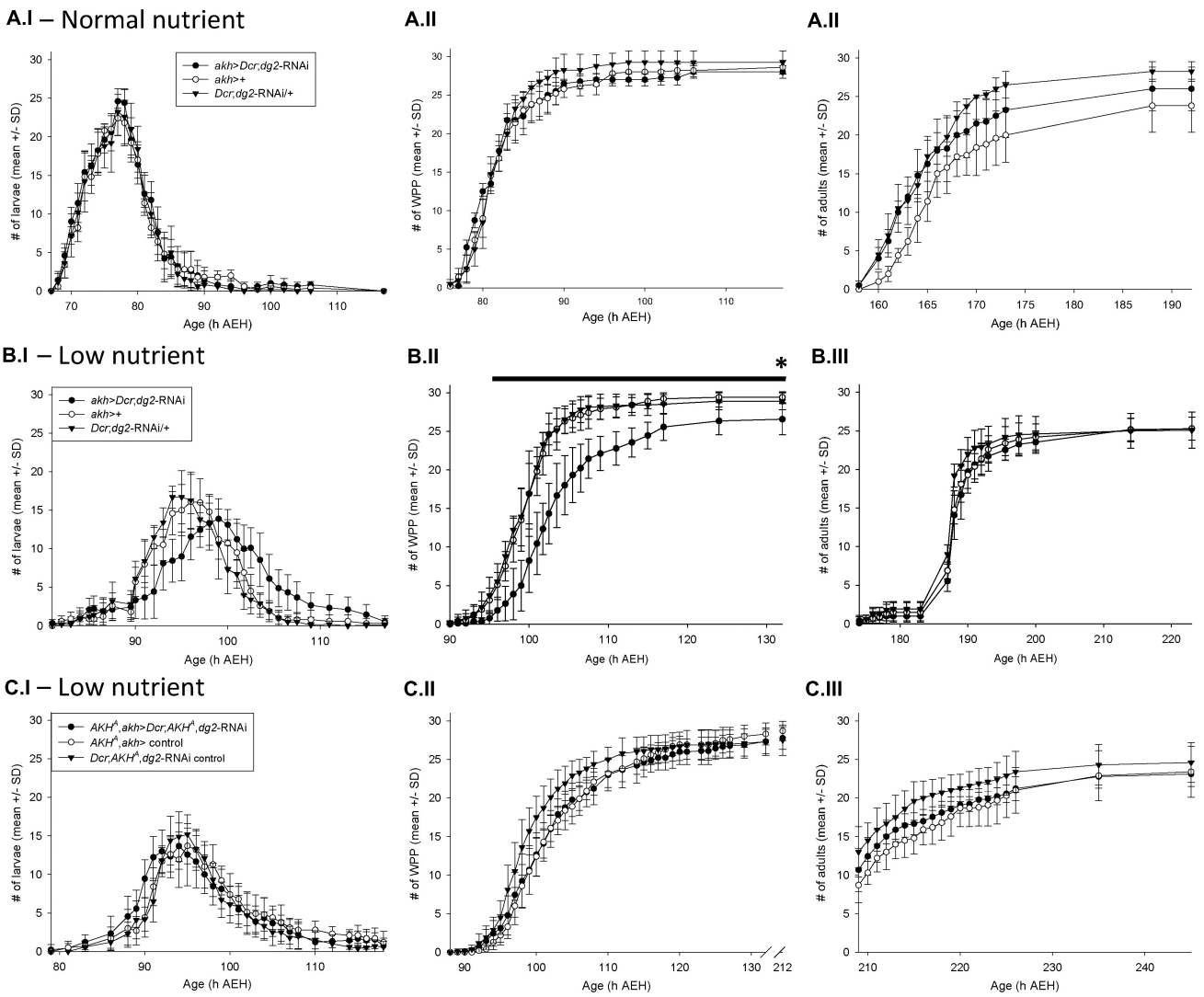

FIGURE 1 | *akh* > *Dcr;dg2-RNA* interacted with low nutrient stress to prolong development via AKH signaling Developmental timing of wandering, pupariation, and eclosion. The number of individual wandering larvae **(I panels)**, white prepuparia (WPP) **(II panels)** and adults eclosed **(III panels)** is recorded on the *y*-axis; the age of the flies (hours AEH) is on the *x*- axis. Each vial contained $n = 30$ newly hatched larvae att = 0h. Data are reported as mean ± standard deviation (SD). **(A.I–III)** In 100% standard nutrient rearing conditions, *akh* > *Dcr;dg2-RNA* did not significantly affect wandering, pupariation or eclosion. $n = 10$ vials/genotype-treatment. **(B.I–III)** In 25% low nutrient rearing conditions, *akh* > *Dcr;dg2-RNA* prolonged larval wandering, delayed pupariation, decreased survival to pupariation, and proportionately increased survival to eclosion. $n = 10$ vials/genotype-treatment. *Indicates significantly decreased survival in *akh* > *Dcr;dg2-RNA* at 132h AEH ($p < 0.05$), black line indicates significant differences between *akh* > *Dcr;dg2*- RNAi and controls from 96h to 132h AEH ($p < 0.05$). **(C.I–III)** In 25% low nutrient rearing conditions, the effect of *akh* > *Dcr;dg2-RNA* in a wild type AKH^+ background was lost in the AKH^A single mutant background. $n = 8$ vials/genotype-treatment. See section "Materials and Methods" for details of statistical testing.

We used a low nutrient food containing 25% of the sucrose and yeast contained in our normal nutrient fly food for larval rearing.

CC-*dg2* and Nutrient Stress Prolonged Larval Development

akh > *Dcr*;*dg2*-RNAi in normal nutrient rearing conditions did not affect larval wandering (**Figure 1A.I**), pupariation (**Figure 1A.II**), or eclosion (**Figure 1A.III**). However, in low nutrient rearing conditions *akh* > *Dcr*;*dg2*-RNAi prolonged larval wandering (**Figure 1B.I**) and significantly delayed pupariation (**Figure 1B.II**). Larvae that showed prolonged wandering alternated between wandering and feeding before either dying in the food or as elongated prepupae on the vial walls.

Survival through larval development to pupariation was significantly reduced by *akh* > *Dcr*;*dg2*-RNAi ($p < 0.05$). In

the GAL4-UAS treatment group (i.e., *akh* > *Dcr*;*dg2*-RNAi), an average (±SD) of 26.6 ± 2.0 larvae out of the 30 larvae placed in each vial at t = 0 h AEH survived to pupariation (**Figure 1B.II**). In contrast, 29.4 ± 0.7 out of 30 larvae in the *akh*-GAL4 control group and 28.9 ± 1.1 out of 30 larvae in the UAS-*dg2*-RNAi control group survived (**Figure 1B.II**). Proportionately, 26.6/30 (i.e., 85%) *akh* > *Dcr*;*dg2*-RNAi larvae survived vs. 29.4/30 (i.e., 98.0%) *akh*-GAL4 control larvae and 28.9/30 (i.e., 96.3%) UAS-*dg2*-RNAi control larvae.

akh > *Dcr*;*dg2*-RNAi affected survival through pupal metamorphosis to adult eclosion (**Figure 1B.III**). Out of 26.6 ± 2.0 larvae that survived to pupariation in the *akh* > *Dcr*;*dg2*-RNAi treatment group, 25.3 ± 1.5 of these survived to eclosion as adults (i.e., 25.3/26.6, or 95.2%) (**Figure 1B.III**). In contrast, 25.3 ± 1.5 out of 29.4 ± 0.7 larvae (86.0%) in the *akh*-GAL4 control group and 25.1 ± 2.3 out of 28.9 ± 1.1 larvae (86.5%) in the UAS-*dg2*-RNAi control group survived (**Figure 1B.III**). This indicated that although the total number of eclosions did not differ between the three genotype groups, *akh* > *Dcr*;*dg2*-RNAi proportionately increased survival through metamorphosis to eclosion.

These developmental effects were largely absent in response to the expression of *gfp*-RNAi in the CC, and were thus not an artifact of activating RNAi machinery (**Supplementary Figure 1Ai–iii**). *dg2* expression in the CC influenced larval development in a nutrient stress-dependent manner. The data reported hereafter were collected from flies reared as larvae on low nutrient food, and as adults on standard nutrient food.

CC-*dg2* Developmental Effects Were Dependent Upon AKH

We hypothesized that the effects of *akh* > *Dcr*;*dg2*-RNAi in low nutrient rearing conditions were mediated by AKH signaling. To test this, we drove *akh* > *Dcr*;*dg2*-RNAi in *akh* genetic mutant backgrounds. Bioactive AKH is synthesized from a prepropeptide from which the APRP is also produced. Because APRP putatively regulates the developmental transitions between larval, pupal, and adult life stages in insects, we investigated the effect of *akh* > *Dcr*;*dg2*-RNAi in AKH single (AKH^{A}) and AKH-APRP double (AKH^{AP}) mutant backgrounds (Clynen et al., 2004; Gàlikovà et al., 2015). The statistically significant developmental delays seen with *akh* > *Dcr*;*dg2*-RNAi in a wild type AKH^{+} background were lost in both the AKH^{A} (**Figure 1C.I–III**) and AKH^{AP} (**Supplementary Figure 1Bi–iii**) mutant backgrounds. These data demonstrated that AKH mediated the developmental effects of *akh* > *Dcr*;*dg2*-RNAi in a low nutrient rearing environment.

We tested our prediction that *akh* > *Dcr*;*dg2*-RNAi increased CC secretion using *dTrpA1*. *dTrpA1* encodes a Ca^{2+}-permeable cation channel that stimulates depolarization in neural and neuroendocrine tissues at 30°C, and as such provided an appropriate means of promoting secretion from the CC (Hamada et al., 2008). We drove *dTrpA1* expression at 30°C with *akh*-GAL4 (i.e., *akh* > *dTrpA1*) and phenocopied the developmental effects of *akh* > *Dcr*;*dg2*-RNAi in a low nutrient environment (**Supplementary Figure 1Ci–iii**). These effects were significantly reduced in larvae reared in normal nutrient conditions (**Supplementary Figure 1Di–iii**).

AKH May Mediate CC-PG Paracrine Signaling

Immunohistochemistry experiments using an AKH antibody revealed the influence of *akh* > *Dcr*;*dg2*-RNAi on AKH biodynamics. The larval CC was reported to contain 119 ± 21 fmol of AKH peptide, and AKH synthesis was independent of *akh* expression (Noyes et al., 1990). Heat mapping revealed significantly more AKH-immunoreactivity (IR) in CC tissues from 92h AEH control larvae (**Figures 2A,C**) as compared to *akh* > *Dcr*;*dg2*-RNAi (**Figures 2B,C**).

akh > *Dcr*;*dg2*-RNAi caused AKH-dependent developmental delays in wandering and pupariation beginning at 92h AEH (**Figures 1B,C**). Temporally age-matched *akh* > *Dcr*;*dg2*-RNAi 92 h AEH larvae displayed developmental delay and arrest in the first and second instar, accompanied by the transparent body "glassy" phenotype (**Figure 2D**). Variation in developmental age was absent in 92 h AEH control larvae. This "glassy" phenotype, the developmental delays, terminal arrest and failed pupariation in third instar larvae are diagnostic of ecdysteroid dysregulation (Mirth and Riddiford, 2007). Significantly reduced CC AKH content (**Figures 2A–C**) coincided with the onset of developmental delay at 92 h AEH (**Figures 1B.I–II**, **2D**). AKHergic projections from the CC that terminate on the PG were reported previously (Kim and Rulifson, 2004; Lee and Park, 2004). In light of this report, our data led us to hypothesize that AKH might influence ecdysteroid physiology through an unidentified CC-PG paracrine signaling pathway. We investigated CC axonal projections to the PG for evidence that AKH may be secreted into the PG.

We drove GFP-tagged neuronal synaptobrevin (UAS-*nSyb.eGFP*) using *akh*-GAL4 in conjunction with a UAS-*cd4:td.Tom* membrane-bound red fluorescent protein (RFP) to mark CC cell bodies and axons. GFP-tagged nSyb was reported to label synaptic vesicles and dense core granules and to mark putative sites of secretion at perisynapses (Estes et al., 2000; Zhang et al., 2002; Nässel, 2009; Shimada-Niwa and Niwa, 2014). We identified synaptobrevin clustered along RFP-labeled CC axonal projections into the PG (**Figure 3AI–IV**). Notably, nSyb-IR and AKH-IR colocalized in these regions. These data identified the potential for AKH secretion into the PG and suggested the existence of an unidentified CC-PG paracrine signaling pathway.

AKH Affected Intracellular Calcium Signaling in the PG

We suspected that the putative effect of AKH signaling in the PG would be different from its catabolic activity in the fat body because the PG does not contain lipid or glycogen stores. Ecdysteroids are actively secreted from the PG via calcium-mediated vesicle exocytosis, and this signaling pathway is stimulated by an unidentified G-protein-coupled receptor

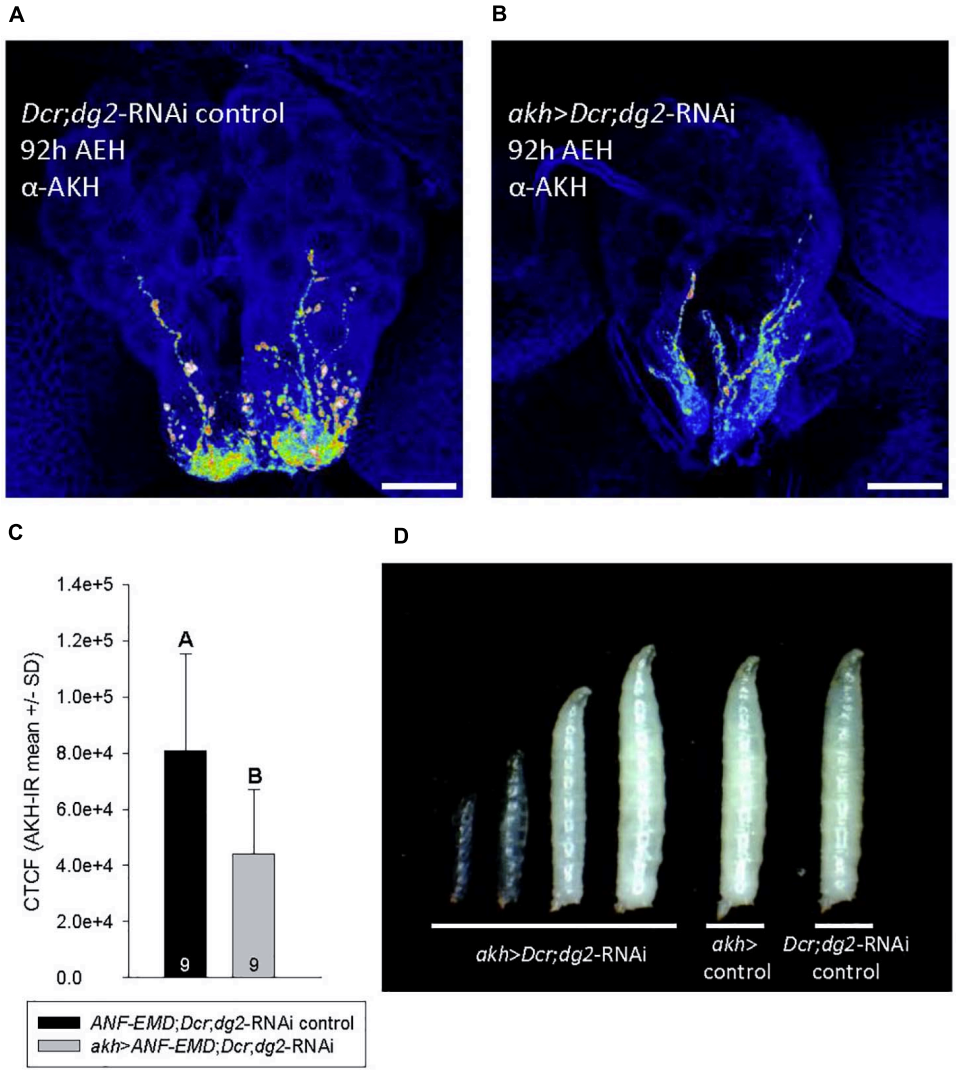

FIGURE 2 | *akh > Dcr,dg2-RNM* altered AKH abundance and caused developmental arrest in low nutrient conditions. **(A–C)** Heat mapping projections from a-AKH revealed AKH-IR in CC cell bodies and axons in control 92h AEH L3 **(A)**, but AKH- IR was significantly reduced ($p = 0.010$) in *akh > Dcr;dg2-RNA* larvae **(B,C)**. Corrected total cell fluorescence (CTCF) of AKH-IR was shown in panel **(C)**. $n = 9$ samples/genotype. Scale bar in panels **(A,B)** 20 μm. **(D)** Temporally age-matched larvae (92 h AEH) displayed developmental arrest at LI and L2 in *akh > Dcr;dg2-RNA* larvae and a transparent "glassy" phenotype. See section "Materials and Methods" for details of statistical testing.

(GPCR) (Yamanaka et al., 2015). The AKH receptor (AKHR) is a GPCR (Staubli et al., 2002). From these reports, we hypothesized that AKH may act through a paracrine signaling mechanism to stimulate increased cytosolic free calcium levels in the PG.

We investigated the effect of AKH signaling on PG intracellular calcium dynamics in larvae carrying either a wild type allele, $AkhR^{+}$, or a loss-of-function deletion mutant allele, $AkhR^{1}$, of the *AkhR* locus (Grönke et al., 2007). We conducted *in vivo* calcium imaging experiments in both $AkhR^{+}$ wild type and $AkhR^{1}$ mutant backgrounds using a PG-specific driver, *spok*-GAL4, to express the UAS-*GCaMP6m* calcium reporter line (**Figure 4A**; Chen et al., 2013; Shimell et al., 2018). Although we hypothesized that AKH acts via paracrine signaling in the PG, we were unable to inject AKH directly into the PG in order to simulate this mechanism. Instead, we incubated dissected CNS-ring glands (CNS-RG) with AKH and recorded over an hour in order to allow time for AKH to diffuse into the PG tissue. We quantified macro and microspikes of calcium activity throughout the PG, as reported previously (Yamanaka et al., 2015).

We found no significant difference between $AkhR^{+}$ and $AkhR^{1}$ calcium spike activity during the first two 15 min blocks of the 1h experiment (**Figure 4D**). Spike frequency in $AkhR^{+}$ increased significantly over the course of the entire experiment; $AkhR^{+}$ spike frequency was significantly greater than that of $AkhR^{1}$ in the 30–45 min and 45–60 min blocks (**Figure 4D**). These effects are shown in representative images of $AkhR^{1}$ (**Figure 4BI–II**) and $AkhR^{+}$ (**Figure 4CI–II**) for 0–15 min (**Figures 4BI,CI**) and 45–60 min (**Figures 4BII,CII**) blocks.

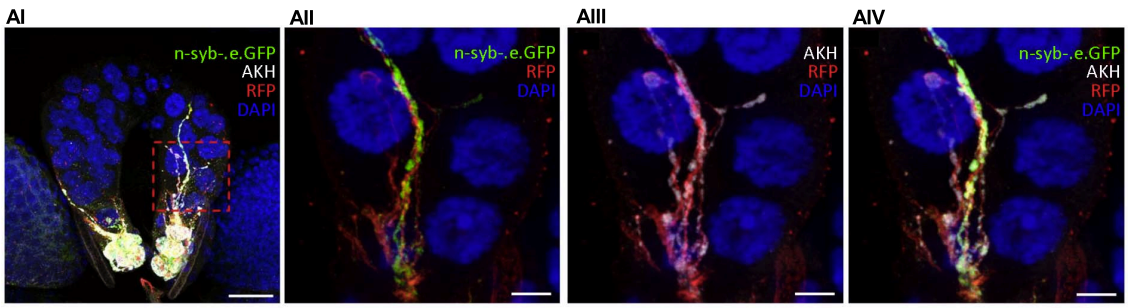

FIGURE 3 | AKH might be secreted from the CC directly into the PG through a novel paracrine mechanism. **(AI–IV)** In the ring gland of 92h AEH *akh* > *td.Tom;nSyb.eGFP* larvae, GFP-tagged neuronal synaptobrevin and AKH-IR colocalize within CC axonal projections to the PG. Region of interest (red dashed box) in panel **(AI)** is magnified in panels **(AII–IV)**. Split GFP-IR [**(AII)** – green] and AKH-IR [**(AIII)** – white] channels are merged in panel **(AIV)**. DAPI (blue) and RFP intensity (red) were modified in order to better identify neuronal projections. Scale bars: **(AI)** 20 μm; **(AII–IV)** 5 μm.

Because AKH stimulated an increase in cytosolic free calcium levels, we quantified ecdysteroid titers in order to see if *akh* > *Dcr*;*dg2*-RNAi affected this trait. We were unable to detect changes in either circulating ecdysteroid titers (**Supplementary Figure 4A**) or in ecdysteroid content of dissected CNS-RG (**Supplementary Figure 4B**).

Regions of the CNS that project to the ring gland are themselves targets of AKH signaling (Ikeya et al., 2002; Wicher et al., 2006; Kim and Neufeld, 2015). In order to ensure that PG calcium spike activity reported in **Figure 4D** was a direct result of AKH signaling in the PG we used tetrodotoxin (TTX) to inhibit synaptic transmission from the CNS to the PG. In $AkhR^{+}$ PG cells, the AKH + TTX treatment significantly increased the frequency of spikes relative to what was observed in response to AKH only (**Supplementary Figure 4C**). Notably, the number of spikes observed in the first block of the AKH + TTX experiment was not significantly different from that observed in the last block of the experiment with AKH only. These results indicated that the slow response seen in **Figure 4D** was due in part to antagonism of the AKH response by an unidentified CNS-derived factor. The same data for wild type with AKH only are shown in **Figure 4D** and **Supplementary Figure 4C**.

Representative videos of $AkhR^{1}$ and $AkhR^{+}$ (with and without TTX) responses to AKH are available online. Supplementary Videos demonstrate changes in PG intracellular calcium levels that were recorded during *in vivo* imaging experiments: $AKHR^{+}$ versus $AKHR^{1}$ in block 1 (**Supplementary Video 1**); $AKHR^{+}$ versus $AKHR^{1}$ in block 4 (**Supplementary Video 2**); and $AKHR^{+}$ without TTX versus $AKHR^{+}$ with TTX in block 4 (**Supplementary Video 3**). Note that the $AKHR^{1}$ data shown in **Figures 4BI,II** are from the same $AKHR^{1}$ tissue sample that is shown in **Supplementary Videos 1 and 2**; note also that the $AKHR^{+}$ data shown in **Figures 4CI,II** are from the same $AKHR^{+}$ tissue sample that is shown in **Supplementary Videos 1, 2,** and **3**. See **Supplementary Video** captions for more details.

We further demonstrated the developmental role played by AKHR in the PG by driving the expression of *AkhR*-RNAi with *Spok*-Gal4. This manipulation delayed time to pupariation (**Figure 4E**). Finally, we compared larval developmental timing between $AkhR^{1}$, AKH^{A}, AKH^{AP} mutants and the wild type control genotype and found that mutation of the *AkhR* and *akh* loci delayed wandering and significantly delayed pupariation (**Supplementary Figure 4Di–ii**). These data demonstrated that AKH acted through AKHR to stimulate increased intracellular calcium levels in the PG, and that dysregulated *AkhR* function caused developmental delay.

Larval Nutrient Experience Altered Adult Metabolic Traits

Early life nutritional stress is strongly associated with adverse outcomes for adult health (Sullivan and Grove, 2010; Wang et al., 2017). We reared flies as larvae in low nutrient conditions and as adults in normal nutrient conditions, and found that *akh* > *Dcr*;*dg2*-RNAi increased adult starvation resistance significantly in virgin females (**Figure 5A**) and males (**Supplementary Figure 5A**). These results were replicated in females (**Supplementary Figure 5B**) and males (**Supplementary Figure 5C**) using another *dg2*-RNAi construct (VDRC GD38320). Consistent with the effect on larval development of *akh* > *Dcr*;*dg2*-RNAi (**Figure 1A.I–III**), starvation resistance in adults that were reared on normal nutrient food during larval life was not affected (**Figure 5B**), and was not attributable to the activation of RNAi machinery (**Supplementary Figures 5A,D**).

We used AKH^{A} and AKH^{AP} mutants to implicate AKH signaling in the effect of CC-*dg2* on adult starvation resistance. Whereas *akh* > *Dcr*;*dg2*-RNAi in a wild type AKH^{+} background increased adult female starvation resistance (**Figure 5A**), *akh* > *Dcr*;*dg2*-RNAi starvation resistance decreased significantly in the AKH^{A} single mutant background where AKH was inactive but bioactive APRP was produced (**Figure 5C**). The effect of *akh* > *Dcr*;*dg2*-RNAi was more severe in the AKH^{+} than in AKH^{A}. There was no effect of *akh* > *Dcr*;*dg2*-RNAi in the AKH^{AP} double mutant background (**Supplementary Figure 5E**).

Starvation resistance influences a fly's need to search for and ingest food, where greater resistance confers a less immediate need to feed (Dethier, 1976). The proboscis extension response (PER) assay quantifies the likelihood that a fly will ingest sucrose (i.e., SR) (Hughson et al., 2018). Starvation modulates

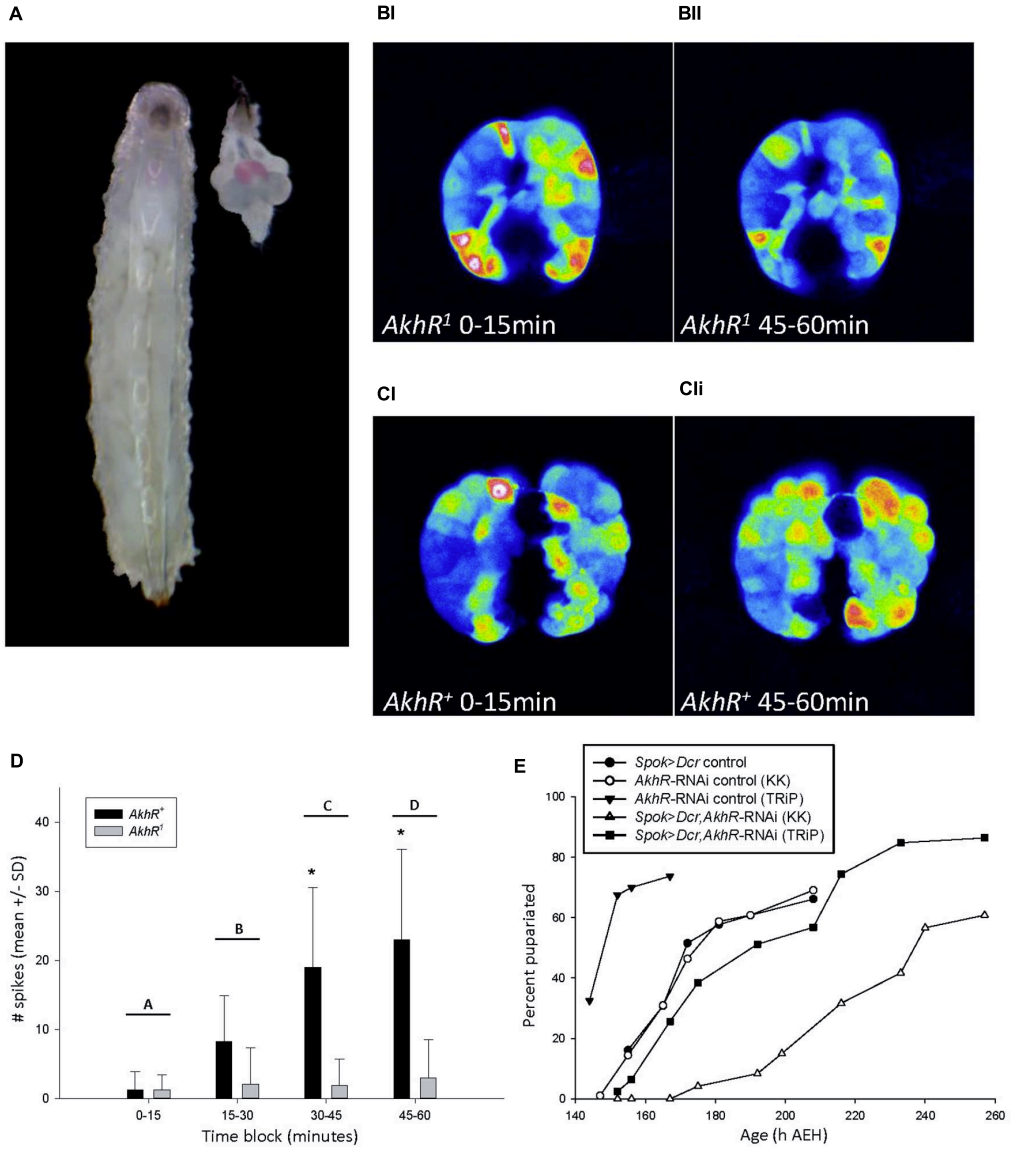

FIGURE 4 | AKH signaling in the PG increased intracellular cytosolic free calcium levels. **(A)** 90hAEH L3 and a dissected CNS-RG positioned to match its anatomical location in the larva. The PG was stained pink by a chemical reaction caused by *spok-GAL4* driving the co-expression of *UAS-GCaMP6m* and *UAS-CD4-td. Tom*. **(B,C)** Maximum intensity projections of PG intracellular calcium activity recorded *in vivo* from 88 to 90 h AEH larvae. Maximum intensity projections of PG calcium spike activity representative of $AkhR^1$ **(BI,II)** and $AkhR^+$ **(CI,II)** *spok > GCaMP6m* larvae during the 0–15 min **(BI,CI)** and 45–60 min **(BII,CII)** blocks. Representative videos of changes in calcium spiking can be found in online supplementary information. **(D)** Calcium spike activity did not differ between $AkhR^+$ vs. $AkhR^1$ during the 0–15 or 15–30 min block, but increased significantly in $AkhR^+$ in each subsequent block. $^*p < 0.001$ denotes statistically significant differences between genotypes within a time block; letters A vs. C and D ($p < 0.001$), B vs. C ($p = 0.006$), B vs. D ($p < 0.001$), A vs. B ($p = 0.079$), and C vs. D (0.237) denote statistically significant differences between time blocks in $AkhR^+$ ($p < 0.05$). **(E)** Reduced *AkhR* expression with KK (VDRC KK109300) in the PG caused significant developmental delay to pupariation in low nutrient food ($p < 0.001$). Reduced *AkhR* expression with TRiP (BDSC 29577) did not cause significant developmental delay ($p = 1.0$). See section "Materials and Methods" for details of statistical testing.

higher-order gustatory circuits to promote PER and increase SR (Kain and Dahanukar, 2015). *akh > Dcr;dg2*-RNAi caused a significant decrease in virgin female SR following 48h starvation (**Figure 5D**). These data supported our finding that *akh > Dcr;dg2*-RNAi increased adult starvation resistance.

Starvation resistance correlates with whole body lipid content, and whole body lipid content is typically directly proportional to body size (Chippindale et al., 1996; Vermeulen et al., 2006). Adult wing surface area is directly proportional to body size, and *akh > Dcr;dg2*-RNAi significantly decreased female body size (**Figures 5E,F**). In *D. melanogaster* literature, the assumption that body size is always directly proportional to whole body protein content underlies the practice of standardizing TAG data to protein content. In contrast to the significant

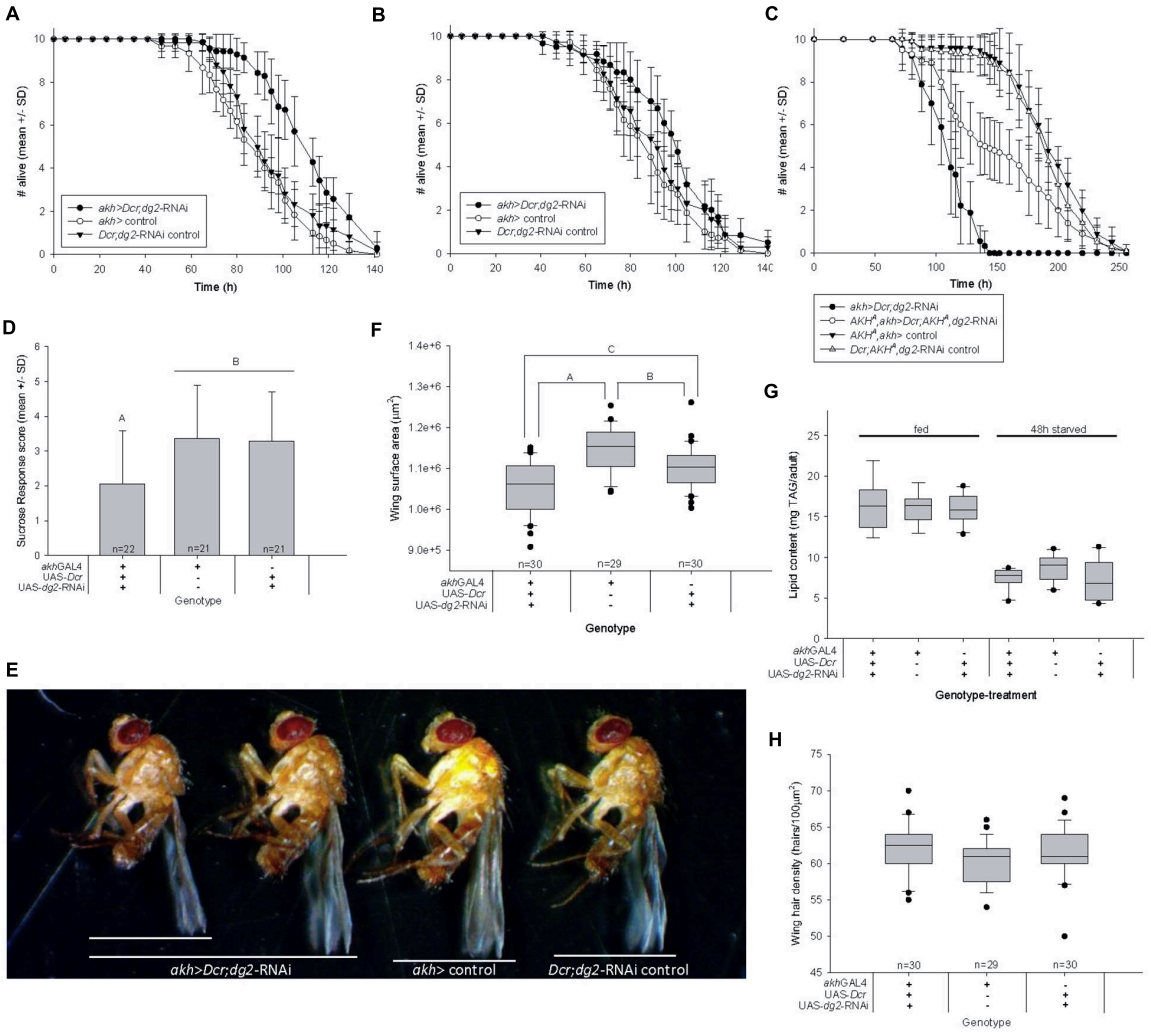

FIGURE 5 | Reduced *CC-dg2* interacts with juvenile metabolic stress to alter adult metabolism and cause obesity. **(A)** Adult female starvation resistance increased significantly ($p < 0.001$) in flies reared as larvae on low nutrient food. **(B)** Adult female starvation resistance was not significantly affected ($p = 0.146$) when flies were reared as larvae on standard nutrient food. **(C)** The effect of reducing *CC-dg2* expression in a wild type AKH^{+} background on adult female starvation resistance is reversed in the AKH^{A} single mutant background. **(D)** Female sucrose response decreased significantly following 48 h starvation. Letters denote statistically significant differences ($p = 0.011$). Data are shown as mean ± standard deviation (SD). **(E)** Representative images of adult females showing body size range within *akh > Dcr;dg2-RNA* genotype. **(F)** Adult female body size is significantly reduced relative to controls ($n = 40$/genotype). Letters denote statistically significant differences: A $p < 0.001$; B $p = 0.004$; C $p = 0.006$ (One way ANOVA, Holm-Sidak). **(G)** Whole body TAG content per adult body was not significantly affected by reduced *CC-dg2* expression in fed ($p = 0.966$) or 48 h starved ($p = 0.111$) females. $n = 7$–9 for fed samples, $n = 9$ for 48 h starved samples. **(H)** Wing cell density is not significantly affected ($p = 0.073$). See section "Materials and Methods" for details of statistical testing.

reduction in adult wing surface area (**Figure 5F**), we found that *akh > Dcr;dg2*-RNAi did not affect whole body protein content in fed flies (**Supplementary Figure 5F**). Furthermore, 48 h starvation significantly altered whole body protein content between genotypes (**Supplementary Figure 5F**). Whole body protein content was neither an appropriate surrogate for body size in our experiments, nor was whole body protein content stable across feeding treatments. We report whole body TAG content per individual.

Human obesity was clinically defined as a disproportionately high body mass relative to body height, where height is used as a surrogate measure of body size (Gutin, 2018). Obesity can be characterized in flies by examining whole body TAG content in proportion to body size. TAG content per individual fly was the same across genotypes (**Figure 5G**), and this indicated that – in proportion to body size (**Figure 5F**) – there was more TAG in the small-bodied adults that experienced *akh > Dcr;dg2*-RNAi and nutrient stress during larval life. These data suggested that adult obesity was a developmental outcome of this life stage-specific transgenic and nutritional manipulation. This may underlie the reported increase in adult starvation resistance.

Adult body size is determined by both cell proliferation and cell growth/size during larval life, and ecdysteroids influence these processes. Wing cells each produce one hair, and differences

in wing hair density thus reflect differences in cell size. *akh* > *Dcr*;*dg2*-RNAi did not affect wing hair density in a 100 μm^2 area (**Figure 5H**). The small body size of *akh* > *Dcr*;*dg2*-RNAi adults was not a consequence of reduced cell growth during larval development.

DISCUSSION

We identified a nutrient-dependent developmental role for AKH; this is the first evidence of its kind in *D. melanogaster*. Downregulation of CC-*dg2* expression in low nutrient rearing environments increased larval lethality and delayed the developmental transition from larval to pupal life. Flies that survived this treatment were smaller and more resistant to nutrient stress during adulthood. We discovered that AKH increased PG cytosolic free calcium levels, and this supported previous work that identified the potential for CC-PG paracrine signaling (Kim and Rulifson, 2004; Lee and Park, 2004; Yamanaka et al., 2015). Here we discuss the major findings and implications of our research: (1) *dg2*/PKG as a regulator of AKH activity and nutrient stress responsivity, (2) a novel developmental role for AKH, (3) the effect of AKH on PG intracellular calcium levels, and (4) a model for AKH as a nutrient-responsive prothoracicotropic factor, and its relevance to human development and metabolism.

dg2 Regulated AKH Nutrient Stress Responsivity

In starving flies, AKH is secreted from the CC and acts on various peripheral targets. AKH stimulates catabolism of glycogen and lipid reserves for an immediate source of energy (Kim and Rulifson, 2004; Isabel et al., 2005;(Lee and Park, 2004; Grönke et al., 2007; Stoffolano et al., 2014; Gàlikovà et al., 2015), stimulates locomotion in order to promote foraging behavior (Yu et al., 2016), increases sweet gustatory receptor neuron excitability so that starving flies will ingest low quality food (Dethier, 1976; Jourjine et al., 2016), and regulates post-prandial insulin secretion (Kim and Neufeld, 2015). The effect of metabolic stress on aging and longevity is also mediated by AKH (Waterson et al., 2014). These diverse functions implicate AKH in orchestrating a suite of changes in physiology and behavior that promote survival and restore metabolic homeostasis. Our work contributed this model: AKH signaling modified larval development in response to low nutrient stress, and *dg2* expression in the CC regulated this effect.

dg2 Altered AKH Activity

dg2 expression in the CC interacted with AKH to mediate the developmental response to low nutrient stress. Although we did not report definitive evidence of altered AKH secretion in response to *akh* > *Dcr*;*dg2*-RNAi, this is consistent with the *D. melanogaster* literature. Previous reports assayed the same phenotypes that we did for providing surrogate evidence of changes in AKH secretion. These included changes in the CC intracellular AKH content (Braco et al., 2012; Kim and Neufeld, 2015), altered lifespan during starvation (Braco et al., 2012; Gàlikovà et al., 2015), changes in metabolism and behavior (Lee and Park, 2004; Isabel et al., 2005), and *in vivo* imaging assays (Kim and Rulifson, 2004; Jourjine et al., 2016). Altogether, our data supported a role for *dg2* as a negative regulator of AKH secretion.

akh > *dTrpA1* stimulated secretion from the CC and phenocopied the developmental effect of *akh* > *Dcr*;*dg2*-RNAi. Increased activity of Ca^{2+} channels promotes AKH secretion from the CC, and the DTRPA1 Ca^{2+}-permeable cation channel provides a strong secretory stimulus (Pannabecker and Orchard, 1989; Hamada et al., 2008). The stronger effect of *akh* > *dTrpA1* might be attributable to the ability of its strong secretory stimulus to override other regulatory inputs that mitigated the effect of *dg2*-RNAi (Braco et al., 2012).

Future investigations into the means whereby *dg2* regulates AKH activity will focus on the influence of PKG activity on CC intracellular Ca^{2+}. AMPK and cAMP signaling promote CC cell excitability and increases AKH secretion by mediating an increase in intracellular Ca^{2+} in both *D. melanogaster* and *Locusta migratoria* (Pannabecker and Orchard, 1989; Braco et al., 2012). AMPK and cAMP signaling likewise promote intracellular Ca^{2+} and glucagon secretion from murine α cells, and PKG activity inhibits glucagon secretion by preventing Ca^{2+}-mediated membrane depolarization (Leiss et al., 2011). This promising avenue of research is supported by the data we report herein.

New methods of haemolymph extraction permit precise sampling required for hormone titer analysis (MacMillan and Hughson, 2014). The establishment of *D. melanogaster* as a model organism in metabolic syndrome research now requires the development of bioassays sensitive enough to quantify biologically significant changes in AKH titers.

AKH Altered Larval Development

Larval development in low nutrient rearing conditions was delayed by 6 h in response to *akh* > *Dcr*;*dg2*-RNAi in an AKH^{+} genetic background. Delays of only 3 h exert significant effects on growth and survival (Bakker, 1961). The developmental delay caused by *akh* > *Dcr*;*dg2*-RNAi in the AKH^{+} background was lost in both the AKH^{A} single mutant (where bioactive APRP is produced) and AKH^{AP} double mutant backgrounds (where neither AKH nor APRP are bioactive). From these data, *dg2* acted in the CC to regulate AKH signaling and this mediated a developmental response to low nutrient stress. This fits with the established role of the CC as a stress-responsive tissue (Vogt, 1946). Consistent with our findings, previous studies reported that AKH was dispensable during larval development in nutrient-abundant conditions (Kim and Rulifson, 2004; Lee and Park, 2004; Isabel et al., 2005; Grönke et al., 2007; Bharucha et al., 2008; Gàlikovà et al., 2015).

Insulin signaling affects larval development by acting directly on the PG to alter ecdysteroid biosynthesis (Caldwell et al., 2005; Colombani et al., 2005; Mirth et al., 2005). AKH altered insulin signaling through protein-dependent secretion of DILP3 (Kim and Neufeld, 2015). Yeast – the protein source in our low nutrient diet – provides cholesterol for ecdysteroid synthesis. From this, the possibility that *akh* > *Dcr*;*dg2*-RNAi and low nutrient diet

influenced development through AKH signaling to the IPCs must be further investigated; this is discussed in section 4.3.2.

Adipokinetic hormone precursor-related peptide was hypothesized to regulate developmental transitions (Clynen et al., 2004; De Loof et al., 2009). Seminal work on the AKH^{A} and AKH^{AP} mutants reported increased starvation resistance in these mutant lines relative to controls (Gàlikovà et al., 2015). Our data unexpectedly demonstrated that adult starvation resistance was significantly reduced in *akh* > *Dcr*;*dg2*-RNAi flies when AKH was inactive but APRP was active (i.e., AKH^{A}; **Figure 5C**), and there was no effect when both AKH and APRP were inactive (i.e., AKH^{AP}, **Supplementary Figure 5E**). The work reported by Gàlikovà et al. (2015) used flies reared as larvae in a nutrient-abundant environment and APRP did not alter adult starvation resistance. In light of this seminal report, we emphasize that our data must not be viewed as evidence of a direct role for APRP but rather of the complexity of tissue-specific gene function during early life development and its responsivity to a stressful nutrient environment. We propose that a putative role for APRP during pupal metamorphosis be investigated.

AKH Altered PG Calcium Dynamics

Adipokinetic hormone increased cytosolic free calcium levels in the PG. We hypothesized that AKHR might be an unidentified GPCR that stimulated the signaling cascade for vesicle-mediated ecdysteroid secretion from the PG (Yamanaka et al., 2015). While AKHR might not be present in the PG and it is possible that AKH acts indirectly on the PG, our neuroanatomical data and TTX experiments suggested that AKH might act directly on the PG. Here we propose a model wherein AKH acted directly on the PG to alter development in response to low nutrient stress.

AKHR mediated a stimulatory effect of AKH on PG calcium dynamics, but the response to AKH was slower than expected for GPCR signaling. We are not first to report slow intracellular calcium responsivity to stimulated GPCR signaling. In *Rhodnius*, malphighian tubules incubated in a serotonin solution exhibited changes in intracellular calcium levels that occurred over the order of 100–200 s (Gioino et al., 2014).

This slow response can be explained by our method for AKH treatment in this assay. Our model proposed a paracrine mechanism through which AKH was secreted directly into the PG. In contrast, we incubated dissected CNS-RG tissues in an AKH solution; this required the passive diffusion of AKH into the PG. It is thus possible that delayed and/or reduced AKH delivery to target cells in the PG caused the slow response. AKH injection into pupae was reported to increase heart rate slowly and only at concentrations of AKH two to five times greater than what is contained in the CC (Noyes et al., 1990). This was explained by the inability of AKH injection to replicate the high potency of endogenous paracrine secretion of AKH from the CC directly onto the aorta. Additionally, the long duration of our assay required that the CNS-RG be removed from the cuticle. As with Yamanaka et al. (2015), we found that this reduced spontaneous calcium spike frequency in the PG; cuticle removal may similarly have reduced PG sensitivity to AKH. Finally, it is possible that AKH acts indirectly on the PG by stimulating chemical-mediated exocytosis of a secreted factor that then acts on the PG to affect intracellular calcium dynamics.

Other CNS-RG-Derived Factors Influenced PG Calcium Dynamics

Another possibility for the slow calcium response to AKH might be that AKH signaling acts indirectly to make the gland competent to receive another GPCR signal, or that the response is modulated by other signals. Consistent with this view is our observation that application of TTX with AKH in our calcium imaging experiments significantly increased spike activity in $AkhR^{+}$ PGs relative to the application of AKH alone. This suggests that the CNS produces a signal that antagonizes the stimulatory effect of AKH in the PG.

Multiple prothoracicotropic and prothoracicostatic factors target the PG in order to regulate ecdysteroid physiology, and their interactions during development are not well characterized. Hormones like PTTH, insulin and serotonin have tropic effects on ecdysteroidogenesis in insects, while prothoracicostatic peptide (PTSP) inhibits this process (Colombani et al., 2005; McBrayer et al., 2007; Yamanaka et al., 2010; Shimada-Niwa and Niwa, 2014). PTTH, insulin, and serotonin communicate nutritional information to the PG in order to modify development in response to the environment. AKH may interact with one or more prothoracicotropic and/or –static factors in order to coordinate ecdysteroid biosynthesis and secretion. Whether or not AKH indeed interacts with another factor, and whether or not this interaction directly regulates ecdysteroid secretion or indirectly permits PG competency, are subjects for future investigations.

Is AKH a Novel Prothoracicotropic Factor?

The PG is a decision-making center that regulates ecdysteroid physiology so as to modify growth and development in response to nutritional inputs (Yamanaka et al., 2013). IIS and PTTH provide nutritional information to the PG pertaining to the anabolic status of the larva (Caldwell et al., 2005; Colombani et al., 2005; Mirth et al., 2005). We hypothesize that AKH is a nutrient stress-responsive factor that communicates catabolic status to the PG. The precise effect of AKH on ecdysteroid physiology must be investigated in future work.

When essential nutrients are deficient, starving larvae must make the decision to pupariate. Starvation inhibits anabolism, and larvae cannot mount an adaptive response through IIS/TOR (Layalle et al., 2008). Starvation promotes catabolism, which stimulates AKH secretion. We showed that AKH signaling in the PG stimulated cytosolic free calcium levels in a manner reminiscent of that reported for the active secretion of ecdysteroids. We propose that *dg2*/PKG-mediated AKH secretion from the CC stimulates ecdysteroid secretion in response to low nutrient stress. Possible evidence for this model lies in the reduction in wing cell proliferation caused by *akh* > *Dcr*;*dg2*-RNAi (**Figure 5H**), as this effect was associated with a modest increase in haemolymph ecdysteroid titers throughout larval life (Colombani et al., 2005).

We were unable to detect a change in circulating ecdysteroid titers in response to *akh* > *Dcr*;*dg2*-RNAi, and there are several possible explanations for this. First, quantification of both ecdysone and 20-hydroxyecdysone may be required to detect changes in ecdysteroid secretion, as in Yamanaka et al. (2015). Second, more frequent sampling of ecdysteroid titers during the third larval instar might increase the resolution of ecdysteroid titer analysis. Third, calcium imaging experiments with TTX identified a putative prothoracicostatic factor(s) that targeted the PG and attenuated the effect of AKH; the effects of competing inputs were attributed to slower cardioacceleratory response to AKH (Noyes et al., 1990). In the future, the influence of multiple signaling inputs to the PG must be controlled for in the characterization of ecdysteroid secretory dynamics.

Loss of *AkhR* in the PG caused developmental delay (**Figure 4E**), but AKH signaling also caused developmental delay (**Figures 1B,C**, **4E**). This may be explained by functional redundancy in the regulatory input of nutritional information to the PG. Decreased serotonin signaling in the PG delayed development in response to low nutrient stress (Shimada-Niwa and Niwa, 2014). Serotonin can cause developmental delay in response to low nutrient stress independently of AKH signaling in the PG. Chronically dysregulated systemic AKH signaling in *akh* > *Dcr*;*dg2*-RNAi larvae might also contribute to the delay.

In a model where AKH signaling in the PG stimulated ecdysteroid secretion, why were larvae developmentally delayed in response to *akh* > *Dcr*;*dg2*-RNAi We suggest that *akh* > *Dcr*;*dg2*-RNAi stimulated ecdysteroid secretion throughout larval life and depleted PG ecdysteroid content. Support for this comes from Yamanaka and colleagues, who observed first and second instar larval lethality in response to activated GPCR signaling in the PG: precise temporal regulation of GPCR signaling is essential for developmental progression through larval life (Yamanaka et al., 2015).

AKH and Metabolic Syndrome

Chronic dysregulation of glucagon and insulin signaling underlie the pathogenesis of type 2 diabetes mellitus T2DM, and the activities of both hormones must be studied together (Unger and Orci, 1975). DILPs have been the primary focus of metabolic disease modeling in *D. melanogaster* (Owusu-Ansah and Perrimon, 2014). Our work demonstrates that the CC-specific role of PKG as a regulator of AKH activity must be considered in the development of fly models for metabolic syndrome.

In humans, pre-natal, childhood, and pubertal malnutrition perturb GnRH signaling in the HPG axis, and thereby contribute to the pathogenesis of metabolic syndrome both within and across generations (Habtu et al., 1999; Painter et al., 2008; Jang et al., 2013; Wang et al., 2017). We reported that CC-*dg2*-mediated disruption of AKH signaling during embryonic, larval, and pupal development – in conjunction with larval nutrient stress – increased the whole body lipid to body size ratio in a manner suggestive of obesity: this suggests a functional parallel between AKH and GnRH. The GnRHR ortholog, *AkhR*, has been implicated in the intergenerational transmission of nutrient stress effects on lipid homeostasis (Palu et al., 2017). Glucagon and GnRH are evolutionarily related (Lindemans et al., 2009; Zandawala et al., 2017). The dual functionality of AKH as a glucagon-like and a GnRH-like peptide presents great potential for understanding the etiological basis of metabolic syndrome, as well as the means whereby the effects of nutrient stress are transmitted across generations through altered HPG axis activity.

DATA AVAILABILITY STATEMENT

The raw data supporting the conclusions of this article will be made available by the authors, without undue reservation.

AUTHOR CONTRIBUTIONS

MS and MBO carried out the developmental timing assays in **Figure 4E** and ecdysteroid titer quantification in **Supplementary Figures 4A,B**. BNH performed the other experiments. All authors contributed to the article and approved the submitted version.

FUNDING

BNH was supported by a Natural Science and Engineering Council of Canada and Canadian Institute for Advanced Research grant (to Marla B. Sokolowski), and MS and MBO were supported by the NIH grant R35GM-118029.

ACKNOWLEDGMENTS

We thank Professor J. Dason for assistance with the conception, troubleshooting, design, and analysis of calcium imaging experiments, Anders Vesterberg for wing size and cell quantification. We thank all three reviewers for their insightful and productive input.

SUPPLEMENTARY MATERIAL

The Supplementary Material for this article can be found online at: https://www.frontiersin.org/articles/10.3389/fphys.2021.619219/full#supplementary-material

Supplementary Video 1 | wild type *AKHR*$^{+}$ (left panel) and *AKHR*^{1} mutant (right panel). Video shows changes in PG intracellular calcium levels during block 1 (0 to 15 minutes). AKH was added at t = 5 minutes. The warmer colours indicate higher levels of calcium.

Supplementary Video 2 | wild type *AKHR*$^{+}$ (left panel) and *AKHR*^{1} mutant (right panel). Video shows changes in PG intracellular calcium levels during block 4 (45 to 60 minutes). The warmer colours indicate higher levels of calcium. Note that these block 4 *AKHR*$^{+}$ and *AKHR*^{1} samples are the same tissues as shown for block 1 *AKHR*$^{+}$ and *AKHR*^{1} samples in **Supplementary Video 1**.

Supplementary Video 3 | wild type *AKHR*$^{+}$ without TTX (left panel) and wild type *AKHR*$^{+}$ with TTX (right panel). Video shows changes in PG intracellular calcium levels during block 4 (45 to 60 minutes). The warmer colours indicate higher levels of calcium. Note that the *AKHR*$^{+}$ without TTX block 4 sample shown here in the left panel is the same dataset as shown for the block 4 *AKHR*$^{+}$ sample in **Supplementary Video 2**.

REFERENCES

Allen, A. M., Anreiter, I., Neville, M. C., and Sokolowski, M. B. (2017). Feeding-related traits are affected by dosage of the foraging gene in *Drosophila melanogaster*. *Genetics* 205, 761–773. doi: 10.1534/genetics.116.197939

Bakker, K. (1961). An analysis of factors which determine success in competition for food among larvae of *Drosophila melanogaster*. *Arch. Neerlandaises Zool.* 14, 200–281. doi: 10.1163/036551661x00061

Bernard, C. (1854). 'Cours de physiologie générale de la Faculté des Sciences'. *Le Moniteur des Hôpitaux* 2:409.

Bharucha, K. N., Tarr, P., and Zipursky, S. L. (2008). A glucagon-like endocrine pathway in *Drosophila* modulates both lipid and carbohydrate homeostasis. *J. Exp. Biol.* 211, 3103–3111. doi: 10.1242/jeb.016451

Braco, J. T., Gillespie, E. L., Alberto, G. E., Brenman, J. E., and Johnson, E. C. (2012). Energy-dependent modulation of glucagon-like signaling in *Drosophila* via the AMP-activated protein kinase. *Genetics* 192, 457–466. doi: 10.1534/genetics.112.143610

Brand, A. H., and Perrimon, N. (1993). Targeted gene expression as a means of altering cell fates and generating dominant phenotypes. *Development* 118, 401–415.

Caldwell, P. E., Walkiewicz, M., and Stern, M. (2005). Ras activity in the *Drosophila* prothoracic gland regulates body size and developmental rate via ecdysone release. *Curr. Biol.* 15, 1785–1795. doi: 10.1016/j.cub.2005.09.011

Cannon, W. B. (1929). Organization for physiological homeostasis. *Physiol. Rev.* 9, 399–431. doi: 10.1152/physrev.1929.9.3.399

Chen, T.-W., Wardill, T. J., Sun, Y., Pulver, S. R., Renninger, S. L., Baohan, A., et al. (2013). Ultra-sensitive fluorescent proteins for imaging neuronal activity. *Nature* 499, 295–300.

Chippindale, A. K., Chu, T. J. F., and Rose, M. R. (1996). Complex trade-offs and the evolution of starvation resistance in *Drosophila melanogaster*. *Evolution* 50, 753–766. doi: 10.1111/j.1558-5646.1996.tb03885.x

Clynen, E., De Loof, A., and Schoofs, L. (2004). New insights into the evolution of the GRF superfamily based on sequence similarity between the locust APRPs and human GRF. *Gen. Comp. Endocrinol.* 139, 173–178. doi: 10.1016/j.ygcen.2004.07.006

Colombani, J., Bianchini, L., Layalle, S., Pondeville, E., Dauphin-Villemant, C., Antoniewski, C., et al. (2005). Antagonistic actions of ecdysone and insulins determine final Size in *Drosophila*. *Nature* 310, 667–670. doi: 10.1126/science.1119432

Dason, J. S., Cheung, A., Anreiter, I., Montemurri, V. A., Allen, A. M., and Sokolowski, M. B. (2019). *Drosophila melanogaster foraging* regulates a nociceptive-like escape behaviour through a developmentally plastic sensory circuit. *PNAS* 117, 23286–23291. doi: 10.1073/pnas.1820840116

de Belle, S. J., Hilliker, A. J., and Sokolowski, M. B. (1989). Genetic localization of a foraging (for) – a major gene for larval behaviour in *Drosophila melanogaster*. *Genetics* 123, 157–163. doi: 10.1093/genetics/123.1.157

De Loof, A., Vandersmissen, T., Huybrechts, J., Landuyt, B., Baggerman, G., Clynen, E., et al. (2009). APRP, the second peptide encoded by the adipokinetic hormone gene(s), is highly conserved in evolution. *Trends Comp. Endocrinol. Neurobiol.* 1162, 376–378. doi: 10.1111/j.1749-6632.2008.03638.x

Delcour, J., and Lints, F. A. (1967). Environmental and genetic variations of wing size, cell size and cell division rate, in *Drosophila melanogaster*. *Genetica* 37: 543–556. doi: 10.1007/BF01547152

Dethier, V. G. (1976). *The Hungry Fly: A Physiological Study of the Behavior Associated With Feeding*. Cambridge, MA: Harvard University Press.

Estes, P. S., Ho, G. L., Narayana, R., and Ramaswami, M. (2000). Synaptic localization and restricted diffusion of a *Drosophila* neuronal synaptobrevin-green fluorescent protein chimera *in vivo*. *J. Neurogenet.* 13, 233–255.

Flybase Id FBal0193987 *Dmel\lilli[189Y]. FB2020_06. General Information; Also Known As*. Avaliable at: http://flybase.org/reports/FBal0193987.html (accessed January 18, 2021).

FlyBase Id FBgn0000721 *Dmel\for. FB2020_06. Alleles, Insertions, and Transgenic Constructs; Classical and Insertion Alleles (84) (see: page 6, for[189Y])*. Avaliable at: https://flybase.org/reports/FBgn0000721.html (accessed January 18, 2021).

FlyBase Id FBti0007080 *Dmel\P{GawB}lilli[189Y]. FB2020_06. General Information; Also Known As*. Avaliable at: https://flybase.org/reports/FBti0007080 (accessed January 18, 2021).

Gàlikovà, M., Diesner, M., Klepsatel, P., Hehlert, P., Xu, Y., Bickmeyer, I., et al. (2015). Energy homeostasis control in *Drosophila* adipokinetic hormone mutants. *Genetics* 201, 665–683.

Gioino, P., Murray, B. G., and Ianowski, J. P. (2014). Serotonin triggers cAMP and PKA-mediated intracellular calcium waves in Malpighian tubules of *Rhodnius prolixus*. *Ame. J. Physiol. Regul. Integrat. Comp. Physiol.* 307, R828–R836.

Grönke, S., Mildner, A., Fellert, S., Tennagels, N., Petry, S., Müller, G., et al. (2005). Brummer lipase is an evolutionary conserved fat storage regulator in *Drosophila*. *Cell Metab.* 1, 323–330. doi: 10.1016/j.cmet.2005.04.003

Grönke, S., Muller, G., Hirsch, J., Fellert, S., Andreou, A., Haase, T., et al. (2007). Dual lipolytic control of body fat storage and mobilization in *Drosophila*. *PLoS Biol.* 5:e137. doi: 10.1371/journal.pbio.0050137

Gutin, I. (2018). In BMI we trust: reframing the body mass index as a measure of health. *Soc. Theory Health* 16, 256–271. doi: 10.1057/s41285-017-0055-0

Habtu, E., Gill, G., and Tesfaye, S. (1999). Characteristics of insulin-requiring diabetes in rural northern Ethiopia – a possible link with malnutrition? *Ethiopian Med. J.* 37, 263–267.

Hamada, F. N., Rosenzweig, M., Kang, K., Pulver, S. R., Ghezzi, A., Jegla, T. J., et al. (2008). An internal thermal sensor controlling temperature preference in *Drosophila*. *Nature* 454, 217–222. doi: 10.1038/nature07001

Hofmann, F., Feil, R., Kleppisch, R., and Schlossmann, J. (2006). Function of cGMP-dependent protein kinases as revealed by gene disruption. *Physiol. Rev.* 86, 1–23. doi: 10.1152/physrev.00015.2005

Hughson, B. N., Anreiter, I., Jackson Chornenki, N. L., Murphy, K. R., Ja, W. W., Huber, R., et al. (2018). The adult foraging assay (AFA) detects strain and food-deprivation effects in feeding-related traits of *Drosophila melanogaster*. *J. Insect Physiol.* 106, 20–29. doi: 10.1016/j.jinsphys.2017.08.011

Ikeya, T., Galic, M., Belawat, P., Nairz, K., and Hafen, E. (2002). Nutrient dependent expression of insulin-like peptides from neuroendocrine cells in the CNS contributes to growth regulation in *Drosophila*. *Curr. Biol.* 12, 1293–1300. doi: 10.1016/s0960-9822(02)01043-6

Isabel, G., Martin, J.-R., Chidami, S., Veenstra, J. A., and Rosay, P. (2005). AKH-producing neuroendocrine cell ablation decreases trehalose and induces behavioral changes in *Drosophila*. *Am. J. Physiol. Regul. Integr. Comp. Physiol.* 288, R531–R538.

Jang, X., Ma, H., Wang, Y., and Liu, Y. (2013). Early life factors and Type 2 Diabetes Mellitus. *J. Diabetes Res.* 2013:485082.

Jékely, G. (2013). Global view of the evolution and diversity of metazoan neuropeptide signaling. *PNAS* 110, 8702–8707. doi: 10.1073/pnas.1221833110

Jourjine, N., Mullaney, B. C., Mann, K., and Scott, K. (2016). Coupled sensing of hunger and thirst signals balances sugar and water consumption. *Cell* 166, 1–12.

Kain, P., and Dahanukar, A. (2015). Secondary taster neurons that convey sweet taste and starvation in the *Drosophila* brain. *Neuron* 85, 819–832. doi: 10.1016/j.neuron.2015.01.005

Kalderon, D., and Rubin, G. M. (1989). cGMP-dependent protein kinase genes in *Drosophila*. *J. Biol. Chem.* 264, 10738–10748. doi: 10.1016/s0021-9258(18)81684-2

Kim, J., and Neufeld, T. P. (2015). Dietary sugar promotes systemic TOR activation in *Drosophila* through AKH-dependent selective secretion of Dilp3. *Nat. Commun.* 6:6846.

Kim, S. K., and Rulifson, E. J. (2004). Conserved mechanisms of glucose sensing and regulation by *Drosophila* corpora cardiaca cells. *Nature* 431, 316–320. doi: 10.1038/nature02897

Layalle, S., Arquier, N., and Léopold, P. (2008). The TOR pathway couples nutrition and developmental timing in *Drosophila*. *Dev. Cell* 15, 568–577. doi: 10.1016/j.devcel.2008.08.003

Lee, G., and Park, J. H. (2004). Hemolymph sugar homeostasis and starvation-induced hyperactivity affected by genetic manipulations of the adipokinetic hormone-encoding gene in *Drosophila melanogaster*. *Genetics* 167, 311–323. doi: 10.1534/genetics.167.1.311

Leiss, V., Friebe, A., Welling, A., Hofmann, F., and Lukowski, R. (2011). Cyclic GMP kinase I modulates glucagon release from pancreatic α-cells. *Diabetes* 60, 148–156. doi: 10.2337/db10-0595

Lindemans, M., Liu, F., Janssen, T., Husson, S. J., Mertens, I., Gade, G., et al. (2009). Adipokinetic hormone signaling through the gonadotropin-releasing hormone receptor modulates egg-laying in *Caenorhabditis elegans*. *Proc. the Natl. Acad. Sci. U.S.A.* 106, 1642–1647. doi: 10.1073/pnas.0809881106

Macleod, G. T., Hegstrom-Wojtowicz, M., Charlton, M. P., and Atwood, H. L. (2002). Fast calcium signals in *Drosophila* motor neuron terminals. *J. Neurophysiol.* 88, 2659–2663. doi: 10.1152/jn.00515.2002

MacMillan, H. A., and Hughson, B. N. (2014). A high-throughput method of hemolymph extraction from adult *Drosophila* without anesthesia. *J. Insect Physiol.* 63, 27–31. doi: 10.1016/j.jinsphys.2014.02.005

McBrayer, Z., Ono, H., Shimell, M., Parvy, J. P., Beckstead, R. B., Warren, J. T., et al. (2007). Prothoracicotropic hormone regulates developmental timing and body size in *Drosophila*. *Dev. Cell* 13, 857–871. doi: 10.1016/j.devcel.2007.11.003

Mirabeau, O., and Joly, J.-S. (2013). Molecular evolution of peptidergic signaling systems in bilaterians. *PNAS* 110, E2028–E2037.

Mirth, C., Truman, J. W., and Riddiford, L. M. (2005). The role of the prothoracic gland in determining critical weight for metamorphosis in *Drosophila melanogaster*. *Curr. Biol.* 15, 1796–1807. doi: 10.1016/j.cub.2005.09.017

Mirth, C. K., and Riddiford, L. M. (2007). Size assessment and growth control: how adult size is determined in insects. *BioEssays* 29, 344–355. doi: 10.1002/bies.20552

Nässel, D. R. (2009). Neuropeptide signaling near and far: how localized and timed is the action of neuropeptides in brain circuits? *Invert. Neurosci.* 9, 57–75. doi: 10.1007/s10158-009-0090-1

Noyes, B. E., Katz, F. N., and Schaffer, M. H. (1990). Identification and expression of the *Drosophila* adipokinetic hormone gene. *Mol. Cell. Endocrinol.* 109, 133–141. doi: 10.1016/0303-7207(95)03492-p

Osborne, K. A., Robichon, A., Burgess, E., Butland, S., Shaw, R. A., Coulthard, A., et al. (1997). Natural behaviour polymorphism due to a cGMP-dependent protein kinase of *Drosophila*. *Science* 277, 834–836. doi: 10.1126/science.277.5327.834

Owusu-Ansah, E., and Perrimon, N. (2014). Modeling metabolic homeostasis and nutrient sensing in *Drosophila*: implications for aging and metabolic diseases. *Dis. Models Mech.* 7, 343–350. doi: 10.1242/dmm.012989

Painter, R. C., Osmond, C., Gluckman, P., Hanson, M., Phillips, D. I. W., and Roseboom, T. J. (2008). Transgenerational effects of prenatal exposure to the Dutch famine on neonatal adiposity and health later in life. *BJOG* 115, 1243–1249. doi: 10.1111/j.1471-0528.2008.01822.x

Palu, R. A. S., Praggastis, S. A., and Thummel, C. S. (2017). Parental obesity leads to metabolic changes in the F2 generation in *Drosophila*. *Mol. Metab.* 6, 631–639. doi: 10.1016/j.molmet.2017.03.012

Pannabecker, T., and Orchard, I. (1989). Ionic dependence of depolarization-mediated adipokinetic hormone release from the locust corpus cardiacum. *Brain Res.* 477, 38–47. doi: 10.1016/0006-8993(89)91392-9

Shimada-Niwa, Y., and Niwa, R. (2014). Serotonergic neurons respond to nutrients and regulate the timing of steroid hormone biosynthesis in *Drosophila*. *Nat. Commun.* 5, 1–13. doi: 10.1016/j.mce.2003.11.003

Shimell, M., Pan, X., Martin, F. A., Ghosh, A. C., Léopold, P., O'Connor, M. B., et al. (2018). Prothoracicotropic hormone modulates environmental adaptive plasticity through the control of developmental timing. *Development* 145:dev159699. doi: 10.1242/dev.159699

Shiraiwa, T., and Carlson, J. R. (2007). Proboscis extension response (PER) assay in *Drosophila*. 2007. *J. Vis. Exp.* 193, 193. doi: 10.3791/193

Sokolowski, M. (2006). *189Y update. FlyBase ID FBrf0198702. Data From Reference; Alleles (2)*. Avaliable at: https://flybase.org/reports/FBrf0198702 (accessed January 18, 2021).

Sokolowski, M. B. (1980). Foraging strategies of *Drosophila melanogaster*: a chromosomal analysis. *Behav. Genet.* 10, 291–302. doi: 10.1007/bf01067774

Staubli, F., Jorgensen, T. J. D., Cazzamali, G., Williamson, M., Lenz, C., Sonfergaard, L., et al. (2002). Molecular identification of the insect adipokinetic hormone receptors. *Proc. Natl. Acad. Sci. U.S.A.* 99, 3446–3451. doi: 10.1073/pnas.052556499

Stoffolano, J. G. Jr., Croke, K., Chambers, J., Gade, G., Solari, P., and Liscia, A. (2014). Role of Phote-HrTH (*Phormia terraenovae* hypertrehalosemic hormone) in modulating the supercontractile muscles of the crop of adult *Phormia regina* Meigen. *J. Insect Physiol.* 71, 147–155. doi: 10.1016/j.jinsphys.2014.10.014

Sullivan, E. L., and Grove, K. L. (2010). Metabolic imprinting of obesity. *Forum Nutr.* 63, 186–194. doi: 10.1159/000264406

Unger, R. H., and Orci, L. (1975). The essential role of glucagon in the pathogenesis of diabetes mellitus. *Lancet* 1, 14–16. doi: 10.1016/s0140-6736(75)92375-2

Vermeulen, C. J., Van De Zande, L., and Bijlsma, R. (2006). Developmental and age-specific effects of selection on difergent virgin life span on fat content and starvation resistance in *Drosophila melanogaster*. *J. Insect Physiol.* 52, 910–919. doi: 10.1016/j.jinsphys.2006.05.014

Vogt, M. (1946). Inhibitory effects of the corpora cardiaca and of the corpus allatum in *Drosophila*. *Nature* 157:512. doi: 10.1038/157512b0

Wang, N., Cheng, J., Han, B., Li, Q., Chen, Y., Xia, F., et al. (2017). Exposure to severe famine in the prenatal or postnatal period and the development of diabetes in adulthood: an observational study. *Diabetologia* 60, 262–269. doi: 10.1007/s00125-016-4148-4

Wang, Z., Pan, Y., Li, W., Jiang, H., Chatzimanolis, L., Chang, J., et al. (2008). Visual pattern mamory requires *foraging* function in the central complex of *Drosophila*. *Learn. Mem.* 15, 133–142. doi: 10.1101/lm.873008

Waterson, M. J., Chung, B. Y., Harvanek, Z. M., Ostojic, I., Alcedo, J., and Pletcher, S. D. (2014). Water sensor *ppk28* modulates *Drosophila* lifespan and physiology through AKH signaling. *Proc. Natl. Acad. Sci. U.S.A.* 111, 8137–8142. doi: 10.1073/pnas.1315461111

Wicher, D., Agricola, H.-J., Sohler, S., Gundel, M., Heinemann, S. H., Wollweber, L., et al. (2006). Differential receptor activation by cockroach adipokinetic hormones produces differential effects on ion currents, neuronal activity, and locomotion. *J. Neurosci.* 95, 2314–2325. doi: 10.1152/jn.01007.2005

Yamamoto-Hino, M., and Goto, S. (2013). *In vivo* RNAi-based screens: studies in model organisms. *Genes* 4, 646–665. doi: 10.3390/genes4040646

Yamanaka, N., Hua, Y.-J., Roller, L., Spalovska-Valachova, I., Mizoguchi, A., Kataoka, H., et al. (2010). *Bombyx* prothoracicostatic peptides activate the sex peptide receptor to regulate ecdysteroid biosynthesis. *Proc. Natl. Acad. Sci. U.S.A.* 107, 2060–2065. doi: 10.1073/pnas.0907471107

Yamanaka, N., Marqués, G., and O'Connor, M. B. (2015). Vesicle-mediated steroid hormone secretion in *Drosophila melanogaster*. *Cell* 163, 907–919. doi: 10.1016/j.cell.2015.10.022

Yamanaka, N., Rewitz, K. F., and O'Connor, M. B. (2013). Ecdysone control of developmental transitions: lessons from research in *Drosophila*. *eAnnu. Rev. Entomol.* 58, 497–515. doi: 10.1146/annurev-ento-120811-153608

Yu, Y., Huang, R., Ye, J., Zhang, V., Wu, C., Cheng, G., et al. (2016). Regulation of starvation-induced hyperactivity by insulin and glucagon signaling in adult *Drosophila*. *eLife* 5:e15693.

Zandawala, M., Tian, S., and Elphick, M. R. (2017). The evolution and nomenclature of GnRH-type and corazonin-type neuropeptide signaling systems. *Gen. Comp. Endocrinol.* 264, 64–77. doi: 10.1016/j.ygcen.2017.06.007

Zhang, Y. Q., Rodesch, C. K., and Broadie, K. (2002). Living synaptic vesicle marker: synaptotagmin-GFP. *Genesis* 34, 142–145. doi: 10.1002/gene.10144

Conflict of Interest: The authors declare that the research was conducted in the absence of any commercial or financial relationships that could be construed as a potential conflict of interest.

Advantages of publishing in Frontiers

OPEN ACCESS
Articles are free to read for greatest visibility and readership

FAST PUBLICATION
Around 90 days from submission to decision

HIGH QUALITY PEER-REVIEW
Rigorous, collaborative, and constructive peer-review

TRANSPARENT PEER-REVIEW
Editors and reviewers acknowledged by name on published articles

Frontiers
Avenue du Tribunal-Fédéral 34
1005 Lausanne | Switzerland

Visit us: www.frontiersin.org
Contact us: frontiersin.org/about/contact

REPRODUCIBILITY OF RESEARCH
Support open data and methods to enhance research reproducibility

DIGITAL PUBLISHING
Articles designed for optimal readership across devices

FOLLOW US
@frontiersin

IMPACT METRICS
Advanced article metrics track visibility across digital media

EXTENSIVE PROMOTION
Marketing and promotion of impactful research

LOOP RESEARCH NETWORK
Our network increases your article's readership